Universidad del País Vasco
Euskal Herriko Unibertsitatea

Haizea Ziarrusta Intxaurtza

October 2018

Integrated analytical approaches to study the adverse effects of pharmaceuticals and personal care products on aquatic ecosystems

Universidad del País Vasco
Euskal Herriko Unibertsitatea

IBeA
Ikerkuntza eta Berrikuntza Analitikoa

Analytical Chemistry Department

Integrated analytical approaches to study the adverse effects of pharmaceuticals and personal care products on aquatic ecosystems

Haizea Ziarrusta Intxaurtza

2018

A thesis submitted for the international degree of Philosophiae Doctor
in Environmental Contamination and Toxicology

supervised by

Dr. Olatz Zuloaga Zubieta
Dr. Maitane Olivares Zabalandikoetxea

(c)2018 HAIZEA ZIARRUSTA INTXAURTZA

Bekak eta Finantziazioa

Tesi hau Hezkuntza, kultura eta kirol ministerioaren doktore berrien prestakuntzarako diru-laguntzari esker egin da, unibertsitate-irakasleen formaziorako (Formación de Profesorado Universitario, FPU, delakorako) programa nazionalaren barruan. Era berean, Hezkuntza, kultura eta kirol ministerioak doktorego-ikasleei bideraturiko mugikortasun-bekari esker posible izan da Estokolmoko Unibertsitatean (Suedia) 5 hilabeteko egonaldia egitea 2016an, eta bide batez Nazioarteko Tesiaren aipamena eskuratu ahal izatea. Bestalde, Kultur Paisaien eta Ondarearen UNESCO katedrak emandako mugikortasun-bekari esker Kataluniako Unibertsitate Politeknikoan (Bartzelona) 2 hilabeteko egonaldia egin ahal izan da 2017an.

Horretaz gain, tesi honetan bildu diren lanak egin ahal izateko hurrengo ikerketa-proiektuen diru-laguntza eskertu nahi dugu:

(i) Nuevas metodologías para evaluar el impacto de los contaminantes emergentes en ecosistemas marinos y el consumo de alimentos (CTM2014-56628-C3-1-R) 2015-2017. Ikerlari Nagusia: Nestor Etxebarria Loizate.

(ii) A-motako Talde kontsolidatua (IT-742-13) Eusko Jaurlaritza, 2012-2018. Ikerlari Nagusia: Juan Manuel Madariaga Mota.

Esker onak

Aitite-amamak sarriten esan doskue denporea arin pasetan dala… Eta zelan ez, arrazoia! Nire eredu zaren horrek, eskutxotik hartute, bideak zabaldu jostezuzen oin dala zazpi bet urte eta ez dekot esperientzi zoragarri hau biziteko aukerea aprobetxau izinen damurik! Hainbeste aholku, eta beste horrenbeste ebatzi. Gauze asko ezin leiz diruegaz pagau. Eta, hamaika abenturen ostean, honaino punturaino heldute… zuri eta beste guztiori eskerrak emotea baino ez jata gelditan.

Lehenengo ta behin, zuzendarieri, eskerrak nigez batera *montaña rusa* honetara igoten animetearren. Ez dau modurik, arlo pertsonalean zein akademikoan, in dozuezan zuzendari, zientzialari, psikologo, lagun, guraso eta beste infinito roletan zuokandik jaso doten laguntasune eta babesa eskertuteko. Txikitetik, barneratute dekot, ekinde lortuten direla gauzek; eskerrik asko talde-lana errealidade bihurtuteagaitik.

Praktiketan batu ginenetik, beti inguruen egon zarien beste hirurori be milesker! Oingoan be, argi gelditu de, danok apurtxu bet emonda lortuten dala gitxi batzuk dana emon behar ez izitea. Eskerrik asko, arrain handiaua zein txikiaua izitea, ez dozuelako gehau edo gitxiau iziteagaz lotuten. Eta hemen be, arkalengandik hur gu! Urrin egon arren, ederto akordetan naz klaseko lehenengo egunegaz! Eskerrik asko juerga, bije eta terapia guztiekaitik!

IBeA taldeko beste kide guztiori be, eskerrik asko aholku guztiekaitik. Laborategien zein laborategitik kanpo, danokandik jaso dot zeozer lehenengo “egun on”-etik azken txanpako proposamenetaraino. Eta mintegi people! Zorragarrie da horrenbeste persona eta personaje ezetuteko aukerea aukitea. Betidanik hor egon dan saltseratik hasi eta etorri barrietaraino. Erdi ahiztute deku zer dan sardinek latan moduen egotea, eh? Eskerrik asko barrealdi guztiekaitik! Nozko hurrungo *social activity*? Gure hizkuntzeari bere lekutxue iten lagundu dostezuenori zein dekanotzako arbelari begire palmeratxuek nigez batera jan dozuezenori, besarkada fuerte bana. Mosu bana PiE-tar danori be, eta eskerrik asko esperimentuekaz eta disekziñoakaz esku bet bota dostezuen danori. Danok barik ez dauelako osorik.

Atzerriko bi estantziekaitik be, zer esan! It was a stressful but at the same time very enriching experience! Tack ACES people and Skarpnäck family! Y qué decir a los de big bang theory… Moltes gràcies frikis de s2lab por vuestra paciencia con la novata de R!

Unibersidadean zein unibersidadetik kanpo, bidean in dodazen laguneri be mosu handi bana! Ez noa izenak banan banan esaten, bea eskerrik asko aloha, friemly, la banda del terror eta konpañia, kontinental, ex“milan-paeshi basqui”… Garbikerrekoakaz, giputxilandiako bulegokoakaz, papelak inprimidu edo eskaneu dostezuezenokaz, kirola ereinazo dostezuenokaz, muskuloak soltauostezuenokaz, eta auzokoakaz be izin ahiztu! Auzolanean beste gauze batzun artean nire

n-garren etxeari bizie emon dotsezuenok be bazarie honen parte. Eskerrik asko irribarrea zein negarra ataratearren, aterrizetan lagundutearren eta batzutan burue beste mundu batera eroanazotearren. Zuotako bakotzan begiradeak itzelezko energie emoten dau… Eta zuon laguntasun barik, batzutan ez zan posible izingo gauze ez hain onari alde positiboa topetea.

Eta zelan ez, etxeko danantzat, eta etxeko moduen sentiduazo nozuen danontzat besarkada beroenak Makaztuire, Urkuzure, Munetxara, Altzustera, eta teilatupe bardine nigez konpartidu dozuenokana. Istori honen parte zarien danori ez jatsuez helduko eskerrok, bea danon *maitasunegaz, epeltasunegaz, errespetuegaz, esker onagaz, laguntasunegaz* eta *gozotasunegaz* gelditan naz. Eskerrik asko kendu dotsuodazen minutu guztiekaitik, zuon pazientziegaitik, eta begiek zabaltan lagunduteagaitik. Eskerrik asko emoneko bazkari guztiekaitik! Ogie emoten doskun hori zelan itzi aititu barik! Bea zuok emoneko energie janetik harau doa!

Munduen pazientzi gehien dekon horreri zelan eskertu beti hor egotea! Ia, tesie akabaute gero, azeitunetxoak ze atxaki topetan dauen. Eta zer esan zuokaitik biokatik? Lurpean egon arren eguzki izpiek ikusi leiz kartetan zein kantetan! Ez daigun umorea galdu! Bizie emon eta mundu zoro honetara ekarri nozuenori be eskerrik asko, berbaz zein begiradeagaz emoneko babesagaitik. Edozeinek ez dauz holango eredu bi aukin. Hau ez zan bardine izingo zuokandik barneratu dodazen balore barik, ezinbestekoak diren gauze batzuk ez dire tesi beten ikisten eta. Ikisi beharrean, aplikau iten dire. Eta zenbet sensaziño, emoziño... batzutan kanpoan, ta beste askotan ondiño barruen!

Ta batan bat ez bada identifikaute sentidu ilada honeitan, lasai! Nire espresiño faltea da, idaztea ez da danon puntu fuerteena-eta.... Eskerrik asko zuri be! Duderik ez, testu honen irakurle hutse baino gehau zarela nitzako! Eta, momenturen baten, ez badotsuet behadan beste kasu in, parkatu!

Asko ikisi doten arren, askoz gehau ikisteko gogoagaz segitan dot, kuriosidadeak dakarrelako jakiturie, eta alrebes. Beti ikisten da zeozer, eta etapa honetatik argi gelditu jatana hauxe da, gatza gatzau bihurtuteak ez dekola zentsurik… eta *gatza bada, ez dala ezinezkoa*! Ekine baragarrie da, ta urrintxuau ikusi arren, beste gauze batzuk be lortukoguz herri honetan: "*Bihotza, Burue, Eskue! Sentitu, Pentsatu, Ekin!*".

Ba horixe, eskerrik asko danori eta batuko gara mendien, etxean, laborategien, herriko plazan zein munduko beste punten! Eta momentuz, ez dakit arrainek zoriontsuek diren Euskal Herriko erreketan, bea ni zuori danori esker, bai! Asko gure zaituziet!

Diman, 2018ko Irailaren 7an

Aurkibidea / Table of contents

Abbreviations / Laburdurak

A

ACN	acetonitrile / *azetonitriloa*
AIF	all ion fragmentation / *ioi guztien apurketa*
AMI	amitriptyline / *amitriptilina*
ANOVA	analysis of variance / *bariantza-analisia*
AOP	adverse outcome pathway / *ondorio kaltegarrien bidea*
APCI	atmospheric pressure chemical ionization / *presio atmosferikoko ionizazio kimikoa*
ASCA	analysis of variance-simultaneous component analysis / *bariantza-analisia - aldibereko osagaien analisia*
au	arbitrary units / *unitate arbitrarioak*

B

BCF	bioconcentration factor / *biokontzentrazio-faktorea*
BPs	by-products / *azpiproduktuak*

C

C_{18}	octadecylsilyl / *oktadezilsilil*
CCD	central composite design / *diseinu konposatu zentrala*
CID	collision induced dissociation / *talkak bultzatutako disoziazioa*
CIPRO	ciprofloxacin / *ciprofloxacin*
CLO	clomipramine / *klomipramina*
CPCA	common principal components analysis / *osagai nagusi komunen analisia*
CX	cation exchanger / *katio-trukatzaile*

D

DANO	danofloxacin / *danofloxacin*
ddMS2	data dependent MS/MS / *datuen menpeko MS/MS ekorketa*

D (Continuation / Jarraipena)

DHB	2,4-dihydroxybenzophenone / *2,4-dihidroxibenzofenona*
DHMB	2,2'-dihydroxy-4-methoxybenzophenone / *2,2'-dihidroxi-4-metoxibenzofenona*
DIA	data independent acquisition / *datuen menpekotasunik gabeko eskuratze-modua*
DIMS	direct infusion mass spectrometry / *sarrera zuzeneko masa-espektrometria*

E

EDA	effect-directed analysis / *efektuek bideratutako analisia*
EDCs	endocrine disruptor compounds / *disruptore endokrinoak*
EDTA	ethylendiaminetetraacetic acid / *azido etilendiaminotetraazetikoa*
EMEA	European Medicine Evaluation Agency / *medikamentuen ebaluaziorako europar agentzia*
ENO	enoxacin / *enoxacin*
ENRO	enrofloxacin / *enrofloxacin*
EQSs	environmental quality standards / *ingurumeneko kalitate-arauak*
ERA	environmental risk assessment / *ingurumenerako arriskuen ebaluazioa*
ESI	electrospray ionization / *elektroesprai-ionizazioa*
EtOAc	ethyl acetate / *etil azetatoa*
EtOH	ethanol / *etanola*

F

FBSC	feature-based signal correction / *elementuetan oinarritutako seinale-zuzenketa*
FC	fold-change / *aldaketa-maila*
FDR	false discovery rate / *aurkikuntza faltsuen tasa*
FQs	fluoroquinolones / *fluorokinolonak*
Full MS-ddMS2	full scan – data dependant MS/MS / *ekorketa osoa - datuen menpeko MS/MS*
FUSLE	focused ultrasound solid–liquid extraction / *ultrasoinu fokatuen bidezko solido-likido erauzketa*

G

GABA	gamma-aminobutyric acid / *gamma-aminobutiriko azidoa*
GC	gas chromatography / *gas-kromatografia*
GC-MS	gas chromatography coupled to mass spectrometry / *masa-espektrometriari akoplatutako gas-kromatografia*

H

HCD	higher-energy collisional dissociation / *energia altuko talka-disoziazioa*
HESI	heated electrospray ionization / *elektroesprai-ionizazio berotua*
HILIC	hydrophilic interaction liquid chromatography / *elkarrekintza hidrofilikoan oinarritutako likido-kromatografia*
HLB	hydrophilic–lipophilic balanced / *hidrofiliko-lipofiliko orekatua*
HOAc	acetic acid / *azido azetikoa*
HRMS	high resolution mass spectrometry / *bereizmen altuko masa-espektrometria*
HSI	hepatic somatic index / *indize hepatosomatikoa*

I

IMI	imipramine / *imipramina*

K

K	condition factor / *egoera-faktorea*
KNN	k-nearest neighbor / *k-nearest neighbor*

L

LC	liquid chromatography / *likido-kromatografia*
LC-FLD	liquid chromatography coupled to fluorescence detector / *likido-kromatografia - fluoreszentzia-detektagailua*
LC-MS	liquid chromatography - mass spectrometry / *masa-espektrometriari akoplatutako likido-kromatografia*

L (Continuation / Jarraipena)

LC-MS/MS	liquid chromatography – tandem mass spectrometry *likido-kromatografia tandem masa-espektrometria*
LC-QqQ	liquid chromatography - triple quadrupole mass spectrometry / *likido-kromatografia kuadrupolo hirukoitzeko masa-espektrometria*
LEVO	levofloxacin / *levofloxacin*
LLE	liquid-liquid extraction / *likido-likido erauzketa*
LOD	limit of detection / *detekzio-muga*
LOME	lomefloxacin / *lomefloxacin*
LOQ	limit of quantification / *kuantifikazio-muga*
LOQ_{proc}	procedural limit of quantification / *kuantifikazio-muga prozedurala*

M

MAE	microwave-assisted extraction / *mikrouhinen bidezko erauzketa*
MDL	method detection limit / *metodoaren detekzio-muga*
MeOH	methanol / *metanola*
MEW	mass extraction-window / *masaren erauzketa-leihoa*
MIP	molecularly imprinted polymer / *molekularki inprimatutako polimeroa*
MLR	multiple linear regression / *aldagai askotariko erregresio lineala*
MoA	mode of action / *ekintza-modua*
MS	mass spectrometry / *masa-espektrometria*
MS/MS	tandem mass spectrometry / *tandem masa-espektrometria*
MSPD	matrix solid-phase dispersion / *fase solidoan dispertsatutako matrizearen bidezko erauzketa*

N

NCE	normalized collision energy / *normalizatutako talka-energia*
NMDAR	N-methyl-D-aspartate receptor / *N-metil-D-aspartato errezeptorea*
NMR	nuclear magnetic resonance / *errezonantzia magnetiko nuklearra*
NOR	nortriptyline / *nortriptilina*
NORF	norfloxacin / *norfloxacin*
NP-SPE	normal-phase solid phase extraction/*fase normaleko fase solidoko erauzketa*

O

OECD	Organization for Economic Co-operation and Development / *Lankidetza eta Garapen Ekonomikorako Erakundea*
OFLO	ofloxacin / *ofloxacin*
OXY	oxybenzone / *oxibenzona*

P

PA	polyamide / *poliamida*
PCA	principal component analysis / *osagai nagusien analisia*
PCPs	personal care products / *zaintza pertsonalerako produktuak*
PEC	predicted environmental concentration / *aurresandako ingurumeneko kontzentrazioa*
PEFLO	pefloxacin / *pefloxacin*
PhACs	pharmaceutical active compounds / *farmakologikoki aktiboak diren konposatuak*
PhCs	pharmaceutical compounds / *farmakoak*
PLE	pressurized liquid extraction / *presiopeko likidoen bidezko erauzketa*
PLS-DA	partial least squares-discriminant analysis / *karratu txiki partzialen bidezko analisi diskriminatzailea*
PNEC	predicted no effect concentration / *aurresandako efektu gabeko kontzentrazioa*
POPs	persistent organic pollutants / *kutsatzaile organiko iraunkorrak*
PP	polypropylene / *polipropilenoa*
PPCPs	pharmaceuticals and personal care products / *farmakoak eta zaintza pertsonalerako produktuak*

Q

QC	quality control / *kalitate-kontrola*
QC_{ext}	extraction quality control sample / *erauzketaren kalitate-kontrolerako lagina*
QC_{seq}	sequence quality control sample / *sekuentziaren kalitate-kontrolerako lagina*
QOrbitrap	quadrupole-Orbitrap mass spectrometer/ *kuadrupolo-Orbitrap masa-analizatzailea*
QqQ	triple quadrupole mass spectrometry/ *kuadrupolo hirukoitzeko masa-espektrometria*

R

RF	radio frequency / *irrati-frekuentzia*
ROS	reactive oxygen species / *oxigenoaren espezie erreaktiboak*
RP-SPE	reverse-phase solid phase extraction / *alderantzizko faseko fase solidoko erauzketa*
RSD	relative standard deviation / *desbiderazio estandar erlatiboa*

S

S/N	signal to noise ratio / *seinale-zarata erlazioa*
SPAR	sparfloxacin / *sparfloxacin*
SPE	solid phase extraction / *fase solidoko erauzketa*
SRM	selected reaction monitoring / *ioi aitzindarietatik apurketa-ioietarako trantsizioen jarraipena*
SSRIs	selective serotonin reuptake inhibitors / *serotoninaren xurgapen selektiboaren inhibitzaileak*

T

TCAs	tricyclic antidepressants / *antidepresibo triziklikoak*
THB	2,3,4-trihydroxybenzophenone / *2,3,4-trihidroxibenzofenona*
TOC	total organic content / *materia organiko osoa*
TOF	time-of-flight / *hegaldi-denbora*
TPs	transformation products / *transformazio-produktuak*

U

UHPLC	ultrahigh performance liquid chromatographic / *ultra-bereizmen altuko likido-kromatografia*
UHPLC-qOrbitrap	ultra high performance liquid chromatography coupled to tandem quadrupole-Orbitrap / *ultra-bereizmen altuko likido-kromatografia - tandem kuadrupolo-Orbitrap*
UHPLC-QqQ-MS/MS	ultra high performance liquid chromatography coupled to triple quadrupole mass spectrometry / *kuadrupolo hirukoitzeko masa-espektrometriari akoplatutako ultra-bereizmen altuko likido-kromatografia*

U (Continuation / Jarraipena)

US EPA	United States Environmental Protection Agency / *Ameriketako Estatu Batuetako Ingurumenaren Babeserako Agentzia*
USE	ultrasound extraction / *ultrasoinuen bidezko erauzketa*

V

VIP	variables importance on projection / *aldagaiek proiekzioan duten garrantzia*

W

WFD	Water Framework Directive / *Ur-Esparru Zuzentaraua*
USE	World Health Organization / *Munduko Osasunaren Erakundea*
WWTP	wastewater treatment plant / *ur-araztegi*

X

XIC	extracted ion chromatogram / *erauzitako ioien kromatograma*

1. Kapitulua

Sarrera

1.1 Farmakoak eta zaintza pertsonalerako produktuak ur-ingurumenean

Farmakoak eta zaintza pertsonalerako produktuak (*pharmaceuticals and personal care products*, PPCP, delakoak) funtzionalitate, propietate fisiko-kimiko eta aktibitate biologiko desberdinak dituzten molekula konplexuak dira [1]. Farmakoak giza zein animalia-gaixotasunak saihesteko edo tratatzeko kontsumitzen diren konposatuak diren bitartean, zaintza pertsonalerako produktuak bizi-kalitatea hobetzeko erabiltzen dira [2]. PPCP-en ekoizpena mundu mailan $2{\cdot}10^7$ tonara hel daiteke urtero [3]. Konposatu horien erabilera zabalak, batez ere herrialde garatuetan, PPCP-ak ur-ingurumenerako kutsadura-iturri nagusienetako bat bilakatzea eragin du [4–8]. PPCP-ak kutsatzaile iraunkor gisa sailkatzen ez diren arren, haien isuria ur-ingurumenera etengabekoa da, eta ng/L-µg/L kontzentrazio-mailan detektatzen dira sarri. Ondorioz, kutsatzaile iraunkorrak bailiran jokatzen dute [5] eta, beraien kontzentrazioak maila kaltegarriak izateraino heltzen badira, uretako organismoetan albo-ondorioak sor ditzakete [9–15]. Hori dela eta, azken urteotan, arazo horren inguruko kezka zientifikoa eta soziala areagotu egin da.

PPCP-en ingurumeneko agerpen zabalak sortutako kezka zenbait legeditan islatzen da ere. Farmakoen ingurumeneko arautzearen lehen urratsak Europar Batasunak (EB-ak) eman zituen. Alde batetik, hiru farmako (17-α-etinilestradiol eta 17-β-estradiol hormonak eta minaren kontrako diklofenak konposatua) "zaintza-zerrenda" delakoan sartu zituen [16]. Beste alde batetik, Europako Ur-Esparru Zuzentarauan (*Water Framework Directive*, WFD, delakoan) PPCP batzuk etorkizuneko lehentasunezko hautagai emergente gisa izendatu zituzten [17]. Esaterako, karbamazepina, iopamidola eta musketa sintetikoak. Horrez gain, WFD-eko orientazio teknikoko dokumentuak biota urtarrean ingurumeneko kalitate-mailak emateko jarraitu beharreko prozedura azaltzen du [18]. Prozedura horrek organismo urtarrentzako eta giza osasunerako arriskuak kontuan hartzen ditu. Aldi berean, Ameriketako Estatu Batuetako Ingurumenaren Babeserako Agentziak (*Environmental Protection Agency*, EPA, delakoak) 14 farmako gehitu zituen hirugarren kutsadura-hautagaien zerrendan [19]. Gainera, PPCP batzuk disruptore endokrino gisa sailkatuta daude [12]. Munduko Osasunaren Erakundearen (*World Health Organization*, WHO, delakoaren) arabera, disruptore endokrinoak sistema endokrinoko funtzioak aztoratzen dituzten substantzia exogenoak edo euren nahasteak dira eta, ondorioz, organismoetan, haien ondorengoetan edo azpi-

biztanlerian albo-ondorioak dituzte. Bestalde, Europako sendagaien ebaluazio-agentziak ezarritako jarraibideetan PPCP-en ingurumenerako arriskuen ebaluazioa aipatzen da [20]. Bertan, izaera kimiko anitzeko konposatuei beraien arrisku-ratioetan oinarritutako lehentasuna nola ezarri deskribatzen da. Hala ere, ratio horiek kalkulatzeko eskuragarri dauden PPCP-en inguruko datu ekotoxikologikoak oso mugatuak dira. Hortaz, PPCP-en erabilera zabala eta ingurumeneko presentzia kontuan izanda, segimendua egiteko planteamendu berriak garatzea beharrezkoa da legedi berrietan aurkeztu ahal izateko. EPA-ren arabera [21], PPCP-en arautzea bermatzeko ezinbesteko baldintza da haien ingurumeneko agerraldiaren eta arriskuen inguruko informazio nahikoa izatea. Izan ere, arriskuen ebaluazio-prozesuan, politikoki bideratutako arrisku-kudeaketa burutu edo neurri arautzaileak ezarri ahal izateko, beharrezkoa da arriskuen azterketa zientifikoa egitea (arriskuen identifikazioa, efektuen ebaluazioa, esposizioaren ebaluazioa eta arriskuen karakterizazioa, besteak beste) [22].

PPCP-ak, dagokien erabileraren ondoren, ur-hondakinetan isuri eta, ur-araztegietako ohiko tratamenduetan guztiz eliminatzen ez direnez, ur-ekosistemetan nonahi agertzen dira [3–5,7,12,23]. Arestian esan bezala, PPCP-en taldea konposatu organikoen hainbat familia desberdinek osatzen dute [5]. Farmakoen artean antibiotikoak, antidepresiboak, hormonak, antiinflamatorioak, epilepsiaren kontrako konposatuak, odoleko lipidoen erregulatzaileak, β-blokeatzaileak eta droga zitostatikoak aurki ditzakegu. Eta zaintza pertsonalerako produktuei dagokienez, antimikrobianoak, musketa sintetikoak, intsektuen aurkako konposatuak, kontserbatzaileak eta ultramore (UM) iragazkiak aipa ditzakegu, besteak beste.

Farmakoen artean, arreta berezia jarri izan zaie antibiotikoei, 90. hamarkadaren amaieratik behatu izan den antibiotikoekiko erresistentziaren areagotze azkarra dela eta [2,24–26]. Ingurumenean nagusiki detektatzen diren antibiotikoen artean fluorokinolonak daude [27,28]. Ur-ekosistemetan ng/L-µg/L kontzentrazio-mailan aurki ditzakegun konposatu horiek arnas-aparatuko gaixotasunen eta bakterio-infekzioen aurka erabiltzen dira medikuntzan zein albaitaritzan. Bestalde, antidepresiboak ere, ingurumenean sarri agertzen diren farmakoak, bereziki kezkagarriak dira espezie urtar ez-zuzenduen portaera alda dezaketelako [10]. Luzaroan depresioa eta buruko gaitzak (adibidez, antsietatea eta fobia) tratatzeko erabili izan diren antidepresibo triziklikoak ingurumenean aurkitu izan dira [29]. Antidepresibo trizikliko batzuk serotoninaren xurgapen

selektiboaren inhibitzaile (*selective serotonin reuptake inhibitor*, SSRI, delako) gisa jokatzen dute eta, nahiz eta ez dagoen guztiz argituta SSRI-ekiko uretako organismoen erantzuna zein den, hainbat ikerketek albo-ondorioak eragiten dituztela baieztatu dute. Besteak beste, agresibitatearen gutxitzea, elikadura-erantzunen inhibizioa, ugalketaren murriztea, enbrioien garapenaren anomaliak eta garapen fisiologikoaren eta sexu-heldutasunaren atzeratzea [10,30].

Farmakoekin erkatuta, zaintza pertsonalerako produktuak kontzentrazio-maila altuagoan aurkitu ohi dira ingurumenean [31] igeri egitean edota bainu bat hartzean zuzenean ur-azalera isurtzen direlako [32]. Adibidez, UM iragazkiek eguneroko bizitzan erabilera anitz dituzte, hala nola eguzki-babeseko produktuetako, larruazaleko kremetako, ileko espraietako eta tintetako eta gainontzeko kosmetikoetako osagai garrantzitsuak baitira [32,33]. Konposatu horiek arreta zientifiko handia bereganatu dute organismo urtarren sistema endokrinoa oztopatzen dutelako [31,34].

PPCP-en ingurumeneko agerpenaren ikerlan gehienak ur-hondakinen araztegietako isurietan eta azaleko uretan fokatzen dira [1,4,7,14,23,35] eta biotan metatzearen inguruko ikerketa gutxi daude eskuragarri [13,15,36–38]. Hala eta guztiz ere, nahiz eta aztarna-mailan egon, beraien etengabeko isuria mehatxu izan liteke uretako organismo ez-zuzenduentzat [38]. Izan ere, esposizioaren eraginak ebaluatzeko ohiko modua da organismoetan kutsatzaileen biometatzea aztertzea. Orokorrean, arrainak, hauen ingurumeneko nonahikotasunagatik, organismo bideragarritzat hartzen dira biometatze-azterketetarako edota ur-sistemen segimendua egiten duten programetarako [39]. Arrainetan, zein beste organismo urtar batzuetan, PPCP-en presentziaren inguruan eskuragarri dagoen informazioa PPCP-ek duten biometatze-gaitasunaren adierazgarri da [5,9,12,15,35–37,40].

Testuinguru honetan, PPCP-en segimendua egitean, kutsatzaileen analisia ur-laginetara mugatu beharrean, lagin biologikoetara ere hedatzen da gaur egun. Horrek, aztarna-mailan dauden PPCP-ak matrize desberdinetan kuantifikatu ahal izateko metodo analitiko sendoak eta sentikorrak garatzeko beharra sortzen du [41]. Gainera, PPCP-en metatzea eta ehun-distribuzioa sakon aztertu ahal izateko, arrain osoa batera bere osotasunean aztertu edo soilik ehun bakarrera mugatu beharrean, aipatutako metodoak ehun eta jariakin biologiko desberdinetara zabaldu beharko lirateke. Izan ere, PPCP-ak askotan mintz biologikoak zeharkatzeko diseinatuta daude eta,

ondorioz, euren metatzea ehunekiko espezifikoa izan daiteke [13].

1.1.1 Metodo analitikoen garapena

Kutsatzaile organiko iraunkorrekin alderatuta PPCP-ak polarragoak izanik, normalean kontzentrazio baxuagotan aurkitzen dira [41]. Azken urteotan PPCP-ak aztarna-mailan detektatzeko metodo analitikoak nabarmen aurreratu diren arren, oraindik gainditu gabe daude erronka analitiko batzuk, besteak beste, biota bezalako ingurumeneko matrizeen konplexutasunarekin loturikoak. Ondorioz, matrize konplexuetako PPCP-en analisian beharrezkoak izan ohi dira laginaren aurretratamendu egokia egin eta sentikortasun altuko detektagailu selektiboak erabiltzea [5,6,36,42]. Azken urteotan, ingurumeneko laginak aztertzeko hainbat aztarna anitzen analisi-metodo garatu dira [23,40,41,43–46]. Hala ere, erauzketaren eraginkortasun falta nabari daiteke, konposatu batzuentzat aztergai diren laginak konplexuak izateaz gain, aztergai diren konposatuen propietate fisiko-kimikoak (polaritatea, disolbakortasuna, eta egonkortasuna, adibidez) oso ezberdinak baitira [6,42]. Ondorioz, metodo analitiko gehienak konposatu bakarraren edo familia bakarreko konposatuen azterketan oinarritzen dira [36].

Ingurumeneko matrizeetako konposatu organikoen analisian, laginaren prestaketa edo aurretratamendua urrats garrantzitsuenetakoa da [6,47,48]. Orokorrean, erauzketa- eta garbiketa-urratsek osatzen dute laginaren prestaketa. Bibliografiaren arabera, PPCP-ak lagin solidoetatik erauzteko erabilitako erauzketa-metodo nagusienak hurrengoak dira: ohiko solido-likido erauzketa-teknikak, ultrasoinuen bidezko erauzketa, mikrouhinen bidezko erauzketa, presiopeko likidoen bidezko erauzketa eta fase solidoan dispertsatutako matrizearen bidezko erauzketa [36,41,42,49]. Erauzketaren eraginkortasuna hobetzeko asmoz, ultrasoinu fokatuen bidezko solido-likido erauzketa (*focused ultrasound solid-liquid extraction*, FUSLE, delakoa) nabarmendu da biotatik konposatu organikoak erauzteko ahalezko teknika gisa [50,51]. FUSLE-ren eraginkortasuna kabitazio-fenomenoaren bidez lortutako presio eta tenperatura altuen ondorioz lortzen da. Hain zuzen, titaniozko mikropunta zuzenean erauzian murgilduta eratzen diren ahalmen handiko ultrasoinu-uhinetan datza FUSLE. Horrez gain, erauzketa-teknika horrek lagin- eta disolbatzaile-kantitate txikiak behar ditu analitoak kuantitatiboki erauzteko prozesu errazaren, azkarraren eta errepikakorraren bidez.

Arestian deskribatutako erauzketa-metodo gehienen selektibitate falta dela eta, erauzketaren ondoren, garbiketa-urratsa behar izaten da orokorrean. Garbiketa-metodo ohikoena fase solidoko erauzketa (*solid phase extraction*, SPE, delakoa) da. Teknika horrek PPCP-en isolamendua edota aurrekontzentrazioa baimentzen ditu ingurumeneko ur-lagin zein biota bezalako matrize desberdinetan [4,23,41,47–49]. Bibliografian, ur-lagin/erauzien garbiketarako gehien aplikatzen diren hurbilketek alderantzizko faseko fase geldikorrak erabiltzen dituzte, beti ere, aurretiaz laginaren pH-a egokituta konposatu azidoen edo basikoen desprotonazioa edo protonazioa, hurrenez hurren, ekiditeko [41,48]. Egun, dibinilbentzenoz eta binilpirrolidonaz osatutako kopolimeroa da alderantzizko faseko fase geldikor erabiliena [41,49]. Hala ere, kasu batzuetan modu mistoko anioi- edo ioi-trukatzaileak eta molekularki inprimatutako polimeroak (*molecularly imprinted polymers*, MIPs, delakoak) aurki daitezke [41,48]. Izan ere, fase geldikor horiek duten erretentzio-mekanismo selektiboagoak erauzi garbiagoak lortzea ahalbidetzen du. Bestalde, gantz ugari dituzten laginen kasuan, lipido eta beste interferentzia ez-polarrak kentzeko, fase normalean burutu ohi da SPE [36]. Horretarako, Florisil, silika edo alumina bezalako fase geldikor polarrak erabiltzen dira.

PPCP-en analisian sarri erabiltzen diren teknika analitikoak likido- (LC) edo gas-kromatografia (GC) dira, biak ala biak detektagailu desberdinei lotuta [23,36,47,49]. Dena den, nagusiki LC erabiltzen da, konposatu polarrekin eta ez-hegazkorrekin duen bateragarritasunagatik [6,42,52]. Aurrerapen teknologiko desberdinek, PPCP-en banaketa nabarmenki hobetu dute matrize konplexutan, besteak beste, ohiko instrumentazioek baino presio altuagotan lan egitea baimendu dute 2 µm azpiko partikulaz paketatutako zutabeen eskuragarritasunaren handitzeak eta hardware-aren hobetzeak [41].

Nahiz eta frogatuta dagoen LC-ri lotuta UM absorbantzia- edo fluoreszentzia-detektagailuak teknika errentagarriak direla, PPCP-en analisian hobetsita dago masa-espektrometria (MS) [23,36,41]. Izan ere, LC-MS metodoak dituen selektibitate, zehaztasun eta sentikortasun altuek matrize konplexuetan aztarna-mailan dauden PPCP-en analisia laguntzen dute. Gainera, PPCP-en analisian erabilitako fluoreszentzia bezalako beste detektagailu batzuekin alderatuta, nahiz eta kromatografikoki banatzea ezinezkoa izan, MS-ak isotopikoki markatutako analogoak erabiltzea ahalbidetzen du emaitza zehatzak lortzeko. MS-ak barne hartzen dituen teknologia desberdinen

artean, azken hamarkadetan tandem masa-espektrometriak (MS/MS) arrakasta handia lortu du [36,43–45,49]. Hurbilketa horrek matrize-interferentziak gutxitzeko edo ezabatzeko gaitasuna du ioi aitzindari eta apurketa-ioi egokiak aukeratuta. Hala ere, LC-MS/MS teknikaren desabantaila nagusia, bereziki elektroesprai-ionizazioa (*electrospray ionization*, ESI, delakoa) erabilita, matrize-interferentziek analitoekin batera eluitzeagatik gertatu daitekeen kromatografia-seinalearen txikitzea/handitzea da [6,41,42,49,52]. Detekzioko matrize-efektua zuzentzeko estrategia ezagunena barne-estandarrak erabiltzea da [36] baina batzuetan ez daude merkatuan eskuragarri edo garestiak dira. Barne-estandarrak erabiltzearen alternatiba gehitze estandarrak dira, nahiz eta hurbilketa horrekin nabarmen handitzen den analisi-denbora [41]. Ondorioz, ionizazio eskasak, hondoaren zaratak eta LC sistemako akatsek eragindako okerreko emaitzak saihestu nahi badira, beharrezkoa izan ohi da interferentziak gutxitzeko prozeduran garbiketa-urratsak sartzea [23].

MS detektagailuen funtzionamenduan ematen ari diren hobekuntzek ere eragin handia dute laginaren aurretratamendu/aurrekontzentrazio prozeduretan [41]. Egungoekin alderatuta, prozedurak askoz sinpleagoak eta laburragoak izan daitezke. Esate baterako, bereizmen altuko masa-espektrometriako (*high resolution MS*, HRMS, delako) analizatzaileak dituzten masa-espektrometro hibridoen erabilerak selektibitatea hobetzen du eta positibo faltsuak saihesten ditu [53]. Gainera, HRMS analisian, erreferentziazko estandarrak erabilita egindako analisi bideratuaz gain, erreferentziazko estandarrak erabili gabeko hurbilketak egitea ere posible da, hots, susmagarrien analisia eta analisi ez-bideratua [54,55]. Susmagarrien analisian, identifikazio tentagarria burutu ahal izateko, espero diren konposatuen (“susmagarrien”) inguruko informazio espezifikoa eskuragarri dago. Bestalde, analisi ez-bideratua aldez-aurretiko inongo informaziorik gabe hasten da.

1.2 Farmakoen eta zaintza pertsonalerako produktuen esposizioa organismo urtar ez-zuzenduetan

Biotaren segimenduaz gain, *in vivo* esposizio-esperimentuak beharrezkoak dira organismo urtarretan PPCP-en metatzea, ehunen arteko banaketa, metabolizazioa eta kanporatzea ulertzeko. Uretako organismo ornodunen artean, arrainak dira PPCP-en eraginak pairatzeko arrisku handiena

dutenak, ekosisteman duten tokiaz gain, ugaztunekin prozesu fisiologiko askotan dituzten antzekotasunengatik [11]. Kutsatzaileak arrainetara sartzeko bide desberdinak daude: PPCP-ak dituen ura zein sedimentuak arrainaren azalarekin eta zakatzekin kontaktuan jarrita, dietaren bidez ahoratuta, edo amarengandik arrautzetako lipidoetan kutsatzaileak transferituta [11]. Biometatze terminoa zehaztasunez definitu gabe egon arren, biota-lagineko eta azken hori inguratzen duen eremuko konposatu kimikoaren kontzentrazioen arteko zatiketatik kalkulatzen da [15,37]. Kutsatzaileak ingurumeneko uretan disolbatuta dauden kasuan, arrainen ehunetan gertatzen den biometatzea biokontzentrazio-faktorearen (*bioconcentration factor*, BCF, delakoaren) bidez adierazi ohi da [15]. BCF-a organismoko eta orekan dagoen uretako konposatu kimikoaren kontzentrazioen arteko erlazioa da. Horrez gain, kutsatzaileen biometatzea eta xedea hobeto ulertzeko, BCF proportzionalak kalkula daitezke organismoaren ehun/organo desberdinak kontuan hartuta [15]. Izan ere, hainbat arrazoi daude ehunetan biometatze espezifikoa behatzeko. Esate baterako, farmako jakin batzuk organo/ehun espezifiko batzuetara iristeko diseinatuta daude. Hala nola, antidepresiboek burmuinean dituzte euren helburu molekularrak [13]. Hori dela eta, ahal den heinean, kutsatzaileak duen ehunen arteko banaketa espezifikoa zehaztu behar da. Izan ere, organismo guztia batera bere osotasunean aztertuta, edo soilik ehun bakarrera mugatuta, kontzentrazio osoa gutxiesteko arriskua dago eta ondorio lokalizatuek eragindako arriskuen okerreko ebaluazioa egin daiteke [13].

Lankidetza eta Garapen Ekonomikorako Erakundearen (*Organisation for Economic Co-operation and Development*, OECD, delakoaren) arabera, ehun biologikoetan biometatzeko gaitasun handia dute ur-oktanol banaketa-koefizientearen (log K_{OW}-aren) balioa 3 edo handiagoa duten substantziek (hau da, konposatu hidrofobikoek) [37]. Hala eta guztiz ere, ohiko konposatu organikoekin alderatuta, PPCP-ak nahiko hidrofilikoak dira eta, ondorioz, OECD-ak proposatutako metatze-irizpideak ez du egokitasunez azaltzen PPCP-en biometatzeko-gaitasuna [15,38]. Hori dela eta, PPCP-en biometatzea soilik euren lipofilikotasunaren bidez azaldu beharrean, bestelako prozesuak izan behar dira kontuan [9,36,39], besteak beste, animalia-homeostasia, arnasketa-esposizioa, metabolizazioa eta iraizketa-zinetika. Gainera, kutsatutako organismoetatik PPCP-en hondakinak ez dira soilik euren polaritateagatik kanporatzen [15], iraizketaren bidez ere azkar kanporatzen dira jatorrizko forman edo organismoak biotransformatuta [39].

Egun organismo ez-zuzenduetan PPCP-en biotransformazioaren eta biodegradazioaren inguruko ezagutza eza funtsezko arazoa da eta informazioa oso mugatua. Izatez, oso lan gutxi daude PPCP-en biometatzea ikertu dutenean metabolitoak eta transformazio-produktuak (TP-ak) ere kontuan hartu dituztenak [15,36]. Egoera horretan, gai horren inguruan azterketa zabalagoa egitea beharrezkoa da. PPCP-en metabolitoek eta TP-ek konposatu aitzindariak bestekoa edo handiagoa den arriskua sor dezaketenez, garrantzitsua da euren eraketa ebaluatzea esposizioaren benetako eragin osoa ez gutxiesteko [2,39,54,56]. Europako REACH konposatu kimikoen araudiaren arabera, substantzia kimikoetatik eratorritako degradazio-produktuen edo azpiproduktuen (*by-products* delakoen) iraunkortasuna eta toxikotasuna aztertu eta ebaluatu behar dira efektu toxikoak eta biometatze-gaitasuna kontuan hartuta [56].

1.2.1 Azpiproduktuen karakterizazioa

Metabolito edo TP garrantzitsuak identifikatu eta karakterizatzeko beharrizana Europako zenbait zuzentarautan eta gidaliburutan ere aipatzen da. Horren adibide da giza erabilerarako medikuntza-produktuen ingurumeneko arriskuen ebaluazioaren inguruko gidaliburua [20]. Dena den, irizpide zehatz gutxi ematen dira azpiproduktu garrantzitsuenak identifikatzeko [57] eta, PPCP-en ingurumeneko analisian, ahalegin gehienak oraindik ere konposatu aitzindarien detekzioan fokatzen dira, aldibereko metabolitoen edo TP-en analisian fokatu beharrean [45]. Hala eta guztiz ere, kontuan izan behar da prozesu desberdinen bidez konposatu aitzindaria apurtzeak edo ezabatzeak ez duela bermatzen toxikotasuna desagertzea, oraindik ur-ingurumenean toxikotasun eta iraunkortasun ezezaguneko azpiproduktu asko daudela uste baita. Hori dela eta, ikerketa berri asko hasi dira PPCP-en egitura-eraldaketa horiek eta degradazio-bide konplexuak karakterizatzeko asmotan.

Konposatu kimiko jakin batetik abiatuta azpiproduktuen eratzea aitzindariaren egitura kimikoaren menpekoa izateaz gain, bere ingurumeneko konpartimentu desberdinetako banaketaren eta ingurumeneko baldintza nagusien menpekoa ere bada [56]. PPCP-en degradazio-ikerketa gehienak araztegietako eta azaleko uretako prozesu espezifiko jakinetan (adibidez, oxidazioan, hidrolisian, erredox erreakzioetan, fotolisian eta mikrobioen degradazioan) eratutako TP-ak karakterizatzera mugatzen dira [7,54,56,58]. Kontrara, PPCP-ek arrainen gisako organismo

ez-zuzendutan jasan dezaketen metabolizazioaren inguruko informazioa urria da. Dena den, txosten desberdinek argi adierazten dute PPCP-ak potentzialki bioaktiboak diren metabolito desberdinetara zeharo metabolizatzen direla [2,7,59]. Metabolito terminoa giza edo animalia-gorputzean emandako PPCP-en egitura-aldaketaren ondorioz sortutako konposatuak definitzeko erabiltzen da [7], prozesu horretan gertatutako erreakzio biokimikoa edozein dela ere. Ornodunetan PPCP-en metabolizazioa, neurri handi batean, 1. Faseko eta 2. Faseko erreakzioek gidatzen dute [5]. 1. Faseak monooxigenasak (adibidez, P450 zitokromoak), erreduktasak eta hidrolasak erabiltzen ditu molekuletan funtzio-talde erreaktiboak gehitzeko. Bestalde, 2. Faseko erreakzioak glikosiltransferasen, sulfotransferasen, glutation S-transferasen, azetiltransferasen eta aminoaziltransferasen bidez katalizatzen dira. 2. Faseak konposatu aitzindaria baino polarragoa den metabolitoa eratu eta iraizketa laguntzeko glukuronidazioa bezalako konjokazio kobalentea erabiltzen du.

Bestalde, beharrezkoa da espezieen arteko aldakortasuna kontuan hartzea PPCP-en metabolizazioan [5,60,61]. Kasu batzuetan soilik espezieen menpeko aldaketa kuantitatiboak behatzen diren arren, konposatu askorentzat aldaketa kualitatiboak erakusten dituzte, baita bi ugaztunen (gizakiaren eta arratoiaren) arteko erkaketan ere [61]. Horrez gain, ikerlari batzuren esanetan, aurreikusteko zailak diren ondorio farmakologikoak edota toxikologikoak izan ditzake espezieen arteko aldakortasun horrek [61]. Gainera, *in vitro* ikerketetatik ondorioztatutako degradazio-bide guztiak ez dira *in vivo* esperimentuen adierazgarri [60,62]. *In vitro* esperimentuen arazoetako bat inkubazioaren prestaketa da, non entzima-iturria hautatu behar den. Adibidez, konposatu batzuren egonkortasuna eta metabolizazioa aztertzeko, mikrosomak eta homogeneizatuak egokiak izan daitezke. Hala eta guztiz ere, mikrosomek, entzima-iturri gisa, ez dituzte 2. Faseko metabolitoen gehiengoa sortzen [61]. Beraz, entzima-iturri gisa homogeneizatuen ordez mikrosomak aukeratzeak ondorio okerretara eraman gaitzake, eta ondorio oker horien neurria eta garrantzia aurresatea zaila da. Horregatik, garrantzitsua da esperimentuak ingurumen-baldintza desberdinetan gauzatzea, horrek ahalbidetuko baitu inoiz deskribatu gabeko azpiproduktu espezifiko posibleak detektatzea. Gainera, azpiproduktu horiek toxikotasunean eragin dezaketenez, arriskuen ebaluaziorako datu fidagarrienak eskaintzeko beharrezkoa da azken froga *in vivo* izatea [63].

Oro har, azpiproduktuen ur-ingurumeneko presentzia ez da arbuiagarria eta azpiproduktuek zeresan nabarmena dute PPCP-en ingurumeneko arriskuetan [54,56,64]. Horrenbestez, ingurumenean PPCP-en iturriak, garraioa, patua eta efektuak finkatzeko, ezinbestekoa da, azpiproduktuak karakterizatzearekin batera, ingurumen-baldintza desberdinetan esposizio-ebaluazioak egitea. Horrela, "ezezagunak" detektatu, identifikatu eta gaur egun segimendua egiten zaien azpiproduktu “ezagunen” zerrenda luzatzea posible izango da.

Dena den, gerta daitezkeen degradazio-erreakzio kopuru izugarria kontuan izanik, ingurumen-analisian azpiproduktuen identifikazioak erronka nagusienetakoa izaten jarraitzen du [54]. Gainera, analisi bideratua burutzeko erreferentziazko estandarrak eskuragarri ez egoteak are zailago bilakatzen du aipatutako erronka. Hori dela eta, azpiproduktu berrien karakterizazioan HRMS-ak indar handia hartu du. Izan ere, kuadrupolo hirukoitzeko (QqQ) masa-espektrometria bezalako bereizmen baxuko masa-espektrometriarekin erkatuta, HRMS-ak gaitasun handia du ezezagunak detektatu eta egiturak karakterizatzeko [55,64–66].

1.2.1.1 Bereizmen altuko masa-espektrometria

Ingurumeneko mikrokutsatzaile polarren analisian eta azpiproduktuen karakterizazio-ikerketetan, LC-HRMS teknika analitikoa hobetsia da [55,64]. HRMS-aren bidezko neurketen bereizmen eta masa-zehaztasun altuek, masa zehatzak eta profil isotopikoak konposatuaren zalantzarik gabeko formula molekularra ondorioztatzea ahalbidetzen dute [55,57]. Aurreko datuak masa-espektrometro hibridoetan lortutako MS/MS espektroarekin osatuta, azpiproduktuentzako hautagai tentagarriak proposatu daitezke, MS/MS espektroek egituraren inguruko informazioa ematen baitute [66]. Erreferentziazko estandarrak erabilita burutzen den analisi bideratuaren ordez, azpiproduktu berrien karakterizazioan susmagarrien analisia eta analisi ez-bideratua dira hurbilketa ohikoenak [54,55]. Lehenengo hurbilketan, susmagarriaren formula molekularrak masa/karga *(m/z)* erlazio zehatza kalkulatzea posible egiten du eta, ondoren, egiaztatze-urrats desberdinak erabili daitezke: lortutako MS espektroak profil isotopikoarekin bat egiten duen ziurtatu eta MS/MS espektrotik eratorritako egitura-informazioa egiaztatzea. Gainera, molekularen egituratik propietate fisiko-kimikoak eta, ondorioz, erretentzio-denbora kromatografikoa aurreikus daitezke. Susmagarrien analisiarekin erkatuta, analisi ez-bideratuan, masa ez-bideratuaren identifikazio osoa sarritan zaila da eta emaitza arrakastatsua ez dago beti bermatuta. Horregatik,

analisi ez-bideratua analisi bideratuaren edo susmagarrien analisiaren osagarri gisa hartzen da sarritan [64]. Analisi ez-bideratuan, intentsitate altuenekoak izan ez arren, garrantzitsuak diren gailurrak aztertzen dira. Beraz, testuinguru honetan, bibliografiako ikerketa asko bi kategoria horien (susmagarrien analisiaren eta analisi ez-bideratuaren) artean kokatzen dira. Erdibideko egoera horren adibide argia da, esaterako, baldintza kontrolatuetan diseinatutako eta burututako esperimentuetan eratzen diren azpiproduktuen identifikazioa [58,64]. Egoera mugatu horretan, gailur ezezagunen karakterizazioa konposatu aitzindariarekiko (esposizioko konposatuarekiko) antzekotasunak erakusten dituzten egitura kimikoetara mugatuta dago [55,64]. Gainera, kontroleko laginak eta denbora-serieak eskuragarri egoteak, ezezagunaren identifikazioa errazago bilakatzen du.

Egungo HRMS-ko instrumentazio modernoen artean hegaldi-denbora (*time-of-flight*, TOF, delakoa) eta Orbitrap masa-analizatzaileak aurkitzen dira [58]. Kuadrupolo masa-analizatzailearekin alderatuta, TOF eta Orbitrap analizatzaileen baitan dagoen teknologiak nabarmen hobetzen du bereizmen-ahalmena eta masa-zehaztasuna [57]. Kuadrupoloek, eremu elektriko eta magnetiko oszilakorrak erabiltzen dituzte ioiak haien *m/z* erlazioaren arabera egonkortu zein desegonkortu eta irrati-frekuentzia kuadrupolo-eremuan zehar bideratzeko. Bestalde, TOF eta Orbitrap masa-analizatzaileak ioiek eremu elektrostatikoetan duten higiduran oinarritzen dira eta ioietan eragiten duten indarrek ez dute *m/z*-rekiko menpekotasunik [67]. Horren ondorioz, oszilazio- edo hegaldi-denborak *m/z*-rekiko menpekotasun erlatibo txikia erakusten dute. TOF masa-espektrometrian, ioiak eremu elektrikoan azeleratzen dira energia zinetiko berarekin [57]. Ioiaren abiadura bere *m/z*-rekiko menpekoa denez, *m/z* determinatzeko ioiak detektagailura heltzeko behar duten denbora erabiltzen da [57]. Orbitrap analizatzailean, aldiz, ioiak elektrostatikoki harrapatzen dira orbita batean [57]. Ioien maiztasunek euren *m/z* erlazioarekiko duten menpekotasuna kontuan hartuta, ioi bakoitzaren *m/z* kalkulatzen du behin eremu elektrikoan ioi bakoitzak eratzen duen korrontea neurtuta [57]. TOF eta Orbitrap analizatzaileen arteko desberdintasun fisiko horien ondorioz, bakoitzak bere abantailak eta mugak ditu.

TOF instrumentuek masa-espektro osoak lortu ditzakete sentikortasun eta masa-bereizmen altuekin (10.000–100.000 FWHM balioekin, instrumentuaren arabera) eta masa-zehaztasun altuekin (normalean 5 ppm baino txikiagoak) [58]. TOF analizatzaile berrien ekorketa-denbora

10-100 ekorketa/s tartean dago. Balio hori nahikoa eta soberazkoa da ultra-bereizmen altuko likido-kromatografia (*ultra-high-performance liquid chromatography*, UHPLC) banaketaren bidez lortutako gailur kromatografiko estuak jarraitzeko, masa-bereizmena eta sentikortasuna kolokan jarri gabe [58,65]. Dena den, TOF analizatzaileek orokorrean bigarren mailako elektroi-biderkatzaileen bidezko detekzioa erabiltzen dute eta azken horiek detekzio-eraginkortasun maximoa ioien energia zinetiko oso altuetan lortzen dute. Zentzu horretan, nahiz eta bereizmen-ahalmena detekzio-denborarekiko edo *m/z*-rekiko independentea izan, espektroaren tarte dinamikoa detekzio-denborarekiko zuzenki menpekoa da [67]. Izatez, zenbat eta eskuratze-denbora laburragoa edo espektroaren eskuratze-abiadura azkarragoa izan, orduan eta estuagoa da tarte dinamikoa TOF masa-analizatzaileetan. Kontrara, Orbitrap masa-analizatzaileetan bereizmen-ahalmena detekzio-denboraren eta oszilazio nagusien periodoaren arteko erlazioarekiko proportzionala da [67]. Ondorioz, detekzio-denboraren eta tarte dinamikoaren arteko menpekotasuna xamurragoa da, eta Orbitrap masa-analizatzaileak TOF masa-analizatzailearen mugarik garrantzitsuena (detekziorako tarte dinamikoa) gainditzen du. Horrez gain, azken Orbitrap masa-analizatzaileek bereizmen-ahalmen handieneko TOF masa-analizatzaileek baino bereizmen altuagoa eskaini ohi dute (>100.000 FWHM) [58,67]. Hori gutxi balitz, TOF masa-analizatzaileekin erkatuta, Orbitrap instrumentuetan masa-zehaztasuna bermatzeko kanpo-kalibrazioa erabil daiteke eta honek operazio-protokoloa sinplifikatzen du [68]. Dena den, Orbitrap masa-analizatzaileak duen desabantailarik garrantzitsuena masa-bereizmenarekiko alderantziz proportzionala den bere ekorketa-abiadura luzea da [58,65,67]. Nahiz eta Orbitrap masa-analizatzailearen teknologia aurreratzen ari den eskuratze-abiadura azkarragoak lortuz, arreta ezarri behar da kromatografian. Izan ere, gailur-zabalerak segundo gutxi batzutakoak badira, gailurra definitzen duten puntu-kopurua nahikoa ez izatea gerta daiteke [58].

Bai TOF eta bai Orbitrap masa-analizatzaileetan ioien injekzioak edo sarrerak azelerazio bortitza ekartzen duenez, analizatzaileko energia zinetiko altuak ioien apurketa eragin dezake MS^n espektroen kalitatea kaltetuz. Horrek azaltzen du zergatik erabiltzen diren TOF eta Orbitrap masa-analizatzaile gehienak modu hibridoan, bakarkako konfigurazioan beharrean [67]. Bi MS teknika (bata bereizmen altukoa eta bestea baxukoa) konbinatzen dituzten tandem MS hibridoek matrize desberdinetan masa molekular txikiko konposatuen detekzio eta identifikazio azkarra, sentikorra eta fidagarria bermatzen dute [23,55,58]. Esate baterako, kuadrupolo-Orbitrap masa-

espektrometroa oso tresna erabilgarria bilakatu da azpiproduktuen karakterizazioan eta ingurumeneko ikerketetan [59], batik bat, masa zehatzeko neurketaren eta datuen menpeko MS/MS ekorketaren (*data dependent MS/MS*, ddMS2, delako ekorketaren) arteko konbinazioan oinarritutako eskuratze-modua erabilita. Aipatutako ddMS2 eskuratze-moduan, MS/MS espektroa lortzeko apurketa jasango duten ioi aitzindariak aurrez definitutako irizpideak erabilita (ioien ugaritasuna edo lehentasunezko ioi-zerrenda) hautatutako ioiak dira. Bestalde, ioi guztien apurketa (*all ion fragmentation*, AIF, delako) eskuratze-moduan, inongo ioi aitzindarien isolatzerik gabe ioi guztiak apurketa-ekintza bakarrean apurtu eta apurketa-ioi guztiak gordetzen dira espektro misto bakarrean. AIF eskuratze-moduaren abantaila konposatu guztien MS eta MS/MS datu guztiak neurketa bakarrean biltzeko gaitasuna da, laginen injekzio gehigarrien beharrik gabe. Hala ere, aldibereko kromatografia-eluzioak daudenean, datuen interpretazioa asko zailtzen da, apurketa-ioiak batera eluitzen duten ioi aitzindari desberdinen eratorriak izan daitezkeelako. AIF eskuratze-moduarekin alderatuta, datuen menpekotasunik gabeko eskuratze-moduan (*data independent acquisition*, DIA, delakoan), apurketa-ioiak ioi aitzindarien masa-tarte txikiagotik eratorritakoak direnez, selektibitatea hobetzen da. Dena den, datuen interpretazioa oraindik ere ddMS2 eskuratze-moduan baino konplexuagoa da.

HRMS-an erabilitako hurbilketa eta eskuratze-modua edozein direla ere, azpiproduktuen edo beste konposatuen identifikazio bakoitzaren konfiantza-maila desberdina da. Hori adierazteko irizpideak bateratu nahian, Schymanski-k eta lankideek maila desberdinetan antolatutako identifikazio-sistema proposatu dute [66]. Maila baxuena 5. maila da, eta konposatu ezezagunaren masa zehatza soilik ematen du. 4. mailak, 5. mailak ez bezala, informazio nahikoa dauka formula molekularra adierazteko. 3. mailan, aldiz, behin behineko hautagaiak proposatzen dira. Izan ere, egitura posibleak proposatzeko ebidentziak egon arren, eskuragarri dagoen informazioa ez da nahikoa egitura zehatz jakin bat lortzeko. Kontrara, 1.go eta 2. mailetan egitura zehazten da. 1.go mailan egitura erreferentziazko estandarra erabilita egiaztatzen da MS, MS/MS eta erretentzio-denborak bat egiten duela baieztatuz. Bestalde, 2. mailan egitura probablea proposatzeko, erreferentziazko estandarra erabili beharrean, baliabide desberdinak erabiltzen dira: liburutegiekiko konparaketa (2a maila) edo diagnostikatutako MS/MS zatikatzea (2b maila) datu bibliografikorik eskuragarri ez dagoenean.

1.2.2 Metabolomika albo-ondorioen ikerketan

Ingurumenean PPCPen eragina ebaluatzean, ez da nahikoa konposatuen biometatzea aztertzearekin, esposizioak organismoetan dituen efektuak ere kontuan izan behar dira [69]. Azpimarratu beharra dago ikerketa gutxik lotu dituztela organismo ez-zuzenduetako PPCP-en biometatzea eta horrek izan ditzakeen albo-ondorioak. Azken ikerketetako emaitzen arabera, PPCP-en toxikotasunean aldagai desberdinek dute eragina, hala nola kutsatutako organismoak, esposizioko unean organismoaren garapen-mailak, esposizio-denborak eta dosiak [10–15]. Ondorioz, metatze- eta biotransformazio-lanekin batera, zeharo garrantzitsua da PPCP-ek uretako organismoetan sor ditzaketen albo-ondorioak ebaluatzea.

PPCP-ak funtzio jakin baterako diseinatzen dira eta hauek ez-zuzendutako organismoetan duten ekintza-moduaren inguruan informazio gutxi dago eskuragarri. Esate baterako, farmakoak dosi baxuetan beraien aktibitate biologikoa handitzeko diseinatzen dira, zenbait helburu metabolikotara eta entzimatikotara, zein seinaleztapen zelularreko mekanismotara, bideratuta. Aipatutako helburu molekular horietako asko espezie desberdinetan berdinak direnez, PPCP-ak ez-zuzendutako organismoetan farmakologikoki aktiboak izateko aukera nabarmen handitzen da. Beraz, PPCP-en ekintza-modua ez-zuzendutako organismo urtarretara hedatu eta horrek konposatu horien arrisku ekotoxikologikoak handitu ditzake [35]. Hala ere, PPCP batek espezie batean sor ditzakeen eraginak ezin dira zuzenean beste espezie ez-zuzenduetara estrapolatu, desberdintasunak izan ditzaketelako bai PPCP-en biometatze-gaitasunean eta baita espezie/organismo/ehun desberdinetan PPCP-ek duten selektibitatean ere. Hortaz, PPCP-en patuaren eta eraginen arteko korrelazioaren inguruan dagoen informazio-hutsunea osatzeko, beharrezkoa da esposizio-ikerketa gehiago burutzea [31].

Araztegietako PPCP-en isurketen eraginei buruzko ingurumen-ikerketak mugatuak diren arren, adibideek argi uzten dute kutsatzaile horiek oso arriskutsuak izan daitezkeela organismo urtarrentzat [2,5,10,11]. Jadanik deskribatutako albo-ondorioen artean ditugu aldaketa histologikoak, jokabide-efektuak, erantzun biokimikoak eta geneen gorako zein beherako erregulazioa. Erantzun horiek, oro har, ez dira arrisku-ebaluazioko egungo hurbilketetan sartzen, nahiz eta kutsatzaileen oso kontzentrazio baxuetan behatu daitezkeen albo-ondorioak izan. Aldiz, egun araututako azterketekin ebaluatzen diren efektuak behatzeko beharrezkoak diren

kontzentrazioak magnitude-ordena handiagokoetakoak izan daitezke [2]. Ohiko azterketa arautu horien artean aurki ditzakegu hilkortasunean duen eragina behatzen duten azterketa akutuak edo ugaltze- eta hazkuntza-efektuak ebaluatzen dituzten azterketa kronikoak. Dena den, azken ebidentziek egungo jarraibideetan aplikatzen diren azterketa estandarrak eta ebaluatutako parametro estandarrak ezegokiak izan daitezkeela frogatzen dute [70]. Ondorioz, PPCP-en ingurumeneko kontzentrazio baxuek organismo urtarretan eragiten dituzten albo-ondorioak ebaluatzeko, erantzun sentikorragoak erabiltzearen beharra azpimarragarria da.

Horretarako, azken hamarkadetan, teknika "omikoak" oso erabilgarriak bilakatu dira ingurumenean agertzen diren kutsatzaileek maila ez-hilgarrietan eragiten dituzten efektuak ikertu eta beraien ekintza-modua ulertzeko [71]. Teknologia “omikoek” lagin biologiko jakin batean geneak (genomika), RNAm (transkriptomika), proteinak (proteomika) eta metabolitoak (metabolomika) jarraitzen dituzte eta euren helburua zelula, ehuna edo organismoa osatzen duten molekulen ikuspegi holistikoa ematea da [72]. Genomikak eta transkriptomikak organismoaren genoma (DNA osoa) eta transkriptoma (RNAm osoa) sistematikoki ikertzen dute, hurrenez hurren. Izan ere, transkriptomak edozein une jakinetan modu aktiboan adierazita dauden geneak islatzen ditu, eta gene-aktibitatearen laburpen gisa gene-adierazpenerako mikromatrizeen bidez paketatutako RNAm neurtzen da. Nahiz eta genomikak eta transkriptomikak interes berezia sortzen duten determinazio genetikoarekin lotutako gaixotasunen aurrean, badute muga garrantzitsu bat. Gene-adierazpenerako mikromatrizearen bidez ez dira proteinak neurtzen, RNAm ugaritasun-aldaketak baizik eta, horrek, datuen interpretazioan desadostasunak sortzen ditu. Bestalde, proteomikaren helburua zelularen eta organismoaren informazio-fluxua karakterizatzea da, proteina-bideen eta sareen bidez. Proteina-adierazpena aztertuta, proteomikak proteinen garrantzia funtzionala ulertzen laguntzen du, baina oso zaila da bere domeinu-tamaina (100.000 proteina baino gehiagokoa) oso handia delako eta ugaritasun txikiko proteinak ezin direlako zehaztasunez detektatu. Aldiz, metabolomak domeinu txikiena (5000 metabolito inguru) dauka. Metabolomika ikerketa-arloak, oro har, baldintza batzuetan sistemaren (zelularen, ehunaren edo organismoaren) metabolitoen profil orokorrak aztertzen ditu. Izatez, metabolomikak saiakuntza toxikologiko estandarrak maiz detektatzeko gai ez diren maila molekularreko aldaketak antzematen ditu [73–77]. Gainera, metabolitoak adierazle sentikor bihurtzen dira, maila hierarkiko altuagotako (zelula-, ehun-, organismo- edo biztanleria-mailako) eraginen aurretik beti gertatzen

direlako aldaketak prozesu biomolekularretan [78]. Ildo beretik, metaboloma gene-transkripzioaren azken urratseko produktua denez, metabolomako aldaketak areagotu egiten dira, transkriptomako eta proteomako aldaketekin erkatuta [72]. Azken hau, metabolomikaren beste abantaila argia da gainontzeko hurbilketa "omikoekiko". Gainera, metaboloma, produktu eratorri gisa, aztertutako sistema biologikoaren fenotipotik hurbilen dagoena da. Testuinguru horretan, oso esparru erabilgarria da ondorio kaltegarrien bidea (*adverse outcome pathway*, AOP, delakoa). AOP delakoaren helburua ekintza abiarazle molekularraren eta arrisku ekologikorako esanguratsua den organismo mailako behaketen arteko lotura frogatzea da [79]. Arrisku ekologiko horien artean ditugu biziraupeneko, garapeneko, zein ugalketako albo-ondorioak, banakoei eragiteaz gain, populazio-mailara heda daitezkeenak.

Guzti hori dela eta, metabolomika hurbilketa eraginkorra da natura- eta bizitza-zientzien arloko ikerketetan [77]. Metabolomikaren bidez, zelula, ehun zein jariakin desberdinak aztertuta, barneko edo kanpoko estimuluen erantzun gisa espezie desberdinetan gertatzen diren metabolito-mailako (oro har, <1000 Da) aldaketa biologikoak azal daitezke. Esate baterako, gaixotasunen diagnostikorako onarpen zabala lortu du metabolomika klinikoak, ezinbesteko doitasun-baliabide bilakatzeraino [80]. Bestalde, ingurumeneko kutsatzaileen agerpena aurretiaz aipatutako kanpoko estimuluaren adibide argia den arren, oraindik ingurumeneko metabolomikan lan asko dago burutu gabe. Nahiz eta ingurumeneko metabolomikaren aplikazioak zeharo hedatu eta ugaritu diren [81], arlo honetan oraindik erronka izaten jarraitzen dute laginaren prestatzeak, erauzien analisiak eta datuen tratamenduak.

1.2.2.1 Laginaren prestatzea eta analisia metabolomikan

Metabolomikak, profil metabolikoak eratzeko, ehunetatik edo jariakinetatik molekula txiki ugariren erauzketa eta neurketa hartzen ditu bere baitan. Prozedura horren baitan, urrats neketsuena eta denbora aldetik mugatzaileena, ehunetatik edo jariakinetatik metabolitoak erauztea da [82]. Kasu batzuetan, metabolito edo familia konkretu bateko metabolito jakin batzuk aztertzen dira. Baina beste batzuetan, polaritate-tarte zabala duten metabolitoak dira erauzi beharrekoak eta, kasu horietan, zaila da analito guztientzat erauzketaren kuantitatibotasuna bermatzea. Alde batetik, aminoazidoen gisako metabolito hidrofilikoak erauzteko disolbatzaile organiko polarrak (hau da, metanola) erabiltzen dira, normalean urarekin nahastuta. Bestalde,

lipido asko bezalako metabolito hidrofobikoak hobeto erauzteko disolbatzaile ez-polarrekin (hau da, kloroformoa) lan egin behar da [83]. Ildo horretan, metabolomikarako funtsezko metodo bat ezarri nahian, hainbat ikerketek ebaluatu dituzte disolbatzaile desberdinen arteko konbinazioen egokitasuna, eta baita ehunak birrintzeko eta disolbatzailea gehitzeko estrategien eraginkortasuna ere [82,84]. Hala eta guztiz ere, ehunetan propietate fisiko-kimiko oso desberdinak dituzten metabolito asko daudenez, ez dago metodo perfekturik metabolito mota guztiak modu eraginkorrean eta errepikakorrean aldi berean erauzteko [83]. Horrenbestez, garrantzitsua da kasu jakin bakoitzerako metodo egokiena aukeratzea. Gainera, ondorengo neurketan arazoak gutxitu eta emaitza okerrak saihesteko, aldagai desberdinak kontuan izatea komenigarria da, hala nola aztertuko den laginaren izaera edo erabiliko den analisi-hurbilketa (bideratua edo ez-bideratua).

Erauzien analisiari dagokionez, erresonantzia magnetiko nuklearra izan den arren analitoen maila neurtzeko tresna nagusia, ingurumeneko metabolomikan sentikortasun altuagoa duten MS hurbilketek ospea irabazi dute azken urteotan [83,85,86]. Ingurumeneko metabolomikan teknika analitiko erabilienak ondorengoak dira: sarrera zuzeneko MS (*flow injection* edo *direct infusion MS*, DIMS, delakoa) eta GC eta LC, biak MS-ra akoplatuta. DIMS metodoan lagina zuzenean sartzen da masa-espektrometroko ionizazio-iturrira, aldez aurretiko metabolitoen banaketa kromatografikorik gabe. Teknika horretan, nahiz eta lagin-kopuru txikiak sentikortasun altuarekin neurtu daitezkeen, badaude banaketa-urratsaren gabeziak sortutako bi muga nagusi: seinalearen txikitzea/handitzea eta ekidin ezin den metabolitoen gainezarpen isobarikoa [83,85,86]. MS-ari akoplatutako kromatografia-tekniken artean, LC-MS da ohikoena, GC-MS erabili ahal izateko aurretiazko metabolito polarren deribatizazio-urratsa beharrezkoa izan ohi delako [83,85,86]. LC-an, metabolitoen banaketa hobetu nahian, zutabea eta disolbatzaileak aukeratuko dira [85,86]. Normalean, metabolito ez-polarrenen banaketarako alderantzizko faseko LC hobea den bitartean, metabolito polarren banaketarako elkarrekintza hidrofilikoan oinarritutako LC (*hydrophilic interaction liquid-chromatography*, HILIC, delakoa) aukeratzen da [85]. Azken hori, fase normalaren alternatiba da, eta errepikakortasun eta sendotasun hobeak bermatzen ditu.

Metabolomikako lanetan hurbilketa bideratuak zein ez-bideratuak erabiltzen dira [83,86,87]. Hurbilketa bideratuetan, erreferentziazko estandarrak erabilita, metabolito ezagunen analisia burutzen da eta, ondorioz, okerreko bide-metabolikoak interpretatzera eraman

gaitzaketen positibo faltsuak saihesten dira. Aldez aurretik aukeratutako metabolito ezagunen identifikazio eta kuantifikazio fidagarria burutu nahi den kasuetan, MS bideratua da aukeratu ohi den teknika [86]. Gainera, isotopikoki markatutako barne-estandarren erabilerak ere lagundu dezake zehaztasun eta doitasun analitikoan eragin dezakeen matrize-efektua zuzentzen [88]. Zuzenketa horren ondorioz, erantzun biologikoa detektatzeko saiakuntzaren sentikortasuna hobetu egiten da [88]. Analisi bideratuak duen desabantaila nagusiena metabolomaren estaldura mugatua da eta, horrek, interesa duen erantzun metabolikoren bat aintzakotzat ez hartzeko arriskua handitzen du. Analisi bideratuan ez bezala, hurbilketa ez-bideratuen xedea analisi bakarrean ahalik eta metabolito gehien detektatzea da, xenobiotikoen arriskuak ulertzera eraman gaitzaketen metabolito berriak aurkitzeko ahalmena bermatuta [73,83,87]. Metabolito asko polaritate-modu bakarrean ionizatzen direnez, estaldura metabolikoa handitu ahal izateko, datuak ionizazio positiboan eta negatiboan eskuratu behar dira eta analisi kopurua bikoiztu egiten da. Alternatiba gisa, polaritate-aldatze azkarra burutzeko gai diren masa-espektrometroak erabil daitezke, zeintzuk, datuak bi polaritate-moduetan aldi berean eskuratuta, analisi-denbora osoa bi aldiz murriztu dezaketen. Hala eta guztiz ere, polaritate-aldatze modua erabiltzeak baditu desabantailak, hala nola neurketa-ziklo mugatua eta konposatu batzuen sentikortasun-jaitsiera [83]. Azken hori polaritate-aldatze modua erabiltzerakoan metabolito guztientzat (azidoak zein baseak) fase mugikor bera erabiltzearekin lotuta dago, metabolitoak ionizatzeko eraginkortasuna murrizten baita.

Hurbilketa ez-bideratuetan, erreferentziazko estandarren faltan metabolitoen identifikazioan positibo faltsuak saihesteko, oso gomendagarria da arestian aipatutako HRMS erabiltzea [83]. Gainera, azken HRMS hibridoak analisi ez-bideraturako erabiltzeaz gain, kuantifikaziorako ere baliagarriak dira [87]. Hau da, HRMS hibridoen moldakortasunak LC-MS analisi guztietarako MS teknologia bera erabiltzea ahalbidetzen du, lan-prozedurak sinplifikatuta eta produktibitatea hobetuta [87]. Horregatik, metabolomikaren arloan lan egiten duten laborategi gehienetan funtsezko tresna bihurtzen ari da.

Oro har, hurbilketa bideratuak zein ez-bideratuak baliagarriak dira ingurumeneko kutsatzaileek organismoetan eragiten dituzten erantzun azpihilgarriak ebaluatzeko [83,86,87]. Erabiltzen den analisirako hurbilketa edozein dela ere, emaitzak eskuratu ondorengo lehen urrats

garrantzitsua datu gordinak prozesatzea da. Orokorrean, dimentsio askotariko eta korrelazio anitzeko datuak lortzen direnez lagin errepikatu gutxi batzuentzat, datuak prozesatu ondoren, beharrezkoa da datuen tratamendu estatistiko egokia burutzea [89,90].

1.2.2.2 Datuen tratamendua metabolomikan

1.2.2.2.1 Datuen prozesatzea

Datu gordinen prozesatzea software libretan edo komertzialetan garatutako lan-fluxu desberdinen bitartez aurrera eraman daiteke eta ondorengo urratsak izaten dituzte bere baitan: datuen iragazketa, gailurren detekzioa, falta diren balioen inputazioa, gailurren lerrokatzea eta datuen normalizazioa, besteak beste [85,91]. Iragazte-metodoek seinale gordina prozesatzen dute zarata eta oin-lerroa ezabatuta eta, jarraian, gailurrak detektatzen dira benetako ioiek sortutako seinale guztiak identifikatu eta positibo faltsuen detekzioa saihestuz. Gainera, datu-multzoak hutsuneak dituen kasuetan, datuen prozesatzeko urrats oso garrantzitsua bihurtzen da "hutsune-betetze" algoritmoa ere [89,92]. Falta diren balioak inputatzeko metodoen artean, *k-nearest neighbor* (KNN) delako metodoak sendotasun onenetarikoa erakutsi du metabolomikako datuentzat [93]. Bestalde, lerrokatze-metodoak beharrezkoak dira injekzio desberdinen arteko erretentzio-denboraren aldaketak zuzendu eta lagin desberdinen neurketen datuak bateratzeko. Azkenik, normalizazio-urratsean desbiderazio edo alboratze sistematikoak sortzen dituzten faktoreak ezabatzen dira. Zuzenketa hori aplikatu ezean, emaitza estatistiko okerretara hel gaitezke joera-efektu horiek datuen aldakortasunaren iturri nagusi izan daitezkeelako [94–96]. Besteak beste, joera horiek laginaren prestatzetik edo neurketa desberdinen artean sor daitekeen ioi-intentsitate aldaketetatik etor daitezke, azken hau ohikoena delarik. Metabolomikako lanetan seinaleen joera horiek gutxitu edo ezabatzeko estrategia erabilgarri desberdinak daude, hala nola kalitate-kontrolerako (*quality control*, QC, delakorako) laginak erabili eta laginen analisia zoriz burutzea [83,85,96,97]. QC laginei dagokienez, esperimentuan aztertuko diren laginekiko biologikoki berdin-berdinak izan beharko lirateke, konposizio metaboliko eta matrize antzekoarekin [97].

Ikerketan QC laginak erabiltzeak datuen kalitatearen jarraipena egitea bermatzen duen bitartean, auzi biologiko jakina erantzuteko datuak lortu ahal izateko beharrezkoa da diseinu

esperimental egokia ezartzea [97]. Adibidez, lagin-kopurua diseinu esperimentalean zehaztu beharreko ezaugarri garrantzitsua da [96]. Izan ere, ikerketaren oinarrian dagoen auzi biologikoari buruzko ebidentzia fidagarriak ematerako orduan porrot egiteko arrazoi desberdinak daude. Arrazoi horietako bat aztertutako lagin-kopuru murritza izan daiteke. Ondorioz, ikerketa zientifiko on bat beti diseinu esperimental zorrotz batekin hasi beharko litzateke [89]. Garrantzitsua da, adibidez, kobarianterik edo nahaste-faktorerik ez egotea edo, behintzat, horiek ondo karakterizatuta egotea. Horrela ez bada, ezin da ziurtatu behaketa biologikoekin erlazionatutako bariantza ikerketa burutzean sortu dugun bariantza baino nabarmenki handiagoa denik. Gainera, analisi estatistikoan, nahaste-faktoreekin lortutako informazioa kontuan izan behar da ondorio biologiko faltsuak ekiditeko [97].

Helburu esperimentalek gidatu beharko lukete diseinu esperimentala eta, lortutako emaitzekin batera, diseinu esperimentalak baldintzatuko luke jarraitu beharreko analisi estatistikorako hurbilketa [98,99]. Datuen egituraren eta banaketaren arabera, beharrezkoak izan daitezke normalizazio- eta eskalatze-urratsak baliabide estatistiko batzuk aplikatu aurretik [89,92]. Eskalatzeak neurtutako erantzunen aldakortasunaren desberdintasun handiek sortutako metabolitoen arteko aldaketa-mailen desberdintasunak doitu ditzake [92]. Eskalatze-metodoen artean Pareto eta autoeskalatzea delakoak aurki ditzakegu [90,92]. Autoeskalatzea da metabolomikan gehien erabiltzen den metodoetako bat, eta metodo horretan aldagaiaren ugaritasunak ez du eraginik. Izan ere, metabolito bakoitzaren desbideratze estandarra 1 bihurtzen du gailur bakoitza batezbestekora erdiratu eta zutabeko desbideratze estandarrarekin zatituta [92].

1.2.2.2.2 Analisi estatistikoa

Datuen analisi estatistikoan, aldagai bakarreko [90,96] zein aldagai anitzeko [75,88,90,99,100] hurbilketak aplikatu izan dira ikerketa-auzia kontrolekotik bereizten duten metabolitoak identifikatu eta begi bistaz datuak analizatzeko. Metabolomikako datu-multzoek izan ohi dituzten dimentsio handiak direla eta, ikerketa gehienek aldagai anitzeko ereduak erabiltzen dituzte aurkikuntza nagusiak azaltzeko. Hala eta guztiz ere, metabolomikako datu-multzoetan aldagai-kopurua lagin-kopuruarekin erkatuta oso handia izan ohi da eta horrek datuen tratamenduan arazoak sortzen ditu [91,96,99]. Horrek funtsezko akatsak sor ditzake, ereduen aurresateko gaitasuna murriztuz [96]. Ondorioz, kasu batzuetan egokiagoa izan daiteke aldagai

bakarreko analisian oinarritutako baliabide estatistikoak aukeratzea. Gainera, hurbilketa bat erabiltzeak ez du zertan bestea kanpoan utzi behar eta ikertzaile batzuk aldagai bakarreko eta aldagai anitzeko hurbilketak konbinatzea gomendatzen dute metabolomikako datu-multzoetatik informazio garrantzitsua hobeto ateratzeko [89,96]. Izatez, aldagaiak hautatzeko eta arestian aipatutako aldagai-kopuru handia nabarmenki murrizteko, sarritan erabiltzen dira aldagai bakarreko metodoak iragazki gisa aldagai anitzeko ereduekin batera [101,102]. Oro har, aldagaien hautatze horrek berebiziko eginkizuna du metabolomikan eta bioadierazleen miaketa gisa ere ezaguna da. Laburki, bioadierazleen miaketa metabolomikako datu-multzotik metabolito garrantzitsuenak ateratzean datza eta metabolito horiek ikerketaren oinarrian dagoen galdera biologikoa erantzuten lagunduko digute [90]. Bioadierazleak, definizioz, zelulak, ehunak edo organismoak egoera osasuntsuan edo asaldatuan dauden adierazteko erabil daitezkeen entitate biologikoak dira [90]. Beraz, bioadierazleek kontrol- eta auzi-laginak bereizten dituzte euren kontzentrazio-mailari erreparatuta. Hala eta guztiz ere, zoritxarrez, nahiko erraza da esanguratsuak iruditu arren okerrekoak diren adierazleak aurkitzea [90]. Hori dela eta, datuen tratamenduan erabilitako baliabide estatistikoa edozein dela, garrantzitsua da I. motako erroreak (positibo faltsuak) kontrolatzea tratamenduen arteko aldibereko erkatze anitz egiten diren datu-multzoetan [88,96].

- **Aldagai bakarreko datuen analisia**

Aldaketak jasan dituzten metabolitoak hautatzeko aldagai bakarreko analisia erabiltzen denean, hipotesi-froga estatistikoak aplika daitezke [90,96], beti ere diseinu esperimentalaren eta datuen banaketaren ezaugarriak kontuan hartuta. Esate baterako, datuek banaketa normala badute, t-froga edo bariantza-analisia (*analysis of variance*, ANOVA, delakoa) bezalako froga parametrikoak erabili ohi dira. Dena den, erregresio-analisia ere erabil daiteke eta, besterik esan ezean, erregresio linealtzat ulertzen da [103]. Nahiz eta ANOVA eta erregresio-analisia funtsean ez diren analisi-mota desberdinak, erregresio-analisian beharrezkoa da aldagai askea(k) aldagai jarrai gisa hartzea.

Erregresio-analisiarekin datuak malda eta ordenatu parametroekin azaltzen direnez, muga nagusiena aldagaien eta erantzunen arteko erlazioa ahalik eta zuzenena izatea da [103], horrela izango ez balitz ahalmen estatistikoa galtzen baita. Hala ere, ANOVA-rekin erkatuta, erregresio-

analisian ereduaren bi parametro bakarrik (ordenatua eta malda) determinatzen direnez, ANOVA-k baino askatasun-gradu gehiago ditu eta, ondorioz, ahalmen estatistiko handiagoa du [103]. Horrez gain, aldagai aske bat baino gehiago dituzten diseinu esperimentalen kasuan, banatutako erregresio-zuzen bat eratzen da bigarren aldagai askeko talde bakoitzarentzat [103]. Esate baterako, kontroleko eta kutsatutako taldeen metabolismoaren erantzuna denboran zehar kontrolatzen duten metabolomikako esperimentuetan, kontrol-taldeak erregresio-zuzen bat izango luke eta kutsatutako-taldeak beste erregresio-zuzen bat. Gainera, erregresio-analisiak aldagai azaltzaileen arteko elkarrekintzak ere kontuan har ditzake [98]. Aldagai askotariko erregresio linealeko (*multiple linear regression*, MLR, delako) ekuazioan, elkarrekintza aurreko aldagaien produktua den aldagai berri bat bailitzan gehitzen da. Arestian aipatutako adibidean, aurresate-erregresioaren ekuazioa ondorengoan bilakatzen da: "Y(denbora,dosia) = β_0 + $\beta_{denbora}$·denbora + β_{dosia}·dosia + $\beta_{denbora·dosia}$denbora·dosia". Dosi-taldea finkatuta dagoenean (α), ekuazioa ondorengora sinplifikatzen da: "Y(denbora,α) = (β_0 + α·β_{dosia}) + ($\beta_{denbora}$ + α·$\beta_{denbora·dosia}$)·denbora". Hortaz, erantzuna denborarekiko lerro zuzena da eta, denbora·dosia elkarrekintzaren gakoa, talde bakoitzak (kontrolak eta kutsatuak) malda desberdina izatean dago [98]. Elkarrekintza horren p-balioa esanguratsua denean (orokorrean p-balioa < 0,05), aldagai horrek erantzunean duen eraginak beste aldagaiaren balioarekiko menpekotasuna duela esan nahi du.

Aurrez aipatu bezala, aldagai bakarreko hipotesi-froga edozein dela, hipotesi nulua zoriz oker baztertzeko (I. motako errorea) probabilitatea handitu egiten da hipotesi-froga kopurua handitzean, eta garrantzitsua da positibo faltsuak kontrolatzea [88,96]. Argitaratutako "omikako" ikerlanen arabera, froga anizkoitzen arazoa kudeatzeko modu ohikoena aurkikuntza faltsuen tasa (*false discovery rate*, FDR, delakoa) kalkulatzea da [88]. Badira beste aukera batzuk ere, hala nola FDR-a baino zorrotzagoa den Bonferroni-ren zuzenketa [96]. Ildo horretan, FDR metodoak oreka bilatzen du emaitza faltsu gehiegi egitearen eta benetako aldaketak aurkitzeko aukera galtzearen artean. FDR zuzenketak p-balio zuzendua edo q-balioa kalkulatzen ditu aztertutako aldagai metaboliko bakoitzarentzat. Aldagai bakoitzari dagokion q-balioak, aldagai hori esanguratsua dela esatean espero daitekeen positibo faltsuen proportzioa adierazten du. Oro har, errore-tasa % 5ean (q-balioa 0,05) finkatzen den arren, hurbilketa honek, errore-tasa ikertzaileak berak ikerketaren eskakizunen arabera hautatzeko aukera ematen du [96].

Aldagai esanguratsuak identifikatzeko beste modua aldagaiaren aldaketa-mailaren (*fold change*, FC, delakoaren) arabera sailkatzea da. FC-aren mozketa-balioa ikerketaren arabera ezartzen den arren, 1,5 balioa nahiko ohikoa da bibliografian [96]. Horrek esan nahi du erkatzen diren bi taldeen artean gutxienez % 50eko aldaketa gertatu dela.

- **Aldagai anitzeko datuen analisia**

Aldagai bakarreko hurbilketak ez direnez gai aldagaien arteko kobariantza kontuan hartzeko, metabolomikako lan askotan aldagai anitzeko analisi estatistikoa burutzen da. Datuen azpian dauden joerak bilatzeko, aldagai anitzeko analisiak aldagai guztiak aldi berean hartzen ditu kontuan eta, datuen interpretazioa errazteko, sarritan patroien antzemate-metodoetan oinarritzen dira [75,81,88,99]. Izatez, datu-multzoen dimentsioak ehundaka aldagaietatik bi edo hiru osagaietara murrizteko gai dira. Metabolomikako datuen tratamenduan erabiltzen diren aldagai anitzeko hurbilketa estatistiko ohikoenak osagai nagusien analisia (*principal component analysis*, PCA, delakoa) eta karratu txiki partzialen bidezko analisi diskriminatzailea (*partial least squares-discriminant analysis*, PLS-DA, delakoa) dira [75,90].

Zalantzarik gabe, PCA da metabolomikan gehien erabiltzen den aldagai anitzeko hurbilketa [75,91,99]. PCA gainbegiratu gabeko metodoa da, hau da, ereduan ez da sartzen laginen klaseari buruzko informaziorik [75]. Beraz, laginetan behatzen diren joerak edo multzokatzeak beraien profil metabolikoen arteko antzekotasunean oinarrituko dira nagusiki. Joera edo multzokatze horiek PCA-ko *scores* grafikoetan behatu eta horietan laginak osagai nagusiek definitutako planoetan kokatuta daude. Hain zuzen, grafiko hori bazterreko balioak edo *outlier-ak* deritzen ez-ohiko balioak detektatzeko ere erabil daiteke, beste estrategia batzuekin batera. Bazterreko puntuak identifikatzea oso garrantzitsua da datu-multzoan adierazgarria ez den aldakortasun handia sartu eta, ondorioz, esanguratsuak diren erantzunen identifikazioa lausotu dezaketelako [75,88,89]. Bestalde, PCA-ko *loadings* grafikoek aldagaiek laginen banaketa horretan duten eraginaren inguruko informazioa ematen dute. Hala ere, objektuen multzokatzeak agerian geratu daitezen, talde barneko aldakortasuna taldeen artekoa baino esanguratsuki txikiagoa izan behar da [99].

Hori dela eta, metabokomikako datuen tratamenduaren hasierako urrats gisa erabiltzen den

gainbegiratu gabeko aldagai anitzeko metodoen adibide da PCA, datu-multzoaren egiturari eta taldeen arteko harremanei lehen begiratua emateko. Ondoren, laginak sailkatzeko eta bioadierazleak aurkitzeko, gainbegiratutako metodoak (hau da, PLS-DA) erabili ohi dira, ereduak eratzeko behaketa bakoitzaren identitatean oinarritzen direnak [75,88,91,99]. PLS-DA hurbilketan, klaseen arteko banaketa handitu eta klaseen banaketarekin zerikusia duten metabolitoen bilaketa errazten da. Aldagaiek proiekzioan duten garrantzian (*variables importance on projection*, VIP, delakoan) oinarritutako metodoa oso hurbilketa erabilia bihurtu da bioadierazle izan daitezkeen konposatuak zehazteko [90,99]. Orokorrean, VIP-aren balioa 1 baino handiago duten hautagaiak aukeratzen dira [90]. Dena den, gainbegiratutako ereduen funtzionamendu egokia bermatzeko eta datuen gehiegizko doitzea saihesteko, beharrezkoa da ereduaren berrespen estatistikoa egitea [75,88,90,99]. Berrespen horren baitan daude zeharkako berrespena eta permutazio-frogak. Zeharkako berrespen metodoak PLS erregresio-ereduko osagai kopuru optimoa zehaztu eta aldagai bakoitzaren ziurgabetasuna estimatzeko erabiltzen dira [90]. Horrez gain, definitutako taldeen arteko bereizmena edo diskriminazioa zein esanguratsua den zehazteko permutazio-frogak erabiltzen dira. Oro har, gainbegiratutako metodoa berretsita egon arren, azpimarratzekoa da egokiagoa dela PLS-DA ereduan agerian geratutako sailkapena PCA-n ere aurreikusi izana [99]. Izan ere, PCA joera gabeko metodoa denez eta zorizko banaketak baztertzen dituenez, beti izango ditu biologikoko esanguratsuak diren emaitzak emateko aukera gehiago.

Hala ere, aldagai anitzeko metodoen muga azpimarragarriena ikerketaren oinarrian dagoen diseinu esperimentala kudeatzeko edo kontuan hartzeko ezintasuna da [90,104]. Arazo horri aurre egin nahian ANOVA-aldibereko osagaien analisia (ANOVA-*simultaneous component analysis*, ASCA, delakoa) garatu da [104]. ASCA erabilita, diseinu esperimentalak sortutako aldakortasuna edo ereduen lausotzea ekiditeaz gain, aldagai bakarreko hurbilketen mugak (aldagaien arteko kobariantza kontuan hartu ezina) ere gaindi daitezke. Aldagai anitzeko hurbilketa horrek kontuan hartzen dituenez diseinu esperimentalaren inguruko informazioa eta datu-multzoen egitura, informazio biologikoa hobeto ulertzeko aukera ematen du [104]. Guzti hori dela eta, ASCA ANOVA-ren orokortze gisa uler daiteke eta, denbora, dosia edo haien konbinazioen gisako faktoreak dituzten esperimentuen datuak tratatzeko erabiltzen da. Hala ere, ASCA-ren muga bat da estimatutako ereduaren parametroen konfiantza-tarteak balioztatzeko metodoaren falta [104].

1.2.2.2.3 Metabolitoen identifikazioa

Analisi estatistikoa metabolitoen kuantifikazioarekin eta identifikazioarekin batera egin ohi da [75]. Analisi bideratuan, oro har, metabolitoen kuantifikazioa analisi estatistikoaren aurretik egiten da. Analisi ez bideratuan, aldiz, metabolitoen identifikazio-urratsa behin aldagai interesgarriak hautatu ondoren egin ohi da [96], metabolomika ez-bideratuko lan-fluxuan denbora gehien kontsumitzen duen urrats neketsuena delako. Hori dela eta, funtsezkoa da datu gordinetatik lehentasuna ematea aldagai-zerrenda bati, aurretiaz aipatutako irizpide estatistiko desberdinetan oinarrituta [96]. Metabolomika ez-bideratuko metabolitoen aniztasun biokimiko zabala medio, MS espektroetatik metabolitoak ziurtasunez identifikatzea erronka esanguratsua da [91,105]; bereziki, LC-MS analisian, non kromatografia-baldintzak eta masa-espektrometriako parametroak nabarmen aldatzen diren esperimentutik esperimentura. Oro har, metabolitoen identifikazioa MS eta MS/MS espektroak aztertuta egiten da, masa zehatza, banaketa isotopikoa eta apurketa-ioiak bezalako ezaugarrietan oinarrituta [105]. Gainera, informazio hori babesteko hainbat metabolitoen identifikazio-baliabide eta datu-base erabil daitezke. Gaur egun metabolomikaren esparruan erabiltzen diren konposatuen datu-baseek egitura kimikoei, propietate fisiko-kimikoei, espektro-profilei, funtzio biologikoei eta metabolito-bideei buruzko informazioa eskaintzen dute [105]. Informazio horren arabera, datu-base horiek bi kategoriatan sailkatzen dira: (i) bide biologikoetan fokatzen diren KEGG [106] bezalako datu-baseak, eta (ii) konposatuetara mugatzen diren giza metabolomaren datu-basea [107], LipidMaps [108] edo mzCloud [109] bezalako datu-baseak. Gainera, mzCloud datu-basea erreferentziazko estandarrekin lortutako MS/MS eta MS^n espektroen informazioarekin aberastuta dago eta, horrek, metabolito ezezagunen identifikazioan asko laguntzen du [105]. Izan ere, aukera ematen du lortutako espektroen eta mzCloud datu-baseko espektroen arteko adostasun-maila erkatzeko. Hala ere, aipatu beharra dago MS/MS eta MS^n liburutegiak oso urrun daudela konposatu kimiko eta metabolito guztien inguruko informazioa izatetik. Ondorioz, liburutegietan hutsuneak dauden kasuetan, Metfrag [110] bezalako baliabideak erabili daitezke, *in silico* apurketek ere lagundu baitezakete metabolitoen masa-espektroak interpretatzen [111].

1.2.2.2.4 Bide metabolikoen aberastea

Metabolomikako lanetako azken urratsa datuen interpretazio biologikoa da, non helburua

kanpoko estimuluaren eta organismoren erantzun metabolikoaren arteko lotura egitea den [75,90]. Horren baitan dago, KEGG bezalako datu-baseak kontsultatuta, identifikatutako metabolitoei edo bioadierazleei lotutako bide metabolikoak zeintzuk diren argitzea [90]. Ildo horretan, bide metabolikoen aberastea lagungarria izan daiteke alterazio metabolikoentzat azalpen biologiko onargarriak aurkitzeko [112]. Bide metabolikoen aberastea burutzeko dauden baliabideek KEGG bezalako datu-baseetan dauden konposatuak, moduluak, entzimak, erreakzioak eta bide metabolikoak hartu ohi dituzte kontuan, eta analisi estatistikoa eta eskema bisualak konbinatzen dituzte. Modu horretan, ikertzaileek errazago identifika ditzakete aztertutako baldintzetan asaldatutako bide metaboliko esanguratsuak. Oro har, bide metaboliko jakin baten eragina handiagoa da zenbat eta bide metaboliko horretan nabarmenki alteratuta dagoen metabolito gehiago egon. Bestalde, nodo batek sare-antolakuntzan duen garrantzia erlatiboa edo rola estimatuta, metabolito baten garrantzia kalkulatzen da sare metaboliko jakinean konposatuak duen zentralitate-neurrietan oinarrituta [113].

1.3 Erreferentziak

1. Brooks Bryan W., Huggett Duane B., Boxall Alistair B. A. 2010. Pharmaceuticals and personal care products: Research needs for the next decade. *Environ. Toxicol. Chem.* 28:2469–2472.
2. Boxall ABA, Rudd MA, Brooks BW, Caldwell DJ, Choi K, Hickmann S, Innes E, Ostapyk K, Staveley JP, Verslycke T, Ankley GT, Beazley KF, Belanger SE, Berninger JP, Carriquiriborde P, Coors A, DeLeo PC, Dyer SD, Ericson JF, Gagné F, Giesy JP, Gouin T, Hallstrom L, Karlsson MV, Larsson DGJ, Lazorchak JM, Mastrocco F, McLaughlin A, McMaster ME, Meyerhoff RD, Moore R, Parrott JL, Snape JR, Murray-Smith R, Servos MR, Sibley PK, Straub JO, Szabo ND, Topp E, Tetreault GR, Trudeau VL, Van Der Kraak G. 2012. Pharmaceuticals and Personal Care Products in the Environment: What Are the Big Questions? *Environ. Health Perspect.* 120:1221–1229.
3. Wang J, Wang S. 2016. Removal of pharmaceuticals and personal care products (PPCPs) from wastewater: A review. *J. Environ. Manage.* 182:620–640.
4. Arpin-Pont L, Bueno MJM, Gomez E, Fenet H. 2016. Occurrence of PPCPs in the marine environment: a review. *Environ. Sci. Pollut. Res.* 23:4978–4991.
5. Daughton CG, Ternes TA. 1999. Pharmaceuticals and personal care products in the environment: agents of subtle change? *Environ. Health Perspect.* 107:907–938.

6. Kot-Wasik A, Dębska J, Namieśnik J. 2007. Analytical techniques in studies of the environmental fate of pharmaceuticals and personal-care products. *TrAC Trends Anal. Chem.* 26:557–568.

7. Kümmerer K. 2009. The presence of pharmaceuticals in the environment due to human use – present knowledge and future challenges. *J. Environ. Manage.* 90:2354–2366.

8. Wilkinson J, Hooda PS, Barker J, Barton S, Swinden J. 2017. Occurrence, fate and transformation of emerging contaminants in water: An overarching review of the field. *Environ. Pollut.* 231:954–970.

9. Ali AM, Rønning HT, Sydnes LK, Alarif WM, Kallenborn R, Al-Lihaibi SS. 2018. Detection of PPCPs in marine organisms from contaminated coastal waters of the Saudi Red Sea. *Sci. Total Environ.* 621:654–662.

10. Brodin T, Piovano S, Fick J, Klaminder J, Heynen M, Jonsson M. 2014. Ecological effects of pharmaceuticals in aquatic systems—impacts through behavioural alterations. *Philos. Trans. R. Soc. B Biol. Sci.* 369.

11. Corcoran J, Winter MJ, Tyler CR. 2010. Pharmaceuticals in the aquatic environment: A critical review of the evidence for health effects in fish. *Crit. Rev. Toxicol.* 40:287–304.

12. Ebele AJ, Abou-Elwafa Abdallah M, Harrad S. 2017. Pharmaceuticals and personal care products (PPCPs) in the freshwater aquatic environment. *Emerg. Contam.* 3:1–16.

13. Miller TH, Bury NR, Owen SF, MacRae JI, Barron LP. 2018. A review of the pharmaceutical exposome in aquatic fauna. *Environ. Pollut.* 239:129–146.

14. Montes-Grajales D, Fennix-Agudelo M, Miranda-Castro W. 2017. Occurrence of personal care products as emerging chemicals of concern in water resources: A review. *Sci. Total Environ.* 595:601–614.

15. Zenker A, Cicero MR, Prestinaci F, Bottoni P, Carere M. 2014. Bioaccumulation and biomagnification potential of pharmaceuticals with a focus to the aquatic environment. *J. Environ. Manage.* 133:378–387.

16. European Commission. 2013. Surface waters: 12 new controlled chemicals, three pharmaceuticals on watch list. [cited 22 April 2018]. Available from http://www.europarl.europa.eu/news/en/press-room/20130701IPR14760/surface-waters-12-new-controlled-chemicals-three-pharmaceuticals-on-watch-list.

17. Water Framework Directive. 2013. *Directive 2013/39/EU*.

18. European Commission. 2011. *WFD-CIS Guidance Document No. 27 Technical Guidance for Deriving Environmental Quality Standards.*

19. USEPA O. 2009. *Contaminant Candidate List (CCL3) and Regulatory Determination*.:51850–51862. [cited 21 April 2018]. Available from https://www.epa.gov/ccl/contaminant-candidate-list-3-ccl-3.

20. EMEA. 2006. *European Medicine Agency Guideline on the Environmental Risk Assessment of Medicinal Products for Human Use. EMEA/CHMP/SWP/4447/00.*

21. USEPA. 2002. *Frequently Asked Questions: PPCPs as Environmental Pollutants. About the National Exposure Research Laboratory (NERL)*. [cited 23 April 2018]. Available from https://www.epa.gov/aboutepa/about-national-exposure-research-laboratory-nerl.

22. Leeuwen CJ van, Hermens JLM. 1995. *Risk Assessment of Chemicals: An Introduction*. Springer Netherlands. [cited 22 April 2018]. Available from //www.springer.com/us/book/9789401585200.

23. Fatta-Kassinos D, Meric S, Nikolaou A. 2011. Pharmaceutical residues in environmental waters and wastewater: current state of knowledge and future research. *Anal. Bioanal. Chem.* 399:251–275.

24. Aryal S. 2001. Antibiotic Resistance: A Concern to Veterinary and Human Medicine. *Nepal Agric. Res. J.* 4:66–70.

25. Carvalho IT, Santos L. 2016. Antibiotics in the aquatic environments: A review of the European scenario. *Environ. Int.* 94:736–757.

26. Levy SB. 2002. Factors impacting on the problem of antibiotic resistance. *J. Antimicrob. Chemother.* 49:25–30.

27. Ashfaq M, Khan KN, Rasool S, Mustafa G, Saif-Ur-Rehman M, Nazar MF, Sun Q, Yu C-P. 2016. Occurrence and ecological risk assessment of fluoroquinolone antibiotics in hospital waste of Lahore, Pakistan. *Environ. Toxicol. Pharmacol.* 42:16–22.

28. Van Doorslaer X, Dewulf J, Van Langenhove H, Demeestere K. 2014. Fluoroquinolone antibiotics: An emerging class of environmental micropollutants. *Sci. Total Environ.* 500–501:250–269.

29. Calisto V, Esteves VI. 2009. Psychiatric pharmaceuticals in the environment. *Chemosphere*. 77:1257–1274.

30. Silva LJG, Lino CM, Meisel LM, Pena A. 2012. Selective serotonin re-uptake inhibitors (SSRIs) in the aquatic environment: An ecopharmacovigilance approach. *Sci. Total Environ.* 437:185–195.

31. Brausch JM, Rand GM. 2011. A review of personal care products in the aquatic environment: Environmental concentrations and toxicity. *Chemosphere*. 82:1518–1532.

32. Balmer ME, Buser H-R, Müller MD, Poiger T. 2005. Occurrence of Some Organic UV Filters in Wastewater, in Surface Waters, and in Fish from Swiss Lakes. *Environ. Sci. Technol.* 39:953–962.

33. Ramos S, Homem V, Alves A, Santos L. 2015. Advances in analytical methods and occurrence of organic UV-filters in the environment — A review. *Sci. Total Environ.* 526:278–311.

34. Kim S, Choi K. 2014. Occurrences, toxicities, and ecological risks of benzophenone-3, a common component of organic sunscreen products: A mini-review. *Environ. Int.* 70:143–157.

35. Fabbri E, Franzellitti S. 2016. Human pharmaceuticals in the marine environment: Focus on exposure and biological effects in animal species. *Environ. Toxicol. Chem.* 35:799–812.

36. Huerta B, Rodríguez-Mozaz S, Barceló D. 2012. Pharmaceuticals in biota in the aquatic environment: analytical methods and environmental implications. *Anal. Bioanal. Chem.* 404:2611–2624.

37. Puckowski A, Mioduszewska K, Łukaszewicz P, Borecka M, Caban M, Maszkowska J, Stepnowski P. 2016. Bioaccumulation and analytics of pharmaceutical residues in the environment: A review. *J. Pharm. Biomed. Anal.* 127:232–255.

38. Ramirez AJ, Brain RA, Usenko S, Mottaleb MA, O'Donnell JG, Stahl LL, Wathen JB, Snyder BD, Pitt JL, Perez-Hurtado P, Dobbins LL, Brooks BW, Chambliss CK. 2009. Occurrence of pharmaceuticals and personal care products in fish: results of a national pilot study in the United States. *Environ. Toxicol. Chem.* 28:2587–2597.

39. van der Oost R, Beyer J, Vermeulen NPE. 2003. Fish bioaccumulation and biomarkers in environmental risk assessment: a review. *Environ. Toxicol. Pharmacol.* 13:57–149.

40. Klosterhaus SL, Grace R, Hamilton MC, Yee D. 2013. Method validation and reconnaissance of pharmaceuticals, personal care products, and alkylphenols in surface waters, sediments, and mussels in an urban estuary. *Environ. Int.* 54:92–99.

41. Buchberger WW. 2011. Current approaches to trace analysis of pharmaceuticals and personal care products in the environment. *J. Chromatogr. A*. 1218:603–618.

42. Vazquez-Roig P, Blasco C, Picó Y. 2013. Advances in the analysis of legal and illegal drugs in the aquatic environment. *TrAC Trends Anal. Chem.* 50:65–77.

43. Baker DR, Kasprzyk-Hordern B. 2011. Multi-residue determination of the sorption of illicit drugs and pharmaceuticals to wastewater suspended particulate matter using pressurised liquid extraction, solid phase extraction and liquid chromatography coupled with tandem mass spectrometry. *J. Chromatogr. A*. 1218:7901–7913.

44. Grabic R, Fick J, Lindberg RH, Fedorova G, Tysklind M. 2012. Multi-residue method for trace level determination of pharmaceuticals in environmental samples using liquid

chromatography coupled to triple quadrupole mass spectrometry. *Talanta*. 100:183–195.

45. Gros M, Petrović M, Barceló D. 2006. Multi-residue analytical methods using LC-tandem MS for the determination of pharmaceuticals in environmental and wastewater samples: a review. *Anal. Bioanal. Chem.* 386:941–952.

46. Togola A, Budzinski H. 2008. Multi-residue analysis of pharmaceutical compounds in aqueous samples. *J. Chromatogr. A*. 1177:150–158.

47. Fatta D, Achilleos A, Nikolaou A, Meriç S. 2007. Analytical methods for tracing pharmaceutical residues in water and wastewater. *TrAC Trends Anal. Chem.* 26:515–533.

48. Pavlović DM, Babić S, Horvat AJM, Kaštelan-Macan M. 2007. Sample preparation in analysis of pharmaceuticals. *TrAC Trends Anal. Chem.* 26:1062–1075.

49. Hao C, Zhao X, Yang P. 2007. GC-MS and HPLC-MS analysis of bioactive pharmaceuticals and personal-care products in environmental matrices. *TrAC Trends Anal. Chem.* 26:569–580.

50. Sanz-Landaluze J, Bartolome L, Zuloaga O, González L, Dietz C, Cámara C. 2006. Accelerated extraction for determination of polycyclic aromatic hydrocarbons in marine biota. *Anal. Bioanal. Chem.* 384:1331–1340.

51. Zabaleta I, Bizkarguenaga E, Iparragirre A, Navarro P, Prieto A, Fernández LÁ, Zuloaga O. 2014. Focused ultrasound solid–liquid extraction for the determination of perfluorinated compounds in fish, vegetables and amended soil. *J. Chromatogr. A*. 1331:27–37.

52. Petrović M, Hernando MD, Díaz-Cruz MS, Barceló D. 2005. Liquid chromatography–tandem mass spectrometry for the analysis of pharmaceutical residues in environmental samples: a review. *J. Chromatogr. A*. 1067:1–14.

53. Wille K, De Brabander HF, Vanhaecke L, De Wulf E, Van Caeter P, Janssen CR. 2012. Coupled chromatographic and mass-spectrometric techniques for the analysis of emerging pollutants in the aquatic environment. *TrAC Trends Anal. Chem.* 35:87–108.

54. Evgenidou EN, Konstantinou IK, Lambropoulou DA. 2015. Occurrence and removal of transformation products of PPCPs and illicit drugs in wastewaters: A review. *Sci. Total Environ.* 505:905–926.

55. Krauss M, Singer H, Hollender J. 2010. LC–high resolution MS in environmental analysis: from target screening to the identification of unknowns. *Anal. Bioanal. Chem.* 397:943–951.

56. Escher BI, Fenner K. 2011. Recent Advances in Environmental Risk Assessment of Transformation Products. *Environ. Sci. Technol.* 45:3835–3847.

57. Hollender J, Singer H, Hernando D, Kosjek T, Heath E. 2010. The Challenge of the Identification and Quantification of Transformation Products in the Aquatic Environment Using High

Resolution Mass Spectrometry. *Xenobiotics Urban Water Cycle*. Springer, Dordrecht, pp 195–211. doi:10.1007/978-90-481-3509-7_11.

58. Hernández F, Ibáñez M, Bade R, Bijlsma L, Sancho JV. 2014. Investigation of pharmaceuticals and illicit drugs in waters by liquid chromatography-high-resolution mass spectrometry. *TrAC Trends Anal. Chem.* 63:140–157.

59. Wang J, Gardinali PR. 2014. Identification of phase II pharmaceutical metabolites in reclaimed water using high resolution benchtop Orbitrap mass spectrometry. *Chemosphere*. 107:65–73.

60. Chiu S-HL, Huskey S-EW. 1998. Species Differences in N-Glucuronidation 1996 ASPET N-Glucuronidation of Xenobiotics Symposium. *Drug Metab. Dispos.* 26:838–847.

61. Pelkonen O, Tolonen A, Rousu T, Tursas L, Turpeinen M, Hokkanen J, Uusitalo J, Bouvier d'Yvoire M, Coecke S. 2009. Comparison of metabolic stability and metabolite identification of 55 ECVAM/ICCVAM validation compounds between human and rat liver homogenates and microsomes - a preliminary analysis. *ALTEX*. 26:214–222.

62. Zhou X, Chen C, Zhang F, Zhang Y, Feng Y, Ouyang H, Xu Y, Jiang H. 2016. Metabolism and bioactivation of the tricyclic antidepressant amitriptyline in human liver microsomes and human urine. *Bioanalysis*. 8:1365–1381.

63. Díaz-Cruz MS, Barceló D. 2009. Chemical analysis and ecotoxicological effects of organic UV-absorbing compounds in aquatic ecosystems. *TrAC Trends Anal. Chem.* 28:708–717.

64. Bletsou AA, Jeon J, Hollender J, Archontaki E, Thomaidis NS. 2015. Targeted and non-targeted liquid chromatography-mass spectrometric workflows for identification of transformation products of emerging pollutants in the aquatic environment. *TrAC Trends Anal. Chem.* 66:32–44.

65. Rousu T, Herttuainen J, Tolonen A. 2010. Comparison of triple quadrupole, hybrid linear ion trap triple quadrupole, time-of-flight and LTQ-Orbitrap mass spectrometers in drug discovery phase metabolite screening and identification in vitro – amitriptyline and verapamil as model compounds. *Rapid Commun. Mass Spectrom.* 24:939–957.

66. Schymanski EL, Jeon J, Gulde R, Fenner K, Ruff M, Singer HP, Hollender J. 2014. Identifying Small Molecules via High Resolution Mass Spectrometry: Communicating Confidence. *Environ. Sci. Technol.* 48:2097–2098.

67. Zubarev RA, Makarov A. 2013. Orbitrap Mass Spectrometry. *Anal. Chem.* 85:5288–5296.

68. Lim H-K, Chen J, Sensenhauser C, Cook K, Subrahmanyam V. 2007. Metabolite identification by data-dependent accurate mass spectrometric analysis at resolving power of 60 000 in external calibration mode using an LTQ/Orbitrap. *Rapid Commun. Mass Spectrom.* 21:1821–1832.

69. World Health Organization, International Programme on ChemicalSafety. 1993. Biomarkers and risk assessment : concepts and principles. [cited 22 April 2018]. Available from http://apps.who.int/iris/handle/10665/39037.

70. Aguirre-Martínez GV, Owuor MA, Garrido-Pérez C, Salamanca MJ, Del Valls TA, Martín-Díaz ML. 2015. Are standard tests sensitive enough to evaluate effects of human pharmaceuticals in aquatic biota? Facing changes in research approaches when performing risk assessment of drugs. *Chemosphere*. 120:75–85.

71. Ge Y, Wang D-Z, Chiu J-F, Cristobal S, Sheehan D, Silvestre F, Peng X, Li H, Gong Z, Lam SH, Wentao H, Iwahashi H, Liu J, Mei N, Shi L, Bruno M, Foth H, Teichman K. 2013. Environmental OMICS: Current Status and Future Directions. *J. Integr. OMICS*. 3:75–87.

72. Horgan RP, Kenny LC. 2011. 'Omic' technologies: genomics, transcriptomics, proteomics and metabolomics. *Obstet. Gynaecol.* 13:189–195.

73. Al-Salhi R, Abdul-Sada A, Lange A, Tyler CR, Hill EM. 2012. The Xenometabolome and Novel Contaminant Markers in Fish Exposed to a Wastewater Treatment Works Effluent. *Environ. Sci. Technol.* 46:9080–9088.

74. Bundy JG, Davey MP, Viant MR. 2008. Environmental metabolomics: a critical review and future perspectives. *Metabolomics*. 5:3–21.

75. Lankadurai BP, Nagato EG, Simpson MJ. 2013. Environmental metabolomics: an emerging approach to study organism responses to environmental stressors. *Environ. Rev.* 21:180–205.

76. Lin CY, Viant MR, Tjeerdema RS. 2006. Metabolomics: Methodologies and applications in the environmental sciences. *J. Pestic. Sci.* 31:245–251.

77. Viant MR. 2008. Recent developments in environmental metabolomics. *Mol. Biosyst.* 4:980–986.

78. Bayne BL. 1985. *The Effects of Stress and Pollution on Marine Animals*. Praeger.

79. Ankley GT, Bennett RS, Erickson RJ, Hoff DJ, Hornung MW, Johnson RD, Mount DR, Nichols JW, Russom CL, Schmieder PK, Serrrano JA, Tietge JE, Villeneuve DL. 2010. Adverse outcome pathways: A conceptual framework to support ecotoxicology research and risk assessment. *Environ. Toxicol. Chem.* 29:730–741.

80. Tolstikov V, Akmaev VR, Sarangarajan R, Narain NR, Kiebish MA. 2017. Clinical metabolomics: a pivotal tool for companion diagnostic development and precision medicine. *Expert Rev. Mol. Diagn.* 17:411–413.

81. Samuelsson LM, Larsson DGJ. 2008. Contributions from metabolomics to fish research. *Mol. Biosyst.* 4:974–979.

82. Wu H, Southam AD, Hines A, Viant MR. 2008. High-throughput tissue extraction protocol for NMR- and MS-based metabolomics. *Anal. Biochem.* 372:204–212.

83. Cajka T, Fiehn O. 2016. Toward Merging Untargeted and Targeted Methods in Mass Spectrometry-Based Metabolomics and Lipidomics. *Anal. Chem.* 88:524–545.

84. Lin CY, Wu H, Tjeerdema RS, Viant MR. 2007. Evaluation of metabolite extraction strategies from tissue samples using NMR metabolomics. *Metabolomics*. 3:55–67.

85. Cajka T, Fiehn O. 2014. Comprehensive analysis of lipids in biological systems by liquid chromatography-mass spectrometry. *TrAC Trends Anal. Chem.* 61:192–206.

86. Viant MR, Sommer U. 2012. Mass spectrometry based environmental metabolomics: a primer and review. *Metabolomics*. 9:144–158.

87. Rochat B. 2016. From targeted quantification to untargeted metabolomics: Why LC-high-resolution-MS will become a key instrument in clinical labs. *TrAC Trends Anal. Chem.* 84:151–164.

88. Simmons DBD, Benskin JP, Cosgrove JR, Duncker BP, Ekman DR, Martyniuk CJ, Sherry JP. 2015. Omics for aquatic ecotoxicology: Control of extraneous variability to enhance the analysis of environmental effects. *Environ. Toxicol. Chem.* 34:1693–1704.

89. Goodacre R, Broadhurst D, Smilde AK, Kristal BS, Baker JD, Beger R, Bessant C, Connor S, Capuani G, Craig A, Ebbels T, Kell DB, Manetti C, Newton J, Paternostro G, Somorjai R, Sjöström M, Trygg J, Wulfert F. 2007. Proposed minimum reporting standards for data analysis in metabolomics. *Metabolomics*. 3:231–241.

90. Gorrochategui E, Jaumot J, Lacorte S, Tauler R. 2016. Data analysis strategies for targeted and untargeted LC-MS metabolomic studies: Overview and workflow. *TrAC Trends Anal. Chem.* 82:425–442.

91. Yi L, Dong N, Yun Y, Deng B, Ren D, Liu S, Liang Y. 2016. Chemometric methods in data processing of mass spectrometry-based metabolomics: A review. *Anal. Chim. Acta*. 914:17–34.

92. Di Guida R, Engel J, Allwood JW, Weber RJM, Jones MR, Sommer U, Viant MR, Dunn WB. 2016. Non-targeted UHPLC-MS metabolomic data processing methods: a comparative investigation of normalisation, missing value imputation, transformation and scaling. *Metabolomics*. 12.

93. Hrydziuszko O, Viant MR. 2012. Missing values in mass spectrometry based metabolomics: an undervalued step in the data processing pipeline. *Metabolomics*. 8:161–174.

94. Dubin E, Spiteri M, Dumas A-S, Ginet J, Lees M, Rutledge DN. 2016. Common components and specific weights analysis: A tool for metabolomic data pre-processing. *Chemom. Intell. Lab.*

Syst. 150:41–50.

95. Fernández-Albert F, Llorach R, Garcia-Aloy M, Ziyatdinov A, Andres-Lacueva C, Perera A. 2014. Intensity drift removal in LC/MS metabolomics by common variance compensation. *Bioinformatics*. 30:2899–2905.

96. Vinaixa M, Samino S, Saez I, Duran J, Guinovart JJ, Yanes O. 2012. A Guideline to Univariate Statistical Analysis for LC/MS-Based Untargeted Metabolomics-Derived Data. *Metabolites*. 2:775–795.

97. Dunn WB, Wilson ID, Nicholls AW, Broadhurst D. 2012. The importance of experimental design and QC samples in large-scale and MS-driven untargeted metabolomic studies of humans. *Bioanalysis*. 4:2249–2264.

98. Seltman HJ. 2015. *Experimental Design and Analysis*.

99. Worley B, Powers R. 2013. Multivariate Analysis in Metabolomics. *Curr. Metabolomics*. 1:92–107.

100. Huang SSY, Benskin JP, Chandramouli B, Butler H, Helbing CC, Cosgrove JR. 2016. Xenobiotics Produce Distinct Metabolomic Responses in Zebrafish Larvae (Danio rerio). *Environ. Sci. Technol.* 50:6526–6535.

101. Kenny LC, Broadhurst DI, Dunn W, Brown M, North RA, McCowan L, Roberts C, Cooper GJS, Kell DB, Baker PN. 2010. Robust Early Pregnancy Prediction of Later Preeclampsia Using Metabolomic Biomarkers. *Hypertension*. 56:741–749.

102. Shi B, Tian J, Xiang H, Guo X, Zhang L, Du G, Qin X. 2013. A 1H-NMR plasma metabonomic study of acute and chronic stress models of depression in rats. *Behav. Brain Res.* 241:86–91.

103. Lazic SE. 2008. Why we should use simpler models if the data allow this: relevance for ANOVA designs in experimental biology. *BMC Physiol.* 8:16.

104. Jansen JJ, Hoefsloot HCJ, van der Greef J, Timmerman ME, Westerhuis JA, Smilde AK. 2005. ASCA: analysis of multivariate data obtained from an experimental design. *J. Chemom.* 19:469–481.

105. Vinaixa M, Schymanski EL, Neumann S, Navarro M, Salek RM, Yanes O. 2016. Mass spectral databases for LC/MS- and GC/MS-based metabolomics: State of the field and future prospects. *TrAC Trends Anal. Chem.* 78:23–35.

106. http://www.kegg.jp/kegg/. 2018. KEGG_.

107. http://www.hmdb.ca/metabolites/. 2018. HMDB_.

108. http://www.lipidmaps.org/. 2018. LipidMaps_.

109. https://www.mzcloud.org/. 2018. mzCloud_.

110. https://msbi.ipb-halle.de/MetFragBeta/. 2018. MetFrag_.

111. Wolf S, Schmidt S, Müller-Hannemann M, Neumann S. 2010. In silico fragmentation for computer assisted identification of metabolite mass spectra. *BMC Bioinformatics*. 11:148.

112. Picart-Armada S, Fernández-Albert F, Vinaixa M, Rodríguez MA, Aivio S, Stracker TH, Yanes O, Perera-Lluna A. 2017. Null diffusion-based enrichment for metabolomics data. *PLOS ONE*. 12:e0189012.

113. Xia J, Wishart DS. 2010. MetPA: a web-based metabolomics tool for pathway analysis and visualization. *Bioinformatics*. 26:2342–2344.

2. Kapitulua

Helburuak

Farmakoen eta zaintza pertsonalerako produktuen (*pharmaceuticals and personal care products*, PPCP, direlakoen) ur-ekosistemetako agerpen zabalak eta horiek organismo ez-zuzenduetan eragin ditzaketen albo-ondorioek kezka zientifikoa eta soziala areagotu dute. Orain arte, PPCP-ak eta euren azpiproduktuak identifikatu eta agerpena kontrolatzeko ahalegin handiak egin dira ur-araztegietako isurietan eta ingurumeneko azaleko uretan. Hala ere, PPCP-en presentziaren ebaluazioak erronka izaten jarraitzen du biotan. Izatez, PPCP-ek arrainak bezalako organismo urtarretan biometatzeko gaitasuna dutela frogatu da ingurumeneko biomonitorizazioen bidez. Dena den, PPCP-en metatzearen, ehunen arteko banaketaren, metabolizazioaren eta kanporatzearen ulermena bermatzeko oraindik informazio gutxiegi dago eskuragarri. Esate baterako, PPCP-en transformazioaren eta biodegradazioaren inguruko ezagutza-faltak esposizioaren benetako neurria gutxiestea eragin dezake. Izan ere, PPCP-en azpiproduktuek (transformazio-produktuek eta metabolitoek, konkretuki) konposatu aitzindariek besteko arriskua edo handiagoa sor dezakete. Horrez gain, ingurumenerako arriskuen ebaluazioari dagokionez, oso garrantzitsua da PPCP-ek organismo urtarretan eragin ditzakeen albo-ondorioak ebaluatzea, urriak baitira metatzea eta albo-ondorioak aldi berean aztertu dituzten ikerketak. Azken urteotan, metabolomika teknika oso erabilgarria eta sentikorra bilakatu da ingurumenean maila ez-hilgarrietan agertzen diren kutsatzaileen albo-ondorioak ikertzeko.

Testuinguru horretan, doktorego-tesi honen helburu nagusia ondokoa da: ***PPCP-ek ur-ekosistemetan duten patua eta jokabidea ebaluatzeko hurbilketa holistikoa garatzea, zeinak barne hartzen dituen organismo urtarretako PPCP-en determinazioa, biometatzea, biotransformazioa eta albo-ondorioak***. Helburu nagusi hori lortzeko, ondorengo azpihelburuak definitu dira:

1. Metodo analitiko sendoak eta fidagarriak optimizatu PPCP-ak ingurumeneko matrize desberdinetan determinatzeko eta metodo horiek Bizkaiko kostaldeko lagin errealetan aplikatzea. Ingurumenean aurkitu ohi diren kutsatzaileen adierazgarri diren antidepresibo triziklikoak eta fluorokinolonak aztertu dira uretan (estuarioko, itsasoko eta araztegien irteerako uretan) eta biotan (muskuiluetan eta arrainen ehunetan/jariakinetan).

2. Urraburu arrain (*Sparus aurata*) gazteen ehunak (burmuina, gibela, zakatzak, muskulua) eta jariakinak (plasma, behazuna) aztertuta, amitriptilina antidepresiboaren, *ciprofloxacin* antibiotikoaren eta oxibenzona ultramore iragazkiaren biometatzea eta ehunen arteko banaketa ebaluatu, eta konposatu horien azpiproduktuak karakterizatzea.
3. Maila ez-hilgarrietan amitriptilinaren eta oxibenzonaren *in vivo* esposizioek urraburu arrain gazteen burmuinean, gibelean eta plasman eragin ditzaketen albo-ondorioak ikertzea.

Helburu horiek erdiesteko, beharrezkoa da honako metodologiak garatzea:

i. Metodo bideratuak, instrumentazio analitiko sentikorra (LC-QqQ-MS/MS) erabilita kutsatzaileak kuantifikatzeko ingurumeneko uretan eta ehun/jariakin biologikoetan.
ii. Susmagarrien analisirako estrategiak, bereizmen altuko masa-espektrometria (LC-qOrbitrap) erabilita azpiproduktuak karakterizatzeko itsasoko uretan eta arrainen ehunetan/jariakinetan.
iii. Metabolomikako hurbilketa bideratuak eta ez-bideratuak, PPCP-ek arrainetan eragindako albo-ondorioak azaltzen dituzten profil metabolikoko aldaketak ikertzeko.

Datozen kapituluetan aipatutako helburuen garapena eta lorpena deskribatzen dira.

3. Kapitulua

Antidepresibo triziklikoen determinazioa biotan eta ingurumeneko uretan tandem masa-espektrometriari akoplatutako likido-kromatografiaren bidez

Analytical and Bioanalytical Chemistry

408 (2015) 1205-1216

3.1 Sarrera

Azken hamarkadetan, farmakoak eta zaintza pertsonalerako produktuak ur-ingurumeneko kutsadura iturri garrantzitsu gisa aitortu dira [1] eta, 1990eko hamarkada geroztik, konposatu aktibo batzuk kontzentrazio baxuetan ere (ng/L-an) ekosistemak oztopatzeko gaitasuna dutela dakigu [2]. Ingurunean detektatu diren konposatu farmakologikoki aktiboen artean antidepresibo triziklikoak (*tricyclic antidepressant*, TCA, delakoak) aurkitzen dira, zeinak depresioaren eta gaixotasun psikiatrikoen tratamenduan erabiliak diren [3–12]. TCA-ek neurotransmisore desberdinen xurgapen selektiboaren inhibitzaile gisa jokatzen dute nerbio-sistema zentralean [13]. Nortriptilina amina sekundarioak norepinefrinaren xurgapen selektiboa inhibitzen duen bitartean, amitriptilina, imipramina eta klomipramina amina tertziarioek serotoninaren xurgapena eragozten dute. Farmako horiek oso erabiliak dira, bereziki herrialde garatuetan, eta ur-ingurumenean sartzen dira, batez ere giza iraizketatik [2]. TCA asko ez dira guztiz degradatzen edo ezabatzen araztegietako tratamenduetan eta, nahiz eta 1 ng/mL kontzentraziora arteko mailan aurkitu [5,6,8–11], euren uretarako etengabeko isuria mehatxu bihurtzen da organismo urtar ez-zuzenduentzat bizitza osoko esposizioa pairatzen baitute. Ondorioz, farmakoak sistema biologikoekin elkarreragiteko diseinatzen direnez, ez da harritzekoa immunitatean, ugalketan, garapenean, zein hazkuntzan eragina duten albo-ondorioak plazaratzen dituzten ikerketa-lanak aurkitzea [14,15].

TCA-k ur-araztegietako isurietan [4,6,8,11,12] eta ingurumeneko azaleko uretan detektatu dira [5]. Gainera, konposatu horien ur-oktanol banaketa-koefiziente altuaren (log K_{ow} > 3) ondorioz, TCA-k biotan ere metatu daitezke [7,16,17]. Izatez, intereseko konposatuek organismoetan duten biometatzea aztertzea ohiko prozedura da kutsatzaileen esposizioaren eragina ebaluatzeko. Hala ere, oraindik informazio gutxi dago eskuragarri biotan detekta daitezkeen farmakoen inguruan eta, dakigunaren arabera, ez dago organismo urtarretan TCA-en metatzea aztertzen duen ikerketarik [18]. Organismo urtarren artean, arrainak ur-ingurumenean nonahi aurki daitezkeenez, organismo bideragarritzat hartzen dira farmakoen biometatze-ikerketetarako zein ur-sistemen segimendua egiten duten programetarako [16,18].

Testuinguru horretan, nahiz eta ingurumeneko matrizeetan TCA-en agerpena araututa ez egon, garrantzitsua da ingurumeneko laginetarako, eta bereziki biotarako, haiek determinatzeko

metodo sendoak eta sentikorrak garatzea. Instrumentazio analitiko berriek kutsatzaile askoren segimendua egitea ahalbideratzen duten arren, oraindik badaude TCA-en detekzioarekin eta kuantifikazioarekin lotutako bi zailtasun nagusi, hala nola euren itsas-ingurumeneko kontzentrazio baxuak eta ingurumeneko matrizeen konplexutasuna [3].

TCA-en analisian sarri erabiltzen den teknika analitikoa masa-espektrometriari akoplatutako gas-kromatografia (GC-MS) [6,19] den arren, likido-kromatografia erabiliagoa da, bereziki tandem masa-espektrometriari akoplatuta (LC–MS/MS), aztarna-mailako ingurumeneko farmakoen analisian erakusten dituen fidagarritasuna eta sentsibilitatea direla eta [4,5,7–9,11,12,16,20]. Izan ere, MS/MS hurbilketak, ioi aitzindari eta apurketa-ioi egokiak aukeratuta, matrize-interferentziak minimizatu edo kentzeko gaitasuna du. Hala ere, LC-MS/MS teknikaren desabantaila nagusia, bereziki elektroesprai-ionizazioa (*electrospray ionization*, ESI, delakoa) erabilita, matrize-interferentziek eragindako seinale kromatografikoaren txikitzea/handitzea da [21]. Hori dela eta, emaitza okerrak ekidin nahian, teknika hori erabiltzean, matrize-efektuen aurretiazko azterketa beharrezkoa da [3]. Horrez gain, ingurumeneko matrize konplexuen analisian funtsezkoa da laginaren prestatze egokia burutzea. Hortaz, erauzketa- eta garbiketa-urrats eraginkorrak ezinbestekoak dira ionizazio eskasa, hondoaren zarata eta LC sistemako akatsak ekiditeko.

Bibliografiaren arabera, TCA-k lagin solidoetatik erauzteko erabilitako teknika nagusienak ohiko solido-likido erauzketa-teknikak [7,16], ultrasoinuen bidezko erauzketa [22], presiopeko likidoen bidezko erauzketa [4] eta QuEChERS (*Quick, Easy, Cheap, Effective, Rugged and Safe* delakoa) dira [12,23]. Ohiko ultrasoinu-bainuekin alderatuta, ultrasoinu fokatuen bidezko solido-likido erauzketa (*focused ultrasound solid-liquid extraction*, FUSLE) sinpleak ezaugarri nabarmenak ditu, hala nola erauzketa-denbora laburrak eta lagin- eta disolbatzaile-kantitate txikien beharrizana (0,01–1,0 g eta 5–15 mL, hurrenez hurren). FUSLE-ren eraginkortasuna kabitazio-fenomenoaren bidez lortutako presio eta tenperatura altuen ondorioz lortzen da. Hain zuzen, titaniozko mikropunta zuzenean erauzian murgilduta eratzen diren ahalmen handiko ultrasoinu-uhinetan datza FUSLE. Teknika hori arrakastaz aplikatu den arren biotatik kutsatzaile organiko desberdinak erauzteko [24,25], lan honetan aztertutako matrizeetatik (arrainen gibeletik eta muskulutik eta muskuiluetatik) TCA-k erauzteko ez da inoiz FUSLE erabili.

Aipatutako erauzketa-metodoen selektibitate falta dela eta, beharrezkoa izan ohi da

garbiketa-urratsa. Garbiketarako prozesu ohikoena fase solidoko erauzketa (*solid phase extraction*, SPE, delakoa) da. Teknika horrek TCA-en isolamendua edota aurrekontzentrazioa baimentzen ditu ingurumeneko ur-lagin zein biota bezalako matrize desberdinetan. Nagusiki erabiltzen diren fase geldikorren artean, dibinilbentzenoz eta binilpirrolidonaz osatutako kopolimeroa (*hydrophilic–lipophilic balanced*, HLB, delakoa) [11,20] eta modu mistoko katioi-trukatzaile (*cation exchanger*, CX, delako) sendoak edo ahulak aurki daitezke [5,6,8–10]. Azken horiek erauzi garbiagoak lortzeko abantaila eskaintzen dute erretentzio-mekanismo desberdinen konbinazioagatik.

Esparru horretan, lan honen helburua metodo zehatzak eta doiak garatzea da amitriptilina, nortiptilina, imipramina eta klomipramina antidepresibo triziklikoak determinatzeko ingurumeneko matrize desberdinetan, hala nola uretan (estuarioko, itsasoko eta araztegien irteerako uretan) eta biotan (arrainen gibelean eta muskuluan eta muskuiluetan). Horretarako, intereseko konposatuak lagin solidoetatik erauzteko FUSLE-ren eraginkortasuna ebaluatu da eta garbiketarako SPE modu desberdinak (alderantzizko fasea eta modu mistoa) aztertu dira. Era berean, ur-laginetarako ere SPE prozedura osotasunean optimizatu da. Bai garbiketa-urratseko bai LC-MS/MS (kuadrupolo hirukoitza) analisiko matrize-efektua ere guztiz arakatu da. Azkenik, garatutako metodoak Bizkaiko kostaldeko lagin errealak analizatzeko erabili dira.

3.2 Materiala eta metodoak

3.2.1 Erreaktiboak eta materialak

Imipramina hidrokloruroa (% 99), amitriptilina hidrokloruroa (98 %), nortriptilina hidrokloruroa (98 %) eta klomipramina hidrokloruroa (98 %), eta trazagarri gisa erabiltzeko isotopikoki markatutako $^{2}H_{3}$-amitriptilina hidrokloruroa ($^{2}H_{3}$-AMI; erreferentziazko estandar zertifikatua) eta $^{2}H_{3}$-nortriptilina hidrokloruroa ($^{2}H_{3}$-NOR; erreferentziazko estandar zertifikatua) Sigma-Aldrich (St. Louis, MO, AEB) merkataritza-etxean erosi dira. TCA-en eta trazagarrien egitura kimikoa, ur-oktanol banaketa-koefizientea (log K_{ow}) eta azidotasun-konstantea (pK_a) 3.1 taulan ageri dira.

Amitriptilina, nortiptilina, imipramina eta klomipramina analitoen disoluzio bakunak metanoletan (Fisher Scientific, Loughborough, Erresuma Batua) prestatu dira gutxi gorabehera

5000 mg/L-ko kontzentrazio-mailan. Bestalde, 100 mg/L-ko eta maila baxuagoko diluzioak metanoletan prestatu dira hilabetero eta egunero, hurrenez hurren. $^{2}H_3$-AMI eta $^{2}H_3$-NOR trazagarrien disoluzio bakunak 100 mg/L kontzentrazioan prestatu dira metanoletan. Disoluzio guztiak −20°C-an gorde dira.

3.1 taula: *Intereseko analitoen egitura kimikoak, log K_{ow} eta pK_a balioak* [26].

Analitoa	**Egitura**	**Log K_{ow}**	**pK_a**
Imipramina (IMI)	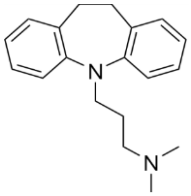	4,28	9,20
Amitriptilina (AMI)	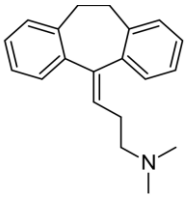	4,81	9,76
Nortriptilina (NOR)	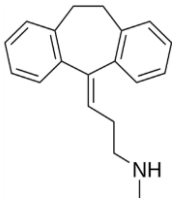	4,43	10,47
Klomipramina (CLO)	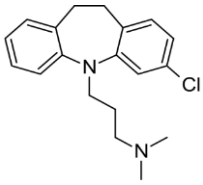	4,88	9,20

Metanola (HPLC kalitatea, % 99,9) eta azetona (HPLC kalitatea, % 99,8) LabScan (Dublin, Irlanda) merkataritza-etxekoak dira, azetonitriloa (HPLC kalitatea, % 99,9) eta amonio azetatoa (NH_4OAc, ≥ % 99) Sigma-Aldrich (Steinheim, Alemania) merkataritza-etxekoak, sodio hidroxidoa (NaOH, ≥ % 99) Merck-ekoa (Darmstadt, Alemania), azido formikoa (HCOOH, ≥ % 98) Scharlau (Bartzelona, Espainia) merkataritza-etxekoa eta amonio hidroxidoa (NH_4OH, % 25) Panreac-ekoa (Bartzelona, Espainia). Ur ultra-purua (Milli-Q ura) ura purifikatzeko sistema (< 0.05 S/cm, Milli-Q 185 modeloa, Millipore, Bedford, MA, AEB) erabilita lortu da.

Lagin solidoak liofilizatzeko Cryodos-50 liofilizatzailea (Telstar Instrument, Sant Cugat del Valles, Bartzelona, Espainia) erabili da eta TCA-k lagin solidoetatik erauzteko 3 mm-ko titaniozko mikropunta duen ultrasoinu-homogeneizatzailea (100 W, 20 kHz; Bandelin Sonopuls HD 3100 sonikatzailea, Bandelin electronic, Berlin, Alemania). Erauzketak Deltalab (Bartzelona, Espainia) merkataritza-etxeko 50 mL-ko polipropilenozko ontzi konikoetan (barne-diametroa 27,2 mm-ko barne-diametroa eta 117,5 mm-ko luzera) egin dira eta erauziak poliamidazko iragazkien (0,45 μm, 25 mm, Macherey-Nagel, Alemania) bidez iragazi dira. Nitrogenoaren (> % 99,999; Messer, Tarragona, Espainia) korrontearen bidez disolbatzailea lurruntzeko Turbo Vap LV lurrungailua (Zymark, Hopkinton, MA, AEB) erabili da.

Garbiketa-urratsean erabilitako SPE egiteko hodi hutsak eta Envi-Carb grafitozko karbonoa (100 m^2/g azalera espezifikoa, 120/400 sare-begia) Supelco (Bellefonte, PA, AEB) merkataritza-etxean erosi dira, Plexa (550 m^2/g azalera espezifikoa, 320 sare-begia) Agilent Technologies merkataritza-etxean eta Evolute-CX (200 mg, 6 mL) SPE kartutxoak Biotage (Uppsala, Suedia) merkataritza-etxean.

Ur-laginak iragazteko Whatman (Maidstone, Erresuma Batua) merkataritza-etxeko bi iragazki-mota aztertu dira: 1,2 μm-ko (90 mm-ko diametroa) beirazko mikrozuntzezkoak eta 0,45 μm-ko (47 mm-ko diametroa) zelulosa nitratozko mintzekin egindakoak.

Lagin guztien erauziak LC-MS/MS-aren bidez analizatu aurretiko iragazketarako iragazki desberdinak frogatu dira: Pall (0,2 μm, 13 mm, AEB) eta Membrane Solutions (0,22 μm, 13 mm, Simplepure, AEB) merkataritza-etxeetako polipropilenozko, Teknokroma-ko (AEB) politetrafluoroetileno (PTFE) hidrofilikozko (0,2 μm, 13 mm) eta Membrane Solutions merkataritza-etxeko polibinilideno polifluorurozko (0,22 μm, 13 mm) iragazkiak.

Fase mugikor gisa, Milli-Q ura eta metanola (Fisher Scientific, Loughborough, Erresuma Batua) erabili dira azido formikoarekin (HCOOH, Formic acid Optima, Fischer Scientific, Gell, Belgika) batera. Talka-gas gisa erabilitako purutasun altuko nitrogenoa (> % 99,999) Messer (Tarragona, Espainia) merkataritza-etxekoa izan da, eta lehortze- eta lainoztatze-gas gisa erabilitako nitrogenoa (% 99,999) AIR Liquide-koa (Madril, Espainia).

3.2.2 Laginak eta laginen prestatzea

Metodoen optimizaziorako eta berrespenerako liofilizatutako arrain-haztegiko muskuiluak, itsas-zapoaren (*Lophius piscatorius*) gibela eta bertako merkatuan lortutako panga arrainaren (*Pangasius hypophthalmus*) muskulua erabili dira, baita Gernikan (Euskal Herria) bildutako ur-laginak (estuarioko, itsasoko eta araztegien irteerako urak) ere. Bestalde, garatutako metodoak 2015eko ekainean Gernikan bildutako ondorengo laginetan aplikatu dira: araztegiko (43,323985 N; -2,674143 W) irteerako uretan, estuarioko (araztegiko irteeratik errekan behera; 43,324036 N; -2,673611 W) uretan eta korrokoien (*Chelon labrosus*) gibeletan eta Laida hondartzako (43,399241 N; -2,685750 W; Ibarrangelu, Euskal Herria) itsasoko uretan eta muskuiluetan (*Mytilus galloprovincialis*).

Analisirako muskuilu-ehuna, arrain-gibela eta arrain-muskulua bereizi eta prestatu dira. Muskuiluetan ehun biguna ozkoletik banatu, eta korrokoi bakoitzetik gibela eta muskulua bereizteko, disekzioa eskalpelo garbia erabilita burutu da. Behin 5 indibiduoren ehunak batu, homogeneizatu, liofilizatu eta anbarrezko ontzietan gorde dira analisira arte -20°C-an. Bestalde, ur-laginak aurretiaz garbitutako anbarrezko beirazko ontzietan bildu eta kutxa hotzetan garraiatu dira laborategira analisia 24 h pasatu baino lehen burutzeko.

3.2.3 Lagin solidoen erauzketa

Lagin solidoetatik TCA-k erauzteko FUSLE-ren baldintzen optimizazioan TCA-ekin indartutako arrain-muskulua (panga-xerra) erabili da. Horretarako, liofilizatutako matrizearen kantitate ezaguna almaizean homogeneizatu, pisatu eta azetonarekin estali ostean, intereseko analitoekin 100 ng/g kontzentrazioan dopatu eta 24 orduz irabiatu da. Ondoren, azetona lurrundu eta lagina aste betez zaharkitu da.

Baldintza optimoetan, 40 mL-ko ontzian lagin liofilizatuaren 0,5 g eta azetonitrilo:Milli-Q ur (95:5, bol/bol) nahastearen 7 mL gehitu ondoren, isotopikoki markatutako estandarrak ($^{2}H_{3}$-AMI eta $^{2}H_{3}$-NOR) gehitu dira (50 ng/mL-ko disoluzioaren 100 μL) trazagarri gisa. FUSLE 30 s-tan gauzatu da (0,8 s-ko pultsu-denborarekin eta 0,2 s-ko pultsu-geldialdiekin), % 10-eko potentziarekin eta izotz-bainuan. Behin erauzita, gaineko likidoa 0,45 μm-ko poliamidazko iragazkien bidez iragazi, nitrogeno-korrontearekin ~1 mL-ra lurrundu eta lortutako erauzia garbiketa-urratsera bideratu da.

3.2.4 Lagin solidoen garbiketa

Matrize-efektua saihesteko, SPE-n oinarritutako garbiketa-modu desberdinak aztertu dira, hala nola alderantzizko fasea (Envi-carb eta Plexa) eta modu mistoa (Evolute-CX modu mistoko katioi-trukatzaile sendoa). Esperimentu guztietan, garbiketa-urratsaren aurretik, dopatu gabeko arrain-muskuluen laginek FUSLE-ren bidez erauzi ostean, erauziak metanoletan dagoen TCA-en (amitriptilinaren, nortiptilinaren, imipraminaren eta klomipraminaren) 2 µg/mL-ko disoluzioaren 25 µL-rekin dopatu dira. Amaieran, LC-MS/MS analisira orduko, garbiketa-urratseko eluzio-disoluzioa nitrogeno-korrontearen laguntzarekin 35°C-an lehorrera eraman, metanol:Milli-Q ur (90:10, bol/bol) nahastearen 200 µL-an berriz disolbatu eta 0,22 µm-ko polipropilenozko iragazkietatik iragazi da.

3.2.4.1 Alderantzizko fasea

FUSLE erauzketaren ondoren, ~1 mL-ra lurrundutako erauzia aldez aurretik NaOH-arekin pH 12-ra doitutako 6 mL Milli-Q ur gehituta diluitu eta alderantzizko-faseko SPE-ren bidezko garbiketa egin da. Urrats hori Envi-Carb edo Plexa fase geldikorren 200 mg-rekin betetako 6 mL-ko kartutxo hutsak erabilita egin da. Bi fase geldikorren kasuan, erauzia kargatu aurretik, kartutxoak egokitu egin dira 5 mL metanol, 5 mL Milli-Q ur eta pH 12-ra doitutako 5 mL Milli-Q ur pasatuta. Kargaren ondoren, garbitzeko 5 mL Milli-Q ur gehitu, ordu betez hutsa eginda, kartutxoak lehortu eta, bukatzeko, analitoak 6 mL metanoletan eluitu dira.

3.2.4.2 Modu mistoa

FUSLE egin ondoren, ~1 mL-ra lurrundutako erauzia Milli-Q uraren 6 mL gehituta diluitu eta 200 mg-ko Evolute-CX kartutxoan kargatu da. Aldez aurretik kartutxoak 5 mL metanol, 5 mL Milli-Q ur eta % 2 HCOOH duen Milli-Q uraren (pH=2) 5 mL pasatuta egokitu dira. Lagina kargatu ondoren eta garbiketarako helburuarekin, Milli-Q uraren eta metanolaren 5 mL, hurrenez hurren, gehitu, kartutxoak 30 min-tan hutsean lehortu eta analitoak % 2,5 NH_4OH duen azetonaren 3 mL-an berreskuratu dira.

3.2.5 Ur-laginen erauzketa eta aurrekontzentrazioa

Ingurumeneko ur-lagin desberdinetatik (estuarioko, itsasoko eta araztegien irteerako

uretatik) TCA-k erauzi eta aurrekontzentratzeko 3.2.4.2 atalean aipatutako modu mistoko SPE-ren protokolo eraldatua erabili da. Hain zuzen, karga-urratsean 500 mL-ko ur-alikuota Evolute-CX kartutxoan zehar pasatu da 3 mL/min-ko abiaduran eta gainontzeko garbiketa- eta eluzio-prozedura aurreko atalean FUSLE-ko erauziei aplikatutako berdina izan da.

3.2.6 LC-MS/MS analisia

TCA-k banatu eta kuantifikatzeko Agilent 1260 serieko HPLC kromatografoa (Agilent Technologies, Palo Alto, CA, AEB) erabili da, zeinak gasgabetzailea, ponpa binarioa eta laginak hartzeko sistema automatikoa dituen. Zutabe kromatografikoa tenperatura konstantean mantentzeko labeari akoplatuta Agilent 6430 kuadrupolo hirukoitzeko (QqQ) masa-espektrometroa du bi ionizazio-iturrirekin, presio atmosferikoko ionizazio kimikoarekin (*atmospheric pressure chemical ionization*, APCI, delakoarekin) eta ESI-rekin.

Lan honetan, analitoen banaketarako bi zutabe kromatografiko aztertu dira. Aurrezutabe-iragazkiari (0,5 μm, Vici Jour, Vici AG International, Schenkon, Suitza) lotutako ACE UltraCore 2,5 SuperC18 (2,1 mm × 50 mm, 2,5 μm) zutabea (Advanced Chromatography Technologies Limited, Aberdeen, Eskozia) eta Kinetex bifenilo 100 Å core-shell aurrezutabeari (2,1 mm x 5 mm, 2,6 μm) lotutako Phenomenex (Torrance, CA, AEB) merkataritza-etxeko Kinetex bifenilo 100 Å core-shell (2,1 mm x 50 mm, 2,6 μm) zutabea. Fase mugikorrari dagokionez, A fasea Milli-Q ur:metanol (95:5, bol/bol) nahasteaz osatuta dago eta B fasea metanol:Milli-Q ur (95:5, bol/bol) nahasteaz, bietan HCOOH % 0,1 gehituta. Banaketa-gradientea ondokoa da: A fase mugikorraren % 45ean hasi eta % 10era jaitsi da 3 minututan, konposizio horretan 6 minutuz mantendu ostean 3 minututan hasierako baldintzetara (A fase mugikorraren % 45era) bueltatu, eta bertan 8 minutuz mantendu da hasierako baldintzak berreskuratzen direla ziurtatzeko. Analitoen banaketa 0,3 mL/min-ko fluxuan burutu eta injekzio-bolumena 2 μL-an ezarri da.

Aukeratutako ioi aitzindarietatik apurketa-ioietarako trantsizioen jarraipena egiten duen eskuratze-modua (*Selected Reaction Monitoring,* SRM, delakoa) erabili da kuantifikaziorako. Nitrogenoa erabili da talka-, lehortze- eta lainoztatze-gas gisa. ESI-ko aldagaiak optimizatu ondoren, ionizazioa modu positiboan egin da, 3000 V-ko tentsio kapilarrarekin, lehortze-gasa 12 L/min-ko fluxuan eta 350°C-an, eta lainoztatze-gasa 45 psi-an. Konposatuak banan banan

injektatuta, ionizazio-iturriko disoziazio-tentsioa eta talka-energia 20–200 V eta 5-60 eV tarteetan optimizatu dira, hurrenez hurren. Baldintza optimoak 3.2 taulan laburbildu dira.

3.2 taula: *Intereseko analitoen eta trazagarrien ioi aitzindariak eta apurketa-ioiak (lehenengoa kuantifikatzeko eta besteak egiaztatzeko) ionizazio-iturriko disoziazio-tentsioaren (V) eta talka-energiaren (eV) balioa optimoetan. Baita determinazio-koefizienteak (r^2), detekzio-muga (limit of detection, LOD, delakoa) eta kuantifikazio-muga (limit of quantification, LOQ, delakoa) instrumentalak.*

Analitoa	Ioi aitzindaria (*m/z*)	Apurketa-ioiak (*m/z*)	Disoziazio-tentsioa (V)	Talka-energia (eV)	r^2	LOD (ng/mL)	LOQ (ng/mL)
IMI	281,2	58,1/86,1/193,1	76	41/13/45	0,99998	0,2	0,5
AMI	278,2	91,1/117,1/191,1	76	29/25/25	0,99993	0,2	0,5
NOR	264,2	233,1/91,1/105,1	102	13/25/17	0,99988	0,1	0,2
CLO	315,2	86,1/58,1/227,0	76	17/41/45	0,99995	0,05	0,1
$^2H_3$-AMI	281,2	91,1/117,1/191,1	76	29/25/25	0,99993	-	-
$^2H_3$-NOR	267,2	233,1/91,1/105,1	102	13/25/17	0,99980	-	-

Neurketak, datuen eskuratzea eta gailurren integrazioa Masshunter Workstation software-arekin (Qualitative Analysis, B.06.00 bertsioa, Agilent Technologies) egin dira.

3.3 Emaitzak eta eztabaida

3.3.1 LC-MS/MS analisiaren optimizazioa

3.3.1.1 Parametro kromatografikoen optimizazioa

Analito guztiak 1 μg/mL kontzentrazioan dituen estandarra erabilita sakon optimizatu dira LC-MS/MS-eko parametroak, hala nola zutabearen fasea, zutabearen tenperatura, fase mugikorraren konposizioa eta fluxua.

Bibliografian C18 zutabeak erabili izan diren arren [8,9,11,16], lan honetan, TCA-en banaketarako bi kromatografia-zutabe (ACE UltraCore 2,5 SuperC18 eta Kinetex bifenilo 100 Å core-shell) aztertu ditugu. Azterketa horien analisia ekorketa osoko eskuratze-moduan egin da

isokratikoan A:B (50:50, bol/bol) fase mugikor nahastea erabilita, non A Milli-Q ur:metanol (95:5, bol/bol) eta B Milli-Q ur:metanol (5:95, bol/bol) nahasteak diren, bietan % 0,1 HCOOH gehituta. 3.1 irudian ikus daitekeen bezala, bereizmenari, gailurren simetriari eta sentikortasunari erreparatuta, Kinetex biphenyl 100 Å core-shell zutabearekin lortu da kromatografia-banaketarik onena. Hortaz, ondoren egindako esperimentu guztietan Kinetex bifenilo 100 Å core-shell zutabea erabili da.

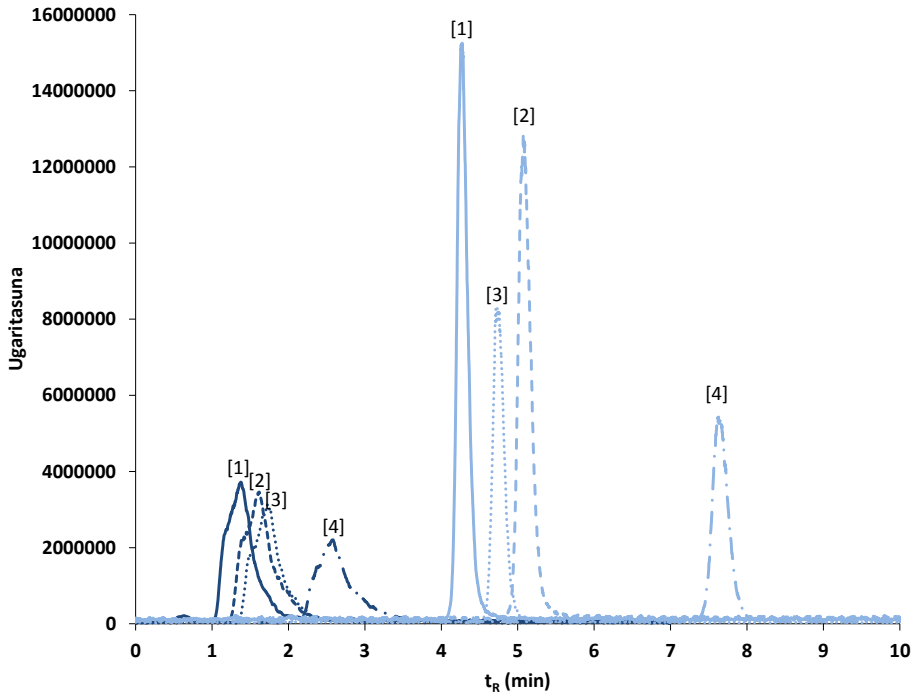

3.1 irudia: *ACE UltraCore 2,5 SuperC18 zutabea (ezkerrean urdin ilunez) eta Kinetex biphenyl 100 Å core-shell* zutabea (*eskuman urdin argiz*) erabilita lortutako kromatogramak gaizenarrita. Analisia ekorketa osoko eskuratze-moduan *eta isokratikoan A:B (50:50) egin da, non A Milli-Q ur:metanol (95:5, bol/bol) eta B Milli-Q ur:metanol (5:95, bol/bol) nahasteak diren, biak % 0,1 azido formikorekin. 1≡ imipramina; 2≡ nortriptilina; 3≡ amitriptilina; 4≡ klomipramina.*

Fase mugikorraren konposizioari dagokionez, metanola eta Milli-Q ura erabiltzeaz gain, A eta B faseetara HCOOH gehitzea aztertu da. Emaitzen arabera, HCOOH gehitu ezean, intereseko analitoak ez dira detektatzen. Beraz, behin betiko metodoan, % 0,1 HCOOH gehitu da Milli-Q ur:metanol (95:5, bol/bol) nahasteaz osatutako A fase mugikorrera eta Milli-Q ur:metanol (5:95, bol/bol) nahasteaz osatutako B fase mugikorrera.

Zutabe-tenperatura desberdinak ere ebaluatu dira, 30 °C, 40 °C eta 50 °C (merkataritza-etxeak ez du tenperatura altuagorik gomendatzen). Hiru tenperaturetan sentikortasuna estatistikoki bereizi ezina izan arren, 40 °C-an eta 50 °C-an egindako analisietako kromatografia-gailurren itxura zertxobait hobea da. Bi horien artean, 40 °C-ko zutabe-tenperatura aukeratu da zutabearen iraupena luzatzeko asmoarekin.

Azkenik, fase mugikorraren fluxu desberdinak aztertu dira, 0,2 mL/min, 0,3 mL/min eta 0,4 mL/min. Fluxurik altuenean kromatografia-gailurren itxura hobetu arren (datuak ez dira txosten honetan erakusten), erantzuna txikiagoa denez, adostasun-balio gisa, 0,3 mL/min aukeratu da.

3.3.1.2 Elektroesprai-ionizazioaren optimizazioa

ESI da LC-MS-aren bidezko TCA-en analisian nagusiki erabiltzen den ionizazio-modua [8,9,16]. ESI-ren eraginkortasuna eta, ondorioz, sentikortasuna hobetzeko beharrezkoa da ionizazio-parametro egokiak aukeratzea. Lan honetan, ESI-MS/MS seinalean eragin dezaketen lau aldagai instrumental aztertu dira Optimizer software erraminta erabilita: tentsio kapilarra (3-6 kV), lainoztatze-presioa (30-50 psi), lehortze-gasaren fluxua (8-12 L/min) eta lehortze-gasaren tenperatura (300-350 °C).

3.2 irudian beha daitekeen bezala, analito guztiek erakusten dute antzeko joera aztertutako parametroen balioak aldatzean. Tentsio kapilarra handitzeak gailurraren seinalean efektu negatiboa eragiten duen bitartean, sentikortasunari dagokionez emaitzak hobeak dira beste hiru parametroak balio altuetan finkatzerakoan. Emaitza horiek aintzat hartuta, tentsio kapilarra 3000 V-ean ezarri da, lehortze-gasaren fluxua 12 L/min-an, lehortze-gasaren tenperatura 350 °C-an eta lainoztatze-presioa 45 psi-an (50 psi-ko emaitzekin estatistikoki bereizi ezina, p-balioa > 0,05).

Aldez aurretik optimizatutako fase mugikorraren fluxua eta ESI-ko baldintzak erabilita masa-espektrometriarekin zerikusia duten ondoko parametroak aztertu dira: disoziazio-tentsioa, talka-energia eta talka-gelaxkako azeleragailua. SRM eskuratze-modurako, Europako jarraibidetako identifikazio-eskakizunen gomendioz [27], hiru ioi-trantsizio aukeratu dira. Sentikorrena kuantifikatzeko eta beste biak egiaztatzeko. 3.2 taulan laburbildu dira konposatu bakoitza neurtzeko jarraitu beharreko ioi-aitzindaria eta apurketa-ioiak disoziazio-tentsioaren eta talka-energiaren balio optimoetan.

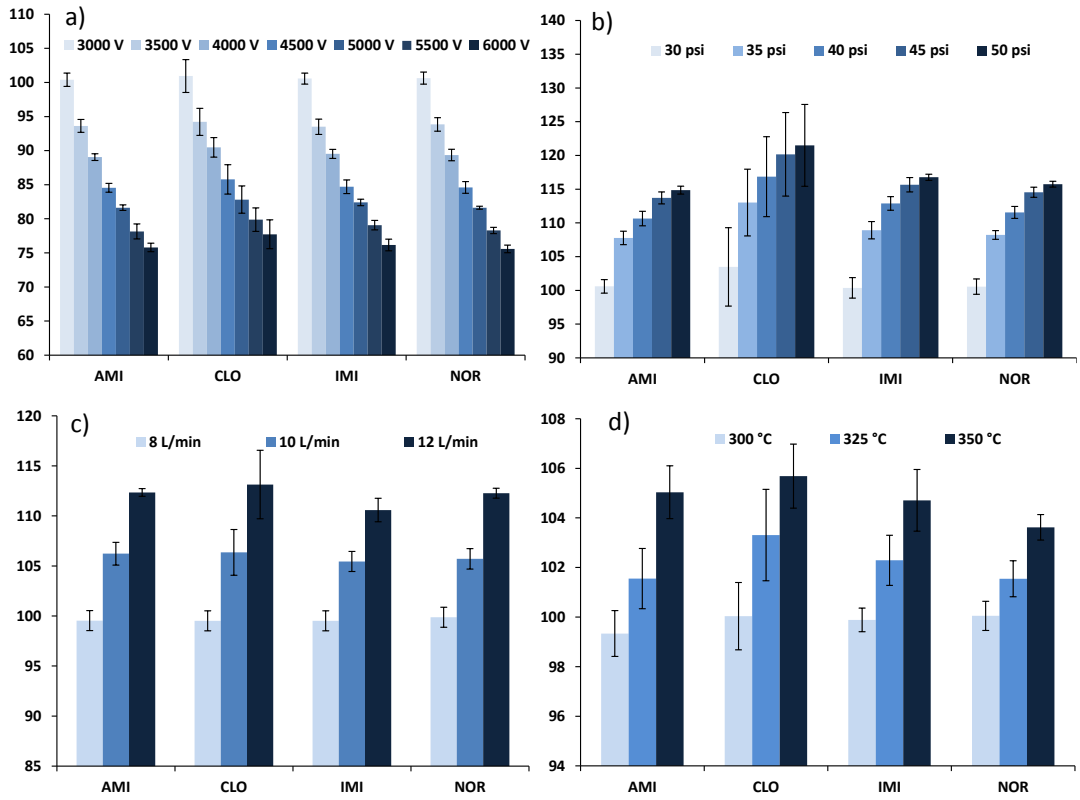

3.2 irudia: *LC-MS/MS analisian zehar parametro desberdinen eragina: (a) tentsio kapilarra, (b) lainoztatze-presioa, (c) lehortze-gasaren fluxua eta (d) lehortze-gasaren tenperatura. Batezbesteko balioa eta desbiderazio estandarrak daude irudikatuta, non seinaleak aldagaiaren balio baxueneko erantzunarekin normalizatuta dauden.*

3.3.1.3 Kalibrazio-tarteak, korrelazio-koefizienteak eta detekzio-muga instrumentalak

Neurketa-baldintza optimoetan, LOQ-2500 ng/mL kontzentrazio-tartean metanoletan prestatutako 10 disoluzio estandarrekin kalibratuak eraiki dira. 3.2 taulan ikus daitekeen bezala, 0,99990-0,99998 bitarteko determinazio-koefizienteak (r^2) lortu dira aztertutako analitoentzat. LOD seinale/zarata arteko erlazioa gutxienez 3 (S/N = 3) duen kontzentrazio baxuenetik ezarri dira. LOQ-ak definitzeko, aldiz, 3 irizpide ezarri dira: (i) kalibratuko tarte linearrean egotea, (ii) gailurraren itxura egokia izatea, eta (iii) gutxienez seinale/zarata arteko erlazioa 10 (S/N = 10) izatea. 3.2 taulan beha daitekeen moduan, lortutako LOD-ak eta LOQ-ak 0,2 ng/mL eta 0,5 ng/mL azpitik daude, hurrenez hurren. Balio horiek bibliografian argitaratutakoen antzekoak dira [5,8,19].

Disoluzio estandar eta lagin guztiak iragazi dira LC-MS/MS analisiaren aurretik. Iragazkiak erabiltzearen ondorioz sor daitekeen kutsadura gurutzatua edota analitoen galera ekiditeko asmoarekin, 0,2 µm-ko iragazki desberdinak frogatu dira: polipropilenozkoak (Pall eta Membrane Solutions merkataritza-etxeetakoak), tefloizkoak eta polibinilideno fluorurozkoak. 3.3 irudian ikus daitekeen bezala, tefloizko eta Membrana Solutions merkataritza-etxeko polipropilenozko iragazkiak soilik dira analitoen erretentzioa pairatzen ez duten bakarrak. Bien arteko emaitzak estatistikoki bereizi ezinak (p-balioa> 0,05) izanik, merkeagoak diren Membrana Solutions merkataritza-etxeko polipropilenozko iragazkiak erabili dira ondorengo esperimentuetan.

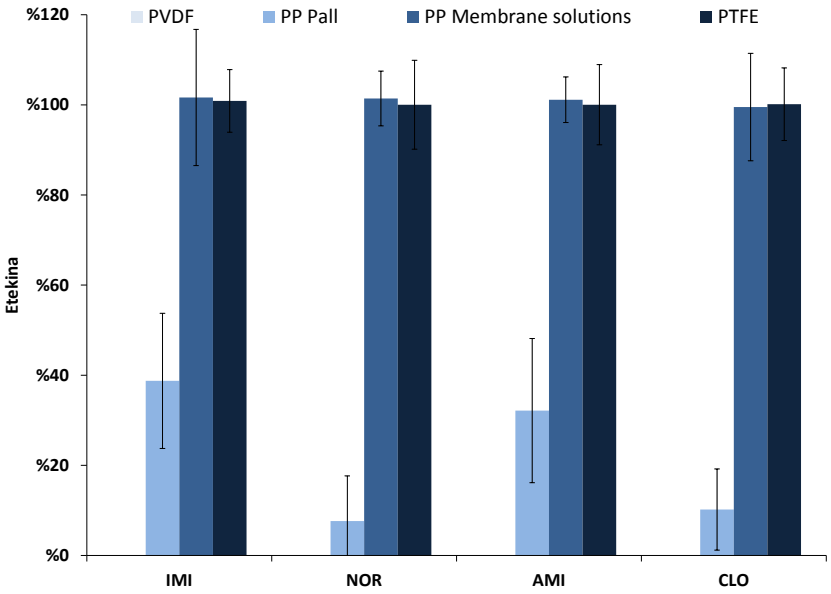

3.3 irudia: *Polibinilideno fluorurozko (PVDF), Pall eta Membrane Solutions merkataritza-etxeetako polipropilenozko (PP) eta tefloizko (PTFE) 0,2 µm –ko iragazki desberdinetatik iragazita lortutako etekin absolutuak.*

3.3.2 Lagin solidoen erauzketa eta garbiketa

3.3.2.1 Lagin solidoetarako erauzketa-parametroen optimizazioa

Lehenik eta behin, bibliografiaren arabera [9,12,16,23], hiru erauzketa-disolbatzaile nahaste desberdin aztertu dira: metanol:HOAc (99:1, bol/bol), azetonitrilo:HOAc (99: 1, bol/bol) eta azetonitrilo:Milli-Q ura (99:1, bol/bol). Erauzketa-urratsaren ostean, erauzia 0,45 µm-ko poliamidazko iragazkiarekin iragazi eta, arestian deskribatutako garbiketa-prozedura (ikus 3.2.4.1

atala) jarraitu da 200 mg Plexa fase geldikorra erabilita. LC-MS/MS-aren bidezko analisira orduko, SPE-ko eluitua nitrogeno-korrontea erabilita lehorreraino 35 °C-an lurrundu, metanol:Milli-Q ur (1:1, bol/bol) nahastearen 200 µL-an berriz disolbatu eta 0,22 µm-ko polipropilenozko iragazkiekin iragazi da. Azterketa guztiak hiru aldiz errepikatu dira. Emaitzek erakutsi dute azido azetikoak arrain-muskuluko proteinak desnaturalizatzen dituela [28] eta metanolak poliamidazko iragazkiak degradatzen dituela (datuak ez dira erakusten txosten honetan). Hori dela eta, erauzketa-disolbatzailean metanolaren eta azido azetikoaren erabilera baztertu da.

Horrez gain, berreraketa-disolbatzailean uraren portzentaje altuak (> % 50) erauzietan uherdura sortarazten duela behatu da. Horren arrazoia uretan disolbagaitzak diren matrizeko osagaien presentzia izan daiteke, zeina proteinen presentziarekin erlazionatuta egon daitekeen [29]. Beraz, zenbait esperimentu egin dira uraren zenbatekoa optimizatzeko. Aurreko esperimentuetan bezala prozesatutako arrain-muskulu laginak metanol:Milli-Q ur konposizio (bol/bol) desberdinen 200 µL-an berriz disolbatu dira. Hain zuzen, metanol:Milli-Q ur 80:20, 85:15, 90:10, 95: 5 eta 100:0 (metanol purua) nahasteetan. Emaitzen arabera, amaierako berreraketa-disolbatzaileko edukiak ezin du uraren % 10a baino gehiago izan, baldin eta erauzietan uherdura saihestu nahi bada (datuak ez dira erakusten txosten honetan). Bestalde, berreratzeko disolbatzaile gisa metanol purua erabilita uherdurarik behatu ez arren, bereizmen kromatografikoa zeharo kaltetzen da. Izan ere, metanolak indar eluotropiko handiegia du fase mugikorraren hasierako konposizioarekin (metanol: Milli-Q ur (55:45, bol/bol) nahastearekin) alderatuta. Hortaz, hurrengo esperimentuetan metanol: Milli-Q ur (90:10, bol/bol) nahastea erabili da berreraketan, amaierako erauziko uherdura ezaren eta bereizmen kromatografiko egokiaren adostasun gisa.

Aurreko emaitzak kontuan hartuta, erauzketa-disolbatzaile gisa azetonitrilo:Milli-Q ur nahastean uraren ehuneko desberdinak (hau da, % 0,% 1, % 5 eta % 10) aztertu dira. 3.4 irudian ikus daitekeen moduan, konposatu guztientzat azetonitrilo:Milli-Q ur (95:5, bol/bol) nahastea erabilita lortu direnez emaitza kromatografiko onenak eta etekin altuenak, nahaste hori ezarri da optimo gisa.

FUSLE-ren eraginkortasuna hobetzeko, erauzketa-denboraren eta ultrasoinuen pultsu-denboraren eragina aldi berean optimizatu dira diseinu konposatu zentralaren (*central composite design*, CCD, delakoaren) bidez Statgraphic Centurium XV software-a erabilita. Horretarako,

ondorengo faktore-tarteak hartu dira kontuan: 0,5 eta 5 min arteko erauzketa-denbora eta 1 s-ko zikloan 0,2 s eta 0,8 s arteko pultsu-denbora. Ikerketa-taldearen esperientzia aintzat hartuta [24], disolbatzailearen bolumena eta sonikazio-potentzia aldagaien balioak konstante mantendu dira 7 mL-an eta % 10ean, hurrenez hurren. Analito bakoitzaren erantzun-azalerak eraikitzeko, esperimentu bakoitzean (erdiko puntuaren 3 erreplikak kontuan izanda, guztira 11 esperimentuetan) lortutako erantzun kromatografikoak erabili dira. Emaitzek agerian utzi dute pultsu-denborak eragin positiboa duela nortriptilina analitoarentzat, baina ez dela esanguratsua gainerako analitoentzat (p-balioa> 0,05). Hori dela eta, ebaluatutako balio altuenean ezarri da, hau da, 0,8 s-an.

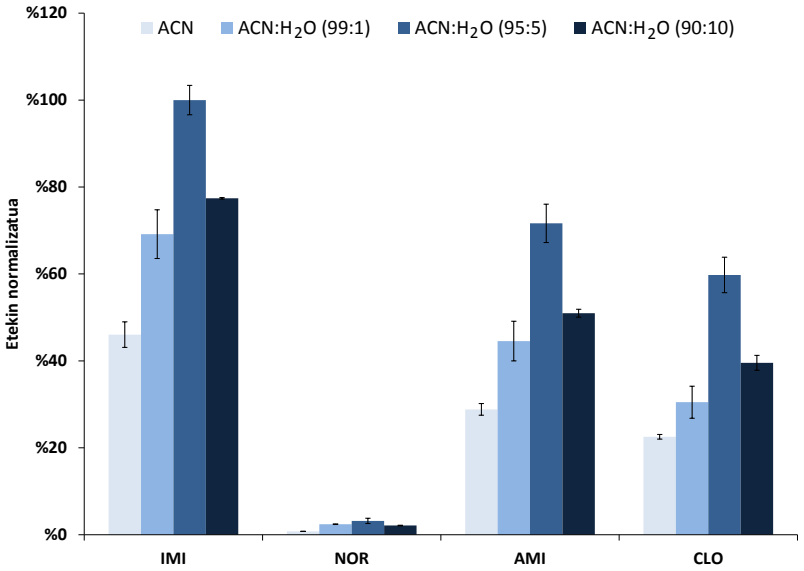

3.4 irudia: *Arrain-muskuluan FUSLE urratsean disolbatzaile motak duen eragina. Batezbesteko balioa eta desbiderazio estandarrak (n = 3) daude irudikatuta, non seinaleak erantzun kromatografiko altuenera normalizatuta dauden.*

Azkenik, erauzketa-denbora ez denez esanguratsua (p-balioa > 0,05) CCD hurbilketan aztertutako tartean, erauzketa jarraiak egin dira CCD-an aztertutako erauzketa-denboraren balio maximoan (5 min) eta minimoan (30 s). Esperimentu bakoitza 3 aldiz egin da. Analito guztientzako lortutako etekinak estatistikoki bereizi ezinak izan dira bi erauzketa-denboretan (p-balioa > 0,05) eta bigarren erauzketa jarraian lortutako berreskurapenak arbuiagarriak (< % 5). Horregatik, erauzketa-denbora balio minimoan (hau da, 30 s-an) ezarri eta bigarren erauzketa jarraia ez egitea erabaki da hurrengo erauzketetarako.

3.3.2.2 Lagin solidoetarako garbiketa-parametroen optimizazioa

Lehenik eta behin, arestian deskribatu den bezala (ikus 3.2.4.1 eta 3.2.4.2 atalak), bibliografian beste matrize batzuetarako erabilitako antzeko baldintzetan [10,20] hiru fase geldikorren (Envi-Carb, Plexa eta Evolute-CX faseen) eraginkortasuna ebaluatu da etekinen bidez. 3.5 irudian ikus daitekeen bezala, erabilitako eluzio-baldintzetan intereseko analitoak ez dira Envi-Carb kartutxoetatik berreskuratzen. Horren arrazoia fase geldikorraren eta analitoen Π elektroien artean sortutako elkarrekintza izan daiteke, analitoaren erretentzioa itzulezina bilakatu daitekeelarik. Kontrara, Plexa eta Evolute-CX faseekin analitoak berreskuratzea lortu da. Bi fase horietan amitriptilina, imipramina eta klomipramina analitoen etekinak estatistikoki bereizi ezinak izan arren, Plexa fase geldikorrarekin nortriptilinarentzat etekin baxuagoan lortu dira. Beraz, modu mistoko SPE aukeratu da optimo gisa. Horrez gain, SPE garbiketan Evolute-CX modu mistoko fase geldikorra erabiltzeak matrize-interferentziak hobeto ezabatu eta erauzi garbiagoak lortzea ahalbideratzen du erretentzio-mekanismo desberdinen konbinazioagatik (hau da, banaketa eta ioi-trukatzaile moduen konbinazioagatik).

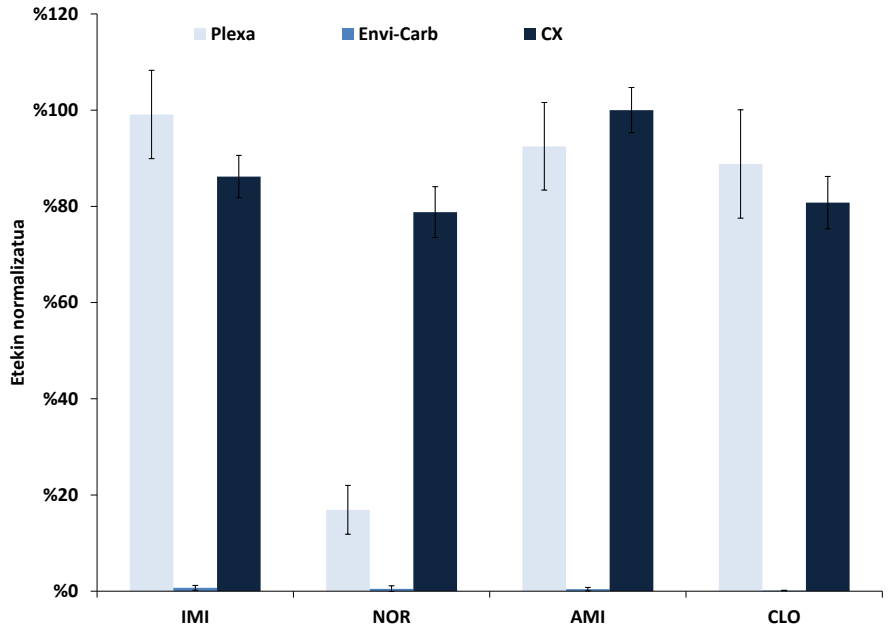

3.5 irudia: *Alderantzizko faseko (Plexa eta Envi-Carb) eta modu mistoko (CX) SPE-ren bidezko garbiketa-estrategia desberdinen eragina. Emaitzak garbiketaren ondorengo etekin gisa adierazten dira, balio altuenera normalizatuta eta desbiderazio estandarrekin (n=3, % 95 konfiantza-maila).*

Modu mistoko katioi-trukatzaile fase geldikorretik analitoak hobeto eluitzeko, indar eluotropiko desberdina duten bi disolbatzaile aztertu dira: % 2,5 NH_4OH duen metanola eta % 2,5 NH_4OH duen azetona. Horretarako, 50 ng TCA-ekin dopatutako arrain-muskuluaren FUSLE-ko erauziak erabili dira, 3 erreplika baldintza bakoitzeko. Gainera, 12 mL-ko bolumen osoaren eluzio-profila lortzeko, eluzio-disolbatzailearen 3 mL-ko 4 frakzio jarrai bildu dira ontzi desberdinetan. Frakzio guztiak, bakoitza bere aldetik, lehorreraino lurrundu, metanol:Milli-Q ur (90:10, bol/bol) nahastearen 200 µL-an berriz disolbatu eta 0,22 µm-ko polipropilenozko iragazkiekin iragazi dira LC-MS/MS-aren bidez analizatzeko.

Disolbatzailea edozein izanda, 3. eta 4. frakzioetan ez da analitorik detektatu. Bestalde, 3.6 irudian laburbiltzen diren emaitzen arabera, % 2,5 NH_4OH duen azetona erabilita, oro har, hobeto berreskuratzen dira analitoak, eta azken hori azetonaren indar eluotropiko handiagoari atxiki dakioke. Gainera, eta analitoak kuantitatiboki berreskuratzeko % 2,5 NH_4OH duen azetonaren 3 mL-rekin nahikoa denez, baldintza horiek erabili dira hurrengo saiakuntzetan.

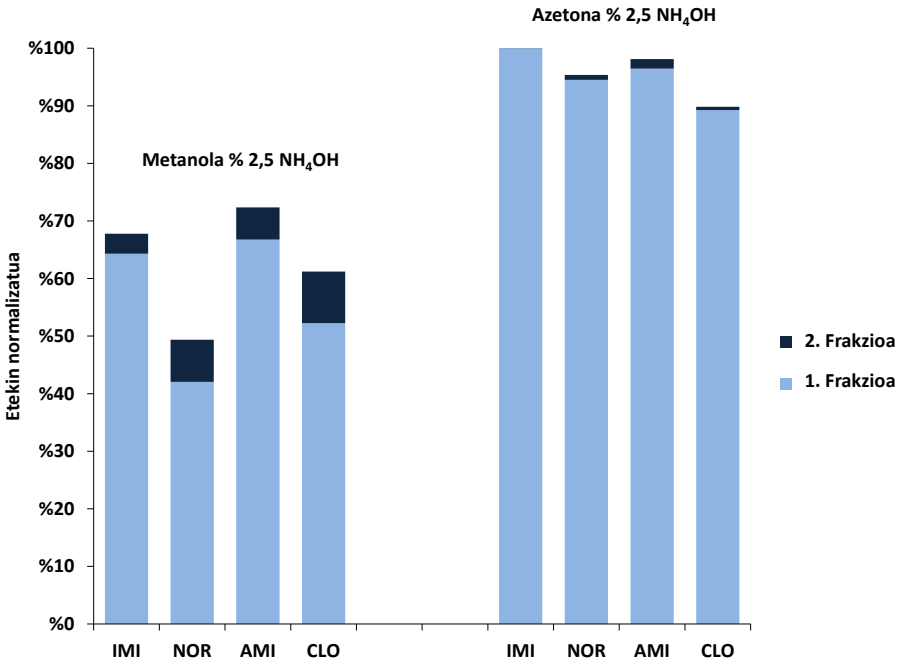

3.6 irudia: *SPE-ko eluzio-urratseko disolbatzailearen eta bolumenaren (frakzio bakoitza 3 mL) eragina. Eluitzaile gisa % 2,5 NH_4OH duen metanola eta % 2,5 NH_4OH duen azetona erabilita lortutako analito bakoitzarentzako etekinak adierazi dira, seinale altuenera normalizatuta.*

3.3.2.3 Matrize-efektua lagin solido desberdinetan

Erauzketaren eraginkortasunean lagineko matrizeak eragin handia izan dezake. Izan ere, matrizeko konposatuek material fase geldikorraren puntu aktiboekin lehiatu edo, ionizazioko eraginkortasunean erasanda, LC-MS/MS-aren bidezko determinazioan matrize-efektua eragin dezakete.

Horregatik, nahiz eta lagin biologiko solidoentzako metodoaren optimizazioa arrain-muskuluarekin egin den, matrize-efektuaren ebaluazioa arrain-muskulura, arrain-gibelera eta muskuiluetara hedatu da.

LC-MS/MS-aren bidezko analisiaren eragina alde batera utzita eta, soilik garbiketa-urratsari dagokion matrize-efektua ebaluatzeko, ondorengoak erkatu dira: laginaren FUSLE-ko erauziak (n=3) garbiketa-urratsaren aurretik eta ostean dopatuta (TCA-en 200 ng/mL-ko disoluziotik 200 μL gehituta). Garbiketa-urratsaren aurretik eta ondoren dopatutako erauzietako analitoen arteko kontzentrazio-zatiketa % 75-95 tartean egon da analito zein matrize guztientzat (ikus 3.7a irudia), eta, hortaz, garbiketa-urratseko matrize-efektua arbuiagarritzat har daiteke.

Beste aldetik, LC-MS/MS detekzioan gertatzen diren matrize-efektuak ebaluatu dira. Horretarako, garbiketa-urratsaren ondoren dopatutako erauziaren eta kontzentrazio berdineko disoluzio estandarraren kontzentrazioak erkatu dira. Oro har, 3.7b irudian beha daitekeenez, analitoa eta aztertutako lagin solidoa (muskulua, gibela edo muskuilua) edozein izanda, detekzioko matrize-efektua % 100 baino pixka bat baxuagoa izan da analito guztientzako. Hortaz, matrizeko interferentzien eraginez, analito guztiek antzeko seinalearen txikitzea pairatzen dutela ondoriozta daiteke. Matrizeen arteko erkaketatik esan daiteke matrize-efektua muskuiluetan (% 92 gehien kaltetutako imipramina analitoarentzat) baino nabarmenagoa dela arrain-laginetan (% 59 eta % 69 imipraminarentzat muskuluan eta gibelean, hurrenez hurren). Detekzioko matrize-efektuak zuzentzeko ohiko bidea metodoaren berrespeneko atalean aztertuko den isotopikoki markatutako barne-estandarren erabilpena da.

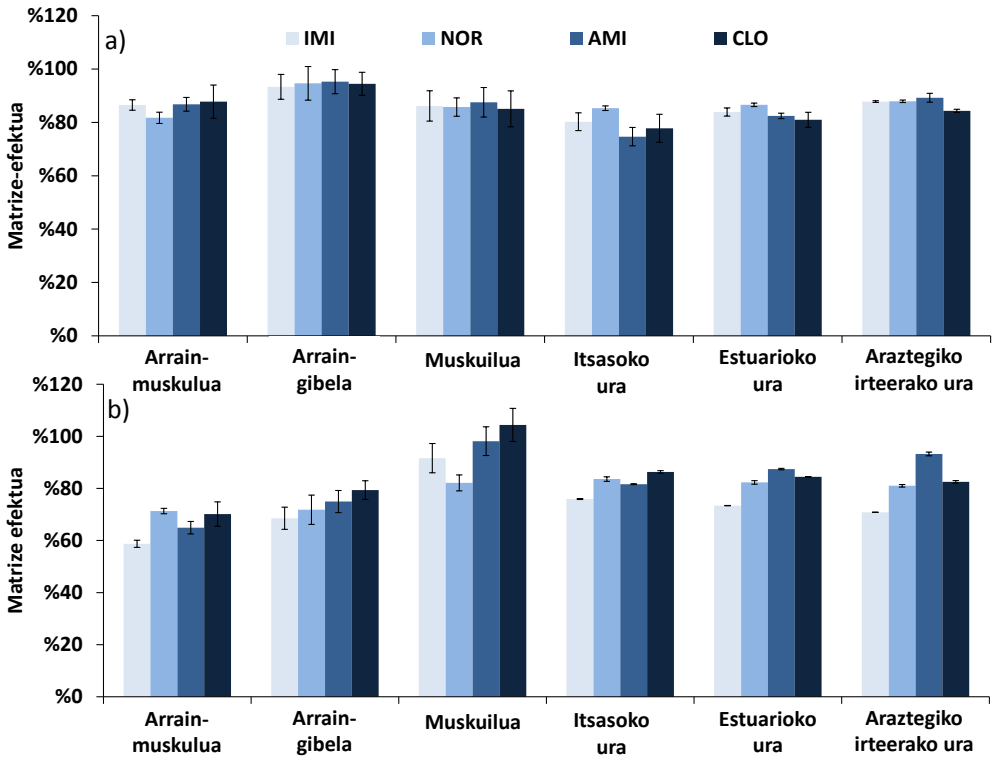

3.7 irudia: *Matrize-efektua a) garbiketa-urratsean eta b) LC-MS/MS-aren bidezko detekzioan. Batezbesteko balioa (n = 3) eta desbiderazio estandarrak daude irudikatuta. Garbiketa-urratseko matrize-efektua garbiketaren aurretik eta ondoren dopatutako (200 ng/mL-ko disoluziotik 200 µL gehituta) laginen arteko kontzentrazioen zatiketatik kalkulatu da. Detekzioko matrize-efektua, aldiz, garbiketaren ondoren dopatutako (200 ng/mL-ko disoluziotik 200 µL gehituta) laginaren eta kontzentrazio bereko estandarraren arteko zatiketatik.*

3.3.2.4 Metodoaren berrespena lagin solido desberdinetan

TCA-entzako erreferentziazko materialik eskuragarri ez dagoenez, lagin solidoen (arrain-muskuluaren, arrain-gibelaren eta muskuiluen) berrespenerako kutsatu gabeko laginak aztarna-mailako kontzentrazio ezagunean indartu dira. Lehenengo hurbilketan, lagina indartzeko azetonatan nahastu dira liofilizatutako lagina eta analitoak. Baina lagin koipetsuetan (arrain-gibeletan eta muskuiluetan) azetona disolbatzailearen gehitzeak matrizeen gehiegizko eraldaketa sortzeaz gain, analitoen galera ere eragin du (datuak ez dira erakusten txosten honetan). Ondorioz, berrespeneko saiakuntzak analitoen disoluzio estandarren bolumen txikia momentuan laginetara gehituta egin dira. Nahiz eta laginen momentuko dopatzea ez den beti hurbilketarik onena lagin

kutsatuak simulatzeko, bibliografian [30,31] arrakastaz aplikatu izan da disolbatzaileen bolumen handiak erabilitako indartutako laginak bideragarriak ez direnean.

Metodoen egokitasuna ebaluatzeko etekin gordinak (zuzendu gabeak) eta dagokion isotopikoki markatutako estandarrarekin zuzendutako etekinak, doitasuna eta metodoen detekzio-mugak (*method detection limit*, MDL, direlakoak) kalkulatu dira (ikus 3.3 taula). Matrize solido desberdinen etekin gordinak bi kontzentrazio-mailatan kalkulatu dira, 10 ng/g-an (n=5) eta 80 ng/g-an (n=3). Etekin gordin onargarriak (% 39-64) lortu dira intereseko konposatu guztientzat eta matrize guztietan (ikus 3.3 taula). Salbuespena maila altuan dopatutako gibela izan da, zeinetan etekin gordin baxuagoak lortu diren (% 22–27).

Nahiz eta isotopikoki markatutako estandarrak erabilita emaitzen zehaztasuna zuzendu daitekeen, azken saiakera bat egin da arrain-gibel laginetatik TCA-en erauzketaren eraginkortasuna hobetzeko. Horretarako, zehaztutako erauzketa-baldintzetan aldaketa txikiak suposatzen dituzten bi estrategia frogatu dira. Lehen saiakeran, erauzketa-disolbatzaile desberdinak (azetona, azetonitriloa, azetonitriloa:Milli-Q ura 95:5 (bol/bol) eta azetonitriloa:Milli-Q ura 80:20 (bol/bol)) ebaluatu dira gainontzeko aldagaiak finko mantenduta. Azetonarekin lortutako erauzietan, garbiketa-urratsaren ondoren, hondar lehor asko gelditu denez (seguruenik gibeleko gantz azidoei dagozkienak), disolbatzaile horren erabilera baztertu da. Gainontzeko disolbatzaileekin egindako esperimentuetan estatistikoki bereizi ezinak (p-balioa> 0,05) diren etekin gordinak lortu dira. Hori dela eta, erauzketaren kuantitatibotasuna ebaluatu nahian, bigarren estrategia bat frogatu da, lagin berdinaren bi erauzketa jarrai eginda azetonitrilo:Milli-Q ur (95:5 ,bol/bol) nahastea erabilita. Arestian aipatutako arrain-muskuluarekin egindako saiakuntzen antzera, bigarren erauzketan analitoen % 10-a baino ez da detektatu gibelean. Ondorioz, nahiz eta bi erauzketen batura egin etekin osoak baxuak izaten jarraitzen duenez, analisiaren bideragarritasuna bermatzeko erauzketa jarrairik ez egitea erabaki da.

Gainera, etekinak zuzentzeko, FUSLE urratsaren aurretik analitoen kontzentrazio berean gehitutako $^{2}H_{3}$-AMI eta $^{2}H_{3}$-NOR trazagarriak erabili dira. Isotopikoki markatutako estandarrak erauzketan behatutako eraginkortasun eza zein detekzioko seinalearen txikitzea arrakastaz zuzentzeko gai dira. Oro har, 3.3 taulan beha daitekeen gisa, etekin zuzenduak % 86-114 tartean daude aztertutako konposatu guztientzat.

3.3 taula: *10 ng/g and 80 ng/g mailetan dopatutako arrain-muskuluarentzako, arrain-gibelarentzako eta muskuiluentzako etekin gordinak eta zuzenduak, eta metodoen detekzio-mugak (ng/g).*

Analitoa	Arrain-muskulua					Arrain-gibela					Muskuiluak				
	Etekin gordina		Etekin zudendua		MDL (ng/g)	Etekin gordina		Etekin zudendua		MDL (ng/g)	Etekin gordina		Etekin zudendua		MDL (ng/g)
	10 ng/g	80 ng/g	10 ng/g	80 ng/g		10 ng/g	80 ng/g	10 ng/g	80 ng/g		10 ng/g	80 ng/g	10 ng/g	80 ng/g	
IMI	39	51	94[a]	103[a]	2	57	22	96[a]	89[a]	2	43	45	89[a]	86[a]	3
NOR	39	54	102[b]	96[b]	1	47	23	102[b]	98[b]	2	48	47	101[b]	100[b]	1
AMI	44	50	107[a]	102[a]	3	63	26	106[a]	103[a]	2	49	52	100[a]	99[a]	3
CLO	42	56	102[a]	114[a]	2	64	27	107[a]	109[a]	2	51	53	104[a]	102[a]	2

(a) $^{2}H_{3}$-AMI trazagarriarekin zuzendua; (b) $^{2}H_{3}$-NOR trazagarriarekin zuzendua.

Metodoaren errepikakortasuna ebaluatzeko desbiderazio estandar erlatiboa (*relative standard deviation*, RSD, delakoa) kalkulatu da egun berean aztertutako errepliketatik. RSD-aren balioak % 1-9 bitartekoak dira, eta matrizeen konplexutasuna kontuan izanda ontzat hartu da. Balio horiek, beste erauzketa-teknika batzuen bidez TCA-k lagin solidoetan aztertu dituzten beste lan batzuekin aldaragarriak dira [12,16,23].

MDL-ak determinatzeko, AEBetako Ingurumenaren Babeserako Agentziaren (*United States Environmental Protection Agency*, US EPA, delakoaren) gomendioei jarraiki [32], matrize-zuri bakoitzaren 5 erreplika kontzentrazio baxuenean (10 ng/g solidoarentzat) dopatu dira. MDL-ak $MDL = t_{(n-1,\,1-\alpha=0.99)} \times s_d$ ekuazioaren bidez kalkulatu dira, non t = 3,75 Student-en t balioa den % 99-ko konfiantza-mailan lau askatasun-gradurentzat eta s_d 5 errepliken (n=5) desbiderazio estandarrari dagokion. 3.3 taulan beha daitekeen bezala, arrain-gibeleko, arrain-muskuluko eta muskuiluetako MDL balioak 1-3 ng/g tartean daude.

3.3.3 Ur-laginen aurrekontzentrazioa eta garbiketa

Aurreko atalean modu mistoko SPE erabilita lortutako emaitza onak oinarri hartuta, ingurumeneko ur-laginen (estuarioko, itsasoko eta araztegien irteerako uren) aldibereko aurrekontzentraziorako eta garbiketarako ere modu mistoko SPE aztertu da.

Katioi-trukatzaile sendoak erabilita, modu mistoko SPE teknika bibliografian aplikatu izan da TCA-k ur gezako laginetatik isolatzeko [5,8,10], baina itsasoko uretako aplikazioak mugatuak dira [6]. Itsasoko uretan kontzentrazio altutan dauden gatz ez-organikoen presentziak ioi-truke mekanismoa oztopa dezakeenez, modu mistoa aplikatu nahi bada, beharrezkoa da aurretiazko ebaluazioa. Izatez, badaude itsasoko urarekin arazoak izan dituzten ikerketa-lanak [33], nahiz eta araztegiko irteerako eta estuarioko uretarako emaitza onak eta erauzi garbiak lortu. Hori dela eta, lan honetan, katioi-trukatzaile sendoa erabilita TCA-k ur-lagin desberdinetatik bereizteko erauzketaren eraginkortasuna, apurketa-bolumena eta matrize-efektua sakontasunez ebaluatu dira.

3.3.3.1 Erauzketa-etekinak

Estuarioko, itsasoko eta araztegien irteerako uretatik TCA-en erauzketaren eraginkortasuna

aztertzeko, 100 mL-ko laginei (1,2 μm-ko beira-zuntzezko iragazkietatik eta 0,45 μm-ko zelulosa nitratozko mintz-iragazkietatik iragazitakoei) TCA-k gehitu zaizkie 400 ng/L mailan. Aldi berean, kontzentrazio-maila berdinean indartutako Milli-Q ura ere analizatu da. Esperimentuak hiru aldiz errepikatu dira. Erauzketaren etekinak % 61-83 bitartekoak izan dira, baita itsasoko uretan ere, eta matrize guztietako emaitzak Milli-Q urarekin lortutakoekin estatistikoki bereizi ezinak dira (p-balioa > 0,05). Hortaz, modu mistoko SPE aztertutako ur-matrize guztientzat erabiltzea posible dela ondoriozta daiteke.

3.3.3.2 Apurketa-bolumena

SPE-ko kartutxoetan laginaren bolumen oso handiak kargatzen direnean, kartutxoaren "apurketa" gerta daiteke eta analitoak fase geldikorrean harrapatuta geratu beharrean zutabean zehar barreiatu daitezke. Analitoak Evolute-CX kartutxoan (200 mg) zehar barreiatzen hasten diren bolumena ebaluatzeko 1,2 μm-ko beira-zuntzezko iragazkietatik eta 0,45 μm-ko zelulosa nitratozko mintz-iragazkietatik iragazitako araztegi irteerako ura erabili da, hau baita aztergai diren laginetatik zikinena. Horretarako, bi Evolute-CX kartutxo seriean elkarri lotuta jarrita egin dira erauzketak eta 100 ng/L mailan indartutako araztegiko irteerako uraren 100 mL, 250 mL eta 500 mL kargatu dira. Lagina kargatu ondoren, seriean dauden kartutxoak desmuntatu eta analitoak berreskuratu dira kartutxo bakoitzetik %2,5 NH_4OH duen azetonaren 3 mL erabilita. Analitoak bereziki goiko kartutxoan detektatu dira, eta kasu guztietan, bigarren kartutxoan detektatu diren analitoen etekina % 2,5 baino baxuagoa izan da. Beraz, nahiz eta 500 mL ur pasatu karga-urratsean ez denez kartutxoan zeharreko analitoen barreiatzerik behatu, aztertutako bolumen handiena kargatzea erabaki da aurrekontzentrazio-faktorerik (2500 aldiz) handiena lortzeko.

3.3.3.3 Matrize-efektua ur-lagin desberdinetan

Ur-lagin desberdinetan garbiketa-urratseko eta LC-MS/MS-aren bidezko detekzioko matrize-efektua aztertzeko lagin solidoetarako erabilitako estrategia bera erabili da (ikus 3.3.2.3 atala) eta laginak kontzentrazio-maila berdinean dopatu dira (200 ng/mL-ko disoluziotik 200 μL gehituta). 3.7 irudian ikus daitekeen moduan, ur-mota guztientzat matrize-efektua arbuiagarria da (% 71-93) garbiketa-urratsen zein detekzioan.

3.4 taula: *10 ng/L eta 80 ng/L mailetan dopatutako itsasoko, estuarioko eta araztegiko irteerako urentzako etekin gordinak eta zuzenduak, eta metodoen detekzio-mugak (ng/L).*

Analitoa	Itsasoko ura					Estuarioko ura					Araztegiko irteerako ura				
	Etekin gordina		Etekin zuzendua		MDL (ng/L)	Etekin gordina		Etekin zuzendua		MDL (ng/L)	Etekin gordina		Etekin zuzendua		MDL (ng/L)
	10 ng/L	80 ng/L	10 ng/L	80 ng/L		10 ng/L	80 ng/L	10 ng/L	80 ng/L		10 ng/L	80 ng/L	10 ng/L	80 ng/L	
IMI	57	74	93[a]	99[a]	2	52	74	93[a]	100[a]	1	60	75	89[a]	95[a]	1
NOR	62	76	107[b]	100[b]	1	62	76	107[b]	100[b]	1	75	76	116[b]	104[b]	2
AMI	73	73	119[a]	98[a]	1	64	80	114[a]	107[a]	1	119	97	176[a]	122[a]	2
CLO	69	78	113[a]	105[a]	1	65	79	115[a]	106[a]	1	79	81	117[a]	102[a]	1

(a) $^{2}H_{3}$-AMI trazagarriarekin zuzendua; (b) $^{2}H_{3}$-NOR trazagarriarekin zuzendua

3.3.3.4 Metodoaren berrespena ur-lagin desberdinetan

Metodo optimoaren kalitate-parametroak 3.4 taulan laburbildu dira. Etekinak iragazitako 10 ng/L (n=5) eta 80 ng/L (n=3) mailetan dopatutako 500 mL-ko ur-laginak erabilita kalkulatu dira. Ingurumeneko lagin errealetan TCA-k agertzea espero denez, dopatu gabeko ur-laginek ere prozedura bera pairatu dute. 3.4 taulan beha daitekeen bezala, dopatu gabeko laginen erantzuna kendu eta trazagarriekin zuzendu ondoren, etekin zuzendu egokiak (% 93-112) lortu dira. Salbuespen bakarra maila baxuan dopatutako amitriptilinaren emaitzak izan dira eta horren arrazoia gehitutako kantitatea (5 ng) jadanik laginean zegoena (12,5 ng) baino baxuagoa izana da. % RSD moduan adierazita dagoen % 1-7 arteko (n = 3) metodoaren doitasuna, argitaratutako beste lan batzuetan aurkitutakoaren antzekoa da [5,8,11,19,23]. MDL-ak lagin solidoentzako azaldutako moduan kalkulatu dira (ikus 3.3.2.4 atala), matrize bakoitzaren bostna zuri kontzentrazio baxuenean dopatuta (10 ng/L). Itsasoko, estuarioko eta araztegiko irteerako ur-laginen MDL balioak 1-2 ng/L tartean daude (ikus 3.4 taula). Bibliografian ere antzeko emaitzak lortu dira [6,8,23].

3.3.3.5 Iragazketa

Lan honetan egin den gisara, konposatu organiko emergenteen analisiaren inguruko lan gehienek ere ur-laginak iragazita aztertzen dituzten arren [5,6,8–10], eztabaida handia dago laginak iragaztearen inguruko egokitasunaren inguruan [34–36]. Izatez, Europar Batasuneko Ur-Esparru Zuzentarauak [37] ur-lagin gordinak, iragazi gabeak, erabiltzea gomendatzen du aztertu nahi diren analitoen kontzentrazio osoa determinatzea beharrezkoa denean. Gainera, iragazkien aukeraketa desegokiak konposatu batzuk iragazkian atxikiturik geratzea eragin dezake [38].

Azken puntu horretan sakondu nahian, bibliografian asko erabiltzen diren bi iragazki desberdinen egokitasuna ebaluatu da: 1,2 μm-ko beira-zuntzezko iragazkiak eta 0,45 μm-ko zelulosa nitratozko mintz-iragazkiak. Saiakuntzak burutzeko, aurretiaz optimizatutako prozedura aplikatu zaie hasieran (iragazi aurretik) analitoekin eta trazagarriekin indartutako (400 ng/L) 100 mL-ko ondoko laginei: iragazi gabeko Milli-Q urari, 0,45 μm-ko zelulosa nitratozko mintz-iragazkiekin iragazitako Milli-Q urari eta 1,2 μm-ko beira-zuntzezko iragazkiekin iragazitako Milli-Q urari. Emaitzek erakutsi dute bai analitoak bai trazagarriak, guztiak atxikitzen direla bi iragazkietan,

baina maila desberdinean. Izan ere, 1,2 µm-ko beira-zuntzezko iragazkietan eta 0,45 µm-ko zelulosa nitratozko mintz-iragazkietan erretenitzearen ondoriozko analitoen galerak % 64,4-68,1 eta % 99,0-99,4 bitartekoak izan dira, hurrenez hurren.

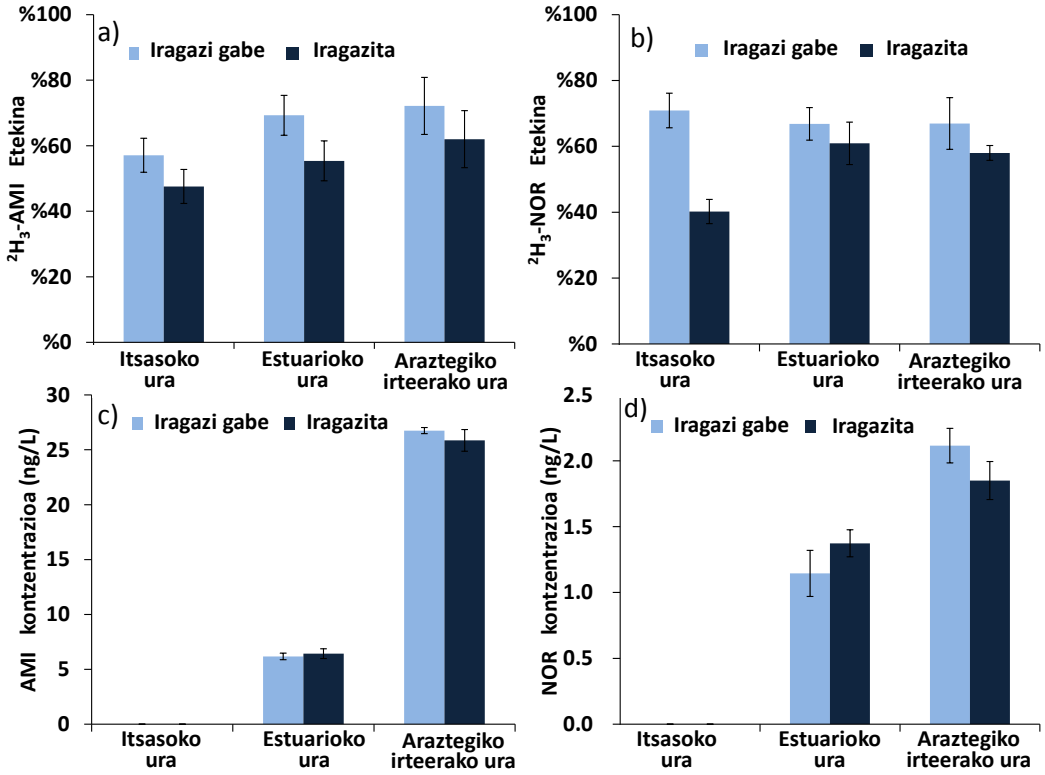

3.8 irudia: *1,2 µm-ko beira-zuntzezko iragazkitik ur-laginak iragaztearen eragina. $^2H_3$-AMI (a) eta $^2H_3$-NOR (b) trazagarrien etekin absolutuak konparatzen dira laginak iragazita edo iragazi gabe. Amitriptilina (AMI, c) eta nortriptilina (NOR, d) analitoen kontzentrazioak laginetan, dagokien trazagarriarekin zuzendu ondoren.*

Analitoen galera txikiena 1,2 µm-ko beira-zuntzezko iragazkietan pairatu denez eta bibiografian gehien erabiliak direnez [5,6,8–10,38], $^2H_3$-AMI eta $^2H_3$-NOR trazagarriekin indartutako (20 ng/L) ur-matrize ezberdinen (itsasoko, estuarioko eta araztegiko irteerako uren) 500 mL aztertu dira (n=3) 1,2 µm-ko beira-zuntzezko iragazkien bidez iragazita eta iragazi gabe. 3.8 (a-b) irudiko emaitzetan erakusten den moduan, laginek duten materia organiko kantitatearen araberako bi erantzun desberdin behatu dira. Alde batetik, iragazitako estuarioko eta araztegiko irteerako uretan trazagarrien etekinak estatistikoki bereizi ezinak dira iragazi gabekoekin. Hortaz, esan

daiteke materia partikulatuaren presentzian beira-irazgazkietan gutxitu egiten dela analitoen atxikipena. Bestalde, $^{2}H_{3}$-NOR trazagarriaren etekinean jaitsiera argia (% 31) behatu da laginak iragazi direnean. Dena den, 3.8 (c-d) irudiko emaitzei erreparatuta, trazagarria lagina iragazi aurretik gehitzen bada, TCA guztientzat (baita nortriptilinarentzat ere) kontzentrazio zehatzak eman daitezke, intereseko analitoen eta trazagarrien joera konparagarria baita. Horrelako joerak beste farmako batzuekin ere behatu izan dira beste ikerketa-lan batzuetan [38].

3.3.4 Metodoen aplikazioa lagin errealetan

Garatutako metodoak 2015eko ekainean Gernikan bildutako zenbait laginetan aplikatu dira, zehazki, araztegiko irteerako uretan, estuarioko (araztegiko irteeratik errekan beherako) uretan eta korrokoien (*Chelon labrosus*) gibeletan, eta baita Laida hondartzako (Ibarrangelu) itsasoko uretan eta muskuiluetan (*Mytilus galloprovincialis*) ere. 3.9 irudian LC-MS/MS-aren bidez lortutako araztegiko irteerako ur-laginaren eta korrokoi-gibelaren erauzien kromatogramak ageri dira, 10 ng/mL-ko disoluzio estandarrarekin batera.

Laburki, aztertutako TCA-etatik imipramina da analizatutako lagin batean ere detektatu ez den bakarra. Klomipramina araztegiko irteerako uretan soilik detektatu da kontzentrazio-maila oso baxuan (1,6 ± 0,3 ng/L) eta nortriptilina ere antzeko kontzentrazioan behatu da araztegiko irteerako (1,85 ± 0,03 ng/L) eta estuarioko (1,37 ± 0,02 ng/L) uretan. Azkenik, nabarmentzekoa da amitriptilina dela aztertutako laginetan kontzentrazio altuenean detektatutako TCA. Kontzentrazio altuenak estuarioko (6,4 ± 0,2 ng/L) eta araztegiko irteerako (26 ± 1 ng/L) uretan aurkitu dira. Izatez, beste leku batzuetan egin duten uren segimenduaren programetan ere amitriptilina izan da kontzentrazio altuenean behatu den TCA [4,5,8,9]. Gainera, amitriptilina korrokoien gibelean detektatu izanak (1,8 ± 0,2 ng/g) eta ez korrokoien muskuluan, konposatu honek ehun espezifiko (gibel) horretan metatzeko duen gaitasuna argi adierazten du. Antzeko emaitzak behatu izan dira bibliografian [16]. Bestalde, aztertutako muskuiluetan TCA-k MDL-tik behera egon diren arren, eta itsasoko uretan TCA-k aurkitu ez direnez, ezin da atera espezie horretan TCA-ek biometatzeko duten gaitasunaren inguruko ondoriorik. Edonola ere, aipatutako emaitzak aintzat hartuta, gomendagarria da, bai biotan bai ur-laginetan, TCA-en segimendua egiten jarraitzea.

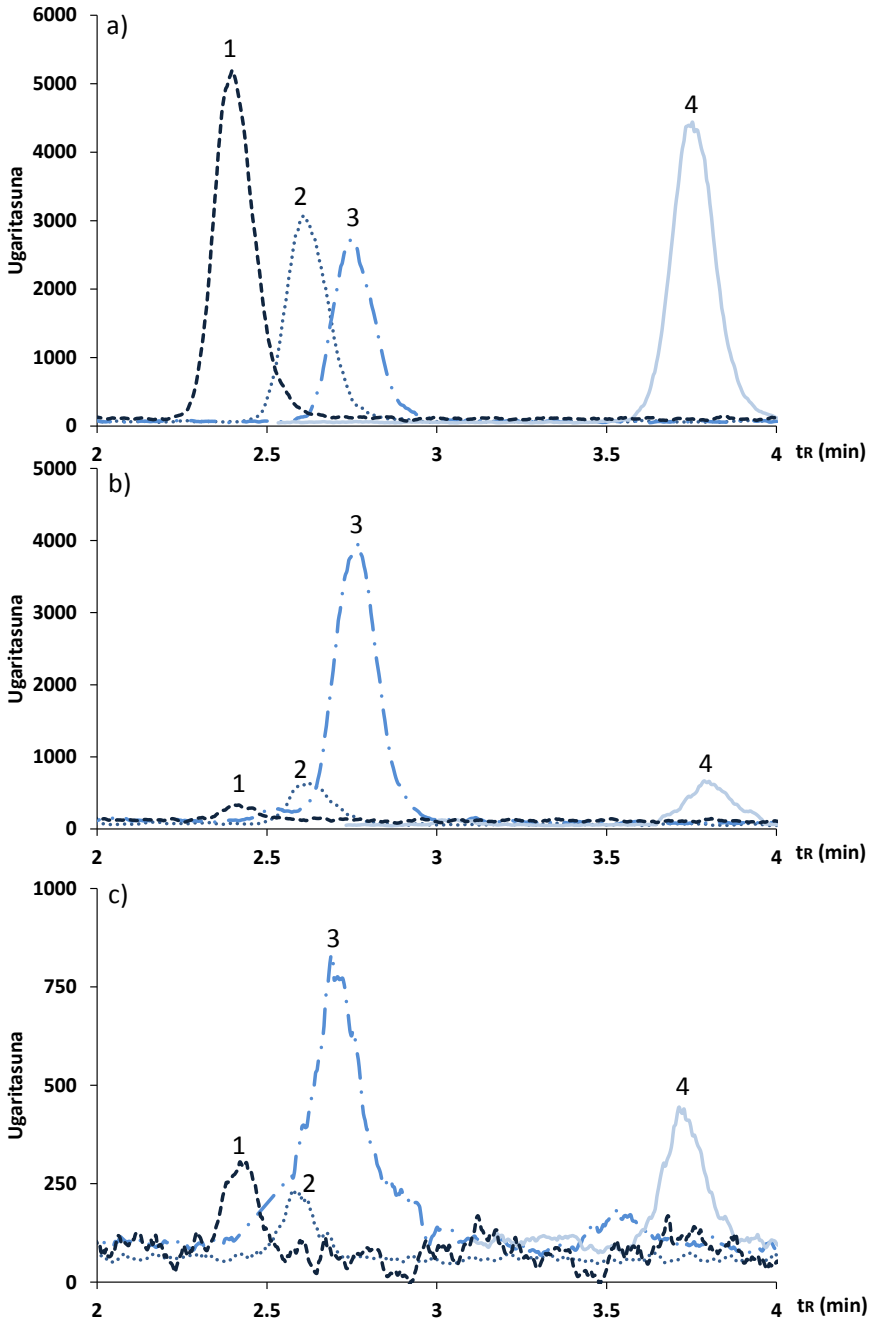

3.9 irudia: *LC-MS/MS analisiaren bidez lortutako SRM kromatogramak aztertutako laginentzat: a) 10 ng/mL-ko disoluzio estandarra; b) araztegiko irteerako ur-lagina; eta c) korrokoi-gibelaren lagin erreala. 1≡ imipramina; 2≡ nortriptilina; 3≡ amitriptilina; 4≡ klomipramina.*

3.4 Ondorioak

Ur laginetan TCA-en segimendua egiten duten ikerketa lan anitz daude bibliografian, baina ez ordea konposatu horiek matrize biologikoetan aztertzen dituztenak. Lan honetan, amitriptilina, nortiptilina, imipramina eta klomipramina TCA-k ingurumeneko uretan (estuarioko, itsasoko eta araztegien irteerako uretan) eta biotan (arrainen gibelean eta muskuluan eta muskuiluetan) determinatzeko metodo sentikorren eta errepikakorren garapena aurkeztu da. Helburu horretarako, analisiaren egokitasunarekin lotutako urrats guztiak sakonki optimizatu dira, hala nola erauzketa, garbiketa eta detekzioa. Lehenik eta behin, aztertutako analitoentzat LC-MS/MS-aren bidezko analisiaren optimizazio osoa burutu da, kromatografia-zutabea, fase mugikorra, ionizazio-baldintzak eta masa-espektrometriako aldagaiak aztertuta. Azpimarratu beharra dago Kinetex biphenyl 100 Å core-shell zutabearekin lortu dela kromatografia-banaketarik onena gailurren bereizmenari, gailurren simetriari eta sentikortasunari dagokionez. FUSLE erauzketan, emaitza optimoak denbora laburreko (30 s) erauzketa bakarrean lortu dira azetonitrilo:Milli-Q ur (95:5, v/v) nahastearen 7 mL erabilita. Lagin solidoen garbiketarako eta ur-laginen aurrekontzentraziorako, katioi-trukatzaile sendoa erabilita burututako modu mistoko SPE prozedurarekin erauzi garbiak lortu dira, matrize-efektu arbuiagarriarekin eta etekin egokiekin, trazagarriekin zuzendu ondoren. Bukatzeko, Bizkaiko kostaldeko ur-lagin desberdinetan zein biotan TCA-k behatu izanak argi erakusten du inguru horretan kutsatzaileen segimendua egiten jarraitzeko beharrizana dagoela.

3.5 Erreferentziak

1. Kümmerer K. 2009. The presence of pharmaceuticals in the environment due to human use – present knowledge and future challenges. *J. Environ. Manage.* 90:2354–2366.
2. Halling-Sørensen B, Nors Nielsen S, Lanzky PF, Ingerslev F, Holten Lützhøft HC, Jørgensen SE. 1998. Occurrence, fate and effects of pharmaceutical substances in the environment- A review. *Chemosphere*. 36:357–393.
3. Calisto V, Esteves VI. 2009. Psychiatric pharmaceuticals in the environment. *Chemosphere*. 77:1257–1274.
4. Baker DR, Kasprzyk-Hordern B. 2011. Multi-residue determination of the sorption of illicit drugs and pharmaceuticals to wastewater suspended particulate matter using pressurised liquid extraction, solid phase extraction and liquid chromatography coupled with tandem

mass spectrometry. *J. Chromatogr. A*. 1218:7901–7913.

5. Baker DR, Kasprzyk-Hordern B. 2011. Multi-residue analysis of drugs of abuse in wastewater and surface water by solid-phase extraction and liquid chromatography–positive electrospray ionisation tandem mass spectrometry. *J. Chromatogr. A*. 1218:1620–1631.

6. Togola A, Budzinski H. 2008. Multi-residue analysis of pharmaceutical compounds in aqueous samples. *J. Chromatogr. A*. 1177:150–158.

7. Klosterhaus SL, Grace R, Hamilton MC, Yee D. 2013. Method validation and reconnaissance of pharmaceuticals, personal care products, and alkylphenols in surface waters, sediments, and mussels in an urban estuary. *Environ. Int.* 54:92–99.

8. Lajeunesse A, Gagnon C, Sauvé S. 2008. Determination of Basic Antidepressants and Their N-Desmethyl Metabolites in Raw Sewage and Wastewater Using Solid-Phase Extraction and Liquid Chromatography−Tandem Mass Spectrometry. *Anal. Chem.* 80:5325–5333.

9. Lajeunesse A, Smyth SA, Barclay K, Sauvé S, Gagnon C. 2012. Distribution of antidepressant residues in wastewater and biosolids following different treatment processes by municipal wastewater treatment plants in Canada. *Water Res.* 46:5600–5612.

10. Sheng L-H, Chen H-R, Huo Y-B, Wang J, Zhang Y, Yang M, Zhang H-X. 2014. Simultaneous determination of 24 antidepressant drugs and their metabolites in wastewater by ultra-high performance liquid chromatography-tandem mass spectrometry. *Molecules*. 19:1212–1222.

11. Yuan S, Jiang X, Xia X, Zhang H, Zheng S. 2013. Detection, occurrence and fate of 22 psychiatric pharmaceuticals in psychiatric hospital and municipal wastewater treatment plants in Beijing, China. *Chemosphere*. 90:2520–2525.

12. Peysson W, Vulliet E. 2013. Determination of 136 pharmaceuticals and hormones in sewage sludge using quick, easy, cheap, effective, rugged and safe extraction followed by analysis with liquid chromatography–time-of-flight-mass spectrometry. *J. Chromatogr. A*. 1290:46–61.

13. Alves C, Fernandes C, Neto AJ dos S, Rodrigues JC, Queiroz MEC, Lanças FM. 2006. Optimization of the SPME Parameters and Its Online Coupling with HPLC for the Analysis of Tricyclic Antidepressants in Plasma Samples. *J. Chromatogr. Sci.* 44:340–346.

14. Minguez L, Farcy E, Ballandonne C, Lepailleur A, Serpentini A, Lebel J-M, Bureau R, Halm-Lemeille M-P. 2014. Acute toxicity of 8 antidepressants: What are their modes of action? *Chemosphere*. 108:314–319.

15. Yang M, Qiu W, Chen J, Zhan J, Pan C, Lei X, Wu M. 2014. Growth inhibition and coordinated physiological regulation of zebrafish (Danio rerio) embryos upon sublethal exposure to antidepressant amitriptyline. *Aquat. Toxicol.* 151:68–76.

16. Lajeunesse A, Gagnon C, Gagné F, Louis S, Čejka P, Sauvé S. 2011. Distribution of

antidepressants and their metabolites in brook trout exposed to municipal wastewaters before and after ozone treatment – Evidence of biological effects. *Chemosphere*. 83:564–571.

17. OECD Guideline 315. 2008. Test No. 315: Bioaccumulation in Sediment-dwelling Benthic Oligochaetes. [cited 28 June 2018]. Available from https://www.oecd-ilibrary.org/environment/test-no-315-bioaccumulation-in-sediment-dwelling-benthic-oligochaetes_9789264067516-en.

18. Huerta B, Rodríguez-Mozaz S, Barceló D. 2012. Pharmaceuticals in biota in the aquatic environment: analytical methods and environmental implications. *Anal. Bioanal. Chem.* 404:2611–2624.

19. Xu R, Lee HK. 2014. Application of electro-enhanced solid phase microextraction combined with gas chromatography–mass spectrometry for the determination of tricyclic antidepressants in environmental water samples. *J. Chromatogr. A*. 1350:15–22.

20. Valcárcel Y, González Alonso S, Rodríguez-Gil JL, Gil A, Catalá M. 2011. Detection of pharmaceutically active compounds in the rivers and tap water of the Madrid Region (Spain) and potential ecotoxicological risk. *Chemosphere*. 84:1336–1348.

21. Kot-Wasik A, Dębska J, Namieśnik J. 2007. Analytical techniques in studies of the environmental fate of pharmaceuticals and personal-care products. *TrAC Trends Anal. Chem.* 26:557–568.

22. Aznar R, Sánchez-Brunete C, Albero B, Rodríguez JA, Tadeo JL. 2013. Occurrence and analysis of selected pharmaceutical compounds in soil from Spanish agricultural fields. *Environ. Sci. Pollut. Res.* 21:4772–4782.

23. Cerqueira MBR, Caldas SS, Primel EG. 2014. New sorbent in the dispersive solid phase extraction step of quick, easy, cheap, effective, rugged, and safe for the extraction of organic contaminants in drinking water treatment sludge. *J. Chromatogr. A*. 1336:10–22.

24. Zabaleta I, Bizkarguenaga E, Iparragirre A, Navarro P, Prieto A, Fernández LÁ, Zuloaga O. 2014. Focused ultrasound solid–liquid extraction for the determination of perfluorinated compounds in fish, vegetables and amended soil. *J. Chromatogr. A*. 1331:27–37.

25. Sanz-Landaluze J, Bartolome L, Zuloaga O, González L, Dietz C, Cámara C. 2006. Accelerated extraction for determination of polycyclic aromatic hydrocarbons in marine biota. *Anal. Bioanal. Chem.* 384:1331–1340.

26. https://www.chemicalize.org/. 2018. chemicalize_.

27. Commission Decision, 2002/657/EC, SANCO/10684/2009 Guideline. 2009. Commission Decision, 2002/657/EC; SANCO/10684/2009 Guideline.:1–55.

28. López-Alonso JP, Bruix M, Font J, Ribó M, Vilanova M, Jiménez MA, Santoro J, González C,

Laurents DV. 2010. NMR Spectroscopy Reveals that RNase A is Chiefly Denatured in 40% Acetic Acid: Implications for Oligomer Formation by 3D Domain Swapping. *J. Am. Chem. Soc.* 132:1621–1630.

29. Griebenow K, Klibanov AM. 1996. On Protein Denaturation in Aqueous−Organic Mixtures but Not in Pure Organic Solvents. *J. Am. Chem. Soc.* 118:11695–11700.

30. Villaverde-de-Sáa E, Valls-Cantenys C, Quintana JB, Rodil R, Cela R. 2013. Matrix solid-phase dispersion combined with gas chromatography–mass spectrometry for the determination of fifteen halogenated flame retardants in mollusks. *J. Chromatogr. A*. 1300:85–94.

31. Ziarrusta H, Olivares M, Delgado A, Posada-Ureta O, Zuloaga O, Etxebarria N. 2015. Multiscreening determination of organic pollutants in molluscs using matrix solid phase dispersion. *J. Chromatogr. A*. 1391:18–30.

32. http://www.epa.gov/waterscience/methods/det/rad.pdf. 2018. US EPA_water.._.

33. Villaverde-de-Sáa E, Fernández-López M, Rodil R, Quintana JB, Racamonde I, Cela R. 2015. Solid-phase extraction of perfluoroalkylated compounds from sea water. *J. Sep. Sci.* 38:1942–1950.

34. Coquery M, Morin A, Bécue A, Lepot B. 2005. Priority substances of the European Water Framework Directive: analytical challenges in monitoring water quality. *TrAC Trends Anal. Chem.* 24:117–127.

35. Ademollo N, Patrolecco L, Polesello S, Valsecchi S, Wollgast J, Mariani G, Hanke G. 2012. The analytical problem of measuring total concentrations of organic pollutants in whole water. *TrAC Trends Anal. Chem.* 36:71–81.

36. Vignati DAL, Valsecchi S, Polesello S, Patrolecco L, Dominik J. 2009. Pollutant partitioning for monitoring surface waters. *TrAC Trends Anal. Chem.* 28:159–169.

37. Water Framework Directive. 2013. *Directive 2013/39/EU*.

38. Sturini M, Speltini A, Pretali L, Fasani E, Profumo A. 2009. Solid-phase extraction and HPLC determination of fluoroquinolones in surface waters. *J. Sep. Sci.* 32:3020–3028.

4. Kapitulua

Amitriptilinaren biokontzentrazioa eta biotransformazioa urraburu arrainetan

Environmental Science & Technology

51 (2017) 2464-2471

4.1 Sarrera

Depresioa eta gaixotasun psikiatrikoak tratatzeko gehien errezetatzen diren farmakoen artean aurki dezakegu amitriptilina [1]. Beste antidepresibo triziklikoen (*tricyclic antidepressant*, TCA, delakoen) antzera, amitriptilinaren ekintza-modua nerbio-sistema zentraleko norepinefrinaren edota serotoninaren xurgapen selektiboaren inhibizioan oinarritzen da eta, ondorioz, burmuineko neurotransmisoreen kontzentrazioak igo egiten dira [2,3]. Amitriptilina ur-hondakinetara giza iraizketaren ondorioz heltzen da nagusiki. [4]. Hondakin-uren tratamenduan zehar nahikotxo ezabatzen den arren [5], amitriptilina 72 ng/L kontzentrazio-mailaraino detektatu da azaleko uretan, eta 223 ng/L kontzentrazio-mailaraino araztegien irteerako uretan [3,5–8].

Amitriptilinaren jokabidea ugaztunetan nahiko aztertuta dago, giza farmakoen segurtasun-ebaluazioko urratsa delako [9–11]. Hala ere, informazio gutxi dago ingurumenean nahi gabe esposizioa paira dezaketen organismo ez-zuzenduen inguruan. Adibidez, espezie urtarretan, amitriptilinak 10 ng/L bezalako kontzentrazio baxuetan sistema immunologikoa asalda dezake eta ugalketetan, garapenean eta hazkundean eragina izan dezake [12–14]. Amitriptilinak biotan metatzeko gaitasuna du [15] (log K_{ow} = 4,81, pK_a = 9,8 [16]), eta korrokoien (*Chelon labrosus-en*) gibelean [8] zein muskuiluetan [17] behatu izan da 8 ng/g eta 0,2 ng/g mailan, hurrenez hurren. Nahiz eta oraindik ez den azterketa sistematikorik egin amitriptilinaren biometatzea eta ehunen arteko banaketa espezie urtarretan ebaluatzeko, amuarrainak (*Salvelinus fontinalis*) amitriptilinarekin (3,7 ng/L mailan) kutsatutako uretan egon ondoren, amitriptilina gibelean detektatu zuten (0,29 ng/g), baina muskuluan eta burmuinean ez [18]. Dena den, beste espezie batzuekin burututako lanetan joera desberdinak behatu dira, eta burmuinerako banaketa gibelerakoa baino handiagoa izan da [9,10].

Ugaztunekin egindako ikerketek amitriptilina, zitokromo P450 2D6 (CYP2D6) entzimen bidez, biologikoki aktiboak izan daitezkeen metabolito desberdinetara zeharo biotransformatzen dela adierazi dute [2]. Giza gibeleko mikrosomekin burututako *in vitro* inkubazioetan amitriptilinaren 50 azpiproduktu behatu diren bitartean [19,20], beste 12 glukuronido-konjugatu gehiago aurkitu dira giza gernuan [20]. Horrez gain, espezieen arteko aldakortasun handia dago amitriptilinaren metabolizazioan [2,21,22] eta, guk dakigula, ez dago daturik eskuragarri organismo

urtarretako amitriptilinaren biotransformazioaren inguruan. Horregatik, soilik amitriptilinan edo ugaztunen metabolito mugatuetan arreta jartzen duten ingurumeneko esposizio-ebaluazioek ur-faunako esposizioaren benetako neurria gutxietsi dezakete.

Testuinguru honetan, amitriptilinaren ur-ingurumeneko agerraldiarekin lotutako arriskuen ebaluazioan laguntzeko asmoz, lan honen helburua arrainetan kutsatzaile horren biometatzea, ehunen arteko banaketa eta biotransformazioa ikertzea da. Helburu hori lortzeko, urraburu arrainak (*Sparus aurata*) 7 egunez amitriptilinaren bi kontzentraziotara (0,2 µg/L and 10 µg/L) kutsatu dira itsasoko uretan. Ehun bakoitzeko biokontzentrazio-faktore espezifikoak kalkulatzeaz gain, amitriptilinaren metabolitoak karakterizatu dira susmagarrien analisirako estrategia erabilita bereizmen altuko masa-espektrometriaren (*high resolution MS*, HRMS, delakoaren) bidez. Gure ezagutzaren arabera, hau da arrainetan amitriptilinaren metatzea eta biotransformazioa sakontasunez ikertzen den lehen aldia. Datu horiek oso lagungarriak dira organismo urtarretan amitriptilinaren eta bere metabolito bioaktiboen esposizioa ebaluatzeko.

4.2 Materiala eta metodoak

4.2.1 Estandarrak eta erreaktiboak

Amitriptilina hidrokloruroa (% 98), nortriptilina hidrokloruroa (% 98), eta trazagarri gisa erabiltzeko isotopikoki markatutako $^{2}H_{3}$-amitriptilina hidrokloruroa ($^{2}H_{3}$-AMI; erreferentziazko estandar zertifikatua) eta $^{2}H_{3}$-nortriptilina hidrokloruroa ($^{2}H_{3}$-NOR; erreferentziazko estandar zertifikatua) Sigma-Aldrich (St. Louis, MO, AEB) merkataritza-etxeari erosi zaizkio. Amitriptilina, nortriptilina, $^{2}H_{3}$-AMI eta $^{2}H_{3}$-NOR konposatuen disoluzioak metanoletan (Fisher Scientific, Loughborough, Erresuma Batua) prestatu dira gutxi gorabehera 5000 mg/L kontzentrazio-mailan eta metanolarekin diluitu dira kalibrazio-kurba eta dopaketarako disoluzioak prestatzeko. Bestalde, tankeak dosifikatzeko amitriptilinaren disoluzioak (5000 mg/L) etanoletan (% 99,9, Scharlab, Bartzelona, Espainia) prestatu eta Milli-Q urarekin diluitu dira 4,26 mg/L eta 85,2 µg/L mailetaraino dosi altuko eta baxuko esperimentuetarako, hurrenez hurren. Dosifikatze-disoluzioan etanolaren kontzentrazioa % 0,1 baino baxuagoa da. Disoluzio guztiak −20˚C-an gorde dira.

Metanola (HPLC kalitatea, % 99,9) eta azetona (HPLC kalitatea,% 99,8) LabScan (Dublin,

Irlanda) merkataritza-etxekoak dira, azetonitriloa (HPLC kalitatea, % 99,9) eta etil-3-aminobenzoato metanosulfonatoa (trikaina, ≥ % 98) Sigma-Aldrich (Steinheim, Alemania) merkataritza-etxekoak, sodio hidroxidoa (NaOH, ≥ 99%) Merck-ekoa (Darmstadt, Alemania), azido formikoa (HCOOH, ≥ % 98) Scharlau (Bartzelona, Espainia) merkataritza-etxekoa, eta amonio azetatoa (NH_4OAc, ≥ % 99), azido etilendiaminotetraazetikoa (EDTA, ≥ % 99) eta sodio hidrogenokarbonatoa ($NaHCO_3$, ≥ % 99,9) Panreac-ekoak (Bartzelona, Espainia). Ur ultra-purua (Milli-Q ura) purifikatzeko sistema (< 0.05 S/cm, Milli-Q 185 modeloa, Millipore, Bedford, MA, AEB) erabilita lortu da. Fase mugikor gisa metanola (Fisher Scientific, Loughborough, Erresuma Batua) erabili da azido formikoarekin (HCCOH, Optima, Fischer Scientific, Gell, Belgika) batera.

Likido-kromatografia – kuadrupolo hirukoitzeko tandem masa-espektrometrian (LC-QqQ-MS/MS analisian) talka-gas gisa eta Turbo Vap LV lurrungailua (Zymark, Hopkinton, MA, AEB) nitrogeno-korronterako erabilitako purutasun handiko nitrogeno gasa (> % 99,999) Messer (Tarragona, Espainia) merkataritza-etxekoa izan da, eta lehortze- eta lainoztatze-gas gisa erabilitako nitrogenoa (% 99,999) AIR Liquide-koa (Madril, Espainia).

4.2.2 Arrainen esposizioa

Plentziako itsas-estazioko (PiE-UPV/EHU) akuarioetan esposizio-esperimentuak egiteko ~40 g-ko eta ~13 cm-ko urraburu arrain (*Sparus Aurata*) gazteak Groupe Aqualande arrain-haztegitik (Roquefort, Frantzia) lortu dira. Arrainak heldutako egunetik bi astez eduki dira bertako girora egokitzeko eta, ondoren, esperimentuak hasi orduko, esperimentuko tankeetan ere beste 48 orduz egon dira ontzietara egokitzeko. Arrainen bizi-irautea ziurtatzeko laborategiko tenperatura 18 °C-an mantendu da, 14:10-h argitasun/iluntasun zikloak bermatu dira, ura etengabe aireztatu da eta egunero 0,10 g arrain-jaki/arrain eman zaie. Esperimentuek iraun duten bitartean, uraren tenperatura (13,5 ˚C) eta pH-a (7,3 ± 0,3) konstante mantendu dira. Bestalde, uraren kalitatea ziurtatzeko, disolbatutako oxigenoaren, nitritoen, nitratoen eta amonioaren kontrola egin da esposizioan zehar.

7 eguneko esposizio-esperimentuak bi kontzentrazio-mailatan egin dira. Lehenengoa, dosi altuan (10 µg/L nominala) amitriptilinaren metabolitoak eta biokontzentrazio-faktoreak determinatzeko helburuarekin. Horretarako, 800 × 600 × 412 mm-ko polipropilenozko bi ontzi

(bata kontrola eta bestea dosifikatua) erabili dira, bakoitza itsasoko uraren 100 L-rekin eta 35 urraburu arrainekin. Bigarren esperimentua, aldiz, dosi baxuagoan (0,20 µg/L nominala) egin da, metatzeaz gain, amitriptilinak ingurumenean aurkitzen den kontzentrazio horretan eragin ditzakeen albo-ondorioak ere aztertzeko. Hurrengo kapituluan (5. Kapituluan) eztabaidatzen diren albo-ondorio horiek aztertu ahal izateko, dosi baxuko esperimentuan arrain-kopuru handiagoa (145 arrain ontziko) behar izan da. Ondorioz, erabilitako tankeak ere handiagoak (1000 × 700 × 650 mm) izan dira, bakoitza itsasoko uraren 250 L-rekin (bata kontrola eta bestea dosifikatua).

Bi esposizio-esperimentuak fluxu jarraiko sistemaren bidez egin dira. Horretarako, ponpa peristaltikoak erabilita tanke guztietara itsasoko ura 8,5 L/h-ko fluxuan gehitu da eta kutsatutako tankeetara amitriptilinaren dosifikatze-disoluzioa 20 mL/h-ko fluxuan. Dosifikatze-disoluzio horiek 48 orduro berriztatu dira.

4.2.3 Lagin-biltzea

Arrainen lagin-biltzea eta disekzioa Euskal Herriko Unibertsitateko (UPV/EHUko) Bioetika-Batzordeak ebaluatu eta, egungo araudien arabera, tokiko agintaritzak onartutako prozedura (CEEA/380/2014/ETXEBARRIA LOIZATE) jarraituta egin dira. Kutsatutako zein kontroleko edukiontzitik 10 urraburu jaso dira esposizioa hasi eta bigarren, laugarren eta zazpigarren egunetan. Lagin-biltzeko egunetan, uretan amitriptilinaren kontzentrazioa determinatzeko, 2,5 L itsasoko ur ere bildu dira esposizioko ontzi bakoitzetik. Arrainak berehala anestesiatu dira 200 mg/L trikaina eta 200 mg/L $NaHCO_3$ itsasoko uretan (10 L) disolbatuta dituen ontzian. 5 minutu igaro ondoren, arrainak pisatu, neurtu eta disekzionatu dira jariakin biologikoak (plasma eta behazuna) eta ehunak (gibela, burmuina, zakatzak eta muskulua) biltzeko. Aurretiaz 0,5 mol/L EDTA (NaOH-arekin pH-a 8-ra doituta) disoluzioarekin bustitako xiringa erabilita itsats-arteriatik odola atera da. Ondoren, plasma lortzeko, odola 5 minutuz zentrifugatu da 1000 bira/min-an. Bereizitako jariakin biologikoak eta ehunak disekzioan zehar nitrogeno likidotan mantendu eta, ondoren, -80°C-ko izozkailuan gorde dira aztertu arte.

4.2.4 Laginen tratamendua

Ehun biologikoak (gibela, burmuina, zakatzak eta muskulua) Cryodos-50 liofilizatzailean (Telstar Instrument, Sant Cugat del Valles, Bartzelona, Espainia) 48 orduz liofilizatu dira.

10 arrainen ehunak elkartuta lagin homogeneoa prestatu da esposizio-tanke (kontrola eta kutsatua) eta laginketa-egun (2, 4 eta 7 egunak) bakoitzerako. Lagin homogeno horren 3 alikuota erauzi eta aztertu dira.

Laginetan amitriptilinaren eta nortriptilinaren kontzentrazioak determinatzeko aurretiaz garatutako metodo analitikoak erabili dira [8]. Laburki, liofilizatutako gibela (0,5 g), muskulua (0,5 g), zakatzak (0,1 g) edo burmuina (0,1 g) isotopikoki markatutako barne-estandarrekin dopatu eta azetonitrilo:Milli-Q ur (95:5, bol/bol) nahastearen 7 mL-rekin erauzi dira. Ultrasoinu-homogeneizatzailea (100 W, 20 kHz; Bandelin Sonopuls HD 3100 sonikatzailea, Bandelin electronic, Berlin, Alemania) erabilita ultrasoinu fokatuen bidezko solido-likido erauzketa (*focused ultrasound solid-liquid extraction*, FUSLE, delakoa) 30 s-tan burutu da (0,8 s-ko pultsu-denborarekin eta 0,2 s-ko pultsu-geldialdiekin), % 10-eko potentziarekin eta 0 °C-an ur-izotz bainuan. Erauziaren gaineko likidoa 0,45 μm-ko poliamida iragazkien (25 mm, Macherey-Nagel, Alemania) bidez iragazi, nitrogeno-korrontearekin ~1 mL-ra lurrundu eta 6 mL Milli-Q ur gehituta diluitu da, ondoren, fase solidoko erauzketaren (*solid phase extraction*, SPE, delakoaren) bidez garbitzeko. Bestalde, plasma, behazuna (100 μL eta 250 μL, hurrenez hurren, 6 mL Milli-Q uretan diluituta) eta itsasoko ura (500 mL) barne-estandarrekin dopatu dira SPE-aren bidezko garbiketa/aurrekontzentrazioa burutu aurretik.

Lagina kargatu aurretik, modu mistoko 200 mg-ko Evolute-CX kartutxoak (6 mL, Biotage, Uppsala, Suedia) 5 mL metanol, 5 mL Milli-Q ur eta 5 mL % 2 HCOOH duen Milli-Q ur (pH=2) pasatuta egokitu dira. Erauzia/lagina kargatu ondoren, garbiketarako 5 mL Milli-Q ur eta 5 mL metanol gehitu eta kartutxoak 30 min-z lehortu dira hutsa eginda. Jarraian, eluzio-urratsean, bi frakzio bildu dira: 5 mL metanola pasatuta (1. frakzioa) eta 3 mL % 2,5 NH_4OH duen azetona pasatuta (2. frakzioa). Bi frakzioak nitrogeno-korrontearen laguntzarekin 35 °C-an lehorrera eraman, metanol:Milli-Q ur (90:10, bol/bol) nahastearen 200 μL-an bereizita berriz disolbatu eta 0,22 μm-ko polipropilenozko iragazkietatik (13 mm, Pall Corp., NY, AEB) iragazi dira analisira orduko.

4.2.5 Analisi instrumentala

Amitriptilina eta bere nortriptilina metabolitoa 2. frakzioan kuantifikatu dira LC-QqQ-MS/MS

teknikaren bidez aurretiaz garatutako metodoa erabilita [8]. Horretarako, Agilent 1260 serieko HPLC kromatografoa (Agilent Technologies, Palo Alto, CA, AEB) erabili da, Phenomenex (Torrance, CA, AEB) merkataritza-etxeko Kinetex bifenilo 100Å core-shell (2,1 mm x 50 mm, 2,6 μm) zutabea eta Kinetex bifenilo 100Å core-shell aurrezutabearekin (2,1 mm x 5 mm, 2,6 μm). Fase mugikorrari dagokionez, A fasea Milli-Q ur:metanol (95:5, bol/bol) nahasteaz osatuta dago eta B fase metanol:Milli-Q ur (95:5, bol/bol) nahasteaz, bietan HCOOH % 0,1 gehituta. Banaketa-gradientea A fase mugikorraren % 45-ean hasi eta % 10-era jaitsi da 3 minututan konposizio horretan 6 minutuz mantenduta; ondoren, 3 minututan hasierako baldintzetara (A fase mugikorraren % 45-era) bueltatu eta bertan 8 minutuz mantendu da hasierako baldintzak berriz lortzen direla ziurtatzeko. Analitoen banaketa 0,3 mL/min fluxuan burutu eta injekzio-bolumena 2 μL-an ezarri da. Kromatografoa Agilent 6430 kuadrupolo hirukoitzeko (QqQ) masa-espektrometroari akoplatuta dago elektroesprai-ionizazioko (*electrospray ionization*, ESI, delako) iturriarekin. Kuantifikaziorako aukeratutako ioi aitzindarietatik apurketa-ioietarako trantsizioen jarraipena egiten duen eskuratze-modua (*Selected Reaction Monitoring,* SRM, delakoa) erabili eta ionizazioa modu positiboan egin da, 3000 V-ko tentsio kapilarrarekin, lehortze-gasaren 12 L/min-ko fluxuarekin eta 350 °C-an, eta lainoztatze-gasaren 45 psi-ko presioarekin. Amitriptilina kuantifikatzeko *m/z* 278,2/191,1 ioi aitzindaritik apurketa-ioirako ioi-trantsizioa erabili da eta konfirmatzeko ioi-trantsizio gisa *m/z* 278,2/117,1 eta *m/z* 278,2/91,1. Nortriptilina kuantifikatzeko, berriz, *m/z* 264,2/233,1 ioi-trantsizioa erabili da eta konfirmatzeko *m/z* 264,2/105,1 eta *m/z* 264,2/91,1 ioi-trantsizioak. Neurketak, datuen eskuratzea eta gailurren integrazioa Masshunter Workstation software-arekin (Qualitative Analysis, B.06.00 bertsioa, Agilent Technologies) egin dira.

Amitriptilinaren metabolitoen identifikazioa, aldiz, 1. eta 2. frakzioetan burutu da. Horretarako, bereizmen altuko qOrbitrap masa-espektrometroa (Thermo Scientific ™ Q Exactive ™ HF kuadrupolo-Orbitrap hibridoa, Thermo, CA, USA) erabili da, merkataritza-etxe berdineko berotutako elektroesprai-ionizazio (*heated electrospray ionization*, HESI, delako) iturriaren bidez bereizmen altuko likido-kromatografoari (Thermo Scientific Dionex UltiMate 3000 UHPLC) akoplatuta. Erauziak Thermo merkataritza-etxeko Hypersil GOLD aQ (2,1 mm x 100 mm, 1,9 μm) zutabean banatu dira, aurrezutabea (2,1 mm-ko barne-diametroa, 0,2 μm) erabilita. Fase mugikorrari dagokionez, Milli-Q ura (A fasea) eta azetonitriloa (B fasea) erabili dira, bietan HCOOH

% 0,1 gehituta. Banaketa-gradientea B fase mugikorraren % 10-ean hasi eta % 50-era igo da 9 minututan; ondoren, beste 3 minututan % 95 konposiziora igo da. Baldintza horietan 1,5 min mantendu ondoren, hasierako baldintzetara bueltatu da 1,5 min-tan. Analitoen banaketa 0,4 mL/min fluxuan burutu da 35 °C-ko zutabe-tenperaturan. Injekzio-bolumena 5 μL-an ezarri eta lagingailu automatikoa 5 °C-an mantendu da.

Orbitrap masa-analizatzailean erabilitako eskuratze-modua ekorketa osoa - datuen menpeko MS/MS (*full scan – data dependant MS2*, Full MS-ddMS2, delakoa) izan da. Ekorketa osoa *m/z* 100-600 tartean egin da 120.000 bereizmenarekin *m/z* 200-eko masari dagokion maximoaren erdiko zabalera osoan (*full width at half maximum,* FWHM, delakoan). Ekorketa oso bakoitzaren jarraian 5 ddMS2 neurketekin burutu dira 15.000 FWHM bereizmenarekin (*m/z* 200-ean), eta isolatze-leihoa 0,4 Da-ean ezarrita. Energia altuko talka-disoziazioko gelaxkan talka-energia normalizatua (*normalized collision energy*, NCE, delakoa) 35 eV-an ezarri da. MS/MS apurketa zein ioiek pairatuko duten zehazteko barne-zerrenda bat eratu da. Zerrenda horretan aurretiaz bibliografian deskribatutako amitriptilinaren metabolitoen ioiak [19] sartzeaz gain, 12 laginen (matrize bakoitzeko kontrol baten eta kutsatu baten) aurreanalisitik lortutako emaitzetako ioiak ere gehitu dira. Aurreanalisi horiek ekorketa osoa - ioi guztien apurketa (*full scan – all ion fragmentation*, Full MS-AIF, delako) eskuratze-moduan egin dira, ekorketa osoa 120.000 bereizmenarekin, eta ioi guztien apurketa 60.000 bereizmenarekin eta 35 eV-ko NCE-arekin. Hain zuzen, *m/z* 108 eta *m/z* 90 ioiez osatutako barne-zerrendak eratu dira, modu positiboan eta negatiboan, hurrenez hurren. Dena dela, ekorketa osoan ez bada barne-zerrenda horietako ioirik detektatu, ugaritasun handieneko ioiak aukeratu dira apurketarako. ddMS2 neurketan $2{,}7 \times 10^4$-ko intentsitate-muga eta 5 s-ko baztertze-denbora dinamikoa finkatu dira. Kontuan izanda bereizmen altuko ekorketa oso bakoitzeko (256 ms) 32 ms-ko bost ddMS2 neurketa egin direla, ziklo bakoitza ~ 0,4 s-koa dela ondoriozta daiteke. HESI iturriko parametroak ondoko balioetan ezarri dira: esprai-tentsioa 4,5 kV-an, kapilarraren tenperatura 350 °C-an, zorro-gasa 45 unitate arbitrariotan, gas-laguntzailea 5 unitate arbitrariotan eta gas-laguntzailearen berogailua 300 °C-an. Instrumentua Xcalibur 3.1 (Thermo) software-aren bidez kontrolatu eta, analisiaren aurretik, instrumentuaren kanpo-kalibrazioa burutu da Pierce LTQ ESI kalibrazio-disoluzioak (Thermo Scientific, Waltham, Massachusetts, Estatu Batuak) erabilita.

4.2.6 Datuen tratamendua

Arrainaren osasunaren ebaluazio orokor gisa, egoera-faktorea K = (arrainaren pisua × 100)/arrainaren luzera^3) eta indize hepatosomatikoa (HSI = (gibelaren pisua × 100)/ arrainaren pisua) determinatu dira. Kutsatutako eta kontroleko taldeen artean K eta HSI estatistikoki erkatzeko, aldagai bakarreko (*analysis of variance*, ANOVA, delakoa) erabili da. Bestalde, dosifikazio-maila bakoitzerako biometatze-faktoreak (*bioconcentration factor*, BCF, delakoak) kalkulatu dira [23]. Horretarako, esposizio-egun bakoitzean arrainaren ehunean dagoen amitriptilinaren kontzentrazioa dagokion esposizio-eguneko uretako batezbesteko kontzentrazioarekin zatitzen da.

Amitriptilina eta nortriptilina 10 puntuko kalibrazio-zuzenarekin kuantifikatu dira Agilent Masshunter software-a erabilita. Metabolitoen identifikazioa, aldiz, Compound Discoverer 2.0 (Thermo) erabilita egin da. Gailurren detekzioa eta lerrokatzea 5 ppm-ko masa-tolerantziarekin eta 0,5 min-ko erretentzio-denboren desbideratzearekin burutu da. Programak amitriptilinaren metabolitoak aurresaten ditu 1.go eta 2. Faseko erreakzioak (ikus I. eranskina) erabilita. Ondoren, aurresandako metabolito horien *m/z* balioak gailurren zerrendan bilatzen dira 5 ppm-ko masa-tolerantziarekin eta isotopo-bilaketarako % 40ko intentsitate-tolerantziarekin. Gailurrak eskuz txekeatu dira eta soilik MS/MS espektroa eskuragarri eta 100.000 baino seinale handiagoa duten, eta kontroleko laginetan aurkitzen ez diren gailurrak hartu dira kontuan aurrerantzean. Lan honetan, soilik modu positiboan detektatutako gailurrak hartu dira aintzat, modu negatiboko gailurrek ez dutelako amitriptilinarekiko antzekotasunik erakutsi egiturari dagokionez. Egituren esleipena software-ak markatutako ddMS2 apurketa-ioietan oinarrituta egin da.

4.3 Emaitzak eta eztabaida

4.3.1 Metodoen kalitate kontrola

Amitriptilina eta nortriptilina urraburu arrainen ehun eta jariakin biologikoetan aztertzeko erabilitako metodoen berrespena egin da inolako analisirik egin aurretik. Konposatu horiek ingurumeneko uretan zein arrainen muskuluan eta gibelean determinatzeko metodoa aurreko lan batean zehaztu eta berretsi da [8]. Aurretiaz optimizatutako metodoa, beste zenbait matrizetara

hedatu eta berretsi da, hala nola zakatzetara, burmuinera, plasmara eta behazunera. Metodo analitikoa berresteko analitorik ez duten matrize errealak (muskulua, gibela, zakatzak, plasma, behazuna eta burmuina) amitriptilinarekin eta nortriptilinarekin dopatu dira: muskulu eta gibela 10 ng/g-an, burmuina eta zakatzak 50 ng/g-an, plasma 20 ng/mL-an eta, azkenik, behazuna 50 ng/mL-an. Trazagarri modura, erauzketaren aurretik $^{2}H_3$-AMI eta $^{2}H_3$-NOR deuteratuak gehitu dira kontzentrazio berdinetan. 4.1 taulan ikus daitekenez, metodoen kalitate-kontrola bermatu da, emaitza zehatzak eta doiak lortu baitira.

***4.1 taula**: Amitriptilina eta nortriptilina ehun/jariakin biologikoetan kuantifikatzeko erabilitako metodoen etekin gordinak, etekin zuzenduak eta desbiderazio estandar erlatiboak (relative standard deviation, RSD, delakoak).*

Matrizea	Amitriptilina			Nortriptilina		
	Etekin gordina (%)	Etekin zuzendua[a] (%)	RSD (%) (n=3)	Etekin gordina (%)	Etekin zuzendua[b] (%)	RSD (%) (n=3)
Muskulua	44	107	2	39	102	3
Gibela	63	106	1	47	102	2
Zakatzak	30	110	4	18	131	7
Burmuina	72	107	1	58	104	2
Plasma	51	107	2	46	104	2
Behazuna	61	101	2	48	105	2

(a) $^{2}H_3$-AMI trazagarriarekin zuzendua; (b) $^{2}H_3$-NOR trazagarriarekin zuzendua.

4.3.2 Esposizio-esperimentuak eta amitriptilinaren metatzea arrainetan

Kutsatutako tankeetako amitriptilinaren denboran zeharreko batezbesteko kontzentrazioak 12 ± 3 µg/L eta 0,12 ± 0,02 µg/L izan dira dosi altukoan eta baxukoan, hurrenez hurren. Kontroleko ontzietan, berriz, amitriptilinaren eta bere metabolitoa den nortriptilinaren kontzentrazioak metodoaren detekzio-mugen (< 1 ng/L) azpitik egon dira. Salbuespen bakarra dosi altuko kontroleko arrainen plasma izan da, zeinak nortriptilina 7,7 ng/mL-ko mailan (kutsatutako arrainetako kontzentrazioa baino % 30 baxuagoa) duen. Analisian eta zurietan ez denez zeharkako kutsadurarik egon, kasu horretako nortriptilinaren jatorria disekzio-, liofilizazio-, laginen elkartze- edo erauzketa-urratsetako zeharkako kutsaduran egon liteke.

Bizi-irauteari dagokionez, ez da arrainik hil esposizioek iraun duten tarte osoan, eta arrainen osasun orokorraren adierazgarri diren K eta HSI aldagai fisiologikoen balioak estatistikoki bereizi ezinak izan dira (p-balioa > 0,05) kontroleko eta kutsatutako arrainen artean dosi altuko zein baxuko esperimentuan aztertutako egun guztietan.

4.1(a-b) irudian beha daitekeen moduan, amitriptilinaren ehunen arteko banaketa antzekoa izan da bi dosietako esperimentuen artean. Nortriptilinari dagokionez, dosi altuko esperimentuan amitriptilinaren antzeko ehunen arteko banaketa erakutsi du (ikus 4.1c irudia), baina dosi baxuko esperimentuan metodoen detekzio-mugetatik behera egon da. Bi dosietan, amitriptilinaren kontzentrazio altuenak, esposizioko 7. egunean aurkitu dira. Batez ere burmuinean eta zakatzetan metatu da amitriptilina, ondoren gibelean, plasman, behazunean eta, azkenik, maila baxuagoan muskuluan. Amitriptilinaren hidrofobikotasuna kontuan hartuta (log K_{ow} =4,81 [16]), lipidotan aberatsak diren ehunetan metatze altuagoa espero zitekeen arren, lipidikoak ez diren zakatzetan ere aurkitu dira kontzentrazio altuenetarikoak. Hortaz, ondoriozta daiteke amitriptilinaren metatzean bere propietate fisiko-kimikoez gain, metabolismoa bezalako bestelako faktoreek ere garrantzia dutela. Amitriptilina droga psikoaktiboa dela kontuan hartuta, burmuinean behatutako kontzentrazioak logikoak dirudite. Gainera, emaitza horrek Lajeunesse-k eta lankideek lortutakoekin bat egin ez arren [18], bibliografian depresioaren kontrako beste hainbat farmakorekin egindako esperimentuetan lan honetan lortu diren antzeko emaitzak aurkitu dira, hau da, drogaren metatzea burmuinean gertatu den bitartean, metabolizazioa gibelean nagusitu da [24–27]. Bestalde, amitriptilinaren burmuineko kontzentrazioak plasmakoak baino 2,7 aldiz altuagoak izateak, hau da, burmuin-plasma banaketa koefizientea 2,7 izateak, amitriptilina arrain-burmuinera barreiatzen dela adierazten du. Bibliografian eragile psikotropiko batzuentzako 3,0 baino burmuin-plasma banaketa-koefiziente altuagoak argitaratu diren bitartean, neuroaktiboak ez diren konposatuentzako balio baxuagoak (0,4 - 1,8) behatu dira [27]. Izatez, amitriptilinaren hidrofobikotasun nabarmenak iradokitzen du amitriptilinak muga hematoentzefalikoa zeharkatzeko mekanismo nagusia difusio pasiboa dela.

Horrez gain, kontuan hartuta amitriptilinaren plasmako kontzentrazioak zakatzetakoak baino altuagoak izan direla eta bi kontzentrazioen artean korrelazio positibo altua behatu dela ($r > 0,98$), amitriptilinaren absortzioa nagusiki zakatzetatik eman dela ondoriozta daiteke eta ez hesteetatik [28]. Bibliografian, zenbait farmakorekin kutsatutako hondakin-uretan egondako arrainetan antzeko emaitzak argitaratu dira metatzearen inguruan [27]. Nahiz eta konposatu ionizagarrien metatzeak eta ehunen arteko banaketak pH-arekiko menpekotasun handia izan ohi duen [29–32], amitriptilina hidrofobikotasun nahiko handiko (log K_{ow} =4,81, log D 2,39 pH 7,3-an [16]) base ahula (pK_a 9.8) da eta, ondorioz, pH fisiologikoan beti positiboki kargatuta dago.

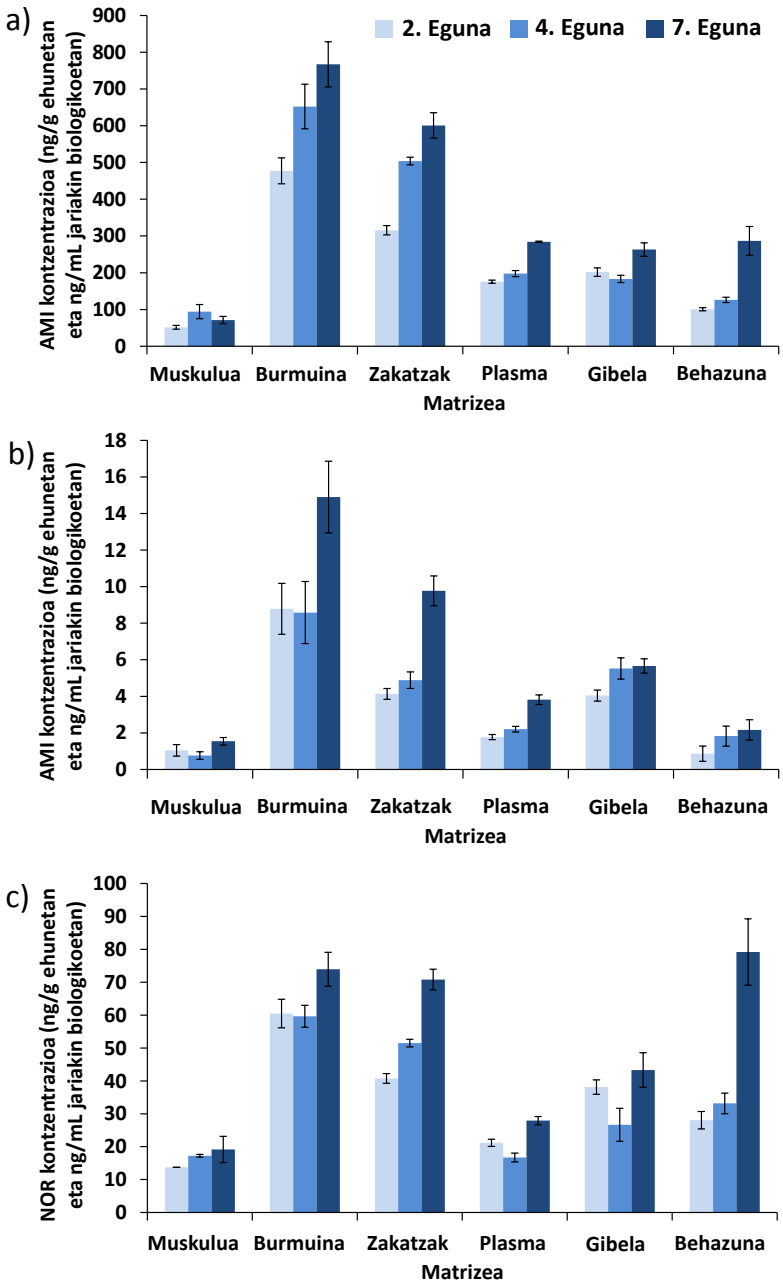

4.1 irudia: *Amitriptilinaren (AMI-ren) 10 µg/L-ra (a) eta 0.2 µg/L-ra (b) kutsatutako arrainen ehun (ng/g) eta jariakin (ng/mL) biologiko desberdinetan detektatutako amitriptilinaren kontzentrazioak eta konfiantza-tarteak (bi aldiz desbideratze estandarra, n=3, % 95 konfiantza-mailan). Nortiptilinaren (NOR-en) kontzentrazioak (c) amitriptilinaren 10 µg/L-ra kutsatutako arrainetan.*

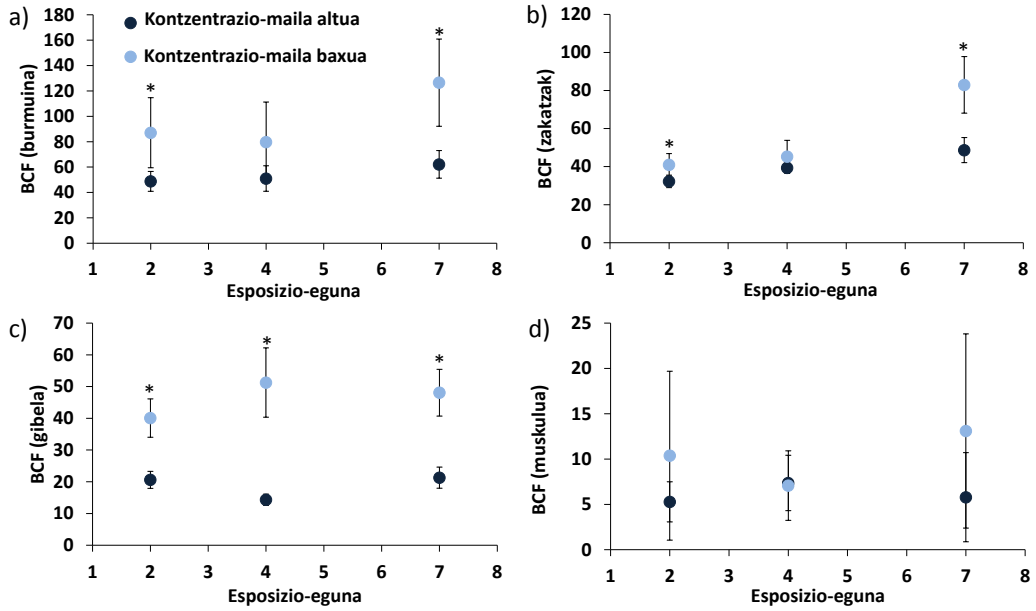

4.2 irudia: *Esposizio-esperimentuko egun desberdinetan burmuineko (a), zakatzetako (b) gibeleko (c) eta muskuluko (d) BCF balioak eta konfiantza-tarteak (bi aldiz desbideratze estandarra, n=3, % 95 konfiantza-mailan). Oharra: kasu batzuetan egoera egonkorrera iritsi ez arren, BCF-ak arrainaren ehuneko eta uretako amitriptilinaren kontzentrazioaren arteko zatiketatik kalkulatu dira. Izartxoek dagokion eguneko dosi altuko eta dosi baxuko esperimentuetako BCF balioen artean desberdintasun esanguratsuak daudela adierazten dute aldagai bakarreko ANOVA-ren arabera (p-balioa < 0,05).*

4.2 irudian beha daitekeenez, oro har, ehunetako BCF-ak denboran zehar konstanteak dira (p balioa> 0,05), eta horrek aditzera ematen du 7 egunetan egoera egonkorrera heltzen dela dosi-maila bietan. Salbuespen bakarra dosi baxuko zakatzen kasua da. Dosi baxuko burmuineko, zakatzetako eta gibeleko BCF-ak altuagoak direnez, amitriptilinaren arrainetako metatzeak kontzentrazioarekiko menpekotasuna duela esan daiteke. Emaitza horrek ez du bat egiten farmakoen metatzean esposizio-kontzentrazioak duen eragina aztertu duten beste lan batzuekin [33], nahiz eta badauden kontzentrazioa eta BCF-en kontrako erlazioa deskribatzen duten ikerketak [34]. Kutsatzailearen kontzentrazio altuagoek oxigeno-espezie erreaktiboen igoera sortzean egon daiteke azken horren arrazoia eta, ondorioz, dosi altuagoetan amitriptilinaren biotransformazioa nabarmenagoa [35] eta amitriptilinaren (jatorrizko farmako metabolizatu gabearen) BCF-ak baxuagoak izatea. Muskuluko BCF-etan, aldiz, ez da berdina gertatu, baina horren arrazoia ehun

horretan behatutako kontzentrazio baxuak izan daitezke. Izan ere, kontzentrazio-maila baxuko esperimentuan, muskuluko amitriptilinaren kontzentrazioak detekzio-mugatik hurbil egon dira eta, ondorioz, aldakortasuna handiagoa izan da.

Bibliografian, adibide gutxi daude amitriptilinaren ehunetako BCF espezifikoak determinatzen dituztenak [18], eta eskuragarri dauden datuek iradokitzen dute amitriptilinaren BCF-ak espezieen arteko desberdintasunen eta esposizio-baldintzen menpekoak direla. Adibidez, lan honetan kalkulatutako gibeleko BCF-en balioak (21 dosi altuan eta 48 dosi baxuan) bestelako lan batean lortutako amuarrain-gibeleko BCF balioaren (BCF=78) magnitude-ordena berdinean daude [18]. Aldiz, amitriptilinarekin kutsatutako araztegiko irteerako ura jasotzen duen ibaiko muskuiluetan determinatu diren BCF balioak askoz altuagoak (BCF= 6028) behatu dira [36]. Horrez gain, azpimarratzekoa da 4.2 irudiko BCF-ek metabolizatu gabeko amitriptilina soilik hartzen dutela kontuan. Ondorioz, BCF-ek konposatu psikoaktiboek ehun jakin baten duten zama osoa gutxietsi dezakete, ez baitute efektu gehigarriak izan ditzaketen metabolito bioaktiboen presentzia kontuan hartzen.

4.3.3 Metabolitoen identifikazioa

Amitriptilinaren metabolizazio-bidean adierazitako 1. eta 2. Faseko metabolitoen egiturak 4.3 irudian ikus daitezke. Egiturak definitzeko 4.2 taulan laburbiltzen diren masa zehatzetan eta apurketa-ioien datuetan oinarritu da. Detektatutako metabolito guztientzat ez daudenez erreferentziazko estandarrak eskuragarri, Schymanski-k eta lankideek ezarritako 2b-3 konfiantza-mailara heldu gara [37] eta egitura probableak edo behin behineko hautagaiak proposatu ditugu. Isomero asko egon daitezkeenez, egitura batzuen determinazioa zalantzazkoa izan daiteke eta adituen justifikazioetan oinarritua izan da. Kasu guztietan, neurtutako masaren eta masa teorikoaren arteko aldea 3,3 ppm baino baxuagoa izan da. Guztira amitriptilinaren 33 metabolito determinatu dira eta, gure ezagutzaren arabera, haietatik 10 (M12, M13, M15, M16, M20, M21, M22, M23, M27 eta M28) lehen aldiz deskribatu dira lan honetan. Atal honetan, egitura horietako bakoitzaren identifikazioko xehetasunak bildu dira.

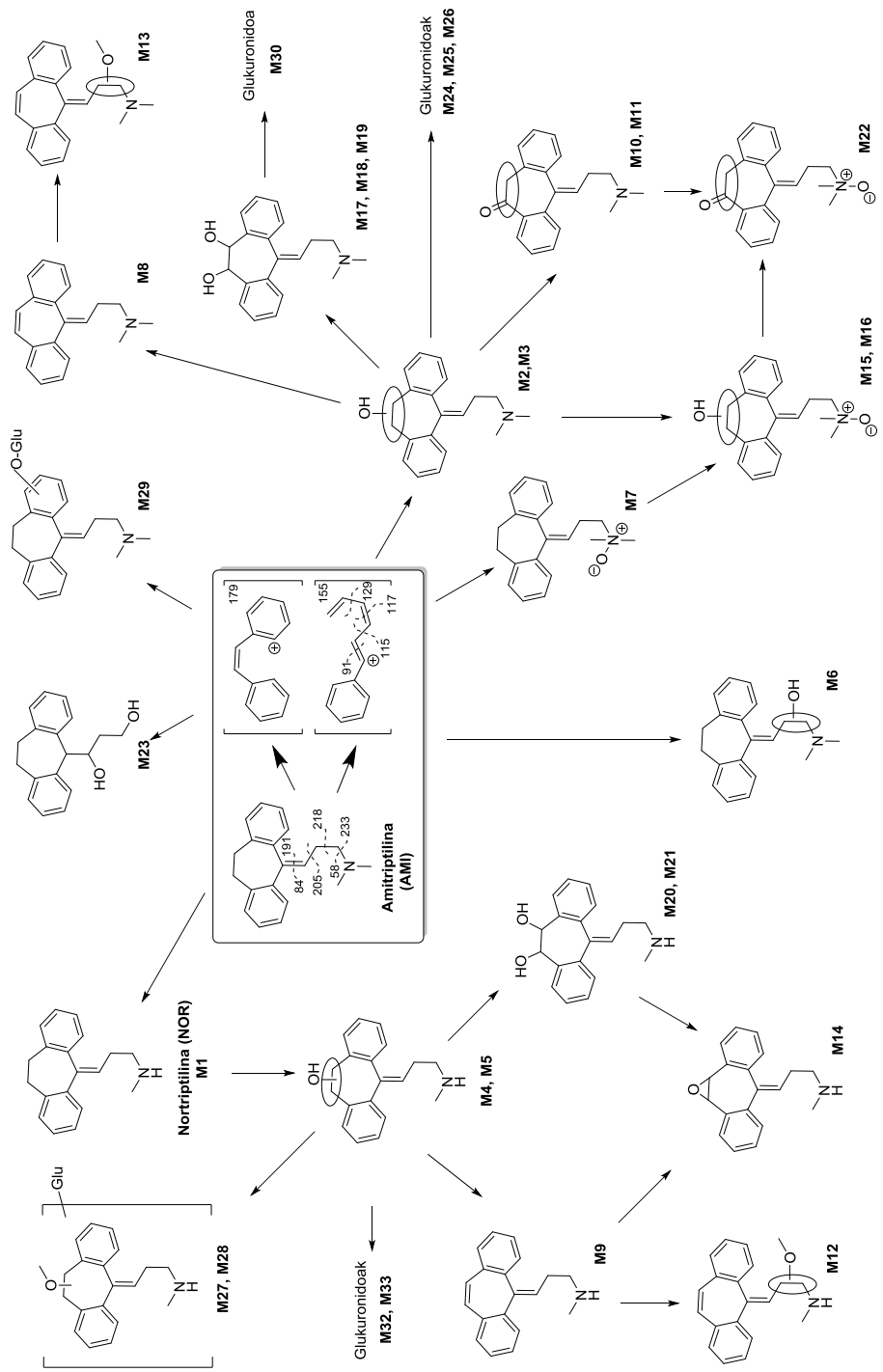

4.3 Irudia: *Amitriptilinaren biotransformazio-bidea urraburu arrainean. Zirkuluek lotura edozein lekutan egon daitekeela adierazten dute.*

4.2 taula: *Amitriptilinaren eta identifikatutako metabolito guztien formula molekularra, $[M+H]^+$ ioiaren m/z teorikoa eta ehun/jariakin bakoitzerako dagokion Δmasa (ppm-an), MS/MS espektroko apurketa-ioiak eta erretentzio-denbora (R_t min-an).*

Konposatua	Formula molekularra (M)	m/z teorikoa ($[M+H]^+$)	MS/MS espektroko apurketa-ioi ugarienak	ΔMasa (ppm)						R_t (min)
				Gibela	Plasma	Behazuna	Burmuina	Muskulua	Zakatzak	
Amitriptilina	$C_{20}H_{23}N$	278,1903	278,1899; 233,1323; 91,0542; 105,0698; 117,0698; 191,0854; 84,0807; 155,0855; 218,1088; 205,1010; 58,0653; 179,0855; 129,0697	0,62	2,28	0,51	2,04	1,27	1,16	7,79
M1; Nortriptilina	$C_{19}H_{21}N$	264,1747	233,1323; 91,0542; 105,0698; 117,0698; 264,1741; 191,0854; 155,0854; 218,1088; 205,1010; 70,0651; 179,0854; 129,0697	1,02	0,55	-0,14	1,36	0,90	1,13	7,61
M2	$C_{20}H_{23}NO$	294,1853	276,17438; 231,11673; 58,06536; 216,09325; 84,08076; 191,08553; 205,10109; 294,18396; 233,13249; 117,06985; 229,10129; 203,08531; 249,12743	1,03	2,59	0,62	1,66	0,83	0,93	4,69
M3	$C_{20}H_{23}NO$	294,1853	276,1730; 231,1167; 58,0654; 216,0929; 191,0853; 84,0808; 193,1011; 205,1013; 233,1324; 294,2057; 117,0702	0,20	1,86	1,55	1,35	1,03	0,83	5,55
M4	$C_{19}H_{21}NO$	280,1696	231,1167; 262,1588; 216,0932; 191,0855; 70,0652; 205,1011; 229,1012; 153,0698; 115,0542; 215,0855; 203,0855	0,45	0,78	0,23	1,76	1,43	1,31	4,55
M5	$C_{19}H_{21}NO$	280,1696	231,1168; 262,1588; 216,0933; 191,0855; 70,0652; 205,1012; 193,1010; 153,0698; 229,1010; 115,0543; 215,0853	0,45	1,00	1,54	1,32	-	1,11	5,39
M6	$C_{20}H_{23}NO$	294,1853	276,1741; 231,1167; 58,0654; 180,1746; 98,0964; 216,0932; 84,0808; 294,1826; 191,0855; 205,1012; 249,1273	-	-	-0,11	-	-	-	4,62
M7	$C_{20}H_{23}NO$	294,1853	233,1323; 91,0542; 105,0699; 117,0698; 191,0855; 155,0855; 218,1088; 205,1011; 58,0653; 179,0862; 129,0701	0.83	1.45	0.00	-	-	0.72	8,13

(-): ez da detektatu

4.2 taula: *(Jarraipena).*

Konposatua	Formula molekularra (M)	m/z teorikoa ($[M+H]^+$)	MS/MS espektroko apurketa-ioi ugarienak	ΔMasa (ppm)						R_t (min)
				Gibela	Plasma	Behazuna	Burmuina	Muskulua	Zakatzak	
M8	$C_{20}H_{21}N$	276,1747	276,1741; 231,1167; 58,0654; 216,0932; 84,0808; 205,1011; 191,0855; 229,1013; 117,0699; 233,1321; 203,0855; 91,0542; 98,0964	1,52	2,08	-	-	-	1,19	4,69
M9	$C_{19}H_{19}N$	262,1590	231,1167; 262,1585; 216,0933; 191,0855; 70,0652; 205,1011; 229,1010; 153,0699; 215,0855; 115,0542; 203,0854	0,70	-	-	-	-	1,39	4,55
M10	$C_{20}H_{21}NO$	292,1696	84,0808; 292,1688; 229,1010; 219,1167; 58,0654; 247,1116; 91,0542; 274,1585; 203,0854; 178,0776; 191,0853; 68,0497; 72,0808	0,96	3,25	-	1,79	0,85	0,54	5,77
M11	$C_{20}H_{21}NO$	292,1696	84,0808; 292,1694; 229,1012; 219,1168; 58,0654; 247,1116; 91,0542; 274,1587; 178,0777; 203,0855; 191,0856	-	1,27	1,16	-	-	-	6,04
M12	$C_{20}H_{21}NO$	292,1696	229,1010; 260,1430; 203,0853; 232,1119; 70,0651; 292,1692; 82,0650; 231,1169; 292,2253; 179,0855	0,43	-	0,43	1,48	1,37	1,48	7,74
M13	$C_{21}H_{23}NO$	306,1853	274,1585; 84,0807; 229,1009; 203,0852; 58,0653; 231,1165; 306,1845; 261,1269; 216,0931; 96,0807	0,50	1,29	0,00	0,99	-2,11	0,99	7,94
M14	$C_{19}H_{19}NO$	278,1540	229,1010; 247,1115; 70,0651; 219,1166; 91,0542; 278,1534; 219,0800; 260,1431; 203,0853; 178,0775; 191,0854	0,47	1,90	1,02	0,80	0,25	0,91	5,63
M15	$C_{20}H_{23}NO_2$	310,1802	231,1166; 216,0932; 58,0654; 191,0857; 229,1008; 219,1162; 292,1692; 115,0543; 153,0698; 178,0776; 91,0542; 84,0807; 249,1293	1.61	0.52	0.43	-	-	-	4,92

(-): ez da detektatu

4.2 taula: *(Jarraipena).*

Konposatua	Formula molekularra (M)	m/z teorikoa ($[M+H]^+$)	MS/MS espektroko apurketa-ioi ugarienak	ΔMasa (ppm)						R_t (min)
				Gibela	Plasma	Behazuna	Burmuina	Muskulua	Zakatzak	
M16	$C_{20}H_{23}NO_2$	310,1802	231,1164; 216,0931; 58,0653; 191,0852; 219,1165; 229,1006; 292,1682; 91,0541; 178,0779; 203,0844; 84,0806; 264,1750; 249,1270	-	0,72	0,92	-	-	-	5,98
M17	$C_{20}H_{23}NO_2$	310,1802	219,1167; 264,1744; 191,0854; 178,0776; 292,1692; 91,0542; 58,0654; 84,0808; 310,1792; 247,1115; 229,1011	1,41	0,72	0,23	-	-	1,51	4,23
M18	$C_{20}H_{23}NO_2$	310,1802	219,1167; 264,1744; 310,1780; 191,0855; 58,0654; 292,1651; 178,0775; 91,0542; 84,0808; 229,1012; 247,1119	1,61	0,82	1,02	-	-	1,41	3,32
M19	$C_{20}H_{23}NO_2$	310,1802	292,1693; 247,1116; 58,0654; 219,1167; 310,1798; 264,1744; 84,0808; 221,0961; 229,1010; 207,0803; 232,0878	-	-	0,62	-	-	-	3,29
M20	$C_{19}H_{21}NO_2$	296,1645	219,1166; 191,0854; 250,1587; 178,0776; 193,1011; 91,0542; 70,0651; 229,1010; 247,1111; 278,1527; 260,1430	0,98	-	-1,08	-	-	1,50	4,16
M21	$C_{19}H_{21}NO_2$	296,1645	219,1166; 250,1591; 191,0854; 178,0776; 91,0542; 193,1012; 264,2070; 247,1116; 296,2331; 70,0652; 229,1010; 278,1507	1,91	-	-	-	-	-	3,20
M22	$C_{20}H_{21}NO_2$	308,1645	229,1010; 219,1166; 91,0542; 58,0653; 247,1115; 217,1010; 178,0776; 191,0854; 207,0802; 308,1629; 84,0807; 290,1537	-	1,44	0,35	-	-	-	6,15
M23	$C_{18}H_{20}O_2$	269,1536	116,1070; 58,0654; 137,0458; 154,0533; 99,0805; 228,2322; 211,1105	3,33	-	-	-	-	-	0,72
M24	$C_{26}H_{31}NO_8$	470,2174	276,1743; 231,1167; 58,0653; 294,1849; 216,093; 84,0808; 191,0855; 205,1010; 203,0849; 117,0697; 249,1276	0.55	-	1.26	-	-	-	3,90

(-): ez da detektatu

4.2 taula: *(Jarraipena).*

Konposatua	Formula molekularra (M)	m/z teorikoa ($[M+H]^+$)	MS/MS espektroko apurketa-ioi ugarienak	ΔMasa (ppm)						R_t (min)
				Gibela	Plasma	Behazuna	Burmuina	Muskulua	Zakatzak	
M25	$C_{26}H_{31}NO_7$	470,2174	276,1743; 231,1167; 58,0654; 294,1849; 216,0931; 191,0855; 84,0808; 205,1011; 249,1277; 117,0698; 203,0861	-	0,16	0,81	-	-	-	3,95
M26	$C_{26}H_{31}NO_7$	470,2174	276,1742; 231,1167; 58,0654; 294,1850; 216,0932; 84,0808; 191,0853; 205,1015; 249,1287; 203,0852; 117,0695	0,48	-0,10	0,87	-	-	-	3,74
M27	$C_{26}H_{31}NO_7$	470,2174	231,1167; 262,1588; 216,0932; 191,0855; 70,0651; 276,1744; 205,1011; 229,1012; 153,0698; 115,0542; 294,1844	-	-	0,09	-	-	-	4,64
M28	$C_{26}H_{31}NO_7$	470,2174	231,1167; 262,1588; 216,0933; 191,0854; 70,0652; 205,1011; 153,0698; 229,1015; 115,0543; 276,1757; 203,0851	-	-	-0,69	-	-	-	5,03
M29	$C_{26}H_{31}NO_7$	470,2174	294,1849; 249,1272; 470,2184; 105,0699; 155,0855; 84,0808	-	-	-0,69	-	-	-	3,48
M30	$C_{26}H_{31}NO_8$	486,2123	292,1693; 247,1116; 58,0654; 310,1799; 468,2013; 207,0803; 84,0808; 219,1181	-	-	-0,20	-	-	-	2,22
M31	$C_{26}H_{31}NO_8$	486,2123	231,1168; 250,1589; 219,1168; 58,0654; 191,0856; 216,0935; 278,1540; 310,1805; 292,1697; 178,0777	-	-	-0,83	-	-	-	4,22
M32	$C_{25}H_{29}NO_7$	456,2017	262,1588; 231,1167; 216,0933; 191,0855; 70,0652; 205,1010; 153,0703; 219,1163; 115,0541	-	-	0,04	-	-	-	3,91
M33	$C_{25}H_{29}NO_7$	456,2017	262,1588; 231,1168; 216,0933; 191,0856; 70,065; 205,1012; 153,0698; 219,1165; 115,0542	-	-	0.31	-	-	-	3,77

(-): ez da detektatu

M1 metabolitoa nortriptilina izenez ezagutzen den amitriptilinaren *N*-desmetilazio gisa identifikatu da. Nortriptilinaren egitura erreferentziazko estandarra erabilita konfirmatu dugu, 4.2 taulako masa zehatzak (*m/z*), erretentzio-denborak eta MS/MS espektroak bat egiten dutela egiaztatuta. M1 metabolitoaren identifikazioa *m/z* 233, 218, 205, 191, 179, 155, 129, 115, 117, 105, 91 eta 70 apurketa-ioien arabera burutu da. Apurketa-ioi gehienak amitriptilinaren berdinak (ikus amitriptilinaren apurketa 4.3 irudian) diren arren, bi desberdintasun nagusi azpimarratu behar dira. Alde batetik, *m/z* 70 ($[C_4H_6N]^+$) apurketa-ioiak iradoki du egiturako albo-katean amitriptilinak baino metilo talde bat gutxiago daukala ($[84 - CH_2]^+$). Beste aldetik, *m/z* 58 apurketa-ioia ez egoteak amina taldea eraldatua izan dela adierazi du.

Lan honetan nortriptilina ehun eta jariakin biologiko guztietan behatu den arren, ez da inoiz metabolito ugariena izan. Emaitza hori harrigarria izan da kontuan hartuta amitriptilinaren *N*-desmetilazioa dela metabolizazio-bide nagusiena giza gibeleko mikrosometan [19]. Era berean, giza gibeleko mikrosometan behatu den *N,N*-didesmetilazioa [19,20] ez dugu lan honetan detektatu. Desberdintasun horiek espezieen arteko aldakortasunari egotzi ahal zaizkio, edo baita *in vivo* eta *in vitro* metabolizazio-bideen arteko desberdintasunei. Nahiz eta desberdintasun horiek egon daitezkeen, giza behaketekin bat eginda [2], urraburu arrainetan ere oxidazioa izan da amitriptilinaren metabolizazio-bide nagusiena. Amitriptilinaren eta nortriptilinaren 5 eratorri monohidroxilatu (M2-M6) eta amitriptilinaren metabolito *N*-oxidatua (M7) behatu dira (ikus 4.3 irudia). Egitura guzti horiek bat datoz amitriptilinarekin burututako *in vitro* esperimentuetan behatutakoekin [19,20]. Azpimarratzekoa da, lan honetan, M2 eta M3 izan direla metabolito guztietatik ugarienak, gailur-azaleren erkaketa erlatiboan oinarrituta (ikus 4.3.3 atala).

M2-M3 (*m/z* 294,1857) eta M4-M5 (*m/z* 280,1701) amitriptilinaren eta nortriptilinaren erdiko eraztuneko etileno talde endoziklikoaren metabolito monohidroxilatu gisa identifikatu dira, hurrenez hurren. M2-M3 metabolitoen egituren esleipena 4.4a irudian ikus daitezkeen honako apurketa-ioietan oinarrituta egin da: *m/z* 276 ($[294 - H_2O]^+$), *m/z* 249 ($[294 - C_2H_7N]^+$), *m/z* 231 ([amitriptilina - C_2H_7N-H_2]$^+$), *m/z* 216 ([amitriptilina – $C_3H_{10}N$-H_2]$^+$), *m/z* 203 ([amitriptilina – $C_4H_{11}N$-H_2]$^+$) eta *m/z* 84 ($[C_5H_{10}N]^+$). Izatez, *m/z* 276, *m/z* 249 eta *m/z* 231 apurketa-ioiek ez dute zehazten hidroxilazioa amitriptilinaren etileno talde exoziklikoan edo endoziklikoan gertatu den, baina *m/z* 216 ($[218\text{-}H_2]^+$) eta *m/z* 203 ($[205\text{-}H_2]^+$) apurketa-ioiak behatzeko aukera bakarra hidroxilazioa

erdiko eraztunean gertatu izana da. Gainera, *m/z* 84 apurketa-ioiak albo-katea eraldatu ez dela eta amitriptilinaren egituran bezala jarraitzen duela (ikus amitriptilinaren apurketa 4.3 irudian) adierazten du. Bestalde, *m/z* 249 ([294 – C_2H_7N]$^+$) apurketa-ioia amitriptilinan dagoen *m/z* 233 apurketa-ioiaren oxidazioari dagokio (([233+O]$^+$) = *m/z* 249), oxidazioa molekularen erdiko eraztunean edo albo-katean (nitrogeno atomoaren eta erdiko eraztunaren arteko hiru karbonoko gunean) gertatu den zehaztu gabe. Amitriptilinaren etileno talde endoziklikoaren hidroxilazioa oso ondo deskribatuta dago bibliografian [2]. Era berean, M4-M5 metabolitoek antzeko apurketa-patroia erakutsi dute, eta etileno talde endoziklikoan ur-galera gertatu dela adierazten duten *m/z* 262 (ur-galera), *m/z* 231 ([233-H_2]$^+$) eta *m/z* 216 ([218-H_2]$^+$) apurketa-ioien presentziak hidroxilazioa erdiko eraztunean gertatu dela aditzera ematen du. Azkenik, eraldatu gabeko *m/z* 70 apurketa-ioiak adierazten du nortriptilinaren hidroxilazioa erdiko eraztuneko etileno taldean gertatu dela.

Bestalde, M6 (*m/z* 294,1857) ere amitriptilinaren metabolito monohidroxilatu gisa identifikatu da, baina etileno talde exoziklikoan. 4.4b irudian beha daitekeenez, M2-M3 metabolitoen apurketarekin erkatuz, M6 metabolitoarenean *m/z* 98 apurketa-ioiaren presentzia nabarmendu behar da. Beste behin, nahiz eta *m/z* 276, *m/z* 249 eta *m/z* 231 apurketa-ioiek ez duten zehazten hidroxilazioa amitriptilinaren etileno talde exoziklikoan edo endoziklikoan gertatu den, *m/z* 98 ([$C_6H_{14}N$]$^+$) apurketa-ioiak albo-katea eraldatu dela adierazten du. M6 metabolitoaren apurketa-ioien espektroan (ikus 4.4b irudia) *m/z* 216 ([amitriptilina – $C_3H_{10}N$-H_2O]$^+$) eta *m/z* 84 ([$C_5H_{10}N$]$^+$) apurketa-ioiak ere beha daitezkeen arren, *m/z* 98 apurketa-ioiaren ugaritasun handiagoari lehentasuna eman zaio egitura proposatzeko.

M7 (*m/z* 294,1857) amitriptilinaren *N*-oxidazioaren metabolito gisa identifikatu da, amitriptilinoxido izenez ezagutzen dena. Horretarako, apurketetan ur-galerarik behatu ez izana eta amitriptilinaren eskeletoa berdin mantentzearen adierazgarri diren *m/z* 233 eta *m/z* 218 apurketa-ioien presentzia (ikus amitriptilinaren apurketa 4.3 irudian) hartu dira kontuan. *N*-metilo taldearen oxidazio-produktua beharrean, M7 *N*-oxidazioaren azpiproduktua dela uste da *m/z* 58 ([C_3H_8N]$^+$) apurketa-ioiaren presentziak amina tertziarioaren eraldaketa gertatu ez dela adierazten duelako eta ez delako *m/z* 264 ([amitriptilina +O-CH_2O]$^+$) apurketa-ioia ageri.

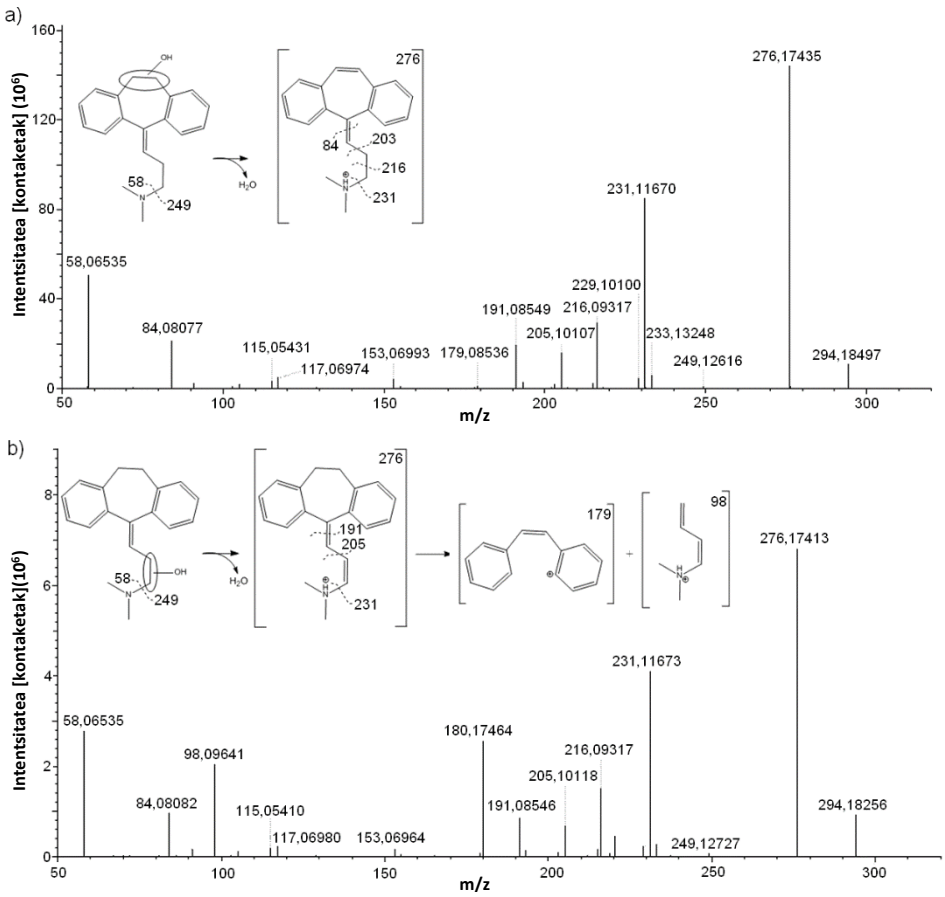

4.4 irudia: *a) M2-M3, eta b) M6 metabolitoen MS/MS espektroak eta apurketa-mekanismoak.*

M8 (*m/z* 276,1752), apurketa-patroian behatutako antzekotasunengatik, M2-M3 metabolitoen deshidrataziotik eratu da. Amitriptilinaren metabolito deshidrogenatu bat dela ondorioztatzera *m/z* 276 ($[278\text{-}H_2]^+$), *m/z* 231 ($[233\text{-}H_2]^+$) eta *m/z* 216 ($[218\text{-}H_2]^+$) apurketa-ioiek eraman gaituzte. Nahiz eta *m/z* 276 eta *m/z* 231 apurketa-ioiek ez duten zehazten deshidrogenazioa etileno talde endoziklikoan edo exoziklikoan gertatu den, *m/z* 216 ($[218\text{-}H_2]^+$) apurketa-ioia azaltzeko aukera bakarra deshidrogenazioa erdiko eraztuneko etileno taldean gertatu izana da. Deshidrogenazioa albo-kateko etileno taldean gertatu dela ondorioztatzera eraman gaitzakeen *m/z* 98 apurketa-ioiaren seinalea *m/z* 216 eta *m/z* 84 apurketa-ioiena baino askoz baxuagoa denez, deshidrogenazioa erdiko eraztunean gertatu dela ondorioztatu da. M8 metabolitoaren antzera, M9 (*m/z* 262,1595) nortriptilinaren metabolito hidroxilatuen (hau da, M4-M5 metabolitoen) deshidrataziotik eratu izana aukerarik probableena da. Nortriptilinaren

deshidrogenazio-metabolitoa dela ondorioztatzera *m/z* 262 ($[264\text{-}H_2]^+$, *m/z* 231 ($[233\text{-}H_2]^+$) eta *m/z* 216 ($[218\text{-}H_2]^+$) apurketa-ioiek eraman gaituzte. Horrez gain, MS/MS espektroan *m/z* 70 apurketa-ioia agertzeak nortriptilinaren albo-katea eraldatu ez dela adierazten du eta, ondorioz, deshidrogenazioa erdiko eraztunean gertatu dela. Bai M8 eta bai M9 metabolitoak giza gibeleko mikrosomak erabilita burututako *in vitro* esperimentuetan identifikatu dira [20].

M10 eta M11 (*m/z* 292,1701) amitriptilinaren erdiko eraztuneko keto-deribatu gisa identifikatu dira, *in vitro* esperimentuetan behatutako metabolitoen antzera [19,20]. 4.5a irudiko MS/MS espektroari erreparatuta, ugaritasun baxuko *m/z* 274 apurketa-ioia bat dator ur-galerarekin ($[292\text{-}H_2O]^+$), eta ur-galera hori keto taldearen forma enolikoari egokitu dakioke. Era berean, *m/z* 247 ($[233+O\text{-}H_2]^+$), *m/z* 229 ($[233\text{-}H_2\text{-}H_2]^+$) eta *m/z* 219 ($[233\text{-}CH_2]^+$) apurketa-ioiek oxigenazio-deshidrogenazio batekin konbinatuta gertatu dela adierazten dute. Dena dela, apurketa-ioi horiek ez dute zehazten keto taldea etileno talde endoziklikoan edo exoziklikoan kokatuta dagoen. Hala ere, amitriptilinaren albo-katea eraldatu ez denaren adierazgarri diren *m/z* 84 eta *m/z* 58 apurketa-ioien ugaritasun altuek keto taldea erdiko eraztunean kokatuta dagoela aditzera ematen dute.

M12 metabolitoak M10-M11 metabolitoen masa zehatz berdina du (*m/z* 292,1701) eta haren MS/MS espektroan oinarrituta (ikus 4.5b irudia), nortriptilinaren deshidrogenazio gehi metoxilazio produktua proposatu da. M10-M11 metabolitoen apurketarekin erkatuta, ur-galeraren ezak, *m/z* 84 ($[C_5H_{10}N]^+$) eta *m/z* 58 ($[C_3H_8N]^+$) apurketa-ioien faltak, eta *m/z* 260 ($[C_{19}H_{18}N]^+$), *m/z* 203 ($[C_{16}H_{11}N]^+$), *m/z* 82 ($[C_5H_8N]^+$) eta *m/z* 70 ($[C_4H_8N]^+$) apurketa-ioien presentziak etileno taldeko deshidrogenazioa gehi metanol taldearen galera gertatu direla iradokitzen dute. Esaterako, *m/z* 203 ($[205\text{-}H_2]^+$) apurketa-ioiak deshidrogenazioa erdiko eraztuneko etileno talde endoziklikoan gertatu dela adierazten du. Horrek, eraztunetan oxigenazioa gertatu dela adierazten duen apurketa-ioien ezarekin batera, M12 metabolitoan behatutako deshidrogenazioa erdiko eraztunean egon behar dela adierazten du. Gainera, *m/z* 70 apurketa-ioia ohikoa da nortriptilinaren apurketan. Beraz, honek, CH_3OH-ren galerarekin lotuta dagoen *m/z* 260 apurketa-ioiaren presentziarekin batera, metoxi taldearen presentzia etileno talde exoziklikoan dagoela esan nahi du. Hala ere, egitura horrekin ez gara gai *m/z* 82 ($[C_5H_8N]^+$) eta *m/z* 232 apurketa-ioien presentzia azaltzeko.

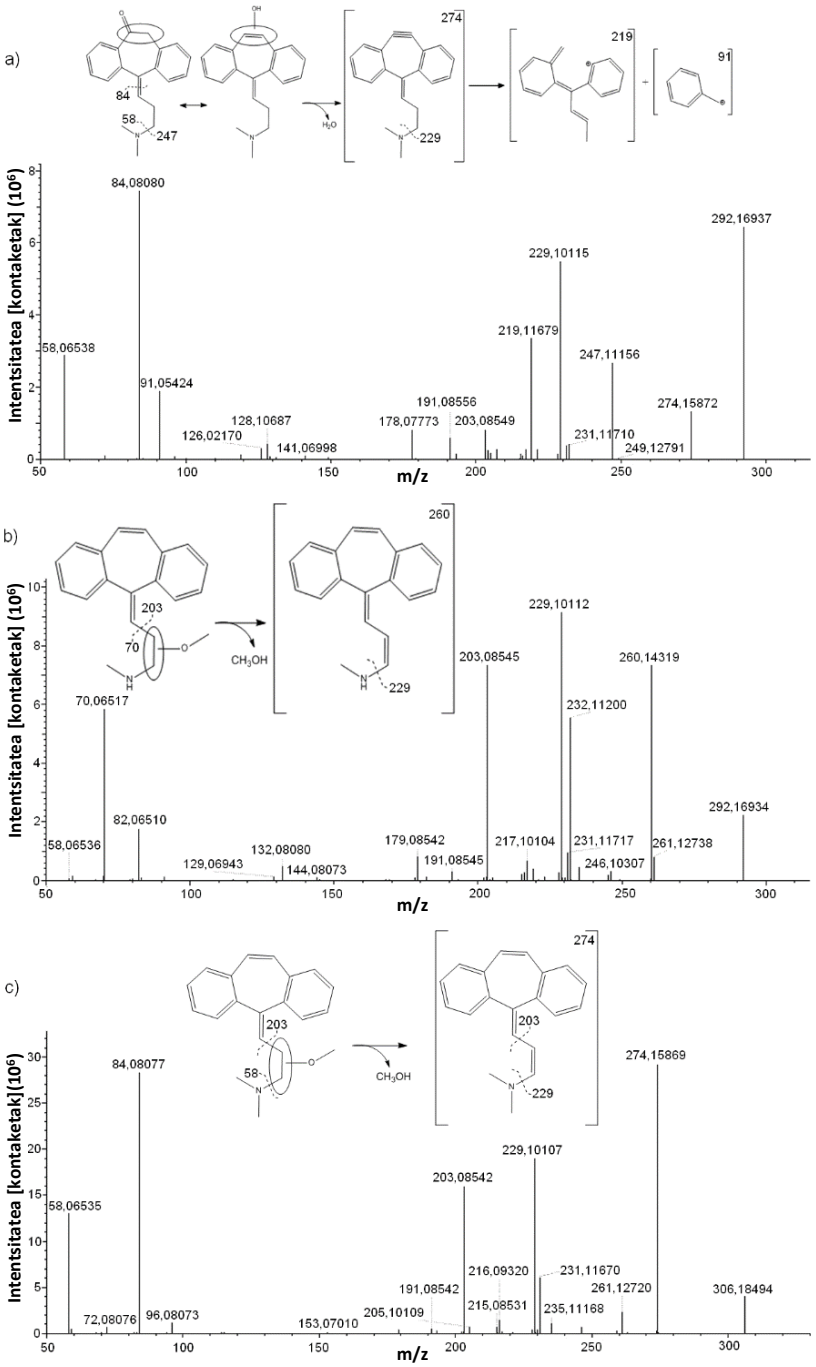

4.5 irudia: *a) M10-M11, b) M12 eta c) M13 metabolitoen MS/MS espektroak eta apurketa-mekanismoak.*

M13 metabolitoak, *m/z* 306,1857 masa zehatzarekin ($C_{21}H_{23}NO$), M12 metabolitoaren antzeko egitura erakutsi du, baina amina tertziarioa amitriptilinan bezala (*m/z* 58), eraldatu gabe. 4.5c irudian beha daitekeenez, *m/z* 274 (306-$[CH_3OH]^+$), *m/z* 229 eta *m/z* 203 ($[205\text{-}H_2]^+$) apurketa-ioiak dira M13 metabolitoaren bereizgarri. Esaterako, *m/z* 203 ($[205\text{-}H_2]^+$) apurketa-ioiak lotura bikoitzaren presentzia adierazten du erdiko eraztuneko etileno talde endoziklikoan. Hala ere, egitura horrekin ez gara gai *m/z* 84 apurketa-ioia azaltzeko.

M14 metabolitoa (*m/z* 278,2544) M9 metabolitoaren epoxidazioari dagokio, *m/z* 260 (278-$[H_2O]^+$), *m/z* 247, *m/z* 219, *m/z* 203 eta *m/z* 70 apurketa-ioien presentziagatik. Zhou-k eta lankideek ere deskribatu dituzte epoxidazio-metabolitoak bitartekari gisa [20] eta ziklobenzaprinaren degradazioaren inguruko ikerketa batean ere behatu dira epoxidazio-metabolitoak [38].

Beste alde batetik, muskuluan eta burmuinean izan ezik, gainontzeko matrize biologiko guztietan identifikatu dira metabolito dioxidatuak. Amitriptilinaren bost metabolito dioxidatu (M15-M19; *m/z* 310,18066) eta nortriptilinaren beste bi (M20 eta M21; *m/z* 296,1650). Zhou-ren eta lankideen emaitzekin erkatuta [20], lan honetan ez dugu aurkitu metabolito dihidroxilaturik non hidroxilo taldeetako bat erdiko eraztuneko etilenoan dagoen eta bestea eraztun aromatikoan. Horren arrazoia espezieen arteko aldakortasunetik edo *in vivo* eta *in vitro* metabolizazio-bideen arteko desberdintasunetatik etor daiteke [20].

M15 eta M16 metabolitoek oso antzeko apurketa-patroia erakutsi dute, ur-galera bakarrarekin (*m/z* 292) eta *m/z* 249, *m/z* 231, *m/z* 216, *m/z* 84 eta *m/z* 58 apurketa-ioien presentziarekin. Ur-galerak eta *m/z* 249 eta *m/z* 231 apurketa-ioiek hidroxilazio bat etileno taldeetako batean gertatu dela adierazten duten bitartean, *m/z* 216 apurketa-ioiak erdiko eraztuneko etilenoari dagokiola zehazten du. Bigarren oxidazioari dagokionez, *m/z* 231 eta *m/z* 216 apurketa-ioien presentzia ez denez bateragarria hidroxilazio aromatikoarekin, bigarren oxigenoa amitriptilinaren amina tertziarioan kokatuta egon behar da. Gainera, *m/z* 84 eta *m/z* 58 apurketa-ioiak behatu direnez, *N*-oxidazioa proposatu da.

M17-M19 amitriptilinaren etileno talde endoziklikoko dihidroxi-metabolito gisa identifikatu dira *m/z* 292 ($[310\text{-}H_2O]^+$), *m/z* 247 ($[233+O\text{-}H_2]^+$), *m/z* 264 ($[C_{19}H_{22}N]^+$), *m/z* 219 ($[C_{17}H_{15}N]^+$), *m/z* 84 ($[C_5H_{10}N]^+$) eta *m/z* 58 ($[C_3H_8N]^+$) apurketa-ioietan oinarrituta (ikus 4.6a irudia). Ur-galerak (*m/z* 292) eta eraldatu gabeko albo-kateak (*m/z* 84 eta *m/z* 58) hidroxilo taldea erdiko eraztuneko

etileno taldean dagoela iradokitzen dute. Bigarren hidroxilo taldea kokatzeko *m/z* 264 ([amitriptilina-CH_2]$^+$) eta *m/z* 219 ([233-CH_2]$^+$) apurketa-ioiak nabarmendu behar dira. Hain zuzen, 4.6a irudian ikus daitekeen bezala, apurketa-ioi horiek erdiko eraztuna apurtzearen ondoren eragindako desmetilazioari dagozkio. Bestalde, bigarren ur-galera ez detektatzeko arrazoia intentsitate baxuari atxiki dakioke. Izan ere, erdiko eraztunean, bigarren ur-galeraren ondorioz, egonkortasun baxuko lotura hirukoitza eratzen da. Horregatik, bigarren ur-galerari dagokion apurketa-ioia ez behatzerakoan, bigarren hidroxilo taldea ere erdiko eraztuneko etilenoan dagoela ondorioztatu dugu. Egitura hauek *in vitro* esperimentuetan ere behatu dituzte [20].

M20-M21 nortriptilinaren etileno talde endoziklikoko dihidroxi-metabolito gisa identifikatu dira. M17-M19 metabolitoen antzera, bi hidroxilo taldeak erdiko eraztuneko etileno taldean kokatuta daudela ondorioztatu da ondoko apurketa-ioiak kontuan izanda: *m/z* 278 ([296-H_2O]$^+$), *m/z* 260 ([278-H_2O]$^+$), *m/z* 247 ([233+OH-H_2]$^+$), *m/z* 250 ([$C_{18}H_{20}N$]$^+$≡[nortriptilina-CH_2]$^+$), *m/z* 219 ([233-CH_2]$^+$) eta *m/z* 70 (albo-katea eraldatu gabe). M20 metabolitoan bigarren ur-galera adierazten duen apurketa-ioia (*m/z* 260) oso ahula denez, eta *m/z* 250 eta *m/z* 219 apurketa-ioiak erdiko eraztunaren etileno taldea apurtzearekin erlazionatuta daudenez, bi hidroxilo taldeak etileno endoziklikoan kokatzea proposatu da (ikus 4.6b irudia). M21 metabolitoak antzeko apurketa erakutsi du, baina bigarren ur-galeraren apurketa-ioia ez da behatu, ziurrenik M21 metabolitoaren MS/MS espektroko apurketa-ioien intentsitate baxuagoagatik. Beraz, M21 ere nortriptilinaren erdiko eraztuneko dihidroxi-metabolito gisa definitu da.

M22 metabolitoak (*m/z* 308,1650) M10-M11 metabolitoen antzeko apurketa-patroia erakutsi du eta, nahiz eta seinale oso baxuan agertzen den, ur-galerari dagokion apurketa-ioia (*m/z* 290 =[308-H_2O]$^+$) detektatu da. Metabolito horrek keto taldea dauka etileno talde endoziklikoan eta bigarren oxidazioa *N*-oxidazio gisa determinatu da ez delako bigarren ur-galerarik behatu eta albo-katea ez delako eraldatu. Ondorioz, M22 metabolitoa M15-M16 metabolitoen deshidrogenazio-produktua edo M10-M11 metabolitoen *N*-oxidazio-produktua izan daiteke.

M23 metabolitoa (*m/z* 269,1541) amitriptilinatik zein nortriptilinatik eratorritakoa izan daiteke, (-C_2H_6N) edo (-CH_3N) taldeak galdu ondoren, hurrenez hurren, jarraian dihidroxilazioa pairatuta. Hala ere, lortutako MS/MS apurketa-espektroa oso pobrea izan denez, metabolito horretan ezin izan dugu zehaztu bi hidroxilo taldeen kokapena.

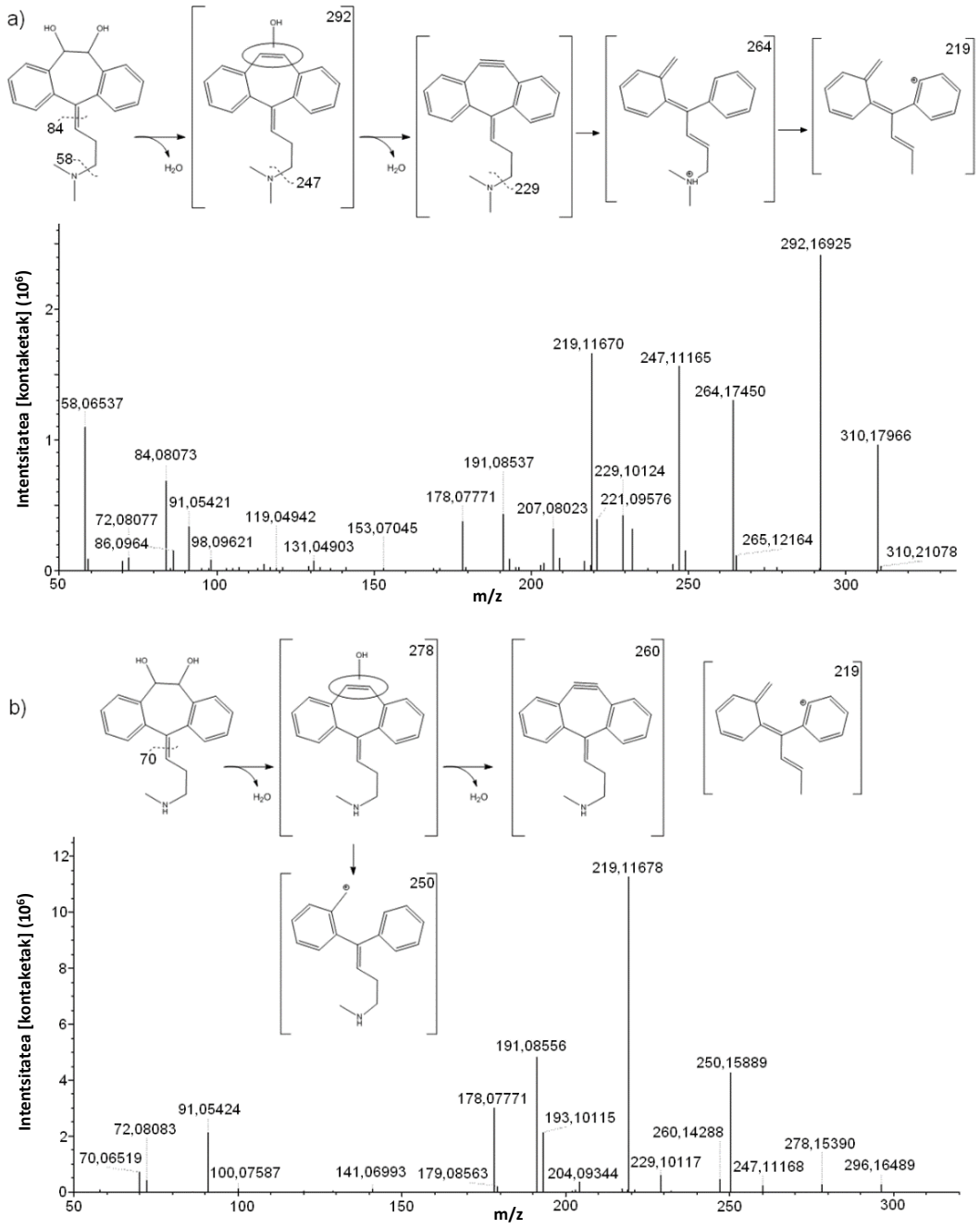

4.6 irudia: *a) M17-M18-M19 eta b) M20 metabolitoen MS/MS espektroak eta apurketa-mekanismoak.*

Azkenik, hamar glukuronido-eratorri behatu dira, nagusiki behazunean (M24-M33), eta horietatik zazpi (M24-M26, M29, M30, M32 eta M33) Zhou-k eta lankideek giza gernuan aurkitutakoak dira [20]. Bestalde, bibliografian deskribatuta dagoen arren [2,19,20], lan honetan ez dugu behatu amitriptilinaren *N*-glukuronidaziorik. Diferentzia hori ugaztunen metabolismoan glukuronidazio-prozesua desberdina izatetik [21] edo *in-vivo* eta *in-vitro* azterketen arteko aldakortasunetik etor daiteke. Zenbait kasutan glukuronido taldearen posizioa zehaztu ahal izan dugun arren, kasu guztietan ez da posible izan konjugazioa non gertatu den (*N*- edo *O*-glukuronidazioa) determinatzea eta hori ohikoa da bibliografiaren arabera [39].

M24-M26 (*m/z* 470,2178) metabolitoak M2-M3 metabolitoen glukuronido gisa identifikatu dira, behin glukuronido taldea galduta (-176 Da) M2-M3 metabolitoen apurketa-patroi berdina dutelako. Emaitza horrek bat egiten du bibliografiarekin, Zhou-k eta lankideek ere hiru glukuronido-eratorri aurkitu baitzituzten hidroxiloa posizio horretan egonda [20]. Edonola ere, apurketa-ioietatik ezin izan da ondorioztatu konjugazioa non (*N*- edo *O*- glukuronidazioa) gertatu den.

Bestalde, M27 eta M28 metabolitoen (*m/z* 470,2178) *m/z* 276 (ugaritasun baxukoa) eta *m/z* 216 apurketa-ioiek erdiko eraztunean hidroxilo taldea dagoela adierazten dute (ikus 4.7 irudia). Hala ere, oxidazio-posizio horretan egonda ezin dira azaldu ugaritasun altuko *m/z* 262 eta *m/z* 70 apurketa-ioiak. Izatez, nortriptilinaren ohikoa den *m/z* 70 apurketa-ioia eta *m/z* 262 azaltzeko modu bakarra M27-M28, amitriptilinaren glukuronidoak beharrean, nortriptilinaren etileno talde endoziklikoan metoxi taldea duen metabolitoaren *N*-glukuronidoak izatea da. Modu horretan, metoxi taldearen galerarekin, intentsitate altuko *m/z* 261 (294-$[CH_3OH]^+$) apurketa-ioia azaldu daiteke.

Nahiz eta lan honetan amitriptilinaren metabolito monohidroxilaturik ez den behatu eraztun aromatikoan, M29 metabolitoa (*m/z* 470,2178) amitriptilinaren eraztun aromatikoaren metabolito hidroxilatuaren glukuronido gisa identifikatu da *m/z* 249 ($[233+O]^+$) apurketa-ioia behatu delako baina ur-galerarik ez. M30 metabolitoa (*m/z* 486,2127) M17-M19 metabolitoen glukuronidazioari egotzi zaio *m/z* 292 (ur-galera) eta *m/z* 247 ($[231+O]^+$) apurketa-ioien presentziagatik. M31 (*m/z* 486,2127) glukuronidoaren egitura ezin izan dugu definitu. Nahiz eta *m/z* 292 eta *m/z* 216 apurketa-ioiek aditzera ematen duten hidroxilo taldeetako bat erdiko eraztuneko etileno taldean

kokatzen dela, ezin izan dugu azaldu *m/z* 250 eta *m/z* 278 apurketa-ioien presentzia. Azken hori hobeto azaltzen da M31 nortriptilinaren metoxi-metabolitoaren glukuronidoa bada. Azkenik, soilik behazunean behatutako M32-M33 metabolitoak (*m/z* 456,2022) M4-M5 metabolitoen (nortriptilinaren monohidroxilatuen) glukuronidoei lotu zaizkie apurketa-patroian erakutsitako antzekotasunean oinarrituta.

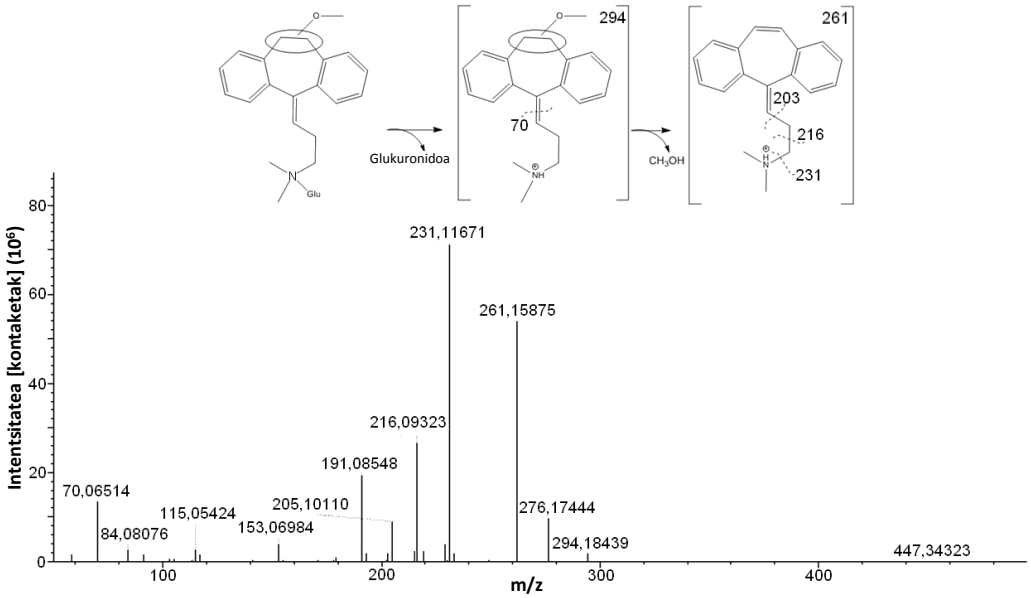

4.7 irudia: *M27-M28 metabolitoen MS/MS espektroa eta apurketa-mekanismoa.*

4.3.4 Metabolito-profilen aldaketak denborarekin eta ehun desberdinetan

Amitriptilinaren metabolitoak behazunean (29), gibelean (21) eta plasman (19) behatu dira nagusiki (ikus 4.2 taula). Hau ez da harritzekoa kontuan izanik gibela dela farmakoen metabolizazioaren gune nagusia eta bertan sortutako metabolitoek zirkulazio sistemikoa (plasmaren bidez, adibidez) edo eliminazioa (behazunaren bidez) pairatuko dutela. Behazunak hesteetan eta gibelean sortutako metabolitoak biltzen ditu eta normala da bertan metabolito gehien behatzea.

Ehun/jariakin biologiko desberdinetan amitriptilinaren eta bere metabolitoen ugaritasuna erkatu ahal izateko hurbilketa bat egin behar izan dugu, metabolitoen estandarrak ez baititugu eskuragarri. Hurbilketa horretan, konposatu bakoitzak duen seinalea hartu dugu erantzun analitiko

gisa, eta ugaritasunak zehazterako orduan detektagailuak konposatu bakoitzarentzat duen sentikortasuna edo seinale instrumentala berdintzat jo dugu. Beraz, emaitza hauek kualitatibotzat hartu behar dira, konposatu bakoitzaren analisiko erantzuna desberdina izan daitekeelako. 4.8 irudian ikus daitezke esposizio-egun bakoitzerako ehun eta jariakin desberdinetan kalkulatutako amitriptilinaren eta metabolitoen abundantzia erlatiboak (gailurren azaleren batuketaren portzentaje gisa kalkulatuta). Gailurren azalera guztiak laginaren kantitatea eta isotopikoki markatutako estandarra ($^2H_3$-NOR) erabilita zuzendu dira. Ehunen eta jariakinen artean metabolito-profiletan desberdintasun nabarmenak behatu diren bitartean, ehun/jariakin bakoitzeko profil erlatiboa nahiko konstante mantendu da esperimentuan zehar.

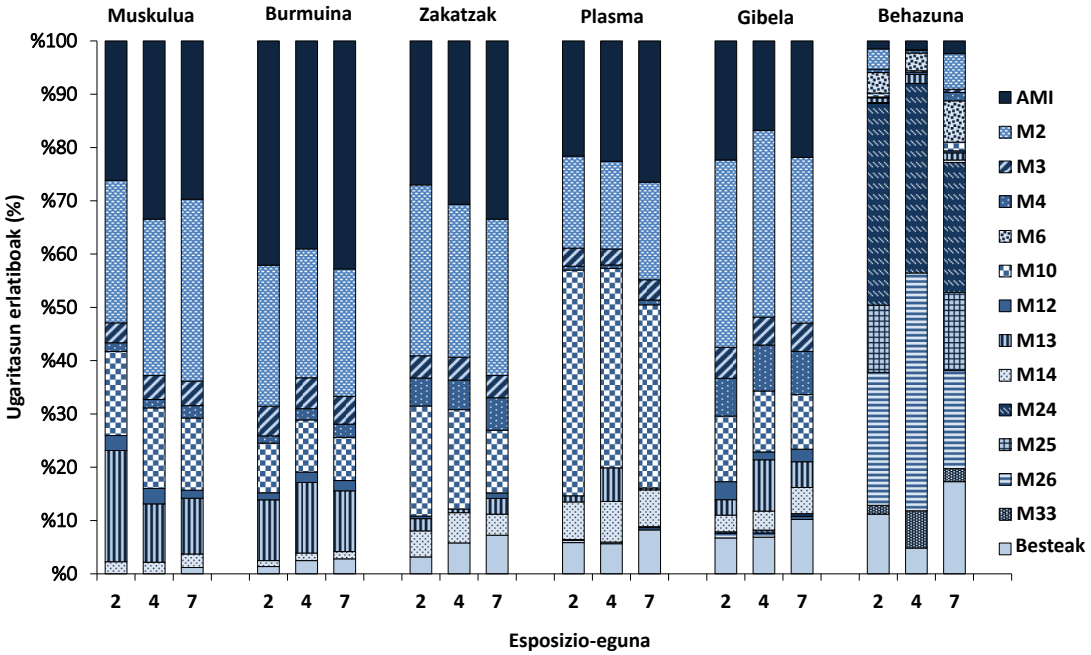

4.8 irudia: *Esposizio-esperimentuan zehar (2., 4. eta 7. egunetako) amitriptilinaren (AMI-ren) eta bere metabolitoen abundantzia erlatiboak (gailurren azaleren batuketaren portzentaje gisa kalkulatuta) ehun (muskulu, burmuin, zakatz eta gibel) eta jariakin (plasma eta behazun) biologikoetan.*

Haren metabolitoekin alderatuta, zakatzetan eta burmuinean konposaturik ugariena amitriptilina bera dela (% 30 eta % 40, hurrenez hurren) ikusi da. Zakatzetan amitriptilinaren absortzioa gertatzen da eta, ondorioz, konposatuaren kontzentrazio altuak espero dira. Bestalde, burmuinera heltzeko amitriptilinak eta bere metabolitoek muga hematoentzefalikoa zeharkatu

behar dute difusioz, eta prozesu hori errazago gertatzen da amitriptilinarentzat 1. Faseko eta 2. Faseko metabolito polarragoentzat baino [10]. Amitriptilinaren ondoren, M2 (% 24) eta M13 (% 11) izan dira burmuinean ugaritasun handieneko metabolitoak. Gibelean eta plasman, konposatu guztien azaleren baturaren % 20 inguru hartzen du amitriptilinak, gibelaren metabolizazio-funtzioa eta plasmaren banaketa-funtzioa azpimarratuta. Gibelaren kasuan M2 amitriptilinaren eratorri monohidroxilatua izan da metabolitorik ugariena (% 30), eta plasman, ordea, M2 metabolitoaren deshidrogenazio-produktua den M10 metabolitoa (% 33). Kontrara, behazunean, amitriptilina oso portzentaje txikian agertu da (% 2) eta 2. Faseko M24 eta M26 glukuronido eratorriak izan dira ugarienak (% 30), hain zuzen ere, M2-M3 monohidroxi-metabolitoen eratorriak direnak.

4.4 Ondorioak

Biologikoki aktiboak izan daitezkeen azpiprodukturen agerpenak zaildu egiten du ur-ingurumeneko farmakoen agerpenarekin lotutako arriskuen ebaluazioa. Gainera, konposatu horiek ez dute zertan hasierako farmakoen segurtasun-ebaluazioetan aurkitutakoen berdinak izan behar. Izan ere, ingurumenean gertatzen diren erreakzio-motak oso desberdinak eta ingurumeneko baldintzen menpekoak edota biotransformazioa eragin duen espeziearen araberakoak izan daitezke. Uretako faunan farmakoen esposizioa osotasunean karakterizatzeko, beharrezkoa da bioaktiboak izan daitezkeen egitura anitzak eta haien ehunen arteko banaketa ezagutzea. Lan honetan, amitriptilina nagusiki burmuinean metatu da eta, bertan, soilik 10 metabolito aurkitu diren bitartean, gibelean 21 metabolito detektatzeaz gain, amitriptilinak % 20 inguruko ugaritasun erlatiboa du soilik. Ondorioz, soilik muskuluan edo gibelean fokatzen diren ur-ingurumeneko ohiko esposizio-azterketek larriki gutxietsi lezakete amitriptilinaren kontzentrazioa bere jomuga-organoan (burmuinean). Bestalde, soilik amitriptilinan fokatzen diren ohiko esposizio-azterketek ez dituzte inondik inora aintzat hartzen organismoaren ehun/jariakin desberdinetako azpiprodukturen kontzentrazioak nahiz eta biologikoki aktiboak izan daitezkeen. Izatez, azken datuek iradokitzen dute nortriptilinaren eta amitriptilinaren metabolito hidroxilatuak eta *N*-oxidatuak aktiboak izan daitezkeela ugaztunetan [2,40–42]. Datu guzti horietatik nabarmendu daiteke funtsezkoa dela farmakoen azpiprodukturen determinazioa burutu eta haien

efektuen azterketa ingurumeneko arriskuen ebaluazioan egitea. Dena den, erronka hori zailago bihurtzen da azpiproduktu askorentzat ez dagoelako eskuragarri erreferentziazko estandarrik. Hala ere, erreferentziazko estandarren faltan, bioaktiboak izan daitezkeen metabolito berrien identifikazio kualitatiboa burutzeko eraginkorra izan daiteke doktorego-tesi honetan erabili den susmagarrien analisirako hurbilketa. Gainera, hurbilketa horren bitartez identifikatutako egitura garrantzitsuak aurrerago konfirmatu eta erdi-kuantifikatu ahal izango dira estandarrak eskuragarri daudenean.

4.5 Erreferentziak

1. Petrie B, Barden R, Kasprzyk-Hordern B. 2015. A review on emerging contaminants in wastewaters and the environment: Current knowledge, understudied areas and recommendations for future monitoring. *Water Res.* 72:3–27.
2. Breyer-Pfaff U. 2004. The Metabolic Fate of Amitriptyline, Nortriptyline and Amitriptylinoxide in Man. *Drug Metab. Rev.* 36:723–746.
3. Lajeunesse A, Gagnon C, Sauvé S. 2008. Determination of Basic Antidepressants and Their N-Desmethyl Metabolites in Raw Sewage and Wastewater Using Solid-Phase Extraction and Liquid Chromatography−Tandem Mass Spectrometry. *Anal. Chem.* 80:5325–5333.
4. Halling-Sørensen B, Nors Nielsen S, Lanzky PF, Ingerslev F, Holten Lützhøft HC, Jørgensen SE. 1998. Occurrence, fate and effects of pharmaceutical substances in the environment- A review. *Chemosphere*. 36:357–393.
5. Baker DR, Kasprzyk-Hordern B. 2011. Multi-residue analysis of drugs of abuse in wastewater and surface water by solid-phase extraction and liquid chromatography–positive electrospray ionisation tandem mass spectrometry. *J. Chromatogr. A*. 1218:1620–1631.
6. Calisto V, Esteves VI. 2009. Psychiatric pharmaceuticals in the environment. *Chemosphere*. 77:1257–1274.
7. Lajeunesse A, Smyth SA, Barclay K, Sauvé S, Gagnon C. 2012. Distribution of antidepressant residues in wastewater and biosolids following different treatment processes by municipal wastewater treatment plants in Canada. *Water Res.* 46:5600–5612.
8. Ziarrusta H, Mijangos L, Prieto A, Etxebarria N, Zuloaga O, Olivares M. 2016. Determination of tricyclic antidepressants in biota tissue and environmental waters by liquid chromatography-tandem mass spectrometry. *Anal. Bioanal. Chem.* 408:1205–1216.
9. Ohshima N, Kotaki H, Sawada Y, Iga T. 1994. Tissue distribution and metabolism of

amitriptyline after repeated administration in rats. *Drug Metab. Dispos.* 22:21–25.

10. Uhr M, Grauer MT, Yassouridis A, Ebinger M. 2007. Blood–brain barrier penetration and pharmacokinetics of amitriptyline and its metabolites in p-glycoprotein (abcb1ab) knock-out mice and controls. *J. Psychiatr. Res.* 41:179–188.

11. Saito K, Maekawa K, Ishikawa M, Senoo Y, Urata M, Murayama M, Nakatsu N, Yamada H, Saito Y. 2014. Glucosylceramide and Lysophosphatidylcholines as Potential Blood Biomarkers for Drug-Induced Hepatic Phospholipidosis. *Toxicol. Sci.* 141:377–386.

12. Fong PP, Ford AT. 2014. The biological effects of antidepressants on the molluscs and crustaceans: A review. *Aquat. Toxicol.* 151:4–13.

13. Minguez L, Farcy E, Ballandonne C, Lepailleur A, Serpentini A, Lebel J-M, Bureau R, Halm-Lemeille M-P. 2014. Acute toxicity of 8 antidepressants: What are their modes of action? *Chemosphere*. 108:314–319.

14. Yang M, Qiu W, Chen J, Zhan J, Pan C, Lei X, Wu M. 2014. Growth inhibition and coordinated physiological regulation of zebrafish (Danio rerio) embryos upon sublethal exposure to antidepressant amitriptyline. *Aquat. Toxicol.* 151:68–76.

15. Zenker A, Cicero MR, Prestinaci F, Bottoni P, Carere M. 2014. Bioaccumulation and biomagnification potential of pharmaceuticals with a focus to the aquatic environment. *J. Environ. Manage.* 133:378–387.

16. https://www.chemicalize.org/. 2018. chemicalize_.

17. Klosterhaus SL, Grace R, Hamilton MC, Yee D. 2013. Method validation and reconnaissance of pharmaceuticals, personal care products, and alkylphenols in surface waters, sediments, and mussels in an urban estuary. *Environ. Int.* 54:92–99.

18. Lajeunesse A, Gagnon C, Gagné F, Louis S, Čejka P, Sauvé S. 2011. Distribution of antidepressants and their metabolites in brook trout exposed to municipal wastewaters before and after ozone treatment – Evidence of biological effects. *Chemosphere*. 83:564–571.

19. Rousu T, Herttuainen J, Tolonen A. 2010. Comparison of triple quadrupole, hybrid linear ion trap triple quadrupole, time-of-flight and LTQ-Orbitrap mass spectrometers in drug discovery phase metabolite screening and identification in vitro – amitriptyline and verapamil as model compounds. *Rapid Commun. Mass Spectrom.* 24:939–957.

20. Zhou X, Chen C, Zhang F, Zhang Y, Feng Y, Ouyang H, Xu Y, Jiang H. 2016. Metabolism and bioactivation of the tricyclic antidepressant amitriptyline in human liver microsomes and human urine. *Bioanalysis*. 8:1365–1381.

21. Chiu S-HL, Huskey S-EW. 1998. Species Differences in N-Glucuronidation 1996 ASPET N-Glucuronidation of Xenobiotics Symposium. *Drug Metab. Dispos.* 26:838–847.

22. Pelkonen O, Tolonen A, Rousu T, Tursas L, Turpeinen M, Hokkanen J, Uusitalo J, Bouvier d'Yvoire M, Coecke S. 2009. Comparison of metabolic stability and metabolite identification of 55 ECVAM/ICCVAM validation compounds between human and rat liver homogenates and microsomes - a preliminary analysis. *ALTEX*. 26:214–222.

23. Nallani GC, Paulos PM, Constantine LA, Venables BJ, Huggett DB. 2011. Bioconcentration of ibuprofen in fathead minnow (Pimephales promelas) and channel catfish (Ictalurus punctatus). *Chemosphere*. 84:1371–1377.

24. Brooks BW, Chambliss CK, Stanley JK, Ramirez A, Banks KE, Johnson RD, Lewis RJ. 2005. Determination of select antidepressants in fish from an effluent-dominated stream. *Environ. Toxicol. Chem.* 24:464–469.

25. Nallani GC, Edziyie RE, Paulos PM, Venables BJ, Constantine LA, Huggett DB. 2016. Bioconcentration of two basic pharmaceuticals, verapamil and clozapine, in fish. *Environ. Toxicol. Chem.* 35:593–603.

26. Schultz MM, Painter MM, Bartell SE, Logue A, Furlong ET, Werner SL, Schoenfuss HL. 2011. Selective uptake and biological consequences of environmentally relevant antidepressant pharmaceutical exposures on male fathead minnows. *Aquat. Toxicol.* 104:38–47.

27. Tanoue R, Nomiyama K, Nakamura H, Kim J-W, Isobe T, Shinohara R, Kunisue T, Tanabe S. 2015. Uptake and Tissue Distribution of Pharmaceuticals and Personal Care Products in Wild Fish from Treated-Wastewater-Impacted Streams. *Environ. Sci. Technol.* 49:11649–11658.

28. Qiao P, Gobas FA, Farrell AP. 2000. Relative contributions of aqueous and dietary uptake of hydrophobic chemicals to the body burden in juvenile rainbow trout. *Arch. Environ. Contam. Toxicol.* 39:369–377.

29. Meredith-Williams M, Carter LJ, Fussell R, Raffaelli D, Ashauer R, Boxall ABA. 2012. Uptake and depuration of pharmaceuticals in aquatic invertebrates. *Environ. Pollut.* 165:250–258.

30. Nakamura Y, Yamamoto H, Sekizawa J, Kondo T, Hirai N, Tatarazako N. 2008. The effects of pH on fluoxetine in Japanese medaka (Oryzias latipes): Acute toxicity in fish larvae and bioaccumulation in juvenile fish. *Chemosphere*. 70:865–873.

31. Erickson RJ, McKim JM, Lien GJ, Hoffman AD, Batterman SL. 2006. Uptake and elimination of ionizable organic chemicals at fish gills: I. Model formulation, parameterization, and behavior. *Environ. Toxicol. Chem.* 25:1512–1521.

32. Zhao J-L, Liu Y-S, Liu W-R, Jiang Y-X, Su H-C, Zhang Q-Q, Chen X-W, Yang Y-Y, Chen J, Liu S-S, Pan C-G, Huang G-Y, Ying G-G. 2015. Tissue-specific bioaccumulation of human and veterinary antibiotics in bile, plasma, liver and muscle tissues of wild fish from a highly urbanized region. *Environ. Pollut.* 198:15–24.

33. Steele IV WB, Garcia SN, Huggett DB, Venables BJ, Barnes III SE, La Point TW. 2013. Tissue-specific bioconcentration of the synthetic steroid hormone medroxyprogesterone acetate in the common carp (Cyprinus carpio). *Environ. Toxicol. Pharmacol.* 36:1120–1126.

34. Wu M, Pan C, Yang M, Xu B, Lei X, Ma J, Cai L, Chen J. 2016. Chemical analysis of fish bile extracts for monitoring endocrine disrupting chemical exposure in water: Bisphenol A, alkylphenols, and norethindrone. *Environ. Toxicol. Chem.* 35:182–190.

35. Xu H, Yang M, Qiu W, Pan C, Wu M. 2013. The impact of endocrine-disrupting chemicals on oxidative stress and innate immune response in zebrafish embryos. *Environ. Toxicol. Chem.* 32:1793–1799.

36. de Solla SR, Gilroy ÈAM, Klinck JS, King LE, McInnis R, Struger J, Backus SM, Gillis PL. 2016. Bioaccumulation of pharmaceuticals and personal care products in the unionid mussel Lasmigona costata in a river receiving wastewater effluent. *Chemosphere*. 146:486–496.

37. Schymanski EL, Jeon J, Gulde R, Fenner K, Ruff M, Singer HP, Hollender J. 2014. Identifying Small Molecules via High Resolution Mass Spectrometry: Communicating Confidence. *Environ. Sci. Technol.* 48:2097–2098.

38. Liu Y, Zhao D, Zhao Z (Zack). 2014. Study of degradation mechanisms of cyclobenzaprine by LC-MS/MS. *Anal. Methods*. 6:2320.

39. Holčapek M, Kolářová L, Nobilis M. 2008. High-performance liquid chromatography–tandem mass spectrometry in the identification and determination of phase I and phase II drug metabolites. *Anal. Bioanal. Chem.* 391:59–78.

40. Gillman PK. 2007. Tricyclic antidepressant pharmacology and therapeutic drug interactions updated. *Br. J. Pharmacol.* 151:737–748.

41. Nałęcz-Jawecki G. 2007. In Vitro Biotransformation of Amitriptyline and Imipramine with Rat Hepatic S9 Fraction: Evaluation of the Toxicity with Spirotox and Thamnotoxkit F™ Tests. *Arch. Environ. Contam. Toxicol.* 54:266–273.

42. Hicks JK, Swen JJ, Thorn CF, Sangkuhl K, Kharasch ED, Ellingrod VL, Skaar TC, Müller DJ, Gaedigk A, Stingl JC. 2013. Clinical Pharmacogenetics Implementation Consortium Guideline for CYP2D6 and CYP2C19 Genotypes and Dosing of Tricyclic Antidepressants. *Clin. Pharmacol. Ther.* 93:402–408.

5. Kapitulua

Amitriptilinaren ondorio metabolikoak urraburu arrainetan; 1.go atala: monoaminetatik haratago doazen aldaketak ingurumenean esanguratsua den dosian

Environmental Toxicology & Chemistry

aldizkarira bidalita

5.1. Sarrera

Depresioaren eta gaixotasun psikiatrikoen tratamendurako gehien errezetatzen den antidepresibo triziklikoa amitriptilina da [1,2]. Beste farmako batzuen antzera, amitriptilina eta bere azpiproduktuak ez direnez guztiz ezabatzen hondakin-uren tratamenduan [3], ingurumenean agertzen dira. Hain zuzen, amitriptilina 72 ng/L eta 1,8 ng/g kontzentrazio-mailetaraino detektatu izan da azaleko uretan [3–5] eta organismo urtarretan [6,7], hurrenez hurren.

Depresioaren tratamenduan, amitriptilinaren dosi terapeutikoek (75 mg/eguneko helduetan) serotoninaren eta norepinefrinaren xurgatzea inhibitzen dute gizakietan [8]. Horrez gain, Vismari-ren eta lankideen arabera [9], amitriptilinak hantura-zitokinen askatzea inhibituta oxido nitrikoaren ekoizpena ere murrizten du immuno-zelulen bitartez. Bestalde, ugaztunetan amitriptilinak eragindako albo-ondorio desberdinak ere deskribatu dira [8,10,11]. Esate baterako, kaspasa-entzimek lagundutako apoptosiari [10] edo amitriptilinak duen detergentearen gisako egiturari [11] egotzi dakieke amitriptilinak sortutako neurotoxikotasuna. Neurotoxikotasunaz gain, amitriptilinaren esposizioak zelula barneko lipidoen peroxidazioa eta oxigeno-espezie erreaktiboen ugaritzea ere eragiten du, hau da, estres oxidatiboa [8].

Ur-ekosistemetan antidepresiboen agerpena eta horrek organismo ez-zuzenduetan izan ditzakeen albo-ondorioek kezka handia sortu dute [12–17]. Antidepresiboek organismo urtarretan dituzten arriskuak ikertzen dituzten lan gehienek, fluoxetina eta *venlafaxina* bezalako serotoninaren xurgapen selektiboaren inhibitzaileetan (*selective serotonin reuptake inhibitor*, SSRI, delakoetan) jarri dute arreta [18–22]. Lan horiek, SSRI-en ekintza-mekanismo ezaguna den monoaminen xurgapen-inhibizioarekin lotutako parametroak aztertu dituzte nagusiki. Hala eta guztiz ere, ekintza-mekanismo horretatik haratago doazen errezeptoreetan ere eragin dezakete SSRI-ek [23] eta, ondorioz, beste bide biokimiko batzuk asalda ditzakete, hala nola energia-metabolismoa, aminoazidoen metabolismoa eta hormona-seinaleztapena [24]. Organismo urtarretan antidepresibo triziklikoekin burututako ikerketak oso mugatuak dira eta, aukitu duguz informazioaren arabera, amitriptilinak organismo urtarretan duen toxikotasunaren inguruko lan bakarra argitaratu da [25]. Lan horretan, hipotalamo-hipofisi-adrenal ardatzean eta antioxidatzaile-sisteman aldaketak behatu dira amitriptilinaren 100 ng/L bezalako kontzentrazio baxuetan.

Ingurumenean maila ez-hilgarrietan agertzen diren kutsatzaileen eraginak ikertzea erronka izugarria da. Izatez, egungo jarraibideetan aplikatzen diren azterketa estandarrak sarritan ez dira gai kutsatzaileek hain maila baxuetan eragiten dituzten efektuak detektatzeko. Testuinguru horretan, lagin biologikoetan masa molekular txikiko molekula endogenoen analisian oinarritzen den metabolomika oso erabilgarria bilakatu da [26]. Izan ere, maila hierarkiko altuagotako (zelula-, ehun-, organismo- edo biztanleria-mailako) albo-ondorioen aurretik beti gertatzen baitira maila molekularreko aldaketak eta, ondorioz, hurbilketa metabolomikoek kutsatzaileak dosi baxuetan eragiteko gai diren aldaketa biokimiko goiztarren inguruko ideia eskaintzen dute [27]. Zehazki, metabolomikaren helburua metabolitoen multzo zabaletik ikerketapean dagoen auzia definitzeko gai diren konposatu biokimiko konkretuak identifikatzea da [28,29].

Metabolomikako datu-multzoek dimentsio handiak izan ohi dituzte, eta horien tratamenduan aldagai bakarreko [30,31] zein aldagai anitzeko [27,31,32] hurbilketak aplikatu izan dira. Hala ere, bi hurbilketek dituzte mugak. Alde batetik, bariantza-analisia (*analysis of variance*, ANOVA, delakoa) bezalako aldagai bakarreko hurbilketak ez dira gai aldagaien arteko kobariantza kontuan hartzeko. Beste aldetik, osagai nagusien analisia (*principal component analysis*, PCA, delakoa) bezalako aldagai anitzeko metodoen muga azpimarragarriena ikerketaren oinarrian dagoen diseinu esperimentala kudeatzeko edo kontuan hartzeko ezintasuna da [33,34]. Arazo horiei aurre egin nahian, diseinatutako esperimentuetako (adibidez, dosia eta egunak aldagai aske gisa dituzten esperimentuetako) datuak analizatzeko aldagai anitzeko hurbilketa berria garatu da: ANOVA-aldibereko osagaien analisia (ANOVA-*simultaneous component analysis*, ASCA, delakoa) [33]. ASCA-k ANOVA eta PCA konbinatu eta, diseinu esperimentalak sortutako aldakortasuna eta aldagaien arteko kobariantza, biak, kontuan hartzen ditu. Esaterako, Malik-ek eta lankideek ASCA erabili dute tributileztainu kutsatzaileak *Daphnia magna* espeziearen lipido-profilean eragiten dituen aldaketak aztertzeko [35], eta Gómez-Canela-k eta lankideek [36] zebra-arrainetan klorpirifos intsektu-hiltzailearen efektu toxikoak ebaluatzeko.

Kapitulu honen helburu nagusia amitriptilinak, ingurumeneko kontzentrazio esanguratsuan, urraburu-arrain (*Sparus aurata*) gazteetan eragiten dituen albo-ondorioak aztertzea da. Helburu hori lortzeko, burmuineko eta gibeleko metaboloma-aldaketak neurtu dira metabolomikako hurbilketa konbinatua (bideratua/ez-bideratua) erabilita [37]. Hurbilketa horrekin lortzen den

metabolomaren estaldura handiak monoaminetatik haratago doazen aldaketa metabolikoak identifikatzea ahalbidetzen du. Gure dakigunaren arabera, hau da amitriptilinaren dosi baxuko eragin metabolikoak ikertu dituen lehen lana.

5.2. Atal esperimentala

5.2.1. Estandarrak eta erreaktiboak

Amitriptilina hidrokloruroa (% 98) Sigma-Aldrich (St. Louis, MO, AEB) merkataritza-etxean erosi da. Tankeak dosifikatzeko amitriptilinaren disoluzioa (5000 mg/L) etanoletan (% 99,9, Scharlab, Bartzelona, Espainia) prestatu eta Milli-Q urarekin diluitu da 85,2 µg/L mailaraino. Esperimentuko tankean etanolaren kontzentrazioa ‰ 0,0004-koa izan da. Disoluzio guztiak −20 ˚C-an gorde dira.

Azetonitriloa (HPLC kalitatea, % 99,9) eta kloroformoa VWR Chemicals (Radnor, PA, AEB) merkataritza-etxekoak dira eta metanola (HPLC kalitatea) Merck-ekoa (Darmstadt, Alemania). Ura Milli-Q Integral 3 eta Millipak express 40 (0,22 µm) iragazkiak (Millipore, Merck) erabilita iragazi da materia organikoaren kantitatea < 3 ng/mL mailan bermatzeko.

5.1 taulan analisi bideratuko metabolitoen zerrenda ageri da bibliografiatik egokitutako euren laburdurekin batera [37]. Laburbilduz, glizerofosfolipidoak definitzeko ester- edota eter-loturen presentzian (“a” edo “e” bidez adierazita, hurrenez hurren), gantz azidoaren kate-luzeran eta lotura bikoitz kopuruan oinarritu da. Gantz azidoak bi glizerol-posiziotara lotuta daudela adierazteko bi letrak (ae = azil-alkil, aa = diazil) erabili dira. Bestalde, karnitinak karbono eta lotura bikoitz kopuruen arabera izendatu dira. Azkenik, esfingomielinak SM gisa laburtu eta “C” baten ondoren gantz azidoaren kateko karbono eta lotura bikoitz kopuruak zehaztu dira.

5.1 taula: *Analisi bideratuko metabolitoen zerrenda.*

Zenbakia	**Metabolitoa (Laburdura)**
Aminoazidoak	
1	Alanina (Ala)
2	Serina (Ser)
3	Prolina (Pro)
4	Valina (Val)
5	Aloisoleuzina (Aleu)

5.1 taula: *(Jarraipena).*

Zenbakia	Metabolitoa (Laburdura)
6	Isoleuzina (Ile)
7	Leuzina (Leu)
8	Asparagina (Asn)
9	Aspartatoa (Asp)
10	Glutamina (Gln)
11	Lisina (Lys)
12	Glutamatoa (Glu)
13	Metionina (Met)
14	Histidina (His)
15	Fenilalanina (Phe)
16	Arginina (Arg)
17	Tirosina (Tyr)
18	Triptofanoa (Trp)
Amina biogenikoak	
19	β-alanina (β-Ala)
20	Kreatinina
21	Azido fumarikoa
22	Azido sukzinikoa
23	Homoserina
24	Taurina
25	Ornitina
26	Azido malikoa
27	Espermidina
28	Zitrulina
29	Homozisteina
Neurotransmisoreak	
30	azido γ-aminobutirikoa (GABA)
31	Dopamina
32	Tiroxina
Base nukleikoak	
33	Adenina
34	Zitosina
35	Uraziloa
36	Timina
37	Guanina
Karnitinak	
38	Karnitina (C0)
39	L-Azetilkarnitina (C2)
40	Malonilkarnitina (C2-COOH & C4-OH)

5.1 taula: *(Jarraipena).*

Zenbakia	Metabolitoa (Laburdura)
41	Propionilkarnitina (C3)
42	Hidroxipropionilkarnitina (C3-OH)
43	Metilmalonilkarnitina (C3-COOH)
44	Butirilkarnitina (C4)
45	Butenilkarnitina (C4:1)
46	2-etilakriloilkarnitina (C4-Et)
47	Glutarilkarnitina (C4-COOH)
48	Balerilkarnitina (C5, C4-M)
49	O-Adipoilkarnitina (C5-COOH)
50	Hexanoilkarnitina (C6)
51	2-Hexenoilkarnitina (C6:1)
52	Heptanoilkarnitina (C7)
53	Oktanoilkarnitina (C8)
54	Oktenoilkarnitina (C8:1)
55	Nonanoilkarnitina (C9)
56	O-sebakoilkarnitina (C9-COOH)
57	O-dekanoil-R-karnitina (C10)
58	Keto-dekanoilkarnitina (C10-ket)
59	Dezenoilkarnitina (C10:1)
60	2-trans,4-cis-Dekadienoilkarnitina (C10:2)
61	Dekatrienoilkarnitina (C10:3)
62	C11 (C9-DM, C10-M)
63	Dodekanedioilkarnitina (C11-COOH)
64	Dodekanoilkarnitina (C12)
65	Hidroxilauroilkarnitina (C12-OH)
66	Hidroxidodezenoilkarnitina (C12:1-OH)
67	(C13-COOH)
68	Tetradekanoilkarnitina (C14)
69	Hidroxi-Tetradekanoil karnitina (C14-OH)
70	Tetradezenoilkarnitina (C14:1)
71	Tetradekadienkarnitina (C14:2)
72	Hidroxitetradekadienkarnitina (C14:2-OH)
73	Palmitoilkarnitina (C16)
74	Palmitoleoilkarnitina (C16:1)
75	Hidroxihexadezenoilkarnitina (C16:1-OH)
76	Hexadekadienoilkarnitina (C16:2)
77	Hidroxihexadekadienoilkarnitina (C16:2-OH)
78	Karboxiheptadekanoilkarnitina (C17-COOH)
79	C17:1-COOH
80	Estearoilkarnitina (C18)

5.1 taula: *(Jarraipena).*

Zenbakia	Metabolitoa (Laburdura)
81	Hidroxioktadekanoilkarnitina (C18-OH)
82	Elaidiko karnitina (C18:1)
83	Hidroxioleoilkarnitina (C18:1-OH)
84	Hexadekadienoilkarnitina (C18:2)
85	Hidroxilinoleilkarnitina (C18:2-OH)
86	Hidroxioktadekatrienoilkarnitina (C18:3-OH)
87	Estearidonil karnitina (C18:4)
Fosfatidilkolinak	
88	PC aa C20:0
89	PC aa C24:0
90	PC aa C26:0
91	PC aa C28:0
92	PC aa C28:1
93	PC aa C28:2
94	PC aa C30:0
95	PC aa C30:2
96	PC aa C32:0
97	PC aa C32:1
98	PC aa C32:2
99	PC aa C32:3
100	PC aa C34:0
101	PC aa C34:1
102	PC aa C34:2
103	PC aa C38:0
104	PC aa C38:1
105	PC aa C38:2
106	PC aa C38:3
107	PC aa C38:4
108	PC aa C38:5
109	PC aa C40
110	PC aa C40:1
111	PC aa C40:2
112	PC aa C40:3
113	PC aa C40:4
114	PC aa C40:5
115	PC aa C40:6
116	PC aa C42:0
117	PC aa C42:1
118	PC aa C42:2
119	PC aa C42:4

5.1 taula: *(Jarraipena).*

Zenbakia	Metabolitoa (Laburdura)
120	PC aa C42:5
121	PC aa C42:6
122	PC ae C30:0
123	PC ae C30:1
124	PC ae C32:1
125	PC ae C32:2
126	PC ae C34:1
127	PC ae C34:2
128	PC ae C34:3
129	PC ae C34:4
130	PC ae C36:0
131	PC ae C36:1
132	PC ae C36:2
133	PC ae C36:3
134	PC ae C36:4
135	PC ae C36:5
136	PC ae C38:0
137	PC ae C38:1
138	PC ae C38:2
139	PC ae C38:3
140	PC ae C38:4
141	PC ae C38:5
142	PC ae C38:6
143	PC ae C40:1
144	PC ae C42:0
145	PC ae C42:1
146	PC ae C42:2
147	PC ae C42:3
148	PC ae C42:4
149	PC ae C42:5
150	PC ae C44:3
151	PC ae C44:4
152	PC ae C44:5
Lisofosfatidilkolinak	
153	lysoPC a C10:0
154	lysoPC a C12:0
155	lysoPC a C14:0
156	lysoPC a C16:0
157	lysoPC a C17:0
158	lysoPC a C18:0

5.1 taula: *(Jarraipena).*

Zenbakia	Metabolitoa (Laburdura)
159	lysoPC a C18:1
160	lysoPC a C18:2
161	lysoPC a C20:0
162	lysoPC a C20:3
163	lysoPC a C20:4
164	lysoPC a C20:5
165	lysoPC a C22:0
166	lysoPC a C22:1
167	lysoPC a C22:5
168	lysoPC a C22:6
169	lysoPC a C24:0
170	lysoPC a C24:1
Esfingomielinak	
171	SM (d18:0/C16:0)
172	SM (d18:0/C16:1)
173	SM (d18:0/C18:0)
174	SM (d18:0/C18:1)
175	SM (OH) (d18:0/C22:2)
176	SM (d18:1/C24:0)
177	SM (d18:1/C24:1)
178	SM (d18:1/C26:0)
179	SM (d18:1/C26:1)

Aminoazidoen, amina biogenikoen, neurotransmisoreen eta base nukleikoen erreaktibo guztiak eta SM C16:0, L-metionina-metiloa ($^{13}C,D_3$) eta C0 (Trimetil-D_9) barne-estandarrak Sigma-Aldrich (San Louis, Missouri, AEB) merkataritza-etxean erosi dira. Karnitina (C2) eta fosfolipidoen estandarrak (PCaaC34:0, PCaaC28:2, lysoPCaC10:0, lysoPCaC24:0) eta barne-estandarrak (lysoPCaC13:0, lysoPCaC17:1, PCaaC25:0, PCaaC31:1, PCaaC43:6 eta SMC12:0) Avanti Polar Lipids (Alabaster, Estatu Batuak) merkataritza-etxekoak dira.

Aminoazidoen, amina biogenikoen, neurotransmisoreen eta base nukleikoen disoluzioak % 1 azido formiko duen Milli-Q ur:metanol (60:40, bol/bol) nahastean prestatu dira, eta L-metionina-metiloa ($^{13}C,D_3$) barne estandarra % 1 azido formiko duen Milli-Q ur:metanol (20:80, bol/bol) nahastean. Karnitinak, lipido guztiak eta haien barne-estandarrak, aldiz, metanoletan disolbatu dira.

5.2.2. Amitriptilinarekin esposizio-esperimentuak

Groupe Aqualande (Roquefort, Frantzia) arrain-haztegitik lortutako urraburu-arrain gazteak, ~40 g-ko pisudunak eta ~13 cm-ko luzerakoak, Plentziako itsas-estaziora (PiE-UPV/EHUra) garraiatu dira, bertan esposizio-esperimentuak burutzeko. Esperimentu osoan zehar, laborategia 18 °C-ko tenperaturan egon da 14:10-h argipe/ilunpe zikloetan, eta uraren tenperatura (13,5 ˚C) eta pH-a (7,3 ± 0,3) konstante mantendu dira. Arrainak heldutako egunetik bi astez eduki dira bertako girora egokitzeko eta, ondoren, esperimentuak hasi aurretik, esperimentuko tankeetan beste 48 orduz egon dira ontzietara egokitzeko. Arrainen bizi-irautea ziurtatzeko ura etengabe aireztatu da eta egunero 0,10 g arrain-jaki/arrain eman zaie (EFICO YM 868, 3 mm, BioMar Group, Danimarka). Uraren kalitatea ziurtatzeko, disolbatutako oxigenoaren, nitritoen, nitratoen eta amonioaren kontrola egin da esposizioan zehar.

Lan hau amitriptilinaren biokontzentrazio/biotransformazio-ikerketarekin batera egin da eta ikerketa horretan (ikus 4. Kapitulua) behatu da amitriptilina burmuinean eta gibelean metatzen dela [38]. Amitriptilina ingurumeneko kontzentrazio esanguratsuan (0,2 µg/L nominalean) dosifikatuta, 7 egun iraun duen esposizio-esperimentua aurrera eramateko 1000 x 700 x 650 mm-ko polipropilenozko bi tanke (bata kontrola eta bestea dosifikatua) erabili dira, bakoitza itsasoko uraren 250 L-rekin eta 145 urraburu arrainekin. Esposizio-esperimentua fluxu jarraiko sistemaren bidez egin da, ponpa peristaltikoak erabilita tanke bietara itsasoko ura 8,5 L/h fluxuan eta kutsatutako tankera dosifikatzeko amitriptilinaren disoluzioa 20 mL/h fluxuan gehituta. Dosifikatzeko amitriptilinaren disoluzioa 48 orduro bete da. Kontroleko tankea baldintza berdinetan mantendu da, baina amitriptilinarik gehitu gabe. Kutsatutako tankean, amitriptilinaren batezbesteko kontzentrazioa 0,12 ± 0,02 µg/L-koa izan da [38]. Tanke bakoitzetik, dosifikazio aurreko (0. eguna) eta osteko 2., 4. eta 7. egunetan 10 arrain bildu dira lan honetako helburua betetzeko. Gure aurreko lanean deskribatutako arrainen lagin-biltzea eta disekzioa [38] Euskal Herriko Unibertsitateko (UPV/EHUko) Bioetika-Batzordeak ebaluatu eta, egungo araudien arabera, tokiko agintaritzak onartutako prozedura (CEEA/380/2014/ETXEBARRIA LOIZATE) jarraituta egin da.

5.2.3. Metabolitoen erauzketa eta analisia

5.2.3.1. Laginaren tratamendua eta analisi instrumentala

Metabolitoen erauzketa eta analisia aurretiaz optimizatu eta berretsitako metodoa erabilita egin dira [37]. Burmuin eta gibel osoen erauzketak 1,5 mL-ko eta 13 mL-ko ontzietan egin dira, hurrenez hurren, laginaren mg bakoitzeko kloroformoa:metanola (20:80, bol/bol) nahastearen 5 µL gehituta eta Next Advance (New York, AEB) merkataritza-etxeko zirkonio oxidozko bolatxoak erabilita (2,0 mm-koak eta 4,8 mm-koak, hurrenez hurren, burmuin- eta gibel-laginetan). Lagin guztiak 1500 bira/min-ko homogeneizatu dira 4 minutuz 1600 MiniG homogeneizatzailean (Spex Sample Prep, New Jersey, AEB). Ondoren, neurketara orduko, laginak metanol purutan diluitu dira barne-estandarra gehituta (200 µg/L diluitutako erauzian). Lortutako erauzi bakoitzaren bina diluzio egin dira, hain zuzen ere, burmuin-laginetan 1:5 eta 1:100 diluzioak eta gibel-laginetan 1:15 eta 1:300 diluzioak.

Erauzien analisia Estokolmoko unibertsitatean egin da, bertan garatutako hurbilketa bideratuak eta ez-bideratuak erabilita [37]. Laburki, lagin diluitu guztien analisi bideratuan erauzi bakoitza (5 µL-ko alikuotak) bi aldiz neurtu da. Alde batetik, analito polarrenak (18 aminoazido, 11 amina biogeniko, 3 neurotransmisore eta 5 base nukleiko) kuantifikatzeko, kuadrupolo hirukoitzeko masa-espektrometroari akoplatutako ultra-bereizmen altuko likido-kromatografoa (UHPLC-QqQ) erabili da, elkarrekintza hidrofilikoan oinarritutako likido-kromatografiako (*hydrophilic interaction liquid chromatography*, HILIC, delako) zutabearekin eta modu positiboan eta negatiboan aldi berean neurtuta. Beste aldetik, lipidoen metabolismoko konposatuak (50 karnitina, 67 fosfatidilkolina, 16 lisofosfatidilkolina eta 9 esfingomielina) neurtzeko, sarrera zuzeneko (*flow injection*, FI, delako) kuadrupolo hirukoitzeko masa-espektrometria (FI-QqQ) erabili da, hau da, lagina zuzenean sartuta ionizazio-iturrira, aldez aurretiko metabolitoen kromatografia-banaketarik gabe. Orotara, 179 metabolito horien (ikus 5.1 taula) analisi bideratuak doitasun eta identifikazioko ziurtasun hobeak ahalbidetzen dituen arren, analisi ez-bideratuaren bitartez metabolitoen estaldura handitu daiteke. Hori dela eta, diluzio baxueneko erauziak (burmuin- eta gibel-laginen 1:5 eta 1:15 diluzio-erauziak, hurrenez hurren) bereizmen altuko masa-espektrometriaren (*high resolution mass spectrometry*, HRMS, delakoaren) bidez analizatu dira tandem kuadrupolo-Orbitrap masa-analizatzaileari akoplatutako UHPLC kromatografoan [37].

Gainera, metabolitoen estaldura maximizatzeko asmoarekin, analisi ez-bideratuko hurbilketa honetan erauzi bakoitzeko lau neurketa burutu dira bakoitzean 5 µL-ko alikuotak injektatuta. Lau neurketa horietarako, bi kromatografia-zutabe desberdin (bata HILIC zutabea eta bestea alderantzizko faseko oktadezilsilil (C18) zutabea) erabiltzeaz gain, analisiak bi ionizazio-moduetan, positiboan ($HILIC_{pos}$ eta $C18_{pos}$) eta negatiboan ($HILIC_{neg}$ eta $C18_{neg}$), egin dira.

5.2.3.2. Kalitate-kontroleko laginak

Lan honetan, analisien arteko kutsadura kontrolatzeko 5 laginetatik behin zuri instrumental bat (metanol purua) injektatu da. Bestalde, prozeduran zehar egon daitekeen albo-kutsadura kontrolatzeko, prozedurako zuriak (burmuin/gibel gabeko laginak) prestatu dira. Horrez gain, kalitate-kontroleko (*quality control*, QC, delako) lagin desberdinak prestatu dira. Alde batetik, burmuin eta gibel indibidualak elkartuta (n=20), lagin-mota bakoitzerako erauzketaren kalitate-kontroleko (*extraction QC*, QC_{ext}, delako) lagin homogeneoak prestatu dira. Erauzketaren errepikakortasuna egiaztatzeko, erauzketa-txanda bakoitzean lagin homogeneo horren erauzketak ere egin dira. Beste aldetik, ehun-mota bakoitzerako sekuentziaren kalitate-kontroleko (*sequence QC*, QC_{seq}, delako) lagina prestatu da. Horretarako, erauzi bakoitzetik bolumen txikia hartu eta, alikuota guztiak nahastu ondoren, lortutako nahastea alikuota desberdinetan banatu da. Alikuota horiek 10 laginetatik behin injektatu dira sekuentzian zehar, seinalearen jarraipena egin eta, beharrezkoa izatekotan, berau zuzentzeko.

Laginen zorizko erauzketa eta analisia egin da eta lagin-mota bakoitzeko erauziak (laginak, QC-ak, zuriak eta disoluzio estandarrak) sei sekuentzia-txandatan analizatu dira, bi analisi bideratukoak (UHPLC-QqQ eta FI-QqQ) eta beste lau analisi ez-bideratukoak ($HILIC_{pos}$, $HILIC_{neg}$, $C18_{pos}$ eta $C18_{neg}$ UHPLC-qOrbitrap bidez). Sekuentzietan zehar ez da analisien arteko kutsadurarik behatu.

5.2.4. Datuen tratamendua eta analisi estatistikoa

Arrainaren osasunaren ebaluazio orokor gisa, egoera-faktorea (K) [39] eta indize hepatosomatikoa (HSI) determinatu dira 5.1 eta 5.2 ekuazioak erabilita, hurrenez hurren.

$$K = \frac{Arrainaren\ pisua\ x\ 100}{Arrainaren\ luzera^3}$$ 5.1 ekuazioa

$$HSI = \frac{Gibelaren\ pisua\ x\ 100}{Arrainaren\ pisua}$$ 5.2 ekuazioa

Kutsatutako eta kontroleko taldeen artean K eta HSI estatistikoki erkatzeko, aldagai bakarreko bariantza-analisia (ANOVA) erabili da. Bestalde, kontzentrazioak nabarmen aldatu zaizkien metabolitoen identifikazioa aparte egin da burmuineko eta gibeleko laginentzat, bai analisi bideratuan, eta baita hurbilketa ez-bideratuan ere.

5.2.4.1. Analisi bideratuko datuen tratamendua

Intereseko metabolitoak XCalibur 4.0 softwarea erabilita detektatu eta kuantifikatu dira. Analisi estatistikora orduko datu-multzoa iragazi egin da, laginen % 50a baino gehiagotan kontzentrazioak detekzio-mugatik behera izan dituzten metabolitoak ezabatuta. Iragazi aurretik, kontroleko eta kutsatutako taldeen artean falta diren balioak orekatuta egon direla ziurtatu da. Gainerako metabolitoetan, *k-nearest neighbor* (KNN) delako metodoa erabili da falta diren balioak inputatzeko [40].

Nahiz eta erauzketa-txanden artean ez den desberdintasunik behatu QC_{ext} laginetako emaitzen arabera, QC_{seq} laginetako emaitzetatik sekuentzian zeharreko ioien intentsitate-aldaketak edo seinaleen joerak identifikatu dira, barne-estandarrak erabilita ezin izan direnak zuzendu. Ondorioz, QC_{seq} laginetako emaitzetan oinarrituta eta lagin bakoitzaren injekzio-hurrenkera kontuan izanda, seinaleak matematikoki zuzendu dira bibliografian deskribatuta dagoen 5.3 ekuazioa erabilita [41]. Ekuazio horretan, $x_{i,j}$ eta $x'_{i,j}$, j lagineko i analitoaren zuzendu gabeko eta zuzendutako seinaleak dira, hurrenez hurren, eta $f_{i,j}$ seinalearen balio teoriko gisa QC_{seq} laginekin i analitoarentzat eratutako erregresio-zuzenean j laginaren injekzio-hurrenkera ordezkatuta kalkulatzen den zuzenketa-faktorea da. Azkenik, emaitza $x'_{i,1}$ balioarekin (injektatu den lehen QC_{seq} laginean i analitoaren zuzendutako seinalearekin) biderkatzen da seinaleek jatorrizko maila berreskuratzeko [41].

$$x'_{i,j} = \frac{x_{i,j}}{f_{i,j}} \cdot x'_{i,1}$$ 5.3 ekuazioa

Asaldatutako bide metabolikoetako metabolitoak identifikatzeko, bi sekuentzietatik (hau da, UHPLC-QqQ eta FI-QqQ analisietatik) lortutako datu zuzenduak elkartu egin dira eta denak erabilita analisi estatistikoa egin da. Datuak autoeskalatu egin dira metabolito guztiek bariantza berdina

izateko, eta bazterreko balioak PCA-ren bidez detektatu [42,43] eta datu-multzo osoaren % 95-eko konfiantza-tartetik kanpo dauden laginak ezabatu dira.

Datuak aldagai askotariko erregresio linealaren (*multiple linear regression*, MLR, delakoaren) bidez ($Y(\text{denbora,dosia}) = \beta_{\text{denbora}}\cdot\text{denbora} + \beta_{\text{dosia}}\cdot\text{dosia} + \beta_{\text{dosia·denbora}}\text{dosia·denbora}$, non Y metabolitoaren erantzuna den) analizatu dira R softwarearen bidez (3.4.3 bertsioa). Lan honen helburua kontroleko eta kutsatutako laginen artean denboran zeharreko kontzentrazioetan joera desberdinak dituzten metabolitoak identifikatzea denez, denboraren eta dosiaren arteko elkarrekintzan (hau da, dosia·denbora osagaian) jarri da arreta. MLR aplikatu eta I. motako erroreak ekiditeko, dosia·denbora elkarrekintzan p-balioa < 0,05 eta aurkikuntza faltsuen tasa (*false discovery rate*, FDR, delakoa) < 0,05 duten metabolitoak aukeratu dira.

Horrez gain, ikerketa honetan bi aldagai askek (esposizio-denborak eta dosiak) definitutako diseinu esperimentala erabili denez, ASCA hurbilketa ere aplikatu da MetaboAnalyst 3.5 erabilita [44]. ASCA-k datuen bariantza osoa aldagai aske bakoitzak eta euren arteko elkarrekintzak eragindako bariantzetan banatzen du. ASCA-k bi aldagai askeentzat eta euren arteko elkarrekintzarentzat eraikitzen dituen azpiereduetan bi parametro erabiltzen ditu metabolitoen jokabidea aurresateko: eragina (*leverage* delakoa) eta aurresate-errorearen karratua (*squared prediction error* delakoa) [34]. Eraginak metabolito batek ASCA-ren ereduan duen garrantzia neurtzen duen bitartean, aurresate-errorearen karratuak metabolito jakin bakoitzarentzako ereduaren egokitasunaren berri ematen du. Hori kontuan izanda, metabolito esanguratsuak eragin altua (eraginaren muga > 0,85) eta aurresate-errorearen karratu baxua (alfa muga < 0,05) erakusten dutenak izango dira. Bestalde, kontzentrazioak nabarmen aldatu zaizkien metabolito horien egun bakoitzeko aldaketa-mailak (*fold change*, FC, delakoak) ere kalkulatu dira. Horretarako, 5.4 ekuazioan oinarrituta, kutsatutako laginetako *i* eguneko *j* metabolitoaren batezbesteko kontzentrazioa kontroleko laginetako egun bereko analito berdinaren batezbesteko kontzentrazioarekin zatitu da.

$$FC_{i\ \text{eguna},\ \ j\ \text{metabolitoa}} = \frac{j\text{−ren kontzentrazioa}_{\text{kutsatutako laginetan i egunean}}}{j\text{−ren kontzentrazioa}_{\text{kontroleko laginetan i egunean}}} \qquad \text{5.4 ekuazioa}$$

5.2.4.2. Analisi ez-bideratuko datuen tratamendua

Analisi ez-bideratuan lortutako kromatogramak Compound Discoverer 2.1 (Thermo-Fisher

Scientific) programa erabilita aztertu dira eta II. eranskinean ageri dira lan-fluxu horretan ezarritako baldintzak. Datuak prozesatu ondoren, metabolito endogenoekin bakarrik gelditzeko, datu-multzoak iragazi dira. Horretarako, datu-multzoko masa zehatzak 4400 konposatu endogeno dituen edo LipidMaps [45] datu-baseetan bilatu eta bat egiten ez dutenak baztertu dira.

Analisi bideratuaren antzera, bazterreko balioak PCA-ren bidez ezabatu dira, erauzketa-txanden artean ez da desberdintasunik behatu QC_{ext} laginetako emaitzen arabera, eta sekuentzian zeharreko seinaleen joera zuzendu behar izan da. Dena den, analisi bideratuan erabilitako hurbilketa (ikus 5.3 ekuazioa) analisi ez-bideratuaren kasuan ez da gai izan joera guztiz zuzentzeko eta, ondorioz, R software-eko intCor paketea [46] erabili behar izan da. Hori erabilita eredua eraikitzeko 3 talde definitu dira (kontrola, kutsatua eta QC_{seq}), eta, seinaleak zuzentzeko, osagai nagusi komunen analisia (*Common Principal Components Analysis*, CPCA, delakoa) eta erdiko balioen metodoa uztartzen dituen bi urratseko hurbilketa erabili da. Behin sekuentzia bakoitzeko seinaleak zuzenduta, analisi ez-bideratuko lau sekuentzietan ($HILIC_{pos}$, $HILIC_{neg}$, $C18_{pos}$ eta $C18_{neg}$) bildutako datuak elkartu eta batera analizatu dira. 5.2.4.1 atalean aipatu den bezala, MLR analisiaren bidez dosia·denbora elkarrekintzan p-balioa < 0,05 eta FDR < 0,05 irizpideak betetzen dituzten gailurrak edo ASCA-ren azpiereduetan eragina > 0,85 eta aurresate-erroreen karratu baxua < 0,05 dituztenak aukeratu dira analisi ez-bideratuan ere.

Analisi ez-bideratuko datuen kasuan, gailur esanguratsuak banaka aztertu dira, batetik, itxura eskaseko edota txarto integratutako gailurrak eta, bestetik, amitriptilinaren azpiproduktuei dagozkienak [38] kentzeko. Azken horiek kentzea funtsezkoa da okerreko ondorioak ekiditeko. Ondoren, FC balioak 5.4 ekuazioaren arabera kalkulatu eta metabolitoen identifikazioa [47] burutu da ondoko hurbilketa hau erabilita. Metabolitoen esleipenerako, masa zehatza, profil isotopikoa, apurketa-espektroa eta ugaritasunak mzCloud liburutegiko konposatuekin konparatu dira. Liburutegi horretan metabolitoa eskuragarri egon ez denean, behin behineko metabolitoen hautagaiak KEGG [48] eta LipidMaps [45] bezalako datu-baseetan bilatu dira eta, gero, lortutako apurketa-espektro esperimentalak MetFrag [49] programaren bidez eskuratutako *in silico* apurketekin erkatu dira adostasun handiena erakusten duen metabolitoa aukeratzeko.

5.3. Emaitzak eta eztabaida

5.3.1. Osasun-egoeraren ezaugarri orokorrak

Bizi-irauteari dagokionez, ez da arrainik hil esposizioak iraun duen tarte osoan eta, arrainen osasun orokorraren adierazgarri diren K eta HSI aldagai fisiologikoen balioak, zein arrainen luzera eta pisua aztertutako egun guztietan estatistikoki bereizi ezinak izan dira (p-balioa > 0,05) kontroleko eta kutsatutako arrainen artean.

5.3.2. Metabolomako aldaketak

MLR-aren bidez ez da FDR < 0,05 irizpidea betetzen duen metabolitorik egon, ez analisi bideratuan ezta analisi ez-bideratuan ere. Aldaketa metabolikoak MLR analisiaren bidez detektatu ahal izateko besteko nabarmenak ez izatearen arrazoia hain denbora laburreko esperimentuan amitriptilinaren kontzentrazioa baxua izan daiteke (0,2 ng/mL). Izan ere, antidepresiboekin bibliografian dauden beste lan batzuetan askoz kontzentrazio altuagoak (23-465 µg/L) aztertu dituzte [18,19,21]. Hala ere, ASCA hurbilketaren bidez asaldatze metaboliko esanguratsuak behatu dira bai analisi bideratuan eta baita ez-bideratuan ere.

5.3.2.1. Analisi bideratuko emaitzak

5.2 taulan ikus daitekeen bezala, burmuineko zein gibeleko emaitzetan dosia azpiereduak ez du permutazio-testa gainditu (p-balioa > 0,05). Aldiz, denbora eta dosia·denbora elkarrekintzaren azpiereduek 1000 permutaziotan oinarritutako testa gainditu (p-balioa < 0,05), eta lehenengo 2 osagai nagusiek (*principal component*, PC, delakoek) bariantzaren ia % 90-a azaldu dute bi azpiereduetan. ASCA-ren arabera, gibelean zein burmuinean metabolitoen mailan gehien eragin duen aldagaia esposizio-denbora da (denbora azpiereduek dute p-balio-rik baxuena). Aldaketa horren atzean dauden metabolitoak ondokoak dira: burmuinean lisina, glutamina, fenilalanina, adenina, tirosina, prolina, azido malikoa, C3, C18:2, C12:1-OH, C14, C16:2-OH, C16:1-OH, C12, C14:2, eta PCaeC38, eta gibelean lisina, glutamina, fenilalanina, aloisoleuzina, balina, arginina, PCaaC40:6 eta PCaeC38:1. Metabolito horiek kontroleko zein kutsatutako arrainetan denboraren menpeko joera erakustea baldintza esperimentalekin lotuta egon daiteke, hala nola esperimentuak aurrera egin ahala ontzi bietako arrain-kopurua gutxitzen joatearekin.

5.2 taula: *ASCA hurbilketaren emaitzak. Burmuineko eta gibeleko analisi bideratu eta ez-bideratuko emaitzekin eraikitako azpiereduen (dosia, denbora eta dosia·denbora elkarrekintza) lehenengo bi osagai nagusien (principal component, PC, delakoen) garrantzia eta azaldutako bariantza.*

Ehuna	Aldagaia	Analisi bideratua			Analisi ez-bideratua		
		Garrantzia (p-balioa)	*Scores azaldutako bariantza (%)*		*Garrantzia (p-balioa)*	*Scores azaldutako bariantza (%)*	
			PC1	PC2	PC1	PC1	PC2
Burmuina	dosia	0,95	-	-	0,70	-	-
	denbora	0,001	60,9	28,3	<0,001	50,1	30,7
	dosia·denbora	0,003	73,7	15,8	0,11	-	-
	Hondarrak		28,2	13,1		19,1	7,9
Gibela	dosia	0,53	-	-	0,48	-	-
	denbora	<0,001	73,9	19,1	0,002	53,8	27,2
	dosia·denbora	0,03	44,2	37,9	0,03	44,5	34,2
	Hondarrak		20,4	14,8		12,3	7,5

Horrez gain, amitriptilinaren dosiak eragindako albo-ondorioak dosia·denbora azpiereduetatik identifikatu dira. Azpieredu horietako lehenengo osagai nagusiaren *scores* diagramak 5.1 irudian beha daitezke, eta azpimarratzekoa da dosi-taldeen (kontrolaren eta kutsatuaren) arteko desberdintasun nabarmenenak esperimentuko azken egunean (7. egunean) behatu direla burmuinean zein gibelean. ASCA-ren arabera amitriptilinaren esposizioaren ondorioz esanguratsuki aldatu diren metabolito horien FC balioak 5.2 irudian ageri dira. Irudi berean, kontroleko eta kutsatutako laginen arteko desberdintasun-maila adierazi da, t-frogaren bidez kalkulatuta.

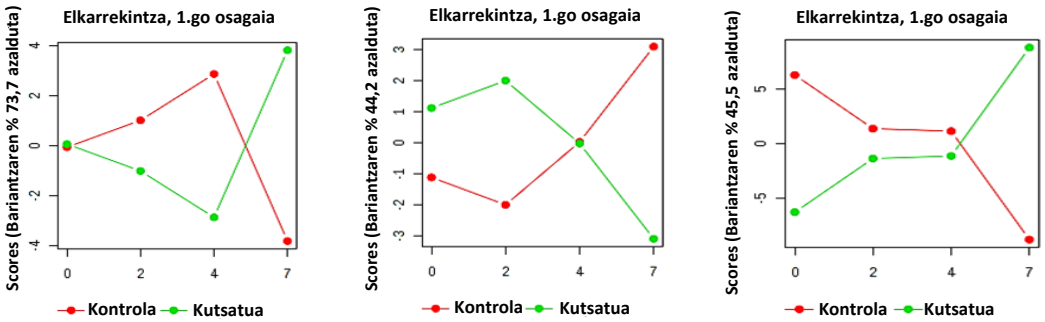

a) Burmuina / analisi bideratua b) Gibela / analisi bideratua c) Gibela / analisi ez-bideratua

5.1 irudia: *Burmuinen analisi bideratuan (a), gibelen analisi bideratuan (b) eta gibelen analisi ez-bideratuan (c) dosia·denbora azpiereduko 1.go osagai nagusiaren scores diagrama. Lerroek talde eta egun bakoitzeko batezbestekoak lotzen dituzte.*

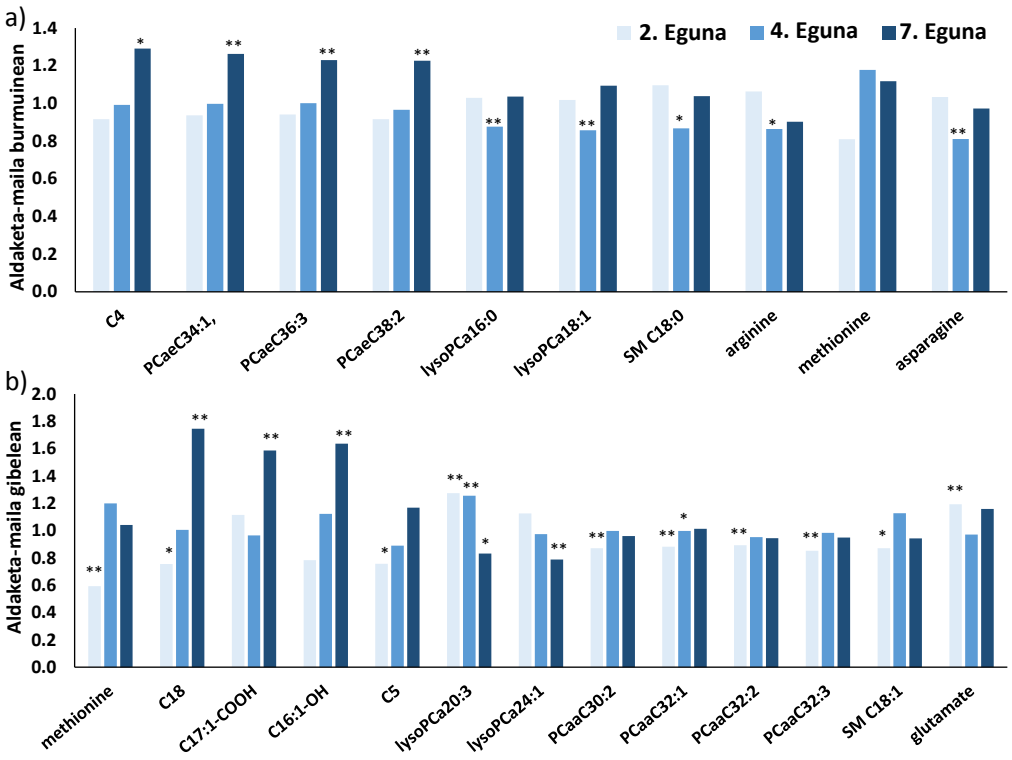

5.2 irudia: *ASCA-ren arabera burmuinean (a) eta gibelean (b) kontzentrazioak nabarmen aldatu zaizkien analisi bideratuko metabolitoen 2., 4. eta 7. egunetako aldaketa-mailak (fold change, FC, delakoak). FC balioak kalkulatzeko kutsatutako laginetako metabolitoaren batezbesteko kontzentrazioa kontroleko laginetako egun bereko analito berdinaren batezbesteko kontzentrazioarekin zatitu da. *: p-balioa < 0,1; **: p-balioa < 0,05.*

Gibelaren kasuan, dosia·denbora azpiereduko emaitzen arabera, 13 metabolitoren kontzentrazioak aldatu dira esperimentuan zehar kontroleko eta kutsatutako arrainetan. Metabolito horien artean daude metionina, glutamatoa eta lipidoen metabolismoko beste 11 konposatu, hala nola azil karnitinak (C18, C17:1-COOH, C16:1-OH eta C5), fosfatidilkolinak (PCaaC30:2, PCaaC32:1, PCaaC32:2 eta PCaaC32:3), lisofosfatidilkolinak (lysoPCa20:3 eta lysoPCa24:1) eta esfingomielina bat (SM C18:1). Bestalde, burmuinean dosia·denbora azpiereduaren arabera ondorengo 10 metabolitoak aldatu dira: arginina, metionina, asparagina eta beste 7 metabolito lipidiko, hala nola C4 azil karnitina, 3 fosfatidilkolina (PCaeC34:1, PCae C36:3 eta PCae C38:2), 2 lisofosfatidilkolina (lysoPCa C16:0 eta lysoPCa C18:1) eta SM C18:0 esfingomielina.

5.3.2.2. Analisi ez-bideratuko emaitzak

Analisi bideratuan bezala, analisi ez-bideratuan ere ASCA-ko dosia azpiereduak ez du permutazio-testa gainditu (p-balioa > 0,05) eta p-balio baxuenak denbora azpiereduan lortu dira (ikus 5.2 taula). Emaitza horien arabera, amitriptilinarekin burututako esposizio-esperimentuan esposizio-denbora da aldagai esanguratsuena. Dosia·denbora azpiereduari dagokionez, permutazio-testa gibelean soilik gainditu da (ikus 5.2 taula). Gainera, 5.1c irudian ageri den bezala, eta analisi bideratuko emaitzekin bat etorrita, kontroleko eta kutsatutako tankeetako arrainen arteko desberdintasun nabarmenenak esposizioko azken egunean (7. egunean) behatu dira. Dosia·denbora azpiereduaren arabera (ikus 5.3 taula) 37 gailurrei dagozkien metabolitoen kontzentrazioak desberdin aldatu dira esperimentuan zehar kontroleko eta kutsatutako arrainetan. 37 metabolito horietatik 3 soilik esleitu ahal izan dira KEGG datu-basearen arabera eta, ondorioz, ezinezkoa izan da bide metabolikoen aberastea burutzea [50]. Izan ere, gainontzeko 34 gailurren masa zehatzak KEGG datu-basean sartuta ez dauden behin-behineko lipido gisa identifikatu dira. Gainera, kasu gehienetan isomeroak detektatu direnez ezin izan da lipidoaren egitura konkretua zehaztu baina posible izan da dagokion lipido-kategoria adieraztea. 5.3 taulan beha daitekeen bezala, behin behineko 34 lipido horietatik 1 gantz aziloa da, 3 esfingolipidoak, 2 esterol lipidoak, 25 glizerofosfolipidoak eta 3 glizerolipidoak dira. Gainera, taula berean amitriptilinaren ondorioz jokabidea esanguratsuki aldatu duten 37 metabolitoen 2., 4. eta 7. esposizio-egunetako FC balioak ageri dira.

Gibelaren kasuan, dosia·denbora azpiereduak analisi bideratuko eta ez-bideratuko emaitzetan izan dira esanguratsuak, eta bi analisi-hurbilketen arabera gehienbat eraldatu diren kontzentrazioak lipidoen metabolismoan barneratzen diren konposatuen kontzentrazioak dira. Hain zuzen, analisi bideratuan 13 metabolitotik 11 izan dira lipidoak, eta analisi ez-bideratuan 37 metabolitotik 34. Hala eta guztiz ere, bi hurbilketetako emaitzetatik identifikatu den metabolito bakarra C18 azil karnitina izan da, estearoilkarnitina gisa ezagutzen dena (ikus 5.3 irudia).

5.3 taula: *ASCA-ren arabera gibeleko mailak esanguratsuki aldatu zaizkien gailurren identifikazioa eta euren aldaketa-mailak (fold change, FC, delakoak) 2., 4. eta 7. egunetan.*

Gailurra	Masa molekularra	Izena edo Formula molekulara	Maila	Kodea (KEGG edo LipidMaps)	Aldaketa-maila (FC)		
					2.eguna	4.eguna	7.eguna
KEGG bidez identifikatuta							
HILICpos_Gailur286	219,1106	Pantotenatoa	2a	C00864	1,78	0,87	1,74
HILICneg_Gailur194	168,02765	Uratoa	2a	C00366	1,95	0,86	1,20
HILICpos_Gailur1	174,06401	Formilisoglutamina / N-Formimino-L-glutamatoa	3	C16674 / C00439	5,18	0,68	3,25
Gantz azilo kategoriako lipidoa (LMFA)							
C18pos_Gailur153	427,36586	C18:0 (Estearoilkarnitina)	2b	7070008	0,70	1,05	1,59
Esfingolipidoen kategoriako lipidoak (LMSP)							
C18pos_Gailur141	309,26659	(9Me;4E;8E;10E-d19:3) esfingosina	2b	1080014	0,94	1,05	0,66
C18pos_Gailur31	647,62106	Zer(d18:1\ /24:1(15Z))	2a	2010009	1,01	1,03	0,81
HILICpos_Gailur319	688,55202	$C_{38}H_{77}N_2O_6P$ (2 hautagai)	3	03010038; 03010037	1,11	1,05	1,44
Sterol lipidoen kategoriako lipidoak (LMST)							
HILICpos_Gailur264	444,36093	$C_{29}H_{48}O_3$ (6 hautagai)	3	01010175; 01010227; 01031087; 03020419; 03020420; 03020421	0,64	0,90	1,01
HILICpos_Gailur79	368,34463	3-Deoxibitamina D3	2b	3020618	0,73	1,14	0,95
Glizerolipidoen kategoriako lipidoak (LMGL)							
C18pos_Gailur42	402,2768	MG(0:0\/22:6 (4Z;7Z; 10Z;13Z;16Z;19Z)\/0:0)	3	1010027	1,54	1,04	0,61
C18pos_Gailur54	616,50614	$C_{39}H_{68}O_5$ (3 hautagai)	3	02010480; 02010064;02010063	1,24	1,15	0,63
C18pos_Gailur75	638,49114	$C_{41}H_{66}O_5$ (2 hautagai)	3	02010174; 02010143	1,17	1,16	0,57

5.3 taula: *(Jarraipena).*

Gailurra	Masa molekularra	Izena edo Formula molekulara	Maila	Kodea (KEGG edo LipidMaps)	Aldaketa-maila (FC)		
					2.eguna	4.eguna	7.eguna
Glizerofosfolipidoen kategoriako lipidoak (LMGP)							
C18neg_Gailur12	777,53107	$C_{44}H_{76}NO_8P$ (4 hautagai)	3	02011139; 02011210; 01012099; 01010512	0,51	0,90	1,09
C18neg_Gailur43	453,28577	$C_{21}H_{44}NO_7P$ (2 hautagai)	3	02050002; 01050001	0,72	1,35	1,18
C18neg_Gailur48	481,31683	$C_{23}H_{48}NO_7P$ (4 hautagai)	3	02050001; 01050016; 01080020; 01080029	0,82	1,12	1,20
C18neg_Gailur50	743,54682	$C_{41}H_{78}NO_8P$ (4 hautagai)	3	02011193; 02010044; 01011618; 01010543	0,95	1,00	1,49
C18neg_Gailur52	479,30127	$C_{23}H_{46}NO_7P$ (2 hautagai)	3	02050004; 01050125	0,78	1,15	1,09
C18neg_Gailur57	748,5257	$C_{40}H_{77}O_{10}P$ (8 hautagai)	3	04010149; 04010484; 04010457; 04010178; 04010127; 04010511; 04010102; 04010530	0,61	0,94	1,04
C18neg_Gailur6	765,53077	$C_{43}H_{76}NO_8P$ (4 hautagai)	3	02010973; 02011201; 01011425; 01011930	0,76	0,99	1,25
C18neg_Gailur70	708,47329	$C_{40}H_{69}O_8P$ (2 hautagai)	3	10010655; 10010240	0,75	1,34	1,74
C18neg_Gailur77	805,56258	$C_{46}H_{80}NO_8P$ (2 hautagai)	3	01011116; 01010650	0,73	1,02	1,10
C18pos_Gailur195	453,28546	$C_{21}H_{44}NO_7P$ (2 hautagai)	3	02050002; 01050001	0,66	1,24	1,35
C18pos_Gailur207	479,30089	PE(18:1(9Z)\/0:0)	2b	2050004	0,81	1,11	1,14
C18pos_Gailur6	763,51454	$C_{43}H_{74}NO_8P$ (13 hautagai)	3	02011161; 02010095; 20020014; 02011172; 02011195; 02010945; 02011192; 02010916; 02010917; 02010887; 02010759; 02010729; 02010701	0,84	1,14	1,21
C18pos_Gailur8	757,5615	$C_{42}H_{80}NO_8P$ (27 hautagai)	3	01010592; 01010585; 01010590; 01010920; 01010588; 01010586; 01010926; 01010932; 01010589; 01011559; 01011504; 01010687; 01010678; 01010887; 01012147; 01010688; 01010727; 01010728; 01010745; 01011398; 01011449; 01011808; 01011761; 01011373; 01011837; 01012035; 01011336	1,38	1,56	0,79
HILICneg_Gailur109	835,51614	PE(22:6(4Z;7Z;10Z;13Z;16Z;19Z) \/ 22:6 (4Z;7Z;10Z;13Z;16Z;19Z))	2b	2010093	1,14	0,95	0,77

5.3 taula: *(Jarraipen).*

Gailurra	Masa molekularra	Izena edo Formula molekulara	Maila	Kodea (KEGG edo LipidMaps)	Aldaketa-maila (FC)		
					2.eguna	4.eguna	7.eguna
HILICneg_Gailur38	803,56873	$C_{43}H_{82}NO_{10}P$ (15 hautagai)	3	00000048, 03010332, 03010462, 03010704, 03010187, 03010157, 03010729, 03010239, 03010536, 03010318, 03010491, 03010221, 03010681, 03010266, 03010516	1,25	1,02	0,80
HILICneg_Gailur58	479,30085	$C_{23}H_{46}NO_7P$ (2 hautagai)	3	02050004; 01050125	0,73	1,11	0,89
HILICpos_Gailur16	805,56144	$C_{46}H_{80}NO_8P$ (22 hautagai)	3	01010650; 01011116; 01012141; 01012140; 01012216; 01010844; 01012201; 01011909; 01012175; 01011880; 01012212; 01012179; 01010907; 01011851; 01012171; 01010943; 01012200; 01011721; 01011662; 01011057; 01011881; 01011691	1,03	1,00	1,42
HILICpos_Gailur17	783,57851	$C_{44}H_{82}NO_8P$ (19 hautagai)	3	01011589; 01011651; 01011588; 01011682; 01011624; 01010895; 01012168; 01010893; 01012149; 01011766; 01011568; 01012194; 01010622; 01011872; 01010624; 01012038; 01011842; 01011490; 01011406	1,03	0,84	1,27
HILICpos_Gailur187	467,30131	$C_{22}H_{46}NO_7P$ (3 hautagai)	3	01050073; 01050012; 01020009	1,28	1,04	1,20
HILICpos_Gailur193	787,51563	$C_{45}H_{74}NO_8P$ (7 hautagai)	3	02011144; 02011191; 02011118; 02010767; 02011173; 02010926; 02010983	1,19	1,04	1,45
HILICpos_Gailur458	819,61213	$C_{48}H_{86}NO_7P$ (3 hautagai)	3	01020110; 01090059; 01030098	1,55	1,17	1,27
HILICpos_Gailur53	769,56366	$C_{43}H_{80}NO_8P$ (24 hautagai)	3	01011602; 01011562; 01011423; 01011870; 02010913; 02011202; 01011533; 01011622; 01011452; 01011840; 02010647; 02010883; 01011507; 01011506; 01011679; 01011648; 02010854; 02010670; 02011078; 02010537; 02010832; 02010726; 02010831; 02010698	0,83	0,86	1,33
HILICpos_Gailur56	763,5154	$C_{43}H_{74}NO_8P$ (13 hautagai)	3	02011161; 02010095; 20020014; 02011172; 02011195; 02010945; 02011192; 02010916; 02010917; 02010887; 02010759; 02010729; 02010701	0,95	1,24	1,89
HILICpos_Gailur57	741,53203	$C_{41}H_{76}NO_8P$ (24 hautagai)	3	02010908; 02011222; 01011444; 01011619; 02010048; 02010663; 02010878; 02010531; 01011867; 01011355; 02010720; 02010629; 02010690; 02010628; 01011482; 01011558; 01011417; 01011416; 01011675; 01011644; 02010608; 02010803; 02011074; 02010449	0,94	1,19	1,83
HILICpos_Gailur87	803,54678	$C_{46}H_{78}NO_8P$ (11 hautagai)	3	01010696; 01012103; 01011306; 01011634; 01011938; 01011882; 01011722; 01011910; 01011663; 01011692; 01011911	1,07	1,07	1,53

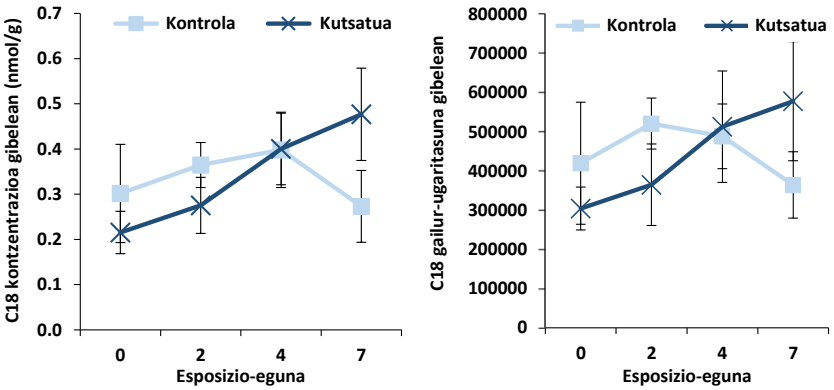

a) Analisi bideratua b) Analisi ez-bideratua

5.3 irudia: *C18 azil karnitinaren gibeleko batezbesteko kontzentrazioak (a, analisi bideratuan) edo gailur-ugaritasunak (b, analisi ez-bideratuan) kontroleko eta kutsatutako arrainetan esperimentuko egun desberdinetan, eta % 95-eko konfiantza tarteak.*

5.3.3. Dosiari lotutako efektuen interpretazio biologikoa

Interpretazio biologikorako analisi bideratuan zein ez-bideratuan ASCA hurbilketatik identifikatutako metabolitoak erabili dira. Laburpen gisa, burmuin- eta gibel-metabolomako aldaketak kontuan izanda, amitriptilinaren dosiak eragindako albo-ondorioak argininan, metioninan, glutamatoan, asparaginan, pantotenatoan, azido urikoan, formilisoglutamina/N-formimino-L-glutamatoan eta lipidoen metabolismoko 51 metabolitotan behatu dira.

Burmuineko argininaren mailako aldaketak oxido nitrikoaren ekoizpena asaldatzearekin lotuta egon daitezke. Izan ere, oxido nitriko sintasak albo-produktu gisa oxido nitrikoa sortzen den argininatik zitrulinarako erreakzioa katalizatu eta, bibliografiaren arabera, antidepresiboen tratamenduak oxido nitrikoaren sistema orekatzen du [51]. Izatez, SSRI-ak entzima horretara lotu daitezke bibliografiaren arabera [23,52]. Horrez gain, beste ikertzaile batzuek zebra-arrainen enbrioietan oxido nitrikoaren edukiaren murriztea behatu dute amitriptilinaren presentzian (< 1 mg/L kontzentrazioan) [25]. Hori dela eta, lan honetan behatutako argininaren aldaketa estres oxidatiboaren kontrako babesaren seinalea izan daiteke, eta emaitza horrek bat egiten du arratoiekin burututako lan bateko ondorioekin, non fluoxetina antidepresiboak oxigeno-espezie erreaktiboen ekoizpena jaisten duela behatu duten [53].

5.2b irudian ikus daitekeen moduan, kutsatutako arrainen gibelean kate luzeko azil karnitinen metatzea behatu da (FC > 1,50). Behaketa hori, kutsatzaileen albo-ondorio nagusia den gibeleko estres oxidatiboaren seinalea izan daiteke [36,54] eta gibeleko zitokromo entzimen bidezko amitriptilinaren metabolizazioak [55] oxigeno-espezie erreaktiboen igoera hori azal dezake. Izatez, hipotesi horrek bat egiten du gure aurreko amitriptilinaren biotransformazio-laneko behaketekin, non amitriptilina nagusiki konposatu monohidroxilatuetara metabolizatu zen kutsatutako arrainen gibelean [38]. Gainera, Kotarsky-ren eta lankideen behaketen antzera [54], metatze hori ez da karnitinan edo kate laburreko azil karnitinetan behatu, baizik eta kutsatutako arrainen gibeleko kate-luzeko azil karnitinetan soilik. Oro har, 5.4 irudian ikus daitekeenez, korrelazio positibo esanguratsua behatu da azil karnitinen kate-luzeraren eta FC-en artean (r^2=0.76), eta horrek erreserba-lipidoen gainkontsumoa iradoki dezake [36].

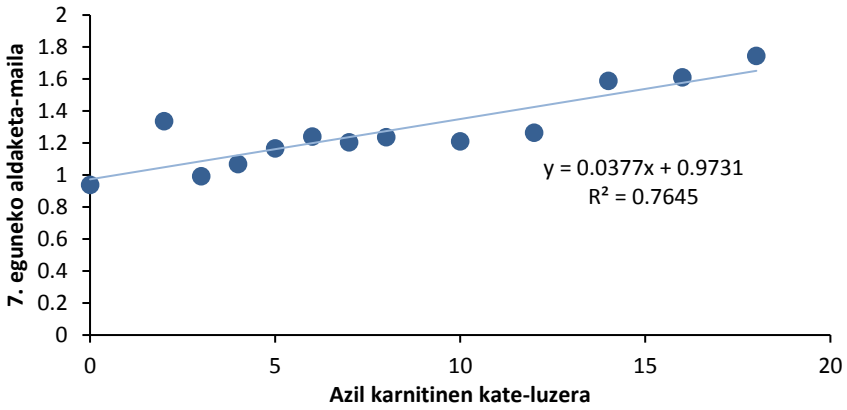

***5.4 irudia**: Asetutako karnitinen kate-luzeraren eta 7. eguneko arrain-gibeleko aldaketa-mailen (fold change, FC, delakoen) arteko korrelazioa. FC balioak kalkulatzeko 7. eguneko kutsatutako laginetako metabolitoaren batezbesteko kontzentrazioa 7. eguneko kontroleko laginetako analito berdinaren batezbesteko kontzentrazioarekin zatitu da.*

Bestalde, amitriptilinak burmuineko eta gibeleko aminoazidoen metabolismoan aldaketak sortu dituela aditzera eman dute 5.2 irudiko eta 5.3 taulako emaitzek. Izan ere, burmuinean metionina eta asparagina aldatu dira, eta gibelean pantotenatoa, azido urikoa eta formilisoglutamina/N-formimino-L-glutamatoa. Karnitinaren aitzindaria den metionina eta asparagina metabolitoen mailetan behatutako aldaketek imipramina antidepresibo triziklikoa eman zaien arratoiekin egindako lanaren behaketekin bat egiten dute [56]. Izan ere, lan horretako

arratoien burmuinean metioninaren, asparaginaren, glutamatoaren eta beste aminoazido batzuen aldaketak behatu dira. Bibliografian, arratoietan, garuneko aminoazidoen metabolismoko perturbazioak estresarekiko duten ahultasunarekin lotu dira [57,58]. Gainera, gibeleko aminoazidoen metabolismoan ere aldaketak behatu ditugu, amitriptilinarekiko esposizioaren ondorioz β-alaninaren metabolismoko, purinen metabolismoko eta histidinaren metabolismoko metabolitoen kontzentrazioak aldatu baitira.

Glutamatoak funtzio garrantzitsua betetzen du gibeleko aminoazidoen metabolismoan. Izan ere, glutationaren aitzindari hau folato-koentzimen katabolismoan eta GABA-ren ezabatze-prozesuan ekoizten da [59]. Gibelean behatutako glutamatoaren kontzentrazio-aldaketak energia-metabolismoarekin lotuta egon daitezke, glutamatoa, glutamato deshidrogenasaren bidez, Krebs zikloko bitartekaria den α-ketoglutaratora eraldatzen delako. Beraz, emaitza horrek erakusten du amitriptilinak energia-metabolismoarekin lotutako aminoazidoen mailetan aldaketak sor ditzakeela, paroxetina SSRI-arekin behatutakoaren antzera [24] eta, ondorioz, antidepresiboek eragindako albo-ondorioak SSRI-ekin burututako lanetan sakon ikertutako monoaminetatik [18,19,21,22] haratago doazela.

Kontrolekin erkatuta, kutsatutako arrainen gibelean behatutako lisofosfatidilkolinen maila baxuagoek (FC < 1,00 esposizioko azken egunean) aditzera ematen dute amitriptilinak lisofosfatidilkolinen eraldatzea areagotzen duela. Izatez, Xia-k eta lankideek adierazi izan dute amitriptilina bezalako farmako anfifilikoek fosfolipidosia (hau da, lipidoen metatze-arazoak) eragin dezaketela organo gehienen zeluletan [60]. Gainera, farmakoek eragindako gibeleko fosfolipidosiaren odoleko adierazle gisa ere deskribatu izan dira lisofosfatidilkolinak [61]. Analisi bideratuko lisofosfatidilkolinez (lysoPCa20:3 eta lysoPCa24:1 metabolitoez) eta fosfatidilkolinez (PCaaC30:2, PCaaC32:1, PCaaC32:2 eta PCaaC32:3 metabolitoez) gain, gibeleko analisi ez-bideratuan beste 25 glizerofosfolipido, 3 glizerolipido, 2 esterol lipido eta 3 esfingolipido ere identifikatu dira kontzentrazioa esanguratsuki aldatuta izan dutenak (ikus 5.3 taula). Oro har, lan honetako emaitzek bat egiten dute metabolomikako ikerketa berriarekin, non lipidoen metabolismoko aldaketen eta estres oxidatiboaren arteko lotura aipatzen den [62].

Lipidoen metabolismoa garunean ere asaldatu da, lipido-klase guztietan (hau da, azil karnitinetan, lisofosfatidilkolinetan, fosfatidilkolinetan eta esfingomielinetan); kutsatutako

arrainetan kontzentrazioak kontrolekoak baino altuagoan izan dira esposizioko azken egunean (FC > 1,00 kasu guztietan). Adibidez, fosfatidilkolinen igoeraren arrazoia amitriptilina bezalako SSRI-ek fosfolipidoei lotzeko duten gaitasunari egotzi dakioke [60]. Izan ere, fosfolipasa entzimen substratu gisa lipidoak duen egokitasuna desberdina izan daiteke lipidoa aske edo SSRI-ari lotuta dagoenean. Bestalde, amitriptilina bezalako antidepresibo triziklikoek esfingomielinasen jarduera ere inhibitzen dutenez [63], horrek esfingomielinen metatzea eragin dezake. Izatez, bibliografian fosfatidilkolinen eta esfingolipidoen kontzentrazioaren eta gaixotasun neurologikoen (antsietatearen eta depresioaren) arteko alderantzizko korrelazioa behatu izan da [64].

5.4. Ondorioak

Lan honen arabera eta, nahiz eta arrainik ez den hil eta urraburu arrainen propietate fisiologiko orokorretan aldaketarik ez den behatu, amitriptilinak ingurumenean esanguratsua den kontzentrazioan 7 eguneko esposizioaren ostean arrainen burmuin- eta gibel-metaboloman aldaketak sortzen dituela ondorioztatu da. Behatutako kate luzeko azil karnitinen metatzeak eta lipidoen metabolismoko konposatuen aldaketek lipidoen gordetzea desorekatuta dagoela adierazten dute. Arazo hori aurretiaz deskribatu izan da SSRI-en albo-ondorio gisa eta kutsatzaileek sortu ohi duten estres oxidatiboarekin lotuta egon daiteke [36]. Dena den, beste mekanismo baten bidez, SSRI-ak estres oxidatiboaren kontrako babesleak ere badira, eta izatez, lan honetan behatutako argininaren kontzentrazio-aldaketak oxido nitrikoaren ekoizpenaren murriztearekin lotuta egon daitezke. Horrez gain, karnitinen aitzindaria den metionina ere gibelean eta burmuinean, bietan, asaldatu da. Izatez, metionina eta beste aminoazidoen aldaketek, bibliografiarekin bat etorrita [56], aminoazidoen metabolismoa perturbatu dela adierazten dute. Bestalde, gibeleko glutamatoaren mailen aldakuntzak energia-metabolismoko aldaketa iradoki dezake, beste antidepresibo batzuekin burututako lanetan behatu den antzera [24]. Behaketa guzti horiek kezkagarriak izan daitezke arrainekin ondorio kaltegarrien bidea (*adverse outcome pathway*, AOP, delakoa) aztertu duten ikerketetan arrainen ehunetan behatutako gertaera espezifikoak (adibidez, estres oxidatiboa eta energia-metabolismoaren aldaketa) indibiduo-mailako (hazte-atzerapena) eta populazio-mailako (biziraupenaren murriztea) albo-ondorioekin lotu baitituzte [65].

Oro har, datu horien arabera amitriptilinaren esposizioak ingurumenean esanguratsua den kontzentrazioan aldaketak sortzen ditu arrainen metaboloman. Gainera, aldaketa metabolikoak sakon aztertutako monoaminetatik haratago doaz. Lan honetako behaketekin, arrainak bezalako organismo ez-zuzenduetan amitriptilinak eragindako albo-ondorioen inguruko informazio mugatua areagotzen den arren, saiakuntza gehiago egitea erabaki da lan honetako emaitzetan oinarrituta. Hain zuzen, ikerketaren bigarren atalerako (ikus 6. Kapitulua) dosi altuagoko eta denbora luzeagoko esposizio-esperimentuak diseinatu dira organismo-mailako aldaketak behatzeko aukera handitzeko. Horrela, posible izango da maila molekularreko ekintza abiarazlearen eta arrisku ekologikorako (hau da, biziraupenerako, garapenerako edo ugalketarako) esanguratsua den organismo mailako behaketen arteko lotura frogatzea [65,66].

5.5. Erreferentziak

1. Bautista-Ferrufino MR, Cordero MD, Sánchez-Alcázar JA, Illanes M, Fernández-Rodríguez A, Navas P, de Miguel M. 2011. Amitriptyline induces coenzyme Q deficiency and oxidative damage in mouse lung and liver. *Toxicol. Lett.* 204:32–37.
2. Calisto V, Esteves VI. 2009. Psychiatric pharmaceuticals in the environment. *Chemosphere*. 77:1257–1274.
3. Lajeunesse A, Gagnon C, Sauvé S. 2008. Determination of Basic Antidepressants and Their N-Desmethyl Metabolites in Raw Sewage and Wastewater Using Solid-Phase Extraction and Liquid Chromatography−Tandem Mass Spectrometry. *Anal. Chem.* 80:5325–5333.
4. Kasprzyk-Hordern B, Dinsdale RM, Guwy AJ. 2008. The occurrence of pharmaceuticals, personal care products, endocrine disruptors and illicit drugs in surface water in South Wales, UK. *Water Res.* 42:3498–3518.
5. Togola A, Budzinski H. 2008. Multi-residue analysis of pharmaceutical compounds in aqueous samples. *J. Chromatogr. A*. 1177:150–158.
6. Klosterhaus SL, Grace R, Hamilton MC, Yee D. 2013. Method validation and reconnaissance of pharmaceuticals, personal care products, and alkylphenols in surface waters, sediments, and mussels in an urban estuary. *Environ. Int.* 54:92–99.
7. Ziarrusta H, Mijangos L, Prieto A, Etxebarria N, Zuloaga O, Olivares M. 2016. Determination of tricyclic antidepressants in biota tissue and environmental waters by liquid chromatography-tandem mass spectrometry. *Anal. Bioanal. Chem.* 408:1205–1216.
8. Moreno-Fernández AM, Cordero MD, de Miguel M, Delgado-Rufino MD, Sánchez-Alcázar JA,

Navas P. 2008. Cytotoxic effects of amitriptyline in human fibroblasts. *Toxicology*. 243:51–58.

9. Vismari L, Alves GJ, Muscará MN, Palermo-Neto J. 2012. A possible role to nitric oxide in the anti-inflammatory effects of amitriptyline. *Immunopharmacol. Immunotoxicol.* 34:578–585.

10. Lirk P, Haller I, Hausott B, Ingorokva S, Deibl M, Gerner P, Klimaschewski L. 2006. The neurotoxic effects of amitriptyline are mediated by apoptosis and are effectively blocked by inhibition of caspase activity. *Anesth. Analg.* 102:1728–1733.

11. Kitagawa N, Oda M, Nobutaka I, Satoh H, Totoki T, Morimoto M. 2006. A proposed mechanism for amitriptyline neurotoxicity based on its detergent nature. *Toxicol. Appl. Pharmacol.* 217:100–106.

12. Brooks BW, Foran CM, Richards SM, Weston J, Turner PK, Stanley JK, Solomon KR, Slattery M, La Point TW. 2003. Aquatic ecotoxicology of fluoxetine. *Toxicol. Lett.* 142:169–183.

13. Fong PP, Ford AT. 2014. The biological effects of antidepressants on the molluscs and crustaceans: A review. *Aquat. Toxicol.* 151:4–13.

14. Guler Y, Ford AT. 2010. Anti-depressants make amphipods see the light. *Aquat. Toxicol.* 99:397–404.

15. Johnson DJ, Sanderson H, Brain RA, Wilson CJ, Solomon KR. 2007. Toxicity and hazard of selective serotonin reuptake inhibitor antidepressants fluoxetine, fluvoxamine, and sertraline to algae. *Ecotoxicol. Environ. Saf.* 67:128–139.

16. Minagh E, Hernan R, O'Rourke K, Lyng FM, Davoren M. 2009. Aquatic ecotoxicity of the selective serotonin reuptake inhibitor sertraline hydrochloride in a battery of freshwater test species. *Ecotoxicol. Environ. Saf.* 72:434–440.

17. Styrishave B, Halling-Sørensen B, Ingerslev F. 2011. Environmental risk assessment of three selective serotonin reuptake inhibitors in the aquatic environment: A case study including a cocktail scenario. *Environ. Toxicol. Chem.* 30:254–261.

18. Bisesi JH, Sweet LE, van den Hurk P, Klaine SJ. 2016. Effects of an antidepressant mixture on the brain serotonin and predation behavior of hybrid striped bass. *Environ. Toxicol. Chem.* 35:938–945.

19. Bisesi Jr JH, Bridges W, Klaine SJ. 2014. Effects of the antidepressant venlafaxine on fish brain serotonin and predation behavior. *Aquat. Toxicol.* 148:130–138.

20. Clotfelter ED, O'Hare EP, McNitt MM, Carpenter RE, Summers CH. 2007. Serotonin decreases aggression via 5-HT1A receptors in the fighting fish Betta splendens. *Pharmacol. Biochem. Behav.* 87:222–231.

21. Gaworecki KM, Klaine SJ. 2008. Behavioral and biochemical responses of hybrid striped bass

during and after fluoxetine exposure. *Aquat. Toxicol.* 88:207–213.

22. Winder VL, Sapozhnikova Y, Pennington PL, Wirth EF. 2009. Effects of fluoxetine exposure on serotonin-related activity in the sheepshead minnow (Cyprinodon variegatus) using LC/MS/MS detection and quantitation. *Comp. Biochem. Physiol. Part C Toxicol. Pharmacol.* 149:559–565.

23. Stahl SM. 1998. Not So Selective Serotonin Reuptake Inhibitors. *J. Clin. Psychiatry*. 59:333–343.

24. Webhofer C, Gormanns P, Tolstikov V, Zieglgänsberger W, Sillaber I, Holsboer F, Turck CW. 2011. Metabolite profiling of antidepressant drug action reveals novel drug targets beyond monoamine elevation. *Transl. Psychiatry*. 1:e58.

25. Yang M, Qiu W, Chen J, Zhan J, Pan C, Lei X, Wu M. 2014. Growth inhibition and coordinated physiological regulation of zebrafish (Danio rerio) embryos upon sublethal exposure to antidepressant amitriptyline. *Aquat. Toxicol.* 151:68–76.

26. Viant MR. 2008. Recent developments in environmental metabolomics. *Mol. Biosyst.* 4:980–986.

27. Huang SSY, Benskin JP, Chandramouli B, Butler H, Helbing CC, Cosgrove JR. 2016. Xenobiotics Produce Distinct Metabolomic Responses in Zebrafish Larvae (Danio rerio). *Environ. Sci. Technol.* 50:6526–6535.

28. Aoki-Kinoshita KF. 2006. Overview of KEGG applications to omics-related research. *J. Pestic. Sci.* 31:296–299.

29. Wishart DS, Tzur D, Knox C, Eisner R, Guo AC, Young N, Cheng D, Jewell K, Arndt D, Sawhney S, Fung C, Nikolai L, Lewis M, Coutouly M-A, Forsythe I, Tang P, Shrivastava S, Jeroncic K, Stothard P, Amegbey G, Block D, Hau DD, Wagner J, Miniaci J, Clements M, Gebremedhin M, Guo N, Zhang Y, Duggan GE, MacInnis GD, Weljie AM, Dowlatabadi R, Bamforth F, Clive D, Greiner R, Li L, Marrie T, Sykes BD, Vogel HJ, Querengesser L. 2007. HMDB: the Human Metabolome Database. *Nucleic Acids Res.* 35:D521–D526.

30. Vinaixa M, Samino S, Saez I, Duran J, Guinovart JJ, Yanes O. 2012. A Guideline to Univariate Statistical Analysis for LC/MS-Based Untargeted Metabolomics-Derived Data. *Metabolites*. 2:775–795.

31. Shi B, Tian J, Xiang H, Guo X, Zhang L, Du G, Qin X. 2013. A 1H-NMR plasma metabonomic study of acute and chronic stress models of depression in rats. *Behav. Brain Res.* 241:86–91.

32. Worley B, Powers R. 2013. Multivariate Analysis in Metabolomics. *Curr. Metabolomics*. 1:92–107.

33. Jansen JJ, Hoefsloot HCJ, van der Greef J, Timmerman ME, Westerhuis JA, Smilde AK. 2005.

ASCA: analysis of multivariate data obtained from an experimental design. *J. Chemom.* 19:469–481.

34. Nueda MJ, Conesa A, Westerhuis JA, Hoefsloot HCJ, Smilde AK, Talón M, Ferrer A. 2007. Discovering gene expression patterns in time course microarray experiments by ANOVA–SCA. *Bioinformatics*. 23:1792–1800.

35. Malik A, Jordao R, Campos B, Casas J, Barata C, Tauler R. 2016. Exploring the disruptive effects of TBT on lipid homeostasis of Daphnia magna using chemometric methods. *Chemom. Intell. Lab. Syst.* 159:58–68.

36. Gómez-Canela C, Prats E, Piña B, Tauler R. 2017. Assessment of chlorpyrifos toxic effects in zebrafish (Danio rerio) metabolism. *Environ. Pollut.* 220, Part B:1231–1243.

37. Ribbenstedt A, Ziarrusta H, Benskin JP. 2018. A Multi-platform Targeted/Non-targeted (TNT) approach for quantitative and discovery-based metabolomics. *PLOS ONE (submitted)*.

38. Ziarrusta H, Mijangos L, Izagirre U, Plassmann MM, Benskin JP, Anakabe E, Olivares M, Zuloaga O. 2017. Bioconcentration and Biotransformation of Amitriptyline in Gilt-Head Bream. *Environ. Sci. Technol.* 51:2464–2471.

39. Fulton WT. 1904. The rate of growth of fishes. *22nd Annu. Rep. Fish. Board Scotl.* 3:141–241.

40. Hrydziuszko O, Viant MR. 2012. Missing values in mass spectrometry based metabolomics: an undervalued step in the data processing pipeline. *Metabolomics*. 8:161–174.

41. Kamleh MA, Ebbels TMD, Spagou K, Masson P, Want EJ. 2012. Optimizing the Use of Quality Control Samples for Signal Drift Correction in Large-Scale Urine Metabolic Profiling Studies. *Anal. Chem.* 84:2670–2677.

42. Gorrochategui E, Jaumot J, Lacorte S, Tauler R. 2016. Data analysis strategies for targeted and untargeted LC-MS metabolomic studies: Overview and workflow. *TrAC Trends Anal. Chem.* 82:425–442.

43. Simmons DBD, Benskin JP, Cosgrove JR, Duncker BP, Ekman DR, Martyniuk CJ, Sherry JP. 2015. Omics for aquatic ecotoxicology: Control of extraneous variability to enhance the analysis of environmental effects. *Environ. Toxicol. Chem.* 34:1693–1704.

44. Xia J, Sinelnikov IV, Han B, Wishart DS. 2015. MetaboAnalyst 3.0—making metabolomics more meaningful. *Nucleic Acids Res.* 43:W251–W257.

45. http://www.lipidmaps.org/. 2018. LipidMaps_.

46. Fernández-Albert F, Llorach R, Garcia-Aloy M, Ziyatdinov A, Andres-Lacueva C, Perera A. 2014. Intensity drift removal in LC/MS metabolomics by common variance compensation. *Bioinformatics*. 30:2899–2905.

47. Schymanski EL, Jeon J, Gulde R, Fenner K, Ruff M, Singer HP, Hollender J. 2014. Identifying Small Molecules via High Resolution Mass Spectrometry: Communicating Confidence. *Environ. Sci. Technol.* 48:2097–2098.

48. http://www.kegg.jp/kegg/. 2018. KEGG_.

49. https://msbi.ipb-halle.de/MetFragBeta/. 2018. MetFrag_.

50. Chagoyen M, Pazos F. 2013. Tools for the functional interpretation of metabolomic experiments. *Brief. Bioinform.* 14:737–744.

51. Park DI, Dournes C, Sillaber I, Ising M, Asara JM, Webhofer C, Filiou MD, Müller MB, Turck CW. 2017. Delineation of molecular pathway activities of the chronic antidepressant treatment response suggests important roles for glutamatergic and ubiquitin–proteasome systems. *Transl. Psychiatry*. 7:e1078.

52. Yaron I, Shirazi I, Judovich R, Levartovsky D, Caspi D, Yaron M. 1999. Fluoxetine and amitriptyline inhibit nitric oxide, prostaglandin E2, and hyaluronic acid production in human synovial cells and synovial tissue cultures. *Arthritis Rheum.* 42:2561–2568.

53. Rebai R, Jasmin L, Boudah A. 2017. The antidepressant effect of melatonin and fluoxetine in diabetic rats is associated with a reduction of the oxidative stress in the prefrontal and hippocampal cortices. *Brain Res. Bull.* 134:142–150.

54. Kotarsky H, Keller M, Davoudi M, Levéen P, Karikoski R, Enot DP, Fellman V. 2012. Metabolite Profiles Reveal Energy Failure and Impaired Beta-Oxidation in Liver of Mice with Complex III Deficiency Due to a BCS1L Mutation. *PLoS ONE*. 7.

55. Breyer-Pfaff U. 2004. The Metabolic Fate of Amitriptyline, Nortriptyline and Amitriptylinoxide in Man. *Drug Metab. Rev.* 36:723–746.

56. Nagasawa M, Otsuka T, Yasuo S, Furuse M. 2015. Chronic imipramine treatment differentially alters the brain and plasma amino acid metabolism in Wistar and Wistar Kyoto rats. *Eur. J. Pharmacol.* 762:127–135.

57. Murakami T, Yamane H, Tomonaga S, Furuse M. 2009. Forced swimming and imipramine modify plasma and brain amino acid concentrations in mice. *Eur. J. Pharmacol.* 602:73–77.

58. Nagasawa M, Ogino Y, Kurata K, Otsuka T, Yoshida J, Tomonaga S, Furuse M. 2012. Hypothesis with abnormal amino acid metabolism in depression and stress vulnerability in Wistar Kyoto rats. *Amino Acids*. 43:2101–2111.

59. Brosnan ME, Brosnan JT. 2009. Hepatic glutamate metabolism: a tale of 2 hepatocytes. *Am. J. Clin. Nutr.* 90:857S-861S.

60. Xia Z, Ying G, Hansson AL, Karlsson H, Xie Y, Bergstrand A, DePierre JW, Nässberger L. 2000.

Antidepressant-induced lipidosis with special reference to tricyclic compounds. *Prog. Neurobiol.* 60:501–512.

61. Saito K, Maekawa K, Ishikawa M, Senoo Y, Urata M, Murayama M, Nakatsu N, Yamada H, Saito Y. 2014. Glucosylceramide and Lysophosphatidylcholines as Potential Blood Biomarkers for Drug-Induced Hepatic Phospholipidosis. *Toxicol. Sci.* 141:377–386.

62. Zhao Y-Y, Wang H-L, Cheng X-L, Wei F, Bai X, Lin R-C, Vaziri ND. 2015. Metabolomics analysis reveals the association between lipid abnormalities and oxidative stress, inflammation, fibrosis, and Nrf2 dysfunction in aristolochic acid-induced nephropathy. *Sci. Rep.* 5.

63. Albouz S, Le Saux F, Wenger D, Hauw JJ, Baumann N. 1986. Modifications of sphingomyelin and phosphatidylcholine metabolism by tricyclic antidepressants and phenothiazines. *Life Sci.* 38:357–363.

64. Demirkan A, Isaacs A, Ugocsai P, Liebisch G, Struchalin M, Rudan I, Wilson JF, Pramstaller PP, Gyllensten U, Campbell H, Schmitz G, Oostra BA, van Duijn CM. 2013. Plasma phosphatidylcholine and sphingomyelin concentrations are associated with depression and anxiety symptoms in a Dutch family-based lipidomics study. *J. Psychiatr. Res.* 47:357–362.

65. Groh KJ, Carvalho RN, Chipman JK, Denslow ND, Halder M, Murphy CA, Roelofs D, Rolaki A, Schirmer K, Watanabe KH. 2015. Development and application of the adverse outcome pathway framework for understanding and predicting chronic toxicity: II. A focus on growth impairment in fish. *Chemosphere*. 120:778–792.

66. Ankley GT, Bennett RS, Erickson RJ, Hoff DJ, Hornung MW, Johnson RD, Mount DR, Nichols JW, Russom CL, Schmieder PK, Serrrano JA, Tietge JE, Villeneuve DL. 2010. Adverse outcome pathways: A conceptual framework to support ecotoxicology research and risk assessment. *Environ. Toxicol. Chem.* 29:730–741.

Chapter 6

Metabolic effects of amitriptyline in gilt-head bream; part 2: linking metabolic and apical endpoints

Submitted to

Environmental Toxicology & Chemistry

6.1 Introduction

There is considerable scientific and societal concern surrounding the effects of pharmaceutical compounds (PhCs) on non-target organisms such as fish. PhCs can enter the aquatic environment following incomplete elimination during wastewater treatment [1]. Among PhCs, the presence of neuroactive compounds such as antidepressants is particularly concerning because these PhCs have been shown to alter behavior in several fish species [1]. The mode of action of most antidepressants involves monoamine increase; however, involvement of other pathways is also possible [2–7]. This includes amino acid metabolism and hormone signalling [7], glutamatergic and ubiquitin–proteasome systems [3], purine and pyrimidine metabolism [4], kynurenine pathway [2], and energy metabolism [5–7].

Amitriptyline, the most widely used tricyclic antidepressant, is less comprehensively studied relative to other selective serotonin reuptake inhibitors (SSRIs). Most studies to date have focused on the effects of amitriptyline and other SSRIs in rodents [8–13]. For instance, amitriptyline at high dose causes toxicity and lipid peroxidation in both liver and brain [12,13]. A similar tricyclic antidepressant, imipramine, was found to alter amino acid levels in brain and plasma [11]. In comparison, research involving the most frequently studied SSRI, fluoxetine, revealed that it is cytotoxic to blood brain barrier endothelial cells [9], modifies the activity of melanin-concentrating hormone and hypocretinergic systems [8], and directs energy metabolism towards the Krebs cycle and causes oxidative phosphorylation [10]. Although recent studies have demonstrated that some antidepressants such as amitriptyline are accumulated in fish tissues [14], the effects of SSRIs in non-target organisms such as fish are not widely studied. The few investigations of adverse effects of neurochemicals in fish have focused on targeted endpoints related to the known mechanism of action of SSRIs, in particular monoamine reuptake inhibition [15–17]. However, the effects of amitriptyline can go beyond the serotonergic system and alter other non-directed biochemical pathways as it has been observed in some studies performed with rodents [2,12,13].

Metabolomics is one of several omic tools which has seen increased usage over the last few decades [18,19] for detecting molecular-level alterations that standard toxicological bioassays are not able to achieve. This approach is particularly useful for investigating the effects of xenobiotics

occurring in the environment at non-lethal levels [20]. In particular, non-targeted metabolomic approaches seek to detect as many distinct features as possible in a single analysis, offering the opportunity to discover novel compounds that can improve our understanding effects of xenobiotics [18,21]. Although non-targeted results are not always fully quantitative, they can be accurate enough for case/control comparisons [3,7,18,22]. Since generally high dimensional and multi-correlated data are obtained for a few replicate samples, both univariate and multivariate approaches [22,23] are applied to identify key metabolites which distinguish case from control groups. In addition, the use of pathway enrichment [24] helps to find plausible biological explanations for those metabolic alterations taking into account compounds, modules, enzymes, reactions and pathways in databases such as KEGG [25].

The present work represents the second of a 2-part study examining the effects of amitriptyline in gilt head bream (*Sparus aurata*). In part 1, an environmentally relevant dose (0.2 µg/L; 7 days) produced significant alterations in the liver and brain metabolome of exposed animals, including lipid, energy and amino acid metabolism (see Chapter 5). The objective of part 2 (the present study) was to verify whether the perturbations observed at low dose were also observable in the presence of an apical endpoint, thereby demonstrating that the effects at low dose were adverse in nature. To achieve this, we utilized a much higher dose (100 µg/L) and longer exposure duration (14 days). In addition to the previously studied liver and brain tissues, plasma was also analyzed by means of a non-targeted metabolomics approach. Collectively, these studies provide a comprehensive picture of the effects of amitriptyline in fish and a connection between metabolic perturbations in the presence and absence of apical effects.

6.2 Experimental

6.2.1 Standards and Reagents

Amitriptyline hydrochloride (98%) was purchased from Sigma–Aldrich (St. Louis, MO, USA). A stock dosing solution of amitriptyline was prepared at 25,000 mg/L in ethanol (EtOH) and diluted down to 1.8 mg/L in Milli-Q water for dosing purposes. The final concentration of EtOH in the tank was 0.004‰. Additional information regarding the reagents of endogenous metabolites purchased from Sigma–Aldrich is provided in Appendix III.

6.2.2 Amitriptyline exposure experiment and sampling

Exposure experiments were carried out in a manner consistent with part 1 of this work (see Chapter 5). Juvenile gilt-head bream weighing ~40 g and measuring ~13 cm in length (Groupe Aqualande, Roquefort, France) were exposed to amitriptyline at 100 µg/L (nominal) for 14 days in the laboratories of the Research Centre for Experimental Marine Biology and Biotechnology (PiE-UPV/EHU).

The exposure was performed using two 1000 × 700 × 650 mm polypropylene tanks (one control, one exposed), each containing 250 L of seawater and 50 fish per tank. Exposures were carried out using a continuous flow-through system with a peristaltic pump delivering 10 L seawater/h and another pump infusing an amitriptyline dosing solution at 0.6 L/h to exposure tanks. The amitriptyline stock dosing solution was refilled every 24 hours. The control tank was maintained at identical conditions as the exposed tank. Ten fish were collected from both exposed and control tanks prior to dosing (day 0) and on exposure days 2, 4, 7 and 14. On these days, 2.5 L water samples were also collected to determine amitriptyline concentrations in both tanks.

The fish were immediately anaesthetized in a tank containing 10 L of seawater with 100 mg/L tricaine and 200 mg/L $NaHCO_3$. After 5 minutes, fish were weighed, measured and dissected. Brain and liver were weighed directly into Precellys vials (2 mL and 7 mL, respectively). Blood was sampled from the caudal vein-artery using a syringe previously rinsed with 0.5 mol/L EDTA solution (pH adjusted to 8.0 using NaOH). Plasma was obtained by centrifuging for 5 minutes at 1000 rpm (Centrifuge 5415 C, Eppendorf, Hamburg, Germany), after which the sample was transferred to a 2-mL Precellys vial and weighed. Plasma and tissues were frozen in liquid nitrogen during dissection and stored at -80 ˚C prior to extraction. Fish processing described herein was evaluated by the Bioethics Committee of UPV/EHU and approved by the Local Authority according to the current regulations (procedure approval CEEA/380/2014/ETXEBARRIA LOIZATE).

6.2.3 Extraction and analysis of metabolites

The analytical method for metabolite extraction and analysis was adapted from Ribbenstedt et al. [26]. Briefly, extraction of whole samples (~100 mg brain, ~400 mg plasma and ~1000 mg liver) was initiated through the addition of 4 µL $CHCl_3$:MeOH (20:80, v/v) per mg sample in the

Precellys tubes used for storage. All samples were homogenized for 3×1.5 min at 4000 rpm (Precellys®, Bertin Instruments, Montigny-le-Breonneux, France) under controlled cooled temperature (4 °C) (Cryolys®, Bertin Technologies, Montigny-le-Bretonneux, France), employing 1.4-mm or 2.8-mm Zirconium oxide beads (Precellys®, Bertin Instruments, Montigny-le-Breonneux, France) in the case of brain and liver, respectively. Extracts were centrifuged for 15 minutes at 18,000 rpm (Centrifuge Allegra X-30R, F2402H, Beckman Coulter, High Wycombe, UK) to get the supernatant.

Non-targeted analysis was carried out using a Thermo Scientific Dionex UltiMate 3000 UHPLC coupled to a Thermo Scientific Q Exactive quadrupole-Orbitrap mass spectrometer (qOrbitrap) equipped with a heated electrospray ionization source (HESI, Thermo, CA, USA), and controlled by Xcalibur 4.0 software (Thermo). To maximize metabolite coverage, 3 injections (5 µL each) were performed per extract using different chromatographic columns and ionization modes: hydrophilic interaction liquid chromatography (HILIC) in positive ($HILIC_{pos}$) and negative ($HILIC_{neg}$) ionization modes, and reverse-phase (octadecylsilyl) liquid chromatography in positive mode ($C18_{pos}$).

In $HILIC_{pos}$ and $HILIC_{neg}$ separation was carried out on an Acquity BEH-Amide column (2.1 × 100 mm, 1.7 µm) equipped with a Vanguard pre-column (2.1 × 5 mm, 1.7 µm) from Waters (Milford, Massachusetts, United States), which was kept at 35 °C during the analysis. Milli-Q water was used as mobile phase A and ACN as mobile phase B, both containing 0.1% HCOOH in $HILIC_{pos}$ and 10 mM of ammonium acetate in $HILIC_{neg}$. The eluent gradient profile, adapted from Ribbenstedt et al. [26], was as follows: 97% of B (hold 3 min), linear change to 85% B up to 5 min, another linear change to 75% B up to 14 min, another linear change to 40% B up to 17 min (hold 3 min) and a final linear change to 97% B up to 23 min (hold 2 min) to regain initial conditions. The flow rate was changed throughout the analysis as follows: 0-3 min at 0.2 mL/min, 3-5 min increase to 0.3 mL/min, 5-23 min at 0.3 mL/min, 23-24 min decrease to 0.2 mL/min and 24-25 min at 0.2 mL/min. Lastly, $C18_{pos}$ method employed a Kinetex C18 100 Å core-shell (3.0 × 150 mm, 2.6 µm) chromatographic column equipped with a Vanguard pre-column (3.0 × 5 mm, 2.6 µm) from Phenomenex (Torrance, CA, USA). Milli-Q water was used as mobile phase A and MeOH as mobile phase B, both containing 0.1% HCOOH. The mobile phase flow rate was set at 0.3 mL/min and the

eluent gradient profile was as follows: 5% of B (hold 1 min), linear change to 95% B up to 16 min (hold 4 min) and a final linear change to 5% B up to 24 min (hold 1 min) to regain initial conditions.

The qOrbitrap was operated in full scan – data dependent MS2 (Full MS-ddMS2) discovery acquisition mode. One full scan at a resolution of 70,000 full width at half maximum (FWHM) at *m/z* 200 over a scan range of *m/z* 70-1000 was followed by three ddMS2 scans at a resolution of 17,500 FWHM at *m/z* 200, with an isolation window of 0.8 Da. The stepped normalized collision energy (NCE) in the higher-energy collisional dissociation (HCD) cell was set to 10, 35 and 75 eV. The HESI source parameters in positive were set to 3.2 kV spray voltage, 300 °C capillary temperature, 35 arbitrary units (au) sheath gas (nitrogen), 10 au auxiliary gas, 1 au sweep gas, 280 °C auxiliary gas heater and S-lens RF level 55.0. The HESI source parameters in negative were set to 3.2 kV spray voltage, 320 °C capillary temperature, 48 au sheath gas, 11 au auxiliary gas, 2 au sweep gas, 310 °C auxiliary gas heater and S-lens RF level 55.0. External calibration of the instrument was conducted immediately prior to analysis using Pierce LTQ ESI Calibration Solutions (Thermo Scientific, Waltham, Massachusetts, United States). The instrument was controlled by Xcalibur 4.0 software (Thermo).

The extraction and analysis of samples was randomized and the samples were analyzed in 9 separate sequences: one per matrix (i.e. liver, brain, plasma) and instrumental condition (i.e. $HILIC_{pos}$, $HILIC_{neg}$, $C18_{pos}$). Instrumental blank samples (pure MeOH) injected every 5 samples ruled out the presence of carryover, and procedural blank samples were prepared to estimate the background concentration of metabolites during sample workup. In addition to this, the sequence quality control sample (QC_{seq}) was prepared for each tissue by pooling a small volume of each extract and splitting into several aliquots. These aliquots were injected after every 10 samples to monitor and correct for signal drift.

6.2.4 Data Handling and Statistical Analyses

Condition factor (K) and hepatic somatic index (HSI) were determined as a general assessment of fish health. K was calculated using the equation $K = (\text{fish weight} \times 100)/(\text{length})^3$) [27], while HSI was determined using the equation HSI = (liver weight × 100)/(fish weight)). K and HSI were statistically evaluated between exposed and control groups using one-way analysis of

variance (ANOVA).

Identification of metabolites involved in altered metabolic pathways was performed separately for plasma, brain and liver following the workflow previously described in non-targeted analysis of part 1 of this research work (see Chapter 5). Briefly, after processing each sequence of chromatograms using Compound Discoverer 2.1 (Thermo-Fisher Scientific) as detailed in Appendix II, outliers in each sequence were identified based on Principal Component Analysis (PCA) and signal drift over the course of the sequence (identified from QC_{seq} data) was subsequently corrected using the package intCor [28] in R software for statistical computing (v3.4.3). Then, the 3 sequences ($HILIC_{pos}$, $HILIC_{neg}$, $C18_{pos}$) of each matrix were merged to perform multiple linear regression analysis (MLR, Y (time, dose) = time + dose + time·dose, where Y is feature response). With the aim of identifying metabolites displaying statistically significant concentration changes over time between exposed and control samples, we selected features with a p-value < 0.05 and a false discovery rate (FDR) < 0.05 in the interaction dose·time. Significant features were then manually checked to discard peaks that had a bad chromatographic peak shape, were incorrectly integrated or corresponded to amitriptyline by-products [14]. The latter is crucial to avoid misleading tendencies. Subsequent metabolite identification was also performed following the steps described in non-targeted analysis of part 1 of this research work (see Chapter 5). Based on the information in different databases and retention time of available standards (see Appendix III), the confidence level of the identification was set [29].

Lastly, in order to identify key affected metabolic processes and a plausible biological explanation for these changes, we performed null diffusion-based enrichment [24] with KEGG annotated compounds using the diffusion method (simulation approximation with 15,000 iterations). The database was built using the KEGG release 84.0+/10-08, Oct 17 2017, with zebrafish (*Danio rerio*) as the organism (organism code "dre") and excluding the unspecific "dre01100" metabolic overview pathway. The network consisted of 161 pathways, 176 modules, 973 enzymes, 4803 reactions and 3450 KEGG compounds. In addition to the metabolites suggested by the enrichment (p-score < 0.05), we also discussed the biological relevance of the lipids identified as significant metabolites but not included in KEGG. Finally, daily fold change (FC) values of the suggested metabolites were calculated as described in part 1 (see Chapter 5), by dividing the

average concentration of each metabolite in the exposed samples with the average concentration of the same metabolite in the control samples at the corresponding day.

6.3 Results and discussion

No significant changes in fish weight and length were observed at the 95% confidence level, regardless of experiment tank or exposure day (p-value > 0.05). There was no mortality and K and HSI were comparable between fish of exposed and control groups (p-value > 0.05) in all the exposure days. However, remarkable differences in feed consumption and animal pigmentation were observed, with exposed fish consuming food 4 times more slowly and becoming paler (see Figure 6.1), than non-exposed animals.

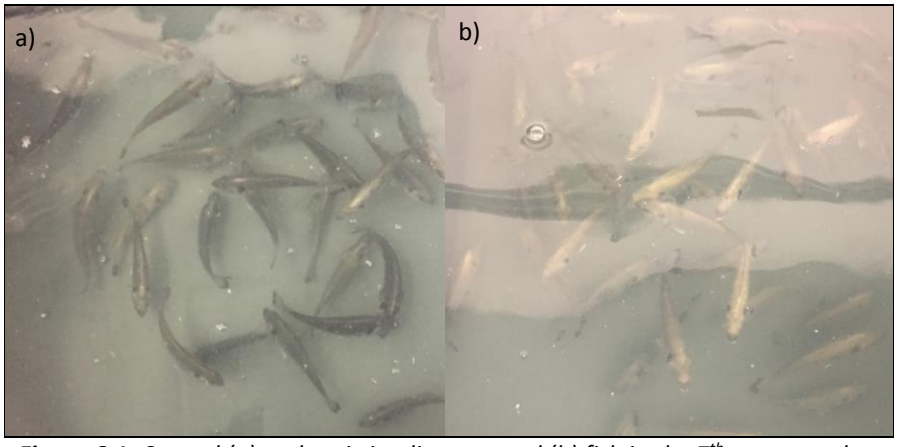

Figure 6.1: *Control (a) and amitriptyline exposed (b) fish in the 7th exposure day.*

Following the data treatment workflow detailed in section 6.2.4, the number of significantly altered features were 114, 26 and 128 in liver, brain and plasma, respectively (see Tables 6.1-6.3) and from them, 83, 22 and 91 were KEGG annotated. The remaining features were either unknown or not included in KEGG. Many lipids (1 in brain, 16 in liver and 28 in plasma) were among the putatively identified metabolites not included in KEGG. The KEGG annotated metabolites suggested by pathway enrichment were involved in alteration of fish behavior, the melatonergic system, oxidative stress, energy metabolism and amino acid metabolism. These metabolites were combined altogether based on KEGG to form a metabolic network (see Figure 6.2), giving a holistic view of metabolic changes occurring in the organism. Overall, the most profound alterations were observed on the last day of exposure and the FC values are shown in Tables 6.1-6.3.

Table 6.1: *Identification of the features whose brain levels were significantly altered after exposure, and their fold change (FC) values at days 2, 4, 7 and 14.*

Brain Peak	Molecular Weight	Name or Molecular formula	KEGG Code	Level	Fold change (Exposed/Control)			
					Day 2	Day 4	Day 7	Day 14
Compounds suggested by the enrichment								
C18pos_Peak809	115.027	Maleamate	C01596	2b	1.28	0.92	0.84	0.65
C18pos_Peak1053	116.0952	5-Aminopentanamide	C00990	2b	0.97	0.9	0.9	0.71
HILICpos_Peak272	123.0322	Picolinic acid / Nicotinic acid	C10164 / C00253	3	1.23	1.02	0.65	0.6
C18pos_Peak1169	125.0954	N-Methylhistamine	C05127	2a	1.04	1.14	1.4	2.34
C18pos_Peak776	160.0847	D-Alanyl-alanine / N-α-acetyl-L-2,4-diaminobutyrate / N-γ-acetyl-L-2,4-diaminobutyrate	C00993 / C06442 / C19929	3	0.73	0.88	0.71	0.61
HILICpos_Peak492	168.09	Pyridoxamine	C00534	2a	0.99	0.95	0.79	0.61
HILICpos_Peak376	173.0688	N-Acetyl-L-glutamate 5-semialdehyde	C01250	2b	1.16	1.46	2.56	1.67
C18pos_Peak674	174.1004	N-Acetylornithine	C00437	2a	0.36	0.62	0.58	0.41
C18pos_Peak1205	183.0895	L-Adrenaline	C00788	2a	0.95	0.88	0.93	0.77
C18pos_Peak901	191.0582	5-Hydroxyindoleacetate	C05635	1	0.68	0.37	0.4	0.46
C18pos_Peak1301	192.0899	2,6-Dihydroxy-N-methylmyosmine	C16151	2b	1.17	0.91	0.77	0.61
C18pos_Peak475	194.1055	6-Hydroxypseudooxynicotine	C01297	2b	0.94	0.88	0.94	0.73
C18pos_Peak1508	248.1159	6-Hydroxymelatonin	C05643	2a	0.98	0.79	0.9	0.73
HILICneg_Peak480	254.1001	3-beta-D-Galactosyl-sn-glycerol	C05401	2b	1.03	0.86	0.75	0.62
C18pos_Peak1464	379.1043	(R)-S-Lactoylglutathione	C03451	2a	1.21	1.49	1.34	1.46

Table 6.1: *(Continuation).*

Brain Peak	Molecular Weight	Name or Molecular formula	KEGG Code	Level	Fold change (Exposed/Control)			
					Day 2	Day 4	Day 7	Day 14
The rest KEGG annotated compounds								
HILICpos_Peak328	115.0636	3-Acetamidopropanal	C18170	2b	1.09	0.71	0.93	0.65
C18pos_Peak668	169.0891	4-Aminobiphenyl	C10998	2a	1.12	1.83	2.65	2.88
HILICpos_Peak656	173.1166	Indospicine	C08288	2b	1.55	1.06	1.48	1.66
C18pos_Peak1139	183.0208	L-Homocysteic acid	C16511	2b	0.99	0.93	0.87	0.75
C18pos_Peak785	186.0326	Psoralen / Angelicin	C09060 / C09305	3	0.83	0.98	0.86	0.7
C18pos_Peak730	186.1156	Calligonine	C09089	2b	1.12	1.9	2.83	3.1
HILICneg_Peak996	374.2097	Jasmolin II	C16781	2b	0.78	0.45	0.44	0.2
Putatively identified/not in KEGG								
C18pos_Peak675	187.1571	$C_{10}H_{21}NO_2$ (4 lipid candidates of Fatty Acyls category)	-	3	0.73	0.91	0.62	0.25
Unknown peaks								
C18pos_Peak1259	128.0951	$C_6H_{12}N_2O$ (Poor MS2)	-	4	1.03	0.85	0.67	0.41
C18pos_Peak1456	260.104	$C_{15}H_{16}O_4$ (Poor MS2)	-	4	0.93	0.72	0.75	0.59
C18pos_Peak1399	276.0971	$C_{10}H_{16}N_2O_7$ (Poor MS2)	-	4	0.89	0.69	0.93	0.65

Table 6.2: *Identification of the features whose liver levels were significantly altered after exposure, and their fold change (FC) values at days 2, 4, 7 and 14.*

Liver Peak	Molecular Weight	Name or Molecular formula	KEGG Code	Level	Fold change (Exposed/Control)			
					Day 2	Day 4	Day 7	Day 14
Compounds suggested by the enrichment								
HILICpos_Peak525	113.059	Creatinine	C00791	1	0.41	0.52	0.43	0.4
C18pos_Peak593	114.043	N-Methylhydantoin	C02565	2a	0.9	0.94	0.68	0.6
C18pos_Peak1188	116.095	5-Aminopentanamide	C00990	2b	0.99	0.94	0.8	0.6
HILICpos_Peak37	129.043	L-1-Pyrroline-3-hydroxy-5-carboxylate	C04281	2b	1.45	1.25	1.14	1.5
HILICpos_Peak1278	129.079	N4-Acetylaminobutanal	C05936	2b	0.51	0.59	0.9	0.5
C18pos_Peak806	130.111	N-Acetylputrescine	C02714	2a	0.71	0.85	0.94	0.7
HILICpos_Peak641	145.038	2-Oxoglutaramate	C00940	2b	0.9	0.48	0.55	0.6
C18pos_Peak379	145.11	Acetylcholine	C01996	2a	0.97	1.02	1.1	2.1
C18pos_Peak12	147.053	D-Glutamate	C00217	1	1.89	1.38	1.1	1.5
HILICpos_Peak513	148.073	(R)-Pantoate	C00522	2b	0.87	0.77	0.66	0.8
C18pos_Peak1059	160.085	D-Alanyl-alanine / N-α-acetyl-L-2,4-diaminobutyrate / N-γ-acetyl-L-2,4-diaminobutyrate	C00993 / C06442 / C19929	3	0.45	0.88	1.02	0.4
HILICpos_Peak210	161.105	(S)-Carnitine	C00318	2a	0.27	0.51	0.67	0.3
HILICpos_Peak1116	162.1	N6-Hydroxy-L-lysine	C01028	2a	2.38	1.6	1.58	1.7
C18pos_Peak559	168.09	Pyridoxamine	C00534	2a	1.18	0.95	0.81	0.6
C18pos_Peak1222	180.042	3-(4-Hydroxyphenyl)pyruvate / 2-hydroxy-3-(4-hydroxyphenyl)propenoate	C01179 / C05350	3	13.4	5.27	5.05	4.1

Table 6.2: *(Continuation).*

Liver Peak	Molecular Weight	Name or Molecular formula	KEGG Code	Level	Fold change (Exposed/Control)			
					Day 2	Day 4	Day 7	Day 14
C18pos_Peak1325	181.074	3-Amino-3-(4-hydroxyphenyl)propanoate	C04368	2b	0.45	0.47	0.49	0.57
C18pos_Peak469	194.106	6-Hydroxypseudooxynicotine	C01297	2b	0.99	0.9	0.9	0.7
HILICneg_Peak1177	204.11	N6-Acetyl-N6-hydroxy-L-lysine	C03955	2b	1.26	1.38	0.68	0.68
C18pos_Peak1459	208.085	L-Kynurenine	C00328	2a	0.31	0.54	0.65	0.54
C18pos_Peak978	210.1	2,6-Dihydroxypseudooxynicotine	C15986	2b	0.84	0.72	0.71	0.5
HILICneg_Peak852	218.126	N2-(D-1-carboxy-ethyl)-L-lysine	C04020	2b	0.99	0.95	0.81	0.54
HILICneg_Peak179	219.11	Pantothenate	C00864	2b	0.9	0.84	0.92	0.75
C18pos_Peak272	219.11	Pantothenate	C00864	2b	0.89	0.98	0.83	0.71
C18pos_Peak1223	224.079	3-hydroxy-L-kynurenine	C03227	2a	0.43	0.44	0.4	0.45
HILICneg_Peak439	240.122	Anserine	C01262	2a	1	0.87	0.61	0.69
HILICneg_Peak738	244.069	Pseudouridine	C02067	2a	1.19	1.68	1.34	1.57
C18pos_Peak1404	299.282	Sphingosine	C00319	2a	1.84	5.5	4.51	2.45
HILICpos_Peak408	299.282	Sphingosine	C00319	2a	1.13	1.19	1.81	1.76
C18pos_Peak75	299.282	3-Dehydrosphinganine	C02934	2b	1.77	2.03	2.75	2.19
C18pos_Peak1013	336.23	12(S)-HPETE	C05965	2b	1.09	1.67	1.16	2.45
HILICneg_Peak397	342.117	Galactinol /Epimelibiose	C01235 / C05400	3	1.19	1.11	0.76	0.32
HILICpos_Peak971	399.335	Palmitoylcarnitine	C02990	2a	1.39	1.86	1	4.36

Table 6.2: *(Continuation).*

Liver Peak	Molecular Weight	Name or Molecular formula	KEGG Code	Level	Fold change (Exposed/Control)			
					Day 2	Day 4	Day 7	Day 14
The rest KEGG annotated compounds								
HILICpos_Peak303	100.053	Tiglic acid	C08279	2a	0.44	0.62	0.64	0.66
HILICpos_Peak553	111.044	Cytosine	C00380	1	0.9	0.69	0.66	0.3
C18pos_Peak400	115.027	Maleamate	C01596	2b	1	0.5	0.6	0.48
HILICpos_Peak50	115.027	Maleamate	C01596	2b	0.85	0.47	0.68	0.57
HILICpos_Peak684	115.064	3-Acetamidopropanal	C18170	2b	0.86	0.61	0.89	0.5
C18pos_Peak878	125.095	N-Methylhistamine	C05127	2a	1.16	2.42	0.6	1.24
C18pos_Peak1422	128.095	(S)-Piperidine-2-carboxamide / D-2-Aminohexano-6-lactam	C02837 / C19809	3	0.56	0.68	0.71	0.55
C18pos_Peak383	132.053	L-Asparagine	C00152	1	0.96	0.47	0.6	0.47
HILICpos_Peak51	132.054	L-Asparagine	C00152	1	0.84	0.52	0.68	0.58
HILICpos_Peak1212	149.07	1-Methyladenine	C02216	2a	2.64	2.16	2.43	2.07
C18pos_Peak398	152.033	Xanthine	C00385	2a	1.02	3.74	2.85	1.6
HILICpos_Peak960	156.054	Imidazole lactate / 4-Imidazolone-5-propanoate	C03817 / C05568	3	0.83	0.44	0.69	0.54
C18pos_Peak217	159.126	Methacholine	C07471	2a	1.53	3.41	3.25	5.75
HILICpos_Peak493	159.126	Methacholine	C07471	2a	1.98	3.48	3.31	6.1
C18pos_Peak1170	162.032	7-Hydroxycoumarine	C09315	2a	15.8	5.84	6.94	4.13
C18pos_Peak583	169.089	4-aminobiphenyl	C10998	2a	1.25	1.83	2.97	3.04
HILICpos_Peak790	173.105	Swainsonine / N-Acetyl-L-leucine	C02710 / C10173	3	1.2	1.66	1.07	1.6

Table 6.2: *(Continuation).*

Liver Peak	Molecular Weight	Name or Molecular formula	KEGG Code	Level	Fold change (Exposed/Control)			
					Day 2	Day 4	Day 7	Day 14
HILICpos_Peak892	174.1	N-Acetylornithine	C00437	2a	0.65	0.67	0.92	0.37
C18pos_Peak1221	183.021	L-Homocysteic acid	C16511	2b	0.89	0.87	0.81	0.64
C18pos_Peak337	183.066	Choline phosphate	C00588	2b	1.12	1.28	1.27	1.42
C18pos_Peak626	184.11	isoproneyl-6-oxoheptanoate / 7-hydroxy-4-isoprenyl-7-methyl-2-oxo-oxepanone / 1,6,6-Trimethyl-2,7-dioxabicyclo[3.2.2]nonan-3-on	C11405 / C06066 / C04718	3	0.79	1.24	0.66	0.53
C18pos_Peak636	186.116	Calligonine	C09089	2b	1.27	1.87	3.01	3.05
HILICneg_Peak776	188.079	Tabtoxinine-beta-lactam	C20918	2b	0.6	0.61	0.62	0.64
HILICpos_Peak733	189.112	L-Homocitrulline	C02427	2b	1.22	0.72	0.62	0.58
HILICpos_Peak1471	195.09	3-Methyl-L-tyrosine / L-Tyrosine methyl ester	C20800 / C03404	3	2.11	2.7	2.44	2.86
HILICneg_Peak96	197.035	Tauropine	C01616	2b	0.97	0.87	0.88	0.57
HILICneg_Peak1321	200.079	Alanylclavam / Dihydroclavaminic acid	C06659 / C17360	3	0.77	0.72	0.54	0.78
HILICpos_Peak1694	200.08	Alanylclavam / Dihydroclavaminic acid	C06659 / C17360	3	0.51	1.05	0.4	0.55
HILICneg_Peak1039	202.095	Proclavaminic acid	C06658	2b	0.76	0.73	0.81	0.66
C18pos_Peak1215	204.09	D-Tryptophan	C00525 / C00806	1	0.97	0.9	0.86	0.65
C18pos_Peak810	222.125	6-Hydroxy-3-oxo-alpha-ionone	C02533	2b	0.4	0.72	0.5	0.57
HILICpos_Peak487	241.106	5-Methyl-2''-deoxycytidine	C03592	2b	1.02	0.64	0.66	0.61
HILICpos_Peak1244	243.104	Biotin amide	C01893	2b	0.9	0.77	0.41	0.52
C18pos_Peak1391	244.089	Biotin	C00120	2a	14.5	18.8	16	15.9

Table 6.2: *(Continuation).*

Liver Peak	Molecular Weight	Name or Molecular formula	KEGG Code	Level	Fold change (Exposed/Control)			
					Day 2	Day 4	Day 7	Day 14
C18pos_Peak884	250.131	N-Caffeoylputrescine	C03002	2b	2.07	1.99	1.69	1.8
HILICpos_Peak1226	250.132	N-Caffeoylputrescine	C03002	2b	2.81	7.82	6.38	3.54
C18pos_Peak1408	251.079	N-Feruloylglycine	C02564	2b	0.23	0.62	0.68	0.37
HILICpos_Peak1729	255.158	L-Pyrrolysine	C16138	2b	1.51	2.25	1.93	2.04
C18pos_Peak781	276.209	Stearidonic acid	C16300	2b	0.84	1.45	1.12	3.26
C18pos_Peak187	281.272	Oleamide	C19670	2a	1.33	1.27	1.83	2.16
C18pos_Peak659	287.209	Octanoylcarnitine	C02838	2b	11.5	4.25	1.03	2.86
HILICpos_Peak1209	290.091	N2-Malonyl-D-tryptophan	C03414	2b	0.43	0.26	0.11	0.08
HILICpos_Peak304	296.14	4-Prenylresveratrol	C10285	2b	0.49	0.35	0.2	0.08
C18pos_Peak1260	308.158	Fructoselysine/Glucoselysine	C16488 / C20978	3	1.1	0.92	0.61	0.69
C18pos_Peak1245	323.115	Stylopine	C05175	2b	15	25.1	27.6	42.6
HILICpos_Peak1588	324.153	2''-Deamino-2''-hydroxyparomamine / Istamycin FU-10	C20353 / C17981	3	1.31	1.2	0.76	0.62
C18pos_Peak1339	328.225	2,3-Dinor-8-iso prostaglandin F1alpha	C14795	2b	1.34	1.17	1.53	3
C18pos_Peak1368	329.052	3',5'-Cyclic AMP / 2'3'-Cyclic AMP / 3,5-Cyclic dGMP	C02507 / C00575 / C02353	3	2.57	1.47	2.17	1.88
HILICneg_Peak961	352.065	4-(4-Deoxy-beta-D-gluc-4-enuronosyl)-D-galacturonate	C06118	2b	9.83	8.26	11.3	29.8
HILICneg_Peak231	358.215	Cannabidiolic acid	C10784	2a	1.34	1.61	1.85	2.41
C18pos_Peak625	589.374	diprenylterpenole I	C20532	2b	0.85	2.21	1.54	1.68

Table 6.2: *(Continuation).*

Liver Peak	Molecular Weight	Name or Molecular formula	KEGG Code	Level	Fold change (Exposed/Control)			
					Day 2	Day 4	Day 7	Day 14
Putatively identified/not in KEGG								
C18pos_Peak1131	159.089	3-Dehydrocarnitine	-	2b	0.43	0.67	0.57	0.5
C18pos_Peak1090	190.099	Dodecapentanoic acid	-	2b	0.44	0.66	0.51	0.59
C18pos_Peak1460	214.135	Farfugin A	-	2b	1.43	0.66	0.55	0.39
C18pos_Peak1345	241.204	(4E,6E,d14:2) sphingosine	-	2b	3.06	6.61	12.3	6.04
C18pos_Peak1236	243.22	2-amino-tetradecanoic acid / C14 sphingosine	-	3	3.42	17.2	18.2	10.9
C18pos_Peak779	277.24	Crucigasterin 277 / Obscuraminol A	-	3	1.25	1.6	1.89	2.69
C18pos_Peak801	285.266	$C_{17}H_{35}NO_2$ (4 lipid candidates of Sphingolipids and Fatty Acyls category)	-	3	1.31	1.63	2.4	2.76
HILICneg_Peak1288	374.21	$C_{25}H_{40}O_4$ (6 lipid candidates of Prenol Lipids and Sterol Lipids category)	-	3	0.5	0.3	0.28	0.16
C18pos_Peak562	404.292	$C_{25}H_{40}O_4$ (3 lipid candidates of Sterol Lipids category)	-	3	0.71	1.66	0.92	4.45
HILICneg_Peak1017	440.148	$C_{24}H_{24}O_8$ (2 lipid candidates of Polyketides category)	-	3	6.74	7.94	10.4	14.3
C18pos_Peak1083	467.301	$C_{22}H_{46}NO_7P$ (4 lipid candidates of Glycerophospholipids category)	-	3	0.65	1.86	1.37	2.67
C18pos_Peak715	481.316	$C_{23}H_{48}NO_7P$ (3 lipid candidates of Glycerophospholipids category)	-	3	0.66	1.9	1.43	2.17
HILICneg_Peak1420	486.445	30,32-dihydroxy-2b-methyl-bishomohopane	-	2b	0.91	0.81	0.69	0.47
HILICpos_Peak1663	739.515	$C_{41}H_{74}NO_8P$ (25 lipid candidates of Glycerophospholipids category)	-	3	1.1	1.13	1.29	1.53
HILICpos_Peak1427	771.576	$C_{43}H_{82}NO_8P$ (30 lipid candidates of Glycerophospholipids category)	-	3	0.98	0.92	0.77	0.67
C18pos_Peak422	990.663	NeuAcα2-3Galβ-Cer(d18:1/16:0)	-	2b	0.83	2.07	2.08	1.85

Table 6.2: *(Continuation).*

Liver Peak	Molecular Weight	Name or Molecular formula	KEGG Code	Level	Fold change (Exposed/Control)			
					Day 2	Day 4	Day 7	Day 14
Unknown peaks								
HILICpos_Peak2	130.027	$C_5H_6O_4$ (Poor MS2)	-	4	1.52	1.3	1.33	1.5
C18pos_Peak1143	131.094	$C_6H_{13}NO_2$ (Poor MS2)	-	4	0.42	0.48	0.61	0.4
C18pos_Peak432	189.119	$C_9H_{19}NOS$ (Poor MS2)	-	4	0.54	0.6	0.45	0.29
HILICneg_Peak1223	210.088	$C_5H_{15}N_4O_3P$ (Poor MS2)	-	4	0.96	0.82	0.61	0.42
HILICneg_Peak237	224.083	$C_{15}H_{12}O_2$ (Poor MS2)	-	4	0.5	0.28	0.13	0.07
HILICpos_Peak649	224.083	$C_{15}H_{12}O_2$ (Poor MS2)	-	4	0.33	0.25	0.13	0.07
HILICneg_Peak1159	238.062	$C_{15}H_{10}O_3$ (Poor MS2)	-	4	1.21	0.68	0.91	1.3
C18pos_Peak1415	302.224	$C_{20}H_{30}O_2$ (Poor MS2)	-	4	1.23	1.24	1.11	1.34
C18pos_Peak761	311.152	$C_{19}H_{21}NO_3$ (Poor MS2)	-	4	44.2	58.8	54.7	78.9
HILICneg_Peak405	316.24	$C_{21}H_{32}O_2$ (Poor MS2)	-	4	0.75	1.37	1.62	2.6
C18pos_Peak770	362.245	$C_{22}H_{34}O_4$ (Poor MS2)	-	4	1.36	1.88	1.22	2.82
C18pos_Peak1351	400.116	$C_{21}H_{20}O_8$ (Poor MS2)	-	4	1.1	1.57	1.73	1.55
HILICneg_Peak1269	412.153	$C_{23}H_{24}O_7$ (Poor MS2)	-	4	12	8.79	10.3	11.2
HILICneg_Peak471	426.169	$C_{24}H_{26}O_7$ (Poor MS2)	-	4	21.9	23.7	36.3	73
HILICpos_Peak988	589.374	$C_{34}H_{53}O_8$ (Poor MS2)	-	4	0.78	1.38	1.56	1.27

Table 6.3: *Identification of the features whose plasma levels were significantly altered after exposure, and their fold change (FC) values at days 2, 4, 7 and 14.*

Plasma Peak	Molecular Weight	Name or Molecular formula	KEGG Code	Level	Fold change (Exposed/Control)			
					Day 2	Day 4	Day 7	Day 14
Compounds suggested by the enrichment								
C18pos_Peak715	105.0428	D-Serine	C00740	1	1.3	0.8	0.6	0.4
HILICpos_Peak112	105.043	D-Serine	C00740	1	1	1	0.7	0.7
C18pos_Peak297	114.0432	N-Methylhydantoin	C02565	2a	1	0.9	0.9	0.5
HILICpos_Peak68	115.027	Maleamate	C01596	2b	0.9	0.8	0.9	0.5
C18pos_Peak822	116.0952	5-Aminopentanamide	C00990	2b	1.1	0.8	0.9	0.7
C18pos_Peak430	119.0584	L-Threonine	C00188	1	1	0.7	0.8	0.4
HILICpos_Peak78	119.0585	L-Threonine	C00188	1	1	1	0.8	0.6
HILICpos_Peak11	129.0426	L-1-Pyrroline-3-hydroxy-5-carboxylate	C04281	2b	0.8	1	0.7	0.7
C18pos_Peak435	130.0631	(S)-3-Methyl-2-oxopentanoic acid	C00671	2b	0.6	0.5	1	0.5
C18pos_Peak898	130.1108	N-Acetylputrescine	C02714	2a	1	0.8	1	0.8
C18pos_Peak117	136.0386	Hypoxanthine	C00262	2a	1.2	1.5	1	1.4
C18pos_Peak686	145.0739	4-Acetamidobutanoate / L-2-Aminoadipate 6-semialdehyde / 2-Amino-5-oxohexanoate	C02946 / C04076 / C05825	3	1	0.7	0.7	0.5
C18pos_Peak748	145.1103	Acetylcholine	C01996	2a	0.6	0.8	1	0.8
HILICpos_Peak13	146.0691	Glutamine	C00819	1	0.8	1	0.7	0.7
C18pos_Peak35	146.0692	D-Glutamine	C00819	1	1	0.8	0.7	0.5
C18pos_Peak123	148.0736	(R)-2,3-Dihydroxy-3-methylpentanoate	C06007	2b	0.6	0.6	0.8	0.5

Table 6.3: *(Continuation).*

Plasma Peak	Molecular Weight	Name or Molecular formula	KEGG Code	Level	Fold change (Exposed/Control)			
					Day 2	Day 4	Day 7	Day 14
HILICpos_Peak71	158.0692	5-Hydroxyectoine	C16432	2b	1	0.9	0.7	0.7
C18pos_Peak440	158.0692	5-Hydroxyectoine	C16432	2b	1.5	0.6	0.6	0.6
C18pos_Peak798	160.0848	D-Alanyl-alanine / N-α-acetyl-L-2,4-diaminobutyrate / N-γ-acetyl-L-2,4-diaminobutyrate	C00993 / C06442 / C19929	3	0.2	0.8	0.8	0.5
C18pos_Peak478	160.0849	D-Alanyl-alanine / N-α-acetyl-L-2,4-diaminobutyrate / N-γ-acetyl-L-2,4-diaminobutyrate	C00993 / C06442 / C19929	3	0.8	0.8	0.7	0.7
C18pos_Peak460	161.0477	4,6-Dihydroxyquinoline	C05639	2a	0.9	1.2	1	1.2
C18pos_Peak464	165.0791	D-phenylalanine	C02265	1	1.1	0.7	0.6	0.5
C18pos_Peak817	168.0897	Pyridoxamine	C00534	2a	1.1	0.8	0.9	0.7
C18pos_Peak463	174.1005	N-Acetylornithine	C00437	2a	0.5	0.5	0.6	0.5
C18pos_Peak386	175.0958	L-Citrulline	C00327	1	1.4	0.8	0.7	0.6
HILICpos_Peak81	175.0958	L-Citrulline	C00327	1	1	0.8	0.7	0.7
C18pos_Peak972	180.09	5-Hydroxykynurenamine	C05638	2a	0.7	0.7	1	0.8
C18pos_Peak818	188.1161	N6-Acetyl-L-lysine	C02727	2a	0.6	0.5	1.3	0.5
C18pos_Peak225	188.1525	N6,N6,N6-Trimethyl-L-lysine	C03793	2a	1.1	0.5	0.6	0.4
C18pos_Peak878	192.0899	2,6-Dihydroxy-N-methylmyosmine	C16151	2b	1.4	0.8	0.9	0.6
HILICpos_Peak402	194.1056	6-Hydroxypseudooxynicotine	C01297	2b	0.9	0.6	0.8	0.6
C18pos_Peak199	194.1057	6-Hydroxypseudooxynicotine	C01297	2b	1	0.7	0.8	0.7

Table 6.3: *(Continuation).*

Plasma Peak	Molecular Weight	Name or Molecular formula	KEGG Code	Level	Fold change (Exposed/Control)			
					Day 2	Day 4	Day 7	Day 14
C18pos_Peak804	195.0533	Dopaquinone / 6-Hydroxy-3-succinoylpyridine / Leucodopaquinone	C00822 / C19631 / C05604	3	1	0.5	1	0.6
C18pos_Peak604	210.1006	2,6-Dihydroxypseudooxynicotine	C15986	2b	0.8	0.7	0.7	0.6
C18pos_Peak677	218.1267	N2-(D-1-carboxy-ethyl)-L-lysine	C04020	2b	0.8	0.6	0.8	0.5
C18pos_Peak766	220.0848	5-Hydroxy-L-tryptophan	C00643	1	1	0.9	0.8	0.7
C18pos_Peak145	268.0807	Inosine	C00294	2a	1.1	1.5	1.1	1.4
HILICpos_Peak500	276.2086	Stearidonic acid	C16300	2b	0.7	0.6	1	0.6
C18pos_Peak688	278.2245	(9Z,12Z,15Z)-Octadecatrienoic acid / (6Z,9Z,12Z)-Octadecatrienoic acid / Crepenynate	C06427 / C06426 / C07289	3	1.2	1.4	1.7	1.4
HILICpos_Peak269	278.2245	(9Z,12Z,15Z)-Octadecatrienoic acid / (6Z,9Z,12Z)-Octadecatrienoic acid / Crepenynate	C06427 / C06426 / C07289	3	0.9	0.8	1	0.7
C18pos_Peak655	292.2036	12,13(S)-EOT / Colnelenic acid / 12-OPDA	C04672 / C16320 / C01226	3	0.8	0.5	0.9	0.7
C18pos_Peak857	294.2193	8-[(1R,2R)-3-Oxo-2-[(Z)-pent-2-enyl]cyclopentyl]octanoate (OPC-8:00)	C04780	2b	1.1	1.6	1.2	1.5
HILICpos_Peak179	296.2351	9(10)-EpOME	C14825	2b	1.2	0.8	0.8	0.4
C18pos_Peak889	299.2823	Sphingosine	C00319	2a	1.7	2.4	2.4	2.5
HILICpos_Peak79	314.2456	9,10-DHOME	C14828	2b	1.1	0.8	0.9	0.4
C18pos_Peak216	328.24	(4Z,7Z,10Z,13Z,16Z,19Z)-Docosahexaenoic acid	C06429	2a	1.5	1.3	1.1	1.8
HILICneg_Peak12	328.2407	(4Z,7Z,10Z,13Z,16Z,19Z)-Docosahexaenoic acid	C06429	2a	1.1	1.3	1.1	1.2
C18pos_Peak877	379.2486	Sphingosine 1-phosphate	C06124	2a	1	0.9	0.9	1.4

Table 6.3: *(Continuation).*

Plasma Peak	Molecular Weight	Name or Molecular formula	KEGG Code	Level	Fold change (Exposed/Control)			
					Day 2	Day 4	Day 7	Day 14
The rest KEGG annotated compounds								
C18pos_Peak679	102.0685	Pentanoate / 2-Methylbutyrate	C00803 / C18319	3	0.6	0.5	0.9	0.6
C18pos_Peak629	116.084	4-Hydroxyhexan-3-one / cis-1,2-Cyclohexanediol / Hexanoic acid	C02948 / C12313 / C01585	3	1	0.8	1	0.8
C18pos_Peak830	128.0951	(S)-Piperidine-2-carboxamide / L-Lysine 1,6-lactam	C19809 / C02837	3	0.6	0.5	0.5	0.5
C18pos_Peak551	131.0947	N,N-Diethylglycine	C16647	2b	0.6	0.5	0.5	0.5
C18pos_Peak609	132.0535	Asparagine	C00152	1	1.2	0.7	0.8	0.4
HILICpos_Peak72	132.0536	Asparagine	C00152	1	0.9	0.8	0.9	0.5
C18pos_Peak585	140.0586	Methylimidazoleacetic acid / Dihydrourocanate	C05828 / C20522	3	0.3	0.5	0.8	0.4
C18pos_Peak443	143.0947	Stachydrine / 2) (E)-4-(Trimethylammonio)but-2-enoate	C10172 / C04114	3	1.1	0.9	0.9	0.5
C18pos_Peak1075	143.0947	Stachydrine / (E)-4-(Trimethylammonio)but-2-enoate	C10172 / C04114	3	0.9	0.8	0.6	0.5
C18pos_Peak930	143.0947	Stachydrine / (E)-4-(Trimethylammonio)but-2-enoate	C10172 / C04114	3	0.9	0.6	0.7	0.5
C18pos_Peak139	148.0736	(R)-Mevalonate / (R)-Pantoate	C00418 / C00522	3	0.6	0.6	0.9	0.6
HILICpos_Peak365	152.0335	Xanthine	C00385	2a	1.1	1.5	1.1	2.2
C18pos_Peak791	159.0896	3-Dehydrocarnitine	C02636	2b	0.9	0.6	0.9	0.6
C18pos_Peak782	171.0895	N-Butyryl-L-homoserine lactone	C11837	2b	0.6	0.6	1.2	0.4
C18pos_Peak750	173.1053	N-Acetyl-L-leucine / Swainsonine	C02710 / C10173	3	0.8	0.7	0.7	0.6

Table 6.3: *(Continuation).*

Plasma Peak	Molecular Weight	Name or Molecular formula	KEGG Code	Level	Fold change (Exposed/Control)			
					Day 2	Day 4	Day 7	Day 14
C18pos_Peak482	174.1005	N5-Ethyl-L-glutamine	C01047	2b	0.6	0.6	0.6	0.6
C18pos_Peak1117	180.0899	3-Hydroxykynurenamine	C05636	2a	0.6	0.6	0.6	0.5
C18pos_Peak577	181.074	gamma-Hydroxy-3-pyridinebutanoate / N-Hydroxy-L-phenylalanine	C19579 / C19712	3	1.8	1.3	1.3	1.7
C18pos_Peak308	187.0845	6-Acetamido-3-oxohexanoate	C03682	2b	0.8	1.1	0.7	0.5
HILICneg_Peak289	197.035	Tauropine	C01616	2b	0.9	0.9	0.4	0.5
C18pos_Peak639	201.1729	11-Aminoundecanoic acid	C19325	2b	1	0.7	0.6	0.4
C18pos_Peak840	203.0794	N2-Acetyl-L-aminoadipate	C12986	2b	1.5	0.8	0.5	0.7
C18pos_Peak958	203.1159	O-Acetylcarnitine	C02571	2a	0.8	1	0.9	0.6
C18pos_Peak678	204.09	Tryptophan	C00525 / C00806	3	1.1	0.8	0.9	0.7
C18pos_Peak955	208.0849	L-Kynurenine	C00328	2a	0.2	0.4	0.7	0.5
C18pos_Peak540	214.1317	Dethiobiotin	C01909	2b	0.8	0.6	0.9	0.4
HILICneg_Peak558	215.0554	sn-Glycero-3-phosphoethanolamine	C01233	2b	1	1.2	0.7	0.8
HILICneg_Peak488	216.0393	2-C-Methyl-D-erythritol 4-phosphate	C11434	2b	0.9	0.9	0.5	0.4
C18pos_Peak426	217.1313	O-Propanoylcarnitine	C03017	2a	0.1	0.4	0.2	0.4
C18pos_Peak1072	248.116	6-Hydroxymelatonin	C05643	2a	1	0.8	0.8	0.7
C18pos_Peak854	264.1044	3-(6'-Methylthio)hexylmalic acid / 2-(6'-Methylthio)hexylmalic acid / Bluensidine	C17227 / C17226 / C17967	3	2.9	1.5	3.2	1.8

Table 6.3: *(Continuation).*

Plasma Peak	Molecular Weight	Name or Molecular formula	KEGG Code	Level	Fold change (Exposed/Control)			
					Day 2	Day 4	Day 7	Day 14
C18pos_Peak789	270.2193	16-Oxopalmitate	C19614	2b	1	1.2	1.1	1.3
C18pos_Peak738	298.1138	N7-Methylguanosine	C20674	2a	0.8	1.9	1.2	1.4
C18pos_Peak1068	300.2087	Retinoate / 4-Oxoretinol	C00777 / C16683	3	1	1.1	1.3	1.5
C18pos_Peak1030	300.2088	Retinoate / 4-Oxoretinol	C00777 / C16683	3	0.6	0.4	0.3	0.3
C18pos_Peak960	308.1582	Glucoselysine / Fructoselysine	C20978 / C16488	3	1	0.6	0.5	0.3
C18pos_Peak681	314.2455	(8E,10S)-10-Hydroperoxyoctadeca-8-enoate / 12,13-DHOME	C20702 / C14829	3	1.1	1.3	1	1.3
HILICneg_Peak344	336.3033	13,16-Docosadienoic acid	C16533	2b	1.4	1.3	1.1	1.1
HILICneg_Peak560	342.1165	Galactinol / Levanbiose / Melibiose / Epimelibiose / Cellobiose / alpha,alpha-Trehalose	C01235 / C01725 / C05402 / C05400 / C00185 / C01083	3	0.7	0.6	1	0.2
HILICneg_Peak406	358.2151	Cannabidiolic acid	C10784	2a	0.9	1.8	1.7	4
C18pos_Peak1063	362.209	Cortisol / 18-Hydroxycorticosterone	C00735 / C01124	3	1	1.4	2.3	3.8
C18pos_Peak727	376.1381	Riboflavin	C00255	2a	0.9	0.6	0.8	0.5
C18pos_Peak244	380.0183	6-Thioxanthine 5'-monophosphate	C16618	2b	0.9	1.2	1.3	1.6
Putatively identified/not in KEGG								
C18pos_Peak780	173.1417	3R-aminononanoic acid / 9-amino-nonanoic acid	-	3	0.7	0.6	0.5	0.3
C18pos_Peak784	187.1573	$C_{10}H_{21}NO_2$ (5 lipid candidates of Fatty Acyls category)	-	3	0.7	0.6	0.4	0.3

Table 6.3: *(Continuation).*

Plasma Peak	Molecular Weight	Name or Molecular formula	KEGG Code	Level	Fold change (Exposed/Control)			
					Day 2	Day 4	Day 7	Day 14
C18pos_Peak518	187.1573	$C_{10}H_{21}NO_2$ (5 lipid candidates of Fatty Acyls category)	-	3	0.8	0.6	0.5	0.3
C18pos_Peak856	187.1573	$C1_0H_{21}NO_2$ (5 lipid candidates of Fatty Acyls category)	-	3	0.5	0.4	0.3	0.2
C18pos_Peak243	231.147	O-Butanoylcarnitine	-	2b	0.3	0.8	0.3	0.8
C18pos_Peak964	241.204	(4E,6E,d14:2) sphingosine	-	2b	1.4	2.1	3	1.9
C18pos_Peak876	243.2197	C14 sphingosine	-	2b	4.7	5.7	6.1	1.9
C18pos_Peak970	271.251	C16 Sphingosine / 2S-aminohexadecanoic acid	-	3	3.4	7.9	5.3	4.2
C18pos_Peak961	342.2193	16,17S-DHA-epoxide / Sinulobatin A	-	3	0.9	3	1.2	4
C18pos_Peak276	345.2665	Anandamide (20:5, n-3)	-	2a	1.4	1.3	1.1	1.8
C18pos_Peak542	350.2819	Furanoid acid - F6	-	2b	1.1	1.1	1.3	1.4
C18pos_Peak790	356.2924	$C_{21}H_{40}O_4$ (3 lipid candidates of Glycerolipids category)	-	3	2.1	1.7	1.8	1.4
C18pos_Peak557	356.2924	$C_{21}H_{40}O_4$ (3 lipid candidates of Glycerolipids category)	-	3	1.3	1.2	1.7	1.6
C18pos_Peak634	389.2929	N-arachidonoyl GABA	-	2b	0.9	0.4	0.6	0.5
C18pos_Peak118	402.2768	$C_{25}H_{38}O_4$ (3 lipid candidates of Glycerolipids, Sterol Lipids and Prenol Lipids category)	-	3	1.1	3.2	1.4	1.9
C18pos_Peak563	404.2925	$C_{25}H_{40}O_4$ (3 lipid candidates of Sterol Lipids category)	-	3	1.1	1.9	1.2	2.1
C18pos_Peak303	426.024	$C_{17}H_{14}O_{11}S$ (3 lipid candidates of Polyketides category)	-	3	0.9	1.3	1.2	1.5
C18pos_Peak1130	429.3093	hexadecanedioic acid mono-L-carnitine ester	-	2b	0.4	0.5	0.2	0.1
C18pos_Peak987	451.3061	PC(P-14:0\/0:0)	-	2b	1.2	1.1	1.2	1.3
C18pos_Peak1099	465.322	$C_{23}H_{48}NO_6P$ (3 lipid candidates of Glycerophospholipids category)	-	3	1.2	1.1	1.3	1.4

Table 6.3: *(Continuation).*

Plasma Peak	Molecular Weight	Name or Molecular formula	KEGG Code	Level	Fold change (Exposed/Control)			
					Day 2	Day 4	Day 7	Day 14
C18pos_Peak839	479.3376	$C_{24}H_{50}NO_6P$ (3 lipid candidates of Glycerophospholipids category)	-	3	1.1	1.2	1.2	1.3
C18pos_Peak329	481.3168	$C_{23}H_{48}NO_7P$ (4 lipid candidates of Glycerophospholipids category)	-	3	1.1	1.2	1.4	1.2
C18pos_Peak186	493.3169	PC(16:1(9E)\/0:0) / PE(19:1(9Z)\/0:0)	-	3	0.9	1.2	1.4	1.3
C18pos_Peak158	733.5618	$C_{40}H_{80}NO_8P$ (25 lipid candidates of Glycerophospholipids category)	-	3	0.7	0.3	0.8	0.2
C18pos_Peak521	777.5284	$C_{44}H_{76}NO_8P$ (22 lipid candidates of Glycerophospholipids category)	-	3	1.8	1.2	1.7	1.9
C18pos_Peak231	815.5824	1-(8-[3]-ladderane-octanoyl)-2-(8-[3]-ladderane-octanyl)-sn-glycerophosphocholine	-	2b	1.1	1.2	1.4	2.5
C18pos_Peak140	831.577	$C_{48}H_{82}NO_8P$ (12 lipid candidates of Glycerophospholipids category)	-	3	1.3	1.4	1.3	2.1
C18pos_Peak220	853.5615	$C_{50}H_{80}NO_8P$ (3 lipid candidates of Glycerophospholipids category)	-	3	1.1	1.2	1.3	1.5
Unknown peaks								
C18pos_Peak553	141.0791	$C_7H_{11}NO_2$ (Poor MS2)	-	4	0.8	1.1	0.7	0.5
C18pos_Peak1098	175.111	$C_{10}H_{13}N_3$ (Poor MS2)	-	4	0.3	0.9	0.5	0.2
C18pos_Peak1007	223.0843	$C_{11}H_{13}NO_4$ (Poor MS2)	-	4	1.7	2.2	0.9	2.4
C18pos_Peak863	223.0843	$C_{11}H_{13}NO_4$ (Poor MS2)	-	4	0.8	0.4	0.8	0.3
C18pos_Peak341	228.1473	$C_{11}H_{20}N_2O_3$ (Poor MS2)	-	4	0.9	1	0.6	0.7
C18pos_Peak502	268.1169	$C_{11}H_{16}N_4O_4$ (Poor MS2)	-	4	1	1.3	1.5	1.7
C18pos_Peak1073	352.2611	$C_{21}H_{36}O_4$ (Poor MS2)	-	4	1.7	1.9	1.6	1.8
C18pos_Peak1093	384.1597	$C_{19}H_{28}O_6S$ (Poor MS2)	-	4	1.7	1.4	1.2	2.3
C18pos_Peak608	401.2777	$C_{21}H_{39}NO_6$ (Poor MS2)	-	4	0.4	0.4	0.5	0.4

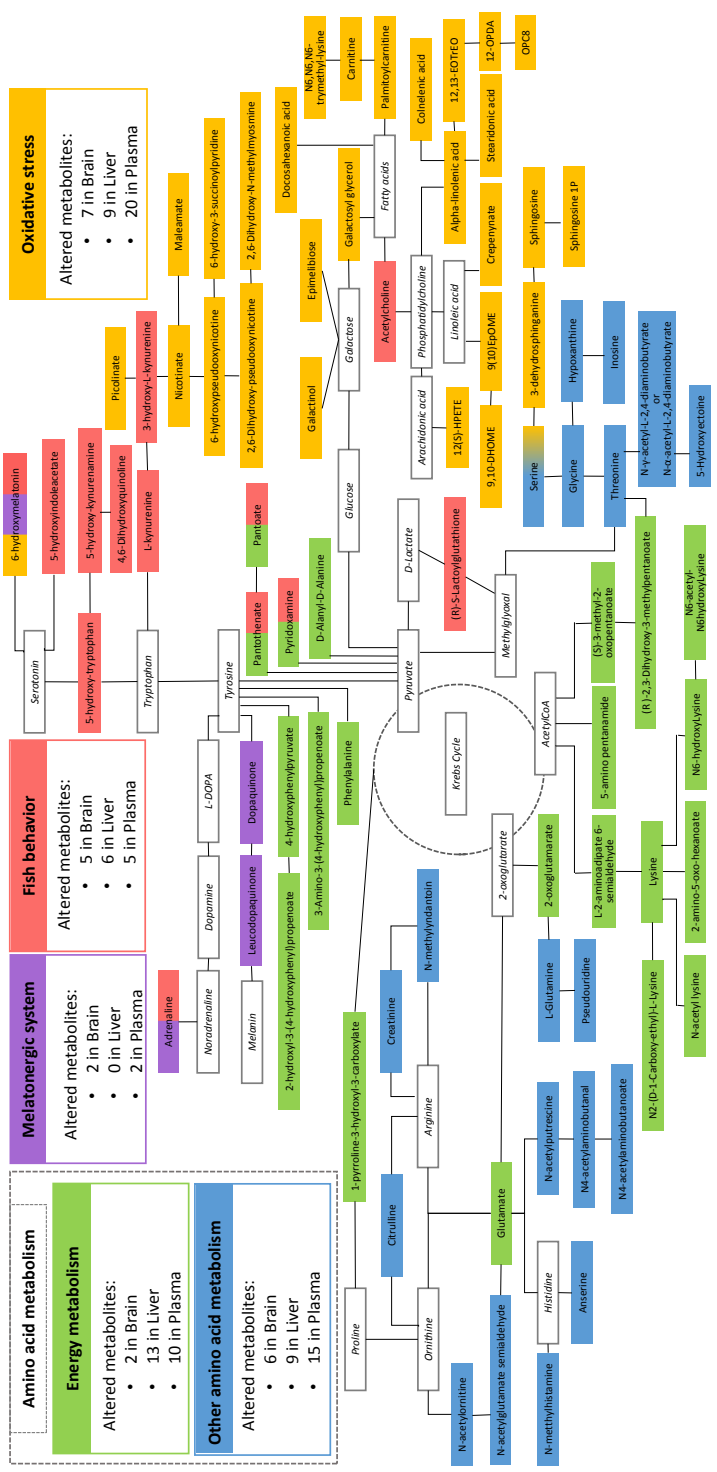

Figure 6.2: *Metabolic network with significantly altered KEGG-annotated compounds suggested by pathway enrichment. Metabolites are involved in the alteration of fish behavior (red), the melatonergic system (purple), oxidative stress (yellow) and amino acid metabolism (blue), which includes energy metabolism (green). The compounds in white, which are useful to link metabolites, have not been observed as altered in the present work.*

6.3.1 Alterations in fish behavior

Amitriptyline is an SSRI, and the alteration of serotonergic activity is reportedly associated with stress [17] since the serotonergic system plays an integral role in many basic systems in vertebrate biology such as wakefulness, aggression and appetite [17]. Serotonin is converted to 5-hydroxyindoleacetate, which displayed significantly reduced concentrations in exposed fish brain in this work (see Figure 6.3). This result suggests a reduction in serotonergic activity, which was also observed in exposure studies involving the SSRI fluoxetine in fish [15,16] and in rodents [30]. Wong and co-workers reported that the reduction in serotonergic activity may occur due to reduced levels of the serotonin precursor 5-hydroxy-L-tryptophan [30]. In our study, 5-hydroxy-L-tryptophan concentrations were lower in plasma of exposed fish (FC = 0.65 at last day of exposure) and two by-products of 5-hydroxy-L-tryptophan (i.e., 5-hydroxy-kynurenamine and 4,6-dihydroxyquinoline) were also perturbed in this biofluid. The reduced appetite of exposed fish can be also linked with the reduction of serotonergic activity, since SSRI treatment suppresses appetite [16]. In addition, the decrease of 6-hydroxymelatonin levels in fish brain after amitriptyline exposure (see Figure 6.4) suggests a similar effect, since melatonin and its related metabolites fall into the complex network between hormones, neurotransmitters and neuropeptides that interact intimately both at the central and peripheral levels to stimulate or inhibit feeding behavior [31].

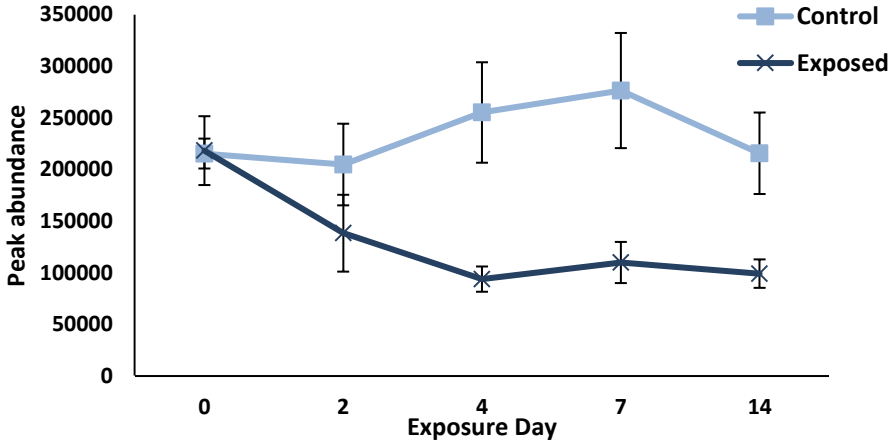

Figure 6.3: *Individual average peak areas for a 95% confidence interval of 5-hydroxyindoleacetate in control and exposed fish brain through the experiment (days 0, 2, 4, 7 and 14).*

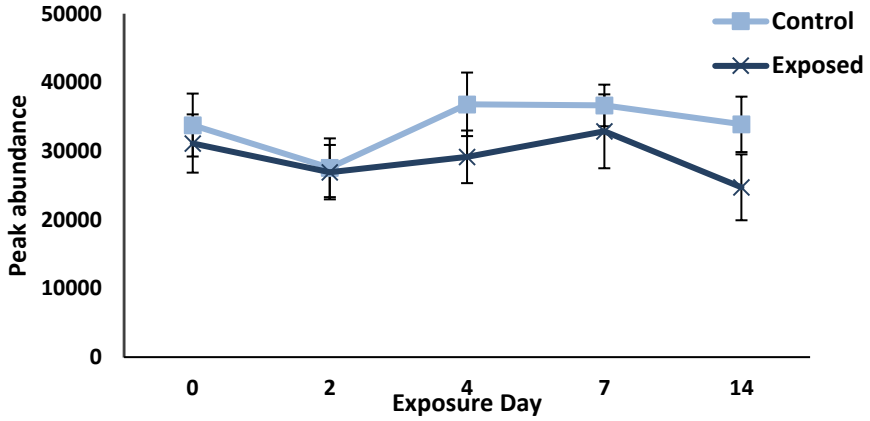

Figure 6.4: *Individual average peak areas for a 95% confidence interval of 6-hydroxymelatonin in control and exposed fish brain through the experiment (days 0, 2, 4, 7 and 14).*

Similar to 5-hydroxy-L-tryptophan, L-kynurenine is a by-product of the amino acid L-tryptophan, and the entry of tryptophan into this pathway is controlled by indoleamine/tryptophan 2,3-dioxygenases. L-kynurenine itself is not considered a neuroactive metabolite, but it is further metabolized down the kynurenine pathway into other neuroactive metabolites, such as 3-hydroxy-L-kynurenine by enzyme kynurenine 3-monooxygenase [32,33]. In this work, lower concentrations of L-kynurenine and 3-hydroxy-L-kynurenine (see Figure 6.5 as example) were detected in the liver of exposed fish, suggesting a decreased dioxygenase activity in liver, consistent with observations in mice [32]. Indeed, this fact has been widely associated with a declining stress [2,32,34–36], pinpointing that amitriptyline has decreased stress in the fish.

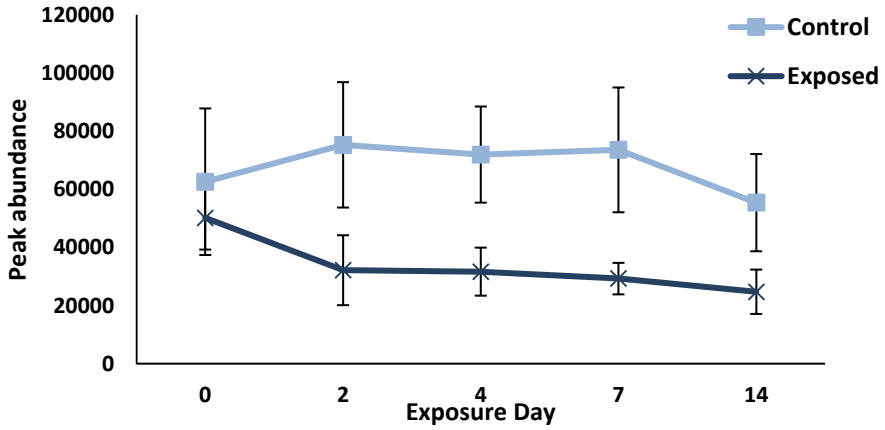

Figure 6.5: *Individual average peak areas for a 95% confidence interval of 3−hydroxy−L−kynurenine in control and exposed fish liver through the experiment (days 0, 2, 4, 7 and 14).*

Additional evidence related to stress episodes is the alteration of catecholamines (e.g. L-adrenaline and noradrenaline) [35,37], and their role in the stimulation of the sympathetic nervous system. Adrenaline is a major stress marker in fish [38,39], and in this work, we observed a decrease of adrenaline levels in brain samples of exposed fish (see Figure 6.6), especially in the last exposure day. According to the observations of Nagappa and coworkers antidepressants can inhibit both the active reuptake and passive uptake of adrenaline [40].

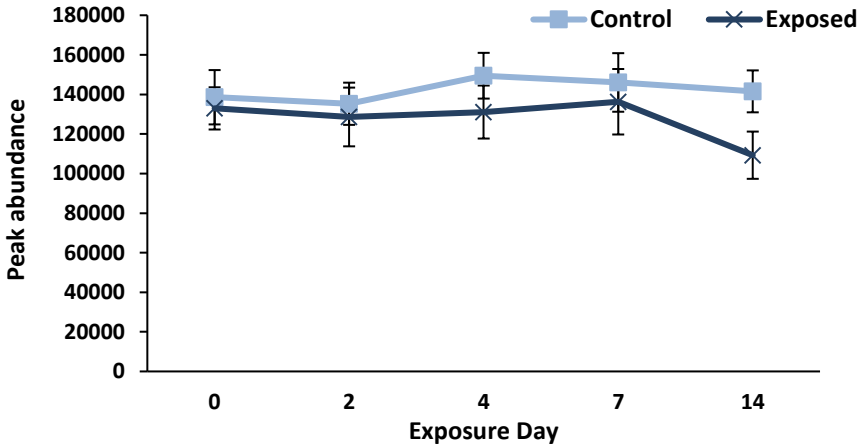

Figure 6.6: *Individual average peak areas for a 95% confidence interval of L−adrenaline in control and exposed fish brain through the experiment (days 0, 2, 4, 7 and 14).*

The decrease in neurotransmitters and related compounds could also be associated with a deficiency in B vitamins, since these substances have an important role in the synthesis of multiple neurotransmitters such as dopamine, serotonin, noradrenaline and the hormone melatonin [41]. In fact, we observed a decrease in pyridoxamine (one form of vitamin B6) levels for the three matrices (last exposure day FC values for brain, liver and plasma are 0.61, 0.57 and 0.68). In addition, in the liver of exposed fish, the levels of pantothenate (vitamin B5) and its precursor pantoate were also decreased, with FC values of 0.71 and 0.83 in the last day of exposure, respectively.

The alteration of acetylcholine levels in fish plasma and liver is also likely to affect fish behavior. It is widely demonstrated that tricyclic antidepressants have high affinity for antagonizing the muscarinic acetylcholine receptors [42,43], and hence, amitriptyline can alter the cholinergic mechanism. Since the parasympathetic nervous system mainly uses acetylcholine as its

neurotransmitter [44], the alterations in fish behavior can be related with the variation of acetylcholine levels in plasma. Furthermore, the alteration of acetylcholine in liver (FC = 2.05 at last day of exposure) may be a side effect of amitriptyline, since increasing acetylcholine concentrations were also observed in the liver of goldfish exposed to the pesticide dichlorvos [45].

Another observation that can be associated with the alteration of fish behavior or mood is the higher levels of (R)-S-lactoylglutathione in the brain of exposed fish (FC = 1.46 at last day of exposure). This suggests activation of the glyoxalase system, wherein the highly cytotoxic methylglyoxal is metabolized into D-lactate by glyoxalase I and II. In fact, glyoxalase is considered a robust and reliable biomarker for anxious versus non-anxious phenotypes [46], and there are several studies that have reported a relationship between enhanced expression of glyoxalase I (lactoylglutathione lyase) and reduced stress in rodents [46–51]. Therefore, the observed increase of (R)-S-lactoylglutathione levels might also be an effect of amitriptyline in fish behavior as suggested by the perturbations in other metabolites (5-hydroxyindoleacetate, 5-hydroxy-L-tryptophan, 6-hydroxymelatonin, L-kynurenine, 3-hydroxy-L-kynurenine, adrenaline and acetylcholine).

6.3.2 Alterations to the melatonergic system

As mentioned above, exposed fish were paler than controls (see Figure 6.1). This phenomena has been widely observed in many fish species, and is attributed to the response of chromatophores to environmental stimuli (e.g. xenobiotics) [52,53]. This observation was also confirmed at the metabolic level based on alterations of adrenaline, 6-hydroxymelatonin and dopaquinone/leucodopaquinone. Catecholamines are known to translocate pigment through receptors on the surface of melanophores. The primary hormones involved in regulating the translocation appear to be the melanocortins, melatonin, melanocyte-stimulating hormone and melanin-concentrating hormone [8,54,55]. It was previously reported that subchronic treatment with fluoxetine altered melanin-concentrating hormone [8], which diminishes the release of melanin and causes aggregation of pigment in the skin cells, making the skin appear paler. Although we have not measured melanin-concentrating hormone and melanin in our samples, we observed that the levels of dopaquinone or leucodopaquinone, which belong to the melanin biosynthesis pathway, were lower in plasma of exposed fish (FC = 0.61 at last day of exposure).

Additionally, a prior study suggested that by-products of melatonin, such as the aforementioned 6-hydroxymelatonin (perturbed by amitriptyline in the present work, see Figure 6.4), showed moderate action in the melatonergic system [56]. Since central melatonin production is regulated by activation of adrenergic receptors and the cutaneous melatoninergic system could also be regulated by locally produced catecholamines, local catecholaminergic and melatoninergic pathways represent a current challenge in skin biology research [55]. In fact, the lower levels of adrenaline detected in exposed fish brain (see Figure 6.6), might play a key role in the regulation of melatonin production. Lastly, a study with fish suggested that 5-HT agonists cause a pigment dispersion and fish skin darkening [54]. Therefore, it is not surprising that the 5-HT antagonist amitriptyline causes the opposite effect; that is, aggregation of the pigment making the fish paler.

6.3.3 Oxidative stress

A number of metabolic alterations, including 6-hydroxymelatonin, picolinic acid, nicotinic acid and other metabolites in nicotinate and nicotinamide pathway, metabolites in the galactose metabolism, metabolites in lipid metabolism and serine, revealed possible oxidative stress in exposed fish. For instance, due to the presence of the phenolic group in the structure, 6-hydroxymelatonin shows an excellent antioxidant activity via radical-trapping and is considered a protector metabolite against oxidative stress [57] and against lipid peroxidation [58]. The reduction observed in 6-hydroxymelatonin levels in exposed fish brain (see Figure 6.4), could pinpoint a sign of oxidative stress, which is consistent with other works where oxidative stress was observed in rodents exposed to antidepressants [9].

Furthermore, the lower levels of picolinic acid found in exposed fish brain (FC = 0.60 at the last day of exposure) can be related as well with higher oxidative stress. Actually, the decrease of picolinic acid could be expected due to the fact that antidepressants reduce the activity of enzymes transforming tryptophan into kynurenine pathway, and further cleavage of the above mentioned 3-hydroxy-L-kynurenine by kynureninase yields 3-hydroxyanthranilic acid, which can be oxidized to adenosine triphosphate (ATP) and to picolinic acid at a lower rate, or can be degraded to quinolinic acid [36]. Although picolinic acid has no radical scavenging ability, it has been reported to inhibit lipid peroxidation, to stimulate nitric oxide production and to prevent the neurotoxic effects of quinolinic acid [59]. The mentioned quinolinic acid can be eventually transformed into nicotinic

acid, which is involved in more than 500 intracellular reactions [36,60]. Actually, in this work, nicotinic acid levels were lower (FC = 0.60 at last day of exposure) in the exposed fish brain, and Tang and coworkers reported the relation between oxidative stress and nicotinic acid deficiency [61]. Another 6 metabolites in nicotinate and nicotinamide pathway (maleamate, 6-hydroxypseudooxynicotine; 6-hydroxy-3-succinoylpyridine; 2,6-dihydroxy-pseudooxynicotine; 2,6-dihydroxy-N-methylmyosmine) were also positively correlated (all of them showed FC value < 1.00 at last day of exposure) with brain nicotinic acid levels in the three matrices (brain, liver and plasma) studied (see Figure 6.7 as example).

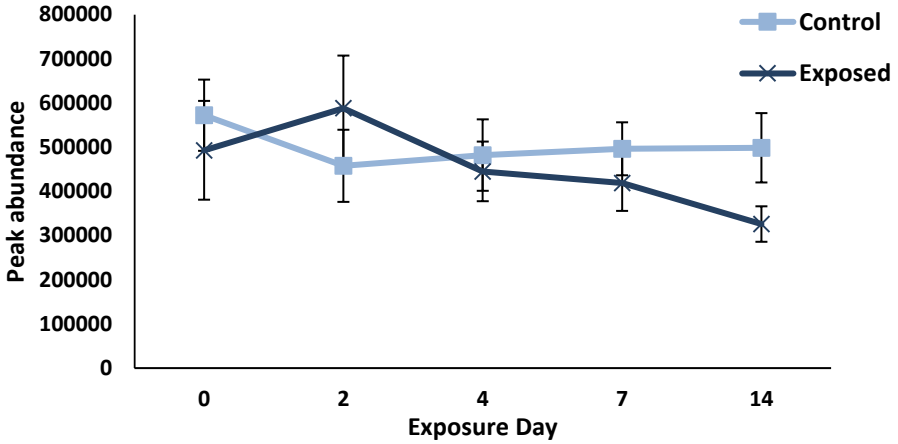

Figure 6.7: *Individual average peak areas for a 95% confidence interval of maleamate in control and exposed fish brain through the experiment (days 0, 2, 4, 7 and 14).*

Furthermore, significantly altered metabolites belonging to the galactose metabolism pathway were perturbed in this work, including galactinol or epimelibiose in liver (FC = 0.32 at last day of exposure) and galactosylglycerol in brain (FC = 0.62 at last day of exposure), which could also be attributed to oxidative stress since D-galactose has been reported to cause symptoms of liver and brain injuries through oxidative stress and apoptosis related processes [62].

Lastly, another sign of oxidative stress was the alteration in lipid metabolism in exposed fish liver and plasma. In fact, the different levels of carnitine (FC = 0.26 at last day of exposure) and long chain acyl carnitines (i.e., L-palmitoylcarnitine) (FC = 4.36 at last day of exposure) in exposed and controlled fish may point out lipid storage disorders in liver. This result is in concordance with the previous observations in part 1 of this research for gilt-head bream exposed to amitriptyline but at

lower concentration levels (i.e., 200 ng/L) (see Chapter 5). Lipid storage disorder in liver, which is highly related to oxidative stress, was already reported as an adverse effect of SSRIs [63–65]. In addition, in this work, the concentration of the carnitine precursor N6,N6,N6-trimethyl-lysine was also decreased in exposed fish plasma (see Figure 6.8).

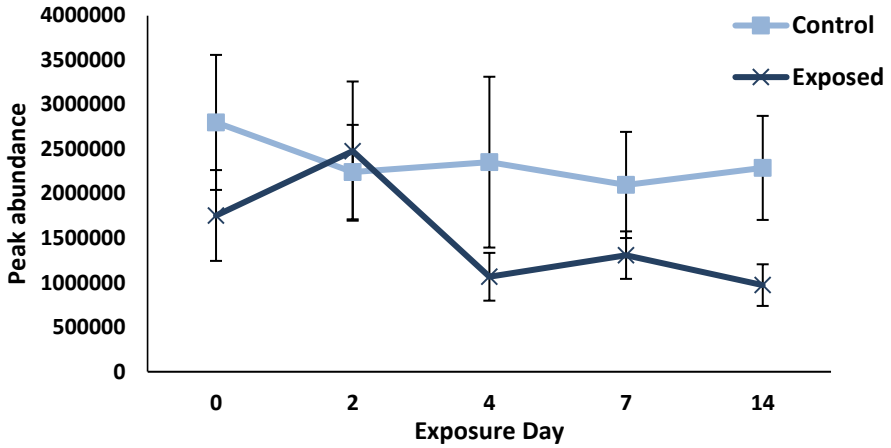

Figure 6.8: *Individual average peak areas for a 95% confidence interval of N6,N6,N6−trimethyl−L−lysine in control and exposed fish plasma through the experiment (days 0, 2, 4, 7 and 14).*

Lipids are susceptible to oxidation and lipid peroxidation products are potential biomarkers for oxidative stress. Some authors have suggested that antidepressants such as amitriptyline induced lipid peroxidation since the proliferation of lysophosphatidylcholines and/or unsaturated fatty acids in microsomal phospholipids may participate in the formation of lipid hydroperoxides [13]. For instance, under the action of lipoxygenase, arachidonic acid is converted into a hydroperoxide: hydroperoxyeicosatetraenoic acid, which will release the hydroxyl radical during its transformation into hydroxyeicosatetraenoic acid. In this work, we observed increased concentrations of intermediate lipoxygenase products such as 12(S)–hydroperoxyeicosatetraenoic acid in exposed fish liver (FC = 2.45 at last day of exposure). Besides deoxygenation of polyunsaturated fatty acids to hydroperoxyeicosatetraenoic acids, lipoxygenases are capable of oxidizing many xenobiotics, such as tricyclic antidepressants, in liver and brain through oxidative N-dealkylation via the lipoxygenase pathway [66]. We also found evidence of the activity of lipoxynesases in our previous work performed at lower amitriptyline exposure levels, since the highest concentrations of amitriptyline degradation products in liver corresponded to

monohydroxylated and dealkylated amitriptyline degradation products [14].

In addition to metabolites involved in arachidonic acid metabolism, docosahexanoic acid and other metabolites belonging to linoleic acid and linolenic acid metabolism are also used to identify oxidative stress episodes [67,68]. In fact, we observed alterations in the levels of lipid peroxidation products of both linoleic acid (e.g., crepenynate, linoleic acid epoxides (9(10)EpOME) and linoleic acid diols (9,10-DHOME)) and linolenic acid (e.g., stearidonic acid, α-linolenic acid, OPC-8:00 and 12,13(S)-EOT / Colnelenic acid / 12-OPDA) pathways in plasma (see FC values in Table 6.3), which are consistent markers of higher oxidative states [69].

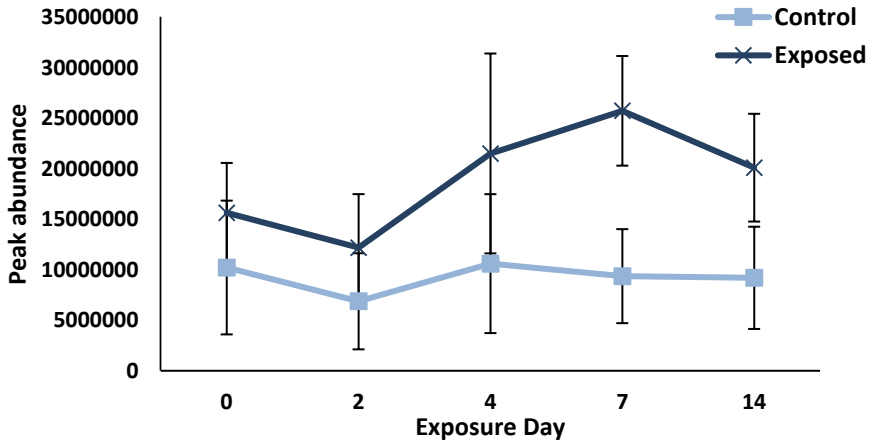

Figure 6.9: *Individual average peak areas for a 95% confidence interval of 3−dehydrosphinganine in control and exposed fish liver through the experiment (days 0, 2, 4, 7 and 14).*

At the same time, we found that sphingolipid metabolism was also perturbed since levels of 3-dehydrosphinganine in liver (see Figure 6.9) and sphingosine and sphingosine-1-phosphate in plasma were altered. A key enzyme in the sphingolipid pathway is acid sphingomyelinase (ASM), which hydrolyses sphingomyelin to ceramide (the precursor of sphingosine), and it can be activated by various stimuli (e.g., reactive oxygen death receptors, stress, infections) [70]. Moreover, some studies show that accumulation of ceramide produce oxidative stress by increasing O_2^- radical generation in endothelial cells, which can rapidly oxidize nitric oxide and reduce the bioactivity of nitric oxide [71]. Therefore, the alteration in sphingolipid metabolism can be another sign of oxidative stress as a side-effect of amitriptyline, because similar sphingosine alterations occurred to fish plasma exposed to effluent wastewater samples [18] or in rat plasma

exposed to dichlorvos [72]. Moreover, apart from those mentioned lipids, another 16 and 28 putatively identified lipids that are not included in KEGG were significantly perturbed in liver and brain, respectively (see Tables 6.1-6.3).

Related to lipid metabolism, we also observed a decrease of the amino acid serine levels in exposed fish plasma (see Figure 6.10). Serine is an essential precursor for the synthesis of lipids [73], and the disruption of the amino acid metabolism related to serine could be indicative of oxidative stress [74]. Therefore, the lower serine levels that we detected after exposure might have caused a more significant cellular response to oxidative stress, which is consistent with other works that observed serine deficiency in plasma under oxidative stress [75]. Actually, in addition to serine, other metabolites in serine, glycine and threonine metabolism (threonine, Nγ-acetyl-L-2,4 diaminobutyrate/Nα-acetyl-L-2,4-diaminobutyrate and 5-hydroxyectoine) showed a decreasing concentration pattern in plasma of exposed fish (see FC values in Table 6.3).

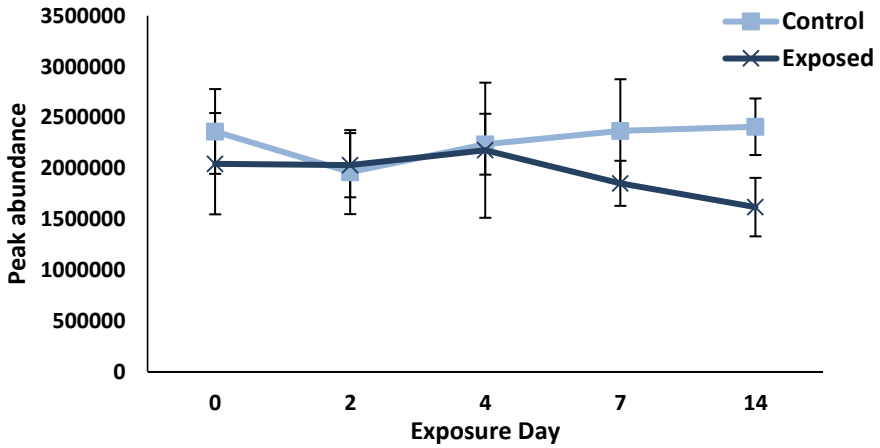

Figure 6.10: *Individual average peak areas for a 95% confidence interval of serine in control and exposed fish plasma through the experiment (days 0, 2, 4, 7 and 14).*

6.3.4 Alterations in amino acid metabolism

The patterns shown by a number of metabolites (22 in liver, 25 in plasma and 8 in brain) are in agreement with a modification in the amino acid metabolism, which is also reported with other xenobiotics [74,76]. Many of those metabolites (13 in liver, 10 in plasma and 2 in brain) are closely linked to energy metabolism. Some of those metabolites (5 in plasma, 4 in liver and 1 in brain) are

connected to the lysine degradation pathway (L-2-aminoadipate-6-semialdehyde, 2-amino-5-oxohexanoate, N-acetyl-lysine, N2-(D-1-carboxy-ethyl)-L-lysine, 5-amino-pentanamide, N6-hydroxylysine and N6-acetyl-N6-hydroxylysine). Additionally, alterations were also observed in metabolites in the biosynthesis of branched chain amino acids valine, leucine and isoleucine biosynthesis ((R)-2,3-dihydroxy-3-methylpentanoate and (S)-3-methyl-2-oxopentanoate) and the tyrosine and pyruvate metabolism (3-amino-3-(4-hydroxyphenyl)-propanoate and 4-hydroxyphenylpyruvate / 2-hydroxy-3-(4-hydroxyphenyl)propenoate), which are also related to the Krebs cycle after their transformation to succinyl-CoA or acetyl-CoA.

Alterations of amino acids linked to the Krebs cycle have already been cited in the literature in relation with depression or depression treatment [5,7,10,22,77,78]. For instance, the downregulation of valine has been linked to a lack of access to pyruvate [22]. Tyrosine metabolism is also linked to the Krebs cycle through pyruvate, and actually, we observed higher concentrations of 4-hydroxyphenylpyruvate/2-hydroxy-3-(4-hydroxyphenyl)propenoate and 3-amino-3-(4-hydroxyphenyl)propanoate in liver of exposed fish (see Figure 6.11), pinpointing a possible lack of pyruvate consumption. Another sign of this effect can be found in the altered levels of 1-pyrroline-3-hydroxy-5-carboxylate in liver (see Table 6.2) and plasma (see Table 6.3) in the arginine and proline metabolism that is linked to pyruvate and, therefore, to the Krebs cycle.

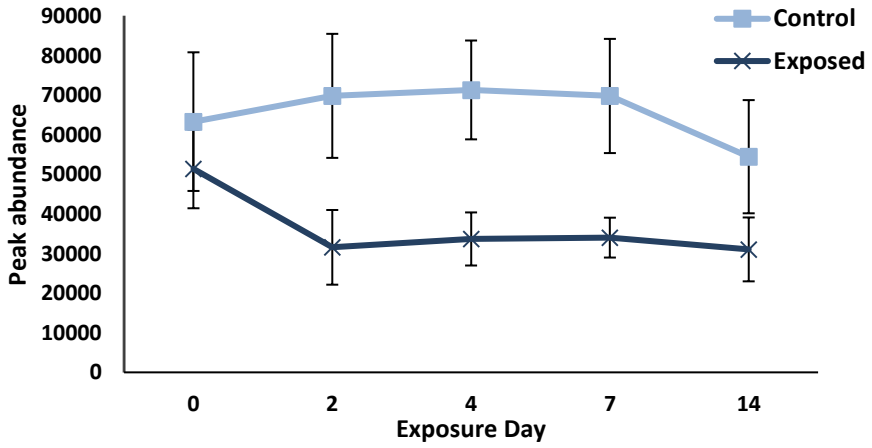

Figure 6.11: *Individual average peak areas for a 95% confidence interval of 3-amino-3-(4-hydroxyphenyl)propanoate in control and exposed fish liver through the experiment (days 0, 2, 4, 7 and 14).*

Additionally, concentrations of phenylalanine in plasma and D-alanyl-D-alanine in brain, plasma and liver (see Tables 6.1-6.3), metabolites related to different alanine pathways, were altered in exposed fish. Alanine concentration was also altered in mice submitted to chronic unpredicted mild stress and reduced levels of glyconeogenesis suggested the obstruction of CoA formation or an energy metabolism disorder [22]. In this aspect, the alterations in the liver levels of pantothenate (vitamin B5), which is involved in both β-alanine metabolism and CoA biosynthesis, and its precursor pantoate might be other signs of energy metabolism perturbation. In fact, the above mentioned B vitamins are clearly involved in every aspect of catabolic energy production [41]. Similarly, the results for the low-dose experiment also pinpointed alteration of pantothenate levels in liver (see Chapter 5).

Another sign of perturbation of the energy metabolism is the alteration of the glutamate amino acid, which is consistent to our previous work where gilt-head bream was exposed to an environmentally relevant concentration (i.e., 200 ng/L) of amitriptyline (see Chapter 5). In this work both glutamate and 2-oxoglutaramate concentrations were altered in liver, with 1.52 and 0.62 FC values at the last day of exposure, respectively. Both glutamate and 2-oxoglutaramate are linked with 2-oxoglutarate through glutamate dehydrogenase and omega-amidase, respectively, and the latter is a Krebs cycle intermediate.

The modification of the amino acid metabolism was not only reflected in the perturbation of energy metabolism. Apart from those amino acids closely linked to energy metabolism, we found that amitriptyline exposure caused alteration of other amino acid metabolisms, especially in plasma (15 metabolites), followed by liver (9 metabolites) and in a lesser extent in brain (6 metabolites). In fact, it has been widely described in the literature the alteration of the amino acid metabolism related to depression or depression treatment [4,6,7,11,22,78].

Similarly to other works in the literature dealing with antidepressants [4,11,78], one of the most altered amino acid pathway in amitriptyline-exposed gilt-head bream plasma was the above mentioned serine, glycine and threonine metabolism. The concentration of the metabolites in this pathway (serine, threonine, Nγ-acetyl-L-2,4 diaminobutyrate/Nα-acetyl-L-2,4-diaminobutyrate and 5-hydroxyectoine) decreased in plasma of exposed fish (see Figure 6.10 as an example). Contrarily, in the exposed fish we observed an increase in the plasma concentration of hypoxanthine

(FC = 1.43 at last day of exposure) and inosine (FC = 1.43 at last day of exposure) metabolites in the purine metabolism, which is closely linked to the serine, glycine and threonine metabolism. In addition to plasma (FC = 0.51), N-acetyl-L-2,4 diaminobutyrate was also decreased in brain and liver, with 0.61 and 0.44 FC values at the last day of exposure, respectively. Other signs of amino acid metabolism alteration were the perturbations in the histidine metabolism, with altered levels of anserine and N-methylhistamine (see Figure 6.12) in liver and brain of exposed fish, respectively. The results for the low-dose experiment also pinpointed alteration of the purine and histidine metabolism since uric acid and formylisoglutamine/N-formimino-L-glutamate in those pathways were perturbed (see Chapter 5).

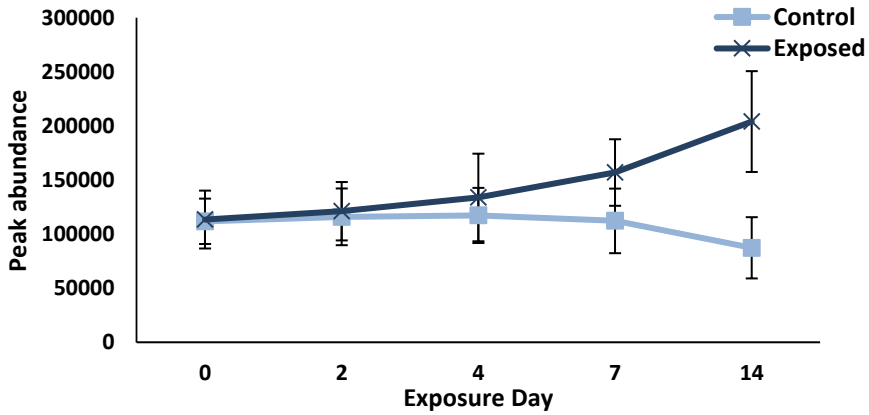

Figure 6.12: *Individual average peak areas for a 95% confidence interval of N−methylhistamine in control and exposed fish brain through the experiment (days 0, 2, 4, 7 and 14).*

Concentration of pseudouridine in the pyrimidine pathway also increased in the liver of exposed fish (FC = 1.57 at last day of exposure). Alterations of the pyrimidine metabolism have already been observed in the literature but the alterations were usually found in brain samples in studies related to depression or the use of antidepressants [4,78–80]. Related to the pyrimidine metabolism, we also observed that glutamine in plasma showed lower concentration in exposed fish (see Figure 6.13). Altered glutamine synthetase protein expression was also observed in mice treated with paroxetine [3] and altered glutamine levels were observed in the hippocampus of mice exposed to paroxetine [6] and in the cerebrospinal fluid of depressed patients [81]. Similarly to glutamine, spermine, spermidine and putrescine in the arginine and proline metabolism are also involved in the N-methyl-D-aspartate receptor (NMDAR) system [46] and in our case N-

acetylputrescine and methylhydantoin in plasma and liver, N4-acetyl-aminobutanal and creatinine in liver, and N4-acetamidobutanoate in plasma (see Figure 6.14) were altered. Moreover, N-acetylputrescine, N4-acetyl-aminobutanal and N4-acetyl-amino-butanoate, all at lower concentrations in exposed fish (FC values < 1.00), are all connected to gamma-aminobutyric acid (GABA) levels (not significantly altered in the present work) through the 4-acetamidobutyrate deacetylase enzyme. Reduced levels of GABA have been related with increased neuronal activity after paroxetine treatment, and it is reported the important role of GABA, together with noradrenaline and glutamate, in antidepressant action [6].

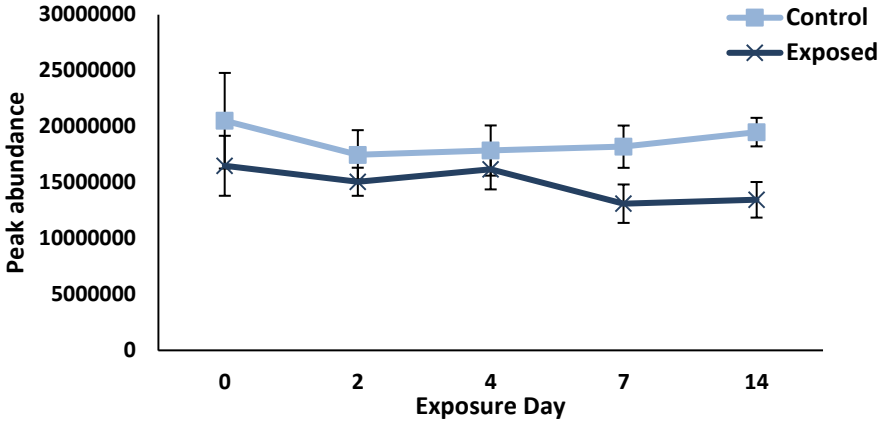

Figure 6.13: *Individual average peak areas for a 95% confidence interval of glutamine in control and exposed fish plasma through the experiment (days 0, 2, 4, 7 and 14).*

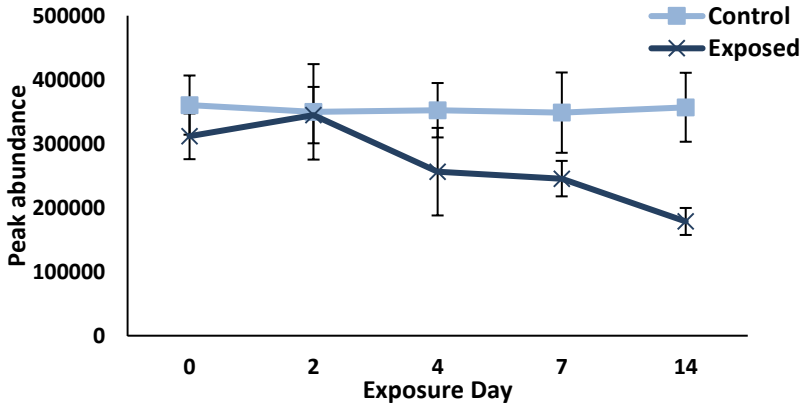

Figure 6.14: *Individual average peak areas for a 95% confidence interval of N4-acetamidobutanoate in control and exposed fish plasma through the experiment (days 0, 2, 4, 7, 14).*

Lastly, similar to the low-dose results in part 1 of this work (see Chapter 5), alterations in metabolites related nitric oxide system were observed in this study. Citrulline was altered in fish plasma (see Figure 6.15), together with N-acetyl-ornithine (both in plasma and brain) and N-acetylglutamate semialdehyde (in brain). Similar observations were made by Park and coworkers [3] who related it to nitric oxide regulations, which is also related to glutamatergic pathways. The nitric oxide system has been often related to the treatment and pathobiology of depression [3].

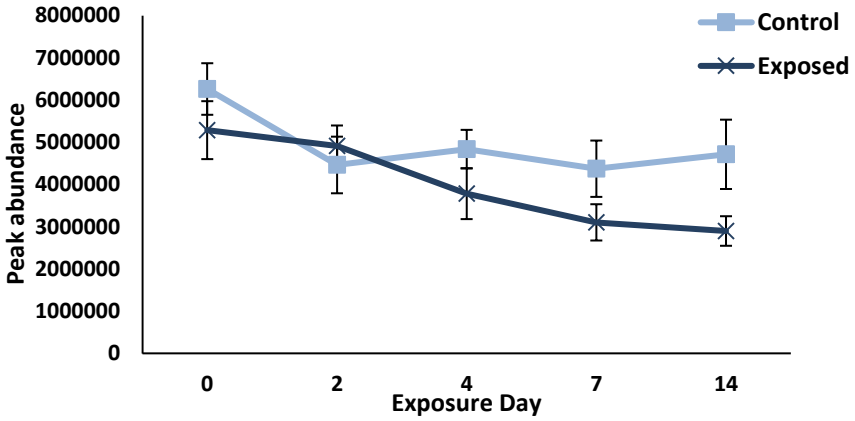

Figure 6.15: *Individual average peak areas for a 95% confidence interval of citrulline in control and exposed fish plasma through the experiment (days 0, 2, 4, 7 and 14).*

6.4 Implications to Environmental Risk Assessment

The observations and effects found in this work support the conclusions described in our previous work (see Chapter 5), where gilt-head bream were exposed to amitriptyline at an environmentally relevant concentration (i.e., 200 ng/L). In both cases, alterations in lipid, energy and amino acid metabolism were observed, which is indicative of adverse effects beyond the mainly studied monoamine reuptake inhibition. In this work, we linked the metabolic changes at both low- and high-dose to apical endpoints, demonstrating that the metabolic changes were associated with adverse outcome, consistent with the known effects of SSRI on feeding rate and other behavioral alterations [1,77].

The above-mentioned metabolic alterations could explain the lower appetite and the altered behavior shown by the exposed fish. Since an acute stress response is necessary for survival

[32] these are troubling results. Acute stress facilitates responses to external stressors and primes the body for the metabolic, physical and cognitive demands of fight-or-flight [82]. Therefore, behavioral changes can have implications for the response to additional environmental stressors and affect population level [17].

Metabolomics also allowed us to confirm the observation of melatonergic system variation (i.e., exposed fish becoming paler) at metabolome level. The observed paleness could cause difficulties for exposed fish in several ways. Fish not only use their color shifting abilities to communicate but also as a way to protect themselves, as camouflaged fish are more likely to escape predators [53]. Lastly, possible disruption of lipid pathways and other related results suggest that amitriptyline is causing common adverse effects such as oxidative stress [18,72,83].

Collectively, these data have implications for risk assessment because the observed changes might lead to adverse effects at either the individual or population level in fish. It further suggests that environmental monitoring programs that investigate wildlife exposure to behavioral altering pharmaceuticals through bioconcentration alone are underestimating exposure. This study demonstrates the usefulness of metabolomics to assess molecular-level effects of emerging contaminants.

6.5 References

1. Brodin T, Piovano S, Fick J, Klaminder J, Heynen M, Jonsson M. 2014. Ecological effects of pharmaceuticals in aquatic systems—impacts through behavioural alterations. *Philos. Trans. R. Soc. B Biol. Sci.* 369.

2. Kocki T, Wnuk S, Kloc R, Kocki J, Owe-Larsson B, Urbanska EM. 2012. New insight into the antidepressants action: modulation of kynurenine pathway by increasing the kynurenic acid/3-hydroxykynurenine ratio. *J. Neural Transm.* 119:235–243.

3. Park DI, Dournes C, Sillaber I, Ising M, Asara JM, Webhofer C, Filiou MD, Müller MB, Turck CW. 2017. Delineation of molecular pathway activities of the chronic antidepressant treatment response suggests important roles for glutamatergic and ubiquitin–proteasome systems. *Transl. Psychiatry*. 7:e1078.

4. Park DI, Dournes C, Sillaber I, Uhr M, Asara JM, Gassen NC, Rein T, Ising M, Webhofer C, Filiou MD, Müller MB, Turck CW. 2016. Purine and pyrimidine metabolism: Convergent evidence on chronic antidepressant treatment response in mice and humans. *Sci. Rep.* 6.

5. Scaini G, Santos PM, Benedet J, Rochi N, Gomes LM, Borges LS, Rezin GT, Pezente DP, Quevedo J, Streck EL. 2010. Evaluation of Krebs cycle enzymes in the brain of rats after chronic administration of antidepressants. *Brain Res. Bull.* 82:224–227.

6. Webhofer C, Gormanns P, Reckow S, Lebar M, Maccarrone G, Ludwig T, Pütz B, Asara JM, Holsboer F, Sillaber I, Zieglgänsberger W, Turck CW. 2013. Proteomic and metabolomic profiling reveals time-dependent changes in hippocampal metabolism upon paroxetine treatment and biomarker candidates. *J. Psychiatr. Res.* 47:289–298.

7. Webhofer C, Gormanns P, Tolstikov V, Zieglgänsberger W, Sillaber I, Holsboer F, Turck CW. 2011. Metabolite profiling of antidepressant drug action reveals novel drug targets beyond monoamine elevation. *Transl. Psychiatry*. 1:e58.

8. Calegare BF, Costa A, Fernandes L, Dias AL, Torterolo P, Almeida VD. 2016. Subchronical treatment with Fluoxetine modifies the activity of the MCHergic and hypocretinergic systems. Evidences from peptide CSF concentration and gene expression. *Sleep Sci.* 9:89–93.

9. Elmorsy E, Al-Ghafari A, Almutairi FM, Aggour AM, Carter WG. 2017. Antidepressants are cytotoxic to rat primary blood brain barrier endothelial cells at high therapeutic concentrations. *Toxicol. In Vitro*. 44:154–163.

10. Filipović D, Costina V, Perić I, Stanisavljević A, Findeisen P. 2017. Chronic fluoxetine treatment directs energy metabolism towards the citric acid cycle and oxidative phosphorylation in rat hippocampal nonsynaptic mitochondria. *Brain Res.* 1659:41–54.

11. Nagasawa M, Otsuka T, Yasuo S, Furuse M. 2015. Chronic imipramine treatment differentially alters the brain and plasma amino acid metabolism in Wistar and Wistar Kyoto rats. *Eur. J. Pharmacol.* 762:127–135.

12. Taziki S, Sattari MR, Dastmalchi S, Eghbal MA. 2015. Cytoprotective Effects of Melatonin Against Amitriptyline-Induced Toxicity in Isolated Rat Hepatocytes. *Adv. Pharm. Bull.* 5:329–334.

13. Yamamoto A, Itoh S, Hoshi K, Ichihara K. 1996. Chronic effect of phenobarbital, amitriptyline or chlorpromazine on lipid peroxidation in rat liver and brain. *Res. Commun. Biol. Psychol. Psychiatry*. 21:27–36.

14. Ziarrusta H, Mijangos L, Izagirre U, Plassmann MM, Benskin JP, Anakabe E, Olivares M, Zuloaga O. 2017. Bioconcentration and Biotransformation of Amitriptyline in Gilt-Head Bream. *Environ. Sci. Technol.* 51:2464–2471.

15. Clotfelter ED, O'Hare EP, McNitt MM, Carpenter RE, Summers CH. 2007. Serotonin decreases aggression via 5-HT1A receptors in the fighting fish Betta splendens. *Pharmacol. Biochem. Behav.* 87:222–231.

16. Gaworecki KM, Klaine SJ. 2008. Behavioral and biochemical responses of hybrid striped bass during and after fluoxetine exposure. *Aquat. Toxicol.* 88:207–213.

17. Winder VL, Sapozhnikova Y, Pennington PL, Wirth EF. 2009. Effects of fluoxetine exposure on serotonin-related activity in the sheepshead minnow (Cyprinodon variegatus) using LC/MS/MS detection and quantitation. *Comp. Biochem. Physiol. Part C Toxicol. Pharmacol.* 149:559–565.

18. Al-Salhi R, Abdul-Sada A, Lange A, Tyler CR, Hill EM. 2012. The Xenometabolome and Novel Contaminant Markers in Fish Exposed to a Wastewater Treatment Works Effluent. *Environ. Sci. Technol.* 46:9080–9088.

19. Bundy JG, Davey MP, Viant MR. 2008. Environmental metabolomics: a critical review and future perspectives. *Metabolomics*. 5:3–21.

20. Huang SSY, Benskin JP, Chandramouli B, Butler H, Helbing CC, Cosgrove JR. 2016. Xenobiotics Produce Distinct Metabolomic Responses in Zebrafish Larvae (Danio rerio). *Environ. Sci. Technol.* 50:6526–6535.

21. Cajka T, Fiehn O. 2016. Toward Merging Untargeted and Targeted Methods in Mass Spectrometry-Based Metabolomics and Lipidomics. *Anal. Chem.* 88:524–545.

22. Shi B, Tian J, Xiang H, Guo X, Zhang L, Du G, Qin X. 2013. A 1H-NMR plasma metabonomic study of acute and chronic stress models of depression in rats. *Behav. Brain Res.* 241:86–91.

23. Vinaixa M, Samino S, Saez I, Duran J, Guinovart JJ, Yanes O. 2012. A Guideline to Univariate Statistical Analysis for LC/MS-Based Untargeted Metabolomics-Derived Data. *Metabolites*. 2:775–795.

24. Picart-Armada S, Fernández-Albert F, Vinaixa M, Rodríguez MA, Aivio S, Stracker TH, Yanes O, Perera-Lluna A. 2017. Null diffusion-based enrichment for metabolomics data. *PLOS ONE*. 12:e0189012.

25. http://www.kegg.jp/kegg/. 2018. KEGG_.

26. Ribbenstedt A, Ziarrusta H, Benskin JP. 2018. A Multi-platform Targeted/Non-targeted (TNT) approach for quantitative and discovery-based metabolomics. *PLOS ONE (submitted)*.

27. Fulton WT. 1904. The rate of growth of fishes. *22nd Annu. Rep. Fish. Board Scotl.* 3:141–241.

28. Fernández-Albert F, Llorach R, Garcia-Aloy M, Ziyatdinov A, Andres-Lacueva C, Perera A. 2014. Intensity drift removal in LC/MS metabolomics by common variance compensation. *Bioinformatics*. 30:2899–2905.

29. Schymanski EL, Jeon J, Gulde R, Fenner K, Ruff M, Singer HP, Hollender J. 2014. Identifying Small Molecules via High Resolution Mass Spectrometry: Communicating Confidence. *Environ.*

Sci. Technol. 48:2097–2098.

30. Wong DT, Bymaster FP, Engleman EA. 1995. Prozac (fluoxetine, lilly 110140), the first selective serotonin uptake inhibitor and an antidepressant drug: Twenty years since its first publication. *Life Sci.* 57:411–441.

31. Piccinetti CC, Migliarini B, Olivotto I, Coletti G, Amici A, Carnevali O. 2010. Appetite regulation: The central role of melatonin in Danio rerio. *Horm. Behav.* 58:780–785.

32. Dostal CR, Carson Sulzer M, Kelley KW, Freund GG, MCusker RH. 2017. Glial and tissue-specific regulation of Kynurenine Pathway dioxygenases by acute stress of mice. *Neurobiol. Stress*. 7:1–15.

33. Tashiro T, Murakami Y, Mouri A, Imamura Y, Nabeshima T, Yamamoto Y, Saito K. 2017. Kynurenine 3-monooxygenase is implicated in antidepressants-responsive depressive-like behaviors and monoaminergic dysfunctions. *Behav. Brain Res.* 317:279–285.

34. Fuertig R, Azzinnari D, Bergamini G, Cathomas F, Sigrist H, Seifritz E, Vavassori S, Luippold A, Hengerer B, Ceci A, Pryce CR. 2016. Mouse chronic social stress increases blood and brain kynurenine pathway activity and fear behaviour: Both effects are reversed by inhibition of indoleamine 2,3-dioxygenase. *Brain. Behav. Immun.* 54:59–72.

35. Kim Y-K, Won E. 2017. The influence of stress on neuroinflammation and alterations in brain structure and function in major depressive disorder. *Behav. Brain Res.* 329:6–11.

36. Réus GZ, Jansen K, Titus S, Carvalho AF, Gabbay V, Quevedo J. 2015. Kynurenine pathway dysfunction in the pathophysiology and treatment of depression: Evidences from animal and human studies. *J. Psychiatr. Res.* 68:316–328.

37. Barton BA. 2015. IAAAM 1988. *VIN.com*. Available from https://www.vin.com/doc/?id=6692548.

38. Mazeaud MM, Mazeaud F. 1981. Adrenergic responses to stress in fish. *Stress Fish*. [cited 17 February 2018]. Available from http://agris.fao.org/agris-search/search.do?recordID=US201302632784.

39. Peter MCS. 2011. The role of thyroid hormones in stress response of fish. *Gen. Comp. Endocrinol.* 172:198–210.

40. Nagappa AN, Kole PL, Pandi PV, Shanmukha I, Girish K, Mishra RPK. 2003. Role of surface activity in mechanism of actions of tricyclic antidepressants. *Colloids Surf. B Biointerfaces*. 32:169–177.

41. Kennedy DO. 2016. B Vitamins and the Brain: Mechanisms, Dose and Efficacy—A Review. *Nutrients*. 8.

42. Drevets WC, Zarate CA, Furey ML. 2013. Antidepressant Effects of the Muscarinic Cholinergic Receptor Antagonist Scopolamine: A Review. *Biol. Psychiatry*. 73:1156–1163.

43. Stahl SM. 1998. Not So Selective Serotonin Reuptake Inhibitors. *J. Clin. Psychiatry*. 59:333–343.

44. McCorry LK. 2007. Physiology of the Autonomic Nervous System. *Am. J. Pharm. Educ.* 71.

45. Liu Y, Chen T, Li M-H, Xu H-D, Jia A-Q, Zhang J-F, Wang J-S. 2015. 1H NMR based metabolomics approach to study the toxic effects of dichlorvos on goldfish (Carassius auratus). *Chemosphere*. 138:537–545.

46. Turck CW, Landgraf R, Filiou MD, Zhang Y, Webhofer C, Reckow S, Gormanns P, Ditzen C, Maccarrone G, Varadarajulu J. 2011. S.3.01 Biomarkers for anxiety disorders: proteomic and systems biology approaches. *Eur. Neuropsychopharmacol.* 21:S110–S111.

47. Fujimoto M, Uchida S, Watanuki T, Wakabayashi Y, Otsuki K, Matsubara T, Suetsugi M, Funato H, Watanabe Y. 2008. Reduced expression of glyoxalase-1 mRNA in mood disorder patients. *Neurosci. Lett.* 438:196–199.

48. Hambsch B. 2011. Altered glyoxalase 1 expression in psychiatric disorders: Cause or consequence? *Semin. Cell Dev. Biol.* 22:302–308.

49. Jang S, Kwon DM, Kwon K, Park C. 2017. Generation and characterization of mouse knockout for glyoxalase 1. *Biochem. Biophys. Res. Commun.* 490:460–465.

50. Krömer SA, Keßler MS, Milfay D, Birg IN, Bunck M, Czibere L, Panhuysen M, Pütz B, Deussing JM, Holsboer F, Landgraf R, Turck CW. 2005. Identification of Glyoxalase-I as a Protein Marker in a Mouse Model of Extremes in Trait Anxiety. *J. Neurosci.* 25:4375–4384.

51. Yang Y, Yang D, Tang G, Zhou C, Cheng K, Zhou J, Wu B, Peng Y, Liu C, Zhan Y, Chen J, Chen G, Xie P. 2013. Proteomics reveals energy and glutathione metabolic dysregulation in the prefrontal cortex of a rat model of depression. *Neuroscience*. 247:191–200.

52. Kaur R, Dua A. 2015. Colour changes in Labeo rohita (Ham.) due to pigment translocation in melanophores, on exposure to municipal wastewater of Tung Dhab drain, Amritsar, India. *Environ. Toxicol. Pharmacol.* 39:747–757.

53. Lennquist A, Mårtensson Lindblad LGE, Hedberg D, Kristiansson E, Förlin L. 2010. Colour and melanophore function in rainbow trout after long term exposure to the new antifoulant medetomidine. *Chemosphere*. 80:1050–1055.

54. Salim S, Ali AS, Ali SA. 2013. 5-HT receptor subtypes as key targets in mediating pigment dispersion within melanophores of teleost, Oreochromis mossambicus. *Comp. Biochem. Physiol. B Biochem. Mol. Biol.* 164:117–123.

55. Slominski A, Fischer TW, Zmijewski MA, Wortsman J, Semak I, Zbytek B, Slominski RM, Tobin DJ. 2005. On the Role of Melatonin in Skin Physiology and Pathology. *Endocrine*. 27:137–148.

56. Fujii R, Miyashita Y. 1978. Receptor mechanisms in fish chromatophores—IV. Effects of melatonin and related substances on dermal and epidermal melanophores of the siluroid, Parasilurus asotus. *Comp. Biochem. Physiol. Part C Comp. Pharmacol.* 59:59–63.

57. Pérez-González A, Galano A, Alvarez-Idaboy JR, Tan DX, Reiter RJ. 2017. Radical-trapping and preventive antioxidant effects of 2-hydroxymelatonin and 4-hydroxymelatonin: Contributions to the melatonin protection against oxidative stress. *Biochim. Biophys. Acta BBA - Gen. Subj.* 1861:2206–2217.

58. Maharaj DS, Limson JL, Daya S. 2003. 6-Hydroxymelatonin converts Fe (III) to Fe (II) and reduces iron-induced lipid peroxidation. *Life Sci.* 72:1367–1375.

59. González Esquivel D, Ramírez-Ortega D, Pineda B, Castro N, Ríos C, Pérez de la Cruz V. 2017. Kynurenine pathway metabolites and enzymes involved in redox reactions. *Neuropharmacology*. 112:331–345.

60. Viljoen M, Swanepoel A, Bipath P. 2015. Antidepressants may lead to a decrease in niacin and NAD in patients with poor dietary intake. *Med. Hypotheses*. 84:178–182.

61. Tang K, Sham H, Hui E, Kirkland JB. 2008. Niacin deficiency causes oxidative stress in rat bone marrow cells but not through decreased NADPH or glutathione status. *J. Nutr. Biochem.* 19:746–753.

62. Chen P, Chen F, Zhou B. 2018. Antioxidative, anti-inflammatory and anti-apoptotic effects of ellagic acid in liver and brain of rats treated by D-galactose. *Sci. Rep.* 8:1465.

63. Buron N, Porceddu M, Roussel C, Begriche K, Trak-Smayra V, Gicquel T, Fromenty B, Borgne-Sanchez A. 2017. Chronic and low exposure to a pharmaceutical cocktail induces mitochondrial dysfunction in liver and hyperglycemia: Differential responses between lean and obese mice. *Environ. Toxicol.* 32:1375–1389.

64. Gómez-Canela C, Prats E, Piña B, Tauler R. 2017. Assessment of chlorpyrifos toxic effects in zebrafish (Danio rerio) metabolism. *Environ. Pollut.* 220, Part B:1231–1243.

65. Kotarsky H, Keller M, Davoudi M, Levéen P, Karikoski R, Enot DP, Fellman V. 2012. Metabolite Profiles Reveal Energy Failure and Impaired Beta-Oxidation in Liver of Mice with Complex III Deficiency Due to a BCS1L Mutation. *PLoS ONE*. 7.

66. Kulkarni AP. 2001. Lipoxygenase - a versatile biocatalyst for biotransformation of endobiotics and xenobiotics. *Cell. Mol. Life Sci. CMLS*. 58:1805–1825.

67. Niki E. 2008. Lipid peroxidation products as oxidative stress biomarkers. *BioFactors*. 34:171–180.

68. Yoshida Y, Umeno A, Shichiri M. 2013. Lipid peroxidation biomarkers for evaluating oxidative stress and assessing antioxidant capacity in vivo. *J. Clin. Biochem. Nutr.* 52:9–16.

69. Shearer GC, Newman JW. 2008. Lipoprotein Lipase releases esterified oxylipins from Very Low Density Lipoproteins. *Prostaglandins Leukot. Essent. Fatty Acids*. 79:215–222.

70. Beckmann N, Sharma D, Gulbins E, Becker KA, Edelmann B. 2014. Inhibition of acid sphingomyelinase by tricyclic antidepressants and analogons. *Front. Physiol.* 5.

71. Li H, Junk P, Huwiler A, Burkhardt C, Wallerath T, Pfeilschifter J, Förstermann U. 2002. Dual Effect of Ceramide on Human Endothelial Cells: Induction of Oxidative Stress and Transcriptional Upregulation of Endothelial Nitric Oxide Synthase. *Circulation*. 106:2250–2256.

72. Yang J, Wang H, Xu W, Hao D, Du L, Zhao X, Sun C. 2013. Metabolomic analysis of rat plasma following chronic low-dose exposure to dichlorvos. *Hum. Exp. Toxicol.* 32:196–205.

73. Hanada K. 2003. Serine palmitoyltransferase, a key enzyme of sphingolipid metabolism. *Biochim. Biophys. Acta BBA - Mol. Cell Biol. Lipids*. 1632:16–30.

74. Zhang J, Shen H, Xu W, Xia Y, Barr DB, Mu X, Wang X, Liu L, Huang Q, Tian M. 2014. Urinary Metabolomics Revealed Arsenic Internal Dose-Related Metabolic Alterations: A Proof-of-Concept Study in a Chinese Male Cohort. *Environ. Sci. Technol.* 48:12265–12274.

75. Zhou Xihong, He Liuqin, Wu Canrong, Zhang Yumei, Wu Xin, Yin Yulong. 2017. Serine alleviates oxidative stress via supporting glutathione synthesis and methionine cycle in mice. *Mol. Nutr. Food Res.* 61:1700262.

76. Eguchi A, Sakurai K, Watanabe M, Mori C. 2017. Exploration of potential biomarkers and related biological pathways for PCB exposure in maternal and cord serum: A pilot birth cohort study in Chiba, Japan. *Environ. Int.* 102:157–164.

77. Mennigen JA, Sassine J, Trudeau VL, Moon TW. 2010. Waterborne fluoxetine disrupts feeding and energy metabolism in the goldfish Carassius auratus. *Aquat. Toxicol.* 100:128–137.

78. Weckmann K, Labermaier C, Asara JM, Müller MB, Turck CW. 2014. Time-dependent metabolomic profiling of Ketamine drug action reveals hippocampal pathway alterations and biomarker candidates. *Transl. Psychiatry*. 4:e481.

79. Carlezon WA, Mague SD, Parow AM, Stoll AL, Cohen BM, Renshaw PF. 2005. Antidepressant-like effects of uridine and omega-3 fatty acids are potentiated by combined treatment in rats. *Biol. Psychiatry*. 57:343–350.

80. Renshaw PF, Parow AM, Hirashima F, Ke Y, Moore CM, Frederick B deB., Fava M, Hennen J, Cohen BM. 2001. Multinuclear Magnetic Resonance Spectroscopy Studies of Brain Purines in Major Depression. *Am. J. Psychiatry*. 158:2048–2055.

81. Levine J, Panchalingam K, Rapoport A, Gershon S, McClure RJ, Pettegrew JW. 2000. Increased cerebrospinal fluid glutamine levels in depressed patients. *Biol. Psychiatry*. 47:586–593.

82. McEwen BS. 2007. Physiology and neurobiology of stress and adaptation: central role of the brain. *Physiol. Rev.* 87:873–904.

83. Xu M-Y, Wang P, Sun Y-J, Wu Y-J. 2017. Metabolomic analysis for combined hepatotoxicity of chlorpyrifos and cadmium in rats. *Toxicology*. 384:50–58.

Chapter 7

Study of bioconcentration of oxybenzone in gilt-head bream and characterization of its by-products

Chemosphere 208 (2018) 399-407

7.1 Introduction

Pharmaceuticals and personal care products (PPCPs) have raised scientific and public concern since they may reach the aquatic ecosystems at detectable and potentially harmful concentrations [1,2]. UV filters are among the PPCPs which have focused much attention due to their wide range of applications in sunscreen products and daily use cosmetics, skin creams, body lotions and hair sprays and dyes [3,4], as well as food contact materials, including plastics and cartons, and textiles [5]. 28 UV light reflecting and scattering inorganic (TiO_2, ZnO) and UV light absorbing organic UV filters are listed in the EU Cosmetics Directive for commercial cosmetic products, giving good protection against UVB and even UVA radiation [6]. One of the most widely used organic UV filter is (2-hydroxy-4-methoxyphenyl)-phenylmethanone, commonly known as oxybenzone (OXY) or benzophenone-3 [3]. The environmental concern of OXY has increased due to its lipophilicity (log K_{ow}=3.6) and bioaccumulation capability, as well as its potential adverse effects, including slight estrogenic and both strong antiestrogenic and antiandrogenic *in vitro* effects [7–9], induction of vitellogenin and reduction of hatching rated in fish [10], and alterations in liver, kidney and reproductive organ in rodents [11].

Both direct (swimming and bathing) and indirect (mainly wastewater) inputs are responsible for the high levels of UV filters found in the aquatic ecosystems [3,4]. Wastewater inputs of UV filters to the environment are indicative of a lack of efficiency of the commonly used removal techniques in wastewater treatment plants [3,12]. OXY has been found in raw and treated wastewater [3,13–16] and in sewage sludge [17,18], but also in lake and river water [19–21], river sediments [17,22] and fish [3,19,23–25].

Although accumulation of UV filters in biota has been scarcely studied, current knowledge was reviewed by Gago-Ferrero and co-workers, and they reported that fish are important bioindicators in order to understand the possible adverse effects of lipophilic contaminants such as OXY [26]. Additionally, transformation and metabolization of UV filters is of great relevance since some of their by-products might be even more toxic than the parent compound [7,9,9,27–30]. Furthermore, the concentration of intermediates 2,4-dihydroxybenzophenone (DHB), 2,2'-dihydroxy-4-methoxybenzophenone (DHMB) and 2,3,4-trihydroxybenzophenone (THB) in rat

blood decreased much more slowly over time compared to the parent compound OXY, indicating that degradation products might have more significant adverse effects than OXY over the long term [31].

In this context, the aim of the present work was to study the uptake, distribution and metabolization of OXY in tissues (liver, gill, muscle) and biofluids (plasma, bile) of juvenile gilt-head bream (*Sparus aurata*) under controlled dosing experiments. Furthermore, by-products generated from OXY under different environmental conditions (in the presence and absence of fish in seawater) were annotated using a suspect screening strategy involving high-resolution mass spectrometry (HRMS) analysis of the different matrices.

7.2 Materials and methods

7.2.1 Standards and Reagents

OXY (98%) and oxybenzone-(phenyl-d_5) ([$^2H_5$]-OXY, 98%) were purchased from Sigma-Aldrich (St. Louis, MO, USA). Stock solutions of OXY and [$^2H_5$]-OXY were prepared at 5 g/L in methanol (MeOH, 99.9%, Fisher Scientific, Loughborough, UK), and diluted with MeOH to prepare standard solutions for calibration curve and spiking purposes. Stock dosing solution of OXY was prepared at 25 g/L in ethanol (EtOH, 99.9%, Scharlab, Barcelona, Spain) and diluted down to 0.83 mg/L in Milli-Q water. The final concentration of EtOH in the dosing solution was <0.005%. All stock solutions were stored at −20 °C prior to use.

MeOH (HPLC grade, 99.9%), ethyl acetate (EtOAc; 99.8%) and *n*-hexane (95%) were supplied by LabScan (Dublin, Ireland), formic acid (HCOOH, ≥ 98%) by Scharlab, and ethyl 3-aminobenzoate methanesulfonate (tricaine, >98%), ethylendiaminetetraacetic acid (EDTA, >99%) and ammonium hydroxide (NH_4OH, 25%) by Panreac (Barcelona, Spain). Ultra-pure water was obtained using a Milli-Q water purification system (< 0.05 µS/cm, Milli-Q model Integral 5, Millipore, Bedford, MA, USA).

Oasis HLB (200 mg, 6 mL) and Florisil (2 g, 12 mL) cartridges used for preconcentration and clean-up purposes were purchased from Waters Corporation (Milford, MA, USA) and Supelco (Walton-on-Tames, UK), respectively.

MeOH (Fisher Scientific) was used as mobile phase solvent and formic acid (HCOOH, Optima, Fischer Scientific, Geel, Belgium) for mobile phase modification. High purity nitrogen gas (>99.999%) supplied by Air Liquide (Madrid, Spain) was used for evaporation purposes in the XcelVap Automated Evaporation and Concentration System (Horizon Technology, Salem, New Hampshire, USA) and in the electrospray ionization and collision cell of the HRMS equipment.

7.2.2 By-product identification experiments

For uptake and by-product identification experiments, juvenile gilt-head bream, weighing ~ 40 g and measuring ~ 13 cm in length, were used. Fish were obtained from Groupe Aqualande (Roquefort, France) and shipped to the Research Centre for Experimental Marine Biology and Biotechnology of Plentzia (PiE-UPV/EHU), where the exposure experiments were performed. The laboratory was maintained at a constant temperature of 18 °C and a 14:10 h light:dark cycle. Fish were acclimatized for 3 months upon arrival and stabilized for an additional 1 week in the dosing tank before starting the exposure. The water was continuously aerated using aquarium oxygenators and fish were fed daily with 0.10 g pellets/fish. Water temperature (13 °C) and pH (7.4 ± 0.3) were constant during the exposure. Dissolved oxygen, nitrite, nitrate and ammonium content were periodically monitored.

A 14-day exposure experiment was designed both to study OXY uptake and to identify by-products of OXY. Four 1000 × 700 × 650 mm polypropylene tanks containing 250 L of seawater were used: two of them contained 100 fish each and the other two only seawater. One tank containing fish and one tank without fish were continuously fortified at 50 ng/mL (OXY nominal concentration), whereas the other two tanks were used as control (one with fish, one without fish).

OXY dosing was performed using a continuous flow-through system with a peristaltic pump delivering 10 L seawater/h and another pump infusing OXY dosing solution (0.83 mg/L) at 0.6 L/h to exposure tanks. OXY dosing solutions were refilled every 24 h with fresh solution. Control tanks were maintained at identical conditions over the duration of the experiment but only seawater was delivered.

7.2.3 Sample Collection

Fish handling described herein was evaluated by the Bioethics Committee of UPV/EHU and

approved by the Local Authority according to the current regulations (procedure approval CEEA/380/2014/ETXEBARRIA LOIZATE). For uptake and by-product identification purposes, 10 fish were collected from both control and exposed tanks on exposure days 0 (before exposure), 2, 4, 7 and 14. The fish were immediately anaesthetized in a tank holding 10 L of seawater and tricaine and $NaHCO_3$, both at 200 mg/L. After 5 min, fish were length measured, weighed and dissected to collect tissues (gill, liver, muscle) and biofluids (bile, plasma). Blood was taken from the caudal vein-artery using a syringe (previously homogenized with 0.5 mol/L EDTA solution at pH 8.0) and centrifuged for 7 min at 1000 rpm to get the plasma. Biofluids and fish tissues were snap-frozen and kept in liquid nitrogen during dissection and stored at -80 °C freezer prior to analysis.

At the time that fish were removed from the tanks, 2 L of water samples were collected to determine the concentration of OXY and to identify OXY by-products in water. In the same sampling days, 2 L of water aliquots were also collected from the tanks without fish for by-product identification in the absence of fish. Water samples were extracted and analyzed within 24 h to avoid any other kind of degradation.

7.2.4 Sample Handling

Fish tissues (gill, liver, muscle) were freeze-dried for 48 h using a Cryodos-50 laboratory freeze-dryer (Telstar Instruments, Sant Cugat del Valles, Barcelona, Spain). A homogenized pool was prepared for each tissue/biofluid using the 10 fish collected at each sampling day (days 0, 2, 4, 7, and 14). For tissue extraction, based on the research group experience, focused ultrasound solid-liquid extraction (FUSLE) was applied [32] and solid-phase extraction (SPE) clean-up was adapted from literature [33]. Biofluid and seawater extraction and LC-HRMS analysis were adapted from our previous work [34]. The analyses were carried out in triplicate.

Briefly, freeze-dried liver (0.5 g), muscle (0.5 g) or gill (0.1 g) samples were spiked with the isotopically labeled internal standard (20 µL of a 10-mg/L solution of $[^2H_5]$-OXY) and then extracted with 7 mL of EtOAc. FUSLE was performed at 0 °C for 2 min (with a pulsed on/off time of 0.8/0.2 s) and 20% power using a Bandelin Sonopuls HD 3100 sonifier (Bandelin Electronic, Berlin, Germany). The supernatant was filtered through a 0.45-µm polypropylene (PP) filter (Phenomenex; California, USA), evaporated to dryness under a nitrogen stream and then reconstituted in 1 mL of *n*-hexane

in preparation for SPE cleanup using 2-g Florisil cartridges, which were preconditioned with 5 mL of *n*-hexane. After loading the sample, analytes were recovered from the cartridge using 10 mL of EtOAc.

On the other hand, the SPE cleanup/preconcentration of aqueous samples (plasma, bile and seawater) was carried out using 200-mg Oasis-HLB cartridges, previously preconditioned with 5 mL of MeOH, 5 mL of Milli-Q water and 5 mL of Milli-Q water containing 2% HCOOH (pH 2). Plasma, bile (100 and 250 µL, respectively, each diluted with 3 mL of Milli-Q water containing 2% HCOOH) and seawater (200 mL, with 2% of HCOOH) samples were fortified with [$^2H_5$]-OXY (20 µL of a 10-mg/L solution) prior to SPE. After loading the sample, the cartridge was rinsed with 5 mL of Milli-Q water and dried for 30 min under vacuum. The compounds were subsequently eluted with 10 mL of MeOH (for plasma and seawater) or EtOAc (for bile).

In all the cases, the eluents were concentrated to dryness under a stream of nitrogen in a water bath at 35 °C, reconstituted in 200 µL of MeOH:Milli-Q water (90:10, v/v), filtered through 0.22-µm PP filters (Phenomenex; Torrance, California, USA) and stored at -20 °C until analysis. Additionally, procedural blanks were analyzed to discard chromatographic peaks associated to contamination during the identification of by-products.

7.2.5 Instrumental Analysis

OXY quantification and by-product identification were performed using a Thermo Scientific Dionex UltiMate 3000 UHPLC coupled to a Thermo Scientific Q Exactive quadrupole-Orbitrap mass spectrometer equipped with a heated ESI source (HESI, Thermo, CA, USA). 5-µL extracts were injected on a Kinetex biphenyl 100 Å core-shell (2.1 mm × 100 mm, 2.6 µm) column with a Kinetex biphenyl 100 Å core-shell pre-column (2.1 mm × 5 mm, 2.6 µm) from Phenomenex, which was kept at 30 °C during the analysis. Milli-Q water:MeOH (95:5, v/v) mixture was used as mobile phase A and Milli-Q water:MeOH (5:95, v/v) mixture as mobile phase B, both containing 0.1% HCOOH. The mobile phase flow rate was set at 0.3 mL/min and the eluent gradient profile was as follows: 5% of B (hold 0.5 min), linear change to 70% B up to 10 min, and another linear change to 95% B up to 20 min (hold 3 min) and a final linear change to 5% B up to 28 min (hold 2 min) to regain initial conditions.

The Orbitrap was operated in positive ionization mode in full scan – data dependent MS2 (Full MS-ddMS2) acquisition mode. One full scan at a resolution of 70,000 full width at half maximum (FWHM) at *m/z* 200 over a scan range of *m/z* 100-700 was followed by three ddMS2 scans at a resolution of 17,500 FWHM at *m/z* 200, with an isolation window of 0.8 Da. The stepped normalized collision energy (NCE) in the higher-energy collisional dissociation (HCD) cell was set to 20, 55 and 95 eV. The ddMS2 scans were acquired on discovery mode, choosing the most intense ions from the full scan for fragmentation, with an intensity threshold of $8.0x10^3$ and a dynamic exclusion of 10 s. The HESI source parameters were set to 3.2 kV spray voltage, 300 °C capillary temperature, 35 arbitrary units (au) sheath gas (nitrogen), 10 au auxiliary gas and 280 °C auxiliary gas heater. External calibration of the instrument was conducted immediately prior to analysis using Pierce LTQ ESI Calibration Solutions (Thermo Scientific, Waltham, Massachusetts, United States). The instrument was controlled by Xcalibur 4.0 software (Thermo).

7.2.6 Data Handling

Condition factor (K) and hepatic somatic index (HSI) were determined as a general assessment of fish health. K was calculated using the equation $K = (\text{fish weight} \times 100)/(\text{fish length})^3$) [35], while HSI was determined using the equation HSI = (liver weight × 100)/(fish weight)). K and HSI were statistically evaluated between exposed and control groups using one-way ANOVA.

OXY was quantified using a 12-point external calibration curve in 2.5 - 25,000 ng/mL range whereas by-products were identified using Compound Discoverer 2.1 (Thermo). Peak picking and peak alignment were performed with retention time deviation of 0.5 min and mass tolerances of 5 ppm. In the case of metabolites the software considered Phase I and Phase II reactions to predict OXY-derived metabolites (a list of reactions can be found in Appendix I). The *m/z* values of the predicted compounds were searched for in the peak list considering the criteria of 5 ppm for mass tolerance and 30% for the intensity tolerance for the isotope search. The peaks that fulfilled both criteria were manually checked and only those with available MS2 spectra, a maximum signal higher than 10^5 and absent in both control samples and procedural blanks were further considered. Structural assignments were carried out based on ddMS2 fragments annotated by Compound Discoverer 2.1 software.

7.3 Results and discussion

7.3.1 Quality control of the methods

Since the methods applied to determine OXY in gilt-head bream tissues/biofluids were adapted from the literature (see Section 7.2.4), their validation was performed in order to assure their quality control. To validate all the methods, the recoveries were calculated by spiking non-polluted samples at 100 ng/L, 100 ng/mL and 100 ng/g concentrations (adding 20 µL of the corresponding solution at the beginning of the extraction procedure) in seawater, biofluids (bile and plasma) and tissues (liver, muscle and gill), respectively. Table 7.1 shows the significant figures of merit of the methods, being all of them accurate and precise to determine OXY in fish tissues/biofluids.

Table 7.1: *Recoveries for seawater and fish tissue/biofluids after correction with [$^2H_5$]-OXY, relative standard deviations (RSDs), instrumental limit of detection (LOD) and method detection limits (MDLs).*

Matrix	Recovery (%)	RSD % (n=3)	LOD (ng/mL)	MDL
Seawater	100%	1%	0.2	0.00014 ng/mL
Bile	97%	3%		0.32 ng/mL
Plasma	97%	13%		0.12 ng/mL
Liver	97%	7%		0.025 ng/g
Muscle	101%	8%		0.022 ng/g
Gill	102%	4%		0.25 ng/g

7.3.2 OXY accumulation in fish

Even though a continuous-flow dosing was used to keep OXY nominal concentration fixed at 50 ng/mL throughout the experiment, lower experimental free OXY concentration was determined in seawater in the presence of fish (see Table 7.2). The fish uptake together with sorption of OXY to either fish skin or feces seemed to diminish the free concentration of OXY in seawater during the first days of the experiment. In fact, the free concentration of OXY increased with exposure time (from 2.3 ng/mL at day 2, to 22 ng/mL at day 14) when less number of fish were present in the tank (from 80 fish at day 2, to 20 fish at day 14). The concentration of OXY in samples collected before starting the exposure (day 0) and in control samples was bellow method detection limit (see Table 7.1).

No significant changes in fish weight and length were observed at the 95% confidence level, regardless of experiment tank or exposure day (p-value > 0.05). There was no mortality and K and HSI were comparable between fish of exposed and control groups (p-value > 0.05) all the exposure days.

Table 7.2: *OXY concentrations in seawater and fish tissue/biofluids during exposure (n=3, 95% of confidence level).*

Exposure day	Seawater without fish (ng/mL)	Seawater with fish (ng/mL)	Bile (ng/mL)	Plasma (ng/mL)	Liver (ng/g)	Muscle (ng/g)	Gill (ng/g)
Day 2	45 ± 3	2.3 ± 0.2	4000 ± 2000	6 ± 1	9 ± 2	9 ± 2	2.4 ± 0.5
Day 4	52 ± 2	2.7 ± 0.2	1800 ± 100	7 ± 1	160 ± 30	500 ± 100	120 ± 20
Day 7	49 ± 4	4.1 ± 0.1	4000 ± 1000	16 ± 2	80 ± 20	430 ± 90	100 ± 20
Day 14	54 ± 3	22 ± 1	17000 ± 2000	129 ± 5	140 ± 30	600 ± 117	150 ± 30

Regarding tissue/biofluid distribution, OXY was detected in all the analyzed samples, with the highest concentrations at the end of the exposure period (see Table 7.2). These results were not surprising because, with the same water renovation and continuous OXY addition, and less fish in the tank, a higher free concentration of OXY in seawater was available per fish. Bile concentrations (in the 1,800 to 17,000 ng/mL range) were significantly higher in comparison to the concentrations found in the rest of tissues/fluids. Since OXY is a hydrophobic and non-ionizable compound, the lowest concentrations of OXY found in plasma (in the 6 to 129 ng/mL range) could be explained with the aqueous nature of this biofluid that can cause immediate distribution of the pollutant to other less polar compartments. Although liver (highly lipidic tissue) could be an appropriate reservoir of OXY, the low concentration (in the 9 to 160 ng/g range) of non-metabolized OXY found (see section 7.3.2) could indicate a high metabolization/elimination activity in this tissue. On the contrary, the lack of degradation activity in muscle (less lipidic tissue) can explain the second highest concentrations of non-metabolized OXY detected (in the 9 to 600 ng/g range), reaching the equilibrium state in the 4th exposure day. The number of studies addressing the differential tissue accumulation trend of UV filters is quite limited. In a recently published work, OXY was found in liver and muscle tissues of mullets sampled in Brazil at ng/g levels [24]. The presence of non-metabolized OXY was detected in gill throughout the experiment, reaching the maximum concentration (150 ng/g) at 14th day, suggesting that at least part of the uptake occurred

through the gills. Molins-Delgado and coworkers also reported the uptake of OXY through the gills due to the fact of being one of the most exposed parts of the fish in continuous contact with the aquatic environment, acting as one of the main entrances for xenobiotic compounds and outlet of organism wastes [24]. However, other routes of uptake such as dermal absorption should be also studied.

7.3.3 OXY by-product identification

OXY by-product structures were annotated in water (in the presence and absence of fish) and biofluids (bile and plasma) and tissues (liver and muscle) of gilt-head bream. No by-product was detected in gill. Probable or tentative structures were given for the by-products, in a 2b-3 confidence level according to Schymanski and co-workers [36] and with a difference between measured and theoretical masses lower than 3.4 ppm. A total of 20 Phase I and Phase II metabolites were detected and, to the best of our knowledge, 12 were reported for the first time. While Figure 7.1 shows the MS/MS spectra of OXY, Figure 7.2 suggests its possible degradation pathway and Table 7.3 includes the molecular formula, the theoretical *m/z* for the pseudomolecular ion, the mass error (in ppm) and the retention time (in min) of OXY and each by-product.

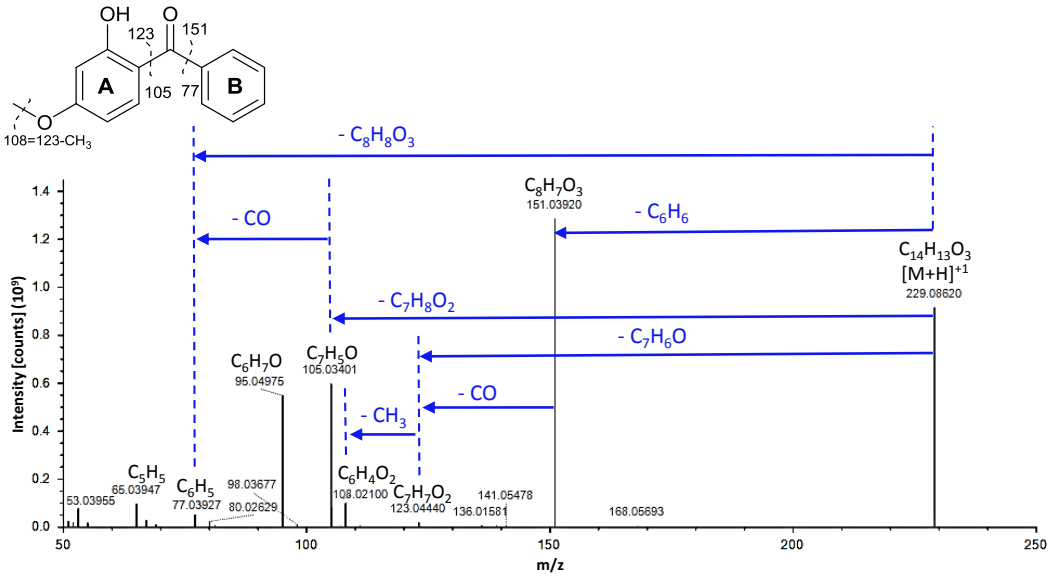

Figure 7.1: *MS/MS spectra of oxybenzone (OXY).*

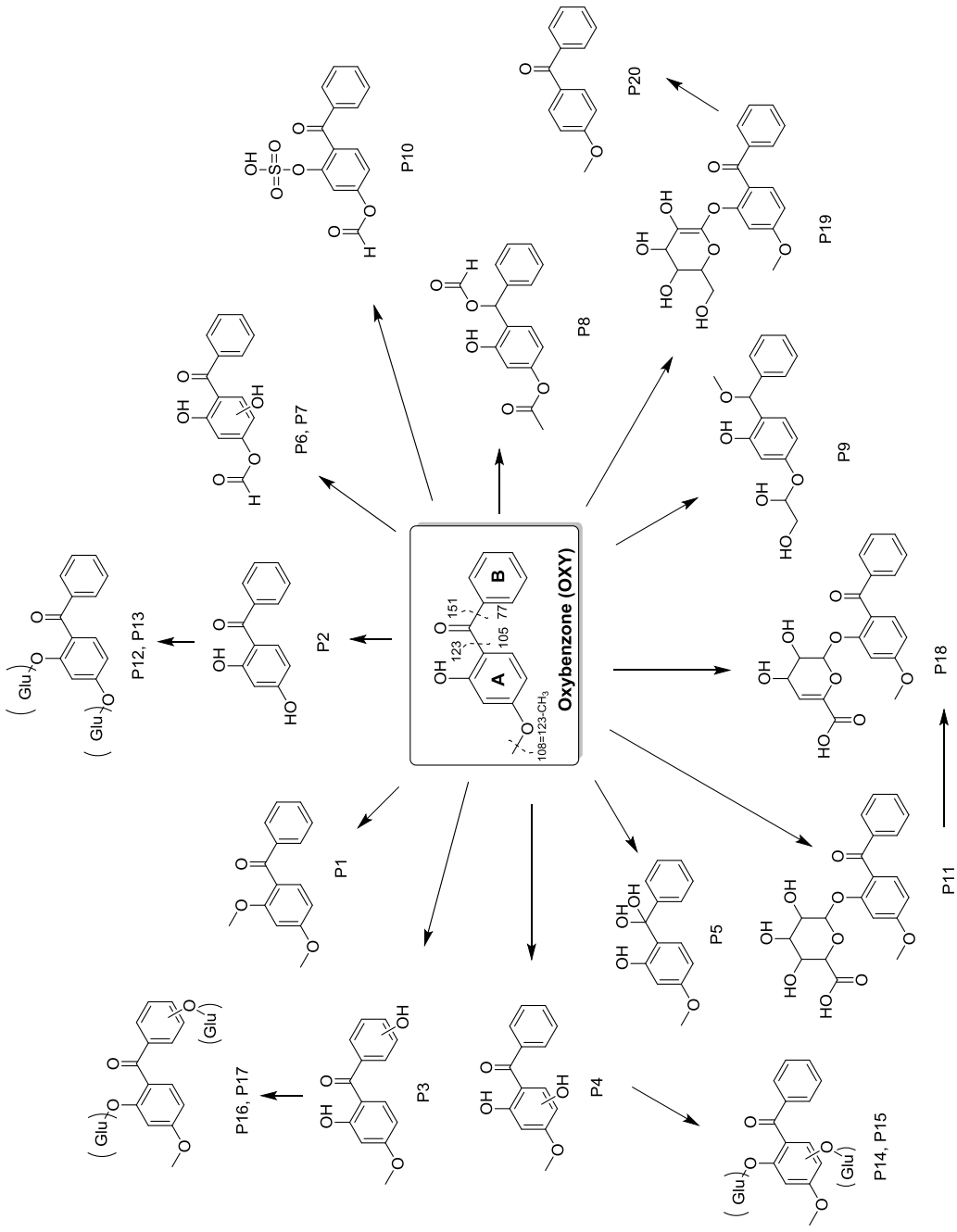

Figure 7.2: *Degradation pathway of OXY. Inset shows MS/MS fragmentation and major m/z ions for OXY.*

Table 7.3: *Molecular formula, theoretical m/z of [M+H]+ and the corresponding ΔMass (ppm) for each matrix, the most abundant fragments in the MS/MS spectra and the retention time for OXY and all annotated by-products (P). When the by-products had already been described, the bibliographic citation has been included.*

Code	Formula (M)	Theoretical m/z $[M+H]^+$	MS/MS fragments	ΔMass (ppm)							Rt (min)	Ref.
				Water*	Water**	Bile	Liver	Plasma	Muscle	Gill		
OXY	$C_{14}H_{12}O_3$	229.0859	151.0392, 105.0340, 95.0497, 108.0211, 65.0395, 53.0396, 105.0444, 77.0393, 67.0551, 123.0443	-0.67	1.13	1.66	1.66	1.79	1.73	2.06	13.63	[12,37–44]
P1	$C_{15}H_{14}O_3$	243.1016	165.0549, 105.0340, 95.04970, 122.03660, 53.03960, 107.0131, 132.0892, 92.0263, 131.0857, 77.0393	-1.03	1.04	-	0.72	-	0.79	-	12.74	[37]
P2	$C_{13}H_{10}O_3$	215.0703	137.0235, 81.0342, 105.0340, 95.0498, 53.0396, 68.9980, 57.0707, 77.0393, 142.0041, 109.0288	-1.05	-0.41	1.22	0.80	-	-	-	11.08	[12,38–43]
P3	$C_{14}H_{12}O_4$	245.0808	151.0390, 95.0496, 121.0287, 65.0394, 111.0443, 108.0208, 67.0550, 55.0551, 83.0862, 80.0263	-	1.04	1.35	-	-	-	-	11.63	[12,38–43]
P4	$C_{14}H_{12}O_4$	245.0808	105.0339, 95.0497, 167.0340, 53.0396, 96.0211, 111.0444, 77.0392, 51.0239, 141.0699, 128.0624	-	-	0.85	-	-	-	-	10.96	[38,44]
P5	$C_{14}H_{14}O_4$	247.0965	91.0548, 229.0857, 219.1013, 95.0496, 191.0702, 79.0549, 105.0701, 115.0545, 163.0753, 123.0440	-	0.63	-	-	-	-	-	13.16	In this work
P6	$C_{14}H_{10}O_5$	259.0601	199.0241, 153.0185, 69.0344, 125.0237, 171.0293, 129.0338, 244.0375, 115.0545, 105.0339, 213.0549	-15.00	-	-	-	-	-	-	8.69	[38]

**Seawater in the absence of fish. **Seawater in the presence of fish.*

Table 7.3: *(Continuation).*

Code	Formula (M)	Theoretical m/z $[M+H]^+$	MS/MS fragments	ΔMass (ppm)							Rt (min)	Ref.
				Water*	Water**	Bile	Liver	Plasma	Muscle	Gill		
P7	$C_{14}H_{10}O_5$	259.0601	199.0237, 153.0185, 125.0234, 181.0131, 68.9980, 92.9977, 244.0369, 171.0290, 115.0544, 97.0288	-1.02	-	-	-	-	-	-	6.75	[38]
P8	$C_{16}H_{12}O_5$	285.0758	270.0523, 118.0416, 242.0574, 168.0574, 197.0598, 141.0701, 115.0546, 225.0544, 169.0644, 214.0624	-	-	0.77	-	-	-	-	9.88	In this work
P9	$C_{16}H_{18}O_5$	291.1227	91.0548, 259.0964, 263.1275, 128.0621, 115.0546, 231.1015, 67.0551, 107.0495, 121.0651, 273.1124	-	-	0.59	-	-	-	-	13.83	In this work
P10	$C_{14}H_{10}O_7S$	323.0220	149.0234, 65.0395, 183.0503, 279.0313, 309.0817, 121.0287, 177.0547, 291.0712, 105.0338, 295.0264	1.03	2.16	-	-	-	-	-	11.21	In this work
P11	$C_{20}H_{20}O_9$	405.1180	229.0859, 151.0390, 105.0339, 95.0497, 85.0290, 65.0395, 53.0395, 108.0209, 73.0291, 77.0393	-	0.82	1.20	0.75	0.07	-	-	10.46	[23]
P12	$C_{19}H_{18}O_9$	391.1024	137.0234, 215.0702, 81.0342, 105.0339, 95.0497, 149.0235, 53.0395, 65.0394, 109.0287, 77.0393	-	0.16	1.18	-	0.63	-	-	9.86	In this work
P13	$C_{19}H_{18}O_9$	391.1024	137.0234, 215.0701, 149.0234, 81.0341, 105.0339, 95.0496, 65.0394, 71.0864, 53.0395, 167.0343	-	2.19	0.71	-	-	-	-	7.56	In this work

**Seawater in the absence of fish. **Seawater in the presence of fish.*

Table 7.3: *(Continuation).*

Code	Formula (M)	Theoretical m/z $[M+H]^+$	MS/MS fragments	ΔMass (ppm)							Rt (min)	Ref.
				Water*	Water**	Bile	Liver	Plasma	Muscle	Gill		
P14	$C_{20}H_{20}O_{10}$	421.1129	245.0789, 105.0340, 95.0496, 167.0344, 171.0055, 85.0289, 263.0888, 53.0396, 96.0210, 73.0292	-	-	3.35	-	-	-	-	9.74	In this work
P15	$C_{20}H_{20}O_{10}$	421.1129	245.0803, 105.0339, 305.1584, 95.0495, 363.1620, 167.0341, 91.5532, 207.6800, 69.4123, 56.9657	-	-	0.16	-	-	-	-	7.71	In this work
P16	$C_{20}H_{20}O_{10}$	421.1129	229.0859, 151.0390, 95.0497, 105.0339, 55.0188, 91.0547, 65.0394, 67.0551, 245.0807, 53.0395	-	1.54	2.27	-	-	-	-	10.42	In this work
P17	$C_{20}H_{20}O_{10}$	421.1129	245.0808, 151.0391, 121.0287, 95.0497, 65.0395, 111.0444, 85.0291, 108.0208, 73.0290, 67.0550	-	-	0.53	-	-	-	-	9.13	In this work
P18	$C_{20}H_{18}O_8$	387.1075	85.0291, 229.0859, 105.0339, 151.0391, 95.0497, 71.0136, 115.0546, 57.0344, 369.0961, 325.1061	-	0.85	2.03	-	-	-	-	10.45	In this work
P19	$C_{20}H_{20}O_8$	389.1231	213.0910, 152.0621, 153.0699, 141.0701, 91.0548, 115.0547, 181.0649, 169.0650, 95.0497, 165.0696	-	0.75	0.59	-	1.38	-	-	9.15	In this work
P20	$C_{14}H_{12}O_2$	213.0910	153.0700, 152.0622, 141.0699, 170.0727, 169.0649, 181.0649, 115.0544, 198.0676, 165.0701, 95.0497	-	-	0.51	-	-	-	-	11.39	[45]

**Seawater in the absence of fish. **Seawater in the presence of fish.*

O-methylation and *O*-demethylation reactions were observed in P1 and P2, respectively. While the presence of *m/z* 165 (151+14) and *m/z* 122 (108+14) pinpointed the addition of a methyl group in ring A in P1, the presence of *m/z* 137 (151-14) and *m/z* 109 (123-14) pinpointed *O*-demethylation in ring A of P2. In both cases, the presence of the fragment *m/z* 105 suggested that ring B was unmodified. P1 was previously described by Vione et al. [37] and P2, also known as DHB, has been widely described in literature [12,38–43]. P1 and P2 were detected in water (both in the presence and in absence of fish) and in fish liver; P1 was also detected in muscle and P2 in bile.

P3 and P4, with the precursor *m/z* 245.08084, corresponded to the monohydroxylation of OXY. In the case of P3, the presence of fragments *m/z* 151 indicated that the hydroxyl group had been introduced in ring B. This was confirmed by the absence of *m/z* 105 and the presence of *m/z* 121 (105+16), with one more oxygen atom. This hydroxylated by-product, commonly known as DHMB, has been reported as one of the main by-products of OXY in the literature [12,38–43]. On the other hand, the absence of the fragment *m/z* 151 and the presence of fragments *m/z* 167 (151+16) and *m/z* 105 in P4 suggested that the hydroxyl group had been added in ring A, as previously reported [38,44]. While both P3 and P4 were detected in bile, only P3 was observed in water in the presence of fish.

P5, corresponding to the hydration of OXY, was only observed in water in the presence of fish. Since a water loss was observed (*m/z* 229=247-18), the formation of gem-diol (see Figure 7.2), which is in equilibrium with OXY in aqueous environment, is the most probable transformation to add a hydroxyl group. Moreover, after dehydration during fragmentation, a fragmentation pattern similar to OXY was observed (*m/z* 229, *m/z* 123 and *m/z* 105).

In the case of regioisomers P6 and P7 (precursor ion *m/z* 259.06010) detected in water in the absence of fish, similar fragments (*m/z* 105, *m/z* 153 and *m/z* 181) to those observed by Gago-Ferrero et al. [38] were detected (see the MS/MS spectra for P6 in Figure 7.3). The *m/z* 105 suggested that ring B had not been modified, while fragment *m/z* 181 ($C_8H_5O_5$), with two oxygen atoms more and two hydrogen atoms less than the common OXY fragment *m/z* 151, pinpointed that a hydroxyl group and a keto group have been included in ring A (*m/z* 181=151+O_2–H_2). In addition, the fragment *m/z* 153 ($C_7H_5O_4$) indicated a CO loss (153=181-CO), a common fragment found in molecules containing aldehyde and ester groups; hence, a modification in the methoxy

group was suggested. This structure also explained the presence of fragments *m/z* 125 ($C_6H_5O_3$) and *m/z* 213 ($C_{13}H_9O_3$).

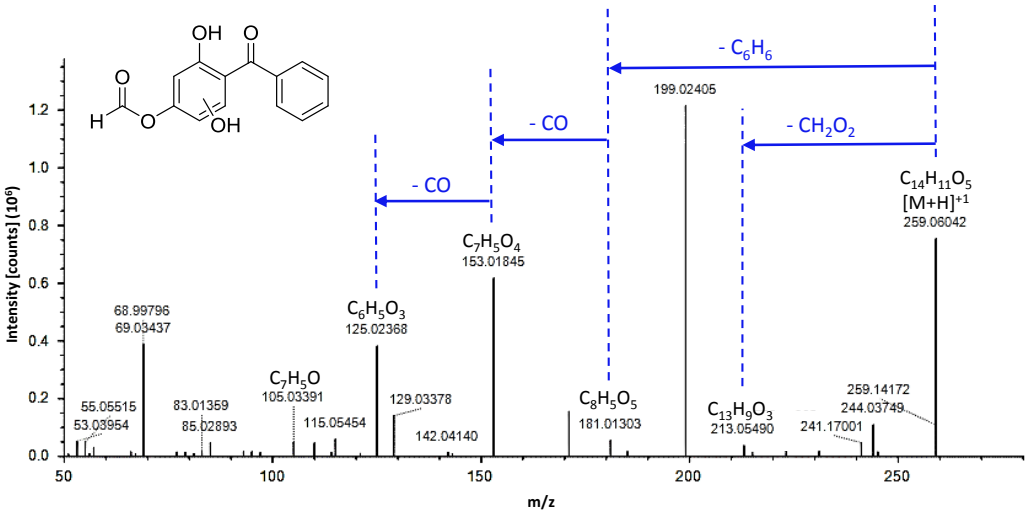

Figure 7.3: *MS/MS of by-product P6.*

P8 (see MS/MS spectra in Figure 7.4) and P9, only detected in fish bile, presented modifications in the keto and methoxy group of OXY. Compared to OXY, P8 showed a +C_2O_2 composition change and, since no hydrogen was introduced, the addition of two keto groups was suggested, being the methoxy group in ring A and the central keto group the most plausible positions to include the two new keto groups. The structure proposed in Figure 7.2 explained the demethylation (*m/z* 270= 285-CH_3), and the CO (*m/z* 242=270-CO) and CO_2H losses (*m/z* 225=270-CO_2H) after the loss of the methyl group. This tentative structure, also explained fragment *m/z* 214, which is the equivalent to P2 after the losses of CO from central ester and C_2OH_3 from ring A. In the fragmentation of P9, a water loss was observed (*m/z* 273=291-H_2O) followed by demethylation (*m/z* 259=273-CH_2) and carbonyl group loss (*m/z* 231=259-CO). Although the fragmentation pattern was complex, the MS/MS spectra could be explained after the addition of a CH_2O_2 group to the methoxy group side, as shown in Figure 7.2. Furthermore, in order to justify the total composition change of +$C_2H_6O_2$, Compound Discoverer 2.1 also proposed the reduction and methylation of OXY. The central keto group was the most probable position to include two hydrogen atoms in the structure without losing the stability of the molecule. This modification of OXY matched with the presence of the fragment *m/z* 107 (105+H_2). Lastly, since fragment *m/z* 121

(107+CH_2) was observed, the methyl group should be attached to the central oxygen.

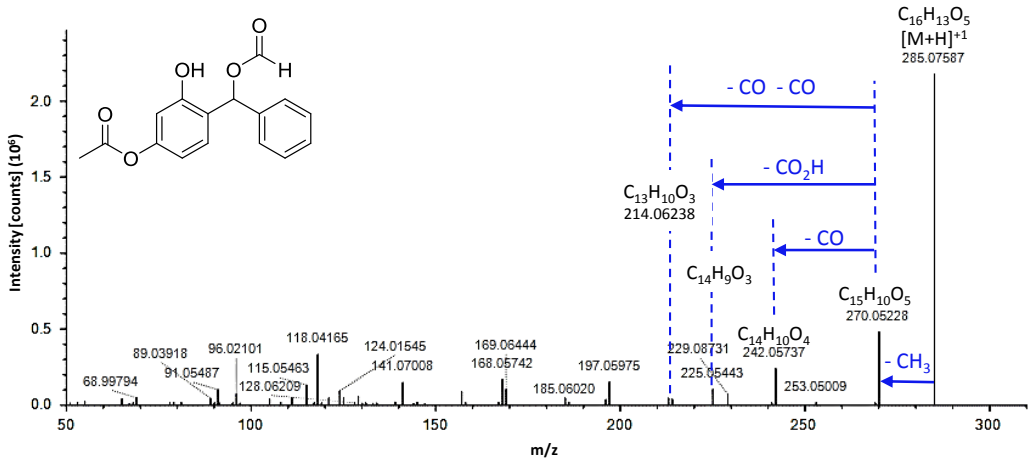

Figure 7.4: *MS/MS of by-product P8.*

In the case of P10 (see MS/MS spectra in Figure 7.5), detected in water in the presence and in absence of fish, a CO_2 (*m/z* 279=323-CO_2) and a CO (*m/z* 295=323-CO) loss from the precursor ion were observed, suggesting the oxidation to an ester of the methoxy group, similar to P6 and P7. The most abundant fragment *m/z* 149 ($C_8H_5O_3$) was the equivalent to *m/z* 151 of OXY, after the loss of sulfonate group due to the fact that the hydroxyl group at ring A became a better leaving group when sulfonating.

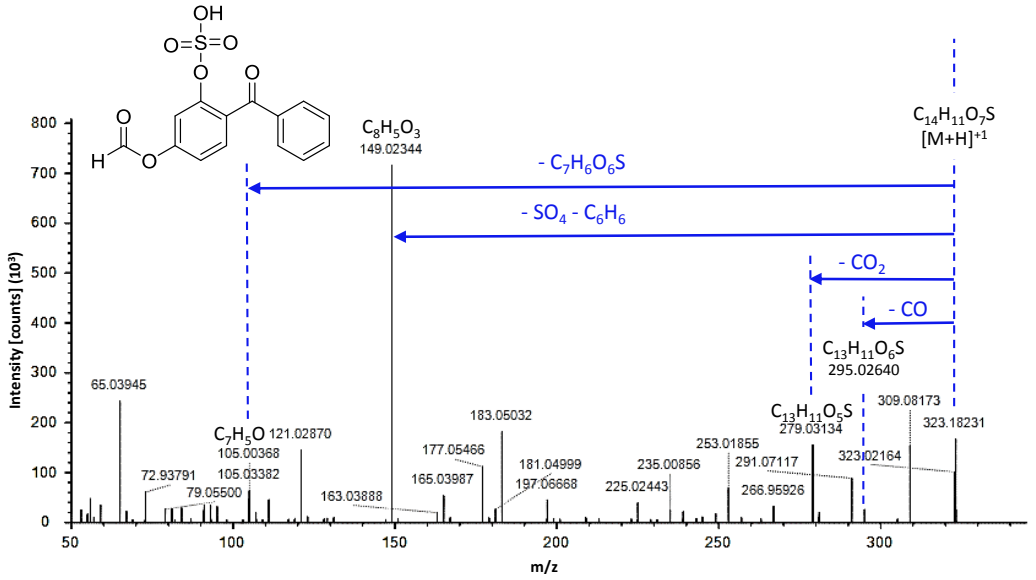

Figure 7.5: *MS/MS of by-product P10.*

P11-P17 corresponded to glucuronide derivates of OXY. P11 (*m/z* 405.11801), detected in bile, liver, plasma and water in the presence of fish, was attributed to the glucuronidation of OXY based on the similar fragmentation observed (*m/z* 229, 151, 108, 105, 95 and 77) after the glucuronide group loss (-176). Oxybenzone glucuronide was also detected in the bile of trout exposed to wastewater treatment effluent [23]. Similarly, P12 and P13 were identified as monoglucuronides of P2, since a similar fragmentation pattern to P2 (*m/z* 137 and *m/z* 105) was observed after the loss of the glucuronide group. With the information available, it was not possible to identify which of the two hydroxyl groups of P2 had suffered glucuronidation in each of the by-products. P12 and P13 were both detected in bile and water (in the presence of fish) and P12 was also detected in plasma. In addition, P14 and P15 were monoglucuronides of P4 and were only detected in bile. Finally, P16 and P17 corresponded to the monoglucuronides of P3 and were observed in bile. P16 was also detected in water in the presence of fish.

P18 and P19 also corresponded to Phase II derivates of OXY. Compared to P11, P18 (*m/z* 387.10745 and detected in bile and water in the presence of fish) had a composition change of $-H_2O$ less in its chemical structure, and instead of a direct loss of the dehydrated glucuronide group, a previous water loss was observed (*m/z* 369=387-H_2O, see MS/MS spectra of P18 in Figure 7.6). Therefore, dehydrated glucuronide conjugation, which was previously reported for other xenobiotics [46,47], was suggested. Additionally, if the dehydration in the glucuronide group was placed in the carbon adjacent to the carboxylic group, the presence of a CO_2 loss could also be explained (*m/z* 325=369-CO_2). However, it is not possible to specify if P18 is formed by conjugation with a dehydrated glucuronide group or by the elimination of a water molecule from P11 even if the cleavage of the ether-linked glucuronide bond is thermodynamically more favorable. For P19 (observed in bile, plasma and water in the presence of fish), with two hydrogen atoms more than P18, glucoside conjugation plus desaturation was suggested by the Compound Discoverer software. In addition to glucuronide conjugation, glucoside conjugation is also reported in the literature for other xenobiotics [46,48]. Hence, in order to explain the molecular formula of P19, the conjugation of the enol equilibrium product of glucono delta-lactone was the tentative approach to form the unsaturated glucoside of OXY. This structure explained the loss of the glucoside moiety (*m/z* 213=389-176) and the most abundant fragment *m/z* 213, equivalent to OXY with one oxygen atom less. Similarly to P10, the presence of the unsaturation of the enol group

conjugated to the oxygen atom linked to ring A made the hydroxyl group at ring A a better leaving group.

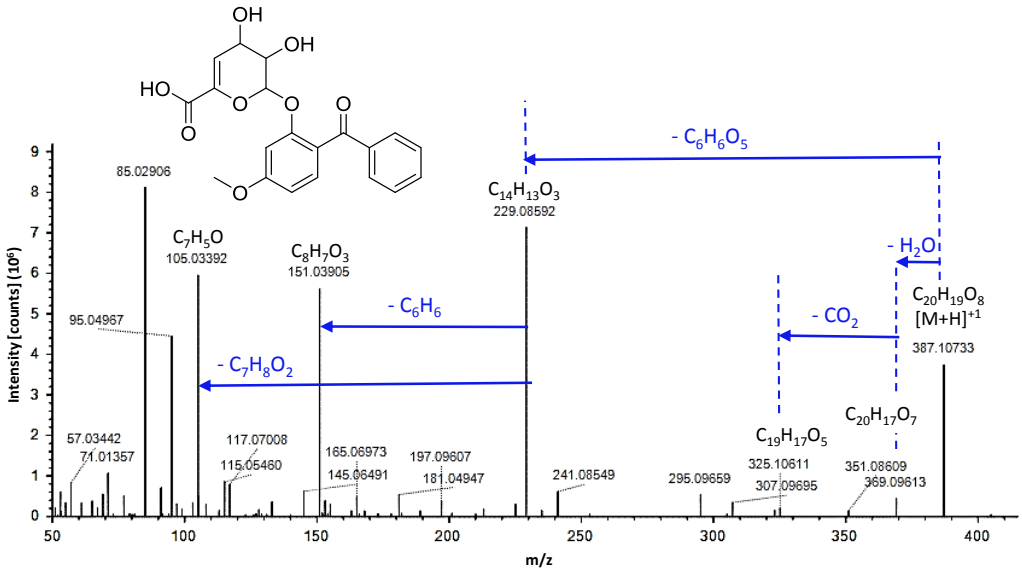

Figure 7.6: *MS/MS of by-product P18.*

Finally, P20 (only detected in bile) contained one oxygen atom less than OXY. P20 was proposed to be formed from P19 (see Figure 7.2), since the presence of a good leaving group is necessary in order to lose the hydroxyl group from the aromatic ring A. This by-product was previously described in the literature [45].

Although in the present work 12 by-products were reported for the first time, we did not detect THB which was described in other works as a common degradation product of OXY together with DHB and DHMB [12,40,41]. Additionally, the fact of identifying 5 by-products in seawater without fish and 11 by-products in seawater in the presence of fish, with only 3 of them in common, clearly indicates that the degradation of OXY is dependent on environmental conditions. It should also be highlighted that bile was the most interesting matrix to identify OXY by-products, with 15 out of the totally annotated 20 by-products, compared to gill (no by-product), muscle (1 by-product), liver (3 by-products) and plasma (3 by-products). According to Molins-Delgado et al. [24] liver can act as detoxifying organ in organisms, and the results in this study confirm that OXY and their by-products are excreted through bile.

7.3.4 Relative abundances of OXY by-products

Equivalent chromatographic signal response factors were assumed for all the by-products in order to discuss their relative abundances in the different matrices studied. Since standards for all the by-products were not available, these results should be considered qualitative. All peak areas were corrected using internal standard ($[^2H_5]$-OXY).

Figure 7.7a and Figure 7.7b show the relative percentage of the annotated by-products in seawater in the absence and in the presence of fish, respectively. While OXY was the compound at the highest percentage in the absence of fish (~ 99%), with P1 (*O*-methylation of OXY at 0.5%), P2 (*O*-demethylation of OXY, also known as DHB, at 0.2%) and P6 (at 0.2%) as the major transformation products, the abundance of OXY decreased to 59-84% range in the presence of fish. Actually, as observed for the free concentration of OXY in seawater (see section 7.3.1), while relative abundance of OXY was constant during the exposure period in the absence of fish, an increase in OXY relative abundance was observed along the experiment when the number of fish was reduced in the tank. In the presence of fish, OXY glucuronide P11 emerged as the most abundant metabolite (13-38%) among all annotated by-products, followed by other glucuronides, including P12-13, P16 and P18-19, but in a much lower abundance.

In the case of fluids and tissues, as can be observed in Figure 7.7c, no metabolite was detected in gill, and OXY accounted almost 100% in muscle and around 95% in the case of liver. For the latter, P11 was again the major metabolite, accounting for up to 6%. In the case of plasma, OXY relative abundance was reduced to approx. 60%, and P11 (35%), P12 (4%) and P19 (2%) glucuronides were the most abundant metabolites. Finally, the highest abundances of metabolites were observed in bile, where OXY was found in the 36-68% range. P11 glucuronide was once more the major metabolite (20-47%), followed by P2 (5%), P3 (2%) and P18 (1%).

To sum up, since the dosing of OXY was carried out in a continuous flow, even though its degradation occurred, OXY still was the main compound detected regardless of the matrix and time. OXY is not fully metabolized and excreted, but it is distributed among the different tissues, as the presence of OXY and its metabolites across all the studied tissues suggests. It is noteworthy that the relative abundance of OXY monoglucuronide (P11) was significantly high in aqueous

matrices (plasma, bile and seawater in the presence of fish) in comparison to the rest of the annotated by-products. The fact of being a Phase II metabolite the most abundant by-product and observing high OXY levels in bile confirm the capacity of fish to eliminate the pollutant and its by-products.

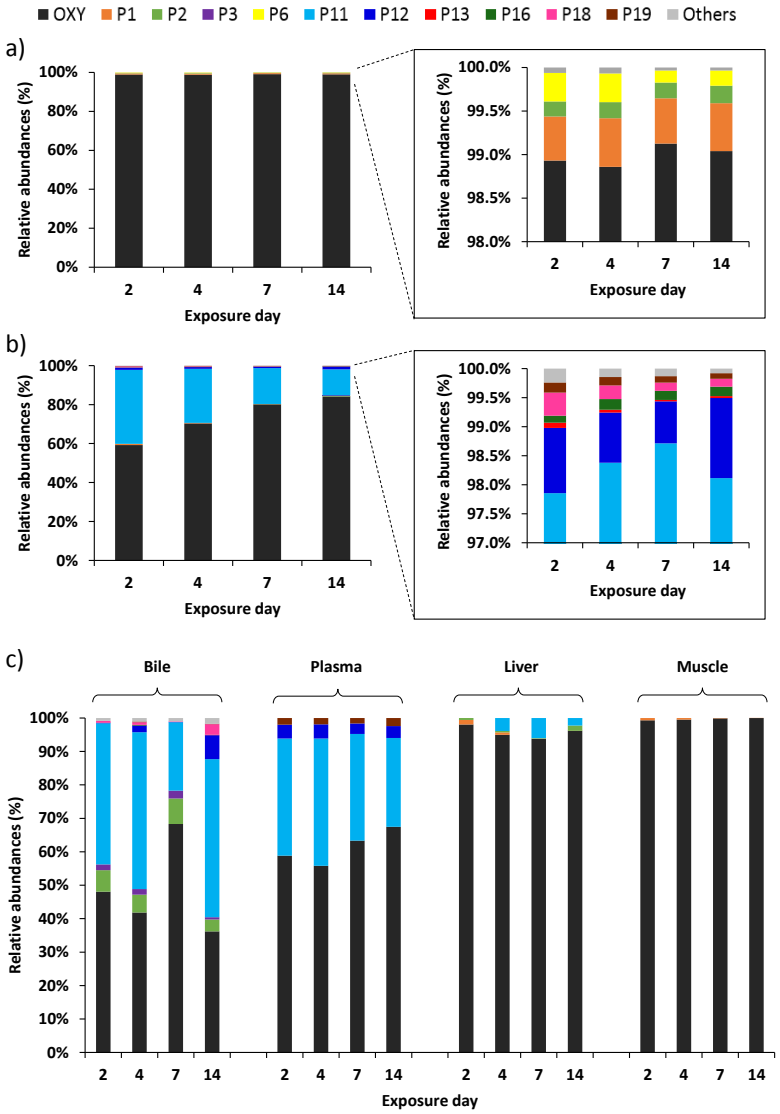

Figure 7.7: *Relative abundances of OXY and its by-products (calculated as the proportion of the sum peak areas) in a) seawater in the absence of fish, b) seawater in the presence of fish, and c) fish biofluid/tissues (bile, plasma, liver and muscle) along the OXY exposure experiment (days 2, 4, 7 and 14).*

7.4 Conclusions

In order to understand the adverse effects that UV filters such as OXY may pose to the aquatic ecosystems, a complete understanding of not only the parent compound but also the potentially bioactive by-products formed is necessary. According to the results of the present work, OXY accumulates especially in bile and in a lower extent in muscle, gill, liver and plasma. OXY by-products were detected in all the matrices studied (seawater in the presence and absence of fish, bile, liver, plasma and muscle), except gill. Up to 20 by-products were annotated: 5 in seawater in the absence of fish, 11 in seawater in the presence of fish, 15 in bile, 3 in liver, 3 in plasma and 1 in muscle. While *O*-methylation and *O*-demethylation of OXY were the major by-products in seawater in the absence of fish, OXY glucuronide P11 was the major metabolite observed in water in the presence of fish, in bile, plasma and liver. Actually, relative abundance of OXY was reduced from a 99% in seawater in the absence of fish to a 59-84% in the presence of fish, which is indicative of the importance of including not only the parent xenobiotic but also the by-products in the monitoring campaigns. The high OXY levels and the high amount of by-products observed in bile suggest that this is the biofluid through which OXY and its by-products were excreted. However, further research should be performed in order to study the elimination through kidney and evaluate if OXY is reabsorbed to plasma in the intestine or completely excreted in faeces. Lastly, not to underestimate the true extent of exposure, it is required to take into account by-products since they might also inhibit 17β-hydroxysteroid dehydrogenase 3 testosterone-forming enzyme [29] or pose estrogenic and antiendrogenic activities like P2 and P3 observed in fish bile and liver [7–9,28,30]. Consequently, identification of novel transformation and metabolization products together with the parent compound, and evaluation of their toxicity, is crucial for a complete environmental risk assessment.

7.5 References

1. Arpin-Pont L, Bueno MJM, Gomez E, Fenet H. 2016. Occurrence of PPCPs in the marine environment: a review. *Environ. Sci. Pollut. Res.* 23:4978–4991.
2. Boxall ABA, Rudd MA, Brooks BW, Caldwell DJ, Choi K, Hickmann S, Innes E, Ostapyk K, Staveley JP, Verslycke T, Ankley GT, Beazley KF, Belanger SE, Berninger JP, Carriquiriborde P,

Coors A, DeLeo PC, Dyer SD, Ericson JF, Gagné F, Giesy JP, Gouin T, Hallstrom L, Karlsson MV, Larsson DGJ, Lazorchak JM, Mastrocco F, McLaughlin A, McMaster ME, Meyerhoff RD, Moore R, Parrott JL, Snape JR, Murray-Smith R, Servos MR, Sibley PK, Straub JO, Szabo ND, Topp E, Tetreault GR, Trudeau VL, Van Der Kraak G. 2012. Pharmaceuticals and Personal Care Products in the Environment: What Are the Big Questions? *Environ. Health Perspect.* 120:1221–1229.

3. Balmer ME, Buser H-R, Müller MD, Poiger T. 2005. Occurrence of Some Organic UV Filters in Wastewater, in Surface Waters, and in Fish from Swiss Lakes. *Environ. Sci. Technol.* 39:953–962.

4. Brausch JM, Rand GM. 2011. A review of personal care products in the aquatic environment: Environmental concentrations and toxicity. *Chemosphere*. 82:1518–1532.

5. Muncke J. 2011. Endocrine disrupting chemicals and other substances of concern in food contact materials: An updated review of exposure, effect and risk assessment. *J. Steroid Biochem. Mol. Biol.* 127:118–127.

6. European Parliament and Council. 2009. *Regulation (EC) No 764/2008 of 30 November 2009 on cosmetic products. ANNEX VI: LIST OF UV FILTERS ALLOWED IN COSMETIC PRODUCTS.* Macmillan Education UK:201–202. [cited 21 May 2018]. Available from https://ec.europa.eu/health/sites/health/files/endocrine_disruptors/docs/cosmetic_1223_2009_regulation_en.pdf.

7. Kunisue T, Chen Z, Buck Louis GM, Sundaram R, Hediger ML, Sun L, Kannan K. 2012. Urinary Concentrations of Benzophenone-type UV Filters in US Women and Their Association with Endometriosis. *Environ. Sci. Technol.* 46:4624–4632.

8. Kunz PY, Galicia HF, Fent K. 2006. Comparison of In Vitro and In Vivo Estrogenic Activity of UV Filters in Fish. *Toxicol. Sci.* 90:349–361.

9. Kunz PY, Fent K. 2006. Multiple hormonal activities of UV filters and comparison of in vivo and in vitro estrogenic activity of ethyl-4-aminobenzoate in fish. *Aquat. Toxicol.* 79:305–324.

10. Coronado M, De Haro H, Deng X, Rempel MA, Lavado R, Schlenk D. 2008. Estrogenic activity and reproductive effects of the UV-filter oxybenzone (2-hydroxy-4-methoxyphenyl-methanone) in fish. *Aquat. Toxicol.* 90:182–187.

11. Nakamura N, Inselman AL, White GA, Chang C-W, Trbojevich RA, Sepehr E, Voris KL, Patton RE, Bryant MS, Harrouk W, McIntyre B, Foster PM, Hansen DK. 2015. Effects of maternal and lactational exposure to 2-hydroxy-4-methoxybenzone on development and reproductive organs in male and female rat offspring. *Birth Defects Res. B. Dev. Reprod. Toxicol.* 104:35–51.

12. Gago-Ferrero P, Badia-Fabregat M, Olivares A, Piña B, Blánquez P, Vicent T, Caminal G, Díaz-Cruz MS, Barceló D. 2012. Evaluation of fungal- and photo-degradation as potential treatments for the removal of sunscreens BP3 and BP1. *Sci. Total Environ.* 427–428:355–363.

13. Hernández Leal L, Vieno N, Temmink H, Zeeman G, Buisman CJN. 2010. Occurrence of Xenobiotics in Gray Water and Removal in Three Biological Treatment Systems. *Environ. Sci. Technol.* 44:6835–6842.

14. Li W, Ma Y, Guo C, Hu W, Liu K, Wang Y, Zhu T. 2007. Occurrence and behavior of four of the most used sunscreen UV filters in a wastewater reclamation plant. *Water Res.* 41:3506–3512.

15. Negreira N, Rodríguez I, Ramil M, Rubí E, Cela R. 2009. Sensitive determination of salicylate and benzophenone type UV filters in water samples using solid-phase microextraction, derivatization and gas chromatography tandem mass spectrometry. *Anal. Chim. Acta*. 638:36–44.

16. Snyder SA, Wert EC, Rexing DJ, Zegers RE, Drury DD. 2006. Ozone Oxidation of Endocrine Disruptors and Pharmaceuticals in Surface Water and Wastewater. *Ozone Sci. Eng.* 28:445–460.

17. Gago-Ferrero P, Díaz-Cruz MS, Barceló D. 2011. Occurrence of multiclass UV filters in treated sewage sludge from wastewater treatment plants. *Chemosphere*. 84:1158–1165.

18. Rodil R, Moeder M, Altenburger R, Schmitt-Jansen M. 2009. Photostability and phytotoxicity of selected sunscreen agents and their degradation mixtures in water. *Anal. Bioanal. Chem.* 395:1513.

19. Fent K, Zenker A, Rapp M. 2010. Widespread occurrence of estrogenic UV-filters in aquatic ecosystems in Switzerland. *Environ. Pollut.* 158:1817–1824.

20. Kameda Y, Kimura K, Miyazaki M. 2011. Occurrence and profiles of organic sun-blocking agents in surface waters and sediments in Japanese rivers and lakes. *Environ. Pollut.* 159:1570–1576.

21. Poiger T, Buser H-R, Balmer ME, Bergqvist P-A, Müller MD. 2004. Occurrence of UV filter compounds from sunscreens in surface waters: regional mass balance in two Swiss lakes. *Chemosphere*. 55:951–963.

22. Zhang Z, Ren N, Li Y-F, Kunisue T, Gao D, Kannan K. 2011. Determination of Benzotriazole and Benzophenone UV Filters in Sediment and Sewage Sludge. *Environ. Sci. Technol.* 45:3909–3916.

23. Al-Salhi R, Abdul-Sada A, Lange A, Tyler CR, Hill EM. 2012. The Xenometabolome and Novel Contaminant Markers in Fish Exposed to a Wastewater Treatment Works Effluent. *Environ. Sci. Technol.* 46:9080–9088.

24. Molins-Delgado D, Muñoz R, Nogueira S, Alonso MB, Torres JP, Malm O, Ziolli RL, Hauser-Davis RA, Eljarrat E, Barceló D, Díaz-Cruz MS. 2018. Occurrence of organic UV filters and metabolites in lebranche mullet (Mugil liza) from Brazil. *Sci. Total Environ.* 618:451–459.

25. Nagtegaal M, Ternes TA, Baumann W, Nagel R. 1997. UV-Filtersubstanzen in Wasser und Fischen. *Umweltwissenschaften Schadst.-Forsch.* 9:79–86.

26. Gago-Ferrero P, Silvia Díaz-Cruz M, Barceló D. 2013. Liquid chromatography-tandem mass spectrometry for the multi-residue analysis of organic UV filters and their transformation products in the aquatic environment. *Anal. Methods*. 5:355–366.

27. Kim S, Choi K. 2014. Occurrences, toxicities, and ecological risks of benzophenone-3, a common component of organic sunscreen products: A mini-review. *Environ. Int.* 70:143–157.

28. Nakagawa Y, Suzuki T. 2002. Metabolism of 2-hydroxy-4-methoxybenzophenone in isolated rat hepatocytes and xenoestrogenic effects of its metabolites on MCF-7 human breast cancer cells. *Chem. Biol. Interact.* 139:115–128.

29. Nashev LG, Schuster D, Laggner C, Sodha S, Langer T, Wolber G, Odermatt A. 2010. The UV-filter benzophenone-1 inhibits 17β-hydroxysteroid dehydrogenase type 3: Virtual screening as a strategy to identify potential endocrine disrupting chemicals. *Biochem. Pharmacol.* 79:1189–1199.

30. Suzuki T, Kitamura S, Khota R, Sugihara K, Fujimoto N, Ohta S. 2005. Estrogenic and antiandrogenic activities of 17 benzophenone derivatives used as UV stabilizers and sunscreens. *Toxicol. Appl. Pharmacol.* 203:9–17.

31. Jeon H-K, Sarma SN, Kim Y-J, Ryu J-C. 2008. Toxicokinetics and metabolisms of benzophenone-type UV filters in rats. *Toxicology*. 248:89–95.

32. Ziarrusta H, Mijangos L, Prieto A, Etxebarria N, Zuloaga O, Olivares M. 2015. Determination of tricyclic antidepressants in biota tissue and environmental waters by liquid chromatography-tandem mass spectrometry. *Anal. Bioanal. Chem.* 408:1205–1216.

33. Negreira N, Rodríguez I, Rodil R, Rubí E, Cela R. 2013. Optimization of matrix solid-phase dispersion conditions for UV filters determination in biota samples. *Int. J. Environ. Anal. Chem.* 93:1174–1188.

34. Rodil R, Quintana JB, López-Mahía P, Muniategui-Lorenzo S, Prada-Rodríguez D. 2008. Multiclass Determination of Sunscreen Chemicals in Water Samples by Liquid Chromatography−Tandem Mass Spectrometry. *Anal. Chem.* 80:1307–1315.

35. Fulton WT. 1904. The rate of growth of fishes. *22nd Annu. Rep. Fish. Board Scotl.* 3:141–241.

36. Schymanski EL, Jeon J, Gulde R, Fenner K, Ruff M, Singer HP, Hollender J. 2014. Identifying Small Molecules via High Resolution Mass Spectrometry: Communicating Confidence. *Environ. Sci. Technol.* 48:2097–2098.

37. Vione D, Caringella R, De Laurentiis E, Pazzi M, Minero C. 2013. Phototransformation of the sunlight filter benzophenone-3 (2-hydroxy-4-methoxybenzophenone) under conditions

relevant to surface waters. *Sci. Total Environ.* 463–464:243–251.

38. Gago-Ferrero P, Demeestere K, Silvia Díaz-Cruz M, Barceló D. 2013. Ozonation and peroxone oxidation of benzophenone-3 in water: Effect of operational parameters and identification of intermediate products. *Sci. Total Environ.* 443:209–217.

39. Gong P, Yuan H, Zhai P, Xue Y, Li H, Dong W, Mailhot G. 2015. Investigation on the degradation of benzophenone-3 by UV/H2O2 in aqueous solution. *Chem. Eng. J.* 277:97–103.

40. Okereke CS, Abdel-Rhaman MS, Friedman MA. 1994. Disposition of benzophenone-3 after dermal administration in male rats. *Toxicol. Lett.* 73:113–122.

41. Okereke CS, Kadry AM, Abdel-Rahman MS, Davis RA, Friedman MA. 1993. Metabolism of benzophenone-3 in rats. *Drug Metab. Dispos. Biol. Fate Chem.* 21:788–791.

42. Pan X, Yan L, Li C, Qu R, Wang Z. 2017. Degradation of UV-filter benzophenone-3 in aqueous solution using persulfate catalyzed by cobalt ferrite. *Chem. Eng. J.* 326:1197–1209.

43. Zúñiga-Benítez H, Aristizábal-Ciro C, Peñuela GA. 2016. Heterogeneous photocatalytic degradation of the endocrine-disrupting chemical Benzophenone-3: Parameters optimization and by-products identification. *J. Environ. Manage.* 167:246–258.

44. Hopkins ZR, Snowberger S, Blaney L. 2017. Ozonation of the oxybenzone, octinoxate, and octocrylene UV-filters: Reaction kinetics, absorbance characteristics, and transformation products. *J. Hazard. Mater.* 338:23–32.

45. Yang B, Ying G-G. 2013. Oxidation of benzophenone-3 during water treatment with ferrate(VI). *Water Res.* 47:2458–2466.

46. Pascal-Lorber S, Despoux S, Jamin EL, Canlet C, Cravedi J-P, Laurent F. 2012. Metabolic Fate of 2,4-Dichlorophenol and Related Plant Residues in Rats. *J. Agric. Food Chem.* 60:1728–1736.

47. Zalko D, Soto AM, Dolo L, Dorio C, Rathahao E, Debrauwer L, Faure R, Cravedi J-P. 2003. Biotransformations of bisphenol A in a mammalian model: answers and new questions raised by low-dose metabolic fate studies in pregnant CD1 mice. *Environ. Health Perspect.* 111:309–319.

48. Chen F, Huber C, Schröder P. 2017. Fate of the sunscreen compound oxybenzone in Cyperus alternifolius based hydroponic culture: Uptake, biotransformation and phytotoxicity. *Chemosphere*. 182:638–646.

Chapter 8

Non-targeted metabolomics reveals alterations in liver and plasma of gilt-head bream exposed to oxybenzone

Chemosphere 211 (2018) 624-631

8.1 Introduction

Benzophenone-3 or oxybenzone is one of the most widely used organic UV filters in sunscreen products and daily use cosmetics. Like other pharmaceuticals and personal care products (PPCPs), oxybenzone and its by-products are incompletely removed during wastewater treatment [1], resulting in their occurrence in many aquatic ecosystems. Oxybenzone has been found in wastewater and surface waters, but also in fish due to its bioaccumulation capacity [2–5]. Preliminary risk assessment studies indicated that oxybenzone discharged from wastewater treatment plants may pose high risk to aquatic organisms in the environment [1].

Consequently, occurrence of UV filters in aquatic ecosystems and their potential effects on non-target organisms is of growing concern [1,6–16]. For instance, developmental and reproductive toxicity of oxybenzone [7,10,11,13] in fish have been attributed to an altered hormonal balance as a result of its endocrine disrupting effects [10–13]. Many studies have reported the complex hormonal activity of UV filters, since many of these xenobiotics show up to three distinct modes of action, including estrogenicity, anti-estrogenicity and anti-androgenicity [6,11–14]. Additionally, the scarce information available regarding their effects on the antioxidant defense system in fish suggests that UV filters have adverse effects beyond hormonal activity [15,16]. For instance, a growing trend in glutathione peroxidase expression was observed in zebrafish (*Danio rerio*) eleuthero-embryos exposed to oxybenzone, which is an indicative of oxidative stress [16]. In the same context, Liu and co-workers also reported that benzophenone UV filters generated oxidative stress in freshwater fish *Carassius auratus* [15].

In addition to this, Coronado and co-workers revealed that the alteration of endocrine and reproduction endpoints in fish are linked to the exposure to oxybenzone, but at levels significantly higher than those measured in the environment [7]. Consequently, acute and chronic toxicity assays are required for a more accurate environmental risk assessment (ERA). Preliminary studies reported that predicted no effect concentration (PNEC) for oxybenzone was derived at 1.32 µg/L [12] and LC_{50} value (48 h) was 1.9 mg/L [9], indicating that individual UV filters should undergo further ecotoxicological analysis, as an environmental risk cannot be ruled out even though the levels observed in water bodies are generally lower. Furthermore, Kim and co-workers stated that

oxybenzone is transformed into benzophenone-1, a more potent estrogen agonist, which needs to be included in ERA in order to have a more realistic estimation of the effects of oxybenzone exposure [11]. On the other hand, although oxybenzone has been frequently detected in aquatic organisms, limited information is available on its *in vivo* toxicity, particularly in fish, and further *in vivo* testing is required since it provides the most reliable data for predictive testing and risk assessment of xenobiotics [8].

Finally, although most of the studies investigating the hazards associated with UV filters in aquatic organisms have focused on receptor binding and gene expression assays [6,7,12,16], complementary approaches are needed for a more thorough ERA. In order to study thoroughly the effects of xenobiotics occurring in the environment at non-lethal levels, it is important to focus on the modes of action. To this end, metabolomics has proven useful by offering insight into early biochemical perturbations at low molecular weight endogenous molecules triggered by low dose of xenobiotics, which may lead to an adverse effect [2,17,18]. For example, Huang et al. revealed that the exposure of multiple class of xenobiotics at environmentally relevant concentrations produces specific biochemical fingerprints in zebrafish [18], indicating that metabolomics can complement toxicity assays with molecular-level information. In particular, a hypothesis-free and non-targeted metabolomic approach allows the identification of many distinct features in a single analysis, offering the opportunity to discover biomarkers that lead to a range of breakthroughs in understanding the risks of xenobiotics [2,17]. Since generally highly dimensional and multi-correlated data are obtained for a few replicate samples, both univariate and multivariate approaches [19] have been applied to identify the metabolites that allow the discrimination of case from control groups. Additionally, pathway enrichment [20] helps to find plausible biological explanations for those metabolic alterations taking into account compounds, modules, enzymes, reactions and pathways in databases such as KEGG [21].

In this framework, the main objective of this work was to evaluate the *in vivo* effects of oxybenzone in juvenile gilt-head bream (*Sparus aurata*) using a non-targeted metabolomic approach to measure perturbations in the brain, liver and plasma metabolome. To our knowledge, this is the first study to investigate metabolic effects of oxybenzone in fish.

8.2 Experimental

8.2.1 Standards and reagents

Stock dosing solution of oxybenzone (98%, Sigma-Aldrich, St. Louis, MO, USA) was prepared at 25,000 mg/L in ethanol (EtOH) and diluted down to 0.83 mg/L in Milli-Q water. The final concentration of EtOH in the dosing solution was <0.005%. Additional information regarding the reagents of endogenous metabolites purchased from Sigma–Aldrich is detailed in Appendix III.

8.2.2 Oxybenzone exposure experiment and sampling

Exposure experiments were designed at the Research Centre for Experimental Marine Biology and Biotechnology (PiE-UPV/EHU) using juvenile gilt-head bream weighing ~40 g and measuring ~13 cm in length (Groupe Aqualande, Roquefort, France). The experiments were carried out at controlled lab temperature (18 °C), water temperature (13.5 ± 0.5 ˚C) and pH (7.3 ± 0.3), and light (14:10 h light:dark cycle). Fish were acclimatized for 1 month upon arrival, stabilized for an additional 1 week in the exposure tanks before the exposure and they were fed daily with 0.10 g pellets/fish (EFICO YM 868, 3 mm, BioMar Group, Denmark). The water in the control and exposed tanks was continuously aerated and the water quality was assured by measuring periodically the dissolved oxygen, nitrite, nitrate and ammonium contents.

This experiment was conducted in parallel with a bioaccumulation/biotransformation study, and it was observed that oxybenzone was accumulated in different tissues and biofluids [5]. A 14-day exposure (50 µg/L nominal) was performed using two 1000 x 700 x 650 mm polypropylene tanks (one control, one exposed), containing 250 L of seawater and 50 fish per tank. Exposures were carried out using a continuous flow-through system with a peristaltic pump delivering 10 L seawater/h and another pump infusing an oxybenzone dosing solution (refilled every 24 hours) at 0.6 L/h to the exposure tank. Identical experimental conditions were maintained for control tank. Ten fish were sampled from both tanks at the beginning of the experiments (day 0) and on exposure days 2, 4, 7 and 14. Additionally, 2.5 L water samples were also collected on the same sampling days to monitor oxybenzone concentrations in both tanks.

Fish taken for dissection were immersed for 5 minutes in a tank containing 10 L of seawater

with 200 mg/L tricaine and 200 mg/L $NaHCO_3$. Each anaesthetized fish was weighed, measured and dissected to collect plasma and brain in 2-mL Precellys vials (Bertin Instruments, Montigny-le-Breonneux, France) and liver in 7-mL Precellys vials. Blood was sampled from the caudal vein-artery using a syringe previously rinsed with 0.5 mol/L EDTA solution (pH adjusted to 8.0 using NaOH) and then centrifuged for 5 minutes at 1000 rpm (Centrifuge 5415 C, Eppendorf, Hamburg, Germany) to get the plasma. Biological fluids and tissues were stored in liquid nitrogen during dissection and kept at -80 ˚C until extraction. Fish processing described herein was evaluated by the Bioethics Committee of the UPV/EHU and approved by the Local Authority according to the current regulations (procedure approval CEEA/380/2014/ETXEBARRIA LOIZATE).

8.2.3 Extraction and analysis of metabolites

Analytical method for metabolite extraction and analysis is fully described elsewhere [22]. In brief, a mixture of 4 µL $CHCl_3$:MeOH (20:80, v/v) per mg sample was added directly into the Precellys vials containing dissected tissues and biofluids (~100 mg brain, ~400 mg plasma and 1000 mg liver) for a single step extraction of both polar and non-polar metabolites. All samples were homogenized for 3x1.5 min at 4000 rpm (Precellys), under controlled cooled temperature (4 °C) (Cryolys, Bertin Technologies, Montigny-le-Bretonneux, France), employing 1.4 mm or 2.8 mm-zirconium oxide beads (Precellys) in the case of brain and liver, respectively. Extracts were centrifuged for 15 minutes at 18,000 rpm (Centrifuge Allegra X-30R, F2402H, Beckman Coulter, High Wycombe, UK) to get the supernatant consisting on a single-phase solution.

Non-targeted analysis was carried using a Thermo Scientific Dionex UltiMate 3000 UHPLC coupled to a Thermo Scientific Q Exactive quadrupole-Orbitrap mass spectrometer equipped with a heated ESI source (HESI, Thermo, CA, USA). Furthermore, to maximize metabolite coverage, 3 runs were performed per extract (aliquots of 5 µL) using different chromatographic columns and ionization modes: hydrophilic interaction liquid chromatography (HILIC) column in positive ($HILIC_{pos}$) and negative ($HILIC_{neg}$) ionization modes, and a reverse-phase octadecylsilyl column in the positive mode ($C18_{pos}$). In $HILIC_{pos}$ and $HILIC_{neg}$ separation was carried out on an Acquity BEH-Amide column (2.1 × 100 mm, 1.7 µm) equipped with a Vanguard pre-column (2.1 × 5 mm, 1.7 µm) from Waters (Milford, Massachusetts, United States), which was kept at 35 °C during the analysis.

Milli-Q water was used as mobile phase A and acetonitrile as mobile phase B, both containing 0.1% formic acid in $HILIC_{pos}$ and 10 mM of ammonium acetate in $HILIC_{neg}$. The eluent gradient profile, adapted from literature [22], was as follows: 97% of B (hold 3 min), linear change to 85% B up to 5 min, another linear change to 75% B up to 14 min, another linear change to 40% B up to 17 min (hold 3 min) and a final linear change to 97% B up to 23 min (hold 2 min) to regain initial conditions. The flow rate was changed throughout the analysis as follows: 0-3 min at 0.2 mL/min, 3-5 min increase to 0.3 mL/min, 5-23 min at 0.3 mL/min, 23-24 min decrease to 0.2 mL/min and 24-25 min at 0.2 mL/min. Lastly, $C18_{pos}$ method employed a Kinetex C18 100 Å core-shell (3.0 × 150 mm, 2.6 µm) chromatographic column equipped with a Vanguard pre-column (3.0 × 5 mm, 2.6 µm) from Phenomenex (Torrance, CA, USA). Milli-Q water was used as mobile phase A and MeOH as mobile phase B, both containing 0.1% formic acid. The mobile phase flow rate was set at 0.3 mL/min and the eluent gradient profile was as follows: 5% of B (hold 1 min), linear change to 95% B up to 16 min (hold 4 min) and a final linear change to 5% B up to 24 min (hold 1 min) to regain initial conditions.

The q-Orbitrap was operated in the corresponding ionization mode in full scan – data dependent MS2 (Full MS-ddMS2) discovery acquisition mode. One full scan at a resolution of 70,000 full width at half maximum (FWHM) at *m/z* 200 over a scan range of *m/z* 70-1000 was followed by three ddMS2 scans at a resolution of 17,500 FWHM at *m/z* 200, with an isolation window of 0.8 Da. The stepped normalized collision energy (NCE) in the higher-energy collisional dissociation (HCD) cell was set to 10, 35 and 75 eV. The HESI source parameters in positive mode were set to 3.2 kV spray voltage, 300 °C capillary temperature, 35 arbitrary units (au) sheath gas (nitrogen), 10 au auxiliary gas, 1 au sweep gas, 280 °C auxiliary gas heater and S-lens RF level 55.0. The HESI source parameters in negative mode were set to 3.2 kV spray voltage, 320 °C capillary temperature, 48 au sheath gas, 11 au auxiliary gas, 2 au sweep gas, 310 °C auxiliary gas heater and S-lens RF level 55.0. External calibration of the instrument was conducted immediately prior to analysis using Pierce LTQ ESI Calibration Solutions (Thermo Scientific, Waltham, Massachusetts, United States). The instrument was controlled by Xcalibur 4.0 software (Thermo).

The extraction of the samples was carried out randomly and the samples were arranged in 9 separate sequences: one per matrix (liver, brain, plasma) and analysis conditions ($HILIC_{pos}$, $HILIC_{neg}$,

$C18_{pos}$). In order to assure the quality assurance/quality control of the instrumental analysis [23], sample extracts were analyzed randomly along the sequence. Instrumental blank samples (pure MeOH) injected every 5 samples ruled out the presence of carryover, and procedural blank samples were prepared to estimate the background concentration of metabolites during sample workup. Sequence quality control sample (QC_{seq}) was also prepared for each tissue by pooling a small volume of each extract and splitting it into several aliquots. These aliquots were injected after every 10 samples to allow signal drift correction.

8.2.4 Data handling and statistical analyses

Condition factor (K) and hepatic somatic index (HSI) were determined as a general assessment of fish health. K was calculated using the equation K = (fish weight × 100)/(fish length)^3) [24], while HSI was determined using the equation HSI = (liver weight × 100)/(fish weight)). K and HSI were statistically evaluated between exposed and control groups using one-way ANOVA.

Identification of metabolites involved in altered metabolic pathways was performed separately for plasma, brain and liver following the workflow shown in Figure 8.1. First, each sequence of chromatograms was processed using Compound Discoverer 2.1 (CD; Thermo-Fisher Scientific). The specific details of the workflow and settings are described in Appendix II. Thereafter, each data set was filtered to keep only endogenous metabolites by searching the detected exact masses in the database containing up to 4400 endogenous compounds or in LipidMaps [25] database.

All statistical analyses were carried out using the R software for statistical computing (v 3.4.3). Firstly, using Principal Component Analysis (PCA) as an unsupervised discrimination approach, possible outliers (i.e., samples outside the 95% confidence regions of the total dataset) were discarded in each sequence. Signal drift over the course of the sequence (identified from QC_{seq} data) was corrected afterwards using the R package intCor [26], via a two-step method that combines Common Principal Components Analysis (CPCA) and the medians method. To create this model, we defined three classes (i.e., control, exposed and QC_{seq}) and the number of components of the model in each specific sequence. Once the drift was corrected, the 3 sequences ($HILIC_{pos}$, $HILIC_{neg}$, $C18_{pos}$) of each matrix were merged to subsequently perform multiple linear analysis

(Y (time, dose) = time + dose + time·dose, where Y is the feature response). Since the objective was to find out the metabolites that showed significantly different concentration evolution during exposure between the exposed and control samples, we paid special attention to the interaction time·dose. Therefore, applying linear analysis and multiple testing, we selected the chromatographic features with a p-value < 0.05 and a false discovery rate (FDR) < 0.05 in the interaction time·dose. We manually checked the features that showed up as significant in order to discard those with bad chromatographic peak shape and/or incorrectly integrated, as well as those features that corresponded to oxybenzone by-products [5].

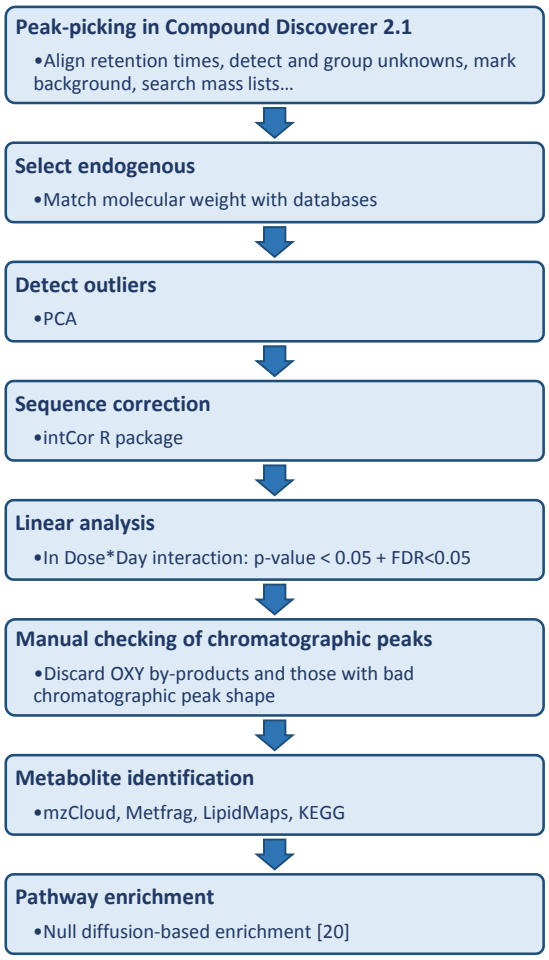

***Figure 8.1**: Workflow followed to identify metabolites involved in altered metabolic pathways.*

After selecting significant features, we performed metabolite annotation [27] comparing the exact mass, isotopic profile, fragmentation and abundances with those available in the mzCloud library [28]. When the metabolite was not available in the mzCloud library, experimental fragmentation pattern was compared against *in silico* fragmentation obtained in MetFrag [29] that uses KEGG [21] and LipidMaps [25] databases for metabolite annotation. Finally, when the standard was available (see Appendix III), retention time was also used for the last confirmation.

In order to identify the key metabolic processes and to find out a feasible biological explanation for the variations observed, null diffusion-based enrichment [20] was run with KEGG annotated compounds based on the following parameters: diffusion method, simulation approximation with 15,000 iterations. The database was built using the KEGG release 84.0+/10-08, Oct 17 2017, the zebrafish (*Danio rerio*) organism (organism code "dre") and excluding the unspecific "dre01100" metabolic overview pathway. The network consisted of 161 pathways, 176 modules, 973 enzymes, 4803 reactions and 3450 KEGG compounds. We also discussed the biological relevance of the lipids identified as significant metabolites but not included in KEGG. Finally, fold change (FC) values (see Equation 8.1) of the suggested metabolites were calculated as described elsewhere [19]:

$$FC = {\bar{X}}/{\bar{Y}} \; when \; \bar{X} > \bar{Y} \;\; or \; FC = -{\bar{Y}}/{\bar{X}} \; when \; \bar{X} < \bar{Y} \qquad \text{Equation 8.1}$$

Where, $\overline{X}$ and $\overline{Y}$ are the average concentrations of the metabolite in the exposed and control samples, respectively.

8.3 Results and discussion

No significant changes in fish weight and length were observed at a 95% confidence level, regardless of experiment tank or exposure day (p-value > 0.05). There was no mortality and K and HSI were comparable between fish of exposed and control groups (p-value > 0.05) at all the exposure days. Furthermore, following the workflow detailed in section 8.2.4, no metabolite concentration was altered significantly in brain, concluding that the brain metabolome was not affected by oxybenzone. Although according to the literature oxybenzone can accumulate in brain and result in neurological effects by disrupting the brain homeostasis in rats [30], in gilt-head

bream we observed no metabolome profile modification in this tissue. Contrarily, in the case of liver and plasma, the number of significantly altered features was 8 and 10, respectively. From those peaks, 4 and 9 were KEGG annotated in liver and plasma, respectively, and the rest of the peaks were putatively identified as lipids that are not included in KEGG (see Tables 8.1 and 8.2). Additionally, pathway enrichment was performed using the significant metabolites previously mapped on KEGG for each matrix. Overall, the largest alterations were observed mainly in the last day of exposure (see the daily FC values and individual average peak areas for each metabolite in liver and plasma in Tables 8.3 and 8.4, respectively).

Table 8.1: *Identification of the features whose liver concentrations were significantly altered after the oxybenzone-exposure.*

Peak	Molecular Weight	MS/MS fragments	R_t (min)	Name	KEGG Code	Identification level
C18pos_Peak1222	180.0421	163.0388; 149.0232; 65.0393	14.04	trans-2,3-dihydroxycinnamate	C12623	2b
C18pos_Peak1293	180.0421	163.0388; 149.0232; 65.0393	10.92	3-(4-Hydroxyphenyl)pyruvate/ 2-hydroxy-3-(4-hydroxyphenyl) propenoate	C01179/ C05350	3
C18pos_Peak529	193.0739	162.0547; 152.0703; 120.0444	11.25	Phenylacetylglycine	C05598	2a
HILICpos_Peak1073	179.0582	162.0550; 105.0335; 95.0491	6.64	Hippurate	C01586	2a
HILICneg_Peak114	791.5487	283.2649; 124.9999; 123.0436	1.67	18 candidates belonging to glycerophospholipids lipid category[a]	*	3
HILICneg_Peak1178	406.1271	243.0670; 227.0714; 123.0436	7.09	5 candidates belonging to polyketides lipid category[b]	*	3
HILICneg_Peak1333	493.3538	311.2956; 283.2649; 184.0733	6.78	2 candidates belonging to glycerophospholipids lipid category[c]	*	3
HILICneg_Peak421	420.1064	123.0436; 108.0200; 93.0328	6.95	7 candidates belonging to polyketides lipid category[d]	*	3

**Putatively identified/not in KEGG. LipidMaps ID: [a]LMGP01011430, LMGP01011544, LMGP01011573, LMGP01011906, LMGP01011935, LMGP01012101, LMGP02010094, LMGP02010678, LMGP02010766, LMGP02010864, LMGP02010894, LMGP02010924, LMGP02010953, LMGP02010981, LMGP02011087, LMGP02011115, LMGP02011142 or LMGP20020015; [b]LMPK13090007, LMPK12020031, LMPK12020264, LMPK12020009 or LMPK12020025; [c]LMGP02070004 or LMGP01070007; [d]LMPK12113361, LMPK12113362, LMPK12113363, LMPK12113382, LMPK12113381, LMPK12113364 or LMPK12113383.*

Table 8.2: *Identification of the features whose plasma concentrations were significantly altered after the oxybenzone-exposure.*

Peak	Molecular Weight	MS/MS fragments	R_t (min)	Name	KEGG Code	Identification level
C18pos_Peak1037	138.1045	121.1013; 97.0657; 93.0703	13.23	3,6-Nonadienal	C16323	2b
C18pos_Peak715	105.0428	88.0398; 70.0295; 60.0453	2.05	D-Serine	C00740	1
HILICneg_Peak29	366.3501	183.1391; 169.1234; 141.0921	1.61	Nervoic acid	C08323	2b
HILICneg_Peak498	172.0141	152.9958; 96.9696; 78.9591	6.66	sn-Glycerol 1-phosphate / sn-Glycerol 3-phosphate	C00623/ C00093	3
HILICneg_Peak12	328.2407	283.2431; 229.1962; 119.0490	2.21	Docosahexaenoic acid	C06429	2a
HILICneg_Peak344	336.3033	95.0862; 85.0277; 57.0710	1.63	Docosadienoic acid	C16533	2b
HILICpos_Peak112	105.0430	88.0399; 70.0295; 60.0453	10.80	D-Serine	C00740	1
C18pos_Peak688	278.2245	261.2217; 243.2115; 95.0859	17.64	γ-Linolenic acid / α-Linolenic acid / Crepenynate	C06426/ C06427/ C07289	3
HILICpos_Peak11	129.0426	102.0554; 84.0451; 56.0505	10.73	5-Oxo-L-proline	C01879	2a
C18pos_Peak158	733.5618	184.0733; 124.9999; 86.0970	21.39	14 candidates belonging to glycerophospholipids lipid category[a]	*	3

**Putatively identified/not in KEGG. [a]LMGP01010463, LMGP01010704, LMGP01010444, LMGP01010564, LMGP01010537, LMGP01011080, LMGP01010997, LMGP01011062, LMGP01010970, LMGP01010739, LMGP01010418, LMGP01010488, LMGP01011267 or LMGP01010397.*

8.3.1 Liver metabolome alterations

Pathway enrichment suggested that the more significantly altered metabolites in liver were those involved in the amino acid metabolism, specifically, in the phenylalanine metabolism and the tyrosine-related metabolites (see Figure 8.2). Phenylacetylglycine, hippurate and trans-2,3-dihydroxycinnamate levels were increased in oxybenzone-exposed fish (see Table 8.3). Apart

from those targets in the phenylalanine metabolism, tyrosine-related metabolites 3-(4-hydroxyphenyl) pyruvate/2-hydroxy-3-(4-hydroxyphenyl)propenoate also showed the same concentration profile. Both pathways are related since phenylalanine-4-hydrolase converts phenylalanine into tyrosine [31]. Therefore, all these perturbations might be associated. Additionally, 4 putatively identified lipid levels were also altered.

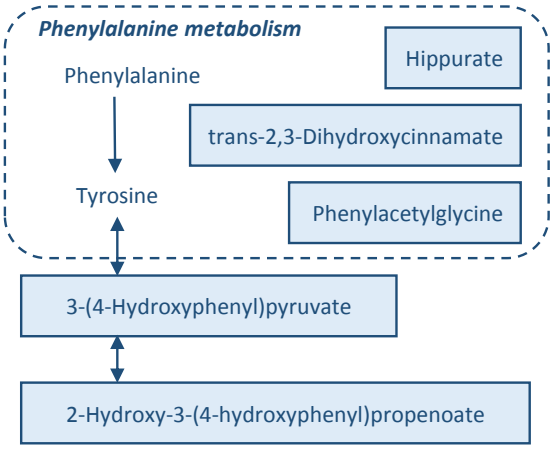

***Figure 8.2**: Altered metabolites and pathway in fish liver.*

The perturbation of the metabolites involved in amino acid metabolism in liver could pinpoint a way to overcome the exposure to oxybenzone, similarly to what occurred with other environmental pollutants [32,33]. Additionally, several studies have shown that the oxidative stress owed to pollutant exposure can induce changes in concentration levels of amino acids and lipid metabolites [34,35]. Furthermore, in this work we have also observed alterations in 4 lipidic metabolites (see Table 8.1), which is consistent with lipid storage disorders observed under exposure to PPCPs [36]. To sum up, the evidences to conclude that the pollutant-exposed fish showed oxidative stress are the alterations in lipidic metabolites [36], the perturbation in hippurate levels [37] and the significant changes in the precursor metabolites of carbohydrate metabolism such as 3-(4-hydroxyphenyl)pyruvate/2-hydroxy-3-(4-hydroxyphenyl)propenoate [34,35].

Oxidative stress has been previously linked to the disruption of energy metabolism [34,35], which is reported to be perturbed by the exposure to pollutants [38,39]. For instance, Colet and co-

workers revealed that the alteration of hippurate was a consequence of a disruption of the energy metabolism in liver mitochondria [39]. In fact, increased hippurate levels after oxybenzone administration (see Table 8.3) are not surprising since it was also observed with other xenobiotics such as toluene or arsenic [37–39], suggesting a non-specific mechanism of action [40]. In addition to hippurate, in the phenylalanine metabolism, we also observed the perturbations of trans-2,3,-dihydroxycinnamate and phenylacetylglycine, and the later was also found as altered metabolite in children exposed to bisphenol A [41]. Therefore, similarly to other xenobiotics [42], we conclude that oxybenzone alters the phenylalanine pathway.

Lastly, although oxybenzone is widely reported to have estrogenic activity [6,7,11–14], we did not observe clear evidences for that adverse effect. It is reported that the estrogenic signaling pathway includes the regulation of tyrosine hydroxylase, which catalyzes the synthesis of catecholamines from tyrosine [43]. Meanwhile, the only perturbation in the tyrosine metabolism was in the above mentioned 3-(4-hydroxyphenyl)pyruvate/2-hydroxy-3-(4-hydroxyphenyl)-propenoate, which is linked to tyrosine. Therefore, this observation might also be associated with the estrogenicity described for oxybenzone.

Table 8.3: *Daily fold change (FC) values and individual average peak areas (n=10, 95% confidence interval) for the metabolites whose concentrations were significantly altered in liver after the oxybenzone-exposure.*

Metabolite	**Fold change (FC)**				**Trends in control and exposed fish (Peak intensity vs Exposure Day)**
	Day 2	**Day 4**	**Day 7**	**Day 14**	
trans-2,3-dihydroxycinnamate	2.93	4.50	5.17	7.17	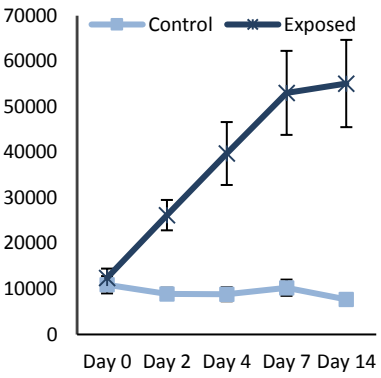

Table 8.3: *(Continuation).*

Metabolite	Fold change (FC)				Trends in control and exposed fish (Peak intensity vs Exposure Day)
	Day 2	Day 4	Day 7	Day 14	
3-(4-Hydroxyphenyl)pyruvate / 2-hydroxy-3-(4-hydroxyphenyl)propenoate	11.14	11.06	18.11	24.75	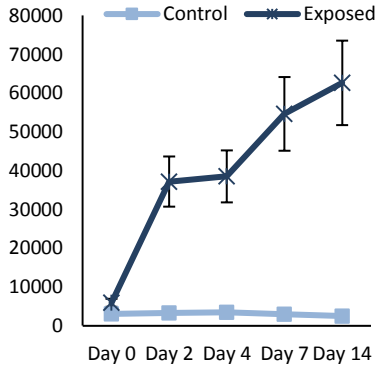
Phenylacetylglycine	1.70	3.36	3.64	1.49	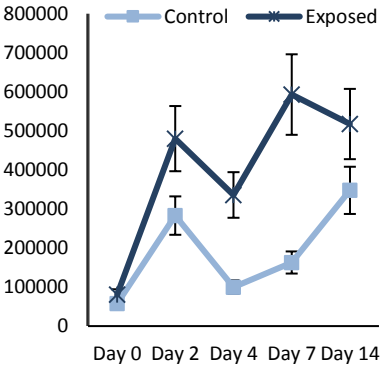
Hippurate	2.98	7.53	17.08	4.37	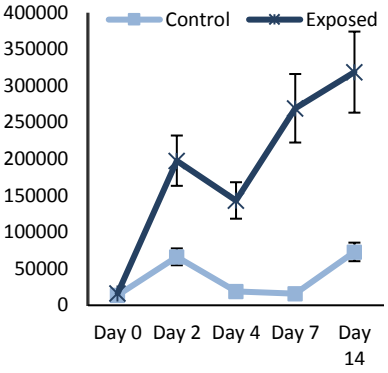

Table 8.3: *(Continuation).*

Metabolite	Fold change (FC)				Trends in control and exposed fish (Peak intensity vs Exposure Day)
	Day 2	Day 4	Day 7	Day 14	
18 candidates belonging to glycerophospholipids lipid category (LMGP01011430, LMGP01011544, LMGP01011573, LMGP01011906, LMGP01011935, LMGP01012101, LMGP02010094, LMGP02010678, LMGP02010766, LMGP02010864, LMGP02010894, LMGP02010924, LMGP02010953, LMGP02010981, LMGP02011087, LMGP02011115, LMGP02011142 or LMGP20020015)	-1.03	1.20	1.02	1.68	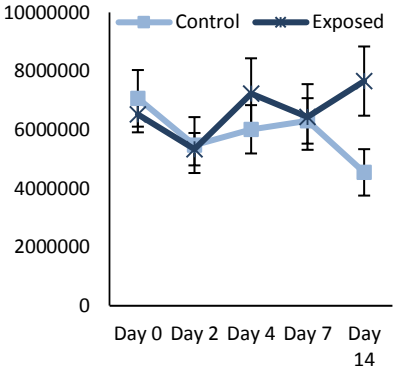
5 candidates belonging to polyketides lipid category (LMPK13090007, LMPK12020031, LMPK12020264, LMPK12020009 or LMPK12020025)	-1.05	1.77	8.36	7.54	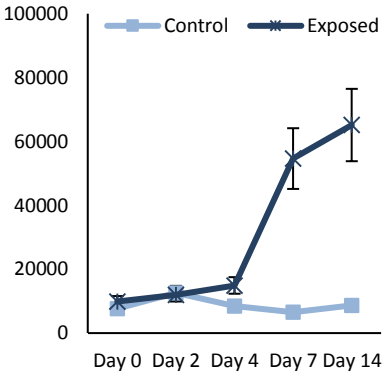
2 candidates belonging to glycerophospholipids lipid category (LMGP02070004 or LMGP01070007)	1.01	1.08	1.18	1.14	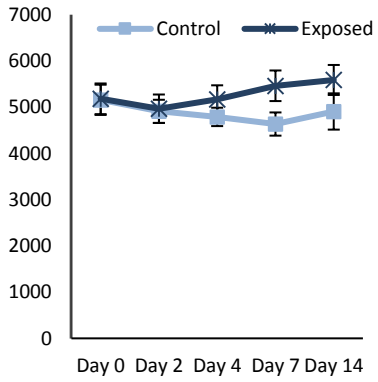

Table 8.3: *(Continuation).*

Metabolite	Fold change (FC)				Trends in control and exposed fish (Peak intensity vs Exposure Day)
	Day 2	Day 4	Day 7	Day 14	
7 candidates belonging to polyketides lipid category (LMPK12113361, LMPK12113362, LMPK12113363, LMPK12113382, LMPK12113381, LMPK12113364 or LMPK12113383; LMGP01010463, LMGP01010704, LMGP01010444, LMGP01010564, LMGP01010537, LMGP01011080, LMGP01010997, LMGP01011062, LMGP01010970, LMGP01010739, LMGP01010418, LMGP01010488, LMGP01011267 or LMGP01010397)	10.31	15.51	66.60	29.52	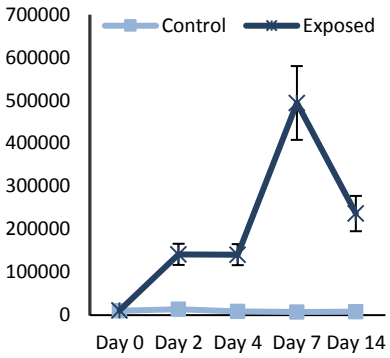

According to literature, liver has been found to be a key organ for absorption, bioaccumulation, energy metabolism, protein biosynthesis, xenobiotic detoxification, endocrine, as well as immune responses in multiple toxicity studies [44]. Therefore, the specific reason behind the alterations found in liver might be the effect of any of them or even the combination of a few ones.

8.3.2 Plasma metabolome alterations

In the case of plasma, the metabolites suggested by pathway enrichment (see Table 8.4) were combined based on KEGG to form a metabolic network, giving a holistic view of metabolic changes in the organism. As can be observed in Figure 8.3, those metabolites are mainly involved in the alteration of the lipid metabolism and the suggested perturbed pathways were: fatty acid elongation, α-linolenic acid metabolism, biosynthesis of unsaturated fatty acids and fatty acid metabolism.

The alterations of 8 metabolites in lipid metabolism can be related to oxidative stress since several authors have reported that UV filters such as oxybenzone generate oxidative stress in fish [15,16]. Similarly to the present work, lipid storage disorder associated with oxidative stress has been already reported as an adverse effect of different xenobiotics [36,45–47]. In this work, the concentrations of 5 unsaturated fatty acids (γ-linolenic acid, α-linolenic acid, docosahexaenoic acid,

nervonic acid and docosadienoic acid) in plasma were altered in oxybenzone-exposed fish. Unsaturated fatty acids serve as substrates for lipoxygenases, which are capable of oxidizing many xenobiotics [48]. Actually, oxidized oxybenzone degradation products were observed in a previous work of our research group [5].

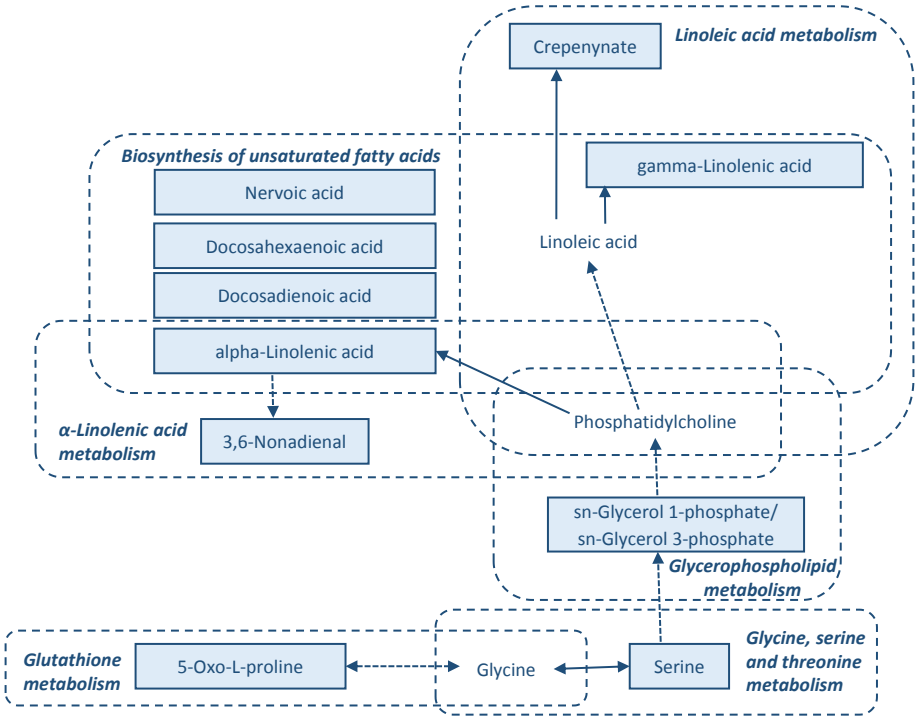

***Figure 8.3**: Altered metabolites and pathways in fish plasma.*

Among the altered fatty acids, docosahexaenoic acid is used for assessing oxidative stress *in vivo* [49], and its alteration was observed with other xenobiotics [46,47]. Metabolites belonging to linoleic acid and linolenic acid metabolism are used to identify oxidative stress episodes [45,49]. Concretely, similarly to other exposure studies [45], we observed alterations in the levels of lipid peroxidation products of both linoleic acid (e.g., γ-linolenic acid and crepenynate) and α-linolenic acid (e.g., α-linolenic acid and 3,6-nonadienal) pathways, which are consistent markers of higher oxidative states [50]. Observing lipid abnormalities in different lipid classes is common [46,51], and we also detected the alteration of *sn*-glycerol 1-phosphate/*sn*-glycerol 3-phosphate in the glycerophospholipid metabolism.

Table 8.4: *Daily fold change (FC) values and individual average peak areas (n=10, 95% confidence interval) for the metabolites whose concentrations were significantly altered in plasma after the oxybenzone-exposure.*

Metabolite	Fold change (FC)				Trends in control and exposed fish (Peak intensity vs Exposure Day)
	Day 2	Day 4	Day 7	Day 14	
3,6-Nonadienal	-1.35	-1.16	-1.04	-1.30	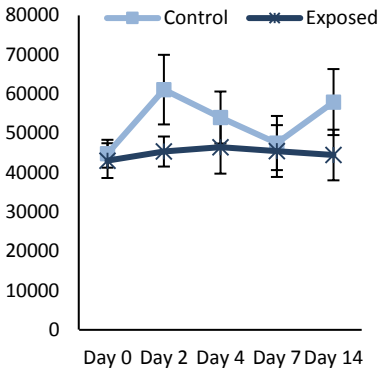
D-Serine	-1.04	-1.06	-1.64	-1.48	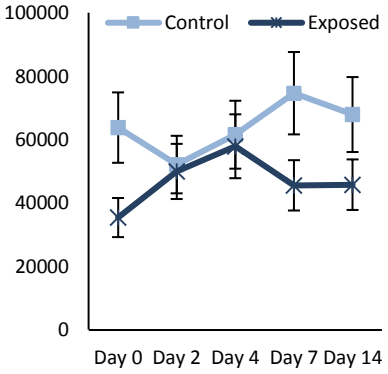
Nervonic acid	-1.11	1.17	1.19	1.15	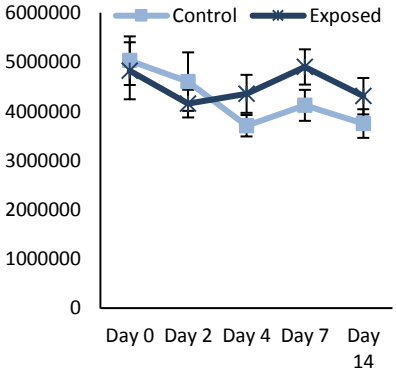

Table 8.4: *(Continuation).*

Metabolite	Fold change (FC)				Trends in control and exposed fish (Peak intensity vs Exposure Day)
	Day 2	Day 4	Day 7	Day 14	
sn-Glycerol 1-phosphate / sn-Glycerol 3-phosphate	1.31	1.58	1.58	1.93	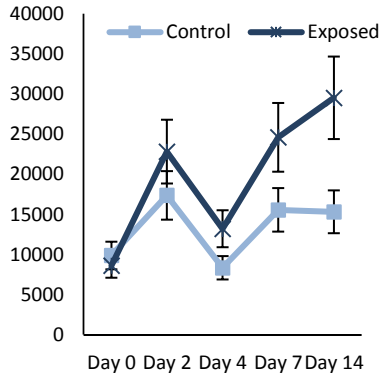
Docosahexaenoic acid	-1.11	1.01	1.02	1.21	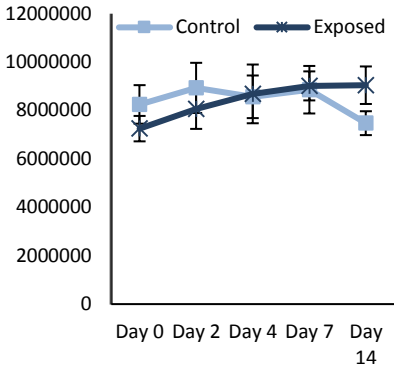
Docosadienoic acid	1.02	1.19	1.29	1.14	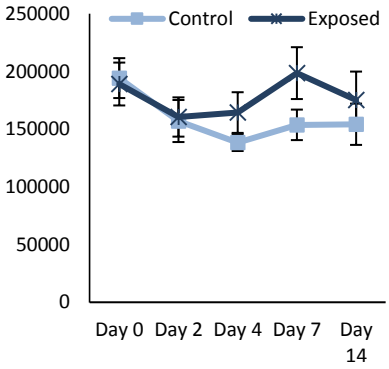

Table 8.4: *(Continuation).*

Metabolite	Fold change (FC)				Trends in control and exposed fish (Peak intensity vs Exposure Day)
	Day 2	Day 4	Day 7	Day 14	
D-Serine	1.23	1.05	-1.11	-1.27	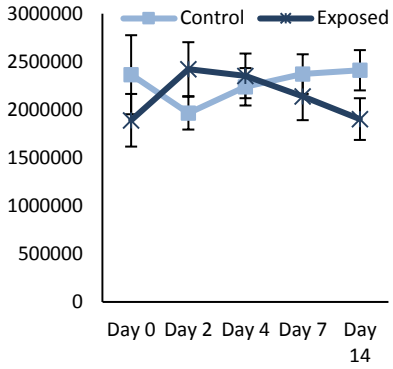
γ-Linolenic acid / α-Linolenic acid / Crepenynate	1.04	1.13	1.25	1.49	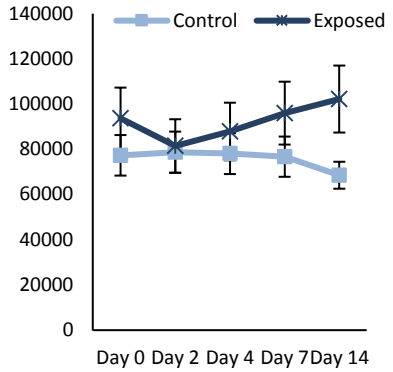
5-Oxo-L-proline	1.07	1.03	-1.20	-1.28	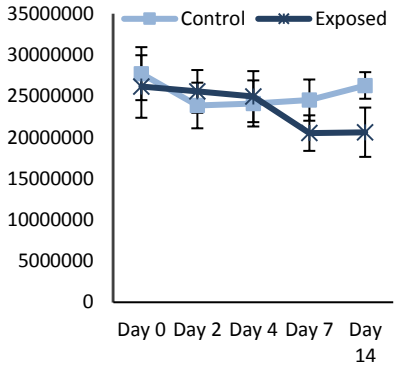

Table 8.4: *(Continuation).*

Metabolite	Fold change (FC)				Trends in control and exposed fish (Peak intensity vs Exposure Day)
	Day 2	Day 4	Day 7	Day 14	
14 candidates belonging to glycerophospholipids lipid category (LMGP01010463, LMGP01010704, LMGP01010444, LMGP01010564, LMGP01010537, LMGP01011080, LMGP01010997, LMGP01011062, LMGP01010970, LMGP01010739, LMGP01010418, LMGP01010488, LMGP01011267 or LMGP01010397)	-1.61	-1.31	-1.01	-3.67	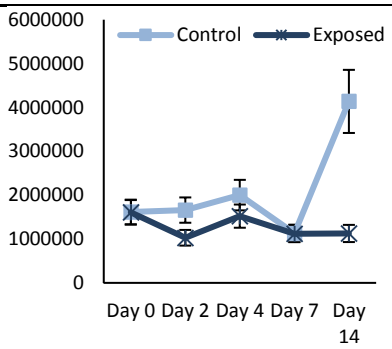

Lastly, we observed the alteration of the amino acid serine, which is an essential precursor for the synthesis of lipids [52]. The alteration of amino acid metabolism, including serine, is also reported with other xenobiotics [37,53]. In fact, Zhang and co-workers stated that the disruption of the amino acid metabolism related to serine is indicative of oxidative stress [37]. Therefore, the lower serine levels that we detected after 14-day oxybenzone exposure (see Table 8.4) might have caused a more significant cellular response to the higher reactive oxygen species (ROS) content, which is consistent with other works that observed serine deficiency in plasma under oxidative stress [54]. The reason behind this might be the role of serine linking biosynthetic flux from glycolysis to the synthesis on antioxidant glutathione [55], because glutathione depletion causes accumulation of ROS [56]. Actually, in the present work there is a sign of glutathione metabolism perturbation since 5-oxo-L-proline was altered in the exposed fish. 5-oxoproline is an intermediate in the biosynthesis of glutathione, and although it is known as a potential biomarker for hepatotoxicity, xenobiotic-induced 5-oxoproline alterations are observed in various biofluids/tissues including liver, urine and plasma [57]. In exposure studies, finding alterations of glutathione-related pathways is common since there are enzymes that are important in xenobiotic metabolism [53]. As an example of glutathione-related pathway disruption, Eguchi and co-workers [53] reported glutathione as possible candidate biomarker for polychlorinated biphenyls exposure. Furthermore, in a study with zebrafish, oxybenzone also perturbed glutathione peroxidase expression involved in cellular redox balance [16], which is consistent with the observation in this work.

8.4 Conclusions

The present study showed that despite an absence of mortality or alterations in general physiological parameters (i.e, fish weight and length, K and HSI) and brain metabolome, oxybenzone produces significant metabolic perturbations in both liver and plasma of fish. Briefly, from the results it can be concluded a possible energy metabolism modification and oxidative stress. The latter has important health implications [51] since it damages cellular structures and functions, significantly influencing life histories of fish through interactions with growth, reproduction and body maintenance and, hence, future fitness and survival [58]. Therefore, this research indicates that oxybenzone has adverse effects beyond the commonly studied hormonal activity [6,11–14], and proves the usefulness of the metabolomic approach to study the modes of action. Consequently, complementary to receptor binding and gene expression assays, ERA should consider metabolomic studies to detect perturbations at molecular level to investigate the effects of xenobiotics at non-lethal levels.

8.5 References

1. Tsui MMP, Leung HW, Lam PKS, Murphy MB. 2014. Seasonal occurrence, removal efficiencies and preliminary risk assessment of multiple classes of organic UV filters in wastewater treatment plants. *Water Res.* 53:58–67.
2. Al-Salhi R, Abdul-Sada A, Lange A, Tyler CR, Hill EM. 2012. The Xenometabolome and Novel Contaminant Markers in Fish Exposed to a Wastewater Treatment Works Effluent. *Environ. Sci. Technol.* 46:9080–9088.
3. Molins-Delgado D, Muñoz R, Nogueira S, Alonso MB, Torres JP, Malm O, Ziolli RL, Hauser-Davis RA, Eljarrat E, Barceló D, Díaz-Cruz MS. 2018. Occurrence of organic UV filters and metabolites in lebranche mullet (Mugil liza) from Brazil. *Sci. Total Environ.* 618:451–459.
4. Ramos S, Homem V, Alves A, Santos L. 2015. Advances in analytical methods and occurrence of organic UV-filters in the environment — A review. *Sci. Total Environ.* 526:278–311.
5. Ziarrusta H, Mijangos L, Montes R, Rodil R, Anakabe E, Izagirre U, Prieto A, Etxebarria N, Olivares M, Zuloaga O. 2018. Study of bioconcentration of oxybenzone in gilt-head bream and characterization of its by-products. *Chemosphere*. doi:10.1016/j.chemosphere.2018.05.154.
6. Blüthgen N, Zucchi S, Fent K. 2012. Effects of the UV filter benzophenone-3 (oxybenzone) at low concentrations in zebrafish (Danio rerio). *Toxicol. Appl. Pharmacol.* 263:184–194.

7. Coronado M, De Haro H, Deng X, Rempel MA, Lavado R, Schlenk D. 2008. Estrogenic activity and reproductive effects of the UV-filter oxybenzone (2-hydroxy-4-methoxyphenyl-methanone) in fish. *Aquat. Toxicol.* 90:182–187.

8. Díaz-Cruz MS, Barceló D. 2009. Chemical analysis and ecotoxicological effects of organic UV-absorbing compounds in aquatic ecosystems. *TrAC Trends Anal. Chem.* 28:708–717.

9. Fent K, Kunz PY, Zenker A, Rapp M. 2010. A tentative environmental risk assessment of the UV-filters 3-(4-methylbenzylidene-camphor), 2-ethyl-hexyl-4-trimethoxycinnamate, benzophenone-3, benzophenone-4 and 3-benzylidene camphor. *Mar. Environ. Res.* 69:S4–S6.

10. Ghazipura M, McGowan R, Arslan A, Hossain T. 2017. Exposure to benzophenone-3 and reproductive toxicity: A systematic review of human and animal studies. *Reprod. Toxicol.* 73:175–183.

11. Kim S, Jung D, Kho Y, Choi K. 2014. Effects of benzophenone-3 exposure on endocrine disruption and reproduction of Japanese medaka (Oryzias latipes)—A two generation exposure study. *Aquat. Toxicol.* 155:244–252.

12. Kim S, Choi K. 2014. Occurrences, toxicities, and ecological risks of benzophenone-3, a common component of organic sunscreen products: A mini-review. *Environ. Int.* 70:143–157.

13. Kinnberg KL, Petersen GI, Albrektsen M, Minghlani M, Awad SM, Holbech BF, Green JW, Bjerregaard P, Holbech H. 2015. Endocrine-disrupting effect of the ultraviolet filter benzophenone-3 in zebrafish, Danio rerio. *Environ. Toxicol. Chem.* 34:2833–2840.

14. Kunz PY, Galicia HF, Fent K. 2006. Comparison of In Vitro and In Vivo Estrogenic Activity of UV Filters in Fish. *Toxicol. Sci.* 90:349–361.

15. Liu H, Sun P, Liu H, Yang S, Wang L, Wang Z. 2015. Hepatic oxidative stress biomarker responses in freshwater fish Carassius auratus exposed to four benzophenone UV filters. *Ecotoxicol. Environ. Saf.* 119:116–122.

16. Rodríguez-Fuentes G, Sandoval-Gío JJ, Arroyo-Silva A, Noreña-Barroso E, Escalante-Herrera KS, Olvera-Espinosa F. 2015. Evaluation of the estrogenic and oxidative stress effects of the UV filter 3-benzophenone in zebrafish (Danio rerio) eleuthero-embryos. *Ecotoxicol. Environ. Saf.* 115:14–18.

17. Cajka T, Fiehn O. 2016. Toward Merging Untargeted and Targeted Methods in Mass Spectrometry-Based Metabolomics and Lipidomics. *Anal. Chem.* 88:524–545.

18. Huang SSY, Benskin JP, Chandramouli B, Butler H, Helbing CC, Cosgrove JR. 2016. Xenobiotics Produce Distinct Metabolomic Responses in Zebrafish Larvae (Danio rerio). *Environ. Sci. Technol.* 50:6526–6535.

19. Vinaixa M, Samino S, Saez I, Duran J, Guinovart JJ, Yanes O. 2012. A Guideline to Univariate

Statistical Analysis for LC/MS-Based Untargeted Metabolomics-Derived Data. *Metabolites*. 2:775–795.

20. Picart-Armada S, Fernández-Albert F, Vinaixa M, Rodríguez MA, Aivio S, Stracker TH, Yanes O, Perera-Lluna A. 2017. Null diffusion-based enrichment for metabolomics data. *PLOS ONE*. 12:e0189012.

21. http://www.kegg.jp/kegg/. 2018. KEGG_.

22. Ribbenstedt A, Ziarrusta H, Benskin JP. 2018. A Multi-platform Targeted/Non-targeted (TNT) approach for quantitative and discovery-based metabolomics. *PLOS ONE (submitted)*.

23. Broadhurst D, Goodacre R, Reinke SN, Kuligowski J, Wilson ID, Lewis MR, Dunn WB. 2018. Guidelines and considerations for the use of system suitability and quality control samples in mass spectrometry assays applied in untargeted clinical metabolomic studies. *Metabolomics*. 14.

24. Fulton WT. 1904. The rate of growth of fishes. *22nd Annu. Rep. Fish. Board Scotl.* 3:141–241.

25. http://www.lipidmaps.org/. 2018. LipidMaps_.

26. Fernández-Albert F, Llorach R, Garcia-Aloy M, Ziyatdinov A, Andres-Lacueva C, Perera A. 2014. Intensity drift removal in LC/MS metabolomics by common variance compensation. *Bioinformatics*. 30:2899–2905.

27. Schymanski EL, Jeon J, Gulde R, Fenner K, Ruff M, Singer HP, Hollender J. 2014. Identifying Small Molecules via High Resolution Mass Spectrometry: Communicating Confidence. *Environ. Sci. Technol.* 48:2097–2098.

28. https://www.mzcloud.org/. 2018. mzCloud_.

29. https://msbi.ipb-halle.de/MetFragBeta/. 2018. MetFrag_.

30. Fediuk DJ, Wang T, Raizman JE, Parkinson FE, Gu X. 2010. Tissue Deposition of the Insect Repellent DEET and the Sunscreen Oxybenzone From Repeated Topical Skin Applications in Rats. *Int. J. Toxicol.* 29:594–603.

31. Li J, Ilangovan U, Daubner SC, Hinck AP, Fitzpatrick PF. 2011. Direct evidence for a phenylalanine site in the regulatory domain of phenylalanine hydroxylase. *Arch. Biochem. Biophys.* 505:250–255.

32. Wang J, Wang Y, Zhang X, Liu J, Zhang Q, Zhao Y, Peng J, Feng Q, Dai J, Sun S, Zhao Y, Zhao L, Zhang Y, Hu Y, Zhang M. 2017. Gut Microbial Dysbiosis Is Associated with Altered Hepatic Functions and Serum Metabolites in Chronic Hepatitis B Patients. *Front. Microbiol.* 8.

33. Zhang H, Zhao L. 2017. Influence of sublethal doses of acetamiprid and halosulfuron-methyl on metabolites of zebra fish (Brachydanio rerio). *Aquat. Toxicol.* 191:85–94.

34. Ling YS, Liang H-J, Chung M-H, Lin M-H, Lin C-Y. 2014. NMR- and MS-based metabolomics: various organ responses following naphthalene intervention. *Mol. Biosyst.* 10:1918–1931.

35. Yuan T-H, Chung M-K, Lin C-Y, Chen S-T, Wu K-Y, Chan C-C. 2016. Metabolic profiling of residents in the vicinity of a petrochemical complex. *Sci. Total Environ.* 548–549:260–269.

36. Buron N, Porceddu M, Roussel C, Begriche K, Trak-Smayra V, Gicquel T, Fromenty B, Borgne-Sanchez A. 2017. Chronic and low exposure to a pharmaceutical cocktail induces mitochondrial dysfunction in liver and hyperglycemia: Differential responses between lean and obese mice. *Environ. Toxicol.* 32:1375–1389.

37. Zhang J, Shen H, Xu W, Xia Y, Barr DB, Mu X, Wang X, Liu L, Huang Q, Tian M. 2014. Urinary Metabolomics Revealed Arsenic Internal Dose-Related Metabolic Alterations: A Proof-of-Concept Study in a Chinese Male Cohort. *Environ. Sci. Technol.* 48:12265–12274.

38. Amorim LC, Alvarez-Leite EM. 1997. Determination of o-cresol by gas chromatography and comparison with hippuric acid levels in urine samples of individuals exposed to toluene. *J. Toxicol. Environ. Health*. 50:401–407.

39. Colet J-M. 2015. Metabonomics in the preclinical and environmental toxicity field. *Drug Discov. Today Technol.* 13:3–10.

40. Robertson DG. 2005. Metabonomics in Toxicology: A Review. *Toxicol. Sci.* 85:809–822.

41. Khan A, Park H, Lee HA, Park B, Gwak HS, Lee H-R, Jee SH, Park YH. 2017. Elevated Metabolites of Steroidogenesis and Amino Acid Metabolism in Preadolescent Female Children With High Urinary Bisphenol A Levels: A High-Resolution Metabolomics Study. *Toxicol. Sci.* 160:371–385.

42. Zhang J, Liu L, Wang X, Huang Q, Tian M, Shen H. 2016. Low-Level Environmental Phthalate Exposure Associates with Urine Metabolome Alteration in a Chinese Male Cohort. *Environ. Sci. Technol.* 50:5953–5960.

43. Maharjan Shreekrishna, Serova Lidia, Sabban Esther L. 2005. Transcriptional regulation of tyrosine hydroxylase by estrogen: opposite effects with estrogen receptors α and β and interactions with cyclic AMP. *J. Neurochem.* 93:1502–1514.

44. Qiao Q, Le Manach S, Sotton B, Huet H, Duvernois-Berthet E, Paris A, Duval C, Ponger L, Marie A, Blond A, Mathéron L, Vinh J, Bolbach G, Djediat C, Bernard C, Edery M, Marie B. 2016. Deep sexual dimorphism in adult medaka fish liver highlighted by multi-omic approach. *Sci. Rep.* 6.

45. Lin Z, Roede JR, He C, Jones DP, Filipov NM. 2014. Short-term oral atrazine exposure alters the plasma metabolome of male C57BL/6 mice and disrupts α-linolenate, tryptophan, tyrosine and other major metabolic pathways. *Toxicology*. 326:130–141.

46. Salihovic S, Ganna A, Fall T, Broeckling CD, Prenni JE, van Bavel B, Lind PM, Ingelsson E, Lind L.

2016. The metabolic fingerprint of p,p'-DDE and HCB exposure in humans. *Environ. Int.* 88:60–66.

47. Wafa T, Amel N, Issam C, Imed C, Abdelhedi M, Mohamed H. 2011. Subacute effects of 2,4-dichlorophenoxyacetic herbicide on antioxidant defense system and lipid peroxidation in rat erythrocytes. *Pestic. Biochem. Physiol.* 99:256–264.

48. Kulkarni AP. 2001. Lipoxygenase - a versatile biocatalyst for biotransformation of endobiotics and xenobiotics. *Cell. Mol. Life Sci. CMLS*. 58:1805–1825.

49. Yoshida Y, Umeno A, Shichiri M. 2013. Lipid peroxidation biomarkers for evaluating oxidative stress and assessing antioxidant capacity in vivo. *J. Clin. Biochem. Nutr.* 52:9–16.

50. Shearer GC, Newman JW. 2008. Lipoprotein Lipase releases esterified oxylipins from Very Low Density Lipoproteins. *Prostaglandins Leukot. Essent. Fatty Acids*. 79:215–222.

51. Chen C-HS, Yuan T-H, Shie R-H, Wu K-Y, Chan C-C. 2017. Linking sources to early effects by profiling urine metabolome of residents living near oil refineries and coal-fired power plants. *Environ. Int.* 102:87–96.

52. Hanada K. 2003. Serine palmitoyltransferase, a key enzyme of sphingolipid metabolism. *Biochim. Biophys. Acta BBA - Mol. Cell Biol. Lipids*. 1632:16–30.

53. Eguchi A, Sakurai K, Watanabe M, Mori C. 2017. Exploration of potential biomarkers and related biological pathways for PCB exposure in maternal and cord serum: A pilot birth cohort study in Chiba, Japan. *Environ. Int.* 102:157–164.

54. Zhou Xihong, He Liuqin, Wu Canrong, Zhang Yumei, Wu Xin, Yin Yulong. 2017. Serine alleviates oxidative stress via supporting glutathione synthesis and methionine cycle in mice. *Mol. Nutr. Food Res.* 61:1700262.

55. Parker SJ, Metallo CM. 2016. Chasing One-Carbon Units to Understand the Role of Serine in Epigenetics. *Mol. Cell*. 61:185–186.

56. Dixon SJ, Stockwell BR. 2014. The role of iron and reactive oxygen species in cell death. *Nat. Chem. Biol.* 10:9–17.

57. Geenen S, Guallar-Hoyas C, Michopoulos F, Kenna JG, Kolaja KL, Westerhoff HV, Thomas P, Wilson ID. 2011. HPLC-MS/MS methods for the quantitative analysis of 5-oxoproline (pyroglutamate) in rat plasma and hepatic cell line culture medium. *J. Pharm. Biomed. Anal.* 56:655–663.

58. Birnie-Gauvin K, Costantini D, Cooke SJ, Willmore WG. 2017. A comparative and evolutionary approach to oxidative stress in fish: A review. *Fish Fish.* 18:928–942.

Chapter 9

Determination of fluoroquinolones in fish tissues, biological fluids, and environmental waters by liquid chromatography tandem mass spectrometry

Analytical and Bioanalytical Chemistry

409 (2017) 6359-6370

9.1 Introduction

Over the last decades, pharmaceuticals and personal-care products have been recognized as a major source of pollution for the aquatic environment [1–3]. Among pharmaceuticals, fluoroquinolones (FQs) [4], which are a group of synthetic, highly potent antibiotics used in human and veterinary medicine for the treatment of respiratory diseases and enteric bacterial infections, are often found in the environment [5]. FQs, like many other pharmaceuticals, are neither completely metabolized in the human body nor completely removed in wastewater treatment plants (WWTPs) [6], leading to different exposure scenarios in water and soil systems [6,7]. Even though FQs are susceptible of photo- and biodegradation [6,7], the presence of a heterocyclic group in their structure makes them resistant to hydrolysis and heat [8]. Consequently, they are persistent in the environment [9], and although they are present at low concentration levels (ng/L level), it cannot be overlooked that these biologically active molecules and their transformation products can be accumulated in the tissues of non-target aquatic organisms and may affect them through long term exposure during their entire life cycle [10]. The concern about the widespread presence of pharmaceuticals in the environment is also reflected in some European legislation. For instance, the EU included ciprofloxacin (CIPRO) and ofloxacin (OFLO) in a regulatory guidance (Directive 2013/39/EU amending Directives 2000/60/EC and 2008/105/EC [11]) and established the Predicted Environmental Concentration (PEC) values for CIPRO and OFLO at 278 ng/L and 90 ng/L, respectively, while the Predicted No Effect Concentration (PNEC) values were fixed at 130 ng/L and 89 ng/L for both analytes, respectively.

Most studies are limited to the monitoring of FQs in environmental waters [6,12–15] whereas the studies focused on the analysis of FQs in biological tissues are scarce or only targeted to a few FQs [16,17]. Exemplarily, Zhao and co-workers [17] investigated the bioaccumulation of only five antibiotics (CIPRO, enrofloxacin (ENRO), norfloxacin (NORF), lomefloxacin (LOME) and OFLO) in bile, plasma, liver and muscle tissues of wild fish from different rivers in the Pearl River Delta region, and all of them (except NORF) were detected in the analyzed tissues and biofluids at concentrations up to 334 μg/L. In another work, Wagil and co-workers [16] proposed a sensitive method to determine only three FQs (ENRO, NORF and CIPRO) in river water and aquatic

organisms, and the three of them were detected in river water at environmentally relevant concentrations (ng/L level) and in fishes at concentrations slightly lower than the maximum residue level (100 ng/g) established by the European Medicine Evaluation Agency (EMEA) [18]. These results indicate that, among aquatic organisms, fish can be considered adequate organisms for bioaccumulation and monitoring studies of FQs [19]. Consequently, the development of robust and sensitive analytical methods to determine more FQs antibiotics in complex environmental samples, especially in biota, is a highly required analytical task [3].

According to the literature, FQs have been extracted from food samples using pressurized liquid extraction [20], from soil and feeding stuffs by ultrasound-assisted extraction [9,21], from soil, sediments and sludge using microwave-assisted extraction [22]**,** from fish tissue and food by solid-liquid extraction [16,17,23,24] and from fish by matrix solid-phase dispersion [25] using pure organic solvents (e.g., methanol, acetonitrile, acetone) [20,22] or diluted acid/basic solutions [9,16,21,23,25]. In order to enhance the extraction yield, focused ultrasound solid-liquid extraction (FUSLE) has recently emerged as a potential technique for the extraction of organic compounds from biota [26,27]. FUSLE needs low amount of sample and solvent to extract the target analytes quantitatively in an easy, fast and reproducible process, but as far as we know, it has never been applied for the extraction of FQs in biota samples.

Regarding the analysis of FQs, even though liquid chromatography coupled to fluorescence detector (LC-FLD) [13] has shown to be adequate for the detection of FQs, liquid chromatography-tandem mass spectrometry (LC-MS/MS) has been the most preferred choice due to its good sensitivity and reliability to work at trace level [16,20,21,28]. Furthermore, LC-MS/MS allows the use of isotopically labeled deuterated analogues to get accurate results even when the chromatographic separation is not possible, while with LC-FLD time-consuming standard addition method is usually required to correct recoveries since labeled standards are not applicable due to chromatographic peak coelution. Electrospray ionization (ESI) in positive mode is the most common ionization source used in FQs analysis by LC-MS/MS [15,29,30] but it cannot reduce matrix effects causing suppression or enhancement of the chromatographic signal, leading to inaccurate results if they are not properly corrected using internal standards [31]. In order to minimize these effects, the sample extracts are often submitted to effective clean-up approaches.

Among them, reverse-phase solid phase extraction (RP-SPE) has been the most applied approach in the literature [9,24,28]. However, some applications using mixed-mode anion [12,17] or cation [14,16] exchange SPE and molecularly imprinted polymers (MIPs) [32] can also be found in the literature since they provide a more selective retention mechanism whereby cleaner extracts are obtained. Lastly, although other authors have proposed alternative extractive phases for the enhanced extraction of FQs [25,33,34], their applicability for routine analysis is limited because they are not often commercially available.

In this framework, the aim of the present work was to develop methods for the accurate and precise determination of ten FQs (NORF, enoxacin (ENO), pefloxacin (PEFLO), OFLO, levofloxacin (LEVO), CIPRO, danofloxacin (DANO), LOME, ENRO and sparfloxacin (SPAR)) in different environmental matrices, such as water (estuarine, seawater, WWTP effluent), fish tissues (muscle and liver) and biofluids (plasma and bile) in order to be applied in further studies dealing with their environmental distribution and accumulation patterns. For the latter, it is important to develop methods to analyze separately each tissue and biofluid, since the reported methods for analyzing FQs in fish are limited to fish homogenate or just muscle tissue [16,24,25]. For the mentioned purpose, the effectiveness of FUSLE was assessed for the extraction of FQs from tissues and different modes of SPE (reverse, mixed-mode and MIPs) were tested with clean-up/preconcentration purposes. Matrix effect was thoroughly studied both in the clean-up and LC-MS/MS analysis steps. Finally, the developed methods were applied to the analysis of real samples from the Biscay Coast.

9.2 Experimental

9.2.1 Reagents and materials

The chemical structures of the target analytes and the isotopically labelled standards, and the acidity constant (as pK_a) values, as well as the precursor and product ions and fragmentor (V) and collision energies (eV) used during the analysis, are included in Table 9.1. NORF (100%), ENO (98%), PEFLO (100%), OFLO (100%), LEVO (100%), CIPRO (98%), LOME (100%), DANO (99.6%), ENRO (98%) and SPAR (99%) and the deuterated analogues used as surrogates [$^2H_8$]–ciprofloxacin

([$^2H_8$]–CIPRO, 99.6%) and [$^2H_5$]–enrofloxacin ([$^2H_5$]–ENRO, 99%) were purchased from Sigma-Aldrich (St. Louis, MO, USA).

FQs were dissolved individually in methanol (MeOH, Fisher Scientific, Loughborough, UK) and two pellets of sodium hydroxide (NaOH, ≥ 99%, Merck, Darmstadt, Germany) were added in order to prepare approximately 500 mg/L stock solutions. Intermediate 50 mg/L dilutions were prepared in MeOH monthly and solutions at lower concentrations were weekly prepared owing to their instability. All stock solutions were stored in the darkness at −20 °C in silanized amber vials to avoid photodegradation [7].

Regarding the chemical reagents, MeOH (HPLC grade, 99.9%) and acetone (HPLC grade, 99.8%) were supplied by LabScan (Dublin, Ireland), acetonitrile (ACN, HPLC grade, 99.9%) and ammonium acetate (NH_4OAc, ≥ 99%) by Sigma–Aldrich, acetic acid (HOAc, 100%) by Merck, formic acid (HCOOH, ≥ 98%) by Scharlab (Barcelona, Spain) and ethylendiaminetetraacetic acid (EDTA, ≥ 99%) and ammonium hydroxide (NH_4OH, 25%) by Panreac (Barcelona, Spain). Ultra-pure water was obtained using a Milli-Q water purification system (< 0.05 µS/cm, Milli-Q model 185, Millipore, Bedford, MA, USA).

A Cryodos-50 laboratory freeze-dryer from Telstar Instrument (Sant Cugat del Valles, Barcelona, Spain) was used to freeze-dry the solid samples. An ultrasonic cell disruptor/homogenizer (100 W, 20 kHz; Bandelin Sonopuls HD 3100 sonifier, Bandelin Electronic, Berlin, Germany) equipped with a 3-mm titanium microtip was used for the extraction of FQs from fish tissues. Fractions were evaporated in a Turbo Vap LV Evaporator (Zymark, Hopkinton, MA, USA) using a gentle stream of nitrogen (> 99.999%; Messer, Tarragona, Spain).

Several SPE cartridges were used for clean-up purposes. Florisil LC cartridges (1 g, 6 mL) were purchased from Supelco (Walton-on-Tames, UK), AFFINILUTE MIP Fluoroquinolones (25 mg, 3 mL), mixed-mode weak anion exchange Evolute-WAX cartridges (200 mg, 6 mL) and mixed-mode strong cation exchange Evolute-CX cartridges (200 mg, 6 mL) from Biotage (Uppsala, Sweeden), and mixed-mode strong anion exchange Oasis-MAX cartridges (150 mg, 6 mL) and Oasis-HLB (200 mg, 6 mL) from Waters Corporation (Milford, USA).

Table 9.1: *pKa values, precursor and product ions (m/z), fragmentor (V), collision energies (eV), determination coefficients (r^2) of the calibration curves (LOQ-2000 µg/L range), instrumental limits of detection (LODs) and quantification (LOQs) for each target analyte and isotopically labelled standards.*

Analyte	pKa_1; pKa_2	Precursor ion (m/z)	Product ions (m/z)	Fragmentor (V)	Collision energy (eV)	r^2	LOD (µg/L)	LOQ (µg/L)
NORF	5.77; 8.68	320	302/231/282	104	17/41/29	0.9973	2	5
ENO	5.50; 8.59	321	303/232/204	104	17/37/45	0.9979	2	5
PEFLO	5.66; 6.47	334	316/290/233	104	17/13/25	0.9993	1	2
OFLO	5.45; 6.20	362	318/261/344	104	17/25/17	0.9997	1	2
LEVO	5.45; 6.20	362	318/261/344	104	17/25/17	0.9997	1	2
CIPRO	5.76; 8.68	332	314/231/288	104	17/41/13	0.9977	2	5
DANO	5.65; 6.73	358	340/82/255	104	21/45/41	0.9987	1	2
LOME	5.64; 8.70	352	265/308/334	104	21/13/17	0.9992	1	2
ENRO	5.69; 6.68	360	342/316/286	104	17/17/37	0.9997	0.5	1
SPAR	5.75; 8.79	393	349/292/375	104	17/21/17	0.9994	0.1	0.2
$[^2H_8]$–CIPRO	-	340	332/296	104	17/17	0.9975	2	5
$[^2H_5]$–ENRO	-	365	347/321	104	37/37	0.9996	0.5	1

All sample extracts were filtered with polypropylene (PP) microfilters (0.22 µm, 13 mm) delivered by Phenomenex (California, USA) before LC-MS/MS. In the LC-MS/MS analysis Milli-Q water and UHPLC-MS MeOH (Scharlau, Barcelona, Spain) were used as mobile phase eluent and formic acid Optima (HCOOH, Fischer Scientific, Gell, Belgium) was used for mobile phase modifications. High purity nitrogen gas (> 99.999%) supplied by Messer (Tarragona, Spain) was used as collision gas and nitrogen gas (99.999%) provided by AIR Liquid (Madrid, Spain) was used as both nebulizer and drying gas.

9.2.2 Samples and sample preparation

For optimization and validation purposes liver, muscle, plasma and bile from gilt-head breams (*Sparus aurata*) obtained from Groupe Aqualande (Roquefort, France) and real water samples (WWTP effluent, seawater and estuarine water) collected in Gernika (Basque Country, Spain) were used. Since FQs are frequently found in real samples, and there were not available water samples free of FQs, water samples were aged for 3 months under sunlight and at room temperature in order to minimize their content in FQs and to be used during the optimization and validation steps.

The liver of thicklip gray mullets (*Chelon labrosus*) collected in Gernika estuary (43.324036, −2.673611) in June 2015 was analyzed using the developed method. Fish liver was separated using a clean scalpel and a pool of 5 individuals was homogenized and freeze-dried in a Cryodos-50 laboratory freeze-dryer. The homogenized freeze-dried samples were stored in amber glass bottles at −20 °C in the fridge until analysis. On the other hand, in the Biscay Coast (Basque Country, Spain) in February 2017 the following water samples were collected in pre-cleaned plastic bottles [1] and transported to the lab in cooled boxes to be analyzed within 24 h: WWTP effluent water (43.323985, −2.674143; Gernika), estuarine water (downstream of the WWTP; 43.324036, −2.673611; Gernika) and seawater (43.399241, −2.685750; Laida beach, Ibarrangelu).

9.2.3 Extraction and clean-up of biological tissues

The extraction of FQs from fish tissues was performed by means of a thoroughly optimized FUSLE. Since the fortification of samples via slurry was not possible [27], the optimization assays

were performed using homogenized and analyte-free biological tissues spiked at 400 ng/g concentration level. Under optimized conditions, 0.5 g of freeze-dried liver or muscle tissue were placed together with 7 mL of MeOH:HOAc (95:5, v/v) mixture in a 40-mL PP vessel and isotopically labelled standards ([$^2H_8$]-CIPRO and [$^2H_5$]-ENRO) were added as surrogates (40 µL of a 1-mg/L solution). The FUSLE was performed for 30 s (with a pulsed time on of 0.8 s and a pulsed time off of 0.2 s) and 10% of power at 0 °C in an ice-water bath. Two consecutive extractions were required to get quantitative recoveries. Once the extraction was over, the FUSLE extracts were centrifuged at 4000 rpm for 10 min, the supernatants were quantitatively recovered, combined, evaporated to ~1 mL under a nitrogen stream and submitted to the clean-up step.

During the optimization of the clean-up of liver and muscle extracts, several SPE modes and liquid-liquid extraction (LLE) were evaluated in terms of extract cleanliness and extraction yields. Regardless of the matrix and the clean-up procedure, the final eluate was evaporated to dryness at 35 °C under a nitrogen stream, reconstituted in 200 µL MeOH and filtered through a 0.22-µm PP filter prior to the LC-MS/MS analysis. Hereinafter, the analytical procedure used in each tested clean-up approach is briefly described.

9.2.3.1 Reverse-phase- SPE (RP-SPE)

For RP-SPE approach (optimum for muscle samples), the extract was adjusted at pH 7 by adding 6 mL of 0.1 M phosphate buffer and loaded onto an Oasis HLB cartridge that was previously conditioned with 5 mL of MeOH, 5 mL of Milli-Q water and 5 mL of phosphate buffer (pH 7). 5 mL of Milli-Q water was added as washing step, the cartridge was completely dried for 1 h under vacuum, and the analytes were recovered using 5 mL of MeOH.

9.2.3.2 Combination of reverse-phase and normal-phase SPE (RP-SPE + NP-SPE)

In this case, the extract was first loaded onto an Oasis-HLB cartridge and submitted to the procedure explained previously (see section 9.2.3.1). The recovered MeOH fraction was afterwards loaded onto a Florisil cartridge (1 g) previously conditioned with 5 mL of acetone and the elution of the FQs was performed with 5 mL of acetone.

9.2.3.3 Mixed-mode anion exchange SPE

The extract was adjusted at pH 10 by adding 6 mL of 0.1 M NH_4OAc. Before sample loading, Oasis MAX cartridge was conditioned with 5 mL of MeOH, 5 mL of Milli-Q water, and 5 mL of Milli-Q water previously adjusted to pH 10. After sample loading, the cartridge was washed first with 5 mL of Milli-Q water and then with 5 mL of MeOH and vacuum-dried for approximately 30 min. Target compounds were recovered with 5 mL of acetone containing 2.5% HCOOH (v/v).

9.2.3.4 Mixed-mode cation exchange SPE

In this case, the extract was diluted in 6 mL of Milli-Q water and the pH was adjusted at pH 4 and pH 6.5 with 0.4 M NaOH. The diluted extract was loaded onto a previously conditioned Evolute CX cartridge (same protocol used for anion exchange cartridges but conditioned at pH 4 or pH 6.5), washed with 5 mL of Milli-Q water and 5 mL of MeOH and the compounds were recovered with 5 mL of acetone containing 2.5% NH_4OH (v/v).

9.2.3.5 Liquid-liquid extraction combined with reverse-phase SPE (LLE + RP-SPE)

In this approach (optimum for liver samples), the FUSLE extract was diluted in 6 mL of Milli-Q water and 3 mL of *n*-hexane were added, vortex-mixed for 2 min and centrifuged at 3500 rpm for 5 min. The organic phase containing lipids was discarded and clean *n*-hexane was added for a second LLE. The fat free aqueous fraction was quantitatively recovered and submitted to an extra clean-up step by means of RP-SPE according to 9.2.3.1.

9.2.4 Extraction and clean-up of biological fluids

In the case of biofluids, 100 µL of bile or 250 µL of plasma were spiked (40 µL of a 1-mg/L solution) with isotopically labelled standards ($[^2H_8]$-CIPRO and $[^2H_5]$-ENRO) and pH was adjusted to 7.4 by addition of 1 mL of 50 mM phosphate buffer before SPE. Two approaches were tested based on: (i) RP- SPE using Oasis HLB (same procedure as in Section 9.2.3.1) and (ii) MIPs.

9.2.4.1 Molecularly imprinted polymers (MIPs)

The protocol recommended by the MIPs' supplier was adapted and used [35]. Briefly, the diluted plasma or bile sample (1 mL) was loaded onto a MIP cartridge that was previously

conditioned with 1 mL of MeOH and 2 mL of Milli-Q water. Three washing steps were applied, including 3 mL of Milli-Q water, 1 mL of ACN and 1 mL of 0.5% HOAc in ACN (v/v), and 1 mL of 0.1% NH_4OH in Milli-Q water. Cartridges were dried for 5 minutes in between each washing step and before the elution with 1 mL of 2% NH_4OH in MeOH (v/v).

9.2.5 Extraction and preconcentration of FQs from environmental aqueous samples

According to the literature, in the case of wastewater effluents, estuarine water and seawater, 0.1% (g/g) of EDTA was added [1,36] and the pH was adjusted to 7 using 0.1 M phosphate buffer before loading to the SPE cartridge. Two clean-up approaches were tested based on (i) RP-SPE (Oasis HLB) and (ii) combined mixed-mode SPE (Oasis WAX) and RP-SPE (Oasis HLB). While the former was adequate for seawater samples, the latter was necessary for samples of wastewater effluent and estuarine water.

9.2.5.1 RP-SPE

A 250-mL aliquot of water was passed through the Oasis HLB cartridge at 3 mL/min in the loading step, and the rest of the procedure was done as described in section 9.2.3.1.

9.2.5.2 Combination of mixed-mode anion exchange SPE and RP-SPE

Oasis WAX and Oasis HLB cartridges were conditioned with 5 mL of MeOH, 5 mL of Milli-Q water and 5 mL of Milli-Q water adjusted at pH 7. Water sample (250 mL) was passed through the in-lined coupled Oasis WAX and Oasis HLB cartridges, and the Oasis WAX cartridge was discarded before the next steps. 5 mL of Milli-Q water was added to the Oasis HLB cartridge as washing step before drying it for 1 h under vacuum and recovering the analytes in 5 mL of MeOH.

9.2.6 LC-MS/MS analysis

An Agilent 1260 series HPLC chromatograph equipped with a degasser, binary pump, autosampler and column oven coupled to an Agilent 6430 triple quadrupole (QqQ) mass spectrometer equipped with an ESI source (Agilent Technologies, Palo Alto, CA, USA) was used for the separation and quantification of FQs.

A Kinetex biphenyl 100 Å core-shell (2.1 mm x 50 mm, 2.6 µm) column with a Kinetex biphenyl 100 Å core-shell pre-column (2.1 mm x 5 mm, 2.6 µm) from Phenomenex (Torrance, CA, USA) column was used at 35 °C and 0.3 mL/min mobile phase flow rate to separate the target FQs. 3 µL of sample were injected in each run. Milli-Q water:MeOH (95:5, v/v) mixture was used as mobile phase A and Milli-Q water:MeOH (5:95, v/v) mixture as mobile phase B, both containing 0.1% HCOOH. The eluent gradient profile was as follows: 20% of B continued with a linear change to 25% in 0.5 min (hold time 3 min) followed with a linear increase to 85% B up to 8.5 min (hold time 3.5 min) and finishing with a linear change to 20% B up to 17.5 min (hold time 7.5 min) until 25 min in order to regain initial conditions.

For the MS detection, the instrument was operated in the positive ESI mode and the acquisition was performed in the selected reaction-monitoring (SRM) mode. The measuring parameters were fully optimized and were set as follows: a capillary voltage of 3000 V, a drying gas flow rate of 8 L/h, a nebulizer pressure of 50 psi and a drying gas temperature of 300 °C. The fragmentor electric voltage and the collision energy were also optimized for ESI in the 20–200 V and 5–60 eV ranges, respectively, by injection of individual compounds. Optimum conditions, as well as the precursor and product ions used, are summarized in Table 9.1 for each target compound. Instrumental operation, data acquisition and peak integration were performed with the Masshunter Workstation Software (Qualitative Analysis, Version B.06.00, Agilent Technologies).

9.3 Results and discussion

9.3.1 Stability of the standard solutions of FQs

The stability of the stock solutions of FQs can be affected mainly by light exposure and the presence of water. Since the effects can be enhanced at low concentration levels and long-term storage periods, the stability of stock solutions was tested at two concentration levels of FQs (50 µg/mL and 1 µg/mL) prepared in two different solvents (pure MeOH and Milli-Q water:MeOH (80:20, v/v) mixture) for 1 day, 2 days, 4 days, 1 week and 1 month stored in darkness and at controlled temperature conditions at -20 °C. All the stock solutions were quantified using

calibration curve built with fresh stock solutions of FQs in MeOH. The standard solutions prepared at the highest concentration level (50 μg/mL) were stable in both solvents for at least one month according to the one-way analysis of variance (ANOVA, p-value > 0.05). However, the standard solutions prepared at the lowest concentration level were only stable in MeOH for a 1-week period (p-value > 0.05). Thus, all the solutions (standards and extracts) were prepared in pure MeOH and the extracts were analyzed within 1 week.

9.3.2 Optimization and figures of merit of the LC-MS/MS analysis of FQs

LC-MS/MS parameters were fully optimized in terms of separation efficiency and sensitivity. Regarding the separation, statistically comparable chromatographic resolution (p-value > 0.05) was obtained for the tested column temperatures (30 °C, 35 °C and 40 °C). However, due to slightly worse chromatographic peak symmetries observed at 30 °C, the column temperature was set at intermediate value (35 °C) in order to enlarge the column lifetime. Similarly, the worst chromatographic peak shapes were obtained at low flow rates (i.e., 0.2 mL/min), whereas adequate peak sensitivity and resolution was obtained at higher flow rates (i.e., 0.3 mL/min and 0.4 mL/min). Thus, the runs were performed at 0.3 mL/min in order to analyze multiple samples in the same run without compromising the dirtying of the source. Even though different gradients were tested, it was not possible to chromatographically separate the enantiomers OFLO and LEVO. Therefore, only OFLO was considered for method development and validation purposes, and the concentration of these compounds in real samples was given as the sum of both. Figure 9.1a shows the chromatographic separation under optimized conditions for a standard solution of the target analytes at 1 μg/L.

Regarding the parameters affecting ESI, the drying gas temperature (300-350 °C), the drying gas flow rate (8-12 L/h), the nebulizer pressure (30-50 psi) and the capillary voltage (3000-6000 V) were studied (data not shown) and were finally fixed at 300 °C, 8 L/h, 50 psi and 3000 V, respectively. The optimum fragmentor voltage (20-200 V) and collision energy (5-60 eV) for each target analyte are included in Table 9.1. The cell accelerator voltage (1-7 V) rendered comparable responses in terms of sensitivity (p-value > 0.05) so that it was kept at the lowest value (1 V).

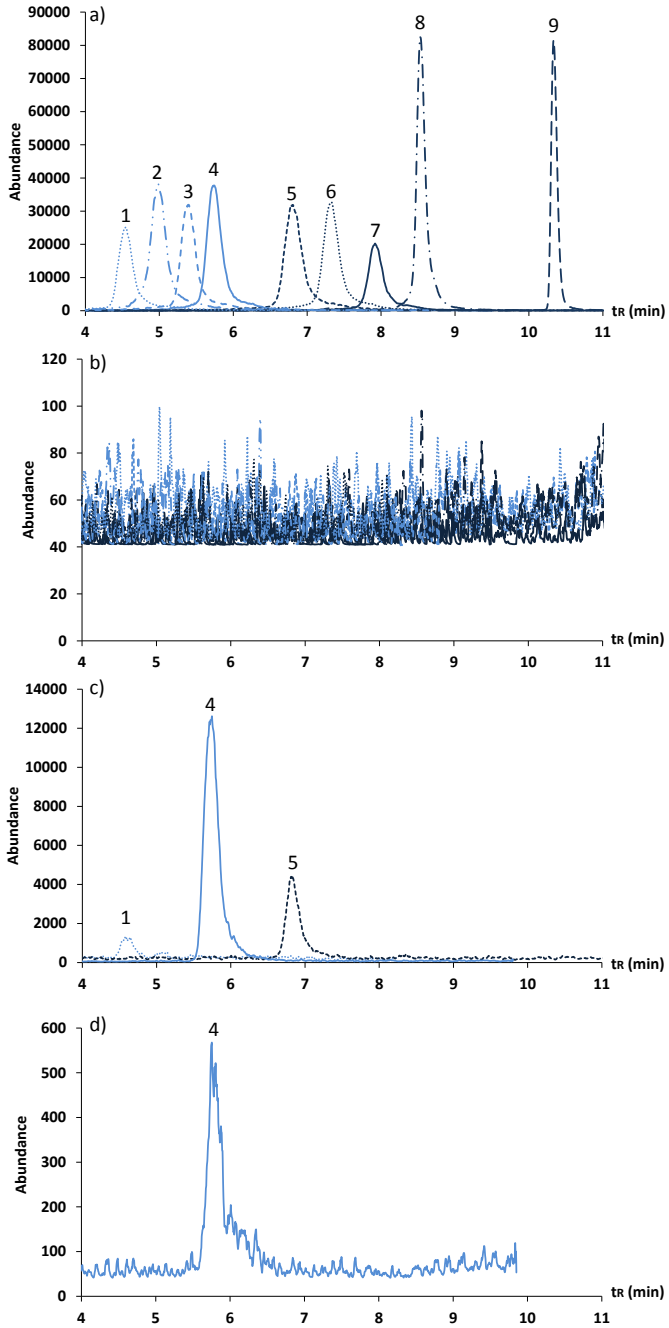

Figure 9.1: *SRM chromatograms of (a) a standard solution of the target FQs at 100 ng/mL, (b) solvent blank, (c) an estuarine water extract and (d) a mullet liver extract. 1≡ NORF; 2≡ ENO; 3≡ PEFLO; 4≡ OFLO/LEVO; 5≡ CIPRO; 6≡ DANO; 7≡ LOME; 8≡ ENRO; 9≡ SPAR.*

Finally, different injection volumes (2 µL, 3 µL, 4 µL, 5 µL and 10 µL) were tested. 3 µL was set as injection volume since it was the highest volume injected without chromatographic peaks being distorted.

Under optimized conditions, calibration curves were built with standard solutions in MeOH in the limit of quantification (LOQ) - 2000 µg/L range and at 10 concentration levels. Determination coefficients (r^2) in the range of 0.997-0.9997 were obtained for all the target analytes without correction with the corresponding labeled standard (see Table 9.1). Instrumental limits of detection (LODs) and quantification (LOQ) were estimated as the lowest concentration for which the peak area was at least three and ten times, respectively, the signal to noise ratio (S/N = 3 for LOD and S/N = 10 for LOQ). As can be observed in Table 9.1, the LODs and LOQs obtained were below 2 µg/L and 5 µg/L, respectively, which are similar to the values reported in other works for FQs using LC-MS/MS [16,20,29,30].

9.3.3 Extraction of FQs from liver and muscle

9.3.3.1 Optimization of FUSLE step

The optimization of FUSLE variables, including solvent type, extraction time and the number of consecutive extractions, was performed using 0.5 g (dry weight) gilt-head bream liver sample spiked with FQs at 400 ng/g. According to the literature, pure organic solvents such as MeOH and ACN or with some modifications such as Milli-Q water [37], HOAc to promote protein precipitation [38] and EDTA to avoid the adsorption of the ionizable compounds in extraction glassware [21] can be used as extraction solvents. In this work, five different extraction solvents were tested based on some procedures found in the literature: (i) pure ACN [37], (ii) a mixture of ACN:Milli-Q water (95:5, v/v) [37], (iii) a mixture of ACN:Milli-Q water containing 0.1% EDTA (95:5, v/v) [21], (iv) a mixture of ACN:HOAc (95:5, v/v) and (v) a mixture of MeOH:HOAc (95:5, v/v) [38]. The spiked liver tissues were extracted with 7 mL of the different solvents mentioned above for 30 s. After the extraction step, the extracts were submitted to a clean-up step with Oasis-HLB RP-SPE cartridges before LC-MS/MS analysis.

The average (n=3) recoveries obtained, normalized to the highest recovery, are summarized in Figure 9.2. Overall, higher recoveries were obtained when a polar modifier was added to ACN

and in the presence of HOAc. In fact, among all the tested combinations, the use of the most polar organic solvent (MeOH) containing HOAc (5%) provided the best extraction yields and it was chosen as extraction solvent for further experiments.

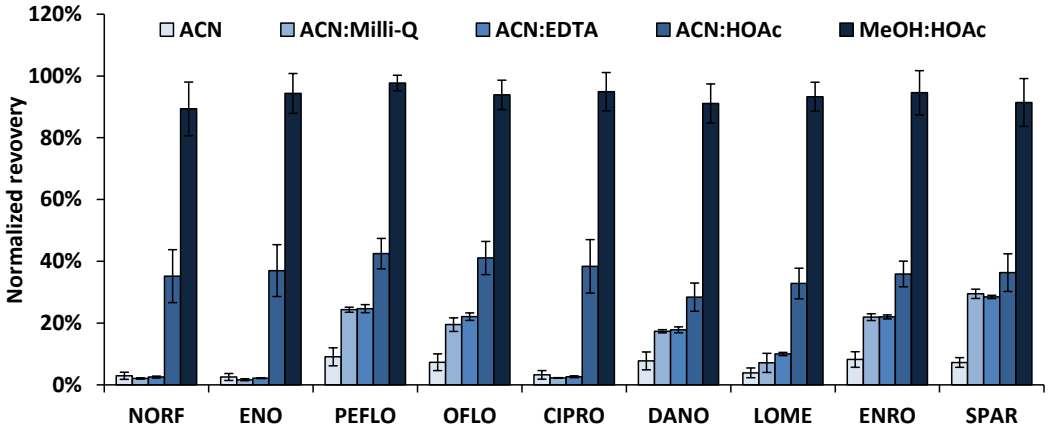

Figure 9.2: *Influence of solvent type during FUSLE extraction of FQs in fish liver. The results are expressed as recovery of the analytes after clean-up step normalized to the highest value and standard deviations (n=3, 95% confidence level).*

The extraction time (30 s and 2.5 min) and the number of consecutive extractions required for quantitative extraction were tested afterwards. Other variables such as the ultrasound pulse time (0.8 s), the solvent volume (7 mL), the sonication power (10%) and the extraction temperature (0 °C) were fixed according to the experience of the research group [26]. The extraction time had no significant effect on the extraction yield (p-value > 0.05), but a single extraction rendered absolute recoveries lower than 80% for all the analytes. Thus, two consecutive 30-s extractions were tested and the sum of the two extraction cycles yielded quantitative extractions (92-115%), except for OFLO (69%), which was not detected in the second extraction. Two consecutive extractions were also necessary in other works dealing with the analysis of FQs in fish tissues [24,39].

9.3.3.2 Optimization of the clean-up step

Due to the high lipid content of fish liver extracts, several clean-up approaches were investigated. In a first attempt, the efficiency of three SPE cartridges (Oasis-HLB, Oasis-MAX and Evolute-CX) was evaluated in terms of recovery and using Milli-Q water at the corresponding pH

and spiked at 400 µg/L. The adjustment of the pH is essential to guarantee good recoveries of the FQs because of their zwitterionic behavior with two ionizable groups in the molecule (the 3-carboxyl group and the N-4 of the piperazine substituent). According to the results shown in Figure 9.3 (normalized to the highest recoveries), the use of Evolute-CX cartridges rendered the lowest recoveries regardless of the pH used (pH 4 and pH 6.5), pointing out that the retention of these compounds by cation exchange mechanism is not strong enough. Slightly better results were obtained by anion-exchange mechanism (Oasis MAX, pH 12) but still inadequate. Oasis-HLB (pH 7) rendered the highest extraction efficiencies and it was selected and used as clean-up purposes.

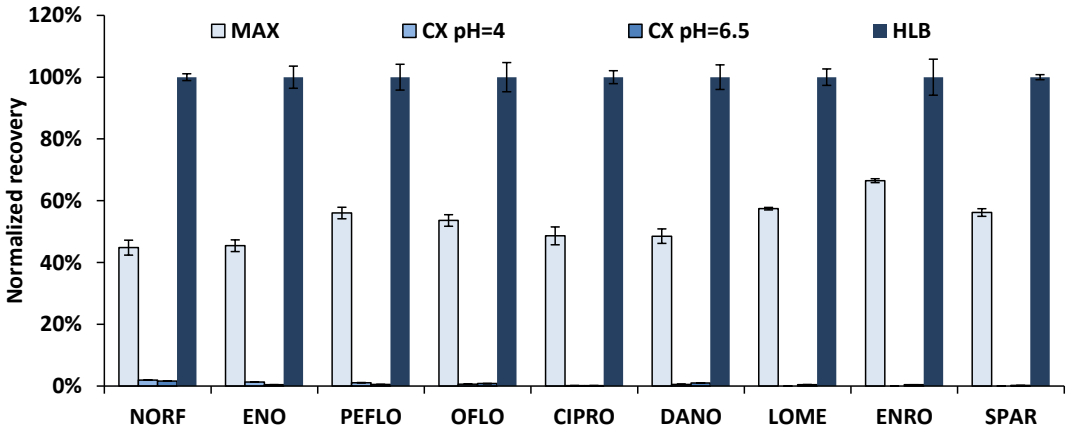

Figure 9.3: *Normalized recovery and standard deviations (n=3, 95% confidence level) of the target compounds from the different sorbents (MAX, CX and Oasis-HLB) assessed.*

200-mg Oasis-HLB cartridges were thereafter used for the clean-up of spiked liver extracts, but the final extracts showed a yellowish color. In addition, the recoveries normalized to the reference recoveries obtained for matrix-free Milli-Q water extracts were in general higher than 150% (see Figure 9.4), showing a large matrix effect. The use of a higher amount of sorbent (400 mg) did not render better results since the recoveries normalized to Milli-Q water were comparable to those obtained with 200 mg of Oasis-HLB (p-value > 0.05). In order to improve the cleanliness of the liver extracts a Florisil cartridge (NP-SPE) was coupled in series to the Oasis HLB cartridge (RP-SPE). In this case, the target analytes were not recovered at all, and this approach was also discarded.

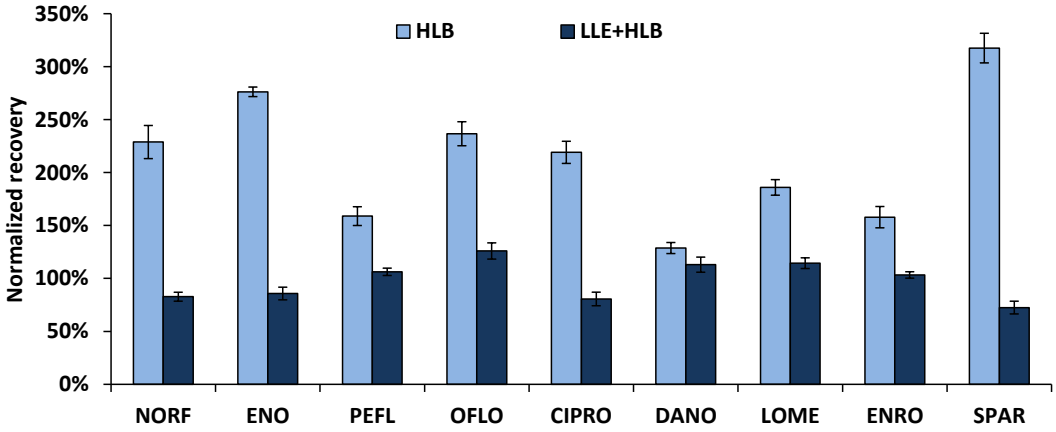

Figure 9.4: *Comparison of the recoveries of FQs after different clean-up strategies in fish liver: a) LLE + HLB and b) HLB. The results are expressed as recovery of the analytes after clean-up step normalized to the responses obtained for Milli-Q water extracts and standard deviations (n=3, 95% confidence level).*

LLE was finally tested in order to eliminate the lipophilic interferences present in the liver extracts. Under ideal conditions, lipids should be extracted to a non-polar solvent (i.e., *n*-hexane), while FQs should remain in the aqueous solvent [23]. When the LLE step was included before the Oasis HLB clean-up, no analytes were detected in the *n*-hexane fraction (with the exception of some traces lower than a 5% for SPAR) and, according to the results in Figure 9.4, the matrix effect was significantly reduced (results shown as responses normalized to the signal obtained for matrix-free Milli-Q water extracts). In addition, the absolute recovery of the combined clean-up steps (LLE + RP-SPE using 200 mg of Oasis HLB) was in the 31-50% range for all the target analytes, except for SPAR (5%). Matrix effects occurring at LC-MS/MS detection were also evaluated by comparing the responses obtained for the final liver extracts spiked at a known concentration with a standard solution prepared in MeOH at the same concentration level (1000 µg/L). The calculated ratios were between 80-120% for all target analytes, except for NORF (140%) and SPAR (69%), proving the low matrix effect in the detection as well as the cleanliness of the extracts.

In the case of the FUSLE muscle extracts, a single clean-up using 200-mg Oasis HLB cartridges rendered acceptable results in terms of absolute recoveries (23-65%) and cleanliness of the extracts (minimum signal suppression/enhancement in the detection step for all the analytes), except for SPAR with a signal suppression of a 36%.

9.3.3.3 Validation of the method for fish tissues

Since reference materials are not available, target analyte fortification at 75 ng/g level of the unpolluted real samples was considered for method validation of fish liver and muscle. Spiking at 75 ng/g level was chosen since the European Union (EU) established maximum residues limits (MRLs) for several FQs in foodstuffs of animal origin through the Council Regulation 2377/90/EEC, specifically 100–300 ng/g for ENRO. The suitability of the method was evaluated in terms of apparent recoveries (corrected with the corresponding labelled standard) and precision. As it can be observed in Table 9.2, satisfactory apparent recoveries (after correction with the deuterated analogues) were obtained for all the target compounds (in the 82-107% range) in both matrices, except for SPAR, which showed apparent recoveries of 162% for muscle and 14% for liver, due to the lack of correction with [$^{2}H_{8}$]-CIPRO. Furthermore, the repeatability of the method can be considered satisfactory, with relative standard deviations (RSD%) between 1 and 10%, taking into account the complexity of the matrices. In addition, procedural LOQs (LOQ_{proc}) have been calculated and, as it can be observed in Table 9.2, tissue LOQ_{proc} values are below the MRL [18].

9.3.4 Extraction and validation of FQs from bile and plasma

Oasis-HLB clean-up of bile was discarded due to the high signal suppression. In the case of biological fluids (plasma and bile), the suitability of MIP cartridges for FQ clean-up and preconcentration was tested. Bile and plasma samples were spiked at 200 µg/L and loaded onto the MIP cartridges according to the manufacturer's conditions [35] (see Section 9.2.4.1). Absolute recoveries higher that 30% were obtained in most of the cases and, as it can be observed in Table 9.2, labeled surrogate correction was satisfactory for all the target compounds (in the 91-115% and 94-106% ranges for plasma and bile, respectively), except for SPAR (70% for bile). RSD% and LOD_{proc} values were also adequate.

Final MIP extracts were also tested for matrix effects in the detection step and no signal suppression/enhancement was observed (p-value > 0.05 according to the one-way ANOVA).

Despite the satisfactory results obtained for biofluids, MIP based clean-up was not tested for liver/muscle tissues since only a small fraction of the extract could be loaded, rendering poor method efficiencies.

Table 9.2: *Apparent recoveries (Rec.%), Relative Standard Deviations (RSD%) and procedural limits of quantification (LOQ_{proc}) for fish tissues and biological fluids.*

Analyte	Tissues						Biological fluids					
	Liver			Muscle			Plasma			Bile		
	Rec. (%)	*RSD (%)*	*LOQ_{proc} (ng/g)*	*Rec. (%)*	*RSD (%)*	*LOQ_{proc} (ng/g)*	*Rec. (%)*	*RSD (%)*	*LOQ_{proc} (µg/L)*	*Rec. (%)*	*RSD (%)*	*LOQ_{proc} (µg/L)*
NORF[a]	107	1	2	96	10	2	93	4	4	96	5	10
ENO[a]	89	1	2	83	3	2	95	3	4	104	2	10
PEFLO[b]	103	1	0.8	89	3	0.8	91	7	1.6	97	1	4
OFLO[b]	96	2	0.8	94	3	0.8	110	3	1.6	105	2	4
CIPRO[a]	92	1	0.8	92	4	0.8	96	2	1.6	97	1	4
DANO[b]	104	1	2	92	2	2	115	6	4	94	4	10
LOME[b]	82	4	0.8	94	7	0.8	103	4	1.6	106	5	4
ENRO[b]	90	1	0.8	94	1	0.8	100	1	1.6	101	1	4
SPAR[a]	14	5	0.4	162	13	0.4	109	20	0.8	70	8	2

[a]Corrected with [$^2H_8$]–CIPRO. [b]Corrected with [$^2H_5$]–ENRO.

9.3.5 Extraction and preconcentration of FQs from environmental water samples

FQ extraction and preconcentration from environmental samples, including effluent samples from WWTPs, estuarine water and seawater, was also studied. Addition of 0.1% (g/g) EDTA was performed according to the literature [1,36]. In a first approach, it was tested whether the samples could be filtered through 1.2-µm microfibre filters [12] without a significant loss of the analyte. Although the absolute recoveries could be corrected using labelled standards added before the filtration step, losses higher than a 50% were observed for most of the target analytes during filtration of Milli-Q water samples spiked at 800 ng/L. According to these results and the recommendation of the EU Water Framework Directive [11], filtration of the samples was rejected.

For preconcentration, in a first approach, Oasis HLB was directly tested for the three aqueous matrices studied. While the final extract was colorless and showed no matrix effect for seawater (matrix enhancement/suppression lower than 18%), estuarine and wastewater effluent samples showed a yellowish final extract and a strong signal suppression (higher than 50% for target analytes such as SPAR, CIPRO, LOME, ENO and NORF) were observed. In order to improve the clean-up of estuarine and wastewater extracts, an Evolute-WAX cartridge was coupled in series to the Oasis HLB cartridge [12]. The purpose of the Evolute-WAX cartridge was not the retention of FQs but the elimination of interferences. While the absolute recoveries for the simple RP-SPE and the combined mixed-mode-RP SPE were similar (p-value > 0.05 according to the one-way ANOVA), the signal suppression/enhancement was improved in the combined approach (p-value < 0.05), with signal suppression/enhancements lower than a 14% and a 33% in the case of estuarine and effluent water, respectively.

The loading sample volume (250 mL and 500 mL) was also tested. In the case of seawater, up to 500 mL were loaded without cartridge breakthrough. However, in the case of wastewater effluents and estuarine, when volumes up to 500 mL were loaded, the Evolute-WAX cartridge was saturated with organic matter, the final extract was dirtier and signal suppression was observed for most of the compounds (p-value < 0.05, according to the one-way ANOVA). Thus, 250 mL was finally selected as loading sample volume in the case of all the water matrices.

9.3.5.1 Validation of the method for water samples

The figures of merit of the optimized method for the different environmental waters are summarized in Table 9.3. The recovery was calculated using 250 mL of samples spiked at 75 ng/L (n=3) and non-spiked water samples were also analyzed using the same extraction procedure. Since the spiked amount was lower than the concentration already present in the sample for NORF, OFLO and CIPRO, the validation was repeated at 200 ng/L. As summarized in Table 9.3, satisfactory apparent recoveries (after subtraction of the responses of the non-spiked samples and correction with the labelled surrogates) between 80% and 126% were obtained for all the target compounds (except SPAR) in seawater, estuarine water and WWTP effluent. The apparent recoveries for SPAR were not successfully corrected with [$^2H_8$]-CIPRO in seawater (67%) nor in estuarine (54%) nor in WWTP effluent (59%). Regardless of the water type, the precision of the method in terms of RSD (%) varied between 1 and 15% (n=3), which is comparable to other reported works [12–14]. In addition, the LOQ_{proc} values showed that the method is enough sensitive to quantify any sample that exceeds the PEC and the PNEC values [2].

Table 9.3: *Apparent recoveries (Rec.%), Relative Standard Deviations (RSD%) and procedural limits of quantification (LOQ_{proc}) for environmental waters.*

Analyte	Seawater			Estuarine water			Effluent water		
	Rec. (%)	***RSD (%)***	***LOQ_{proc} (ng/L)***	***Rec. (%)***	***RSD (%)***	***LOQ_{proc} (ng/L)***	***Rec. (%)***	***RSD (%)***	***LOQ_{proc} (ng/L)***
NORF[a]	90	2	4.00	84	2	4.00	93	1	4.00
ENO[a]	80	1	4.00	82	7	4.00	83	1	4.00
PEFLO[b]	101	2	1.60	109	7	1.60	109	4	1.60
OFLO[b]	105	4	1.60	93	14	1.60	125	15	1.60
CIPRO[a]	87	3	1.60	85	6	1.60	109	1	1.60
DANO[b]	112	4	4.00	109	14	4.00	118	3	4.00
LOME[b]	106	1	1.60	120	15	1.60	126	4	1.60
ENRO[b]	101	2	1.60	97	1	1.60	99	6	1.60
SPAR[a]	67	4	0.80	54	14	0.80	59	3	0.80

[a]Corrected with [$^2H_8$]–CIPRO. [b]Corrected with [$^2H_5$]–ENRO.

9.3.6 Application to real samples

The developed methods were applied to water samples collected in February 2017 in Gernika WWTP effluent, water of the estuary (downstream of the WWTP) and seawater in Laida beach (Ibarrangelu). Briefly, NORF, OFLO/LEVO (as a sum of both enantiomers) and CIPRO were the only target analytes detected (44-278 ng/L). These FQs are highly prescribed for human use and they are mostly found in the environment at the ng/L level [6,13–15]. Furthermore, we should underline that the sampling points were close to a hospital, and hospital wastewaters are one of the sources of pharmaceutical emissions [6]. Exemplarily, Figure 9.1c shows the chromatogram obtained for estuarine water extract. Generally, as reported in other works [6,37], concentrations were higher in WWTP effluent (143 ± 8 ng/L NORF, 160 ± 7 ng/L CIPRO and 234 ± 2 ng/L OFLO/LEVO) than in estuarine water (44 ± 4 ng/L NORF, 79 ± 1 ng/L CIPRO and 280 ± 20 ng/L OFLO/LEVO), just in the exit of the WWTP. Surprisingly, the concentration of OFLO/LEVO was higher at the estuary than at the effluent. This fact could be attributed to the deconjugation of metabolites through microbial activity in the estuary [14]. Lastly, the seawater concentrations were under the LOQs probably due to the high dilution factor.

On the other hand, the presence of OFLO/LEVO (4.0 ± 0.3 ng/g) in thicklip gray mullet liver collected in June 2015 in the same estuary point (see Figure 9.1d) could be indicative of the bioaccumulation capacity of FQs, in accordance with the results observed in the literature [16,17].

9.4 Conclusions

In the present work, methods were thoroughly optimized and validated for 10 FQs (NORF, ENO, PEFLO, OFLO, LEVO, CIPRO, DANO, LOME, ENRO and SPAR) in 7 different matrices, namely fish liver, muscle, bile and plasma, and seawater, estuarine water and effluent wastewater. It should be highlighted that these are the first specific methods for FQs in fish liver, plasma and bile. Satisfactory results were obtained for all the target analytes after correction with labeled analogues, except for SPAR. For the latter, either the use of standard additions or a more suitable surrogate should be applied, but it is worth mentioning that the isotopically labeled analogue of SPAR is not commercially available yet. As far as we know, there are no other works in the

literature dealing with the simultaneous determination of ten FQs in a wide variety of environmental matrices. Due to the complexity of the matrices studied, different clean-up combinations were necessary depending on the matrix. In the case of fish tissues, while simple RP-SPE was sufficient for the clean-up of fish muscle extracts, LLE coupled to RP-SPE was necessary for liver. In the case of biofluids, the strong matrix effect observed in the detection step when using RP-SPE could be avoided using MIP cartridges. Finally, in the case of estuarine and effluent waters, the combination of Oasis WAX and RP-SPE was also necessary for minimizing the signal enhancement/suppression. Lastly, the developed methods were applied to the analysis of real samples from the Biscay Coast, where CIPRO, NORF and OFLO/LEVO were detected in both, water and fish liver samples up to 280 ng/L and 4 ng/g, respectively. These preliminary results suggest that further monitoring of FQs in both fish and water samples is advisable. In addition, the developed methods will be further used in exposure experiments that will be carried out under controlled laboratory conditions in order to study the bioaccumulation and biotransformation of FQs in fish.

9.5 References

1. Vazquez-Roig P, Blasco C, Picó Y. 2013. Advances in the analysis of legal and illegal drugs in the aquatic environment. *TrAC Trends Anal. Chem.* 50:65–77.
2. Besse J-P, Garric J. 2008. Human pharmaceuticals in surface waters: Implementation of a prioritization methodology and application to the French situation. *Toxicol. Lett.* 176:104–123.
3. Seifrtová M, Nováková L, Lino C, Pena A, Solich P. 2009. An overview of analytical methodologies for the determination of antibiotics in environmental waters. *Anal. Chim. Acta*. 649:158–179.
4. Van Doorslaer X, Dewulf J, Van Langenhove H, Demeestere K. 2014. Fluoroquinolone antibiotics: An emerging class of environmental micropollutants. *Sci. Total Environ.* 500–501:250–269.
5. Martinez M, McDermott P, Walker R. 2006. Pharmacology of the fluoroquinolones: A perspective for the use in domestic animals. *Vet. J.* 172:10–28.
6. Speltini A, Sturini M, Maraschi F, Profumo A. 2010. Fluoroquinolone antibiotics in environmental waters: Sample preparation and determination. *J. Sep. Sci.* 33:1115–1131.

7. Andreozzi R, Raffaele M, Nicklas P. 2003. Pharmaceuticals in STP effluents and their solar photodegradation in aquatic environment. *Chemosphere*. 50:1319–1330.

8. Petrović M, Hernando MD, Díaz-Cruz MS, Barceló D. 2005. Liquid chromatography–tandem mass spectrometry for the analysis of pharmaceutical residues in environmental samples: a review. *J. Chromatogr. A*. 1067:1–14.

9. Turiel E, Martín-Esteban A, Tadeo JL. 2006. Multiresidue analysis of quinolones and fluoroquinolones in soil by ultrasonic-assisted extraction in small columns and HPLC-UV. *Anal. Chim. Acta*. 562:30–35.

10. Janecko N, Pokludova L, Blahova J, Svobodova Z, Literak I. 2016. Implications of Fluoroquinolone Contamination for the Aquatic Environment-a Review. *Environ. Toxicol. Chem.* 35:2647–2656.

11. Water Framework Directive. 2013. *Directive 2013/39/EU amending Directives 2000/60/EC and 2008/105/EC*.

12. Sturini M, Speltini A, Pretali L, Fasani E, Profumo A. 2009. Solid-phase extraction and HPLC determination of fluoroquinolones in surface waters. *J. Sep. Sci.* 32:3020–3028.

13. Benito-Peña E, Urraca JL, Sellergren B, Moreno-Bondi MC. 2008. Solid-phase extraction of fluoroquinolones from aqueous samples using a water-compatible stochiometrically imprinted polymer. *J. Chromatogr. A*. 1208:62–70.

14. Lee H-B, Peart TE, Svoboda ML. 2007. Determination of ofloxacin, norfloxacin, and ciprofloxacin in sewage by selective solid-phase extraction, liquid chromatography with fluorescence detection, and liquid chromatography–tandem mass spectrometry. *J. Chromatogr. A*. 1139:45–52.

15. Nakata H, Kannan K, Jones PD, Giesy JP. 2005. Determination of fluoroquinolone antibiotics in wastewater effluents by liquid chromatography–mass spectrometry and fluorescence detection. *Chemosphere*. 58:759–766.

16. Wagil M, Kumirska J, Stolte S, Puckowski A, Maszkowska J, Stepnowski P, Białk-Bielińska A. 2014. Development of sensitive and reliable LC-MS/MS methods for the determination of three fluoroquinolones in water and fish tissue samples and preliminary environmental risk assessment of their presence in two rivers in northern Poland. *Sci. Total Environ.* 493:1006–1013.

17. Zhao J-L, Liu Y-S, Liu W-R, Jiang Y-X, Su H-C, Zhang Q-Q, Chen X-W, Yang Y-Y, Chen J, Liu S-S, Pan C-G, Huang G-Y, Ying G-G. 2015. Tissue-specific bioaccumulation of human and veterinary antibiotics in bile, plasma, liver and muscle tissues of wild fish from a highly urbanized region. *Environ. Pollut.* 198:15–24.

18. EMEA. 2002. Committee for veterinary medicinal products, Enrofloxacin EMEA/MRL/820/02-FINAL. [cited 28 February 2017]. Available from http://www.ema.europa.eu/ema/index.jsp?curl=pages/includes/document/document_detail.jsp?webContentId=WC500014151&murl=menus/medicines/medicines.jsp&mid=WC0b01ac058009a3dc.

19. Huerta B, Rodríguez-Mozaz S, Barceló D. 2012. Pharmaceuticals in biota in the aquatic environment: analytical methods and environmental implications. *Anal. Bioanal. Chem.* 404:2611–2624.

20. Yu H, Tao Y, Chen D, Pan Y, Liu Z, Wang Y, Huang L, Dai M, Peng D, Wang X, Yuan Z. 2012. Simultaneous determination of fluoroquinolones in foods of animal origin by a high performance liquid chromatography and a liquid chromatography tandem mass spectrometry with accelerated solvent extraction. *J. Chromatogr. B*. 885–886:150–159.

21. Boscher A, Guignard C, Pellet T, Hoffmann L, Bohn T. 2010. Development of a multi-class method for the quantification of veterinary drug residues in feedingstuffs by liquid chromatography-tandem mass spectrometry. *J. Chromatogr. A*. 1217:6394–6404.

22. Speltini A, Sturini M, Maraschi F, Profumo A, Albini A. 2011. Analytical methods for the determination of fluoroquinolones in solid environmental matrices. *TrAC Trends Anal. Chem.* 30:1337–1350.

23. Cho H-J, Yi H, Cho SM, Lee DG, Cho K, Abd El-Aty AM, Shim J-H, Lee S-H, Jeong J-Y, Shin H-C. 2010. Single-step extraction followed by LC for determination of (fluoro)quinolone drug residues in muscle, eggs, and milk. *J. Sep. Sci.* 33:1034–1043.

24. Evaggelopoulou EN, Samanidou VF. 2013. HPLC confirmatory method development for the determination of seven quinolones in salmon tissue (Salmo salar L.) validated according to the European Union Decision 2002/657/EC. *Food Chem.* 136:479–484.

25. Sun X, Wang J, Li Y, Yang J, Jin J, Shah SM, Chen J. 2014. Novel dummy molecularly imprinted polymers for matrix solid-phase dispersion extraction of eight fluoroquinolones from fish samples. *J. Chromatogr. A*. 1359:1–7.

26. Zabaleta I, Bizkarguenaga E, Iparragirre A, Navarro P, Prieto A, Fernández LÁ, Zuloaga O. 2014. Focused ultrasound solid–liquid extraction for the determination of perfluorinated compounds in fish, vegetables and amended soil. *J. Chromatogr. A*. 1331:27–37.

27. Ziarrusta H, Mijangos L, Prieto A, Etxebarria N, Zuloaga O, Olivares M. 2015. Determination of tricyclic antidepressants in biota tissue and environmental waters by liquid chromatography-tandem mass spectrometry. *Anal. Bioanal. Chem.* 408:1205–1216.

28. Chiesa L, Nobile M, Arioli F, Britti D, Trutic N, Pavlovic R, Panseri S. 2015. Determination of veterinary antibiotics in bovine urine by liquid chromatography–tandem mass spectrometry.

Food Chem. 185:7–15.

29. Bourdat-Deschamps M, Leang S, Bernet N, Daudin J-J, Nélieu S. 2014. Multi-residue analysis of pharmaceuticals in aqueous environmental samples by online solid-phase extraction–ultra-high-performance liquid chromatography-tandem mass spectrometry: Optimisation and matrix effects reduction by quick, easy, cheap, effective, rugged and safe extraction. *J. Chromatogr. A*. 1349:11–23.

30. Tamtam F, Mercier F, Eurin J, Chevreuil M, Bot BL. 2009. Ultra performance liquid chromatography tandem mass spectrometry performance evaluation for analysis of antibiotics in natural waters. *Anal. Bioanal. Chem.* 393:1709–1718.

31. Calisto V, Esteves VI. 2009. Psychiatric pharmaceuticals in the environment. *Chemosphere*. 77:1257–1274.

32. Rodríguez E, Navarro-Villoslada F, Benito-Peña E, Marazuela MD, Moreno-Bondi MC. 2011. Multiresidue Determination of Ultratrace Levels of Fluoroquinolone Antimicrobials in Drinking and Aquaculture Water Samples by Automated Online Molecularly Imprinted Solid Phase Extraction and Liquid Chromatography. *Anal. Chem.* 83:2046–2055.

33. Speltini A, Sturini M, Maraschi F, Consoli L, Zeffiro A, Profumo A. 2015. Graphene-derivatized silica as an efficient solid-phase extraction sorbent for pre-concentration of fluoroquinolones from water followed by liquid-chromatography fluorescence detection. *J. Chromatogr. A*. 1379:9–15.

34. Prieto A, Schrader S, Bauer C, Möder M. 2011. Synthesis of a molecularly imprinted polymer and its application for microextraction by packed sorbent for the determination of fluoroquinolone related compounds in water. *Anal. Chim. Acta*. 685:146–152.

35. Application note for Biotage - AFFINILUTE™ MIP Fluoroquinolones. [cited 28 February 2017]. Available from http://www.biotage.com/product-page/affinilute-mip-columns.

36. Gros M, Rodríguez-Mozaz S, Barceló D. 2013. Rapid analysis of multiclass antibiotic residues and some of their metabolites in hospital, urban wastewater and river water by ultra-high-performance liquid chromatography coupled to quadrupole-linear ion trap tandem mass spectrometry. *J. Chromatogr. A*. 1292:173–188.

37. Golet EM, Strehler A, Alder AC, Giger W. 2002. Determination of fluoroquinolone antibacterial agents in sewage sludge and sludge-treated soil using accelerated solvent extraction followed by solid-phase extraction. *Anal. Chem.* 74:5455–5462.

38. Tang Q, Yang T, Tan X, Luo J. 2009. Simultaneous Determination of Fluoroquinolone Antibiotic Residues in Milk Sample by Solid-Phase Extraction−Liquid Chromatography−Tandem Mass Spectrometry. *J. Agric. Food Chem.* 57:4535–4539.

39. He X, Wang Z, Nie X, Yang Y, Pan D, Leung AOW, Cheng Z, Yang Y, Li K, Chen K. 2011. Residues of fluoroquinolones in marine aquaculture environment of the Pearl River Delta, South China. *Environ. Geochem. Health*. 34:323–335.

Chapter 10

Ciprofloxacin by-products in seawater environment in the presence and absence of gilt-head bream

Chemosphere 197 (2018) 560-568

10.1 Introduction

There is a growing concern on the presence of pharmaceutical active compounds (PhACs) in the environment since they may exert adverse effects on non-target organisms after they enter into the ecosystems [1–3]. Among PhACs, special attention has been paid to antibiotics specially due to the rapid expansion of antibiotic resistance observed since the late 90's [4–7]. Due to their high use and continuous release to the environment, their transformation and elimination rate is balanced and antibiotics are, therefore, known as "pseudo-persistent" pollutants [8]. For example, fluoroquinolones (FQs) are a class of antibiotics used against respiratory diseases and bacterial infections in human and veterinary medicine [1,9–11]. Although FQs can absorb UV radiation and are photodegradable [1], they are resistant to hydrolysis and elevated temperatures, which increases their persistency in the environment.

Due to the widespread application of FQs such as ciprofloxacin (CIPRO), and the fact of being partially metabolized in the body and not completely removed in wastewater treatment plants, FQs are the most detected antibiotics in the environment, at concentrations in the ng/L-µg/L range in aquatic ecosystems, which may act as sinks for antibiotics through different pathways such as domestic/municipal wastewaters, surface waters and hospital effluents [1]. Although CIPRO is threatening the aquatic organisms at actual environmental concentrations [12], little is known on its distribution, metabolism and elimination in tissues of aquatic organisms.

The determination of antibiotics and their by-products (BPs), namely metabolites and transformations products (TPs), is relevant to establish the sources, transport, fate and effects in the environment [5]. High-resolution mass spectrometry (HRMS) plays an important role on the determination of BPs. The high resolution/high mass accuracy, exact mass and isotopic profile measurements performed by HRMS allow inferring the unequivocal molecular formula. When full MS data information is complemented with the MS/MS spectra obtained in hybrid mass spectrometers, tentative structure candidates can be proposed for the BPs [13].

In this framework, the aim of the present work was to study the uptake, distribution and metabolization of CIPRO in tissues (brain, liver, gill, muscle) and biofluids (plasma, bile) of juvenile gilt-head bream (*Sparus aurata*). Controlled dosing experiments were performed in the presence

and absence of fish in seawater, and the HRMS analysis of the different matrices was performed in a hybrid quadrupole-Orbitrap mass spectrometer to annotate the BPs generated under each condition.

10.2 Materials and methods

10.2.1 Standards and Reagents

CIPRO (98%) and [$^{2}H_{8}$]-ciprofloxacin ([$^{2}H_{8}$]-CIPRO, 99.6%) were purchased from Sigma-Aldrich (St. Louis, MO, USA). CIPRO stock solution was prepared at 500 mg/L in methanol (MeOH, Fisher Scientific, Loughborough, UK) and CIPRO dosing solution was prepared in Milli-Q water at 45.2 mg/L. In both cases, sodium hydroxide (NaOH, ≥ 99%, Merck, Darmstadt, Germany) was added to ease CIPRO dissolution. Stock solutions were stored in the darkness at −20 °C.

Ethyl 3-aminobenzoate methanesulfonate (tricaine, > 98%) and sodium hydrogen carbonate ($NaHCO_3$, > 99%) used for fish anaesthetizing were purchased from Sigma Aldrich and ethylendiaminetetraacetic acid (EDTA, > 99%) from Panreac (Barcelona, Spain).

Ultra-pure water was obtained using a Milli-Q water purification system (< 0.05 µS/cm, Milli-Q model 185, Millipore, Bedford, MA, USA). MeOH was used as mobile phase solvent and formic acid (HCOOH, Optima, Fischer Scientific, Geel, Belgium) for mobile phase modifications.

10.2.2 Metabolite and BP identification experiments

For exposure experiments, juvenile gilt-head bream, weighing ~ 40 g and measuring ~ 13 cm in length, were used. Fish were obtained from Groupe Aqualande (Roquefort, France) and shipped to the Research Centre for Experimental Marine Biology and Biotechnology of Plentzia (PiE-UPV/EHU) to perform the experiments at controlled temperature (18 °C) and light (14:10 h light:dark cycles). Fish were acclimatized for 3 months upon arrival and stabilized for an additional 1 week in the dosing tank before starting the exposure. The water was continuously aerated using aquarium oxygenators and fish were fed daily with 0.10 g pellets/fish. Water temperature (13 °C) and pH (7.4 ± 0.3) were constant during the exposure. Dissolved oxygen, nitrite, nitrate and ammonium content were periodically monitored.

An 8-day exposure experiment was designed to identify BPs of CIPRO. Four 1000 × 700 × 650 mm polypropylene tanks containing 250 L of seawater were used: two of them contained 40 fish each and the other two only seawater. One of the tanks containing fish and one of the tanks without fish were continuously fortified at 200 ng/mL (nominal concentration), whereas the other tanks were used as control (one with fish, one without fish). CIPRO dosing was performed using a continuous flow-through system with a peristaltic pump delivering 9 L seawater/h and another pump infusing CIPRO dosing solution (45.2 mg/L, refilled every 24 h with newly prepared solution) at 40 mL/h to exposure tank. Control tanks were maintained at identical conditions over the duration of the experiment but only seawater was delivered.

10.2.3 Sample Collection

Fish handling and dissection were performed according to the Bioethics Committee rules of UPV/EHU (procedure approval CEEA/380/2014/ETXEBARRIA LOIZATE). 10 fish were collected from control and exposed tanks on exposure days 0 (before exposure), 1, 3 and 8. The fish were immediately anaesthetized in a tank holding 10 L of seawater that contained tricaine and $NaHCO_3$, both at 200 mg/L. After 5 min, fish were length measured, weighed and dissected to collect tissues (brain, gill, liver, muscle) and biofluids (bile, plasma). Blood was taken from the caudal vein-artery using a syringe (previously homogenized with 0.5 mol/L EDTA solution at pH 8.0) and, then, centrifuged for 7 min at 1000 rpm to get the plasma. Biofluids and fish tissues were snap-frozen and kept in liquid nitrogen during dissection and stored at -80 °C freezer prior to analysis.

At the time that fish were removed from the tanks, 2-L water samples were also collected from the four tanks to determine the concentration of CIPRO and to identify CIPRO BPs in water. Water samples were extracted and analyzed within 24 h.

10.2.4 Sample Handling

Fish tissues (brain, gill, liver, muscle) were freeze-dried for 48 h using a Cryodos-50 laboratory freeze-dryer (Telstar Instruments, Sant Cugat del Valles, Barcelona, Spain). A homogenized pool was prepared for each tissue/biofluid using the 10 fish collected at each sampling day. The pools and the seawater samples (100 mL) were extracted and analyzed in

triplicate using a previously developed analytical method [14]. Procedural blanks were analyzed to discard chromatographic peaks associated to contamination during the identification of BPs.

10.2.5 Instrumental Analysis

CIPRO was quantified by liquid chromatography tandem mass spectrometry (LC-QqQ-MS/MS) using a previously developed method [14]. BP identification was performed using a Thermo Scientific Dionex UltiMate 3000 UHPLC coupled to a Thermo Scientific Q Exactive quadrupole-Orbitrap mass spectrometer equipped with a heated ESI source (HESI, Thermo, CA, USA). 3-µL extracts were separated on a Kinetex biphenyl 100 Å core-shell (2.1 mm × 100 mm, 2.6 µm) column with a Kinetex biphenyl 100 Å core-shell pre-column (2.1 mm × 5 mm, 2.6 µm) from Phenomenex (Torrance, CA, USA), which was kept at 30 °C during the analysis. Milli-Q water:MeOH (95:5, v/v) was used as mobile phase A and Milli-Q water:MeOH (5:95, v/v) as mobile phase B, both containing 0.1% HCOOH. The mobile phase flow rate was set at 0.3 mL/min and the eluent gradient profile was as follows: 5% of B (hold 0.5 min), linear change to 95% B up to 20 min (hold 3 min) and a final linear change to 5% B up to 28 min (hold 2 min) to regain initial conditions.

The qOrbitrap was operated in positive ionization mode in full scan – data dependent MS2 (Full MS-ddMS2) acquisition mode. One full scan at a resolution of 70,000 full width at half maximum (FWHM) at *m/z* 200 over a scan range of *m/z* 100-700 was followed by three ddMS2 scans at a resolution of 17,500 FWHM at *m/z* 200, with an isolation window of 0.8 Da. The stepped normalized collision energy (NCE) in the higher-energy collisional dissociation (HCD) cell was set to 25, 50 and 75 eV. The ddMS2 scans were acquired on discovery mode, choosing the most intense ions from the full scan for fragmentation, with an intensity threshold of $8.0 \cdot 10^3$ and a dynamic exclusion of 10 s. The HESI source parameters were set to 3.2 kV spray voltage, 300 °C capillary temperature, 35 arbitrary units (au) sheath gas (nitrogen), 10 au auxiliary gas and 280 °C auxiliary gas heater. External calibration of the instrument was conducted immediately prior to analysis using Pierce LTQ ESI Calibration Solutions (Thermo Scientific, Waltham, Massachusetts, United States). The instrument was controlled by Xcalibur 4.0 software (Thermo).

10.2.6 Data Handling

CIPRO was quantified using a 10-point external calibration curve whereas BPs were identified using Compound Discoverer 2.0 (Thermo). Peak picking and peak alignment were performed with retention time deviation of 0.5 min and mass tolerances of 5 ppm. In the case of metabolites the software considered Phase I and II reactions to predict CIPRO derived metabolites (see Appendix I). The *m/z* values of the predicted compounds were searched for in the peak list considering the criteria of 5 ppm for mass tolerance and 30% for the intensity tolerance for the isotope search. The peaks that fulfilled both criteria were manually checked and only those with available MS/MS spectra, a maximum signal higher than 10^5 and absent in control samples (both exposure and procedural) were further considered. Structural assignments were carried out based on ddMS2 fragments annotated by Compound Discoverer software.

10.3 Results and discussion

10.3.1 CIPRO accumulation in fish

Condition factor (K = (fish weight x 100)/length^3) and hepatic somatic index (HSI = (liver weight x 100)/fish weight) were calculated to assess general fish health [15]. Mortality was not observed in any of the experiments and K and HSI values were not statistically different between control and exposed (p-value > 0.05) at all the exposure days, indicating maintenance of fish health during the exposure.

The average concentration of CIPRO in seawater was consistent with the nominal dosing concentration (200 ng/mL) regardless of the absence (230 ± 20 ng/mL) or presence (208 ± 3 ng/mL) of fish. The concentration of CIPRO in samples collected before starting the exposure (day 0) and in samples from all control tanks was bellow method detection limit (MDL, 2 ng/L, [14]).

Regarding the uptake in fish, CIPRO was only detected in bile whereas it was under MDLs in the rest of analyzed fish biofluid and tissues regardless of the exposure time. The concentrations of CIPRO in bile increased over the exposure time: 70 ± 10 ng/mL, 120 ± 30 ng/mL and 315 ± 4 ng/mL (at 95% of confidence level) in sampling days 1, 3 and 8, respectively. Low uptake factors for CIPRO were also found in the literature in comparison to other non-ionizable pollutants [16]. The low

octanol-water partition coefficient (log K_{ow} = -2.4 at pH 7.4) and the zwitterionic behavior of CIPRO may reduce its uptake rate and accumulation capacity in lipidic tissues. However, its bioavailability and accumulation in biofluids (such as bile) can be increased due to the larger transfer capacity across cell membrane of the ionized form of the compound [17]. Moreover, saline environment can also reduce the accumulation factors of the drug, since some FQs are apparently worse absorbed by fish in saline environment [18]. Finally, the metabolization of CIPRO should be also suggested to explain its low accumulation since it is susceptible to photolysis by dealkylation, defluorination and hydroxylation [11]. CIPRO can go through various Phase I and II metabolisms after entering into fish body and its accumulation without any transformation can be also reduced (see discussion in section 10.3.2).

10.3.2 CIPRO BPs

BPs of CIPRO were studied in seawater (in the presence and absence of fish) and in biological tissues (liver, brain, muscle, gill) and fluids (plasma, bile). Table 10.1 includes the molecular formula, the theoretical *m/z* of the $[M+H]^+$ form and the corresponding ΔMass (ppm) for each matrix, the most abundant fragments in the MS/MS spectra and the retention time for CIPRO and all identified BPs. Figure 10.1 showed the proposed degradation pathway of CIPRO.

For the elucidation of BPs, it is worth mentioning that the fragmentation of CIPRO is conditioned by the two charge isomers, namely CIPRO A and CIPRO B (see Figure 10.2), which show different collision induced dissociation (CID) spectra [19]. CIPRO A corresponds to the isomer where the charge resides in the piperazinyl ring and CIPRO B to the isomer when the proton resides in the keto group. CIPRO A fragmentation begins with a CO_2 neutral loss and CIPRO B loses first H_2O [19].

10.3.2.1 BPs in water in the absence of fish

In a first approach BPs in the absence of fish were studied due to the susceptibility towards photolysis shown by CIPRO [20–22]. Up to 20 BPs (see Figure 10.1) were observed and 16 were reported for the first time.

***Table 10.1**: Molecular formula, theoretical m/z of $[M+H]^+$ and the corresponding ΔMass (ppm) for each matrix, the most abundant fragments in the MS/MS spectra and the retention time for CIPRO and all annotated BPs.*

Compound	Molecular Formula (M)	Theoretical m/z ($[M+H]^+$)	Fragments in MS/MS spectra	ΔMass (ppm)			R_t (min)
				Water*	Water**	Bile	
CIPRO	$C_{17}H_{18}FN_3O_3$	332.1405	231.0565, 245.1084, 203.0612, 204.0692, 314.1295, 288.1505, 312.1344, 249.0669, 217.0774, 70.0659	0.16	0.62	2.28	9.20
BP1	$C_{18}H_{18}FN_3O_4$	360.1354	230.0486, 243.0565, 231.0564, 342.1244, 272.0826, 249.0667, 318.0880, 281.0787, 243.0944, 56.0503	0.10	0.77	-	16.07
BP2	$C_{17}H_{19}N_3O_4$	330.1449	229.0599, 243.1131, 261.0867, 312.1341, 217.0970, 228.0528, 70.0659, 231.0924, 286.1556, 269.0911	0.08	-0.66	-	8.29
BP3	$C_{17}H_{18}FN_3O_4$	348.1354	261.1040, 205.0408, 233.0720, 265.0618, 264.0543, 305.0929, 219.0555, 70.0659, 251.0459, 328.1297	-0.25	-	-	9.97
BP4	$C_{17}H_{18}FN_3O_4$	348.1354	272.0833, 245.1087, 285.1277, 330.1251, 56.0504, 257.1325, 302.1302, 287.1429, 230.1222, 289.0999	-0.51	-0.08	-	13.28
BP5	$C_{17}H_{19}N_3O_4$	346.1398	245.0556, 300.1340, 328.1288, 257.0920, 231.0557, 332.1401, 259.0943, 231.0763, 287.0918, 70.0658	-0.33	-0.42	-	10.07
BP6	$C_{18}H_{20}FN_3O_3$	346.1562	332.1404, 231.0565, 314.1297, 312.1343, 249.0669, 294.1232, 273.0906, 272.1188, 272.0834, 284.1028	1.20	1.29	-	9.23
BP7	$C_{18}H_{20}FN_3O_4$	362.1511	348.1358, 272.0833, 285.1274, 330.1251, 290.0938, 98.0606, 56.0504, 232.1247, 289.0997, 86.0608	0.33	-	-	13.28
BP8	$C_{18}H_{21}N_3O_4$	344.1605	243.0763, 257.1285, 227.0822, 229.0968, 300.1706, 216.0893, 215.0801, 217.0974, 326.1501, 70.0658	-0.65	-0.91	-	10.00
BP9	$C_{18}H_{20}FN_3O_4$	362.1511	302.0932, 330.1245, 271.0746, 229.1134, 256.1233, 162.0711, 262.0749, 86.0607, 231.0786, 68.0503	-0.17	-0.85	-	9.98
BP10	$C_{17}H_{16}FN_3O_3$	330.1249	231.0930, 229.0775, 56.0504, 202.0664, 257.1085, 238.0974, 190.0535, 83.0611, 275.0831, 68.0501	0.00	-0.93	-	8.65
BP11	$C_{17}H_{17}N_3O_3$	312.1343	213.1026, 56.0504, 211.0871, 239.1182, 184.0761, 199.0737, 312.1335, 227.1049, 240.1130, 68.0504	0.17	-	-	9.06

**Seawater in the absence of fish. **Seawater in the presence of fish.*

***Table 10.1**: (Continuation).*

Compound	Molecular Formula (M)	Theoretical m/z ($[M+H]^+$)	Fragments in MS/MS spectra	ΔMass (ppm)			R_t (min)
				Water*	Water**	Bile	
BP12	$C_{18}H_{20}FN_3O_3$	346.1562	332.1403, 231.0564, 70.0659, 312.1341, 245.1084, 314.1299, 249.0669, 58.0661, 204.0694, 203.0611	0.49	0.14	-	9.65
BP13	$C_{19}H_{20}FN_3O_4$	374.1511	243.0568, 231.0567, 360.1357, 230.0489, 249.0672, 272.0836, 261.0673, 248.0596, 215.0250, 342.1250	-0.41	0.49	-	16.30
BP14	$C_{19}H_{22}FN_3O_5$	392.1616	227.1182, 149.0235, 56.0504, 150.0268, 305.0287, 213.1025, 245.1087, 348.1357, 70.0659, 360.1385	-0.30	-	-	11.62
BP15	$C_{18}H_{20}FN_3O_5$	378.1460	275.0826, 346.1196, 257.0719, 189.0822, 289.0969, 378.1462, 215.0259, 229.0780, 328.1081, 215.0601	-0.62	-0.78	-	13.85
BP16	$C_{18}H_{22}FN_3O_5$	380.1616	348.1354, 328.1293, 330.1248, 310.1182, 190.0536, 86.0607, 231.0926, 72.0452, 217.0408, 258.0670	-0.15	-0.55	-	8.67
BP17	$C_{17}H_{16}FN_3O_5$	362.1147	259.0514, 72.0452, 291.0777, 112.0761, 231.0564, 245.0718, 334.1185, 273.0672, 299.0843, 316.1087	-0.20	-0.87	-	11.89
BP18	$C_{18}H_{20}FN_3O_5$	390.1460	330.1250, 234.0438, 289.0986, 275.0824, 55.0426, 285.1274, 235.0518, 216.0333, 276.0908, 174.0713	0.57	-	-	16.94
BP19	$C_{17}H_{14}FN_3O_4$	344.1041	298.0981, 271.0873, 70.0659, 176.0746, 326.0941, 289.0994, 229.0773, 161.0513, 304.0731, 53.0033	-0.31	-	-	12.18
BP20	$C_{19}H_{22}FN_3O_3$	360.1718	245.1086, 72.0815, 204.0693, 203.0614, 84.0814, 286.0987, 316.1823, 231.0928, 285.1267, 70.0660	-0.39	-0.81	-	10.26
BP21	$C_{19}H_{18}FN_3O_3$	356.1405	217.0408, 108.0811, 231.0565, 94.0656, 338.1288, 235.0512, 81.0579, 80.0500, 134.0965, 68.0503	-	0.32	-	16.66
BP22	$C_{19}H_{18}FN_3O_4$	372.1354	110.0603, 372.1351, 82.0657, 230.0485, 217.0407, 247.0511, 235.0511, 354.1242, 344.1400, 68.0503	-	0.59	-	14.91
BP23	$C_{18}H_{20}FN_3O_4$	362.1511	100.0761, 230.0484, 217.0408, 247.0513, 248.0593, 263.0822, 144.0011, 235.0510, 136.0758, 344.1393	-	0.50	-	13.92

**Seawater in the absence of fish. **Seawater in the presence of fish.*

***Table 10.1**: (Continuation).*

Compound	Molecular Formula (M)	Theoretical m/z ([M+H]$^+$)	Fragments in MS/MS spectra	ΔMass (ppm)			R_t (min)
				Water*	Water**	Bile	
BP24	$C_{17}H_{16}FN_3O_4$	346.1198	228.0713, 217.0406, 229.0482, 258.0671, 318.1246, 286.0613, 235.0506, 328.1074, 275.0820, 257.0719	-	-1.21	-	16.22
BP25	$C_{18}H_{18}FN_3O_4$	360.1354	217.0407, 68.0502, 235.05120, 231.0561, 332.1400, 263.0829, 84.0814, 85.0528, 98.0605, 340.1305	-	0.52	-	12.76
BP26	$C_{17}H_{18}FN_3O_3$	332.1405	231.0566, 245.1085, 312.1339, 203.0616, 249.0669, 204.0691, 314.1298, 205.0777, 191.0617, 273.0899	-	-0.02	-	16.57
BP27	$C_{17}H_{19}FN_2O_5$	351.1351	305.0929, 217.0406, 337.1191, 235.0511, 319.1086, 287.0819, 218.0484, 84.0814, 259.0879, 201.0822	-	1.32	-	13.44
BP28	$C_{19}H_{20}FN_3O_6$	406.1409	388.1299, 126.0550, 217.0407, 230.0485, 98.0604, 247.0512, 235.0513, 144.0655, 306.1238, 370.1174	-	-0.25	-	13.02
BP29	$C_{22}H_{22}FN_3O_7$	460.1515	243.0565, 416.1616, 231.0564, 261.0671, 215.0253, 230.0488, 85.0290, 249.0667, 69.0343, 70.0659	-	-0.54	-	16.16
BP30	$C_{19}H_{18}FN_3O_6$	404.1252	306.1246, 217.0405, 124.0394, 286.1185, 230.0485, 235.0512, 247.0515, 386.1144, 231.0566, 263.0822	-	0.22	-	14.04
BP31	$C_{17}H_{19}N_3O_3$	314.1499	268.1437, 254.1281, 255.1361, 240.1126, 67.0549, 226.1334, 238.0967, 239.1051, 240.1488, 296.1388	-	-	3.55	16.02
BP32	$C_{17}H_{20}N_2O_5$	333.1445	241.0965, 226.0731, 255.1123, 240.0887, 227.1174, 213.1016, 212.0917, 210.0910, 229.0965, 225.0657	-	-	2.01	13.00
BP33	$C_{17}H_{18}N_2O_4$	315.1339	227.1174, 255.1121, 240.0887, 210.0910, 212.0923, 199.1228, 136.0756, 241.0956, 243.1121, 287.1385	-	-	2.30	14.77
BP34	$C_{18}H_{20}N_2O_5$	345.1445	283.1069, 284.1143, 256.1197, 285.1227, 299.1387, 271.1071, 327.1333, 74.0606, 317.1491, 86.0604	-	-	2.65	16.65
BP35	$C_{17}H_{18}N_2O_6$	347.1238	241.0965, 84.0812, 70.0658, 226.0867, 86.0968, 198.0911, 259.1072, 273.1227, 301.1187, 287.1028	-	-	1.80	9.45

**Seawater in the absence of fish. **Seawater in the presence of fish.*

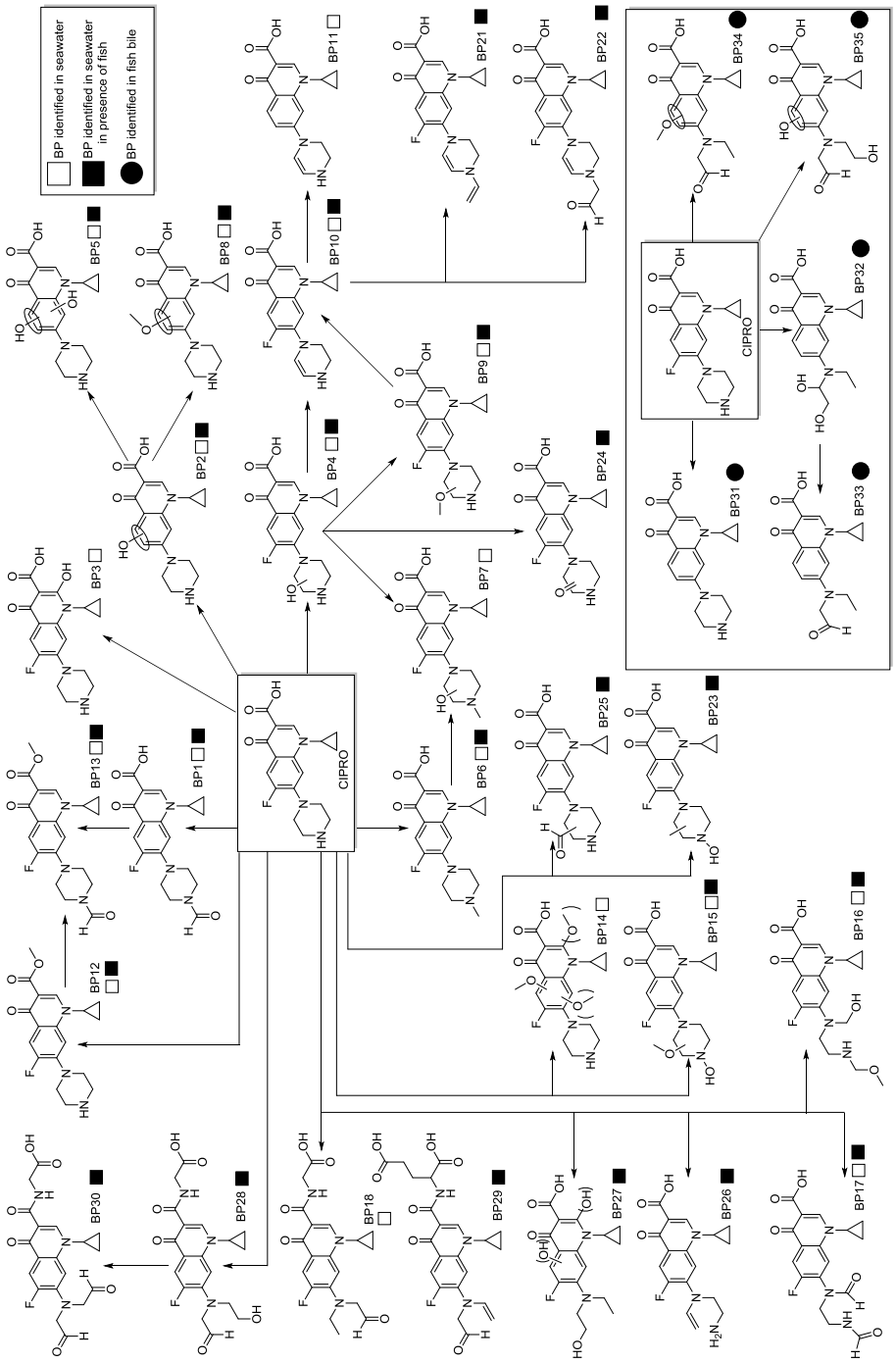

Figure 10.1: *Proposed degradation pathway of CIPRO in seawater (in the absence and presence of gilt-head bream fish) and in fish bile.*

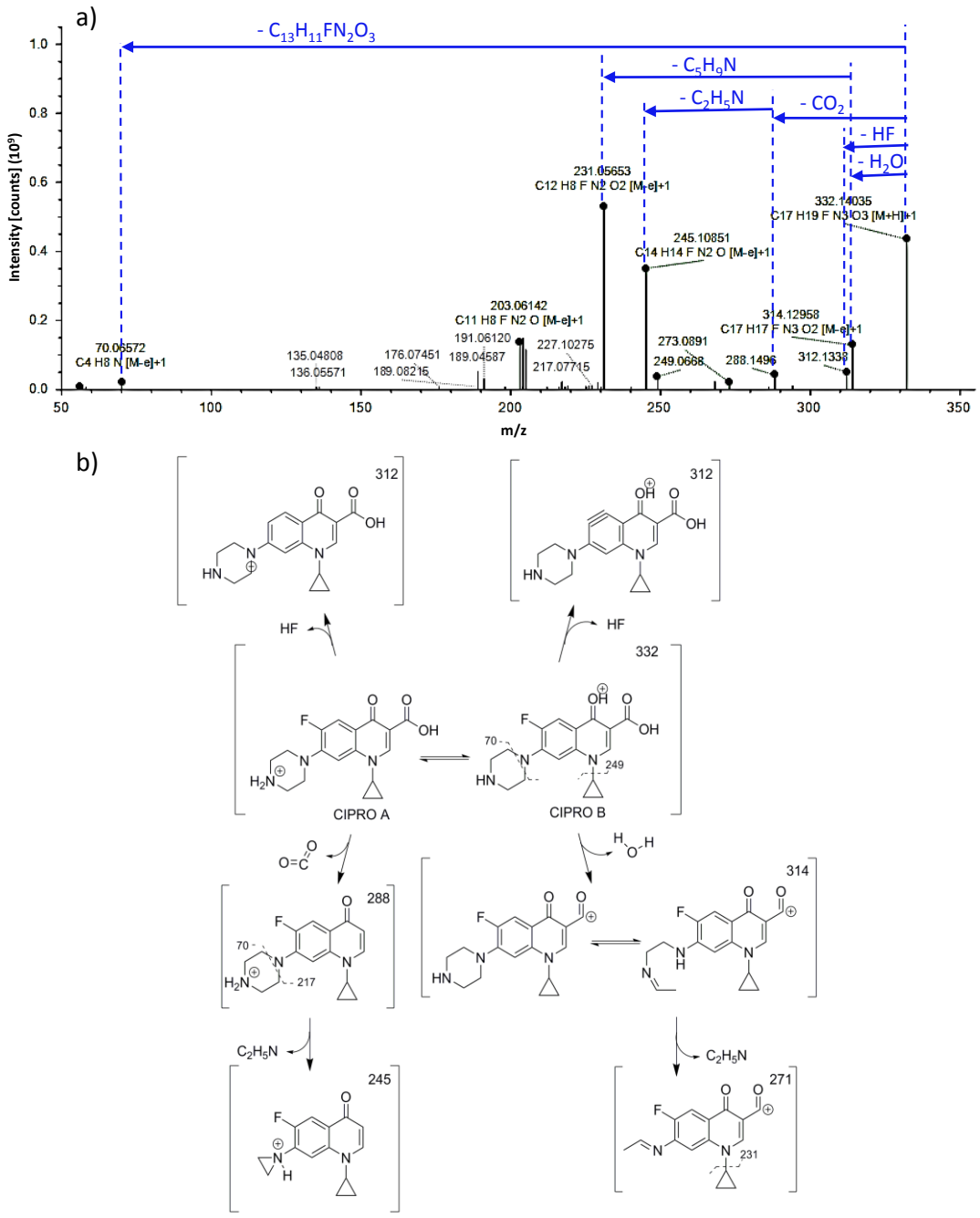

Figure 10.2: *a) MS/MS spectra of CIPRO b) CIPRO A and CIPRO B charge isomer equilibrium and collision induced dissociation fragments observed for each isomer.*

BP1 (*m/z* 360.13541) showed a composition change of +CO with respect to CIPRO (see Figure 10.1). The absence of *m/z* 70 (C_4H_8N) indicated that the modification occurred in the piperazinyl ring (see MS/MS spectra in Figure 10.3). The *N*-formylation of CIPRO could explain the basicity loss of the secondary nitrogen and the favored equilibrium towards the equivalent of CIPRO B structure, as pinpointed by the water loss observed in fragment *m/z* 342. Additionally, the abundant ion *m/z* 243 ($C_{13}H_8FN_2O_2$) suggested the loss of C_5H_9NO moiety (*m/z* 99) in the piperazinyl ring from the dehydrated fragment (*m/z* 342). This BP was previously described in the literature [23,24].

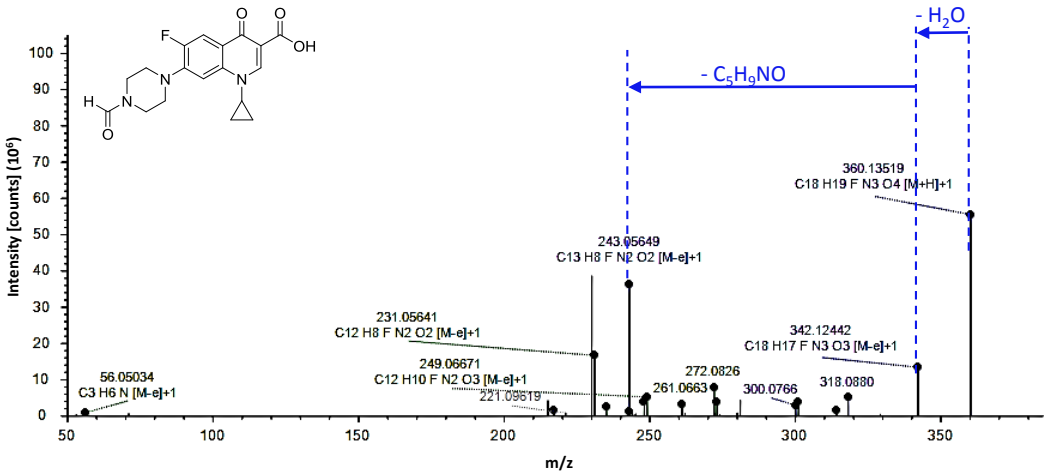

Figure 10.3: *MS/MS spectra of by-product BP1.*

BP2-BP4 consisted on monohydroxylated derivatives of CIPRO. BP2 (*m/z* 330.14484), an oxidative defluorination of CIPRO, has been widely described in the literature [22,23,25–28]. The much lower abundance of fragment *m/z* 286 (loss of CO_2) than fragment *m/z* 312 (loss of water) pinpointed that the equivalent structure of CIPRO B was favored. Fragments *m/z* 70, 217, 231, 243 and 312 (see MS/MS spectra in Figure 10.4a) indicated that an oxidation had caused the loss of the fluorine atom through a nucleophilic aromatic substitution. The lack of loss of water, together with defluorination, pinpointed that the hydroxyl group was introduced in the aromatic ring. However, with the data available, it was not possible to assign the position of the hydroxyl group in the aromatic ring, which could be located in the position left by the fluorine atom or in the adjacent carbon [29]. BP3 (*m/z* 348.13541) also corresponded to the hydroxylation of CIPRO but without defluorination. The presence of *m/z* 70 showed that the piperazinyl ring was unmodified (see

MS/MS spectra in Figure 10.4b). Similar to BP2, the lack of loss of water suggested that the hydroxyl group was located at any carbon with sp^2 hybridation. However, fragment *m/z* 305 ($C_{15}H_{14}FN_2O_4$), with all oxygen atoms and one nitrogen atom less than the precursor (*m/z* 305=348-C_2H_5N), pinpointed that the piperazinyl ring was broken before common dehydration or decarboxylation in the carboxylic group. This difference could be caused if the hydroxyl group was placed in the carbon with the sp^2 hybridation in the piperidin-4-one ring as reported in the literature [23,25]. Lastly, for BP4 (*m/z* 348.13541), the absence of fragment *m/z* 70 and the presence of two losses of water (fragment *m/z* 272 corresponded to the loss of two water molecules of the precursor together with the loss of the cyclopropyl group) suggested that the hydroxylation occurred in the piperazinyl ring (see MS/MS spectra in Figure 10.5a). Moreover, the presence of fragments *m/z* 272 ($C_{14}H_{11}FN_3O_2$) and *m/z* 285 ($C_{16}H_{16}FN_3O$), both maintaining all the N atoms of CIPRO, indicated that this hydroxylation could increase the stability of the piperazinyl ring since the characteristic fragments of piperazinyl ring cleavage in CIPRO (*m/z* 231, *m/z* 249 and *m/z* 217) were not detected.

A single dihydroxylated BP of CIPRO was observed, BP5 (*m/z* 346.13975), which could correspond to an oxidative defluorination plus a second hydroxylation of CIPRO. The presence of *m/z* 70 indicated that the piperazinyl ring was unmodified (see MS/MS spectra in Figure 10.4c). Similarly to BP2, fragments *m/z* 328 (loss of water) and *m/z* 300 (loss of CO) pinpointed that the equivalent structure of CIPRO B was favored, and both -OH groups should be placed in the aromatic ring for larger structural stability. One of the hydroxyl groups should be placed in replacement of the fluorine atom or in the adjacent sp^2 carbon atom, but the position of the second hydroxyl group could not be determined. We discarded that the second hydroxyl group was located at the sp^2 carbon atom in the piperidin-4-one ring since fragment *m/z* 303, corresponding to $C_{15}H_{16}N_2O_5$ and equivalent to fragment *m/z* 305 observed in BP3, was not observed. Similar BPs with two hydroxyl groups in the aromatic ring have been previously described in the literature [23,28].

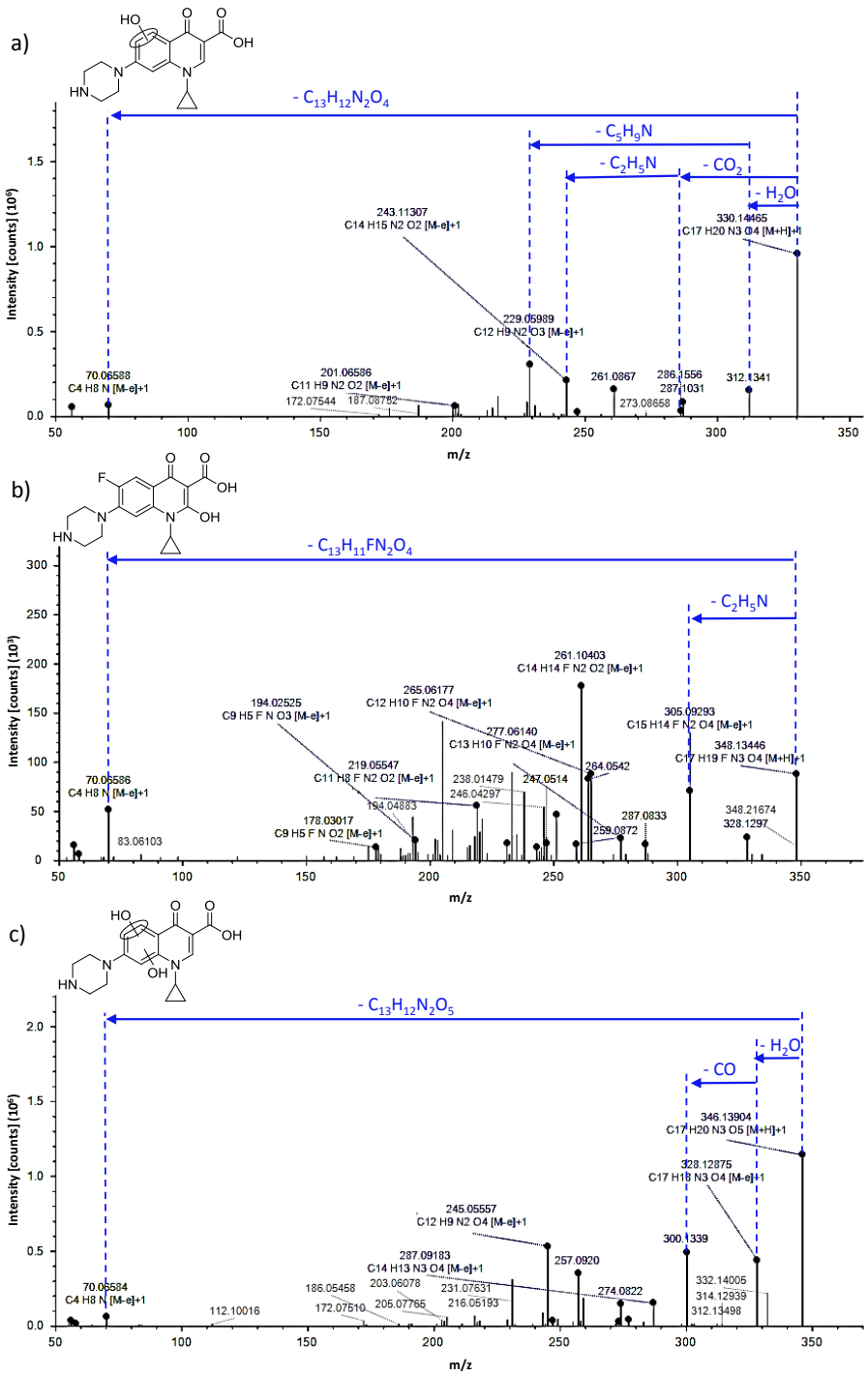

Figure 10.4: *MS/MS spectra of by-products BP2 (a), BP3 (b) and BP5 (c).*

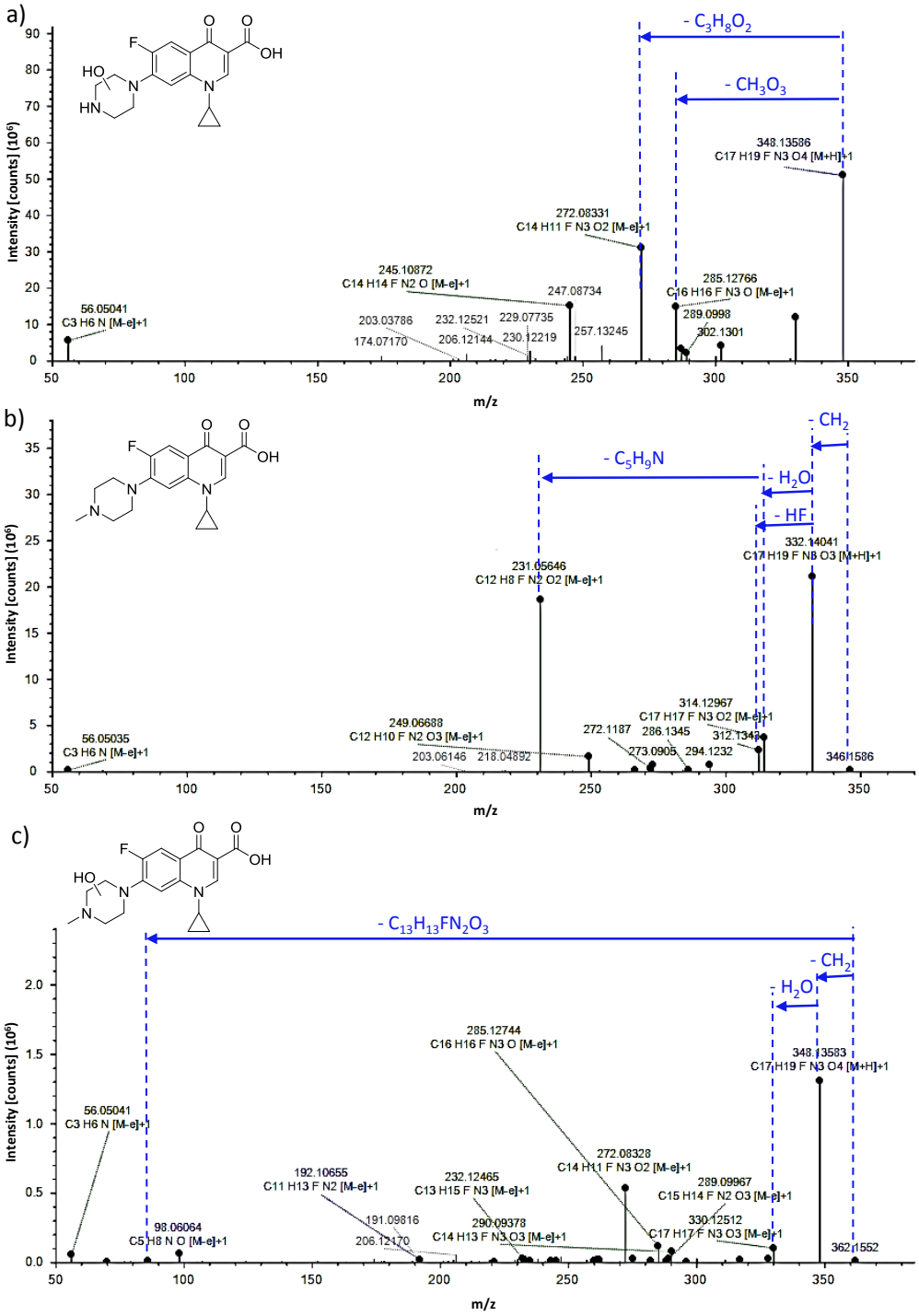

Figure 10.5: *MS/MS spectra of by-products BP4 (a), BP6 (b) and BP7 (c).*

N-methylation of CIPRO was observed in BP6. The absence of *m/z* 70 suggested that the methylation of CIPRO occurred in the piperazinyl ring (see MS/MS spectra in Figure 10.5b). Furthermore, the precursor ion *m/z* 346.15615 was almost completely fragmented and the rest of fragments (*m/z* 332, 314, 312, 249, 231) corresponded to common CIPRO fragmentation. In the case of BP7 (*m/z* 362.15106), hydroxylation plus methylation of CIPRO occurred. The absence of fragment *m/z* 70, and the presence of *m/z* 86 (C_4H_8NO) indicated a modification of the piperazinyl ring by the addition of a hydroxyl group and a methyl group (see MS/MS spectra in Figure 10.5c). Similar to BP6, demethylation (*m/z* 348) was observed in the fragmentation, and the ion *m/z* 330 ($C_{17}H_{17}FN_3O_3$) could correspond to the dehydration of the demethylated fragment rather than to the loss of a methoxy group (-32) from the parent *m/z* 362. In addition, similar to BP4, the presence of fragment *m/z* 272, indicating that something had stabilized the piperazinyl ring, pinpointed that BP7 could be either the methylation product of BP4 or the hydroxylation product of BP6.

Methoxylation of CIPRO was observed in both BP8 and BP9 (see MS/MS spectra in Figure 10.6). BP8 (*m/z* 344.16049) showed both the gain of a methoxy group and the loss of the fluorine atom. Therefore, the most plausible structures were the oxidative replacement of the fluorine atom with the methoxy group or the methoxylation of the adjacent sp^2 carbon atom [29]. This is in agreement with the presence of *m/z* 70 fragment and the lack of a methoxy group loss. Moreover, the loss of water (*m/z* 326) and the decarboxylation (*m/z* 300) suggested that neither the carboxylic group nor the secondary amine of the piperazinyl ring were modified and that the protonation was in equilibrium between these two functional groups. In the case of BP9 (*m/z* 362.15106), in contrast with BP7 and BP8, a loss of a methoxy group was detected in the fragmentation pattern (*m/z* 330). The absence of fragment *m/z* 70 and the presence of *m/z* 68 pinpointed that an unsaturation ($-H_2$) appeared in the piperazinyl ring during fragmentation, most probably during the loss of the methoxy group. Furthermore, fragment *m/z* 86 (C_4H_8NO) could be explained by the presence of the methoxy group in the piperazinyl ring. Lastly, the abundant fragment *m/z* 302 belongs to C_2H_4 loss after demethoxylation.

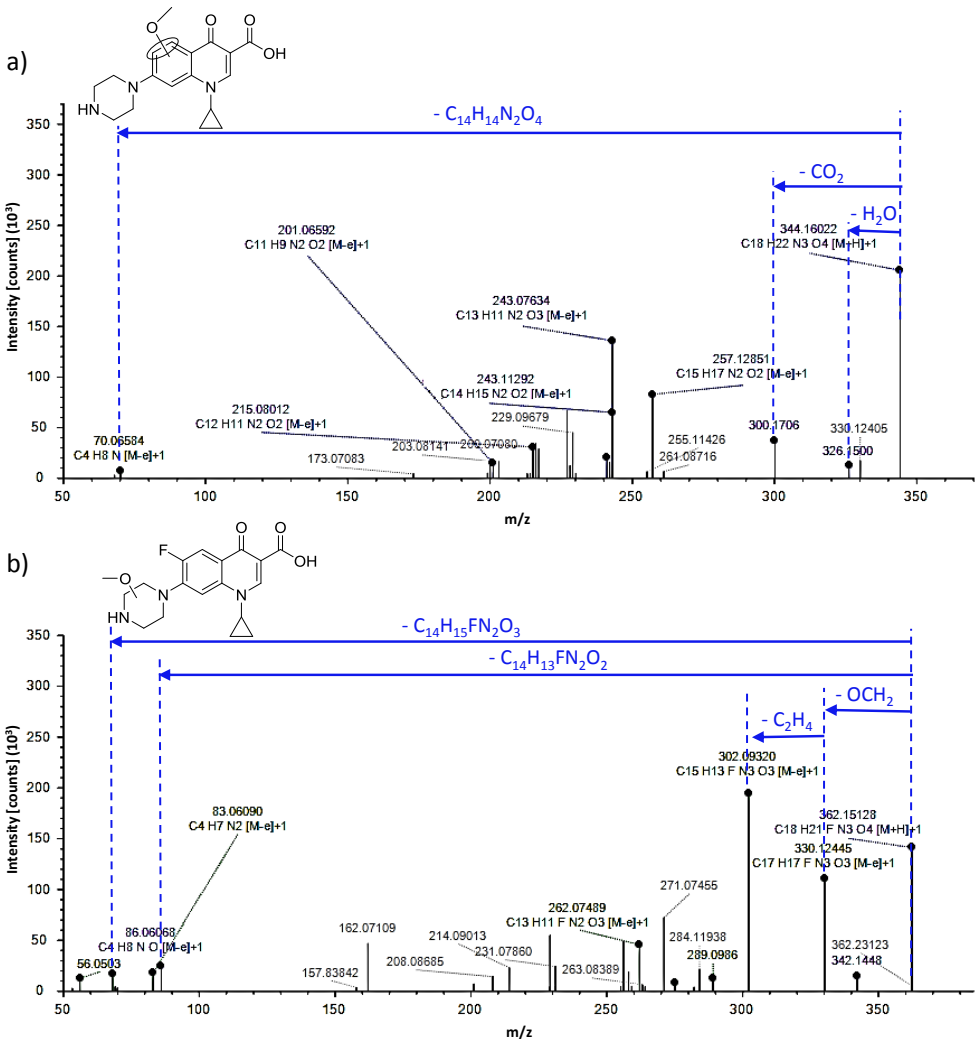

Figure 10.6: *MS/MS spectra of by-products BP8 (a) and BP9 (b).*

In the case of BP10, the precursor ion *m/z* 330.12485 contained one unsaturation (-H_2) more than CIPRO. The absence of fragment *m/z* 70 and the presence of *m/z* 68 pinpointed that the unsaturation should be located in the piperazinyl ring (see MS/MS spectra in Figure 10.7a), caused after dehydration of BP4 or demethoxylation of BP9. The higher stability of alkene function compared to imine group pinpoints that the unsaturation should be located between two carbon atoms. A regioisomer of BP10 with the unsaturation in the imine group has been previously described in the literature [30]. Similar to BP10, BP11 (*m/z* 312.13427) also contained an unsaturation more than CIPRO but, in this case, defluorination had also taken place. The absence

of the fragment *m/z* 70 and the presence of *m/z* 68 pinpointed that the unsaturation should be placed in the piperazinyl ring (see MS/MS spectra in Figure 10.7b).

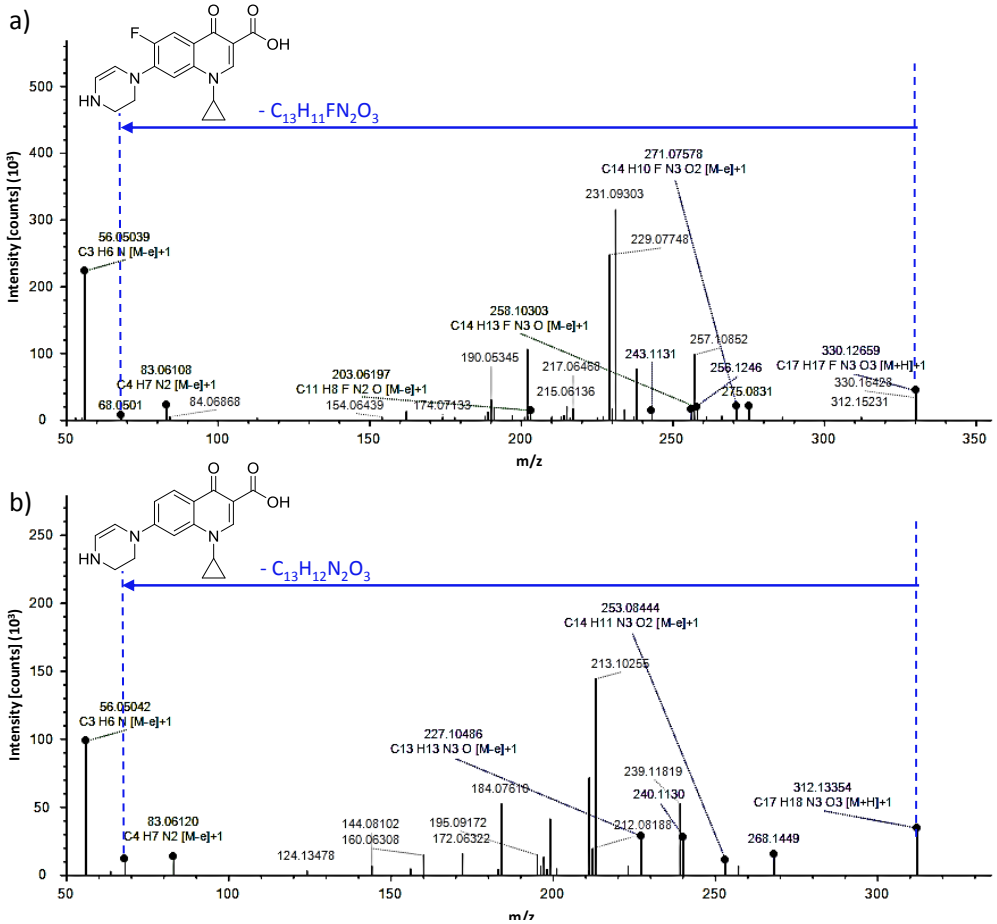

Figure 10.7: *MS/MS spectra of by-products BP10 (a) and BP11 (b).*

Esterification of CIPRO was also observed in BP12 and BP13 (see MS/MS spectra in Figure 10.8). In the case of BP12, the precursor ion *m/z* 346.15615 pinpointed the addition of CH_2 in the molecule. Similar to BP6, the MS/MS spectra contained abundant fragments (*m/z* 332, 314, 312, 249, 245, 231) also present in CIPRO. However, compared to BP6, the presence of the fragment *m/z* 70 suggested that the piperazinyl ring was unmodified and esterification in the carboxylic group of CIPRO was the most tentative structure. However, BP13 (*m/z* 374.15106) could correspond to the *N*-formylation of BP12 or esterification of BP1 since, once the methyl group was lost (*m/z* 360), the fragmentation pattern (*m/z* 342, *m/z* 231, *m/z* 243) corresponded to BP1.

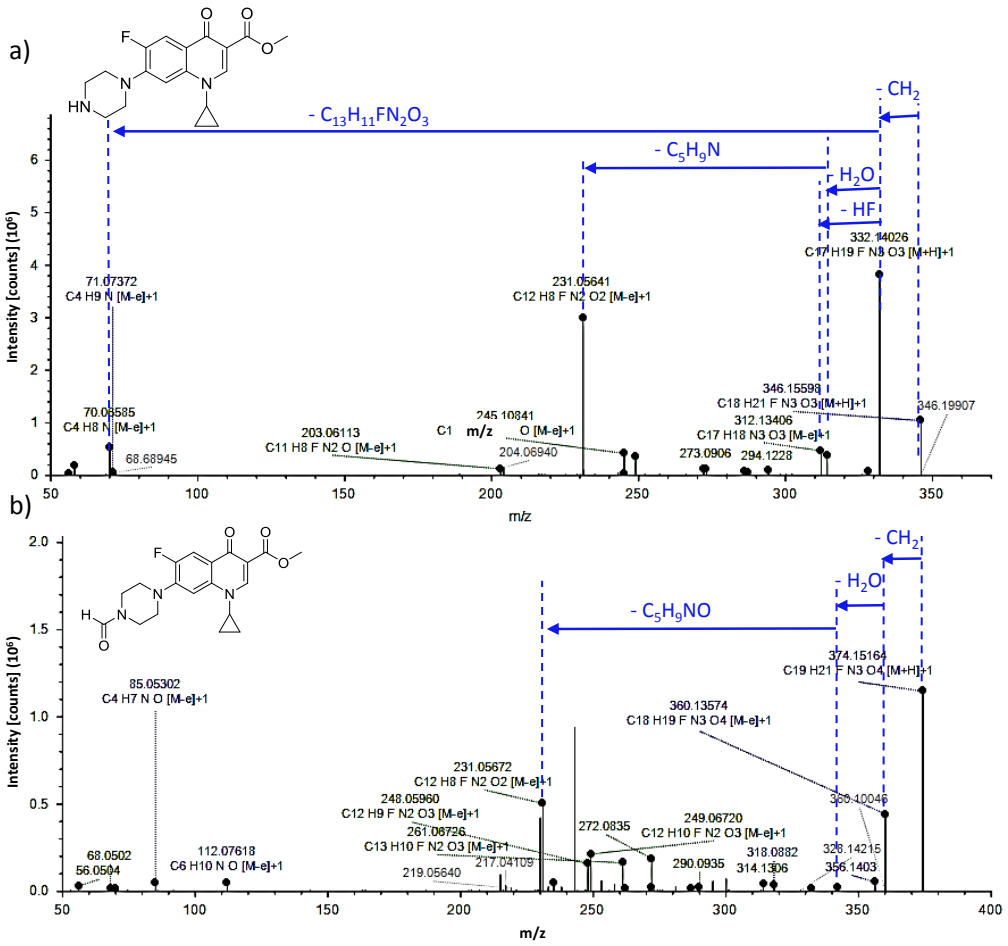

Figure 10.8: *MS/MS spectra of by-products BP12 (a) and BP13 (b).*

Dimethoxylation of CIPRO was observed in BP14. The presence of the fragments *m/z* 70 and *m/z* 348, indicating the decarboxylation of the precursor ion *m/z* 392.16163, pinpointed that the piperazinyl ring was unmodified (see MS/MS spectra in Figure 10.9). The composition change $+C_2H_4O_2$ could come from the introduction of two methoxy groups in CIPRO. However, since only a small fragment showing the methoxy loss was observed (*m/z* 360), the methoxy groups should be located in carbons with sp^2 hybridation, at least one in the aromatic ring and the second one also in the aromatic ring or in the piperidin-4-one ring. Abundant fragment *m/z* 227.11816 could not be explained due to the absence of a molecular formula related with CIPRO that could explain that exact mass.

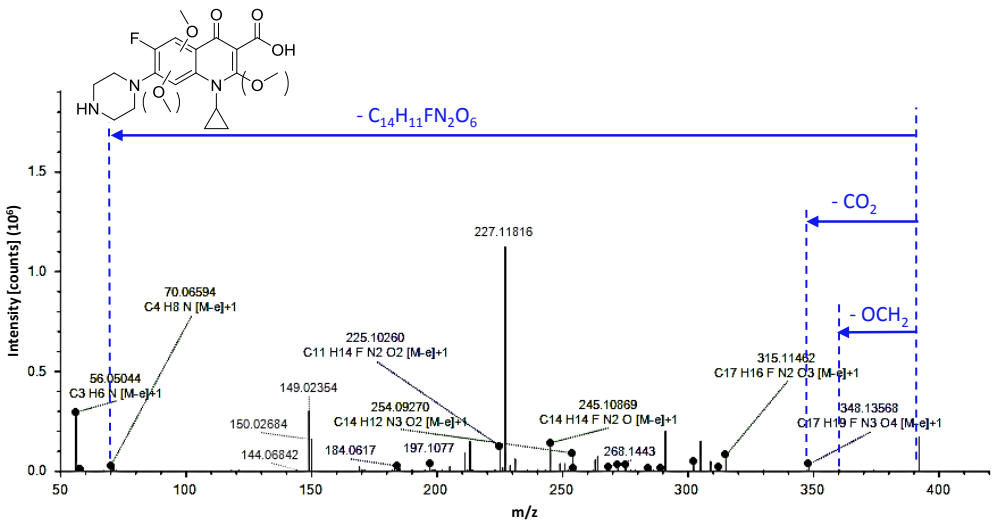

Figure 10.9: *MS/MS spectra of by-product BP14.*

Although the MS/MS spectrum of BP15 was quite poor (see Figure 10.10), the fragment *m/z* 346 corresponded to the loss of a methoxy group from the precursor *m/z* 378.14598. Compared to CIPRO, BP15 contained one more oxygen atom and an unsaturation, which could be explained if the methoxy group was located on the piperazinyl ring and generated an unsaturation when fragmented. This is in agreement with the absence of the *m/z* 70 fragment. Furthermore, after demethoxylation, a small fragment, corresponding to a water loss (*m/z* 328), and a lack of decarboxylation were observed, suggesting that *N*-hydroxylation occurred in the secondary amine group to favor the positive charge equilibrium to the oxygen atom in the piperidin-4-one ring.

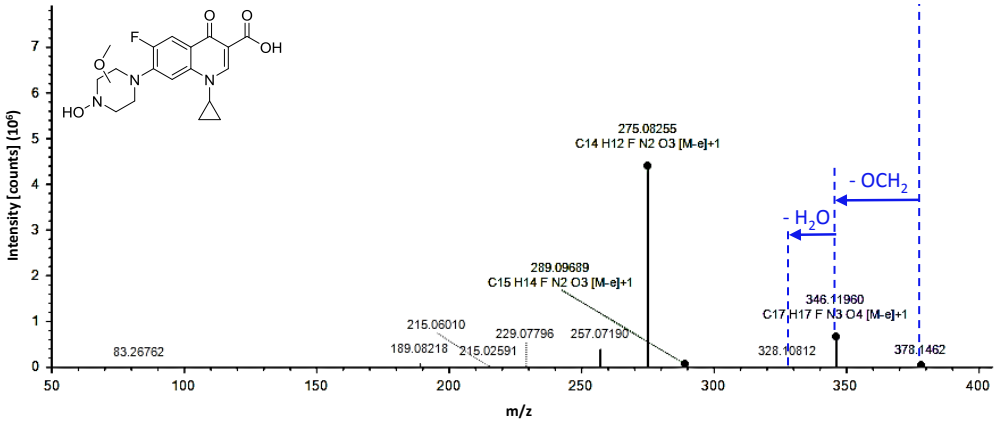

Figure 10.10: *MS/MS spectra of by-product BP15.*

BP16-BP18 (see MS/MS spectra in Figure 10.11) had undergone the cleavage of the piperazinyl ring, which has been previously described in the literature [1,8,22–27,30–33]. BP16 (*m/z* 380.16163) could correspond to the methoxylation and hydroxylation of CIPRO after the cleavage of the piperazinyl ring. The loss of a methoxy group was clearly observed (*m/z* 348), which could be located in the *N*-methyl moiety formed after the cleavage of the piperazinyl ring due to the presence of fragment *m/z* 86 (C_4H_8NO) instead of the fragment *m/z* 70, similar to BP9. On the other *N*-methyl group, obtained after the cleavage of the piperazinyl ring, hydroxylation is proposed in order to explain the presence of the fragment *m/z* 72 (CH_3H_6NO). After demethoxylation, water loss (*m/z* 330) and defluorination (*m/z* 328) were observed in the spectrum. Villegas et al. [27] described a similar BP, but with two hydroxyl groups in the structure. In the case of BP17, the precursor ion *m/z* 362.11468 contained two more oxygen atoms and a single unsaturation. The lack of *m/z* 70 suggested that the piperazinyl ring had been modified. Furthermore, the CO loss before the water loss (*m/z* 334) suggested the presence of at least an aldehyde group. In the absence of a dehydration and in the presence of fragment *m/z* 72 (C_3H_6NO), one possible structure could contain two aldehyde groups after the cleavage of the piperazinyl ring, as already described in the literature [26,31], and the MS/MS fragments observed, including *m/z* 334, 316, 299, 273, 259 and 245, matched with the reported values. Finally, according to the Compound Discoverer 2.0 program, BP18 (*m/z* 390.14598) corresponded to the oxidative deamination to alcohol plus glycine conjugation of CIPRO. Glycine conjugation in the carboxylic acid group of acidic xenobiotics and oxidative deamination of primary amines are common Phase II and Phase I reactions, respectively [34]. In the case of CIPRO, a previous cleavage of the piperazinyl ring is required to form the primary amine. This structure is also in agreement with the lack of fragment *m/z* 70.

BP19 (*m/z* 344.10411, $C_{17}H_{14}FN_3O_4$) contained 4 hydrogen atoms less and an oxygen atom more than CIPRO. The presence of fragment *m/z* 70 suggested no modification in the piperazinyl ring (see MS/MS spectra in Figure 10.12). On the other hand, the loss of water (*m/z* 326) and the consecutive CO loss (*m/z* 298) were attributed to the carboxylic group. Therefore, the most probable position to add an unsaturation and the keto group was the cyclopropyl ring, which was supported by the presence of the fragment *m/z* 53 (C_3HO). However, it was not possible to determine if this oxidation involved the uncommon cleavage of the cyclopropyl moiety.

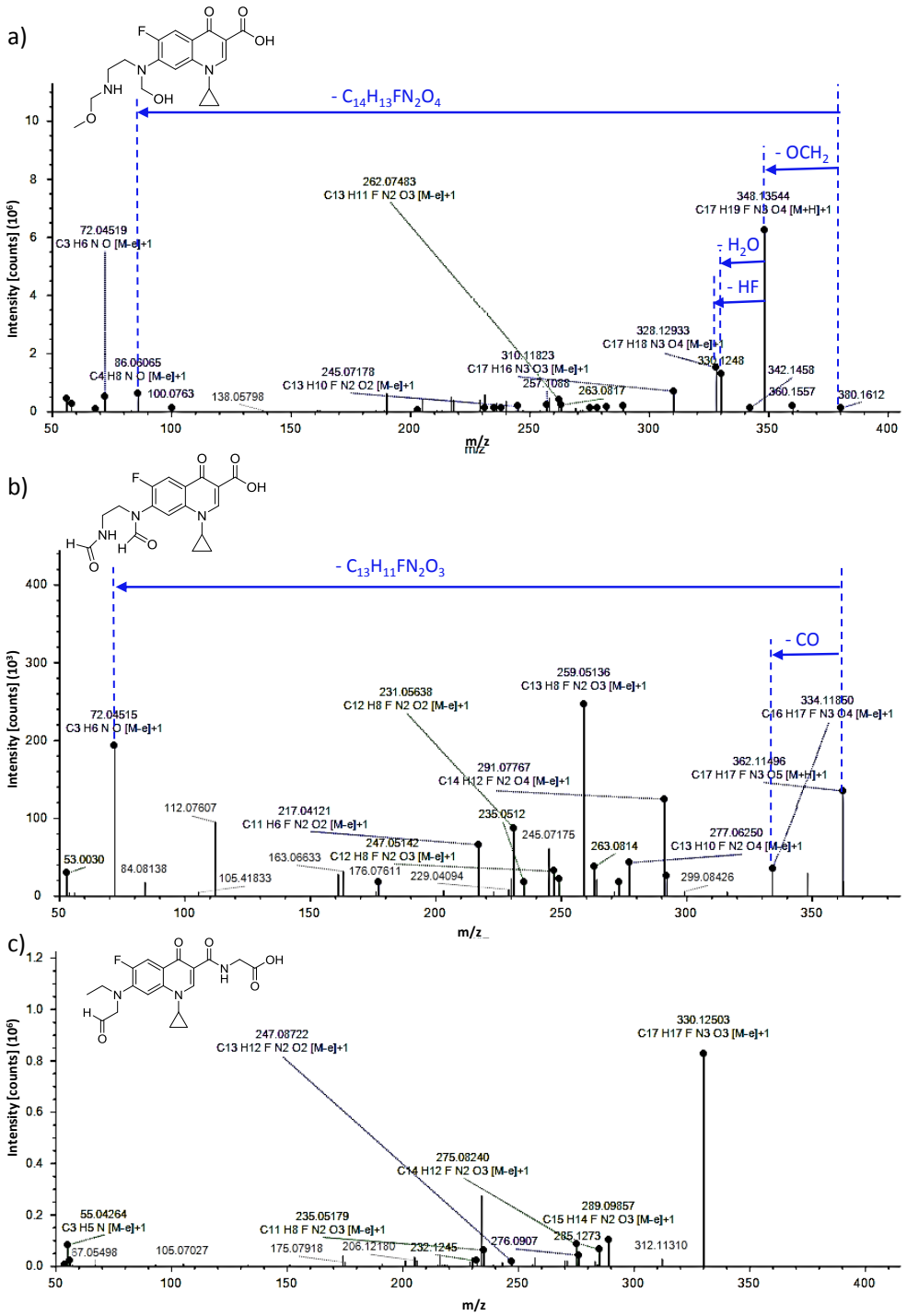

Figure 10.11: *MS/MS spectra of by-products BP16 (a), BP17 (b) and BP18 (c).*

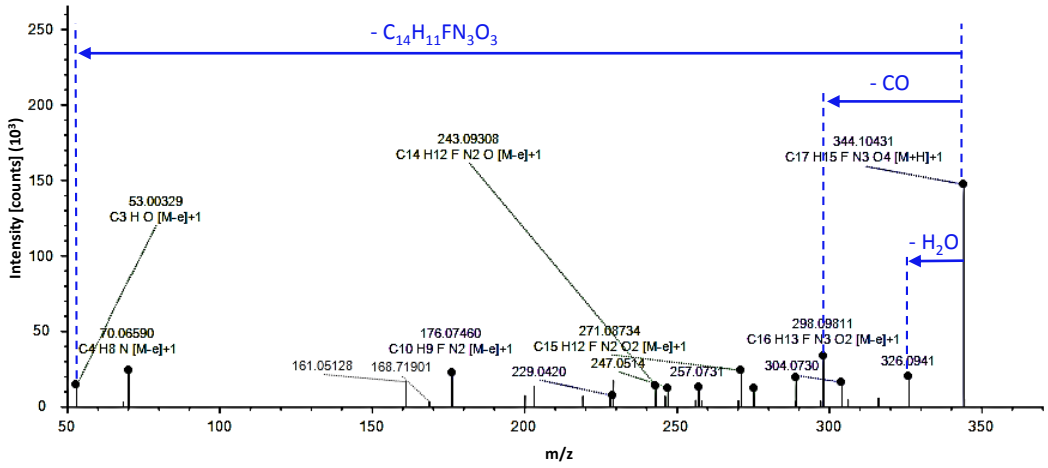

Figure 10.12: *MS/MS spectra of by-product BP19.*

Finally, the structure of BP20 (*m/z* 360.17180) showed a +C_2H_4 composition change compared to CIPRO, but the structure could not be annotated since we did not observe neither a methyl or ethyl loss in the fragmentation, nor a modification of the piperazinyl ring (*m/z* 70), but a decarboxylation (*m/z* 316) of the precursor ion (see MS/MS spectra in Figure 10.13).

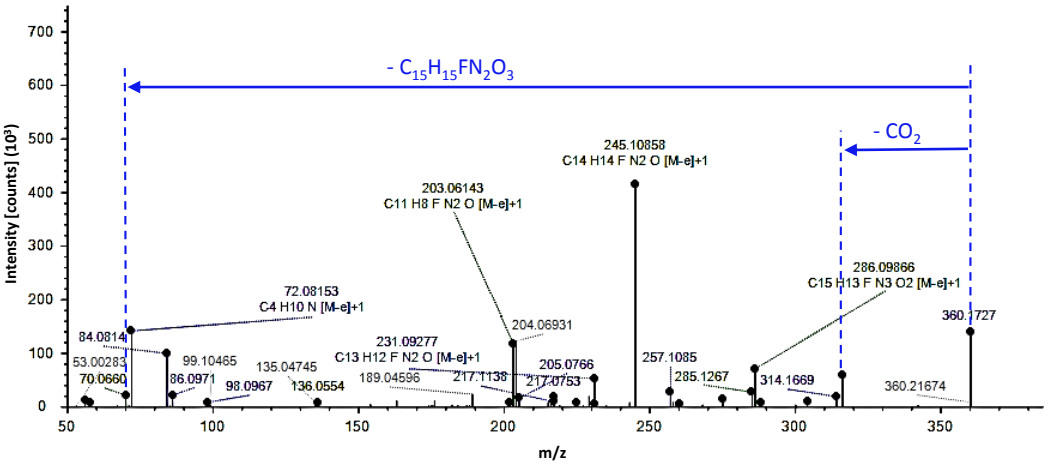

Figure 10.13: *MS/MS spectra of by-product BP20.*

Oxidation, methylation (*N*-, *C*- or *O*-methylation), oxidative defluorination (in 3 BPs out of 20), reductive defluorination (1 BP out of 20), dehydrogenation of the piperazinyl ring (in 2 BPs) and the cleavage of the piperazinyl ring with (1 BP) or without (2 BPs) the loss of the primary amine

formed during the cleavage were the main phase I transformations of CIPRO in seawater. The only Phase II transformation of CIPRO observed was BP18, which suffered oxidative deamination of the piperazinyl ring and glycine conjugation. Regarding toxicology of the BPs, even though most of the annotated BPs were identified in the present work for the first time and scarce information is found in the literature, Toolaram and co-workers reported that BP2, BP5 and BP17 may be genotoxic to bacteria and mammals according to QSAR (Quantitative Structure Activity Relationships) predictions [35]. However, they reported that antagonistic mixture interactions or the low concentration of the BPs in the mixture was not sufficient to cause any observable effect in the bioassays [35].

10.3.2.2 BPs in water in the presence of fish

14 of the previously detected BPs were also observed (BP 1-2, 4-6, 8-10, 12-13, 15-17, 20) and 10 new BPs were annotated in seawater in presence of fish, from which 9 were reported for the first time in the present work (see Figure 10.1).

In BP21, while decarboxylation of precursor ion *m/z* 356.14050 was not observed, the fragment corresponding to the dehydration (*m/z* 338) was one of the main fragments (see MS/MS spectra in Figure 10.14). Dehydration is common when the secondary amine of piperazinyl ring is modified. The absence of the fragment *m/z* 70 and the presence of *m/z* 68 pinpointed that the unsaturation should be in the piperazinyl ring (similar to BP10 and BP11) and fragment *m/z* 94 suggested the presence of an *N*-ethylene group. Therefore, BP21 could be the alkylation product of BP10.

Similarly, in BP22 (*m/z* 372.13541) the introduction of an unsaturation in the CIPRO structure is also required in order to explain the modification of $+C_2O$ (see MS/MS spectra in Figure 10.15). The absence of the fragment *m/z* 70 and the presence of *m/z* 68 pinpointed that the unsaturation was located in the piperazinyl ring, similar to BPs 10, 11 and 21. Fragment *m/z* 344, due to a CO loss before dehydration (common in aldehydes), together with the presence of the abundant fragment *m/z* 110 and the presence of a water loss (*m/z* 354), related to the equivalent of CIPRO B structure, suggested an introduction of an *N*-alkyl aldehyde group in the secondary amine of the piperazinyl ring. Therefore, BP22 could be the alkylation product of BP10.

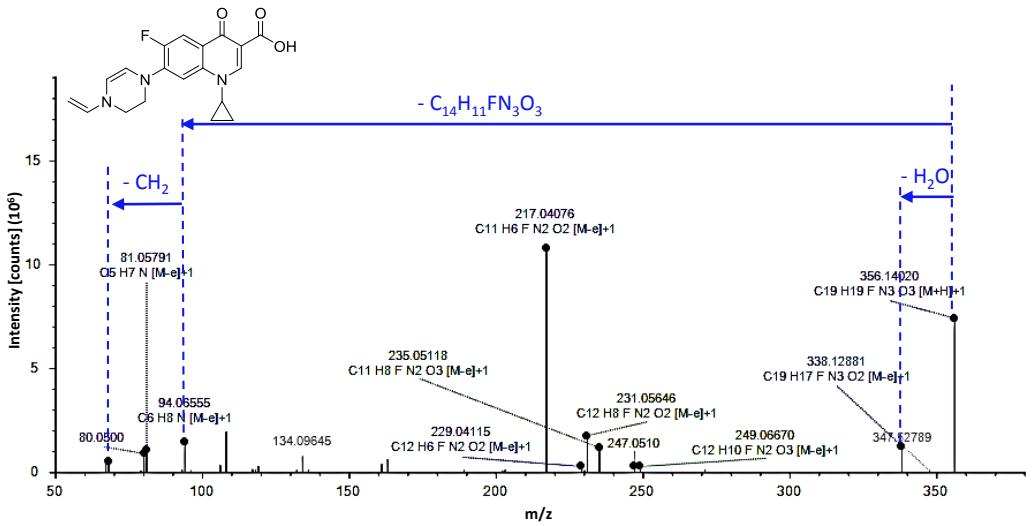

Figure 10.14: *MS/MS spectra of by-product BP21.*

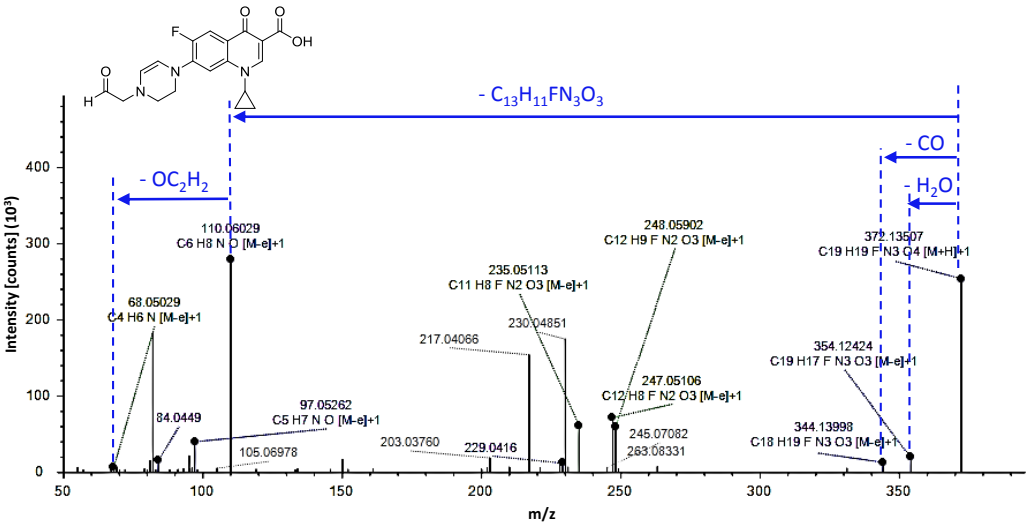

Figure 10.15: *MS/MS spectra of by-product BP22.*

In BP23, the precursor ion *m/z* 362.15106 was poorly fragmented (see MS/MS spectra in Figure 10.16) and the composition change +CH_2O compared to CIPRO could not be attributed to the introduction of a methoxy group because no methoxy loss was observed. The absence of fragment *m/z* 70 pinpointed that the piperazinyl ring was modified and, therefore, the methoxy group could not be located in the aromatic ring. The most abundant fragment *m/z* 100 ($C_5H_{10}NO$)

suggested that both transformations (methylation plus hydroxylation) should be present in the piperazinyl ring. Thus, the addition of +CH_2O should be attributed to a methylation plus hydroxylation of CIPRO. The single water loss observed (*m/z* 344) could be attributed to the common water loss when the secondary amine group has been modified. Hence, *N*-hydroxylation of the secondary amine and methylation of a carbon atom in the piperazinyl ring was suggested to explain BP23.

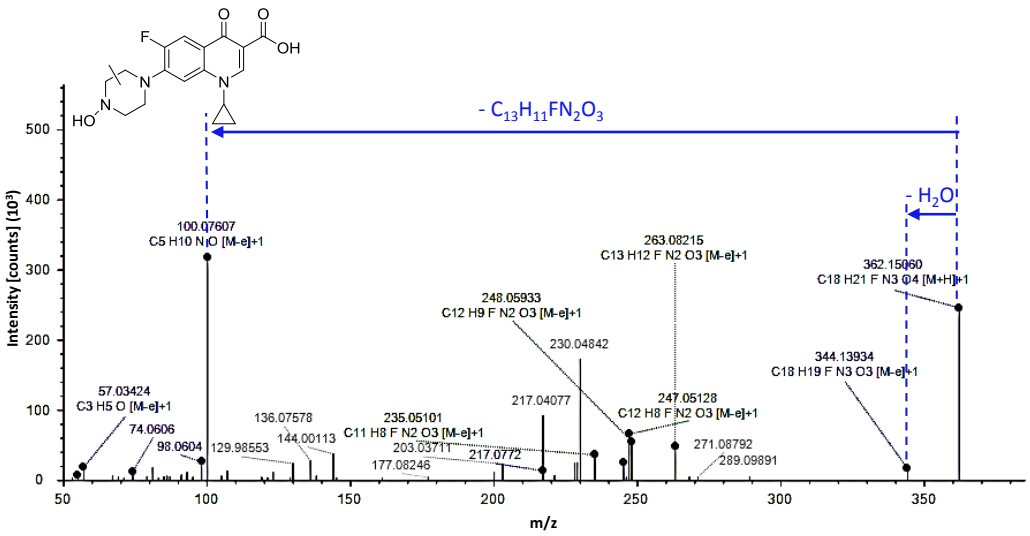

Figure 10.16: *MS/MS spectra of by-product BP23.*

BP24 (*m/z* 346.11976), a keto transformation of CIPRO, could be considered an oxidated product of the monohydroxylated BP4. The absence of *m/z* 70 indicated that the piperazinyl moiety was modified with a carbonyl group in the piperazinyl ring, as described in the literature [24,25,30,31], and the MS/MS fragments observed, including *m/z* 328, 318, 275, 257 and 229, matched with the reported values (see MS/MS spectra in Figure 10.17).

In BP25 (*m/z* 360.13541) fragments *m/z* 340 (360-HF) and *m/z* 332, corresponding to a CO loss before dehydration, were observed (see MS/MS spectra in Figure 10.18). The lack of the *m/z* 70 and the presence of fragment *m/z* 98 indicated that the aldehyde should be in the piperazinyl ring. The fragment *m/z* 68 could correspond to the aldehyde loss and the formation of an unsaturation in the piperazinyl ring. In this case, and on contrary to BP1, the *N*-formylation of CIPRO was discarded because otherwise the equilibrium would be favored towards the equivalent

of CIPRO B structure, causing a water loss not observed in BP25. Therefore, the aldehyde group should be bonded to a sp^3 carbon of the piperazinyl ring.

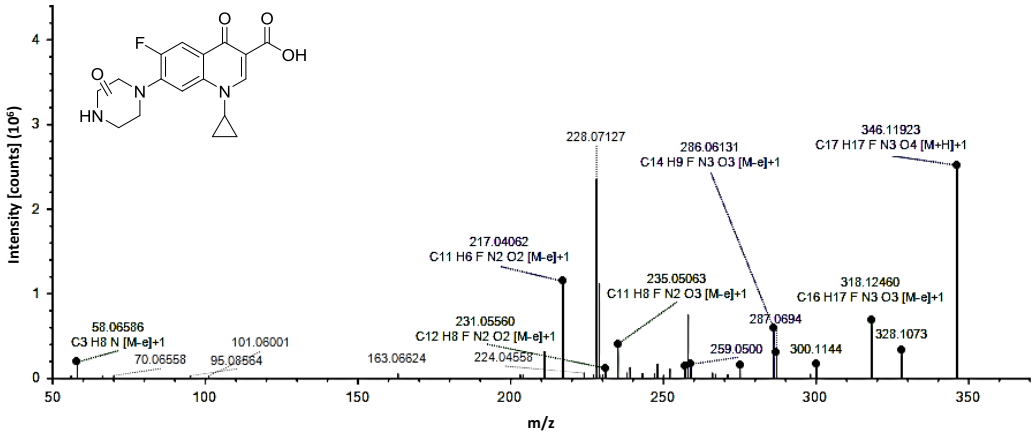

Figure 10.17: *MS/MS spectra of by-product BP24.*

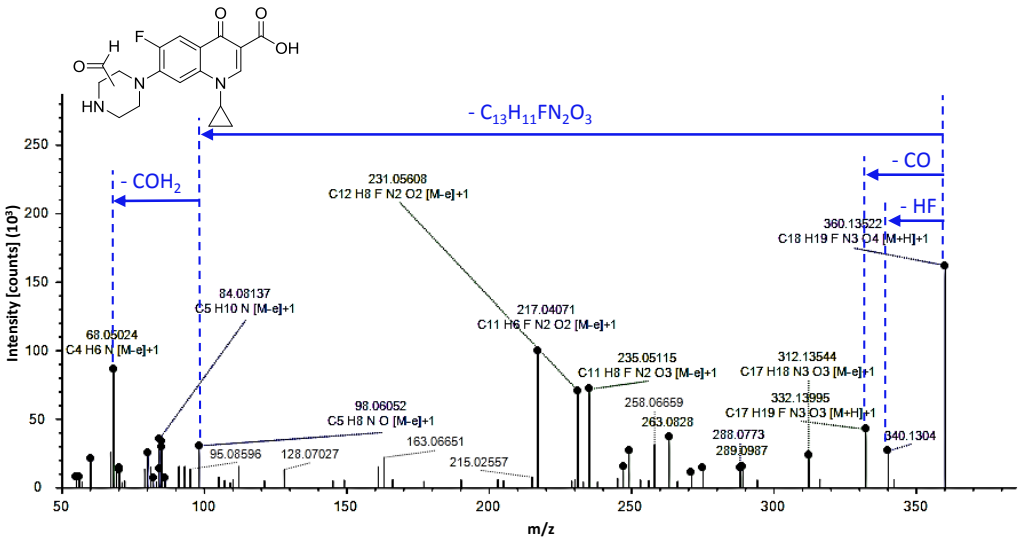

Figure 10.18: *MS/MS spectra of by-product BP25.*

BP26 (*m/z* 332.14050) is a constitutional isomer of CIPRO. Although it presented similar fragmentation to CIPRO (*m/z* 314, 312, 249, 245, 231, 203), the main difference in the MS/MS spectra (see Figure 10.19) is the absence of fragments *m/z* 70 (C_4H_8N) and *m/z* 136 (C_8H_7FN). One option to justify the lack of fragment *m/z* 70 could be the cleavage of the piperazinyl ring, giving place to an unsaturation.

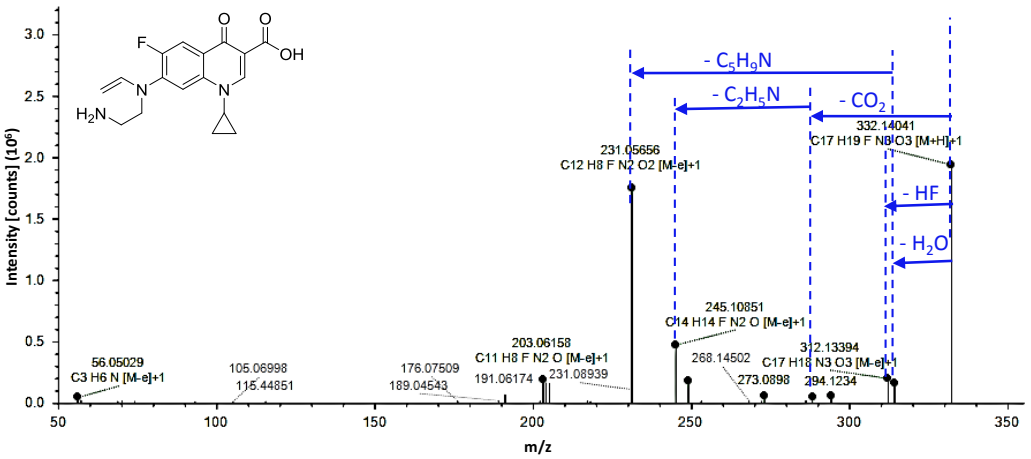

Figure 10.19: *MS/MS spectra of by-product BP26.*

BPs 27-30 suffered the oxidative deamination of the piperazinyl ring of CIPRO when fish were present. In BP27 (*m/z* 351.13508) oxidative deamination of primary amine could explain the loss of nitrogen without losing any carbon atom and, therefore, the cleavage of the piperazinyl ring was suggested, followed by the oxidative deamination to alcohol (see MS/MS spectra in Figure 10.20). Moreover, the two methyl losses observed (fragments *m/z* 337 and *m/z* 305) could correspond to the fragmentation of the *N*-ethyl group. The second hydroxyl group added to the CIPRO structure should be in a sp^2 carbon atom since only two water losses were observed (fragments *m/z* 319 and *m/z* 287), one from the alcohol formed after oxidative deamination and the other one coming from the carboxylic group. However, there was no sufficient information in the MS/MS spectra in order to locate this hydroxyl either in a sp^2 carbon atom of the aromatic ring or in the sp^2 carbon of the piperidin-4-one ring.

BP28 (*m/z* 406.14089) corresponded to the combination of hydration, oxidative deamination to ketone and glycine conjugation of CIPRO. After the cleavage of the piperazinyl ring, while the primary amine suffered oxidative deamination to ketone, the hydroxylation of the other side of the opened ring was suggested. In the MS/MS fragmentation (see Figure 10.21a) two fragments related to water loss were observed (*m/z* 388 and *m/z* 370), one corresponding to the hydroxyl group in the piperazinyl side and the other one corresponding to the carboxyl group. This structure could also explain the absence of fragment *m/z* 70. Additionally, CO loss due to the presence of carbonyl group was observed in small fragments such as *m/z* 98. For BP29

(*m/z* 460.15146) an oxidative deamination plus glutamine conjugation was proposed. A large neutral CO_2 loss was observed (*m/z* 416) related to the two carboxylic groups present in glutamine (see MS/MS spectra in Figure 10.21b). Fragment *m/z* 243 ($C_9H_{11}N_2O_6$) was also related to the glutamine conjugative. Although usually the presence of fragment *m/z* 70 is related to a lack of modification in the piperazinyl ring, this was not the case in BP29, which had suffered oxidative deamination. Finally, three transformations from CIPRO were suggested to annotate BP30 (*m/z* 404.12524) as the dehydrogenated derivate of BP28: oxidation, oxidative deamination to ketone plus glycine conjugation. However, we could not justify fragment *m/z* 306 ($C_{15}H_{17}FN_3O_3$) corresponding to the loss of $C_4H_2O_3$ from the precursor ion (see MS/MS spectra in Figure 10.21c).

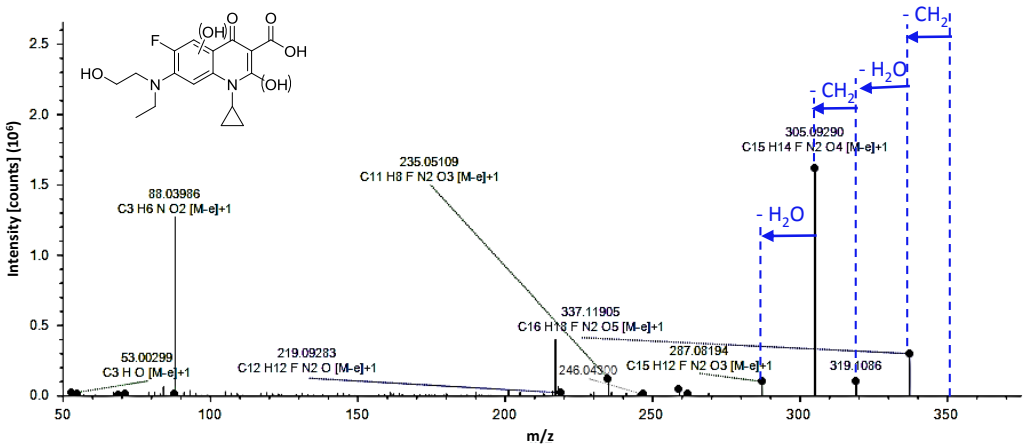

Figure 10.20: *MS/MS spectra of by-product BP27.*

Compared to the BPs annotated in the absence of fish, oxidative deamination and both glycine and glutamine conjugation gained importance in the presence of gilt-head bream since 4 of the 10 new BPs had suffered both transformation reactions (see Figure 10.1).

10.3.2.3 BPs in fish tissues and fluids

Although CIPRO BPs were searched in gilt-head bream liver, brain, muscle, gill, plasma and bile, they were only detected in bile and will be further commented. 5 BPs were found in fish bile and none of them was detected in seawater (see Figure 10.1). The 5 new BPs, named BP31-BP35, had gone through defluorination, which had only been observed in 4 of the 30 BPs previously annotated in water. Moreover, all of them, except BP31, suffered oxidative deamination. Neither glycine nor glutamine conjugates were observed.

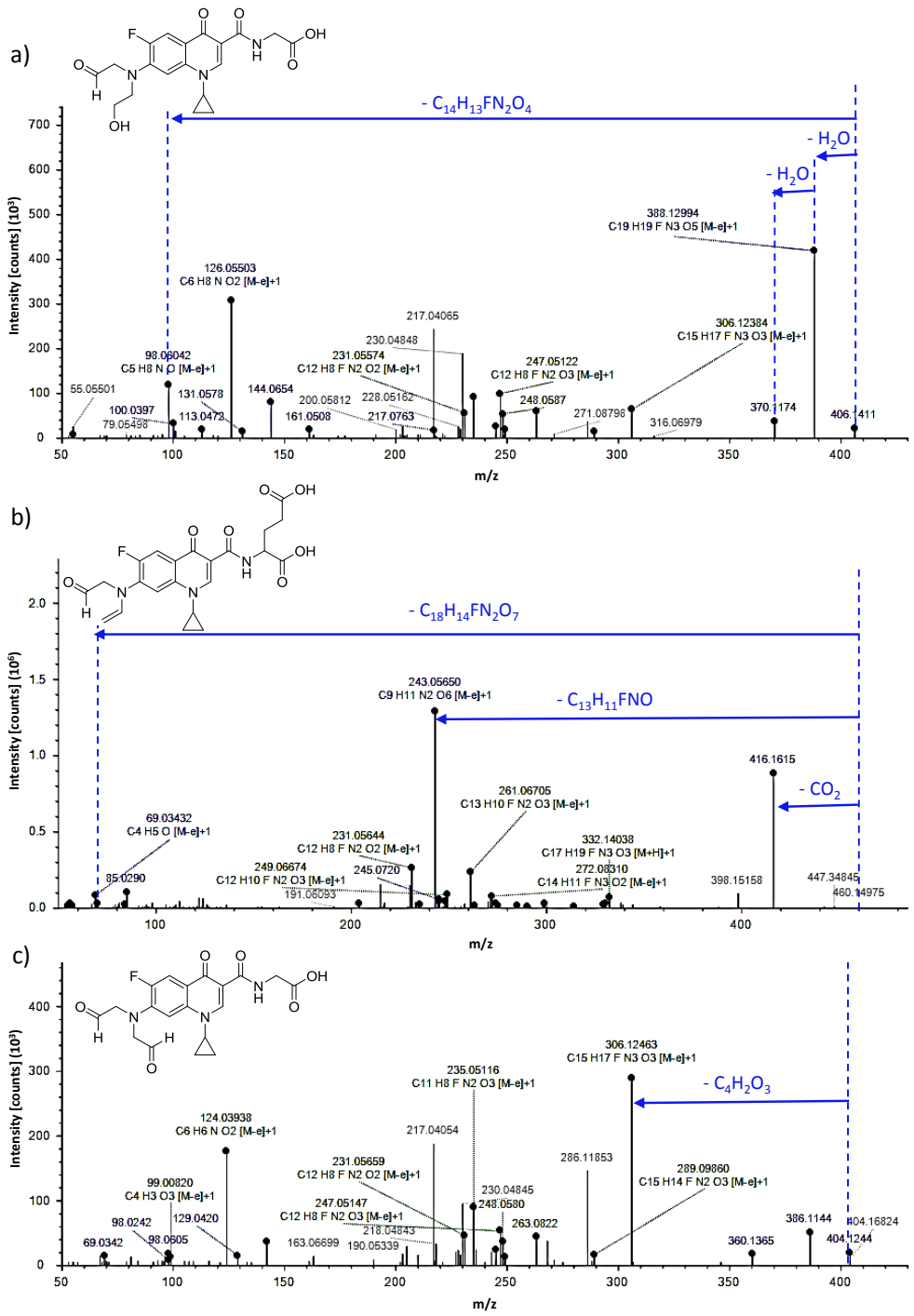

Figure 10.21: *MS/MS spectra of by-products BP28 (a), BP29 (b) and BP30 (c).*

In BP31-33 reductive defluorination took place and the fluorine atom was not replaced by a hydroxyl group in the aromatic ring (see Figures 10.22a-c). BP31 (*m/z* 314.14992) corresponded to the reductive defluorination of CIPRO. Although the MS/MS spectra was poor, fragments *m/z* 296 and *m/z* 268 corresponded to the common water and the consecutive CO losses. In BP32 (*m/z* 333.14450), reductive defluorination, oxidative deamination and hydration of CIPRO were observed, and the structure explained the absence of the fragment *m/z* 70. The presence of the abundant fragment *m/z* 255 ($C_{15}H_{15}N_2O_2$) could be explained as water and CO loss from the carboxylic group, dehydration from one of the hydroxyl groups and demethylation from the alkyl group. Similarly, fragment *m/z* 241 ($C_{14}H_{13}N_2O_2$) corresponded to the demethylation of fragment *m/z* 255. Both fragments suggested that the second hydroxyl group could not be lost, and to match with the reductive defluorination proposed by Compound Discoverer, both OH groups should be placed in adjacent carbons. Finally, oxidative deamination plus reductive defluorination of CIPRO was proposed for BP33 (*m/z* 315.13394). The absence of *m/z* 70, together with the oxidative deamination and the loss of CO (*m/z* 287), pinpointed the introduction of an aldehyde group in replacement of the secondary amine of the piperazinyl ring. Fragment *m/z* 255 could be explained as dehydration in the carboxyl group and demethylation in the *N*-ethyl group of *m/z* 287.

On the contrary to BP31-33, oxidative defluorination of CIPRO was pinpointed in BP34-35. BP34 (*m/z* 345.14450) corresponded to the oxidative deamination, oxidative defluorination plus methylation of CIPRO. Similar to BP32, the fragment *m/z* 317 indicated a CO loss from the precursor, suggesting the presence of an aldehyde formed during the oxidative deamination (see MS/MS spectra in Figure 10.23a). Fragments *m/z* 283 and *m/z* 271 suggested the presence of the *N*-ethyl group formed after the cleavage of the piperazinyl ring. On the other hand, since methoxy group loss was not observed, the methoxy or hydroxyl group plus methyl groups should be located in the aromatic ring, being most probable the addition of the methoxy group to either the sp^2 carbon that contained the fluorine atom or to the adjacent one. Actually, since two regioisomers were detected, one could contain the methoxy group in the sp^2 carbon atom where the fluorine atom had been located and the other one could contain the methoxy group in the adjacent sp^2 carbon atom. Lastly, fragment *m/z* 327 was attributed to a water loss due to the presence of the carboxylic acid group of CIPRO, and this structure also explained the absence of fragment *m/z* 70 (C_4H_8N) and the presence of fragments *m/z* 74 (C_3H_8NO) and *m/z* 86 (C_4H_8NO).

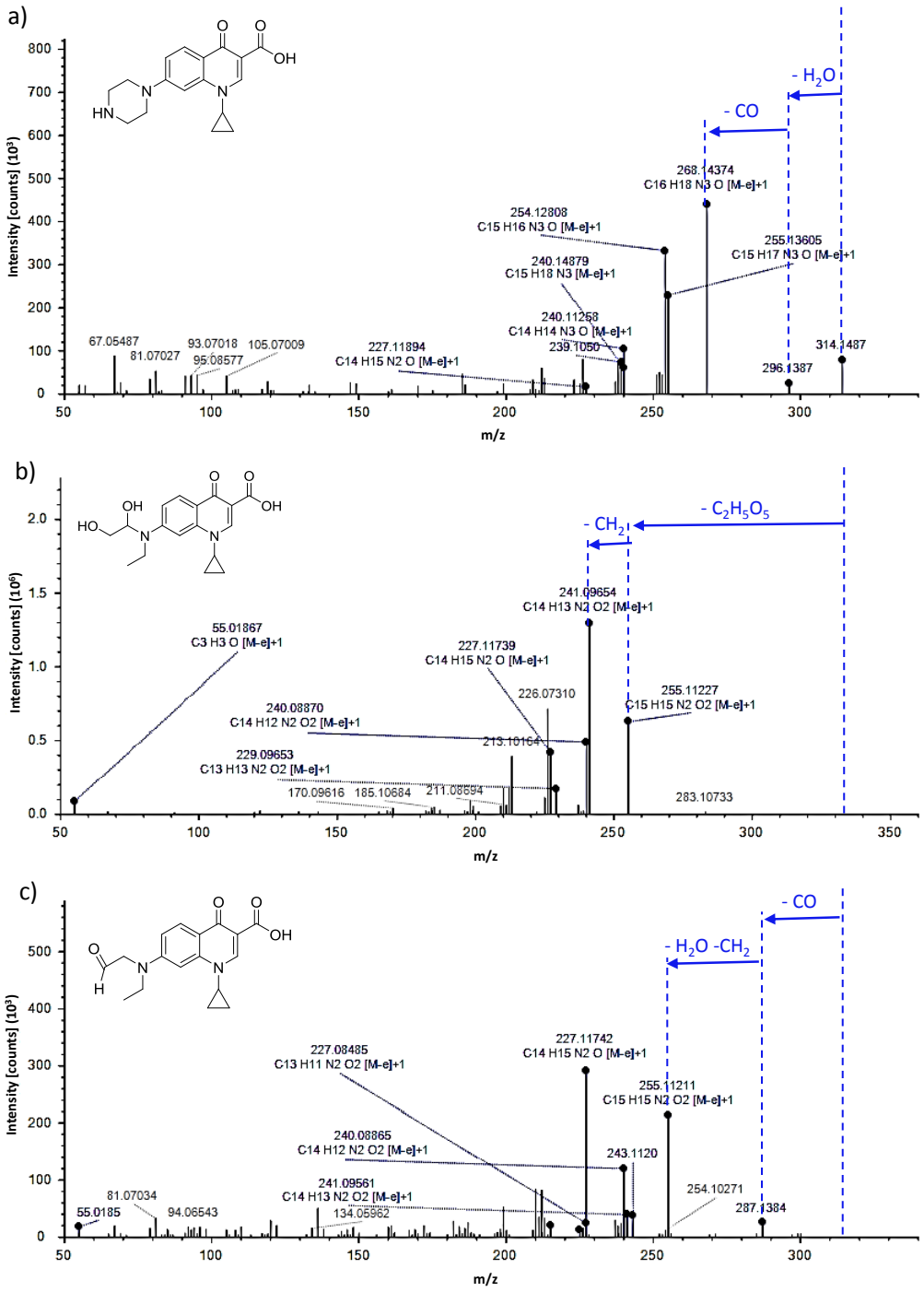

Figure 10.22: *MS/MS spectra of by-products BP31 (a), BP32 (b) and BP33 (c).*

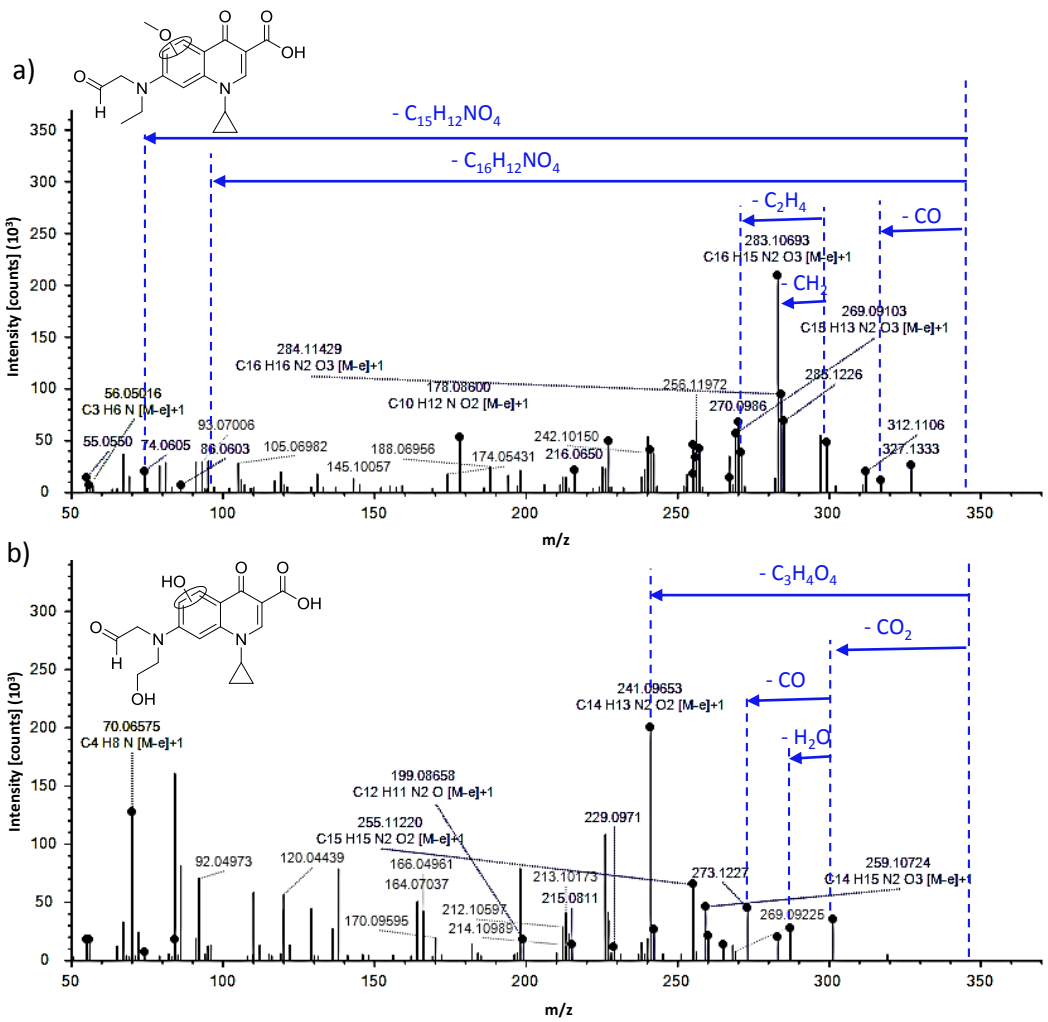

Figure 10.23: *MS/MS spectra of by-products BP34 (a) and BP35 (b).*

Finally, hydration, oxidative deamination to ketone plus oxidative defluorination of CIPRO was suggested to explain the metabolite BP35 (*m/z* 347.12377). The CO loss observed before dehydration (fragment *m/z* 273) suggested the presence of an aldehyde group formed from the cleavage of the piperazinyl ring and the oxidative deamination of the primary amine formed (see MS/MS spectra in Figure 10.23b). The presence of the fragment *m/z* 301 attributed to a decarboxylation and the fragment *m/z* 287, corresponding to a subsequent dehydration, pinpointed that one hydroxyl group should be located in a position where dehydration could occur.

Hence, we suggested a structure with a hydroxyl group in the aromatic ring (no water loss) and another one in the *N*-ethyl group formed during the cleavage of the piperazinyl ring. The -OH group in the aromatic group should be related to defluorination but, with the information available, we could not annotate its position, which could replace the fluorine atom or could be located in the adjacent sp^2 carbon. Lastly, the fragment *m/z* 241 ($C_{14}H_{13}N_2O_2$), which kept both nitrogen atoms of the precursor, could be explained by decarboxylation, CO loss from aldehyde, dehydration of the alcohol plus demethylation.

As above mentioned, defluorination was characteristic of all the BPs observed in bile, and BP31 was the most similar in structure to the 4 defluorinated BPs observed in seawater (BP2, BP5, BP9 and BP11). However, all of them were already present in the seawater in the absence of fish, therefore, BP31 was not necessarily their precursor.

10.3.3 Relative abundances of CIPRO BPs

In order to compare the abundances of BPs in the different scenarios studied, equivalent chromatographic signal response factors were assumed for all the BPs. Since response factors may differ among BPs, these results should be considered semiquantitative. Figure 10.24 shows the relative abundances calculated as the ratio of the individual peak area with respect to the sum of all peak area in the different samples (seawater, seawater with fish and fish bile). All peak areas were corrected using internal standard ([$^2H_8$]-CIPRO).

CIPRO was significantly the most abundant compound in seawater in the absence and presence of fish, accounting for approximately the 95% of all the compounds detected in the aqueous phase. BP1 (*N*-formylation of CIPRO), BP4 (hydroxylation in the piperazinyl ring of CIPRO) and BP13 (*N*-formylation + esterification of CIPRO) were detected both in the absence and presence of fish in approximately 1% of the total compounds. In the presence of gilt-head bream, BP21 and BP24 were also detected at similar levels. The relative profile for CIPRO and BPs in seawater remained fairly consistent over the duration of the experiment regardless of the presence or absence of fish. The BPs in the presence of fish correspond to the most complete scenario since we did not only consider the BPs formed in seawater due to photodegradation or degradation by microorganisms present in seawater but we also took into account those present in

the seawater media due to either fish elimination or formation in the water media in the presence of fish excrements.

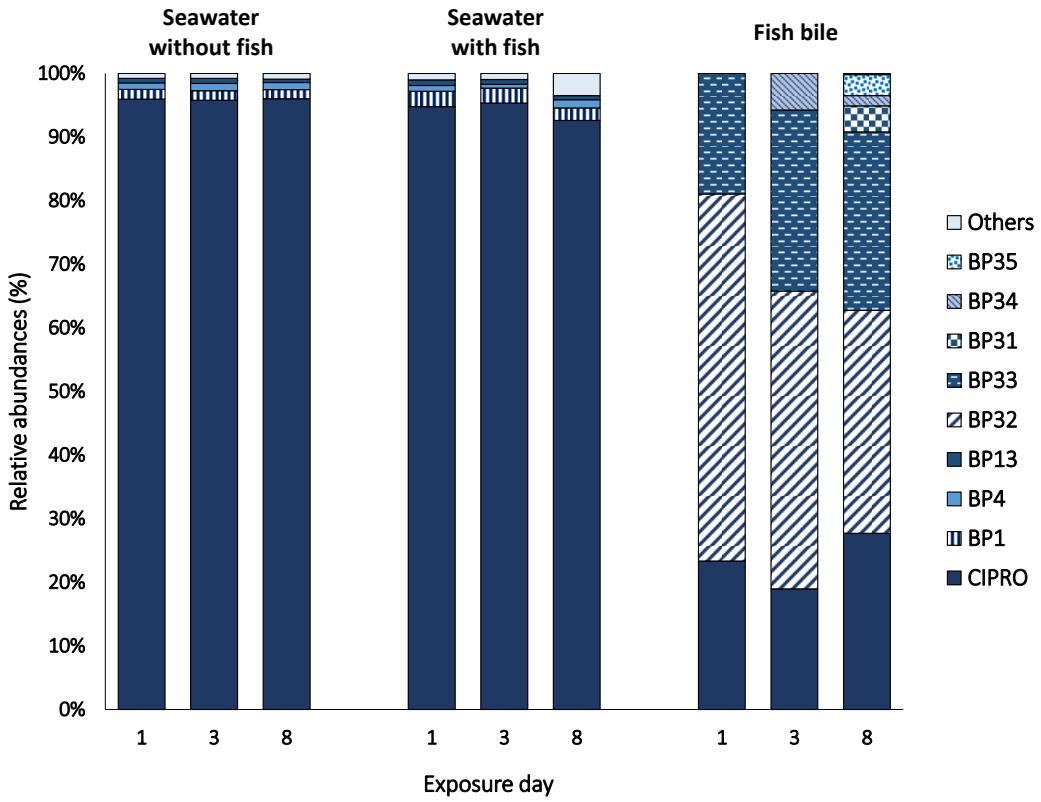

Figure 10.24: *Relative abundances of CIPRO and its BPs (calculated as the ratio of the individual peak area with respect to the sum of all peak areas) in seawater in the absence and presence of gilt-head bream and fish bile along the CIPRO exposure experiment (day 1, 3, and 8).*

In the case of fish bile, BP32 was found at the highest abundance (33-58%), followed by CIPRO (18-26%) and BP33 (19-28%) and the relative profile varied with time. Overall, while a slight decrease of BP32 was observed with time, BP33 increased. An increase of BP34 up to 6% was also observed at day 3 of exposure, and BP31 (4%) and BP35 (3%) also increased in the last exposure day (day 8).

10.4 Conclusions

In order to assess risks associated with the exposure to PhACs in aquatic wildlife, a complete understanding of the uptake of the pharmaceutical together with its potentially bioactive BPs is required. Although this can vary from specie to specie and under different environmental conditions (seawater vs freshwater), in the present work it has been observed that CIPRO is only accumulated in gilt-head bream bile and not in lipidic tissues.

On the other hand, even though CIPRO was significantly the most abundant compound in seawater, accounting for approximately the 95% of all the compounds detected in the aqueous phase, 30 different BPs were detected in water and another 5 different BPs in fish bile. The fact of having just 14 BPs in common in seawater in the absence and presence of fish clearly indicates that the degradation of CIPRO is dependent on environmental conditions. It is worth mentioning that in the BPs annotated in the presence of fish, oxidative deamination and both glycine and glutamine conjugation gained importance. In the case of bile, while glycine or glutamine conjugates were not observed, defluorination and oxidative deamination were relevant, with BP32 being even more abundant than CIPRO. Lastly, with *in-silico* tests that concluded genotoxicity of CIPRO BPs to bacteria and mammals [35], and having reported 30 BPs out of 35 for the first time in the present work, it is suggested that the identification of new BPs is a required challenge in order to include the determination and effects of PhACs BPs in environmental exposure assessment.

10.5 References

1. Babić S, Periša M, Škorić I. 2013. Photolytic degradation of norfloxacin, enrofloxacin and ciprofloxacin in various aqueous media. *Chemosphere*. 91:1635–1642.
2. Van Doorslaer X, Dewulf J, Van Langenhove H, Demeestere K. 2014. Fluoroquinolone antibiotics: An emerging class of environmental micropollutants. *Sci. Total Environ.* 500–501:250–269.
3. Zhao J-L, Liu Y-S, Liu W-R, Jiang Y-X, Su H-C, Zhang Q-Q, Chen X-W, Yang Y-Y, Chen J, Liu S-S, Pan C-G, Huang G-Y, Ying G-G. 2015. Tissue-specific bioaccumulation of human and veterinary antibiotics in bile, plasma, liver and muscle tissues of wild fish from a highly urbanized region. *Environ. Pollut.* 198:15–24.

4. Aryal S. 2001. Antibiotic Resistance: A Concern to Veterinary and Human Medicine. *Nepal Agric. Res. J.* 4:66–70.

5. Carvalho IT, Santos L. 2016. Antibiotics in the aquatic environments: A review of the European scenario. *Environ. Int.* 94:736–757.

6. Levy SB. 2002. Factors impacting on the problem of antibiotic resistance. *J. Antimicrob. Chemother.* 49:25–30.

7. Levy SB. 1997. Antibiotic resistance: an ecological imbalance. *Ciba Found. Symp.* 207:1–9; discussion 9-14.

8. Maia AS, Ribeiro AR, Amorim CL, Barreiro JC, Cass QB, Castro PML, Tiritan ME. 2014. Degradation of fluoroquinolone antibiotics and identification of metabolites/transformation products by liquid chromatography–tandem mass spectrometry. *J. Chromatogr. A*. 1333:87–98.

9. Alcaráz MR, Vera-Candioti L, Culzoni MJ, Goicoechea HC. 2014. Ultrafast quantitation of six quinolones in water samples by second-order capillary electrophoresis data modeling with multivariate curve resolution–alternating least squares. *Anal. Bioanal. Chem.* 406:2571–2580.

10. Ashfaq M, Khan KN, Rasool S, Mustafa G, Saif-Ur-Rehman M, Nazar MF, Sun Q, Yu C-P. 2016. Occurrence and ecological risk assessment of fluoroquinolone antibiotics in hospital waste of Lahore, Pakistan. *Environ. Toxicol. Pharmacol.* 42:16–22.

11. Turiel E, Bordin G, Rodríguez AR. 2005. Determination of quinolones and fluoroquinolones in hospital sewage water by off-line and on-line solid-phase extraction procedures coupled to HPLC-UV. *J. Sep. Sci.* 28:257–267.

12. Gomes MP, Gonçalves CA, de Brito JCM, Souza AM, da Silva Cruz FV, Bicalho EM, Figueredo CC, Garcia QS. 2017. Ciprofloxacin induces oxidative stress in duckweed (Lemna minor L.): Implications for energy metabolism and antibiotic-uptake ability. *J. Hazard. Mater.* 328:140–149.

13. Schymanski EL, Jeon J, Gulde R, Fenner K, Ruff M, Singer HP, Hollender J. 2014. Identifying Small Molecules via High Resolution Mass Spectrometry: Communicating Confidence. *Environ. Sci. Technol.* 48:2097–2098.

14. Ziarrusta H, Val N, Dominguez H, Mijangos L, Prieto A, Usobiaga A, Etxebarria N, Zuloaga O, Olivares M. 2017. Determination of fluoroquinolones in fish tissues, biological fluids, and environmental waters by liquid chromatography tandem mass spectrometry. *Anal. Bioanal. Chem.*:1–12. doi:10.1007/s00216-017-0575-4.

15. Nallani GC, Edziyie RE, Paulos PM, Venables BJ, Constantine LA, Huggett DB. 2016. Bioconcentration of two basic pharmaceuticals, verapamil and clozapine, in fish. *Environ.*

Toxicol. Chem. 35:593–603.

16. Gao L, Shi Y, Li W, Liu J, Cai Y. 2012. Occurrence, distribution and bioaccumulation of antibiotics in the Haihe River in China. *J. Environ. Monit.* 14:1247–1254.
17. Erickson RJ, McKim JM, Lien GJ, Hoffman AD, Batterman SL. 2006. Uptake and elimination of ionizable organic chemicals at fish gills: I. Model formulation, parameterization, and behavior. *Environ. Toxicol. Chem.* 25:1512–1521.
18. Elston RA, Drum AS, Schweitzer MG, Rode RA, Bunnell PR. 1994. Comparative Uptake of Orally Administered Difloxacin in Atlantic Salmon in Freshwater and Seawater. *J. Aquat. Anim. Health*. 6:341–348.
19. Kovačević B, Schorr P, Qi Y, Volmer DA. 2014. Decay mechanisms of protonated 4-quinolone antibiotics after electrospray ionization and ion activation. *J. Am. Soc. Mass Spectrom.* 25:1974–1986.
20. Burhenne J, Ludwig M, Spiteller M. 1997. Photolytic degradation of fluoroquinolone carboxylic acids in aqueous solution. *Environ. Sci. Pollut. Res.* 4:61–67.
21. Pereira VJ, Linden KG, Weinberg HS. 2007. Evaluation of UV irradiation for photolytic and oxidative degradation of pharmaceutical compounds in water. *Water Res.* 41:4413–4423.
22. Vasconcelos TG, Henriques DM, König A, Martins AF, Kümmerer K. 2009. Photo-degradation of the antimicrobial ciprofloxacin at high pH: Identification and biodegradability assessment of the primary by-products. *Chemosphere*. 76:487–493.
23. Haddad T, Kümmerer K. 2014. Characterization of photo-transformation products of the antibiotic drug Ciprofloxacin with liquid chromatography–tandem mass spectrometry in combination with accurate mass determination using an LTQ-Orbitrap. *Chemosphere*. 115:40–46.
24. Morales-Gutiérrez FJ, Hermo MP, Barbosa J, Barrón D. 2014. High-resolution mass spectrometry applied to the identification of transformation products of quinolones from stability studies and new metabolites of enrofloxacin in chicken muscle tissues. *J. Pharm. Biomed. Anal.* 92:165–176.
25. Guo H-G, Gao N-Y, Chu W-H, Li L, Zhang Y-J, Gu J-S, Gu Y-L. 2013. Photochemical degradation of ciprofloxacin in UV and UV/H2O2 process: kinetics, parameters, and products. *Environ. Sci. Pollut. Res.* 20:3202–3213.
26. Paul T, Dodd MC, Strathmann TJ. 2010. Photolytic and photocatalytic decomposition of aqueous ciprofloxacin: Transformation products and residual antibacterial activity. *Water Res.* 44:3121–3132.
27. Villegas-Guzman P, Oppenheimer-Barrot S, Silva-Agredo J, Torres-Palma RA. 2017.

Comparative Evaluation of Photo-Chemical AOPs for Ciprofoxacin Degradation: Elimination in Natural Waters and Analysis of pH Effect, Primary Degradation By-Products, and the Relationship with the Antibiotic Activity. *Water. Air. Soil Pollut.* 228:209.

28. Wetzstein H-G, Stadler M, Tichy H-V, Dalhoff A, Karl W. 1999. Degradation of Ciprofloxacin by Basidiomycetes and Identification of Metabolites Generated by the Brown Rot Fungus Gloeophyllum striatum. *Appl. Environ. Microbiol.* 65:1556–1563.

29. Ramanathan R, Chowdhury SK, Alton KB. 2005. Oxidative metabolites of drugs and xenobiotics: lc-ms methods to identify and characterize in biological matrices, in Chowdhury, S.K. (ed.), Identification and Quantification of drugs, metabolites and metabolizing enzymes by LC-MS. 6, Elsevier, Amsterdam, pp 225–276.

30. Salma A, Thoröe-Boveleth S, Schmidt TC, Tuerk J. 2016. Dependence of transformation product formation on pH during photolytic and photocatalytic degradation of ciprofloxacin. *J. Hazard. Mater.* 313:49–59.

31. Hu L, Stemig AM, Wammer KH, Strathmann TJ. 2011. Oxidation of Antibiotics during Water Treatment with Potassium Permanganate: Reaction Pathways and Deactivation. *Environ. Sci. Technol.* 45:3635–3642.

32. Zhang X, Li R, Jia M, Wang S, Huang Y, Chen C. 2015. Degradation of ciprofloxacin in aqueous bismuth oxybromide (BiOBr) suspensions under visible light irradiation: A direct hole oxidation pathway. *Chem. Eng. J.* 274:290–297.

33. Prieto A, Möder M, Rodil R, Adrian L, Marco-Urrea E. 2011. Degradation of the antibiotics norfloxacin and ciprofloxacin by a white-rot fungus and identification of degradation products. *Bioresour. Technol.* 102:10987–10995.

34. Hop CECA, Prakash C. 2005. *Metabolite identification by LC-MS: applications in durg discovery and development, in Chowdhury, S.K. (ed.), Identification and Quantification of drugs, metabolites and metabolizing enzymes by LC-MS*. Elsevier, Amsterdam, pp. 123-158.

35. Toolaram AP, Haddad T, Leder C, Kümmerer K. 2016. Initial hazard screening for genotoxicity of photo-transformation products of ciprofloxacin by applying a combination of experimental and in-silico testing. *Environ. Pollut.* 211:148–156.

11. Kapitulua

Ondorioak

Doktorego-tesi honetan lortutako emaitzek aurretiaz ezarritako helburuak betetzea bermatu digute. Kapitulu honetan, lan osotik nabarmendu beharreko ondorio nagusiak laburbiltzen dira.

Lehenik eta behin, metodo analitiko sentikor eta errepikakor desberdinak optimizatu eta berretsi dira antidepresibo triziklikoak (*tricyclic antidepressant*, TCA, delakoak) eta fluorokinolona (*fluoroquinolone*, FQ, delako) antibiotikoak ingurumeneko uretan (estuarioko, itsasoko eta araztegien irteerako uretan) eta biotan (muskuiluetan eta arrainen ehunetan/jariakinetan) determinatzeko. Nahiz eta TCA-en eta FQ-en uretako analisia bibliografian aztertuta egon, lan honetan garatu dira lehenengo aldiz arrainen gibela, behazuna eta plasma bezalako matrize konplexuetan lau TCA (amitriptilina, nortriptilina, imipramina and klomipramina) eta hamar FQ (*norfloxacin*, *enoxacin*, *pefloxacin*, *ofloxacin*, *levofloxacin*, *ciprofloxacin*, *danofloxacin*, *lomefloxacin*, *enrofloxacin* and *sparfloxacin*) determinatzeko metodo analitikoak.

Metodoaren etekinean eragina duten urrats guztiak sakonki optimizatu dira, hala nola erauzketa, garbiketa eta analisia. Erauzketari dagokionez, lagin solidoentzako garatutako metodo guztietan ultrasoinu fokatuen bidezko solido-likido erauzketa (*focused ultrasound solid-liquid extraction*, FUSLE, delakoa) erabili da. Izan ere, FUSLE erabilita intereseko konposatuen erauzketa osoa burutzeko nahikoa da disolbatzaile organikoen kantitate txikiarekin (7 mL) eta erauzketa-denbora laburrekin (30 s); beraz, disolbatzaileen gehiegizko kontsumoa eta urrats analitiko luzeak ekidin daitezke. TCA-ekin erkatuta, FQ-en kasuan bigarren erauzketa jarraia beharrezkoa izan da etekin egokiak lortzeko. Horrez gain, laginen konplexutasuna eta FUSLE-ren selektibitate eza direla eta, kasu guztietan optimizatu da garbiketa-urratsa fase solidoko erauzketa (*solid phase extraction*, SPE, delakoa) erabilita. TCA-k determinatzeko metodoetan, katioi-trukatzaile sendoekin modu mistoko SPE erabilita erauzi garbiak eta etekin onak lortu dira, fase geldikor horiek duten erretentzio-mekanismo selektiboaren ondorioz. Dena den, FQ-en analisian, matrize bakoitzaren arabera garbiketa-estrategia desberdina izan da beharrezkoa matrize-efektua gutxitu eta etekinak hobetzeko. Arrainen ehunen kasuan, muskulu-erauzien garbiketarako alderantziko faseko SPE (*reverse-phase SPE*, RP-SPE, delakoa) nahikoa izan den bitartean, gibelerako ezinbestekoa izan da likido-likido erauzketa eta RP-SPE konbinatzea. Bestalde, jariakin biologikoekin molekularki

inprimatutako polimeroak (*molecularly imprinted polymers*, MIPs, delakoak) erabilita lortu da ekiditea RP-SPE erabilita detekzioan behatutako matrize-efektua. Azkenik, estuarioko eta araztegien irteerako uren kasuan, beharrezkoa izan da anioi-trukatzaile ahula eta RP-SPE konbinatzea kromatografia-seinalearen txikitzea/handitzea minimizatzeko likido-kromatografia kuadrupolo hirukoitzeko masa-espektrometroari akoplatuta (LC-QqQ) burututako analisian. Garbiketa-urratsaren optimizazioaz gain, isotopikoki markatutako estandarren erabilerak matrize-efektua zuzendu eta emaitza zuzenak lortzea ahalbidetu du garatutako metodo guztietan.

Gainera, berretsitako metodo horiek Bizkaiko kostaldeko ur- eta biota-laginetan aplikatu ditugu TCA-en eta FQ-en segimendua egiteko. TCA-ei dagokienez, aipagarria da amitriptilina izan dela aztertutako laginetan bereziki detektatutako antidepresiboa. Estuarioko uretan (6,4 ± 0,2 ng/L) eta araztegien irteerako uretan (26 ± 1 ng/L) behatzeaz gaiz, korrokoien gibelean (1,8 ± 0,2 ng/g) ere agertu da amitriptilina. Bestalde, *ciprofloxacin*, *norfloxacin* eta *ofloxacin/levofloxacin* FQ-ak ere detektatu ditugu uretan eta arrainen gibeletan, 280 ± 20 ng/L eta 4,0 ±0,3 ng/g kontzentrazioetara arteko mailan, hurrenez hurren. Hori dela eta, garatutako metodoen bidez lortutako aurretiazko emaitza horiek argi adierazten dute komenigarria dela farmakoak eta zaintza pertsonalerako produktuak (*pharmaceuticals and personal care products*, PPCP, direlakoen) segimendua egiten jarraitzea ur- eta biota-laginetan.

Gainera, garatutako metodoak laborategian baldintza kontrolatuetan urraburu arrain gazteekin burututako esposizio-esperimentuetan ere erabili dira PPCP desberdinen (hau da, amitriptilinaren, *ciprofloxacin*-en eta oxibenzonaren) metatzea eta ehunen/jariakinen arteko banaketa aztertzeko. Analitoaren naturaren eragina argi eta garbi behatu dugu. Izan ere, polaritate txikiagoko amitriptilina ($\log K_{ow}$ = 4,8) eta oxibenzona ($\log K_{ow}$ = 3,6) analizatutako ehun/jariakin guztietan behatu diren bitartean, oso polarra ($\log K_{ow}$ = -0,85) eta zwitterionikoa (pKa_1 = 5,76 eta pKa_2 = 8,68) den *ciprofloxacin* behazunean soilik detektatu da. Amitriptilinaren ehunen arteko banaketari dagokionez, dosi baxuan (0,12 ng/mL) zein altuan (12 ng/mL) emaitza berdintsuak lortu dira. Hau da, kontzentrazio altuenak burmuinean eta zakatzetan aurkitu dira, ondoren gibelean, plasman eta behazunean eta, azkenik, baxuenak muskuluan. Emaitza horietatik ondoriozta daiteke metatzea zakatzetatik gertatu dela, eta antidepresiboa burmuinera heltzeko diseinatuta dagoela. Ondorioz, soilik muskuluan edo gibelean fokatzen diren ur-ingurumeneko ohiko esposizio-

azterketek larriki gutxietsi lezakete amitriptilinaren kontzentrazioa bere jomuga-organoan (burmuinean). Beste alde batetik, oxibenzona nagusiki behazunean metatu da, eta kontzentrazio baxuagoak behatu dira muskuluan, zakatzetan, gibelean eta plasman.

Horrez gain, ur-ingurumeneko PPCP-en esposizioaren benetako neurria osotasunez karakterizatu nahian, biologikoki aktiboak izan daitezkeen PPCP-en azpiproduktuak (transformazio-produktuak eta metabolitoak) identifikatu ditugu. Amitriptilinaren, *ciprofloxacin*-en eta oxibenzonaren 33, 35 eta 20 azpiproduktu karakterizatu ditugu, hurrenez hurren, likido-kromatografia-bereizmen altuko masa-espektrometriaren (LC-qOrbitrap-aren) bidez susmagarrien analisirako hurbilketa erabilita. Nabarmentzekoa da, eraldaketak jasan arren, amitriptilinaren 33 metabolitoek TCA-en eraztun hirukoitzeko egitura mantendu dutela, zeina toxikologikoki esanguratsua izan daitekeen. Horrenbestez, soilik amitriptilinan fokatzen diren ohiko esposizio-azterketek ez dituzte inondik inora aintzat hartzen azpiproduktuen kontzentrazioak nahiz eta biologikoki aktiboak izan daitezkeen. Izan ere, azken datuen arabera, ugaztunetan amitriptilinaren metabolito hidroxilatuak eta *N*-oxidatuak aktiboak izan daitezke. Amitriptilinaren azpiproduktuez gain, gutxienez arrainen gibelean eta behazunean behatutako oxibenzonaren bi azpiproduktuk, konposatu aitzindariaren gisara, aktibitate estrogenikoa eta antiendrogenikoa dute. Horregatik, ez dago zalantzarik, azpiproduktuen agerpenak zaildu egiten duela ur-ingurumeneko PPCP-en agerpenarekin lotutako arriskuen ebaluazioa, eta azpiproduktuen toxikotasuna ikertzea ere ezinbestekoa dela ingurumeneko arriskuen ebaluazio osoa burutu nahi bada.

Oro har, azpiproduktuen ehunen arteko banaketari dagokionez, metabolitoak detektatzeko matrize interesgarrienak behazuna, gibela eta plasma izan dira. Esate baterako, gibelean amitriptilinaren metabolito ugari (21) behatu izanak organo horren metabolizazio-aktibitate altua erakusten du, eta hori izan daiteke nahiko hidrofobikoa den amitriptilina gibel koipetsuan gehiago ez metatzearen arrazoia. *Ciprofloxacin*-en kasuan, konposatu aitzindariaren antzera, bere azpiproduktuak ere behazunean soilik detektatu dira. Azkenik, oxibenzonaren kasuan, behazunean behatutako oxibenzona maila altuak eta azpiproduktu kopuru handiak iradokitzen dute behazuna dela oxibenzona eta bere azpiproduktuak kanporatzeko jariakina. Hala ere, giltzurrunean zeharreko kanporatzea aztertzeko ikerketa sakonagoa burutu beharko litzateke.

Identifikatutako amitriptilinaren, *ciprofloxacin*-en eta oxibenzonaren azpiproduktu

guztietatik 10, 30 eta 12 egitura lehen aldiz deskribatu dira lan honetan, hurrenez hurren. Bibliografian aipatu gabe egotearen arrazoia kasu bakoitzean ingurumenean gertatzen diren erreakzio-mota desberdinekin lotuta egon daiteke. Izan ere, erreakzio horiek ingurumeneko baldintzen menpekoak izan daitezke, hau da, ur-motaren (itsasoko ura edo ur geza) edota espeziearen araberakoa. Izatez, doktorego-tesi honetan, arrainen presentzian zein arrainik gabeko itsasoko uretan identifikatu ditugu azpiprodukuak eta, bakar batzuk bakarrik zeudenez komunean, konfirmatu dugu PPCP-en degradazioa ingurumeneko baldintzen menpekoa dela. Guzti horrek iradokitzen du funtsezko erronka dela azpiproduktu berrien identifikazioa, ondoren, PPCP-en azpiproduktuen determinazioa eta beraien efektuen azterketa ingurumeneko arriskuen ebaluazioan sartu ahal izateko. Baina erronka hori zaildu egiten du azpiproduktu askorentzat erreferentziazko estandarrik eskuragarri ez egoteak. Hala eta guztiz ere, erreferentziazko estandarren faltan, bioaktiboak izan daitezkeen metabolito berrien identifikazio kualitatiboa burutzeko eraginkorra izan daiteke doktorego-tesi honetan erabili den susmagarrien analisirako hurbilketa. Hurbilketa horren bitartez identifikatutako egitura garrantzitsuak aurrerago konfirmatu eta erdi-kuantifikatu ahal izango dira estandarrak eskuragarri daudenean.

Behin PPCP-ak eta beren azpiproduktuak determinatzeko metodo bideratuak eta ez-bideratuak garatuta, konposatu horiek organismo urtarretan sortutako albo-ondorioetan zentratu gara. Amitriptilinarekin eta oxibenzonarekin burututako esposizio-esperimentuetatik ondorioztatu dugu PPCP horiek urraburu arrainen propietate fisiologiko orokorretan (arrainen pisuan eta luzeran, indize hepatosomatikoan eta egoera-faktorean) aldaketarik sortu ez arren, bide metabolikoak asaldatzeko gaitasuna dutela. Zehazki, nahiz eta oxibenzonarekin burmuineko metaboloma ez aldatu, amitriptilinaren kasuan aztertutako hiru matrizeetan (burmuinean, gibelean eta plasman) behatu dira aldaketa metabolikoak. Bi kutsatzaileen kasuan, behatutako albo-ondorioak orokorrean aztertzen diren efektuetatik haratago joan dira, hau da, oxibenzona ultramore (UM) iragazkiarenak aktibitate hormonaletik haratago eta amitriptilina antidepresiboarenak monoaminen xurgapenaren inhibiziotik haratago. Izatez, oxibenzonarekin burutako esposizio-esperimentuko emaitzek energia-metabolismoaren aldaketa eta estres oxidatiboa iradokitzen dituzte. Bestalde, amitriptilinaren esposizioko emaitzei erreparatuta, esan daiteke amitriptilinak ingurumenean esanguratsua den kontzentrazioan ere arrainen metaboloman

aldaketak sortzen dituela, eta dosi baxuko emaitzek dosi altukoekin bat egiten dutela. Bi kasuetan, energiaren, aminoazidoen eta lipidoen metabolismoko aldaketak ikusi dira, eta azken horrek estres oxidatiboa iradokitzen du. Horrez gain, dosi altuko esperimentuan behatutako metabolitoen aldaketek ahalbidetu dute maila molekularreko aldaketak organismo-mailako behaketekin lotzea, hala nola janguraren murriztearekin, jokabide-aldaketarekin eta arrainen zurbiltasunekin. Guzti horrek erakusten du aldaketa metabolikoen eta ondorio kaltegarrien arteko lotura. Oro har, estres akutuko erantzuna bizirauteko beharrezkoa denez, aurresan daiteke amitriptilinaren esposizioak sortutako jokabide-aldaketek ondorioak izan ditzaketela ingurumeneko estres-eragileekiko erantzunean, eta kalteak populazio-mailara heda daitezkeela. Ildo beretik, arrainek kolore-aldaketa komunikatzeko eta euren burua harrapakarietatik babesteko erabiltzen dutenez, kutsatutako arrainetan behatutako zurbiltasunak ere arazoak sortu ahal dizkie.

Organismo-mailako behaketa horiez gain, arrainekin ondorio kaltegarrien bidea (*adverse outcome pathway*, AOP, delakoa) aztertu duten ikerketetan arrainen ehunetan behatutako beste gertaera espezifiko batzuk (adibidez, estres oxidatiboa eta energia-metabolismoaren aldaketa) ere indibiduo- (hazte-atzerapena) eta populazio- (biziraupen murriztea) mailetako albo-ondorioekin lotu izan dira. Izatez, tesi honetan aztertutako PPCP-en (amitriptilinaren eta oxibenzonaren) bi kasuetan behatu ditugu kutsatzaileen ohiko albo-ondorio diren estres oxidatiboa eta energia-metabolismoaren aldaketa. Baina ohikoak izateak ez du esan nahi ez direnik kaltegarriak. Adibidez, oxigeno erradikal askeen produkzioaren eta gorputzeko babes antioxidatzaileen arteko desorekak ondorio garrantzitsuak ditu osasunean. Izan ere, desoreka horrek egitura eta funtzio zelularrak kaltetzen ditu, arrainen hazkuntzan, ugalketan eta gorputzaren mantenuan elkarrekintzak sortuta, eta ondorioz, etorkizuneko osasuna eta biziraupena kaltetuta. Horrez gain, estres oxidatiboaren zantzu nagusiena lipidoen metabolismoaren asaldatzea da. Lipidoen biosintesirako beharrezko diren erreaktiboak eskuragarriago badaude, kolesterola bezalako lipidoen igoera beha daiteke plasman, eta hori arrisku-faktore nagusia da desoreka kardiobaskularretarako zein bestelako gaixotasun askotarako.

Osotasunean, emaitza guzti horiek argi uzten dute metabolomikaren erabilgarritasuna kutsatzaileen ekintza-modua ikertzeko eta indibiduo- zein populazio-mailan albo-ondorioak eragin ditzaketen aldaketa metabolikoak behatzeko. Ondorioz, gene-adierazpenaren eta errezeptore-

loturen azterketen osagarri gisa, ingurumenerako arriskuen ebaluazioak aintzat hartu beharko lituzke metabolomikako lanak. Izan ere, maila ez-hilgarrietan agertzen diren kutsatzaileek eragindako maila molekularreko efektuak detektatzeko baliagarriak lirateke ingurumeneko kutsatzaileen segimendu-programetan.

Hitz bitan, doktorego-tesi honetan lortutako emaitza guztiak kontuan izanda, ondorioztatu da arrainen gisako organismo urtarrek kutsatutako itsasoko uretatik PPCP desberdinak meta ditzaketela, hala nola antidepresiboak, antibiotikoak eta UM iragazkiak. Ondorioz, kutsatzaile horiek elikadura-katean sar daitezke arrainen zein itsaskien bitartez, eta giza osasunerako arriskutsu bihurtu daitezke. Horrez gain, lan honek agerian uzten du PPCP-ek maila molekularreko albo-ondorioak eragiten dituztela aztertutako organismo urtarretan. Hori dela eta, PPCP-en eragina itsas-ekosistemetan eta jaki-kontsumitzaileetan aintzat hartu beharrekoa da, eta arau berriak ezarri beharko lirateke ikertzaileek PPCP-en agerpenaren eta arriskuen inguruko informazioa argitaratu ahala. Izatez, doktorego-tesi honetan, funtsezko informazio hori biltzeko baliagarriak izan daitezkeen hurbilketa analitikoak garatu ditugu. Horiei esker posible izan daiteke neurri arautzaileak ezarri ahal izateko PPCP-ek ur-ekosistemetan dituzten eraginen inguruko ezagutza handitzea.

Laburbilduz, doktorego-tesi honetan hiru PPCP moten (hau da, antidepresiboen, antibiotikoen eta UM iragazkien) organismo urtarretako biometatzea, biotransformazioa eta albo-ondorioak aztertu ditugu, eta etorkizun hurbilean estrategia holistiko berbera erabili liteke beste kutsatzaile edota beste espezie batzuen joerak ikertzeko. Izatez, etorkizunari erreparatuta, oraindik lan asko dago egiteko. Adibidez, esposizio-esperimentuei dagokienez, zebra-arraina (*Danio rerio*) edo Daphnia Magna bezalako eredu-organismoen erabilerak laborategien arteko erkaketak erraztuko lituzke. Horrez gain, arazketa-urratsa ikertzea ere interesgarria litzateke, eta baita giltzurrunak, hestea edo gernua bezalako ehun eta jariakin gehiago analizatzea. Guzti horrek PPCP-en farmakozinetikaren inguruko informazio gehiago eskuratzea bermatu, eta ondorioz, kutsatzaileen xedea hobeto ulertzen lagunduko luke.

Kutsatzaileek organismo urtarretan eragin ditzaketen albo-ondorioei dagokienez, emaitza nabarmenak lortu dira, bereziki, metabolomikako ikerketatik. Doktorego-tesi honetako behaketak babesteko informazio osagarria eman dezakete jokabide-azterketek, ebaluazio histologikoek eta

proteomika edo genomika bezalako beste teknika “omikoek”. Horrez gain, laborategiko baldintza kontrolatuetan burututako esperimentu azpikronikoetara mugatu beharrean, komenigarria da emaitza horiek ingurumeneko baldintza errealetan garatutako esperimentu kronikoekin erkatzea. Gainera, ezin da ahaztu PPCP-ak, beste kutsatzaile batzuekin batera, nahastean agertzen direla ur-ekosistemetan. Hori dela eta, aztarna anitzen analisi-metodo sentikorrak garatzeaz gain, ikerketa sakonagoak egin beharko lirateke nahasteek sor ditzaketen eraginak aintzat hartuta. Ildo horretan, ikerketa taldean burutuko diren hurrengo lanak etorkizun oparoa duen efektuek bideratutako analisian (*effect-directed analysis*, EDA, delakoan) fokatuko dira, zeinak toxikotasun-azterketa biologikoak, zatikapen-prozesuak eta metodo analitikoak konbinatzen dituen.

Eranskinak / Appendix

Appendix I: *Phase I and Phase II reactions that Compound Discoverer takes into account to predict possible by-products from the selected parent compound.*

Phase I reactions	
Dehydration	H_2O ->
Desaturation	H_2 ->
Hydration	-> H_2O
Nitro Reduction	O_2 -> H_2
Oxidation	-> O
Oxidative Deamination to Alcohol	H_2N -> HO
Oxidative Deamination to Ketone	H_3N -> O
Reduction	-> H_2
Thiourea to Urea	S -> O
Phase II reactions	
Acetylation	H -> C_2H_3O
Arginine Conjugation	H O -> $C_6H_{13}N_4O_2$
Glucoside Conjugation	H -> $C_6H_{11}O_5$
Glucuronide Conjugation	H -> $C_6H_9O_6$
Glutamine Conjugation	HO -> $C_5H_9N_2O_3$
Glycine Conjugation	HO -> $C_2H_4NO_2$
GSH Conjugation 1	-> $C_{10}H_{15}N_3O_6S$
GSH Conjugation 2	-> $C_{10}H_{17}N_3O_6S$
Methylation	H -> CH_3
Ornithine Conjugation	HO -> $C_5H_{11}N_2O_2$
Palmitoyl Conjugation	H -> $C_{16}H_{31}O$
Stearyl Conjugation	H -> $C_{18}H_{35}O$
Sulfation	H -> HO_3S
Taurine Conjugation	HO -> $C_2H_6NO_3S$

Appendix II: *Compound Discoverer workflow settings and parameters (Compound Discoverer 2.1).*

1. Select Spectra	
1.1. General Settings	- Precursor Selection: Use MS (N - 1) Precursor - Use New Precursor Reevaluation: True - Use Isotope Pattern in Precursor Reevaluation: True - Store Chromatograms: False
1.2. Spectrum Properties Filter	- Lower RT Limit: 0 - Upper RT Limit: 0 - First Scan: 0 - Last Scan: 0 - Ignore Specified Scans: (not Specified) - Lowest Charge State: 0 - Highest Charge State: 0 - Min. Precursor Mass: 100 Da - Max. Precursor Mass: 5000 Da - Total Intensity Threshold: 0 - Minimum Peak Count: 1
1.3. Scan Event Filters	- Mass Analyzer: (not Specified) - MS Order: Any - Activation Type: (not Specified) - Min. Collision Energy: 0 - Max. Collision Energy: 1000 - Scan Type: Any - Polarity Mode: (not Specified)
1.4. Peak Filters	- S/N Threshold (FT-only): 1.5
1.5. Replacements for Unrecognized Properties	- Unrecognized Charge Replacements: 1 - Unrecognized Mass Analyzer Replacements: ITMS - Unrecognized MS Order Replacements: MS2 - Unrecognized Activation Type Replacements: CID - Unrecognized Polarity Replacements: + - Unrecognized MS Resolution@200 Replacements: 60000 - Unrecognized MSn Resolution@200 Replacements: 30000
2. Align Retention times	
2.1. General Settings	- Alignment Model: Adaptive curve - Alignment Fallback: Use Linear Model - Shift Reference File: True - Maximum Shift [min]: 1 - Mass Tolerance: 5 ppm - Remove Outlier: True

3. Detect Unknown Compounds	
3.1. General Settings	- Mass Tolerance [ppm]: 5 ppm - Intensity Tolerance [%]: 30 - S/N Threshold: 3 - Min. Peak Intensity: 1000000 - Ions: [M+H]+1; [M+K]+1; [M+Na]+1; [M+NH4]+1; [M-H]-1 - Base Ions: [M+H]+1; [M-H]-1 - Min. Element Counts: C H - Max. Element Counts: C90 H190 Br3 Cl4 K2 N10 Na2 O15 P3 S5
3.2. Peak Detection	- Filter Peaks: True - Max. Peak Width [min]: 0.5 - Remove Singlets: True - Min. # Scans per Peak: 5 - Min. # Isotopes: 1
4. Group Unknown Compounds	
4.1. Compound Consolidation	- Mass Tolerance: 5 ppm - RT Tolerance [min]: 0.5
4.2. Fragment Data Selection	- Preferred Ions: [M+H]+1; [M-H]-1
5. Fill Gaps	
5.1. General Settings	- Mass Tolerance: 5 ppm - S/N Threshold: 1.5 - Use Real Peak Detection: True
6. Mark Background Compounds	
6.1. General Settings	- Max. Sample/Blank: 5 - Max. Blank/Sample: 0 - Hide Background: True
7. Search mzCloud	
7.1. Search Settings	- Compound Classes: All - Match Ion Activation Type: True - Match Ion Activation Energy: Match with Tolerance - Ion Activation Energy Tolerance: 20 - Apply intensity threshold: True - Precursor Mass Tolerance: 10 ppm - FT Fragment Mass Tolerance: 10 ppm - IT Fragment Mass Tolerance: 0.4 Da - Search Algorithm: HighChem HighRes --Library: Reference - Post Processing: Recalibrated - Match factor threshold: 50

	- Max. # results per compound and spectrum: 10
8. Predict Composition	
8.1. Prediction Settings	- Mass Tolerance: 5 ppm - Min. Element Counts: C H - Max. Element Counts: C90 H190 Br3 Cl4 N10 O18 P3 S5 - Min. RDBE: -1 - Max. RDBE: 40 - Min. H/C: 0.1 - Max. H/C: 3 - Max. # Candidates: 10 - Max. # Internal Candidates: 200
8.2. Pattern Matching	- Intensity Tolerance [%]: 30 - Intensity Threshold [%]: 0.1 - S/N Threshold: 3 - Min. Spectral Fit [%]: 10 - Min. Pattern Cov. [%]: 90 - Use Dynamic Recalibration: True
8.3. Fragments Matching	- Use Fragments Matching: True - Mass Tolerance: 5 ppm - S/N Threshold: 3
9. Map to KEGG Pathways	
9.1. By Mass Search Settings	- Mass Tolerance: 5 ppm
9.2. By Formula Search Settings	- Max. # of Predicted Compositions to be searched per Compound: 3
9.3. General Settings	- Max. # Pathways in 'Pathways' column: 20
10. Search ChemSpider	
10.1. Search Settings	- Database(s): BioCyc; Human Metabolome Database; KEGG; LipidMAPS - Mass Tolerance: 5 ppm - Max. # of results per compound: 100 - Max. # of Predicted Compositions to be searched per Compound: 3 - Result Order (for Max. # of results per compound): Order By Reference Count (DESC)
10.2. Predict Composition	- Check All Predicted Compositions: False
11. Search Mass Lists	
11.1. Search Settings	- Input file(s): \Endogenous Metabolites database 4400 compounds.csv; \Lipids_LMSD_HZI.csv - Show extra Fields as Columns: False - Consider Retention Time: False - RT Tolerance : 0.5 - Mass Tolerance: 5 ppm

Appendix III: *Reagents of endogenous metabolites.*

Reagent Name	**Purity of Reagent**
Adenine	99.0 %
L-Alanine	99.5 %
L-Alloisoleucine	100 %
L-Arginine	98.5 %
L-Asparagine	100 %
L-Aspartic acid potassium salt	98.0 %
β-Alanine	100 %
Citric Acid	99.0 %
L-Citrulline	99.0 %
Creatine	98.0 %
L-Cysteine	100 %
Cytosine	99.0 %
Levodopa	99.0 %
Dopamine hydrochloride	99.0 %
Fumaric Acid	99.0 %
γ-Aminobutyric acid	99.5 %
L-Glutamic acid monosodium salt monohydrate	99.0 %
L-Glutamine	99.0 %
Guanine	100 %
L-Histidine	98.0 %
L-Homoserine	98.0 %
L-Isoleucine	98.0 %
L-Leucine	99.0 %
L-Lysine	98.0 %
DL-Malic acid	99.5 %
L-Methionine	99.5 %
L-Ornithine monohydrochloride	99.0 %
L-Phenylalanine	100 %
L-Proline	99.0 %
Sodium pyruvate	99.0 %
L-Serine	100 %
Serotonin	98.0 %
Spermidine	99.0 %

Reagent Name	**Purity of Reagent**
Succinic Acid	100 %
Taurine	99.5 %
L-Threonine	98.0 %
Thymine	99.0 %
L-Thyroxine	99.0 %
L-Tryptophan	100 %
L-Tyrosine	99.0 %
Uracil	98.0 %
L-Valine	99.0 %
α-Ketoglutaric acid	99.0 %
DL-Homocysteine	95.0 %
Melatonin	98.0 %
5-Hydroxyindole-3-acetic acid (5-HIAA)	98.0 %
5-Hydroxytryptophan	100.0 %
L-Glutathione oxidized	98.0 %
L-Glutathione reduced	98.0 %

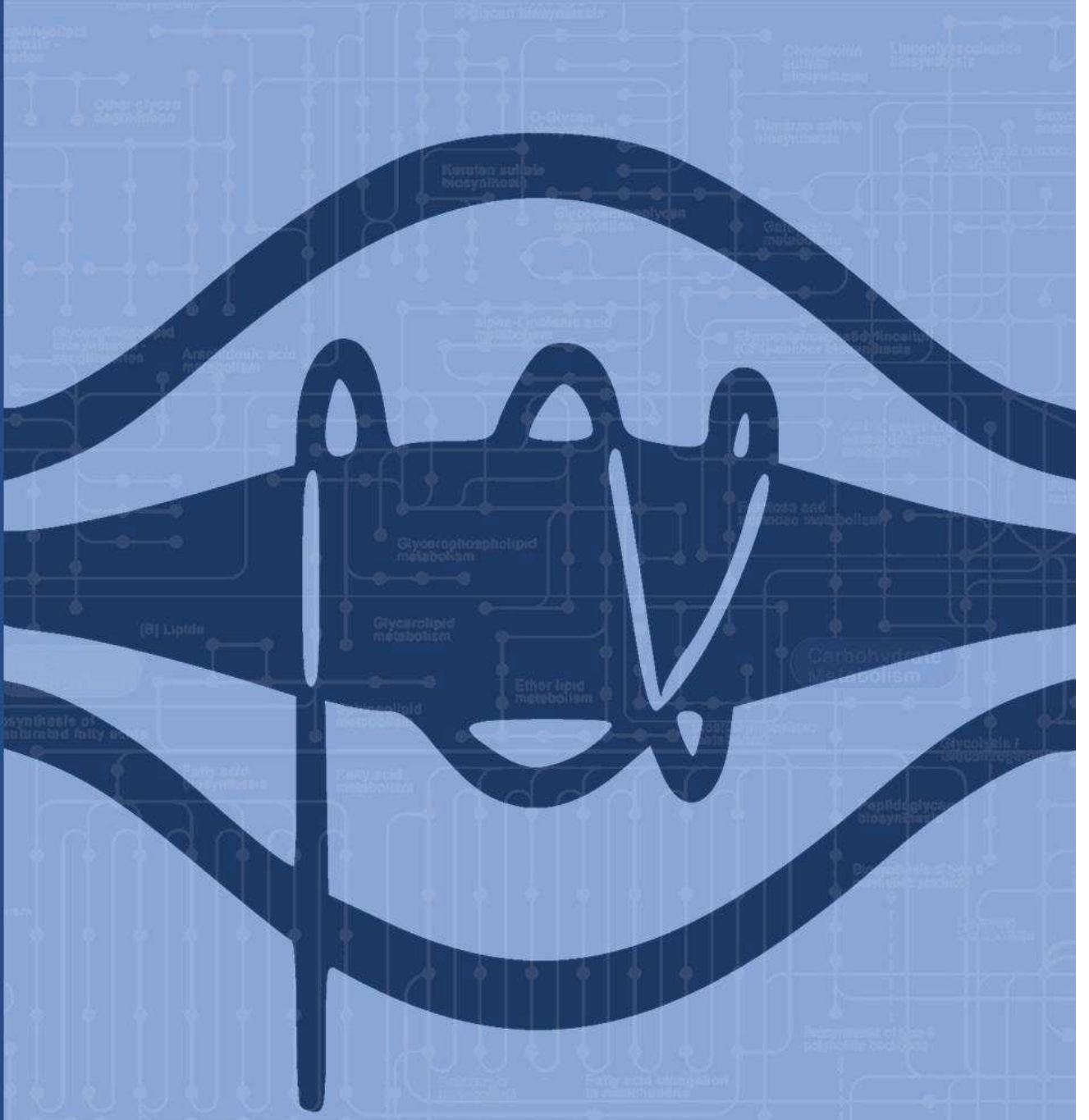

In this PhD work we have developed a holistic strategy to study the adverse effects of pharmaceuticals and personal care products on aquatic ecosystems, focusing on the determination, bioaccumulation and biotransformation of these pollutants on aquatic organisms, as well as on metabolomic studies. The results of this thesis confirm that the antidepressant amitriptyline, the antibiotic ciprofloxacin and the ultraviolet filter oxybenzone can be accumulated by fish, causing molecular-level adverse effects. Moreover, these integrated analytical approaches could be employed in other case studies to gather information required for environmental risk assessment and subsequent regulatory measures.